

Programme for the 14th European Conference on Antennas and Propagation (EuCAP 2020) (ver. 31 Mar 2020)

Application Tracks - Colour Legend															
	T01 LTE and Sub-6GHz 5G	T02 Millimetre wave 5G	T03 Wireless LANs	T04 IoT and M2M	T05 Biomedical and health	T06 Aircraft (incl. UAV, UAS, RPAS) and automotive	T07 Defence and security								
	T08 Positioning, localization & tracking	T09 Space (incl. cubesat)	T10 EM modelling and simulation tools	T11 Fundamental research and emerging technologies	T12 Scientific/Industrial Workshops	T13 Bicentennial Session									
Rooms															
Time	A2	A3	B1	B2	B4	B5	B6	B7	B8	B9	B10	B11	B3	Room 6	see below
Monday, 16 March															
09:00-10:00	OC: Opening Ceremony														
10:00-10:40	IK 01: Keynote 1														
10:40-11:10	Coffee Break (Exhibition Hall)														
11:10-11:50	IK 02: Keynote 2														
11:50-12:30	IK 03: Keynote 3														
12:30-13:30	Lunch (Exhibition Hall)														
13:30-15:30	CS02: Advanced Antenna Arrays for 5G and Beyond	T02-P09: Propagation Channels for Wide-Sense Vehicle-to-X Communications	SW04: COST Session CA18223 (SyMat): Periodic Structures with Higher Symmetries	CS21: Challenges in Leaky Wave Antennas and Novel Approaches to Solve Them	T07-A01: Antenna Theory and System Design	T08-A17: Antennas and Techniques for Positioning and Direction Finding	T05-A12/1: Wearable and Implantable Antennas	CS05: AMTA Session: Automotive Antenna Measurements and Testing	T09-A09: Millimetre-wave Lens Antennas for Space Applications	CS64: Trends and Advances in Machine Learning for Applied Electromagnetics	CS24: Controlling EM Waves with Low- and High-Dimensional Metamaterials	T11-E08: Metamaterials, Metasurfaces and Advanced Materials	IW05: Frontline of 5G Workshop: Insights on 5G Antenna & Propagation R&D from Sony and Regional Partners (Sony)		
15:30-16:00	Coffee Break (Exhibition Hall)														
16:00-18:00	T02-A04/1: Millimetre-wave Arrays for Mobile Communications	T02-P09: (cont'd)	SW04: (cont'd)	T04-A08: IoT Antennas	T07-A17: Multiband, Wideband and Array Antennas	T08-A17: (cont'd)	T05-A12/1: (cont'd)	T06-M03: Near-field, Far-field, Compact and RCS Range Measurement Techniques	T05-E05: Microwave Imaging	CS43: Near- and Far-Field Wireless Power Transfer	CS24: (cont'd)	T11-E08: (cont'd)	IW01: Key Advantages of Combining Measurements and Simulations for Antenna Applications (MVG)		
Tuesday, 17 March															
08:30-10:10	T02-A04/2: Millimetre-wave Arrays for Mobile Terminals	CS35: IET/IRACON Session: Propagation Measurements and Modelling for 5G and Beyond	CS38: ISAP Session: Recent Advances in Asian Antennas and Propagation Research	CS16: Antennas in IoT Wireless Devices: Modelling and Industrial Considerations	T11-M02: Radar Scattering Measurement and Calibration Techniques	CS01: Active Antennas for Onboard Space Applications	CS60: Sensors and Systems for Microwave Biomedical Imaging and Sensing	SW02: COST Session CA17115 (MyWAVE): Developments in Electromagnetic-Based Medical Technologies	T09-P08: Satellite Propagation	CS09: Analytical and Numerical Methods for Metasurface Analysis and Design	CS39: Machine Learning in Antennas	BC/1: History of Electromagnetism 1	SW08: Challenges of Modern Material Measurements		EurAAP 5: WG Active Array Antennas (8:30-10:10, Room: 17)
10:10-10:40	Coffee Break (Exhibition Hall)														
10:40-12:20	T02-A04/2: (cont'd)	CS35: (cont'd)	CS38: (cont'd)	CS16: (cont'd)	T10-M10: General Antenna Measurements	CS01: (cont'd)	CS60: (cont'd)	SW02: (cont'd)	T09-P08: (cont'd)	CS09: (cont'd)	CS39: (cont'd)	T10-E03/1: Computational and Numerical Techniques 1	SW08: (cont'd)		EurAAP 3: WG Software and modelling (10:40-12:20, Room: 17)
12:20-13:20	Lunch (Exhibition Hall)														
13:20-14:50	Convened Poster Sessions 1: Room A2 (Poster Area)							Regular Poster Sessions 1: Exhibition Hall							

	CS08: Analysis, Design and Use of Microwave Techniques, Models, Systems, and Antennas for Snowpack Avalanches Monitoring CS10: Antenna Array and Integrated Systems for 5G Communication Applications CS17: Antennas with Multi-Port/Distributed Feeding and On-Antenna Power-Combining for Efficient Integration and Reconfigurability CS18: Applications of mm-Wave Gap Waveguide Technology-I CS19: Applications of mm-Wave Gap Waveguide Technology-II CS27: Electromagnetics in MRI Applications CS57: Recent Research on Wind Turbines: EM Modelling and Measurements						A07: Dielectric Resonator Antennas A09: Propagation Experimental Methods and Campaigns A17: Array Antennas, Antenna Systems and Architectures (incl. Radomes) A18: Reflector, Feed Systems, and Components A19: Reflectarrays and Transmitarrays A22: MIMO, Diversity, Smart Antennas & Signal Processing				M01: Material Characterisation and Non-destructive Testing M03: Near-field, Far-field, Compact and RCS Range Measurement Techniques M04: Data Acquisition, Imaging Algorithms and Processing Methods P02: Propagation Modelling and Simulation P03: Channel Sounding and Parameter Estimation Techniques P04: Propagation Experimental Methods and Campaigns				EurAAP 1: WG Measurements + AMTA Europe (12:50-14:50, Room: 5), EurAAP 2: WG Small Antennas (12:40-14:00, Room: 17)
14:50-15:30	IS-Tue 1/1: Invited Speaker Session	IS-Tue 2/1: Invited Speaker Session													
15:30-16:10	IS-Tue 1/2: Invited Speaker Session														
16:10-16:40	Coffee Break (Exhibition Hall)														
16:40-18:20	T04-A20: Wireless Power Transfer and Inductive Coupling	CS56: Recent Advances on Electronically Steerable Antenna Arrays at mm-Wave Frequencies	CS58: Reconfigurable Antennas for Compact Devices	T04-A15: RFID and Backscattering Antennas	CS67: Water-Based Microwave Devices	CS28: EuMA/EurAAP Session: From Radiating Section to Digital Interface - Research and Design Trends for an End-To-End Approach of Highly Integrated Active Antenna Systems	SW01: COST Session CA15104 (IRACON): Measurements and Simulations in Channel Modelling in Wireless Body Area Networks	CS03: Advanced Radar Measurements, Modelling and System Solutions for Vehicular Applications	CS15: Antennas for Radio Astronomy	CS32: High-Frequency Methods and Applications	T11-P02/1: Channel Modelling for Massive MIMO and Near-Field Communication Systems	T10-E03/2: Computational and Numerical Techniques 2	IW04: CTG Workshop on Advances in Antenna Measurements for Modern (Antenna Systems S.L.)	IW10: Sophisticated Antenna Development for Modern Hearing Aids (WS Audiology)	
Wednesday, 18 March															
08:30-10:10	T09-A19: Reflectarrays and Transmitarrays	CS06: AMTA/IRACON Session: Over-The-Air Testing of 5G Radios	CS45: New Perspectives and Applications of Characteristic Mode Analysis in Antenna Design	CS62: Small Antenna in a Human Body Environment	CS26: Education in Electromagnetics, Antennas, and Microwaves	CS47: Non-Magnetic Nonreciprocity	SW03: COST Session CA17115 (MyWAVE): Supporting Medical Device Development via Dielectric and Thermal Tissue Characterization	T06-A17: Automotive Antennas	CS55: Recent Advances in Terahertz Antennas for Radio-Astronomy and Space Exploration	CS66: Unconventional Techniques and Applications for Inverse Scattering Problems	T11-P02/2: Machine Learning in Radio Propagation	BC/2: History of Electromagnetism 2	IW06: Active Impedance Assessment and Beamforming Optimization for mm-Wave Antenna Arrays (Optenni Ltd)	IW09: 5G Antenna Array Design and Integration Simulation (ANSYS)	
10:10-10:40	Coffee Break (Exhibition Hall)														
10:40-12:20	T09-A19: (cont'd)	CS06: (cont'd)	CS45: (cont'd)	CS62: (cont'd)	CS26: (cont'd)	CS47: (cont'd)	SW03: (cont'd)	T06-A17: (cont'd)	CS55: (cont'd)	CS66: (cont'd)	T11-P04: Experimental Methods and Campaigns	T06-M10: UAV-Based Antenna Measurements (AMTA)	IW02: Analysis and Design of Advanced Antenna Systems using TICRA Tools (TICRA)	IW07: State-of-the-art in Antenna System Simulation with CST Studio Suite (Dassault Systèmes)	
12:20-13:20	Lunch (Exhibition Hall)														
13:20-14:50	Convended Poster Sessions 2: Room A2 (Poster Area)						Regular Poster Sessions 2: Exhibition Hall								

	CS14: Antennas for Harsh Environment CS29: Exotic Antennas from Nano to Macro Scales CS36: Innovative Lens Antennas for Future Communication Systems CS41: Metasurfaces for Mobile (5G and Beyond) and Satellite Communication Systems CS50: Novel Wave Phenomena in Metamaterials and Metasurfaces Applied to Antennas and Propagation CS61: Signal Processing Techniques for Advanced Electromagnetics Synthesis, Analysis, and Measurements						A01: Antenna Theory A02: Antenna Interactions and Coupling A04: Mm-, Sub-mm-wave, and Nano-optical Antennas A08: Electrically Small Antennas A10: Slotted-waveguide and Leaky-wave Antennas E02: EM Theory and Analytical Techniques E03: Computational and Numerical Techniques E04: Optimisation Methods in EM					E05: Imaging and Inverse Scattering E06: Scattering and Diffraction, E07: Frequency and Polarization Selective Surfaces P05: Mm-wave and UWB Propagation P09: Propagation for Vehicular Communications P10: Propagation in Biological Tissues and Body Area Propagation P12: Radar, Localisation, and Sensing P13: Radio Science and Remote Sensing				
14:50-15:30	IS-Wed 1/1: Invited Speaker Session	IS-Wed 2/1: Invited Speaker Session														
15:30-16:00	Coffee Break (Exhibition Hall)															
16:00-16:40	IS-Wed 1/2: Invited Speaker Session	IS-Wed 2/2: Invited Speaker Session													ESoA: ESoA Meeting (16:00-18:00, Room: 5)	
16:40-17:45																
17:45-18:00	Conference Dinner (Wallmans)															
18:00-23:59																
Thursday, 19 March																
08:30-10:10	T01-A11: Multiband and Wideband Antennas	CS34: IET/AMTA Session: Test and Measurement Challenges for 5G and Beyond	T02-P02: Millimetre-wave Propagation Modelling	CS46: New Trends in Leaky Wave Antennas	CS44: Near-Field Focusing and Pulse Generation Through Localized Waves	CS25: Convergence of Mobile Radio and Radar	T05-A12/2: Point of Care Microwave Sensors	T06-P09: Propagation for Unmanned Aerial Vehicles (UAVs)	CS30: Fundamental Challenges and Novel Methodologies in the Next-Generation Computational Electromagnetics	T10-E05/1: Electromagnetic Methods for Direct and Inverse Scattering Involving Stratified Media	CS07: AMTA/EurAAP Session: Post Processing Techniques in Antenna Measurements	BC/3: History of Electromagnetism 3	SW07: H2020 Project ACASIAS (GA N° 723167) - Antennas for Integration into Aircraft Structure	IW03: Efficiently Simulating and Optimising Antenna Placement in Virtual Test Scenarios (Altair)		
10:10-10:40	Coffee Break (Exhibition Hall)															
10:40-12:20	T01-A02: Terminal Antennas and Interactions with Surroundings	CS34: (cont'd)	T01-P02: Propagation Modelling and Simulation	CS46: (cont'd)	CS44: (cont'd)	CS25: (cont'd)	T05-A12/2: (cont'd)	T11-P10: Propagation in Biological Tissues	CS30: (cont'd)	T10-E05/1: (cont'd)	CS07: (cont'd)	T11-E01: EM Theory	SW07: (cont'd)			
12:20-13:20	Lunch (Exhibition Hall)															
13:20-14:50	Best Paper Awards Poster Sessions: Room A2 (Poster Area)						Regular Poster Sessions 3: Exhibition Hall									
	Antennas Electromagnetics Propagation Measurement Best Student Paper						A06: Conformal Antennas A11: Multiband and Wideband Antennas A12: Wearable and Implantable Antennas A13: Adaptive and Reconfigurable Antennas A14: Active and Integrated Antennas A15: RFID Antennas/Sensors and Systems A16: UWB Antennas and Time-domain Techniques A20: Antennas for Wireless Power Transmission and Harvesting					A21: Additive Manufacturing A23: Other Antenna Topics E08: Metamaterials, Metasurfaces and EBG M07: Satellite and Aerospace Antenna Characterisation M09: MIMO and OTA Testing M10: General Antenna Measurements M11: Other Measurement Topics				
14:50-15:30	IS-Thu 1/1: Invited Speaker Session	IS-Thu 2/1: Invited Speaker Session														
15:30-16:10	IS-Thu 1/2: Invited Speaker Session	IS-Thu 2/2: Invited Speaker Session														
16:10-16:40	Coffee Break (Exhibition Hall)															
16:40-18:00	CS42: Nano and Quantum Antennas	CS49: Novel Techniques for Beam Manipulation at	T03-A11: Antennas for WLAN Applications	T02-A10: Leaky-wave and Traveling-wave Antennas	CS63: State of the Art in Antenna Research in	CS31: GNSS Antennas and Systems for Challenged RF	T05-A12/3: Body Area Antennas and Sensor Systems	T06-P12: Radar, Localisation and Sensing for Aircraft and	T09-P13: Propagation Aspects in Remote Sensing	T10-E05/2: Imaging and Inverse Scattering	CS48: Novel Antenna Measurement Data Analysis	SW05: ESA Session: Selected Papers from the 40th ESA				

18:00-18:20		Millimeter			Russia	Environment		Automotive Applications			and Techniques	Workshop on Antenna Developments for Terrestrial and Small-Space Platforms			EurAAP 4: WG Propagation (18:00-20:00, Room: B8)
18:20-18:40															
18:40-20:00															

Friday, 20 March

08:30-10:10	T01-A22: MIMO, Diversity, Smart Antennas & Signal Processing	CS37: IRACON Spectrum Sharing: Challenges and Opportunities for 5G and Beyond	CS33: IET Session: New Antenna Systems Involving Application of Metamaterials and Metasurfaces	T05-M06: Dosimetry, Exposure, and SAR Assessment	T11-E06: Scattering and Diffraction	T11-M05: EMI/EMC/PIM Chambers, Instrumentation, and Measurements	SW06: H2020 Session ID764479 (EMERALD): Electromagnetic Imaging for a Novel Generation of Medical Devices	T06-A11: Aircraft Antennas	CS59: Reconfigurable Reflectarray and Transmitarrays	T10-P02: Propagation Modelling and Simulation	CS11: Antenna Design and Fundamental Bounds with External Constraints	CS20: Assessment and Modeling of Antennas and Radio Channels Jointly	SW09: Integration Challenges for Low-cost Mm-wave Phased Arrays		
10:10-10:40	Coffee Break (Exhibition Hall)														
10:40-12:20	T01-A22: (cont'd)	CS37: (cont'd)	CS33: (cont'd)	T02-M08: Mm-wave, THz, and Quasi-optical Antenna Measurements	T11-E06: (cont'd)	T11-M01: Material Characterisation and Non-destructive Testing	SW06: (cont'd)	T06-A11: (cont'd)	CS59: (cont'd)	T10-P02: (cont'd)	CS11: (cont'd)	CS20: (cont'd)	SW09: (cont'd)		
12:30-13:30	CC: Closing Ceremony														

Monday, 16 March 9:00 - 10:00

OC: Opening Ceremony

Room: A2

Chairs: Olav Breinbjerg (Technical University of Denmark, Denmark), Cyril Mangenot (Api-Space, France)

Monday, 16 March 10:00 - 10:40

IK 01: Keynote 1

Room: A2

Chairs: Mats Gustafsson (Lund University, Sweden), Katsuyuki Haneda (Aalto University, Finland), Daniel Sjöberg (Lund University, Sweden)

10:00 *The Technology Journey Towards 6G*

[Magnus Frodigh](#) (Ericsson AB, Sweden)

5G is now in the deployment phase. We will see broad roll-out of 5G systems over the next coming years. Extra interesting will be to follow the uptake of new use cases, with richer interactivity for consumers, smarter cities and fully connected manufacturing in Industry 4.0. In a research context, there is still more to be done in the evolution of 5G, work on specific properties to further improve support for the new use cases. But gradually we will start looking into more fundamental additions to connectivity, break-through technology that will be needed to fulfill the visions of the Internet of senses and fully connected intelligent machines, and to continue addressing sustainability targets. To do this, we need to broaden the discussion on the evolution towards 6G to also include, technologies for trustworthiness, fully cognitive networks and fully integrated edge compute capabilities.

10:40 *Microwave Imaging in Real Time*

[Natalia Nikolova](#) (McMaster University, Canada)

Real-time microwave and millimeter-wave imaging methods are the workhorse in applications ranging from synthetic aperture radar, which operates with far-field data, to nondestructive testing and medical imaging, which employ near-field measurements. Research in this field is intensifying due to expansion in numerous applications fueled by the advances in high-frequency electronics and flexible field-programmable platforms. This paper is an attempt to explain, categorize, compare and contrast these methods within a common framework thus making this interdisciplinary subject more comprehensible and accessible to the research community.

Monday, 16 March 11:10 - 11:50

IK 02: Keynote 2

Room: A2

Chairs: Mats Gustafsson (Lund University, Sweden), Katsuyuki Haneda (Aalto University, Finland), Daniel Sjöberg (Lund University, Sweden)

11:10 *Application of Machine Learning to Wireless Channel Modeling*

[Jianhua Zhang](#) and [Li Yu](#) (Beijing University of Posts and Telecommunications, China); [Yuxiang Zhang](#) (Beijing University Of Posts And Telecommunications, China); [Zhen Zhang](#) and [Zhiqiang Yuan](#) (Beijing University of Posts and Telecommunications, China)

With the increasing antenna number, wide frequency range, huge bandwidth, and versatile application scenarios brought by fifth generation (5G) and beyond, channel measurement data will be quite huge. Measurement data processing is very time consuming and channel characteristics are difficult to capture and model accurately. Thanks to machine learning has been successfully demonstrated efficient handling big data and find the hidden rules. Thus, it is reasonable to develop channel models by taking advantage of data mining and machine learning algorithms. In this presentation, some of our attempts of applying big data analytics, especially machine learning algorithms to channel modelling have been principally explained and summarized, including Gaussian mixture model (GMM) based channel multipaths clustering, principal component analysis (PCA) based channel parameter reduction, MIMO channel fading tracking and prediction, and intelligent channel modeling schemes, etc. Finally, the open issues and future research directions of ML application in channel model are discussed.

11:50 *Impact of Spatially Consistent Channels on Digital Beamforming for Millimeter-Wave Systems*

[Harsh Tataria](#) and [Fredrik Tufvesson](#) (Lund University, Sweden)

The premise of massive multiple-input multiple-output (MIMO) is based around coherent transmission and detection. Majority of the vast literature on massive MIMO presents performance evaluations over simplified statistical propagation models. All such models are drop-based and do not ensure continuity of channel parameters. In this paper, we quantify the impact of spatially consistent (SC) models on beamforming for massive MIMO systems. We focus on the downlink of a 28GHz multiuser urban microcellular scenario. Using the recently standardized Third Generation Partnership Project 38.901 SC-I procedure, we evaluate the signal-to-interference-plus-noise ratio of a user equipment and the system ergodic sum spectral efficiency with zero-forcing, block diagonalization, and signal-to-leakage-plus-noise ratio beamforming. Our results disclose that at practical signal-to-noise ratio levels, SC channels yield a significant performance loss relative to the case without SC due to substantial spatial correlation across the channel parameters.

Monday, 16 March 11:50 - 12:30

IK 03: Keynote 3

Room: A2

Chairs: Mats Gustafsson (Lund University, Sweden), Katsuyuki Haneda (Aalto University, Finland), Daniel Sjöberg (Lund University, Sweden)

11:50 *Present and Future Trends in Electromagnetics and Metamaterials*

[Andrea Alù](#) (CUNY Advanced Science Research Center, USA)

In this talk, I will discuss recent trends and opportunities in the context of electromagnetics research and metamaterials, with particular attention on the opportunities offered by nonlinearity, gain and spatio-temporal modulation to overcome some of the outstanding limitations of conventional approaches. We will discuss opportunities stemming from commutated switching networks and from modulation of the electromagnetic properties of artificial materials to enable non-reciprocal responses for guided and radiated waves, as well as to leverage parametric phenomena. We will also discuss possible applications of this technology from radio-waves to nano-optics.

Monday, 16 March 13:30 - 15:30

CS02: Advanced Antenna Arrays for 5G and Beyond

T02 Millimetre wave 5G / Convened Session / Antennas

Room: A2

Chairs: [Y. Jay Guo](#) (University of Technology Sydney, Australia), [Richard Ziolkowski](#) (University of Technology Sydney, Australia & University of Arizona, USA)

13:30 *Beam Steerable Reflectarray Enabling CubeSat Internet of Space: Conceptualization and Design*

[Junbo Wang](#) and [Vignesh Manohar](#) (University of California, Los Angeles, USA); [Yahya Rahmat-Samii](#) (University of California Los Angeles (UCLA) & UCLA, USA)

The vision of Internet of Things (IoT) has evolved the needs of providing seamless connectivity between devices across the globe. A potential solution to this requirement is to launch a CubeSat constellation that can provide broadband Internet access to rural and undeveloped areas (Internet of Space (IoS)). This has escalated the need for low-cost, low-profile antennas with wide angle beam steering capabilities. In this work, we elaborate on the design of a broadband, circularly polarized reflectarray capable of dynamic beam steering in the frequency range of 17.8-20.2 GHz. The reflectarray unit cell consists of a set of four copies of rotated Archimedean spiral arms, and the desired phase shift is obtained by suitably switching between these arms through PIN diodes. Representative prototypes have been fabricated and measured, and beam scans up to 60 have been achieved.

13:50 *A Wideband Differentially Fed Multi-beam Antenna Array*

[He Zhu](#) and [Y. Jay Guo](#) (University of Technology Sydney, Australia)

A differential Butler matrix is presented in this paper using a new type of wideband unbalanced-to-balanced power dividers. The differential Butler matrix has the merit of high levels of common-mode signal suppression. A differential array with four elements is also designed, fabricated and tested. By feeding the differential array with the differential Butler matrix, two beams are produced in the E-plane radiation pattern. The differentially fed array achieves very low cross-polarization level due to the excellent common-mode suppression from the Butler matrix. The design approach is verified experimentally, and the measured result agrees well with the predicted one, demonstrating the application potential for the presented differential beam-forming networks.

14:10 *On the Design of a 27-dBi Phased Array for 5G Point-to-Point Communications*

[Huasheng Zhang](#), [Sjoerd Bosma](#) and [Andrea Neto](#) (Delft University of Technology, The Netherlands); [Ulrik Imberg](#) (Huawei Technologies, Sweden AB, Sweden); [Nuria LLombart](#) (Delft University of Technology, The Netherlands)

In this contribution the design of a 27-dBi gain dual-polarized phased array for point-to-point 5G communications is presented. The 4x4 array achieves the desired gain, thanks to the wide spacing between the feeding elements. Grating lobes are suppressed by using movable dielectric lenses that provide directive and steerable element patterns. The array is also capable of scanning electronically to 10 degree in two main planes, suffering only 2 dB of degradation in gain, thanks to the simultaneous shifting of the lenses by a few millimeters.

14:30 *3-D Printed High-Efficiency Wideband 2X2 and 4X4 Double-Ridged Waveguide Antenna Arrays for Ku-Band Satcom-On-The-Move Applications*

[Francesco Filice](#) (Polytech'Lab, University of Nice & ST Mricroelectronics Crolles, France); [Nour Nachabe](#) (University of Nice Sophia Antipolis, France); [Frédéric Giancesello](#) (STMicroelectronics, France); [Guillermo Alvarez Narciandi](#) (University of Oviedo, Spain); [Jaime Laviada](#) (Universidad de Oviedo, Spain); [Fernando Las-Heras](#) (University of Oviedo, Spain); [Cyril Luxey](#) (University Nice Sophia-Antipolis, France)

The development of Low-Earth-Orbit (LEO) satellite communications aims at delivering low-cost worldwide internet connection. The development of compact and low-cost user terminals on Earth represents a fundamental step to reach the consumer mass-market. Here, we present the design, fabrication and test of a 3D-printed 2x2 double-ridged waveguide (DRWG) antenna array with waveguide feeding network, working at Ku- Band (10.75 - 14.5 GHz) with simulated total efficiency > 70%. A 4x4 array is also designed leveraging the previous concept with simulated total efficiency > 60% and realized gain of ~ 16 dBi, paving the way for innovative low-cost antenna solutions for user's terminal.

14:50 *Circularly Polarized Antenna Array Based on Microstrip Ridge Gap Waveguide at 60 GHz*

[Abdelmoniem Hassan](#) and [Ahmed Kishk](#) (Concordia University, Canada)

A high gain, circularly polarized 4x4 antenna array, is proposed. A circularly polarized magneto-electric (ME) dipole element is used as a radiating element. The 4x4 antenna array excited by slots and feeding networks of microstrip ridge gap waveguide (MRGW). A compact design is archived with including the effect of the mutual coupling. The simulated 4x4 array achieved an impedance bandwidth of 20.8% for $|S_{11}| < -10$ dB with a maximum gain of 20.3 dBi, which is higher than any reported 4x4 array antenna. An axial ratio bandwidth of 18.3% is achieved.

15:10 *Millimeter-Wave Dual-Polarized Slot Array Antenna Using a TE210 and TE120 Mode*

[Qingling Yang](#), [Steven Gao](#), [Lehu Wen](#) and [Qi Luo](#) (University of Kent, United Kingdom (Great Britain)); [Xiaofei Ren](#) (China Research Institute of Radiowave Propagation, China); [Jian Wu](#) (China Research Institute of Radiowave Propagation, P. R. China); [Yong-Ling Ban](#) (University of Electronic Science and Technology of China, China)

This paper presents a millimeter-wave dual-polarized slot antenna array by using a SIW cavity supporting TE210 and TE120 modes. A crossed slot is etched over the cavity. The antenna element can be excited from two orthogonal directions to realize dual-polarization. Thanks to the orthogonality between TE210 and TE120 mode, high isolation and low cross-polarization are achieved in the antenna. A prototype of the designed antenna array is demonstrated at the center frequency of 25 GHz. The measured and simulated results are in good agreement showing that the antenna array has high radiation efficiency, high port isolation and low cross-polarization.

Monday, 16 March 13:30 - 18:00

T02-P09: Propagation Channels for Wide-Sense Vehicle-to-X Communications

T02 Millimetre wave 5G / Regular Session / Propagation

Room: A3

Chairs: [Uwe-Carsten G. Fiebig](#) (German Aerospace Center (DLR), Germany), [Ke Guan](#) (Beijing Jiaotong University, China), [Juan Moreno](#) (Metro de Madrid S.A. & Universidad Politécnica de Madrid, Spain), [Fernando Pérez-Fontán](#) (University of Vigo, Spain)

13:30 *60 GHz V2I Channel Variability for Different Elevation Angle Switching Strategies*

[Herbert Groll](#) and [Erich Zöchmann](#) (TU Wien, Austria); [Markus Hofer](#) (AIT Austrian Institute of Technology, Austria); [Hussein Hammoud](#) (University of Southern California, USA); [Seun Sangodoyin](#) (Georgia Institute of Technology, USA); [Thomas Zemen](#) (AIT Austrian Institute of Technology GmbH, Austria); [Jiri Blumenstein](#) (Brno University of Technology, Czech Republic); [Ales Prokes](#) (Brno University of Technology & Sensor, Information and Communication Systems Research Centre, Czech Republic); [Andreas Molisch](#) (University of Southern California, USA); [Christoph F Mecklenbräuker](#) (TU Wien, Austria)

We report results based on millimeter wave vehicle-to-infrastructure (V2I) channel measurements carried out in an urban street environment, down-town Vienna, Austria. Signal to noise ratios (SNRs) have been acquired at 60 GHz with 100 MHz bandwidth. Two horn antennas were used on a moving transmitter vehicle: one horn emitted a beam towards the horizon and the second horn emitted an elevated beam at 15-degrees up-tilt. This configuration was chosen to assess the impact of beam elevation on V2I communication channel variability. The variability of the V2I channel is shown by density estimates of the channel transfer function magnitudes. The channel changes severely along the vehicle trajectory in an urban street scenario. Density estimates in the region with clear wide-angle view are bimodal and motivate a TWDP fading model for V2I communication with horizontal and elevated antenna beams. We compare three different strategies for beam switching: fixed, geometry-based, and SNR-based.

13:50 *Emulation of End-To-End Communications Systems in Railway Scenarios: Physical Layer Results*

[Juan Moreno](#) (Metro de Madrid S.A. & Universidad Politécnica de Madrid, Spain); [Sofiane Kharbech](#) (University of Lille, France); [Laurent Clavier](#) (Institut Mines-Telecom, Telecom Lille & IEMN / IRCICA, France); [Redha Kassi](#) (University of Lille, France); [Raúl Torrego](#), [Aitor Arriola](#) and [Iñaki Val](#) (IK4-IKERLAN, Spain); [Marion Berbineau](#) (IFSTTAR, COSYS, LEOST & University Lille Nord de France, France); [Jose Soler](#) and [Ying Yan](#) (Technical University of Denmark, Denmark)

The complexity of modern communication systems is remarkable, and the efforts needed to put into service a new one are substantial as well. In some industrial sectors, circumstances are even harder. For example, in railways, the tests to be done are costly due to the integration in the rolling stock plus the need to have physical access to the railway tracks. Therefore, it is worth having a suitable emulator that considers many different radio-access technologies (RAT) in several railway scenarios (viaducts, tunnels, rural, hilly, etc.). Moreover, it should be able to do an end-to-end emulation, absolutely transparent for the application layer (this is, considering not only the physical layer but the network one as well). In this paper, we highlight the physical layer aspects considered in the construction of this emulator. Integration with the network layer is briefly mentioned, as well as the whole architecture.

14:10 *Millimeter-Wave Channel Characteristics for V2V Communications in the Garage Entrance*

[Xue Zhang](#) and [Pan Tang](#) (Beijing University of Posts and Telecommunications, China); [Lei Tian](#) (Beijing University of Posts and Telecommunications & Wireless Technology Innovation Institute, China); [Jianhua Zhang](#) (Beijing University of Posts and Telecommunications, China)

To design fifth-generation (5G) millimeter-wave (mm-wave) vehicle-to-vehicle (V2V) communication systems for the future intelligent transportation system (ITS), the knowledge of channel characteristics in various vehicular communication environments is essential. In this paper, we present a channel measurement at 28 GHz in a common scene, a

typical underground garage entrance, and analyze the channel characteristics, including path loss, shadow fading, and root mean square (RMS) delay spread (DS). Statistical results of these channel characteristics are presented. Differences between our measurement-based channel characteristics and those of the existing results are discussed. Furthermore, we investigate the change trend of the RMS DS along the garage entrance, and find that the special structure of the garage entrance has a apparent effect on the RMS DS. These results are helpful to design the physical layer for the future V2V communication systems.

14:30 *Millimeter-Wave Channel Characterization for Vehicle-to-Infrastructure Communication*

[Lina Wu](#), [Danping He](#), [Ke Guan](#) and [Bo Ai](#) (Beijing Jiaotong University, China); [Junhyeong Kim](#) and [Hee Sang Chung](#) (ETRI, Korea (South))

The vehicle-to-infrastructure (V2I) communication can capture infrastructure data and provide travelers with real-time traffic information, which can significantly improve road safety. Millimeter-wave (mmWave) with large bandwidth has been introduced as a key technology to achieve ultra-reliable, low latency, and high-data-rate V2I communication. In this paper, the V2I communication in mmWave band (22.1GHz-23.1GHz) is characterized for typical urban and highway scenarios. By considering the different deployments involving overtaking and traffic flow, the simulations are conducted by employing the self-developed ray-tracing. The key channel parameters, including received power, Rician K-factor, root-mean-square delay spread and angular spreads, are analyzed and compared between different deployments. Moreover, the impacts of the multiple antennas and beam switching technologies at the vehicle are evaluated as well. This work aims to help the researchers understand the channel characteristics of the V2I communication in mmWave band and support communication system design for vehicular communications.

14:50 *Large Scale Fading Characteristics for Vehicle-to-Cyclist Channel in Urban Environment at 5 GHz*

[Ibrahim Rashdan](#) and [Michael Walter](#) (German Aerospace Center (DLR), Germany); [Wei Wang](#) (Chang'an University, China); [Giuseppe Caire](#) (Technische Universität Berlin, Germany)

Vehicle-to-vulnerable road users (V2VRU) communication provides 360 degree of awareness for both vehicles and vulnerable road users (VRUs). A realistic and accurate channel model for V2VRU in critical accidents scenarios is of great importance for developing reliable V2VRU communication systems. This paper presents a large scale fading characterization based on a wideband channel measurement campaign in urban environment considering a collision scenario between a vehicle and a cyclist. A dual-slope path loss model is proposed, and a zero-mean Gaussian distribution is found to best fit the shadow fading. Additionally, for more realistic system-level simulations, the spatial correlation of shadow fading are calculated. The underlying correlation is captured by using 2-dimensional spatially correlated shadow fading maps.

15:10 *28-GHz High-Speed Train Measurements and Propagation Characteristics Analysis*

[Jae-Joon Park](#), [Juyul Lee](#), [Kyung-Won Kim](#) and [Myung-Don Kim](#) (ETRI, Korea (South))

In this paper, we investigate millimeter-wave propagation characteristics of high-speed moving train based on field measurements in a tunnel and viaduct scenario. The measurements were carried out at 28 GHz emulating for a 3GPP-like high-speed train (HST) deployment scenario where a transmitter is positioned next to a track and a receiver is mounted on the rooftop of a train carriage. Based on the measurement data, we analyzed path loss (PL) and observed the PL is almost constant with respect to distance in the tunnel. Other channel parameters, such as delay spread and Doppler shift were studied as well. Multipaths were periodically observed in the analysis results. It was caused by objects regularly installed along the tracks, such as overhead power line equipments.

15:30 Coffee Break

16:00 *Architecture and Performance of the Base Station Prototype for MN Systems*

[Sung Woo Choi](#) and [Junhyeong Kim](#) (ETRI, Korea (South)); [Seon-Ae Kim](#) (Electrics and Telecommunications Research Institute, Korea (South)); [Hee Sang Chung](#) (ETRI, Korea (South)); [Ilgyu Kim](#) (ETRI of KOREA, Korea (South))

This paper presents current updates of Moving Network (MN) system. The MN has been developed to escalate passenger's Internet access speed in buses. It uses wide spectrum of millimeter waves to get higher network throughput but undergoes severe deterioration of signal in the urban road environment. In this paper, the system architecture and features of physical layer specification are provided. And simulation results of physical uplink channels are given to evaluate the uplink performance. We show the architecture of MN prototypes which have been produced recently. From indoor test, the base-station throughput was estimated to reach 3 Gbps with 6 component carriers. By using these prototypes, all specifications of MN will be tested and outdoor experiment will be started.

16:20 *Shadowing and Multipath-fading Statistics at 2.4 GHz and 39 GHz in Vehicle-to-Vehicle Scenarios*

[Hui Wang](#), [Xuefeng Yin](#) and [José Rodríguez-Piñeiro](#) (Tongji University, China); [Juyul Lee](#) and [Myung-Don Kim](#) (ETRI, Korea (South))

In this paper, a recently conducted measurement campaign aiming at 39 GHz millimeter wave (mmWave) and sub-6 GHz vehicle-to-vehicle (V2V) propagation channel characterization is introduced. Simultaneous signal tracing at both mmWave and sub-6 GHz were performed in the measurements in order to evaluate the different influences of common environments and vehicle-flowing modes on channel characteristics at two distinctive bands. Four typical vehicle flow modes are considered in our measurements. Channel parameters investigated include shadowing, fast fading, and their space coherent behaviors. The results obtained show that most shadowing and fast fading segments follow truncated Gaussian distributions in most vehicle-flow modes and propagation scenarios considered. In most scenarios, the spacial consistency of 2.4 GHz channel can be maintained in larger distances than in the case of 39 GHz.

16:40 *Bi-directional Vehicle-to-Vehicle Radio Channel Characteristics over Bridge at 5.9 GHz*

[Kun Yang](#) and [Ning Zhou](#) (Super Radio AS, Norway); [Terje Røste](#) (NTNU, Norway); [Junyi Yu](#), [Fang Li](#) and [Wei Chen](#) (Wuhan University of Technology, China); [Egil Eide](#) and [Torbjorn Ekman](#) (Norwegian University of Science and Technology, Norway); [Changzhen Li](#) and [Fuxing Chang](#) (Wuhan University of Technology, China)

A V2V radio channel measurement campaign with a maximum distance of 2 km was performed over bridge between two urban areas in Wuhan city, China. In this paper, a detailed description of the channel measurement campaign including antenna setups, channel sounder configurations and other related info is given. The RSL is extracted from the measured data and interpreted. The APDP are demonstrated, from which the mean excess delay and the RMS delay spread are extracted and shown. It can be found that the 90% of the mean excess delay and the RMS delay spread are within 758 ns and 1.18 micro s, respectively. The best-fit amplitude distribution of the small-scale fading is estimated by using a model selection algorithm based on the Akaike Information Criterion (AIC). The TWDP, Rayleigh and Rician model are found to be the best-fit models at different TX-RX distances and the physical interpretation is given.

17:00 *Measurement and Diffuse Multipath Analysis of V2V Propagation Channel at 5.9 GHz in Tunnel Area*

[Suying Jiang](#), [Xu Zhang](#) and [Wei Wang](#) (Chang'an University, China); [Mi Yang](#) and [Ruisi He](#) (Beijing Jiaotong University, China)

Vehicle-to-vehicle (V2V) communication is an essential fundament of intelligent transportation systems (ITS). Therefore, evaluating the influence of the radio propagation channel of ITS is of great interest. So far the diffuse multipath in V2V propagation channel in tunnel area has not been thoughtfully studied. This paper presents channel measurements and analysis of V2V channel characteristics at 5.9 GHz in tunnel. We evaluate and compare the received power and root mean square (RMS) delay spread for outside and inside tunnel. Further, we use the space-alternating generalized expectation-maximization (SAGE) based channel parameter estimator with the autoregressive (AR) filter to estimate the specular and the diffuse multipath components. Results reveal that the diffuse multipath inside tunnel is not dominant in the line-of-sight (LoS) case. The ratio between the diffuse multipath component (DMC) power and the total received power has a mean value of 10.56% and a standard deviation of 8.7%.

17:20 *Comparison of a Fast Analytical Ray Tracer and Channel-Sounder Measurements for V2V Communications*

[Nils Dreyer](#) (TU Braunschweig, Germany); [Thomas Kürner](#) (Technische Universität Braunschweig, Germany)

Ray optical path loss predictions for Ad-hoc networks (Device-to-Device) are still a complex and time consuming task. In past publications we introduced a new predictor concept that is based on visibility analysis, leading to a huge predictor speed up for the computation of reflected rays. In this paper we present our new extensions of the simulation framework, introducing a methodology to apply the same visibility concept on side-building diffraction and non-specular reflection. Our approach is fast enough to be applied on scenarios with a realistic number of communication pairs in the future. We further evaluated our predictor for the first time by applying the model on an intersection scenario and comparing the result with a measurement campaign performed in 2009 in the Swedish city Lund. The result of the Power Delay Profile offers a good agreement between measurement and simulations, however we could observe difference of the power distribution.

17:40 *Path Loss Models and Large Scale Fading Statistics for C-Band Train-to-Train Communication*

[Paul Unterhuber](#), [Ibrahim Rashdan](#) and [Michael Walter](#) (German Aerospace Center (DLR), Germany); [Thomas Kürner](#) (Technische Universität Braunschweig, Germany)

The profound knowledge of wireless propagation is essential for wireless communication between vehicles. To evolve and test communication standards we need channel models in representative environments to neither over-, nor underestimate the effect of the surrounding environment and the movement of the vehicles; typical environments for railway communication are railway station, open field and hilly environments. We introduce train-to-train (T2T) path loss models and large scale fading statistics based on channel sounder measurement data as a first step towards a geometry-based stochastic channel model (GSCM). The models represent the mentioned typical environments for railway applications. We compare the results with previous published intelligent transportation system (ITS-G5) measurement based models and highlight the differences.

SW04: COST Session CA18223 (SyMat): Periodic Structures with Higher Symmetries

T11 Fundamental research and emerging technologies / Convened Session / Electromagnetics

Room: B1

Chairs: [Francisco Mesa](#) (University of Seville, Spain), [Guido Valerio](#) (Sorbonne Université, France), [Pablo Padilla](#) (University of Granada, Spain)

13:30 *High Scanning Rate Leaky Wave Antenna Based on Glide Symmetry for 77 GHz Automotive Radar*

[Adrián Tamayo-Domínguez](#) (Universidad Politécnica de Madrid, Spain); [Jose Manuel Fernández González](#) (Universidad Politécnica de Madrid, Spain); [Oscar Quevedo-Teruel](#) (KTH Royal Institute of Technology, Sweden)

This work presents a leaky wave antenna at W band with glide-symmetric protrusions that enhance the scanning ratio of previous works. Also, a conventional leaky wave is designed for comparing the results in terms of required bandwidth and steering range. Both prototypes are based on gap waveguide technology to prevent the leakage due to air gaps

between layers. In order to reduce the manufacturing cost, the designs are aimed to 3D-printing. A Taylor amplitude modulation is conducted in the two cases to reduce side lobe levels. The glide-symmetric leaky wave provides a variation of the steering angle from 12.14° to 50.84° in a band from 74.2 GHz to 79.8 GHz. The scanning ratio compared with the simple leaky wave is enhanced by a factor of 6.41. This rapid variation of the steering angle in a narrow band (7%) is of interest for automotive radars.

13:50 *Holey Glide-Symmetric Waveguide Filters for 5G Communication Systems at Millimetre Wave Frequencies*

[Alberto Monje-Real](#) (KTH Royal Institute of Technology, Sweden); [Nelson Fonseca](#) (European Space Agency, The Netherlands); [Oskar Zetterstrom](#) (KTH Royal Institute of Technology, Sweden); [Elena Pucci](#) (Ericsson AB, Sweden); [Oscar Quevedo-Teruel](#) (KTH Royal Institute of Technology, Sweden)

In this paper, we present a holey, fully-metallic, glide symmetric waveguide filter. This solution is low-loss, cost-effective, robust and suitable for applications at millimetre wave frequencies (e.g. Ka band). We also explore here the possibility to break the glide symmetry as an additional degree of freedom to control the pass and stopbands. Finally, a denser kind of glide symmetry, named braided glide symmetry, is introduced to enhance the attenuation per unit cell.

14:10 *Ultra-Wide Band Non-Dispersive Leaky-Wave Antenna Based on Glide-Symmetric Meandered Transmission Lines*

[Mahsa Ebrahimpouri](#) and [Oscar Quevedo-Teruel](#) (KTH Royal Institute of Technology, Sweden); [Mauro Ettore](#) (University of Rennes 1 & UMR CNRS 6164, France); [Anthony Grbic](#) (University of Michigan, Ann Arbor, USA)

We present an ultra-wide band planar Luneburg lens based on glide-symmetric meandered transmission lines. In order to make the structure radiate, a non-dispersive leaky-wave structure is designed. The whole structure produces a pencil beam with steering capabilities from -60° to 60° in the azimuth direction from 10 to 20 GHz.

14:30 *A Frequency-Controlled Fast Beam-Scanning Antenna with Glide-Symmetric Feeding*

[Wenxuan Tang](#) and [Qiangqiang Shi](#) (Southeast University, China); [Qiang Cheng](#) (Southeastu University, China); [Tie Jun Cui](#) (Southeast University, China)

This paper presents a frequency-controlled fast beam-scanning antenna fed with a glide-symmetric transmission line of spoof surface plasmon polaritons. Split ring resonators are located close to the transmission line as radiators. Due to the glide-symmetric property, negative-group-velocity waveguiding is supported on the transmission line and continuous beam scanning from backward to forward is realized. Directive beam is observed in simulation to scan from -52 to 32 degree when frequency varies from 9.2 to 10.22 GHz.

14:50 *Holey and Pinned Structures Comparison for Waveguide Phase Shifters*

[Angel Palomares-Caballero](#) (Universidad de Granada, Spain); [Antonio Alex-Amor](#) (Technical University of Madrid, Spain); [Juan Valenzuela-Valdés](#) (Universidad de Granada, Spain); [Pablo Padilla](#) (University of Granada, Spain)

This paper presents the applicability of using structures to control the phase shift in a waveguide phase shifter. By means of dispersion diagrams, different phase shift unit cells are analyzed. Glide symmetry is also applied to some of these unit cells to evaluate its effects in the propagating modes. Then, unit cells with best dispersive behaviour are selected to design two waveguide phase shifters, one by pinned unit cells and the other by holey pinned unit cells. Both waveguide phase shifters are well matched in the frequency range from 50-75 GHz with insertion losses lower than 0.5 dB. The phase shift produced by both waveguide phase shifter is also evaluated. Pinned waveguide phase shifter is more dispersive compared to the holey waveguide phase shifter, producing a phase shift deviation over 180° of +50° and +10°, respectively.

15:10 *Design of Antenna Arrays Using Groove Gap Waveguide Technology Implemented with Glide Symmetric Holes*

[Luis Fernando Herran](#) (University of Oviedo, Spain); [Astrid Algaba Brazález](#) (Ericsson Research, Ericsson AB, Sweden); [Malcolm Ng Mou Kehn](#) (National Chiao Tung University, Taiwan); [Eva Rajo-Iglesias](#) (University Carlos III of Madrid, Spain)

There is an explosion designs of high directive antennas (mainly arrays) based on the use of gap waveguide technology. In most of them, the periodic structure used as Electromagnetic Band Gap (EBG) to control the leakage is the Bed of Nails. We present here another option where glide-symmetrical holes are used as EBG to design Groove Gap Waveguide (GGWG) based antennas. The use of this unit cell that is much bigger than the pins is beneficial for the manufacturing aspects but poses some challenges in the design of compact components or arrays. Two examples of antenna designs will be presented, one of them includes the design of a compact 1 to 4 power divider.

15:30 Coffee Break

16:00 *Reconfigurable Microwave Components Using Glide-symmetric Pin-loaded Parallel Plates*

[Mohammad Bagheriasl](#) (Sorbonne University, France); [Julien Sarrazin](#) and [Guido Valerio](#) (Sorbonne Université, France)

Glide-symmetric structures have recently gained a lot of interest in the design of electromagnetic bandgap materials due to their high attenuation in the stopband region and for their capability to support an almost dispersionless wave propagation. In this paper, we propose a reconfigurable waveguide using a glide-symmetric structure with pins. We show how the wave propagation in this waveguide can be enabled or suppressed by a mere adjustment of the displacement between the two metallic plates of the waveguide. In addition, we demonstrate how this structure can be used to design a phase shifter.

16:20 *Higher-Order Cylindrical Leaky Waves in Planar Structures*

[Paolo Burghignoli](#), [Walter Fuscaldo](#) and [Davide Comite](#) (Sapienza University of Rome, Italy); [Paolo Baccarelli](#) (Roma Tre University, Italy); [Alessandro Galli](#) (Sapienza University of Rome, Italy)

The main features of the recently-introduced class of cylindrical leaky waves having arbitrary azimuthal order (higher-order cylindrical leaky waves, HOCLWs) are presented. Canonical continuous ring sources are described, capable of exciting such waves in general multilayered structures. The relevant electrodynamic potentials are derived and analytical formulas are provided for their radiation patterns in the far-field region. Guidelines for the design of discrete ring sources, i.e., circular phased arrays, for the excitation of HOCLWs up to a desired maximum order are also provided.

16:40 *Mode-matching Analysis of Loaded Transmission Lines with Twist Symmetries*

[Oskar Zetterstrom](#) (KTH Royal Institute of Technology, Sweden); [Guido Valerio](#) (Sorbonne Université, France); [Francisco Mesa](#) (University of Seville, Spain); [Fatemeh Ghasemifard](#), [Martin Norgren](#) and [Oscar Quevedo-Teruel](#) (KTH Royal Institute of Technology, Sweden)

This paper studies the propagation characteristics in twist-symmetric structures by means of a mode-matching approach. The studied structures are coaxial transmission lines periodically loaded with 1- and 3-fold twist-symmetric infinitely thin sectorial sheets. The mode-matching formulation is validated with the commercial software CST Microwave Studio. In addition, the impact of adding twist symmetry to a coaxial line on the coupling of the higher order TM modes is discussed.

17:00 *Dual-band Polarizing Screen Based on Self-Supported Metallic Structures*

[Carlos Molero](#) (IETR-INSA Rennes, France); [Lionel Simon](#) (SWISSto12 SA, Switzerland); [Esteban Menargues](#) (SWISSto12, Switzerland); [Tomislav Debogovic](#) (SWISSto12 SA, Switzerland); [María García-Vigueras](#) (IETR-INSA Rennes, France)

A metallic periodic screen is here proposed that allows for dual-band operation and polarization conversion. The unit-cell structure is monolithic and three-dimensional, and it consists of a section of metallic waveguide loaded with perforations at its lateral walls. The geometry of the unit cell allows for independent control of incident fields with horizontal or vertical orientation. This feature is employed to manipulate the polarization of the illuminating wave. An equivalent circuit is proposed in order to model the cell behavior. Three design examples are proposed with different polarization conversion capabilities. One of the examples concerns a dual-band polarizer providing orthogonal sense of circular polarization at each of the bands. Such a design is manufactured and some preliminary measurements are shown in order to validate the proposed concept.

17:20 *Exceptional Points of Degeneracy in Electromagnetic Waveguides and the Role of Symmetries*

[Tarek Mealy](#), [Mohamed Y Nada](#), [Ahmed F. Abdelshafy](#), [Ehsan Hafezi](#) and [Filippo Capolino](#) (University of California, Irvine, USA)

We show the relation between reflection and glide symmetry in periodic waveguides and the existence of various orders of exceptional points of degeneracy (EPDs). We use an equivalent circuit network to model each unit-cell of the waveguide. Assuming that a coupled mode waveguide supports N modes in each direction we derive the following conclusions. When N is even, we show that a periodic waveguide with reflection symmetry may exhibit EPDs of maximum order N. To obtain a degenerate band edge (DBE) with only two coupled waveguides, reflection symmetry must be broken. For odd N, N+1 is the maximum order that may be obtained, and an EPD of order N is not allowed. We present an example of three coupled microstrip transmission lines and show that by introducing glide symmetry we enable the occurrence of a stationary inflection point (SIP) which is an EPD of order three.

17:40 *Analysis of Glide-Symmetric Dielectric Corrugated Structures - Properties of TE and TM Propagating Modes*

[Zvonimir Sipus](#) and [Marko Bosiljevac](#) (University of Zagreb, Croatia)

Tailoring dispersion properties of different waveguiding structures using glide-symmetric properties has shown huge potential. Our interest in this paper is focused on the analysis and design of such dielectric glide-symmetric structures. The analysis method separates the analyzed structure into different regions and describes the EM field in each region with suitable modes. These representations are then connected using symmetry properties which results in an efficient approach for determining dispersion properties and gives a clear physical insight into the propagation mechanisms in such waveguides. The developed approach is verified using the results of commercial solver and this is followed with the analysis of differences between TE and TM modes and the obtainable properties.

Monday, 16 March 13:30 - 15:30

CS21: Challenges in Leaky Wave Antennas and Novel Approaches to Solve Them

T11 Fundamental research and emerging technologies / Convened Session / Antennas

Room: B2

Chairs: [Darwin Blanco](#) (Ericsson, Sweden), [Eva Rajo-Iglesias](#) (University Carlos III of Madrid, Spain)

13:30 *Quasi-Optical Excitation of a Circularly-Polarized Metasurface Antenna at K-band*

[Jorge Ruiz García](#) (Université de Rennes, France); [Marco Faenzi](#) (Université de Rennes 1, France); [Adham Mahmoud](#) (Institut d'Électronique et de Télécommunications de Rennes, France); [Mauro Ettore](#) (University of Rennes 1 & UMR CNRS 6164, France); [Patrick Potier](#) ((DGA), France); [Pouliguen Philippe](#) (DGA, France); [Ronan Sauleau](#) (University of Rennes 1, France); [David González-Ovejero](#) (Centre National de la Recherche Scientifique - CNRS, France)

This paper presents a new concept of modulated metasurface (MTS) antenna for satellite communications. As opposed to using cylindrical surface waves (SW) to excite circular apertures, we employ a quasi optical beamformer to launch a plane SW. This architecture enables an efficient illumination of rectangular apertures. In addition, the use of anisotropic MTS elements allows us to obtain circularly-polarized beams with excellent characteristics in terms of cross-polarization discrimination. We present the design process of a prototype at K-band and the obtained simulation results, which prove the suitability of this antenna for satellite data links.

13:50 *Leaky Wave Analysis of Periodic Corrugated Metallic Plates with Complex Shapes*

[Despoina Kampouridou](#) and [Alexandros Feresidis](#) (University of Birmingham, United Kingdom (Great Britain))

The leaky wave analysis of corrugated metallic structures is presented in this work. Two known analytical periodic methods are compared with the results of the Matrix Pencil Method, which is applied for the first time for this type of leaky wave antenna. The complex wavenumber of the leaky mode is extracted for two corrugated antenna cases designed for operation around 30 GHz. From the calculated dispersion the farfield characteristics of the leaky wave antenna and its design procedure can be indicated.

14:10 *Near-field Focusing Through Higher-order Cylindrical Leaky Waves*

[Davide Comite](#), [Walter Fuscaldo](#) and [Paolo Burghignoli](#) (Sapienza University of Rome, Italy); [Paolo Baccarelli](#) (Roma Tre University, Italy); [Alessandro Galli](#) (Sapienza University of Rome 1, Italy)

The possibility of generating a higher-order nondiffracting Bessel beam by means of a fast backward spatial harmonic is discussed in this work. The focusing features of the radiated near field are achieved by the excitation of a higherorder cylindrical leaky wave supported by an annular metal-strip grating placed on a grounded dielectric slab, which is excited by a circular arrangement of elementary sources. By properly phasing the array elements, the azimuth order of the radiated beam is controlled, offering the possibility of generating a focused beam of arbitrary order n carrying a nonzero orbital angular momentum. Full-wave simulations of a prototype are developed using a commercial code and the field profiles are compared with the ideal beam supported by an infinite aperture.

14:30 *Near-Field Beamforming in Leaky-Wave Resonant Antennas*

[Sjoerd Bosma](#), [Huasheng Zhang](#), [Andrea Neto](#) and [Nuria LLombart](#) (Delft University of Technology, The Netherlands)

There is a large interest in utilizing lens arrays for many applications in the mm- and submm- wavelength ranges. The efficiency of the excitation of dielectric lenses increases significantly when the feeding structures support leaky-wave radiation mechanisms. Leaky-wave feeding structures based on resonant cavities can generate very high directivity in a dense medium. Many scenarios require lenses of moderate size and typically the focusing surface needs to be in the near field of the radiators. In this contribution, we analyse the near-field radiation mechanism of such leaky-wave feeds and provide guidelines to design moderate size lenses.

14:50 *Prism-based Leaky-Lens Antennas at 60 GHz for 5G Point-to-Point Communication Links*

[Qiao Chen](#) (KTH Royal Institute of Technology, Sweden & State Key Laboratory of Millimeter Wave, Southeast University, China); [Oskar Zetterstrom](#) (KTH Royal Institute of Technology, Sweden); [Francisco Mesa](#) (University of Seville, Spain); [Pablo Padilla](#) (University of Granada, Spain); [Angel Palomares-Caballero](#) (Universidad de Granada, Spain); [Elena Pucci](#) (Ericsson AB, Sweden); [Xiaoxing Yin](#) (State Key Laboratory of Millimeter Waves, China); [Oscar Quevedo-Teruel](#) (KTH Royal Institute of Technology, Sweden)

Two cost-effective implementations of a leaky-lens antenna at 60 GHz are proposed for high-throughput 5G communication links. The leaky-wave feed is realized in gap-waveguide technology, where the radiation from the slit is controlled with glide-symmetric holes. The beam-squint of the leaky-wave radiation is mitigated, owing to the coupling of a complementary-dispersive prism. Here, two prisms are implemented, one with glide-symmetric holes, and another with substrate-integrated-holes (SIHs), both integrated in parallel plates with the leaky-wave feeding. Thanks to glide symmetry, better control of the leakage rate, lower costs, and better tolerance to manufacturing are achieved in comparison with the non-glide hole counterpart. In addition, the SIH-based design exhibits substantially enhanced bandwidth with even better robustness. In the analysis of the leaky-wave feed, more accuracy and reduced computational time is achieved by using a multi-mode method. Both antennas show stable radiation patterns, featuring high efficiency, high gain, and low side lobe levels.

15:10 *Direct Synthesis of Frequency-Scanned Monopulse Half-Width Microstrip Leaky-Wave Antennas*

[Alejandro Gil Martinez](#) (Technical University of Cartagena Cartagena, Spain); [Miguel Poveda-Garcia](#) (Technical University of Cartagena, Spain); [Jose-Luis Gómez-Tornero](#) (Polytechnic University of Cartagena, Spain)

We propose a synthesis technique for half-width microstrip leaky-wave antennas (HWM LWAs) producing frequency-scanned monopulse patterns with two channels. The election of the substrate thickness and dielectric constant is of key importance to obtain the desired angular scanning in the prescribed frequency band, and with high radiation efficiency. Using the two far advertising channels of Bluetooth Low Energy (BLE) protocol in the 2.45 GHz band, we demonstrate that wide and narrow scanning designs can be directly obtained with the proposed approach, while dispensing from any numerical optimization. It is examined how different dielectric laminates and antenna sizes are convenient for each design.

T07-A01: Antenna Theory and System Design

T07 Defence and security / Regular Session / Antennas

Room: B4

Chairs: [Animesh Biswas](#) (IIT Kanpur, India), [Angelo Freni](#) (University of Florence, Italy)

13:30 *Analysis of Compensation Methods and the Capability Boundary for Element Position Errors in Electrically Scanned Arrays*

[Josef Ydreborg](#) (European Space Agency, ESTEC, The Netherlands); [Bengt Svensson](#) (Saab AB, Sweden); [Jian Yang](#) (Chalmers University of Technology, Sweden)

Mechanical translational tolerances have negative effects on the radiation patterns in sensor and antenna arrays. Methods for restoring the radiation pattern of an array with element position errors to the designed one without the position errors have been investigated and the limits of their capabilities in different scenarios of real array configurations explored. A proof of concept has been established by manufacturing an intentionally erroneous antenna array and applying investigated compensation methods. Conclusion is that the possibilities of compensating for mechanical errors are greatly enhanced with increased digitalisation of the array antenna system. Analog systems may achieve a full compensation in a smaller solid angle, while digital systems can achieve a full compensation covering almost the half space.

13:50 *Novel Dual-mode SIHC Based Filtering Antenna*

[Prasun Chongder](#) (NIT Rourkela, India); [Soumava Mukherjee](#) (Indian Institute of Technology Jodhpur, India); [Animesh Biswas](#) (IIT Kanpur, India)

In this paper, a compact dual-mode substrate integrated hexagonal cavity (SIHC) based integrated filtering antenna is proposed. The design utilizes perturbation in a high Q dual-mode cavity to introduce radiation nulls in the antenna response thereby improving selectivity. The measured resonant frequency of the proposed filter is at 8.9 GHz with 290 MHz (-10 dB S11) impedance bandwidth (3.26%) and reflection coefficient is below 15 dB in the filtering passband. The gain of the filtering antenna is flat throughout the operating band (4.33 dBi) and has one radiation null at 8.65 GHz which is at the left side of the passband edge of the filter and thereby improving selectivity. The measured cross-polarization level is below 18 dB. Here the efficient use of higher order mode of SIW cavity to realize compact filtering antenna that makes it suitable for low profile wireless communication applications.

14:10 *Axial-ratio Tuning in Nano-Dielectric Resonator Antenna for Optical Band Applications*

[Shailza Gotra](#) (NIT Delhi, India); [Rajesh Yadav](#) (National Institute of Technology Delhi, India); [Vinay Pandey](#) (NIT Delhi, India); [Rajveer Singh Yaduvanshi](#) (AIACR, India)

A rectangular circularly polarized nano- dielectric resonator antenna (NDRA) is presented in the proposed work. The Gaussian pulse excitation is given through the nanostrp feedline. The excitation position is chosen at the edge of the feedline having width equivalent to the quarter wavelength. This will split the field components into the quadrature phase difference travelling at the sides of the feedline. The travelling field with orthogonal components coupled inside DR resulting in the circular polarization. Further, this technique is utilized to tune the axial-ratio of the antenna within different optical bands by changing the excitation position. The rectangular DR allows the generation of specific mode similar to the analogy of mode in the cylindrical DR. The proposed NDRA is designed for the optical L, C, and S-band applications.

14:30 *Experimental Demonstration of Artificial Magnetic Conductors Constructed of Magnetically Coupled Helices*

[Pavel Petrov](#) and [Alastair Hibbins](#) (University of Exeter, United Kingdom (Great Britain)); [Ian Youngs](#) (Platform Systems Division, Dstl, Salisbury, United Kingdom (Great Britain)); [Mario Lima](#) (Antenna Applied Research, Electronics Division, Leonardo, United Kingdom (Great Britain)); [John Sambles](#) (University of Exeter, United Kingdom (Great Britain))

An Artificial Magnetic Conductor (AMC) is a type of metamaterial that can be used to enhance the performance in several antenna and microwave design applications. In this work we propose a novel geometry of AMC constructed of magnetically coupled helical elements that are smaller than those previously suggested and which may be optimized to achieve a broadband performance. Numerical results (obtained using COMSOL) are shown to be in good agreement with experimental ones.

14:50 **3D Printed Broadband Double-Ridged Waveguide to Coax Transition**

[Karina Hoel](#) (FFI & University of Oslo, Norway); [Stein Kristoffersen](#) (FFI, Norway)

A broadband double-ridged waveguide to coax transition, specifically designed for 3D printing manufacturing is demonstrated. The transition employs a shorted-probe excitation topology. VSWR < 1.8:1 over the entire bandwidth of 6-18GHz is achieved. A sensitivity analysis to the design parameters is presented and some fabrication issues are discussed. Excellent repeatability is obtained with measured results closely resembling theory.

15:10 **Design of a Wide-Scan Lens Based Focal Plane Array for Sub-millimeter Imaging Systems Using Coherent Fourier Optics**

[Shahab Oddin Dabironezare](#), [Muhan Zhang](#) and [Giorgio Carluccio](#) (Delft University of Technology, The Netherlands); [Angelo Freni](#) (University of Florence, Italy); [Andrea Neto](#) and [Nuria LLombart](#) (Delft University of Technology, The Netherlands)

Future sub-millimeter imagers will use large format focal plane arrays (FPAs) of lenses to increase their field of view and the imaging speed. This abstract employs a spectral technique based on Fourier Optics for analyzing lens based FPAs. Here, the method is applied to optimize the scanning performance of an imager with monolithically integratable lens feeds without employing any optimization algorithms, by doing a field match by a tunable leaky resonant antenna. The synthesized FPA achieved scan losses much lower than the ones predicted by standard formulas related to the direct field coming from the reflector. In particular, a FPA with scan loss below 1 dB while scanning up to +17.5° is presented with directivity of 52 dB. A prototype of the described design using realistic antenna feeders is also presented.

Monday, 16 March 13:30 - 18:00

T08-A17: Antennas and Techniques for Positioning and Direction Finding

T08 Positioning, localization & tracking / Regular Session / Antennas

Room: B5

Chairs: [Thomas Kaufmann](#) (U-blox AG, Switzerland), [Richard J. Kozick](#) (Bucknell University, USA)

13:30 **Two-Element Biomimetic Antenna Array Design for Power Extraction / Phase Amplification Tradeoff**

[Richard J. Kozick](#) (Bucknell University, USA); [Fikadu Dagefu](#) (US Army Research Laboratory, USA); [Brian Sadler](#) (Army Research Laboratory, USA)

Two-element arrays composed of closely-spaced antennas with mutual coupling have recently been investigated in conjunction with electrical coupling networks that amplify the phase difference in the measurements. These systems have biomimetic analogies to the hearing mechanism in small insects that exhibit exceptional direction finding capabilities. Several coupling networks have been considered with varying complexity and performance relative to the fundamental tradeoff between power extraction and phase difference amplification. In this paper we present a general design method that establishes the achievable region for the power extraction / phase amplification tradeoff, and we present a four-port Pi coupling network that realizes the entire achievable region. An example illustrates the design method for two closely-spaced dipole antennas at 40 MHz.

13:50 **Axially-Corrugated X-Band Horn Design with Integrated TE21 Monopulse Tracking in Corrugation**

[Christophe Granet](#) (Lyrebird Antenna Research Pty Ltd, Australia); [John Kot](#) (Young & Kot Engineering Research, Australia)

A new concept to generate the TE21 monopulse tracking signal by integrating the tracking coupler into the first corrugation of an axially corrugated horn is presented. This new concept allows for a compact design while maintaining isolation between the communication and tracking networks.

14:10 **Adaptive GNSS Antenna Matching for Low-Cost Applications**

[Thomas Kaufmann](#) and [Rod Bryant](#) (U-blox AG, Switzerland)

This paper presents a methodology for adapting the global navigation satellite systems (GNSS) antenna resonance frequency to different environments at a minimal cost. De-tuning effects of GNSS antennas due to the environment or manufacturing tolerances, especially for very compact narrow band antennas, significantly reduce the carrier-to-noise ratio of navigation signal. This has a detrimental effect on the acquisition, tracking and finally navigation performance of the system. This methodology contains an RF switch with different pre-defined matching components. A supervisory system uses knowledge of the received signal and switches between the matching options to maximize the realized RHCP gain. This increases the signal quality and finally improves the performance of the GNSS receiver. It is shown that the de-tuning of a single-band antenna due to ground plane effects can be successfully compensated. Furthermore, it is demonstrated that the resonances of a dual-band antenna can be shifted independently with the same approach.

14:30 **Element Mutual Coupling Effect in a Wideband Planar Aperiodic Sparse Phased Array**

[Shaoqing Hu](#), [Chao Shu](#) and [Xiaodong Chen](#) (Queen Mary University of London, United Kingdom (Great Britain)); [Kai Wang](#) (East China Research Institute of Electronic Engineering, China)

This paper presents our study on a planar wideband aperiodic sparse phased array and the effect of element mutual coupling. The planar aperiodic sparse array in a circular disk with a diameter of $10\lambda_0$ was optimized by using covariance matrix adaption evolutionary strategy (CMA-ES) together with Danzer tiling to generate the peak SLL (Side Lobe Level) of array factor less than -13 dB without the main beam steered and -9.5dB with the main beam steered to 60° away from the broadside in a band from f_0 to $10f_0$. Then, the array using the rectangular patch antenna as the element has been simulated by using CST Microwave Studio to study the effect of mutual coupling when the elements are separated by $\lambda_0/2$ at f_0 . Basically, the peak gain degrades a little bit, while SLL has large degradation in some specific directions, resulted from the mutual coupling between the array elements.

14:50 **A Broadband Circularly Polarized Antenna with Triple-Mode Characteristics**

[Wei Hu](#), [Xuekang Liu](#) and [Hao Wu](#) (Xidian University, China); [Steven Gao](#) and [Lehu Wen](#) (University of Kent, United Kingdom (Great Britain)); [Yuan-Ming Cai](#) (Xidian University, China)

A novel circularly polarized (CP) antenna based on the triple-mode characteristics is presented in this paper. First, by utilizing three resonant modes, a compact antenna element is designed to realize a wide impedance bandwidth of 80%. Then, for the purpose of obtaining broadband CP radiation, the sequential feeding method is employed in the design. By sequentially exciting four antenna elements with a progressive 90° phase shift, a wideband CP windmill-shaped antenna is developed. The proposed antenna exhibits a wide impedance bandwidth (104%), a wide axial ratio (AR) bandwidth (80%), and a low profile (0.18λ , λ is the wavelength in free space at the lowest operating frequency). Such a wideband and low-profile CP antenna is a promising candidate for modern broadband CP applications.

15:10 **A Method of Side-lobe Suppression for Reactance Modulated Antennas**

[Peng-Yuan Wang](#) (University of Duisburg-Essen, Germany); [Meng Fan-Yi](#) (Harbin Institute of Technology, China); [Yue-Long Lyu](#) (The 14th Research Institute, CETGC, China); [Andreas Rennings](#) and [Daniel Erni](#) (University of Duisburg-Essen, Germany)

This paper reveals the mechanism of the high side-lobe level (SLL) phenomenon in reactance modulated antennas (RMAs) and proposes a method to suppress the sidelobe for RMAs. The wave-guiding mode in RMAs is a surface wave with considerable EM field exposed to the free-space. We found that it is the exposure of EM power results in the slow-wave radiation (SWR) phenomenon deteriorating the SLL. To eliminate the SWR, a 'complementary decoupling' method is proposed by introducing another RMA with inverse periodic variation to the original one. The two parallel antennas are excited with equal amplitude and reversed phase forming a complementary radiation pair. With the proposed method, the SWR is eliminated and the SLL is improved. Meanwhile, all of the even radiation modes are also suppressed. Especially for the -2nd mode, which also carries considerable power and often appears in most RMAs.

15:30 **Coffee Break**

16:00 **Pattern Shifting and Size Control in Offset Reflector Antennas with Microstrip Array as Matched Feed**

[Kaushik Debbarma](#) (IIT Guwahati, India); [Ratnajit Bhattacharjee](#) (Indian Institute of Technology, Guwahati, India)

This paper presents details of a dual-layered microstrip based matched feed array for an offset reflector. The top layer of the proposed feed consists of 9 TM11 mode operating circular microstrip patch antennas (CMPA) arranged in a centered circular array configuration. The second layer contains a CMPA operating in TM21 mode located below the central element of the circular array. The excitation ratio between the TM21 and TM11 mode patches is varied to achieve a low cross-polar level at the asymmetric plane at different array radius. An investigation has been done to show that by exciting selective array antenna elements, beamwidth and beamshift reconfigurability in the reflector pattern can be achieved while maintaining the cross-polar levels below -38 dB by having a proper mode excitation ratio. A maximum beamshift of 0.4 degree (approximately 31% of 3dB beamwidth) from the principal axis has been achieved in the reflector pattern.

16:20 **Frequency Diverse Array Information Geometry Analysis**

[Haifeng Yu](#) and [Qinglong Han](#) (Beijing Institute of Space Craft System Engineering, China); [Xiaoning Ji](#) (Air Force Research Institute, China); [Zhibin Wang](#) (Beijing Institute of Space Craft System Engineering, China); [Wen-Qin Wang](#) (University of Electronic Science and Technology of China, China)

Different classic phased-array that generates only angle-dependent transmit beampattern, frequency diverse array (FDA) offers both angle-dependent and range-dependent transmit beampattern. This paper adopts the information geometry theory to study the fundamental information resolution for a general FDA radar system. The information resolution, associated with the waveform, measurement and noise model and characterized by the Fisher information metric, provides a statistical measure for the FDA radar system. Numerical results show that FDA radar indeed outperforms conventional phased-array radar in information geometry resolution capability.

16:40 **RSS-based AoA Estimation System for IoT Applications Using Rotman Lens**

[Noori BniLam](#), [Arne Aerts](#) and [Dennis Joosens](#) (University of Antwerp - imec, IDLab Research Group, Belgium); [Jan Steckel](#) (University of Antwerp - Cosys-lab Research Group, Belgium); [Maarten Weyn](#) (University of Antwerp - imec, Belgium)

In this paper, we present a new Angle of Arrival (AoA) estimation system for Internet of Things (IoT) applications. The proposed system utilizes the received signal strength (RSS) to estimate the AoA of the received signal in the 868 MHz frequency band. The system consists of two sub-systems: Sub-system 1 utilizes a Rotman lens to provide analog beamforming capabilities and Sub-system 2 utilizes the sparsity-based regularized minimization technique to estimate the AoA of the received signal based on the RSS values. An experiment has been conducted in an anechoic chamber to validate the AoA estimation accuracy. The experimental results reveal that the proposed system can accurately estimate the AoA of the received signals based on the RSS values.

17:00 RSS-Based DoA Estimation Using ESPAR Antenna for V2X Applications in 802.11P Frequency Band

[Damian Duraj](#) (Gdansk University of Technology, Poland); [Mateusz Rzymowski](#) (Gdansk University of Technology & WiComm Center of Excellence, Poland); [Krzysztof Nyka](#) (Gdansk University of Technology, Poland); [Lukasz Kulas](#) (Gdansk University of Technology, Faculty of Electronics, Telecommunications and Informatics, Poland)

In this paper, we have proposed direction-of-arrival (DoA) estimation of incoming signals for V2X applications in 802.11p frequency band, based on recording of received signal strength (RSS) at electronically steerable parasitic array radiator (ESPAR) antenna's output port. The motivation of the work was to prove that ESPAR antenna used to increase connectivity and security in V2X communication can be also used for DoA estimation. The numerical simulation results show that for every proposed radiation pattern we can obtain acceptable DoA estimation results, even with radiation pattern without strong maximum and deep minimum.

17:20 Phase-based Variant Maximum Likelihood Positioning for Passive UHF-RFID Tags

[Chenglong Li](#) and [Emmeric Tanghe](#) (Ghent University, Belgium); [David Plets](#) (Ghent University - imec, Belgium); [Pieter Suanet](#) (Aucxis, Belgium); [Nico Podevijn](#) (University of Ghent, Belgium); [Jeroen Hoebeke](#) (Ghent University - imec, Belgium); [Eli De Poorter](#) (Ghent University & Imec, Belgium); [Luc Martens](#) (Ghent University - imec, Belgium); [Wout Joseph](#) (Ghent University/IMEC, Belgium)

Radio frequency identification (RFID) technology brings tremendous advancement in Internet-of-Things, especially in supply chain and smart inventory management. Phase-based passive ultra high frequency RFID tag localization has attracted great interest, due to its insensitivity to the propagation environment and tagged object properties compared with the signal strength based method. In this paper, a phase-based maximum-likelihood tag positioning estimation is proposed. To mitigate the phase uncertainty, the likelihood function is reconstructed through trigonometric transformation. Weights are constructed to reduce the impact of unexpected interference and to augment the positioning performance. The experiment results show that the proposed algorithms realize fine-grained tag localization, which achieve centimeter-level lateral accuracy, and less than 15-centimeters vertical accuracy along the altitude of the racks.

T05-A12/1: Wearable and Implantable Antennas

T05 Biomedical and health / Regular Session / Antennas

Room: B6

Chairs: [Sema Dumanli](#) (Bogazici University, Turkey), [Daniel Segovia-Vargas](#) (Universidad Carlos III de Madrid, Spain)

13:30 Low-Profile and High-Gain Linear Polarized Loop Antenna

[Ali Khaleghi](#) (Norwegian University of Science and Technology (NTNU) & Oslo University Hospital, Norway); [Ilangko Balasingham](#) (Norwegian Institute of Science and Technology, Norway)

A loop antenna on top of a metal plate can provide a higher gain than that of a dipole antenna. A low depth profile multi-loop antenna geometry is proposed with a thickness of 0.02 wavelength to the back metal plate. The designed loop antenna is self-matched to the 50-ohm impedance of a source and provides a high directional gain of 8.2 dBi. The antenna gain is increased to 10.0 dBi by using a dual multi-loop geometry. Sample antennas are designed and manufactured for operating at 2250 MHz. The antennas are measured and characterized for the return loss, radiation pattern and gain. The proposed antenna can be used as a wearable antenna in wireless body area network (WBAN), in which the backside radiation is reduced and the antenna impedance characteristics are not affected by the background tissues.

13:50 Multilayer Ultra-Miniature Loop Antenna for Insertable Pill Application

[Amine Samoudi](#) (Ghent University & IMEC, Belgium); [Gunter Vermeeren](#) (Ghent University, Belgium); [Denys Nikolayev](#) (Institut d'Électronique et de Télécommunications de Rennes (UMR CNRS 6164), France); [Minyoung Song](#) (Holst Centre/IMEC, The Netherlands); [Yao-Hong Liu](#) (Imec-nl, The Netherlands); [Wout Joseph](#) (Ghent University/IMEC, Belgium); [Luc Martens](#) (Ghent University, Belgium)

An ultra-miniaturized multilayer loop antenna for insertable pill applications is presented. The antenna is designed for the Medical Device Radiocommunications service (MedRadio 401-406 MHz) and makes use of the three metal layers of the antenna board to increase its electrical length within a compact size of 16.2 mm² (3.3 × 4.9 mm). The realized gain is -38.3 dBi in ø10-cm muscle-equivalent spherical phantom, and the radiation efficiency reaches 0.06%. Antenna adaptation to manufacturing (extra Rogers 2929® substrate layer and vias diameter increased) resulted in an efficiency of 0.05%. Finally, different approaches are discussed to increase the antenna efficiency while keeping the space constraint unchanged.

14:10 Body Matched Dipole-Loop Composite Antenna with Reconfigurable Focused Field for Non-Alcoholic Fatty Liver Disease Diagnosis Systems

[Sasan Ahdi Rezaeieh](#) and [Amin Abbosh](#) (The University of Queensland, Australia)

A body matched antenna with reconfigurable field focusing capability for electromagnetic-based non-alcoholic fatty liver diagnosis systems is presented. The antenna utilizes a combination of three distinct methods to achieve unidirectional radiation, miniaturize the size of the antenna and reconfigure field focusing. To achieve unidirectional radiation and wide operating bandwidth, a loop-dipole configuration is utilized to eliminate the need for conventional bulky reflectors. The dipole is matched to the body to miniaturize the size of the antenna. To avoid using dielectric loading to cover the distance between the loop and the dipole, the loop is meandered and designed in a three-dimensional structure. Finally, to alter electric field intensity to scan different regions inside thorax, the dipole is designed as three sub-elements that are electronically switched.

14:30 Robustness Analysis of the Polymer-Conductive-Mesh Composite for the Realization of Transparent and Flexible Wearable Antennas

[Abu Sadat Md. Sayem](#) (Macquarie University, Australia); [Karu Esselle](#) (University of Technology Sydney, Australia); [Raheel Maqsood Hashmi](#) (Macquarie University & IEEE, Australia)

In this paper the morphology of the polydimethylsiloxane (PDMS)-flexible-conductive-mesh composite has been studied to evaluate its suitability in the realization of robust, flexible, transparent, wearable antennas that can withstand multiple bending operations. We have utilized conductive mesh made out of VeilShield from Less EMF which has about 70% light transmittance and is highly flexible. On the other hand, PDMS is a highly flexible and optically transparent polymer. Uncured PDMS is in liquid form and upon curing it transforms to a robust flexible substrate and forms a strong bonding with the conductive mesh, VeilShield. We have examined the composite through Scanning Electron Microscope (SEM) images during and after multiple bending operations. Later, we have designed a simple patch antenna operating at 2.45 GHz band using our selected materials. For performance evaluation the antenna is tested in both free space and under bent conditions and the results are presented in this paper.

14:50 Miniaturized CPW-fed Bowtie Slot Antenna for Wearable Biomedical Application

[Amir Arayeshnia](#) (Imam Khomeini International University, Iran); [Alireza Madannejad](#) (Research Assistant, University of Tehran, Iran); [Javad Ebrahimzadeh](#) (University of Uppsala, Sweden); [Fatemeh Ravanbakhsh](#) (Student, Islamic Azad University, Iran); [Mauricio D Perez](#) (Uppsala University, Sweden & National Technological University, Argentina); [Robin Augustine](#) (Uppsala University, Sweden)

A miniaturized, low-profile, flexible, and wearable ultra-wideband antenna for biomedical applications is proposed. The antenna is designed to operate in wearable conditions with the presence of multilayer biological tissues. A meandering technique is employed to reduce the electrical size of the antenna. The operational band of the proposed antenna is 0.5-4.5 GHz, while its dimensions are as small as 21×19.25×0.025 mm³. The antenna is simulated using a commercial full-wave simulator (CST Microwave Studio), fabricated on Polyethylene terephthalate (PET), and tested in realistic scenarios. The simulation and measurement results are in good compliance with each other

15:10 Coffee Break

15:40 Rectenna at 2.45 GHz for Wearable Applications

[Mónica Borgoños-García](#), [Ana Lopez-Yela](#) and [Daniel Segovia-Vargas](#) (Universidad Carlos III de Madrid, Spain)

This paper presents the design and implementation of a 2.45-GHz wearable integrated rectifier antenna (rectenna) for far-field wireless powering for low-power sensors. A circular patch antenna resonant at 2.45 GHz is designed, manufactured and characterized. The performance of the fabricated antenna is studied when it is placed over body tissues for wearable applications. A Spice model for a Schottky diode, which is part of the rectifier, is implemented and tested in different rectifying circuits for low input powers, ranging from -20dBm to 0 dBm. A rectifying circuit at 2.45 GHz is fabricated and measured in terms of power-conversion efficiency. The rectifier impedance is analyzed as a function of dc load and input power. Finally, the antenna and rectifier are integrated as a rectenna, and the total efficiency evaluated for incident power densities up to 7 μW/cm² at 2.45 GHz.

16:00 A Wide-band Slot-based Frequency Agile Yagi-Like MIMO Antenna System

[Rifaqat Hussain](#) (KFUPM, Saudi Arabia); [Syed Jehangir](#) (United Arab Emirates University, United Arab Emirates); [Muhammad Umar Khan](#) (National University of Sciences and Technology & Research Institute for Microwave and Millimeter-Wave Studies, Pakistan); [Mohammad S. Sharawi](#) (Polytechnique Montreal, Canada)

In this work, we propose a wide-band slot-based frequency agile 2-layer Yagi-like multiple-input-multiple-output (MIMO) antenna system. The MIMO system consists of 4 identical pentagonal slot-line based active antenna elements reactively loaded with varactor diodes to achieve frequency reconfigurability. The proposed antenna could be tuned over a wide frequency band from 1.5 - 2.1 GHz. To achieve Yagi-like directional characteristics of a slot antenna, a parasitic metallic reflector layer was used below the substrate. This helped in suppressing the back-lobe radiation and thus a front-to-back ratio (FBR) of 5 - 13 dB is achieved within the entire frequency band of operation. The proposed 4-element design is compact with an overall size of 100*100*20 mm³, and a reflector size of 110*110 mm². The antenna system also shows good MIMO performance with high port isolation and very low envelope correlation coefficient (ECC) values within the operational band.

16:20 *Applications of Mixed Powder Dielectrics in Prototype 2.45GHz Pendant Antenna Design and Manufacture*

[John Brister](#), [Robert Michael Edwards](#) and [Jacky Brister](#) (Loughborough University, United Kingdom (Great Britain))

In this paper a new type of tissue emulating phantom that is useful in the study of on-body and close to body antennas is presented. The use of pressure agglomerating dielectric powders within a bespoke 3D printed enclosure are discussed for rapid prototyping. Particular attention is given to attempting to avoid the effects of reactive near field de-tuning in antennas constantly in contact with the body. The method of using high permittivity mixed dielectric powders in the size reduction of a common dipole and a compact spherical helical antenna with a balanced feed are discussed.

16:40 *A Biodegradable Implant Antenna Detecting Post-Surgical Infection*

[Kivanc Ararat](#), [Omer Altan](#), [Sanberk Serbest](#), [Oguzhan Baser](#) and [Sema Dumanli](#) (Bogazici University, Turkey)

Biodegradable implants have proven to be attractive where the patient will not need to go through an additional operation for the removal of the implant. Here biodegradability is utilized further where the biodegradation process has been part of the device's operation. An implant antenna is designed to detect post-surgical infections which increase the acidity inside the human body. The implant antenna is provisioned to be located in the operation site where it degrades at different paces depending on the existence of infection or not. The Mg antenna is tested in cow's minced fat where the degradation is monitored using a wearable slot antenna used as a reader. The detection was possible for an implant depth of 1cm with 14 MHz resolution.

17:00 *Protective Coating Methods for Glove-Integrated RFID Tags - A Preliminary Study*

[Zahangir Khan](#), [Han He](#), [Xiaochen Chen](#), [Leena Ukkonen](#) and [Johanna Virkki](#) (Tampere University, Finland)

In this study, machine washing durability of working glove-integrated passive RFID tags is evaluated. These glove-tags are embedded inside 3D-printed thermoplastic polyurethane platforms. The results are compared to platforms embedded inside brush-painted encapsulant platforms. For a preliminary washing reliability evaluation, both types of glove-integrated platforms are washed in a washing machine for 5 times. Although both platforms can protect glove-tags from the effects of water, the main reliability challenge is found to be the fragile antenna-IC attachments. This paper introduces the two platform materials and the achieved washing test results. These preliminary results determine the future direction of this research: The next step is to study suitable methods to strengthen the interconnections, so that these glove-tags can survive the harsh environment inside a washing machine.

17:20 *A Low Profile Button Antenna with Back Radiation Reduced by FSS*

[Bappaditya Mandal](#) (Uppsala University, Uppsala, Sweden); [Ayan Chatterjee](#) (National Institute of Technology Sikkim, India); [Pramod K B Rangaiah](#) (Researcher & Uppsala University, Sweden); [Mauricio D Perez](#) (Uppsala University, Sweden & National Technological University, Argentina); [Robin Augustine](#) (Uppsala University, Sweden)

In this article, a button antenna with a reflective frequency selective surface(FSS) is proposed to reduce its back radiation. The proposed antenna is low in profile, circularly polarized and designed for Wi-Fi and WLAN applications. The radiating element is made of copper sheet, while a transparent acrylic fibre sheet is used as a substrate. The antenna is fed by a coaxial line, and the FSS layer is designed on jeans material. The patch type FSS with split ring shape has also been designed to operate in the Wi-Fi and WLAN frequency band (5.250-5.850 GHz) with the centre frequency of 5.51 GHz. The FSS reduces back radiation of the antenna by 4 dB. The antenna with FSS is fabricated, and a measured gain of 2.9dBi is obtained that matches well with the theoretical value. The antenna is miniaturized by around 61.15% by the slits.

17:40 *Frequency Reconfigurable Multi-Band Antenna Using 1-D EBG Structures with BST Chip Capacitors*

[Jae-Yeong Lee](#) (Pohang University of Science and Technology (POSTECH), Korea (South)); [Kyung-Bin Lee](#) (Gwangju Institute of Science and Technology (GIST), Korea (South)); [Celso Leite](#) (Samsung Electronics, Korea (South)); [Seung-Han Kim](#) (Defense Agency for Technology and Quality, Korea (South)); [Jae-Hyung Jang](#) (Gwangju Institute of Science and Technology, Korea (South))

This paper describes a monopole antenna using one-dimensional electromagnetic bandgap structures with barium strontium titanate chip capacitors for frequency reconfigurable operation in multi-band. Despite the absence of an RF choke and DC blocking capacitor, a frequency reconfigurable antenna featuring high radiation performance with low DC power consumption is realized. The frequency tuning ratios are 25% in low frequency band and 4.6% in high frequency band. The antenna exhibits low power consumption less than 1 uW and high antenna efficiency (more than 40%).

Monday, 16 March 13:30 - 15:30

CS05: AMTA Session: Automotive Antenna Measurements and Testing

T06 Aircraft (incl. UAV, UAS, RPAS) and automotive / Convened Session / Measurements

Room: B7

Chairs: [Philipp Berlt](#) (Technische Universität Ilmenau, Germany), [Lars Foged](#) (Microwave Vision Italy, Italy)

13:30 *Experimental Comparison of Vehicular Antenna Measurements Performed over Different Floors*

[Per Iversen](#) (Orbit/FR, USA); [John Estrada](#) (MVG, USA); [Francesco Saccardi](#) and [Lars Foged](#) (Microwave Vision Italy, Italy); [Francesca Mioc](#) (Consultant, Switzerland); [Michael Edgerton](#) and [Janalee Graham](#) (General Motors, USA)

Large truncated spherical near-field systems with conductive or absorbing floors are typically involved in the measurement of the performances of vehicle installed antennas. The main advantage of a conductive floor systems is the ease of accommodation of the vehicle under test, but their performances are often degraded by the strong interaction with the reflecting floor. Instead, absorbing-based systems emulating free-space conditions ensure better accuracy, but generally require longer setup times, especially at lower frequencies (70-400 MHz), where bulky absorbers are typically used to ensure good reflectivity levels. Considering scaled measurements of a vehicle model, the performance of these two typical implementations are analysed in the 84-1500 MHz range and compared to free-space measurements. Absorbers with different dimensions and reflectivity have been installed in the scaled measurement setup, and measured data have been investigated with proper post-processing to verify the applicability to realistic systems.

13:50 *Exploiting Spatial Derivative Information in Phaseless Near-Field Far-Field Transformations*

[Alexander Paulus](#) (Technical University of Munich, Germany); [Thomas F. Eibert](#) (Technical University of Munich (TUM) & Chair of High-Frequency Engineering (HFT), Germany)

By exploiting information about the spatial derivative of magnitude data, we increase the reliability of phaseless near-field far-field transformations. While existing techniques operate on the measured magnitudes, the presented formulation puts restrictions on the first-order spatial derivative of the measured magnitudes. This potentially allows to utilize hidden information about the antenna near fields and, thus, increase the chances of a successful phaseless transformation. Preliminary simulation results for an implementation based on the fully-analytic equations for the spatial derivatives of the magnitude of fields caused by Hertzian dipoles are presented. The comparison as well as combination with a typical phaseless solver not using the spatial derivatives showcases the potential of the new formulation.

14:10 *Accurate 3D Phase Recovery of Automotive Antennas Through LTE Power Measurements on A Cylindrical Surface*

[Philipp Berlt](#) and [Christian Bornkessel](#) (Technische Universität Ilmenau, Germany); [Matthias Hein](#) (Ilmenau University of Technology, Germany)

Phaseless antenna measurements have been gaining much interest in the past. In the course of increasing integration of antennas with frontends and digital signal processing units on chipsets, the measurement of the phase pattern becomes challenging since a RF connection to the antenna feed point is missing and common measurement methods with a vector network analyzer cannot be applied. This paper deals with a phase recovery technique exploiting intrinsic communication signals from a LTE user equipment, following the approach of indirect holography in spatial domain. Phase recovery is applied on a cylindrical measurement surface, scanning in both vertical and horizontal polarization. Comparison to a conventional phase measurement with a vector network analyzer shows excellent agreement on the entire measured surface. Thus, this approach is a promising alternative and has high potential for further signal processing, e.g. nearfield to far field transformation or localization of the antenna within the measurement volume.

14:30 *Modeling of a Far-Field Automotive Antenna Range Using Computational Electromagnetic Tools*

[Daniel N Aloï](#) and [Ehab Abdul-Rahman](#) (Oakland University, USA)

Vehicle-level antenna performance standards are being established for vehicle-to-everything (V2X) communications that support safety of life applications for automobiles. Once these antenna performance standards are established, there must be confidence that automotive antenna measurement systems can make accurate and repeatable measurements. In this paper, a full-wave, three-dimensional electromagnetic field solver based on the method of moments (MOM) was utilized to create a simulation model of the antenna measurement process at Oakland University's outdoor automotive antenna range. Initial results for the comparison of this model against measurements are provided in this paper for a directive monopole antenna on a one-meter diameter ground plane. This type of tool will be useful to establish uncertainty levels for vehicle-level antenna gain measurements.

14:50 *Recent Developments in Automotive Antenna Measurements*

[Manuel Sierra-Castañer](#) (Universidad Politécnica de Madrid, Spain)

This overview paper summarizes the recent advances in automotive antenna measurements during the last years. This topic has been important in the past, but the development of new communication systems, specially the fifth generation (5G) cellular systems means a huge number of antennas and sensors placed in all the vehicles. During the last year several research groups, connected with the industry have shown advances in measurement architecture, hardware and post-processing algorithms.

15:10 *Wideband Radio Channel Emulation Using Band-stitching Schemes*

[Yilin Ji](#), [Wei Fan](#) and [Gert Pedersen](#) (Aalborg University, Denmark)

In the fifth-generation (5G) new radio specifications, large signal bandwidth e.g. 400 MHz for frequency range 2 (FR2), is expected to be utilized. Therefore, there is a need to develop channel emulators that can support such large bandwidth. In this paper, we revisit the band-stitching scheme, i.e. combining multiple logic channels of small bandwidth to form a larger total bandwidth. We put a focus on the calibration stage of this scheme, and the effect of the phase jump at the junctions of adjacent subbands on the stitching performance is investigated through simulation.

T09-A09: Millimetre-wave Lens Antennas for Space Applications

T09 Space (incl. cubesat) / Regular Session / Antennas

Room: B8

Chairs: [Nelson Fonseca](#) (European Space Agency, The Netherlands), [Andrea Neto](#) (Delft University of Technology, The Netherlands)

13:30 Compressed Lenses via Transformation Optics for Mobile Satellite Communications

[Oskar Zetterstrom](#) (KTH Royal Institute of Technology, Sweden); [Nelson Fonseca](#) (European Space Agency, The Netherlands); [Oscar Quevedo-Teruel](#) (KTH Royal Institute of Technology, Sweden)

In this paper, the design of a volumetric Luneburg lens antenna is described. Transformation optics is used to compress the height of the lens. A moderate compression of 30% is applied to facilitate an all-dielectric realization. A gain of almost 20 dBi is obtained in simulations with a lens diameter of 4 free space wavelengths before compression. Compared to a spherical Luneburg lens antenna with the same height (i.e. with a smaller diameter), the gain of the compressed lens is about 2 dB higher. The antenna is intended for satellite communications on-the-move through low Earth orbit constellations.

13:50 Experimental Validation of the Beam Pattern of a Wide Band Quasi-Optical System for DESHIMA Spectrometer

[Shahab Oddin Dabironezare](#) (Delft University of Technology, The Netherlands); [Kenichi Karatsu](#), [Stephen Yates](#) and [Vignesh Murugesan](#) (SRON, The Netherlands); [David Thoen](#) (Kavli Institute of NanoScience, Delft University of Technology, The Netherlands); [Jochem Baselmans](#) (SRON, The Netherlands); [Nuria LLombart](#) (Delft University of Technology, The Netherlands)

DESHIMA is a spectrometer for astronomical applications targeting sources at sub-mm wavelengths from 240GHz to 720GHz. In this work, the quasi optical system for this spectrometer is presented. This design is based on hyperhemispherical leaky lens antenna. The design procedure is based on a field matching technique in reception. By employing this methodology, the performance of the design is rapidly optimized over the whole 1:3 relative bandwidth. The achieved average illumination efficiency over the band is approximately 70%. The directivity patterns in the sky are also estimated. The leaky lens antenna is fabricated, and the measurement of the system is ongoing. The beam pattern of the system at the beginning of the and is presented in this abstract. This beam pattern is obtained directly from the response of the super conductive Kinetic Inductance Detectors coupled to the antenna. The rest of the measurement will be presented at the conference

14:10 Analysis of Wide Band Wide-Scanning Quasi-Optical Systems Based on Fourier Optics

[Shahab Oddin Dabironezare](#), [Giorgio Carluccio](#), [Andrea Neto](#) and [Nuria LLombart](#) (Delft University of Technology, The Netherlands)

Sub-millimeter imaging systems with wide frequency bandwidth of operation as well as large steering capabilities are required for future security and space imaging applications. In this paper, a Quasi-Optical (QO) system with multiple refractive components is proposed to achieve these requirements. The system which consists of hyper-hemispherical lenses antenna feeders at its focal plane. Double-sided hyperbolic free-standing lenses are then used to link to the rest of QO chain. A fast and accurate method based on Fourier Optics combined with Geometrical Optics is proposed to analyze these type of surfaces. The tool is validated against time consuming multi surface Physical Optics with excellent agreement. As the result, the proposed method can be used to design and optimize the performance of such QO systems. To demonstrate the capability of the method, an example case is also presented, and its performance is evaluated.

14:30 Rotman Lenses with Ridged Waveguides in Q-Band

[Sophie-Abigael Gomanne](#), [Nelson Fonseca](#), [Petar Jankovic](#) and [Jaione Galdeano](#) (European Space Agency, The Netherlands); [Giovanni Toso](#) (European Space Agency, ESA ESTEC, The Netherlands); [Piero Angeletti](#) (European Space Agency, The Netherlands)

This paper provides a discussion on ridged waveguide Rotman lenses for satellite applications in Q-band. Two transition designs from the ridged waveguide feeding ports to the parallel plate waveguide lens cavity are compared. Whereas the longer transition provides slightly better return loss, the shorter transition reduces phase errors in the lens, translating into more accurate beam pointing and lower scan losses. S-parameters and normalised array factors are reported over the frequency range from 37.5 GHz to 42.5 GHz for both lenses, confirming the benefits of shorter transitions.

14:50 Design of an Impedance-Matched Horn Antenna with Enhanced Directivity Using Conformal Transformation Optics

[Hossein Eskandari](#) (Ferdowsi University of Mashhad, Iran); [Tomáš Tyc](#) (Masaryk University, Czech Republic); [Juan Luis Albadalejo-Lijarcio](#), [Oskar Zetterstrom](#) and [Oscar Quevedo-Teruel](#) (KTH Royal Institute of Technology, Sweden)

In this work, conformal transformation optics is employed to enhance the directivity of a horn antenna. The phase error at the horn's aperture is mitigated using a dielectric graded-index lens designed by the conformal transformation. The design not only leads to a negligible phase error at the aperture but also has an excellent impedance match to the vacuum. Simulation results show that for a typical horn antenna with length and aperture width equal to 10 wavelengths, our method can enhance the directivity more than 5 dB.

15:10 All-Metal Graded Index Gutman Lens Antenna - A More Compact Luneburg Lens

[Petros Bantavis](#) (Universite de Rennes 1, France); [Cebrian Gonzalez](#) (Idonial, Spain); [Ronan Sauleau](#) (University of Rennes 1, France); [George Goussetis](#) (Univerity, France); [Ségolène Tubau](#) (Thales Alenia Space, France); [Hervé Legay](#) (Thalès Alenia Space, France)

The present work introduces an all-metal Gutman lens antenna in a parallel plate waveguide (PPW) technology for space applications at Ku band. Compared to the Luneburg lens, the Gutman lens provides more compact size up to 35%. To achieve this compactness an optimized unit cell with glide symmetry is utilized. Single ridge waveguides are proposed to excite the lens along its focal arc to obtain a field of view with high beam overlap level between adjacent beams. Finally, the antenna presents broadband performance up to 40% with low losses and high directivity which makes it an excellent candidate for satellite missions.

CS64: Trends and Advances in Machine Learning for Applied Electromagnetics

T10 EM modelling and simulation tools / Convened Session / Electromagnetics

Room: B9

Chairs: [Sotirios Goudos](#) (Aristotle University of Thessaloniki, Greece), [Marco Salucci](#) (ELEDIA Research Center, Italy)

13:30 Modelling Ray Tracing Propagation Data Using Different Machine Learning Algorithms

[Sotirios Goudos](#) (Aristotle University of Thessaloniki, Greece); [Georgia E. Athanasiadou](#) and [George Tsoulos](#) (University of Peloponnese, Greece); [Vasileios Rekkas](#) (Aristotle University of Thessaloniki, Greece)

In this paper, we apply different machine learning methods for the prediction of path loss in urban environment for cellular communications with UAVs. We generate the training set using a ray tracing technique assuming a flying base station at different heights within the city of Tripolis, Greece. We produce prediction models for the path loss using three different learners the k-Nearest Neighbors (kNN), the Support Vector Regression (SVR) and the Random Forest (RF). The obtained numerical results are compared with the original data from the test dataset using representative performance indicators and overall they exhibit good precision.

13:50 A Comparison of Machine Learning Classifiers for Human Activity Recognition Using Magnetic Induction-based Motion Signals

[Negar Golestani](#) and [Mahta Moghaddam](#) (University of Southern California, USA)

Human activity recognition (HAR) is a growing research field with a wide range of applications. Magnetic induction-based human activity recognition system (MI-HAR) is a wearable-based HAR system proposed for capturing human motions and detecting activities based on the collected data. In this work, we focused on the performance analysis of different machine learning classifiers using synthetic magnetic induction-based motion (MI-motion) signals. The main aim of this analysis is to compare the performances of six commonly used classifiers for HAR applications. Furthermore, we compared the classification performance using MI-motion data with the result reported in other studies using accelerometer data correspond to the same actions. Our results showed that Random Forest obtained the best performance of 91.5% on MI-motion data. Also, k-SVM and KNN models have respectively achieved accuracy of 91.4% and 86.4% on MI-motion data, which are both higher than the reported accuracy of 85.4% and 81.75% on accelerometer data.

14:10 A Learning-by-Examples Method for Rapid Estimation of Surface Currents in Microstrip Antenna Arrays

[Marco Salucci](#) (ELEDIA Research Center, Italy); [Giulia Mansutti](#) (Università degli Studi di Padova, Italy); [Alessandro Polo](#) (ELEDIA Research Center, University of Trento, Italy); [Paolo Rocca](#) (University of Trento, Italy)

An innovative Learning-by-Examples (LBE) methodology is presented to efficiently and accurately predict the surface currents in printed microstrip arrays. More in detail, the proposed technique is based on an orthonormal representation of the surface currents and on the generation of a fast surrogate model with high generalization capabilities. Thanks to such an approach, it is possible to accurately estimate the surface currents on the antenna under test (AUT) without the need for time-consuming full-wave simulations nor a perfect matching of its characteristics with the nominal ones (e.g., due to manufacturing errors/inaccuracies). A preliminary numerical example is shown to assess the effectiveness and potentialities of the proposed LBE methodology.

14:30 Near-Field Multi-Focused Arrays Using Support Vector Regression

[Rafael González Ayestarán](#) (Universidad de Oviedo, Spain); [Fernando Las-Heras](#) (University of Oviedo, Spain)

Support Vector Regression, a powerful framework in the field of Machine Learning, is proposed for Near-Field Focusing using antenna arrays. It allows creating a model of an array relating the weights required in the elements of an array and the corresponding near-field distribution, focused on one or more positions of interest. A previous learning process concentrates the computational cost so that the trained system operates without relevant cost and fast enough for applications where adaptation must be fast, for example because moving devices are involved. The learning capabilities of Support Vector Machines are increased with respect to other machine learning tools, allowing the use of a reduced number of training samples that may be generated with an adaptive system or any full-wave electromagnetic analysis tool, so that realistic effects such as coupling or non-uniformities can be accounted for. Illustrative examples are also presented to test the performance of the method.

14:50 *SNO Optimization Technique Applied to Reflectarray Antennas Design*

[Michele Beccaria](#) (Politecnico di Torino, Italy); [Alessandro Niccolai](#) (Politecnico di Milano, Italy); [Andrea Massaccesi](#) (Politecnico di Torino, Italy); [Riccardo Enrico Zich](#) (Politecnico di Milano, Italy); [Paola Pirinoli](#) (Politecnico di Torino, Italy)

This communication presents some numerical results on the optimized design of a passive reflectarray with scanning beam capabilities. The proposed approach is based on the use of an efficient pseudo-stochastic optimization algorithm, the Social Network Optimization (SNO) and by a definition of a proper cost function, that allow the simultaneous optimization of the antenna radiation pattern for different pointing directions. The results relative to two different configurations, with increasing size, prove the effectiveness of the method, also confirmed by the full-wave analysis of the smallest antenna.

15:10 *Bayesian Active Learning for Electromagnetic Structure Design*

[Jixiang Qing](#), [Nicolas Knudde](#) and [Ivo Couckuyt](#) (Ghent University, Belgium); [Domenico Spina](#) (Ghent University - imec, Belgium); [Tom Dhaene](#) (Ghent University & IMEC, Belgium)

A novel design framework based on Bayesian active learning is presented in this contribution. The proposed approach allows one to identify a set of design configurations satisfying the chosen specification. In particular, the entropy search-based active learning strategy, which relies on a Gaussian Process model, is able to minimize the number of time-consuming computer simulations or expensive design trials necessary to reach this goal. A suitable application example validates the proposed method.

Monday, 16 March 13:30 - 18:00

CS24: Controlling EM Waves with Low- and High-Dimensional Metamaterials

T11 Fundamental research and emerging technologies / Convened Session / Electromagnetics

Room: B10

Chair: [Mario Junior Mencagli](#) (University of North Carolina at Charlotte, USA)

13:30 *A Subwavelength Microwave Bandpass Filter Based on a Chiral Waveguide*

[Maliheh Khatibi Moghaddam](#) (École Polytechnique Fédérale de Lausanne (EPFL), Switzerland); [Romain Fleury](#) (EPFL, Switzerland)

Wave manipulation at subwavelength scale has recently attracted significant interest, especially for low-frequencies. Recently, a few methods using locally resonant metamaterials have been proposed, foreseeing new technologies for ultra-compact passive components, e.g. in satellite communications. In this paper, we aim at exploiting such a technique for designing a miniature microwave filter, which guides modes at the interface between two locally-resonant metamaterials with opposite chirality, so-called chiral waveguide. It has been recently demonstrated that a chiral waveguide has inherent robustness against imperfections in both the position and resonance frequencies of the local resonators, which can be leveraged for realizing robust subwavelength systems. We use this property to realize a bandpass filter with improved RF parameters, by purposely integrating subwavelength resonators directly into the active region of the filter and also dispersion-engineering methods. Therefore we enhance the order of the filter and suppress spurious bands, functionalities conventionally obtained by cascading bulky stages.

13:50 *Broadband Offset-Reflector Beamformer on BCB in the 300-GHz Band*

[Adham Mahmoud](#) (Institut d'Électronique et de Télécommunications de Rennes, France); [David González-Ovejero](#) (Centre National de la Recherche Scientifique - CNRS, France); [Mauro Ettore](#) (University of Rennes 1 & UMR CNRS 6164, France); [Ronan Sauleau](#) (University of Rennes 1, France); [Frédéric Aniel](#), [Nicolas Zerounian](#) and [Anne-sophie Grimault](#) (Université Paris Sud, France)

This paper presents the design of a broadband offset-reflector beamformer on a polymer substrate operating at submillimeter frequency bands. The offset reflector is used to excite a leaky-wave antenna array (LWA). The full system is fabricated in substrate integrated waveguide technology (SIW). Benzocyclobutene (BCB) is used as a substrate due to its excellent electrical properties in this frequency range. A simulated field of view of 58° and a realized gain of more than 14 dBi are achieved over a 25% fractional bandwidth, from 260 GHz to 340 GHz. The antenna efficiency is estimated to be 17%.

14:10 *Matched Waves at Metaboundaries*

[Ari Sihvola](#) (Aalto University, Finland); [Ismo V Lindell](#) (Aalto University, School of Electrical Engineering, Finland)

Electromagnetic boundary conditions require connections between the components of the electric and magnetic at this boundary. In the following, generalized boundary conditions are analyzed which define the connection between combinations of the tangential and normal components of the electric and magnetic fields. In particular, the focus is on matched waves: single waves which by themselves satisfy the given boundary condition.

14:30 *Mini- And Multi-Dimensional Metamaterials*

[Sergei Tretyakov](#) (Aalto University, Finland)

Recently, metamaterial science and technology has been developing fast, with the emphasis on metasurfaces as two-dimensional metamaterials. Also, external time modulations have been actively studied, and this technique can be viewed as expanding the space of design parameters into the fourth dimension, that of time. In this conceptual review talk I will discuss the notion of dimensionality of meta-atoms, metasurfaces, and metamaterials, emphasizing possible different understandings of this term in electromagnetics of complex space-time varying media.

14:50 *A Method for Extending the Bandwidth of Modulated Metasurface Antennas*

[Marco Faenzi](#) (Université de Rennes 1, France); [David González-Ovejero](#) (Centre National de la Recherche Scientifique - CNRS, France); [Stefano Maci](#) (University of Siena, Italy)

Modulated metasurface (MTS) antennas can provide a broadside pencil beam at the frequency where the cylindrical surface wave (SW) wavelength matches the period of the impedance modulation. The mismatch between the SW wavelength and the period of the modulation imposes a limitation on the product bandwidth-gain. Here, we overcome this limitation by acting on the function that provides the local period for a given radial distance. Doing so, we generate annular active regions on the antenna aperture. Such regions typically move from the antenna center to the circular rim as the frequency decreases. This paper shows that one can optimize the profile of the local periodicity function to obtain broadside pencil beams over large bandwidths, while preserving the flatness of the gain versus frequency response. The presented results prove that these antennas can provide high broadside gain over bandwidths difficult to reach by other flat antennas based on printed technology.

15:10 *Analytic Design of Dual-Band, Dual-Polarized LP-to-CP Polarization Converters*

[Michele Del Mastro](#) (University of Rennes 1, France); [Mauro Ettore](#) (University of Rennes 1 & UMR CNRS 6164, France); [Anthony Grbic](#) (University of Michigan, Ann Arbor, USA)

A systematic procedure for the design of dualband, dual-polarized linear-to-circular polarization converters is presented. This class of polarizers can convert linear polarization to orthogonal circular polarizations in two separate frequency bands. The polarization converter is composed of three electric admittance sheets. The frequency response of each sheet is determined using an analytic approach, without relying on any optimization. A representative example is proposed in the Ka-band for Satcom applications. The polarizer converts a 45° linearly-polarized plane-wave to left-handed and right-handed circularly-polarized waves within the downlink and uplink of the Ka-band. Specifically, relative bandwidths of 19% and 7% are achieved within the downlink and uplink, respectively, for normal incidence. Stable responses are demonstrated in simulation under oblique incidence up to 60° in elevation.

15:30 Coffee Break

16:00 *Graphene Plasmonics with a Drift-Current Bias*

[Tiago Morgado](#) (Instituto de Telecomunicações and University of Coimbra, Portugal); [Mario Silveirinha](#) (Universidade de Lisboa - Instituto de Telecomunicações, Portugal)

We present a novel route to achieve strong nonreciprocal responses and regimes of optical gain at the nanoscale. We theoretically demonstrate that the biasing of a graphene sheet with a drift electric current gives rise to the emergence of one-way surface plasmons. Furthermore, we demonstrate that by coupling the drift-current biased graphene sheet to another plasmonic slab (e.g., a semiconductor slab), it is possible to obtain regimes of negative Landau damping wherein the surface plasmons are pumped by the drifting electrons.

16:20 *Stable Positive/negative Capacitor for Use in Active Artificial Structures*

[Silvio Hrabar](#) (University of Zagreb, Croatia); [Dominik Zanic](#) (University of Zagreb, Croatia); [Igor Krois](#) (University of Zagreb, Croatia)

Recently, a 'bandpass' non-Foster negative capacitor with improved stability properties, intended for use in active metamaterials and antennas, has been introduced. Here, a simple extension that enables stable switchable negative/zero/positive capacitance operation, is proposed and verified by realistic SPICE simulation.

16:40 *Virtual Perfect Absorption Through Adiabatically Modulated Cavities*

[Dimitrios Sounas](#) (Wayne State University, USA)

Virtual perfect absorption refers to the complete transfer of the energy an incident wave to a lossless cavity without reflection. However, the approaches proposed so far require either exponentially increasing waves, which are hard to maintain for long times, or extreme forms of time modulation. Here, it is shown that virtual absorption can be achieved for signals of any shape by applying slow adiabatic modulation to the coupling coefficient between a cavity and a waveguide. The proposed approach consists a simple yet efficient way for trapping electromagnetic pulses and it may have applications in energy storage, energy conversion and quantum information processing.

17:00 *Spatial and Spatio-Temporal Modulations for Advanced Wave Control with Metasurfaces*

[Younes Radi](#) and [Adam Overvig](#) (CUNY Advanced Science Research Center, USA); [Yoshiaki Kasahara](#) (University of Texas at Austin, USA); [Andrea Alù](#) (CUNY Advanced Science Research Center, USA)

In this talk, we review our recent work in the context of metasurfaces to control electromagnetic waves. Spatial gradients of surface impedance, and careful engineering of the spatial dispersion, are shown to implement metasurfaces for efficient beam steering, focusing and wavefront control. Adding temporal modulations to this picture provides interesting opportunities to break time-reversal symmetry and reciprocity, frequency mixing and wavefront transformations in space-time. Opportunities for new radio-wave and optical technology, as well as physical insights into the functionality of these metasurfaces, will be discussed during the presentation.

17:20 *Investigation of Surface Waves on Anisotropic Self-Complementary Metasurfaces*

[Vladimir Lenets](#), [Andrey Sayanskiy](#) and [Stanislav Glybovski](#) (ITMO University, Russia); [Enrica Martini](#) (University of Siena, Italy); [Juan Domingo Baena](#) (Universidad Nacional de Colombia, Colombia); [Stefano Maci](#) (University of Siena, Italy)

In this paper, we show through a numerical investigation that an anisotropic self-complementary metasurface constituted by a sequence of capacitive and inductive strips supports at low frequency two degenerating quasi TE- and TM surface-waves modes with identical dispersion characteristics. It is also seen that group velocity drastically changes depending on the direction of propagation of the surface waves, becoming extremely low for direction of propagation orthogonal to the strips. The phenomenon can be used in dual polarized leaky wave antennas

17:40 *High Speed Metasurface Reconfigurability Under Optical Control*

[Houssemeddine Kraoui](#) (ESPCI, France); [Charlotte Tripon-Canseliet](#) (Université Pierre et Marie Curie, France); [Stefano Maci](#) (University of Siena, Italy); [Jean-Maurice Chazelas](#) (Thales Aerospace Division, France)

A contactless technique to configure the Metasurface structure printed on photoconductive semiconductor substrate is proposed. This technique is based on the phenomenon of photon absorption into a high resistivity semiconductor material. A free space bi-static measurement system operating in the 40- 60 GHz frequency range is developed to measure the reflection coefficients of planar samples. The measurement system consists of transmit and receive antennas in the bi-static configuration, two focusing lenses to minimize the diffraction effects at the edges of the sample, piezoelectric, precision coaxial cable, laser source at wavelength of 805 and 971nm and the network analyzer

T11-E08: Metamaterials, Metasurfaces and Advanced Materials

T11 Fundamental research and emerging technologies / Regular Session / Electromagnetics

Room: B11

Chairs: [Christophe Fumeaux](#) (The University of Adelaide & School of Electrical and Electronic Engineering, Australia), [Christophe Caloz](#) (Ecole Polytechnique de Montreal, Canada)

13:30 *Dual-band Anomalous Reflection with Interleaved Metagratings*

[Gengyu Xu](#), [Sean V Hum](#) and [George V. Eleftheriades](#) (University of Toronto, Canada)

A new metagrating topology is proposed to enable perfect anomalous reflection of electromagnetic plane waves at two independent bands at microwave frequencies. Two reactively loaded segmented single-band gratings are interleaved together to form a composite metagrating. The constituent halves are electromagnetically shielded from each other through incorporation of PEC baffles, allowing them to be designed independently. Furthermore, isolation between the two frequency channels is achieved with dual-resonant grating wires which can be tuned to be inactive at prescribed frequencies. A dual-band metagrating that performs perfect anomalous reflection at 10 GHz and 15.11 GHz is designed and numerically verified.

13:50 *Reconfigurable Sparse Metasurface: Beamforming Beyond Phase Gradient Heuristics*

[Vladislav Popov](#) (SONDRA, CentraleSupélec, Université Paris Saclay, France); [Badreddine Ratni](#) (Univ Paris Nanterre, France); [Fabrice Boust](#) (ONERA, France); [Shah Nawaz Burokur](#) (LEME, France)

We present the design of a reconfigurable sparse metasurface operating at microwave frequencies (X-band). The operating principle of the metasurface does not rely on established phase gradient along its surface such that it allows one to overcome common limitations of the phase-gradient-based devices. Instead, we have developed a rigorous microscopic approach that allows one to take into account the interaction between the neighboring elements and engineer the individual response of each scatterer to meet a required functionality. By varying the applied bias voltage, we experimentally demonstrate beam steering as well as generation and steering of two (and more) beams with a single feeding horn antenna.

14:10 *An Efficient Anisotropic Metasurface for Linear and Circular-Polarization Conversion Applications*

[Afzal Ahmed](#) (National University of Sciences and Technology, Pakistan); [Hattan F. Abutarboush](#) (Taibah University & Communications and Electronics Engineering, Saudi Arabia); [Fahad Ahmed](#) (National University Of Science and Technology & School of Electrical Engineering and Computer Sciences, Pakistan); [Farooq A. Tahir](#) (National University of Sciences and Technology, Pakistan)

A reflective metasurface exhibiting both crosspolarization conversion (CPC) and linear-to-circular polarization (LP-to-CP) conversion is presented in this paper. The proposed metasurface is composed of 45° tilted T-shaped unit cell having a circular ring at its center. The proposed metasurface converts linearly-polarized wave into its orthogonal counterpart over two frequency bands; 6.2-9.7 GHz, and 15.5- 16.5 GHz with more than 90% CPC efficiency. The metasurface also transformed linearly-polarized wave into circularlypolarized wave at frequency bands; 5.6-5.8 GHz and 11.5-14.5 GHz. The metasurface is insensitive to incident angles up to 30° for both CPC and LP-to-CP conversion.

14:30 *Cold Sintered CaTiO3-K2MoO4 Microwave Dielectric Ceramics for Integrated Microstrip Patch Antennas*

[Dawei Wang](#) (University of Sheffield, United Kingdom (Great Britain)); [Shiyu Zhang](#) (Loughborough University, United Kingdom (Great Britain)); [Ge Wang](#) (University of Sheffield, United Kingdom (Great Britain)); J (Yiannis) Vardaxoglou, [William Whittow](#) and [Darren Cadman](#) (Loughborough University, United Kingdom (Great Britain)); [Di Zhou](#) (Xi'an Jiaotong University, United Kingdom (Great Britain)); [Kaixin Song](#) (Hangzhou Dianzi University, United Kingdom (Great Britain)); [Ian Reaney](#) (University of Sheffield, United Kingdom (Great Britain))

CaTiO₃-K₂MoO₄ (CTO-KMO) dielectric composites were successfully cold-sintered at 150 °C for 30 min with a uniaxial pressure of 200 MPa. As KMO concentration increased, the temperature coefficient of resonant frequency (TCF) and relative permittivity (ϵ_r) decreased but the microwave quality factor (Q \times f) increased. A near-zero TCF composition was obtained for CTO-0.92KMO composites which exhibited $\epsilon_r \sim 8.5$ and Q \times f $\sim 11,000$ GHz. A microstrip patch antenna was designed and fabricated using the cold sintered CTO-0.92KMO as a substrate (40 \times 40 \times 1.4 mm) with a radiation efficiency of 62.0% at 2.51 GHz.

14:50 Coffee Break

15:20 *Fabrication of Artificial Dielectrics via Stereolithography Based 3D-Printing*

[Jack McGhee](#), [Tom Whittaker](#), [Jacob Moriarty](#), [Jamie Northedge](#), [Shiyu Zhang](#), [Darren Cadman](#), [William Whittow](#) and J (Yiannis) Vardaxoglou (Loughborough University, United Kingdom (Great Britain))

In this research, stereolithography (SLA) based additive manufacturing (AM) has been investigated as a fabrication method for producing artificial dielectrics. Initially, the effect of the curing time on the microwave electromagnetic properties (X-band) on the photoinitiated resin used was measured and found to be negligible after 15 minutes of UV curing. Artificial dielectric isotropic and anisotropic lattice structures were then designed and fabricated, allowing for varying permittivity between 1.23 and 2.80 through the control of the structure's density. As a demonstration of the ability to grade permittivity through a high-resolution printing process, lattice structures were embedded into solid substrates. The ability to do this allowed for the printing of a graded permittivity substrate which is showcased in a design for a circularly polarized patch antenna.

15:40 *Complementary Metasurfaces for Waveguide Applications*

[Xin Ma](#) (Northwestern Polytechnical University, China); [Mohammad Sajjad Mirmoosa](#) and [Sergei Tretyakov](#) (Aalto University, Finland)

Metasurfaces have shown a strong potential for controlling electromagnetic waves in a desired fashion and provided us with different new functionalities. For example, they can be used to design novel waveguide structures for transferring electromagnetic energy. In this talk, we will introduce and discuss guiding structures which consist of two parallel penetrable metasurfaces whose surface impedances are "complementary" to each other. We theoretically investigate guided modes which propagate along the structure and show the corresponding dispersion curves. As one of the study results, we show that there is a possibility to excite two modes with orthogonal polarizations which have the same phase velocity within a broad frequency range.

16:00 *Design and Simulation of Polarization-Sensitive ENNZ-Lined Apertures for Visible-Light Metasurfaces*

[Mitchell Semple](#) and [Ashwin K. Iyer](#) (University of Alberta, Canada)

Many proposed visible-light metasurface designs are limited in their ability to confine light on a subwavelength scale, which reduces their maximum efficiency due to discretization errors. Plasmonic metasurfaces show great promise in this regard, as their unit cells can be made deeply subwavelength. Unfortunately, current designs are limited to simple structures due to fabrication difficulty, and are forced to rely on limited-efficiency polarization conversion effects. In this work, we extend the concept of ENNZ-lined apertures that has been used to create metasurface unit cells in the near-IR regime to the visible regime by relaxing the requirement that the unit cells be polarization-insensitive.

16:20 Propagation Through Metamaterial Temporal Slabs: Transmission, Reflection and Special Cases

[Davide Ramaccia](#) (RomaTre University, Italy); [Alessandro Toscano](#) (University Roma Tre (IT), Italy); [Filiberto Bilotti](#) (University Roma Tre, Italy)

Time-varying metamaterials are artificial materials whose electromagnetic properties change over time. In earlier studies, the equivalent reflection and transmission coefficients at a temporal interface have been derived. Here, we extend the study to a temporal slab, i.e., a uniform homogeneous medium that is present in the space for a limited time. We derive the transmission and reflection coefficients for a metamaterial temporal slab as a function of the refractive indices and application time. Similarly to the role played by the electrical thickness for spatial slabs, we show that the response of the temporal slab can be controlled through the application time. The preliminary results reported here may pave the way to several novel devices based on temporal discontinuities.

16:40 Propagation Characteristics in Substrate Integrated Holey Metasurfaces

[Fateme Ghasemifard](#) (KTH Royal Institute of Technology, Sweden); [Francisco Mesa](#) (University of Seville, Spain); [Guido Valerio](#) (Sorbonne Université, France); [Oscar Quevedo-Teruel](#) (KTH Royal Institute of Technology, Sweden)

In this paper we discuss the dispersion properties of a particular type of holey metasurfaces, named here "substrate integrated holey" (SIH) metasurface. SIH is a metallic holey structure manufactured in printed circuit board (PCB) technology by using densely metallized posts. We demonstrate that, differently to the case of holes fully covered with metal, in SIH, the height of the holes has a significant effect on the dispersion properties. In addition, in SIH metasurfaces, apart from the conventional stopband caused by its periodicity, there are stopbands due to the resonance modes trapped in the hole due to the posts. These stopbands are narrow and have a high rejection.

Monday, 16 March 13:30 - 15:30

IW05: Frontline of 5G Workshop: Insights on 5G Antenna & Propagation R&D from Sony and Regional Partners (Sony)

T12 Scientific / Industrial Workshops

Room: B3

Zhinong Ying, Sony

Monday, 16 March 16:00 - 18:00

T02-A04/1: Millimetre-wave Arrays for Mobile Communications

T02 Millimetre wave 5G / Regular Session / Antennas

Room: A2

Chairs: [Vedaprabhu Basavarajappa](#) (University of Surrey, United Kingdom (Great Britain)), [David González-Ovejero](#) (Centre National de la Recherche Scientifique - CNRS, France)

16:00 Dual-Polarized Dielectric Resonator Antenna Array for 5G Mobile Radio Base Stations

[Jerzy Kowalewski](#) (Karlsruhe Institute of Technology, Germany); [Alisa Jauch](#) (Karlsruhe Institute of Technology (KIT), Germany); [Joerg Eisenbeis](#) (Karlsruhe Institute of Technology, Germany); [Sören Marahrens](#) (Karlsruhe Institute of Technology (KIT), Germany); [Karina Schneider](#) (Karlsruhe Institute of Technology, Germany); [Thomas Zwick](#) (Karlsruhe Institute of Technology (KIT), Germany)

Large-scale antenna arrays operating in the millimetre-wave (mmW) regime are required for mobile radio base stations of the next generation. These arrays should support dual-polarization and cover the large available bandwidths. Two dual-polarized antenna concepts are compared to addressing these challenges. The presented dielectric resonator antenna (DRA) is characterized by 3D printed resonator elements, whereas the stacked patch antenna array features a classical multilayer printed circuit board (PCB) structure. To verify the proper functioning a 2x2 DRA antenna array prototype around 28 GHz is built. The investigations show that both antenna designs can meet the requirements of 5G mmW large-scale antenna arrays, whereby the DRA antenna approach reduces the number of PCB layers and thereby lowers manufacturing costs.

16:20 Dual-band Dual-polarized Antenna for mm-Wave 5G Base Station Antenna Array

[Zeeshan Siddiqui](#) (University of Oulu & Centre for Wireless Communications, Finland); [Marko Sonkki](#) and [Jiangcheng Chen](#) (University of Oulu, Finland); [Markus Berg](#) (University of Oulu & Excellant LTd., Finland); [Marko E Leinonen](#) and [Aarno Pärssinen](#) (University of Oulu, Finland)

A dual-band dual-polarized antenna suitable for 5G millimeter-wave base station antenna array is presented in this paper. It operates on all the commercial millimeter wave frequencies allotted in 5G NR from 24.25 GHz up to 40 GHz. The antenna is based on a novel stacked square ring patches arrangement to achieve wide dual band and stable radiation pattern. The antenna offers a sharp roll-off and a filter like response between the operating bands due to the strongly coupled resonators. Antenna design principle and simulated performance are discussed in detail. The -10 dB impedance bandwidth of the lower band starts from 24.25 GHz to 29.5 GHz while the higher band covers the 37 GHz to 40 GHz. The realized gain remains stable between 5 to 6 dBi at all the operating frequencies. The isolation between the ports and cross-polar discrimination remain better than 20 dB in all the covered frequency range.

16:40 Subarray Antenna Fed by Analog Beamforming Network for 5G Picocell Applications

[Danelys Rodríguez-Avila](#) (Microwave and Antenna Group (MAG), Ecole Polytechnique Fédérale de Lausanne, Switzerland); [Anja K. Skrivervik](#) (EPFL, Switzerland)

In this paper a subarray fed by an analog beamforming network for 5G picocell applications is proposed. Design requirements are presented taking into account frequency band operation, bandwidth, radiation pattern shape and both, antenna element and transmission line technologies. The synthesis and implementation of the analog beamforming network are described, and the final subarray architecture is provided. The proposed antenna, verified by simulation, operates at 26 GHz with a bandwidth larger than 25%. The subarray gain is higher than 16 dB with cross-polarization better than -28 dB. Its radiation pattern in elevation fulfills the desired csc2 shape with side lobe level below -15 dB. The performance of the proposed antenna meets the requirements of the defined application.

17:00 A Photonic Beam-Steerable Mm-wave Antenna Array for Radio over Fiber Applications

[Alvaro J Pascual](#) (University of Rennes 1 & IETR, France); [Muhsin Ali](#), [Luis Enrique García Muñoz](#) and [Guillermo Carpintero](#) (Universidad Carlos III de Madrid, Spain); [David González-Ovejero](#) (Centre National de la Recherche Scientifique - CNRS, France); [Ronan Sauleau](#) (University of Rennes 1, France)

We present a photonic-fed transmitter at E-band for radio over fiber (RoF) applications. The transmitter includes four 2x2 sub-arrays fed independently by four photodiodes. Thus, the proposed configuration enables 2D beam steering. Simulation results on a simplified 2x1 prototype, which is under assembly, show a reflection coefficient below -10 dB between 70.7 GHz and 84.7 GHz, with sidelobe levels better than 10 dB and a minimum gain of 15 dBi in this frequency band.

17:20 Low-profile Millimeter-Wave Wideband Circularly Polarized Spiral Antenna Array

[Huakang Chen](#), [Yu Shao](#), [Keyao Li](#), [Changhong Zhang](#) and [Zhi-Zhong Zhang](#) (Chongqing University of Posts and Telecommunications, China)

A single fed low-profile millimeter-wave (mmW) wideband circularly polarized (CP) spiral antenna 2x2 array is presented. By employing the regular parallel feeding network technique to excite each CP spiral element with equal amplitude and phase, the proposed array achieves the impedance bandwidth (IBW) of 6.47 GHz about 23.1% of 28 GHz. A cross slot is introduced at the bottom layer for decoupling. The bandwidth of axial ratio (AR) lower than 3 dB is 6.95 GHz (24.8% referring to 28 GHz) from 24.87 GHz to 31.82 GHz. The polarization sense at the top side and bottom side are left-hand circular polarization (LHCP) and right-hand circular polarization (RHCP), respectively. The gains of the whole desired frequency band (from 25 GHz to 31 GHz) are higher than 10 dBi with a peak gain of 11.98 dBi at 29.5 GHz.

17:40 28 GHz Millimeter Wave Multibeam Antenna Array with Compact Reconfigurable Feeding Network

[Yihua Zhou](#) (Queen Mary University of London, United Kingdom (Great Britain)); [Vedaprabhu Basavarajappa](#) (University of Surrey, United Kingdom (Great Britain)); [Shaker Alkaraki](#) (Queen Mary University Of London, United Kingdom (Great Britain)); [Yue Gao](#) (University of Surrey, United Kingdom (Great Britain))

A switchable multibeam antenna array with a compact planar feeding network is presented. Operating within 1 GHz bandwidth at 28 GHz, this 4x4 antenna can generate one-beam, two-beam and four-beam patterns based on two phase states, which are controlled by the reconfigurable feeding network. The whole structure is validated by simulating in CST Studio. The antenna is a promising candidate in millimeter-wave Massive MIMO for applications where multiple beams are required simultaneously.

T04-A08: IoT Antennas

T04 IoT and M2M / Regular Session / Antennas

Room: B2

Chairs: [Sandra Costanzo \(University of Calabria, Italy\)](#), [Mohsen Khalily \(University of Surrey & 5G Innovation Centre, Institute for Communication Systems \(ICS\), United Kingdom \(Great Britain\)\)](#)

16:00 *Integrated Design of Dual-Band Antenna with Uni-/Omni-Directional Radiations*

[Chun-Xu Mao](#) (University of Surrey, United Kingdom (Great Britain)); [Mohsen Khalily](#) (University of Surrey & 5G Innovation Centre, Institute for Communication Systems (ICS), United Kingdom (Great Britain)); [Pei Xiao](#) (University of Surrey, United Kingdom (Great Britain))

A multifunctional antenna with diverse radiation patterns in different frequency bands (2.45/5.8 GHz) is presented in this paper. The antenna has a low profile but exhibits an omni-directional radiation pattern in the low-band operation and uni-directional pattern in the high-band operation. For the high-band operation, a 2×2 patch arrays are designed by employing an out-of-phase feeding method. The low-band operation with the omni-directional pattern is achieved by exciting four open-ended slots in-phase. The four slots are slit in the ground of the high-band array and in this way, this footprint of the antenna is maintained. The operating principles of the antenna are studied with the aid of equivalent circuit model and the current distribution. The antenna is prototyped and measured, demonstrating good results in terms of bandwidths, inter-channel isolation, radiation characteristics.

16:20 *On the Way to Green IoT Antennas: Compact Ultra-Thin CPW-Fed Monopole on Tencel*

[María Elena de Cos Gómez](#) and [Alicia Flórez Berdasco](#) (Universidad de Oviedo, Spain); [Humberto Fernandez Alvarez](#) and [Fernando Las-Heras](#) (University of Oviedo, Spain)

A compact ultra-thin eco-friendly antenna for IoT applications around 2.45GHz is presented based on both simulations and measurements. The use of a botanical textile named Tencel is explored and its suitability is evaluated through comparison of the novel antenna's performance using Tencel versus a conventional R03003 dielectric with similar relative dielectric permittivity. A comparison with recently published wearable antenna suitable for IoT at the same band is included to assess the relevance of this contribution, not only in terms of reducing the ecological footprint and skin comfort, but especially in terms of size reduction and radiation efficiency.

16:40 *Miniaturized Planar Inverted-F Antenna Using Minkowski Pre-Fractal Structure*

[Sandra Costanzo](#) and [Adil Masoud Qureshi](#) (University of Calabria, Italy)

In this paper, a Miniaturized Planar Inverted-F Antenna (PIFA) is presented. Miniaturization is achieved by transforming the square radiating element in to a Minkowski Pre- Fractal. As a result, the antenna resonates at a lower frequency, in comparison with a square PIFA of the same size. Simulated and measured return loss values are presented. A brief explanation of the miniaturization effect of the Minkowski pre-fractal is also presented.

17:00 *Inexpensive 3D-Printed Radiating Horns for Customary Things in IoT Scenarios*

[Diogo Helena](#) and [Amélia Ramos](#) (Universidade de Aveiro, Instituto de Telecomunicações, Portugal); [Tiago Varum](#) and [João Matos](#) (Instituto de Telecomunicações, Universidade de Aveiro, Portugal)

The increase of data-traffic capacity demands for better performance of the new generation of mobile communications (5G) drives new antenna technologies. The main challenge is to produce user devices which easily integrate a 5G network and its inherent services, without compromising neither cost nor performance. 3D printing is a good solution for these issues, as it can produce high accuracy objects while maintaining low production costs. This work presents several horn antennas operating in the 28 GHz band, all manufactured with 3D printing technology. Two techniques were used to metallize the antennas: with copper tape and with conductive ink. All prototypes achieved proper results for integrating the upcoming IoT scenarios.

17:20 *3D Antenna-on-Package for Near-Isotropic Radiation Shielded from Embedded Electronics*

[Maria M Bermudez](#), [Kirill Klionovski](#) and [Atif Shamim](#) (King Abdullah University of Science and Technology, Saudi Arabia)

Internet of Things devices can be placed anywhere and with random orientations. This raises a need for an antenna on package design that presents high isotropy, while minimizing interference from the embedded electronics. In this paper we present a microstrip patch based cubic antenna system with near-isotropic radiation pattern. The system is designed with six patch antennas on the faces of a 3D cube. All patches are matched for radiation at 2.45GHz. The cube is a hollow structure with metal covered internal walls. The metal covering acts as both ground for the radiating elements and shielding for the embedded electronics. By applying specific phases to each patch we show high isotropy both in gain pattern (6.6dB of gain variation), and electric field polarization (>90% of LP coverage). Our design allows for planar fabrication, thus making it low cost, and is highly suitable for various IoT applications.

17:40 *Design of an Array Antenna Consisting of Three Dual Antenna Sets with a Narrow Array Distance for Interference Mitigation*

[Tae Heung Lim](#) (Hongik University, Korea (South)); [Byung Jun Jang](#) (Kookmin Univ, Korea (South)); [Hosung Choo](#) (Hongik University, Korea (South))

In this paper, we propose a circular array antenna consisting of three dual antenna sets to maximize the number of the array elements in a limited platform size for interference mitigation application. The dual antenna set contains two radiators of a rectangular loop patch and a monopole antenna, which are integrated almost in the same place. The measured peak gains in the upper hemisphere of the monopole and patch elements are 4.7 dBi and 7.0 dBi, respectively. The nulling performance is observed to mitigate the five interference signals with optimum weights of each element. In this null pattern, the minimum null depth of -64.6 dB and the maximum null width of 15 deg are achieved among the five nulling points.

T07-A17: Multiband, Wideband and Array Antennas

T07 Defence and security / Regular Session / Antennas

Room: B4

Chairs: [Andrés Alayón Glazunov \(University of Twente, The Netherlands & Chalmers University of Technology, Sweden\)](#), [Hugo G Espinosa \(Griffith University, Australia\)](#)

16:00 *A Copper Strip Array Loaded Multiband Square Slot Antenna*

[Princy Paul](#) (NIT, Suratkal, India); [Krishnamoorthy Kandasamy](#) (National Institute of Technology Karnataka, SURATKAL, India); [Mohammad S. Sharawi](#) (Polytechnique Montreal, Canada)

A simple copper strip array loaded multiband square slot antenna with microstrip line feed is proposed in this paper. The slot antenna is designed to radiate at 2.28 GHz. The slot is loaded with a uniform array of rectangular copper strips to produce other resonances at 2.2 GHz, 3.4 GHz, 4.6 GHz, 5.4 GHz, 6.6 GHz. The proposed antenna is modeled and simulated using HFSS. The antenna prototypes are fabricated and tested. Good agreement is obtained between the measured and simulated results. The surface current distributions at the various resonant frequencies are simulated. The principle of operation is explained based on the distributions obtained and using analytic equations. An equivalent circuit model is also studied. Impedance bandwidths of 500 MHz, 300 MHz, 600 MHz, 400 MHz, 600 MHz and a gain of above 3 dB is obtained at the five resonant frequencies.

16:20 *Preliminary Co-Design of L and X-band Stacked Arrays with Scanning Capabilities*

[Brandon Sun](#) (Insa de Rennes, France); [Renaud Loison](#) and [Raphael Gillard](#) (IETR & INSA, France); [Eric Estebe](#) (Thales DMS France, France); [Christian Renard](#) (Thales Systèmes Aéroportés, France)

The design of L and X-band stacked arrays is presented in this paper. The design of the X-band element is first detailed. The use of stacked patches leads to scan angles up to 60° in E-plane, and 54° in H-plane, in the 9.5-10.5 GHz band (active reflection coefficient < -10 dB). Secondly, the design of the L-band source is presented. The use of stacked dipoles results in scan angles up to 60° in the H-plane, for the two Identification Friend or Foe (IFF) bands, at 1.03 and 1.09 GHz (with 3.6 MHz bandwidths). Finally, the L-band dipoles are placed above the X-band array and the performances of the stacked arrays are analyzed in the L and X-bands.

16:40 *Multichannel Dynamic Directional Modulation with Software Defined Radio*

[Edith Annette Cabrera-Hernández](#) and [Josep Parrón Granados](#) (Universitat Autònoma de Barcelona, Spain); [Alan Tennant](#) (University of Sheffield, United Kingdom (Great Britain))

Dynamic Directional Modulation (DDM) has become an attractive option to achieve physical layer security. In this contribution, we evaluate the generation of DDM with software defined radio for transmitting simultaneously two uncorrelated signals along two different observation angles. The generation of DDM relies on the knowledge of the channel vector and an accurate adjustment of the weights that feed the phased array, for that reason, the components of the transmitter need to be characterized accurately. Experimental results that assess the performance of the system for the observation angles under consideration are shown.

17:00 *Research on a Kind of Asymmetric Scanning Phased Array Antenna*

[Hong-yin Zhang](#) (The 14th Institute of China Electronics Technology Group Corporation, China)

In this paper, a technique for asymmetric scanning of phased array antenna by beamforming of antenna elements is discussed, and this technique has been applied in practical engineering. The proposed Ya-gi antenna element centered in the large scale array provides good radiation performance in the range of 0 - 70 degree, thus realizing the asymmetric reshaping of the element pattern. Additionally, a 7×7 array prototype is fabricated. The measured results agree well with the simulated results, which prove its effectiveness.

17:20 *A Distinct Approach Exploiting Collapse Distribution Colligated with Genetic Algorithm for the Synthesis of Thinned Planar Antenna Arrays*

[Veer S Gangwar](#) (LRDE(DRDO), India); [Juhi Modi](#) (IIT(ISM) DHANBAD, India); [Jatin Narde](#) (NIT Rourkela, India); [Kundan Suman](#) (IIT ISM, India); [Ashwin. P](#) ((DRDO), Bangalore, India)

In this paper, authors propose a distinguishable technique, which synthesizes Thinned Planar Antenna (TPA) Arrays with maximally reduced peak side lobe level (PSLL). Authors employed Collapse Distribution Technique amalgamated with Genetic Algorithm (CDT-GA) in order to reduce optimization complexity and to obtain efficient control of PSLL. 8×8- and 10×20-element TPA arrays are numerically analyzed to verify the effectiveness and examine the distinguishable features of the proposed strategy. The numerical results obtained through CDT-GA evidence that it outmatches the similar designs available in the literature. In order to further ascertain and validate the performance of CDT-GA in practical scenarios, authors realized an 8×8-element TPA array and carried out experimental evaluation. The obtained empirical results are found nearly in agreement with corresponding numerically computed and electromagnetically simulated ones. Index terms Collapsed distribution technique combined with genetic algorithm (CDT-GA), peak side lobe level (PSLL), thinned planar antenna (TPA) arrays.

17:40 *High-Performance Wideband Horn Antenna for Direction Finding Arrays*

[Saeed Manshari](#) (Engineering Optimization & Modeling Center, Reykjavik University, Iceland); [Slawomir Koziel](#) (Gdansk University of Technology, Poland); [Leifur Leifsson](#) (Iowa State University, USA); [Andrés Alayón Glazunov](#) (University of Twente, The Netherlands & Chalmers University of Technology, Sweden)

In this paper, a structure and design procedure of a novel double ridged horn antenna with a Gaussian amplitude radiation pattern and stable phase center for two-element direction finding arrays is presented. The radiation properties of the structure are improved through appropriate profiling of the ridge taper and utilization of an elliptical aperture. Furthermore, rigorous numerical optimization is employed to adjust the antenna geometry parameter values. The achieved impedance bandwidth (VSWR < 2) is from 1.5 GHz to 12 GHz (8:1). The antenna exhibits 7 dBi to 20 dBi gain, better than 85% aperture efficiency, > 10 dB side lobe level, as well as low phase center variation (< 5 cm over the operating band). The aforementioned features make the proposed antenna suitable for the amplitude and phase hybrid direction finding applications. The design is validated numerically in CST Microwave Studio.

T06-M03: Near-field, Far-field, Compact and RCS Range Measurement Techniques

T06 Aircraft (incl. UAV, UAS, RPAS) and automotive / Regular Session / Measurements

Room: B7

Chairs: [Manuel Sierra-Castañer](#) (Universidad Politécnica de Madrid, Spain), [Christopher G Hynes](#) (Simon Fraser University, Canada)

16:00 *Experimental Validation of the Translated-SWE Technique Applied to Automotive Measurements over PEC-Floor at Arbitrary Height*

[Francesco Saccardi](#) (Microwave Vision Italy, Italy); [Francesca Mioc](#) (Consultant, Switzerland); [Per Iversen](#) (Orbit/FR, USA); [John Estrada](#) (MVG, USA); [Lars Foged](#) (Microwave Vision Italy, Italy)

Automotive antenna testing performed on large, truncated spherical near-field systems, able to host the entire vehicle under test, are an industry standard. The truncated scanner is often terminated to a conductive floor where the vehicle is staged for testing. Despite the strong interaction with the reflective floor, such systems are often employed because of the ease of car accommodation and measurement setup. Moreover, if the conductive floor lies on the horizon plane, truncation errors can be easily reduced in the near-field to far-field transformation by simply mirroring the measured field (image theory). Due to mechanical constraints, or extension of the operational mode of some systems (e.g. absorber-based systems), sometimes the floor position doesn't correspond to the horizon plane, and advanced techniques are needed to extrapolate the truncated area. The Translated-SWE technique, already presented in the past, is proposed for such purpose and will be validated experimentally considering scaled automotive measurements.

16:20 *Near-field Measurement and Far-field Characterization of a J-band Antenna Based on an Electro-optic Sensing*

[Shintaro Hisatake](#) and [Yusuke Tanaka](#) (Gifu University, Japan); [Cybelle Belem](#) (Université de Lille, France); [Cyril Luxey](#) (University Nice Sophia-Antipolis, France); [Frédéric Giancesello](#) (STMicroelectronics, France); [Guillaume Ducournau](#) (IEMN, University of Lille, France); [Akihiko Hirata](#) (Chiba Institute of Technology, Japan)

In this paper, we present a near-field pattern measurement based on an electro-optic sensing at 300 GHz band. The measurement system is based on a self-heterodyne technique and non-polarimetric frequency down-conversion technique. The far-field radiation pattern of a horn antenna calculated from the measured near-field pattern is compared with the far-field pattern measured with a conventional measurement system using open-ended waveguide probe.

16:40 *A New Method to Measure the Absolute Gain Patterns of a Log-Periodic Antenna at a Reduced Distance Without Considering the Phase Center in a Single-Cut Near-Field Far-Field Transformation*

[Masanobu Hirose](#) and [Satoru Kurokawa](#) (National Institute of Advanced Industrial Science and Technology, Japan)

We propose a new method to measure accurately the absolute gain patterns of a log-periodic antenna over the operating frequency band at a reduced distance and a fixed setup position in a single-cut near-field far-field transformation (called the Kim method). By combining the Kim method and a source reconstruction method, our method does not require the information of the phase-center position of the antenna. Therefore, we can measure the absolute gain patterns accurately over the frequency band without re-setting the antenna position to each frequency. At 1.3 GHz, our method makes it possible to determine the maximum absolute gain within 0.1 dB and the patterns errors below - 20 dB over all angles at a measurement circle radius of 1.5 m.

17:00 *Relative Phase Reconstruction Based on Multiprobe Solutions and Post-Processing Techniques*

[Ruben Tena Sanchez](#) (Technical University of Madrid, Spain); [Manuel Sierra-Castañer](#) (Universidad Politécnica de Madrid, Spain); [Lars Foged](#) (Microwave Vision Italy, Italy)

In a previous paper a referenceless measurement set-up based on a reference antenna was used for characterizing the near-field radiation of antennas in the planar and spherical multiprobe systems. This paper proposes an alternative technique based on exploiting the intrinsic characteristics of multiprobe systems. One of the antennas from the multiprobe arch is used to retrieve the relative phase between measurement points. Post-processing is needed since the relative phase between azimuth cuts is lost. The advantages, limitations and results are shown. The results demonstrate that the technique is very promising for characterizing devices under certain conditions.

17:20 *MetOp-SG Scatterometer Antenna Testing - Golden Standard Measurement 2019*

[Javier Fernández Álvarez](#), [Kyriakos Kaslis](#), [Jeppe Nielsen](#) and [Olav Breinbjerg](#) (Technical University of Denmark, Denmark)

This work presents the 2019 campaign of investigatory measurements, which goal is to assess the robustness of the measurement setup when mounting large masses on the AUT positioner, such as will be the case for the 300 kg MetOp-SG antennas, as well as the long-term reproducibility of the measurements. To this end a full measurement was performed, including complete uncertainty measurements, of the DTU Golden Standard array antenna (GS) in two configurations, unloaded and loaded with 303 kg of dummy weight. The measurements of the unloaded and loaded configurations were compared and it is demonstrated that the AUT positioner is capable of assuming an antenna with a mass comparable to the MetOp-SG without suffering any impact to its accuracy. For the long-term reproducibility, measurements were compared with a previous investigatory campaign of the same antenna dating from 2017.

17:40 *RCS Evaluation by Image-based Near-field to Far-field Transformation*

[Hirokazu Kobayashi](#) (Osaka Institute of Technology, Japan)

There is recently a strong demand to evaluate for Radar Cross-Section (RCS) of electrically large objects such as airplane and for radiation pattern of large antennas. This is because the measurement difficult by the conventional method in far-region. We have proposed the improved novel Near-Field to Far-Field Transformation method in cylindrical scanning, from which RCS can be estimated by pickup near-field data. Our method is featured by the improved focusing factor obtained from the exact integral equation using small spheres, which leads more accurate estimation for strong asymmetrical objects, so that the RCS measurement is available even in a small anechoic chamber. In this paper, by applying Geometrical Theory of Diffraction (GTD) to simple shaped models as a target, and it is shown high agreement between theoretical and measured NFFFT results including antenna pattern. Furthermore, we propose a simple method to suppress the unnecessary wave by the imaging area-limiting method.

18:00 *On the Accuracy of Standard Gain Horn Measurement*

[Maryam Razmhosseini](#), [Christopher G Hynes](#) and [Rodney Vaughan](#) (Simon Fraser University, Canada)

New measurement accuracy results are presented for a Standard Gain Horn in a profession-level system, the MVG Stargate 64. This system offers calibration options, and draws on the user's knowledge to choose the most appropriate one. An ideal measurement in an ideally calibrated system should be perfectly repeatable and independent of the choice of calibration method, but the variations caused by real-world effects are of interest. The measurements include the use of a coaxial feed cable with a multitude of ferrite beads (to suppress any currents on the cable outer), and the cable with no beads, and with an optical fiber feed system for eliminating the scattering contribution of the measurement cable. We also compare patterns taken at different times and temperatures. The pattern comparison basis is the vector pattern correlation coefficient (inner product). The worst-case pattern variations appear to be related to the temperature variation of the system.

T05-E05: Microwave Imaging

T05 Biomedical and health / Regular Session / Electromagnetics

Room: B8

Chairs: [Marco Salucci](#) (ELEDIA Research Center, Italy), [Alessandro Fanti](#) (University of Cagliari, Italy)

16:00 *Robust Multi-Resolution Microwave Imaging Through an Over-Constrained Approach*

[Marco Salucci](#) (ELEDIA Research Center, Italy); [Paolo Rocca](#) and [Andrea Massa](#) (University of Trento, Italy)

This work presents an innovative iterative multi-resolution (MR) methodology to solve fully non-linear inverse scattering (IS) problems. More in detail, an over-constrained (OC) formulation is adopted to enforce additional constraints on the solution in order to mitigate the occurrence of false solutions/local minima at each multi-zooming step. Thanks to such an OC-MR procedure, progressively acquired information on the imaged domain can be effectively exploited to counteract both non-linearity and ill-posedness of the IS problem, yielding accurate and reliable guesses with a remarkable robustness to noise. A preliminary numerical benchmark is presented to assess the potentialities of the proposed method, as well as to compare it with a standard MR solution approach.

16:20 *Multiple Moving Targets Tracking Based on Kernel Localization and Group Trackers for Envisioned Functional Microwave Brain Imaging Applications*

[Mohammad Ojaroudi](#) (University of Limoges/CNRS, France); [Stéphane Bila](#) (XLIM UMR 7252 Université de Limoges/CNRS, France)

This paper presents a new concept of multiple target tracking using hierarchical trackers based on kernel localization for envisioned functional microwave brain imaging application. For this purpose, the performance of brain activated regions tracking using fMRI video is improved. In the first stage, all of the moving regions in the fMRI video frame are detected. Then, by using the group tracking, histogram and distance corresponding to the moving-targets in the previous frame, the directions of moving-regions are determined. After determining the exact number of moving objects and tracking them, one by one, the direction of each vector is extracted. In addition, due to the kernel labelling, the proposed method has capability of separation and merging by group tracking in conditions of motion paths interfere with each other. The simulated results validate the effectiveness of the proposed methods for precisely tracking of the activated regions.

16:40 *Validation of Multilevel 24-Port Microwave Imaging System for Brain Stroke Monitoring on Synthetic Numerical Data*

[Jan Tesarik](#) and [Jan Vrba](#) (Faculty of Biomedical Engineering, Czech Technical University in Prague, Czech Republic)

Microwave imaging (MWI) could provide a great opportunity for early stroke diagnosis and thus reduce the health consequences caused by stroke. Based on different dielectric properties of healthy and stroke hit tissue MWI systems can help to differentiate the type of stroke. The main purpose of this contribution is to validate the newly designed multilevel 24-port MWI system on numerical data. Inside the 3D human head phantom, the different stroke phantom types (HEM - haemorrhagic or ISCH - ischemic) with different diameters were placed. Using the reconstruction algorithm based on Born Approximation and TSVD the stroke phantoms can be followed and distinguish. The numerical analysis of MWI system proved promising results where positions, diameters and types of stroke phantoms were successfully reconstructed. The system showed some limitations as disability to detect objects with size lower than half of used wavelength which can be and will be eliminated in the future.

17:00 *Microwave Imaging of Cervical Myelopathy: A Preliminary Feasibility Assessment*

[Chiara Dachena](#) (University of Genoa, Italy); [Alessandro Fanti](#) (University of Cagliari, Italy); [Alessandro Fedeli](#) (University of Genoa, Italy); [Giuseppe Mazzarella](#) (University of Cagliari, Italy); [Matteo Pastorino](#) and [Andrea Randazzo](#) (University of Genoa, Italy)

Microwave imaging is acquiring a growing importance in several biomedical applications, such as breast and brain stroke diagnosis and monitoring. In this work, a preliminary feasibility analysis concerning the application of such a technique to the monitoring of cervical myelopathy is reported. In particular, suitable working conditions are defined on the basis of a simplified multilayer model of the neck and a first inversion result, aimed at assessing the possibility of retrieving the spinal cord size, is shown.

17:20 *Effectiveness of Folded Quasi Self-Complementary Antenna to Microwave Imaging*

[Yoshihiko Kuwahara](#) and [Akira Nozaki](#) (Shizuoka University, Japan)

We examined the application of Folded Quasi Self-Complementary Antenna (FQSCA) to a microwave imaging system aimed at breast cancer detection. It is presented that FQSCA can reconstruct high-fidelity diagnostic images that are robust to manufacturing errors compared to the printed dipoles.

17:40 *Real-Time Three-Dimensional Electrical Impedance Tomography of the Human Chest*

[Marco Salucci](#) and [Davide Marcantonio](#) (ELEDIA Research Center, Italy); [Alessandro Polo](#) (ELEDIA Research Center, University of Trento, Italy); [Maokun Li](#) (Tsinghua University, China)

An approach for the diagnosis of the human chest in real time based on electrical impedance tomography (EIT) is hereby applied on a fully three-dimensional (3D) imaging scenario. The methodology adopted for performing EIT data inversion is based on the learning-by-examples (LBE) paradigm and exploits a profitable combination of a feature reduction strategy based on partial least squares (PLS) with an adaptive sampling based on the output space filling method (OSF). Some preliminary results are shown to assess how the 3D-EIT problem can be efficiently, accurately, and robustly solved thanks to the proposed methodology.

CS43: Near- and Far-Field Wireless Power Transfer

T11 Fundamental research and emerging technologies / Convened Session / Electromagnetics

Room: B9

Chairs: [Yi Huang](#) (University of Liverpool, United Kingdom (Great Britain)), [Naoki Shinohara](#) (Kyoto University, Japan), [Hubregt J. Visser](#) (imec The Netherlands, The Netherlands)

16:00 *Wireless Power Transfer in Japan: Regulations and Activities*

[Naoki Shinohara](#) (Kyoto University, Japan)

Japan has a long history of research and development (R&D) in wireless power transfer (WPT) technologies. Recently, based on a WPT R&D agreement, there are interesting new WPT R&D and WPT research projects in Japan, and are discussed in the course of this paper. . WPT technologies and its applications can make significant advancements not only through R&D and commercialization, but also in discussion of new radio regulations. Japan not only contributes in discussions of regulation of the WPT within its shores, but also in the International Telecommunication Union Radiocommunication Sector (ITU-R). The status of the discussion in the new regulation of the WPT is further discussed in the course of this paper.

16:20 *High-Efficiency Rectifiers with Wide Input Power Range and Application on Powering Wireless Sensors*

[Xiuyin Zhang](#) and [Jun-Hui Ou](#) (South China University of Technology, China); [Mo Huang](#) (University of Macau, China)

In order to enhance the efficiency stability of a rectifier in MPT application with movable TX/RX systems, this paper proposes several effective approaches for the rectifier to maintain high efficiency when input power varies. The ideas are divided into two types: improve matching performance of the rectifier, or recycle the power which is reflected from the rectifier due to impedance mismatch, when input power varies. Mechanism of these approach is introduced briefly, while a comparison is carried out to illustrate the differences between each approach. To demonstrates the effectiveness of extending input power dynamic range, RF powered wireless sensors are integrated, and an MPT system is formed. The measurement shows that even though the locations of sensors are changed significantly, the rectifiers operates efficiently, and the sensors are successfully function.

16:40 *3D Antenna Array for SWIPT Sensing with WPT Capabilities*

[Diogo Rafael Pinto Pires](#) and [Daniel Belo](#) (Universidade de Aveiro & Instituto de Telecomunicações, Portugal); [Marina Jordão](#) (Instituto Telecomunicações - Universidade Aveiro, Portugal); [Pedro Pinho](#) (IT - Instituto de Telecomunicações & ISEL - Instituto Superior de Engenharia de Lisboa, Portugal); [Nuno Borges Carvalho](#) (University of Aveiro/IT Aveiro, Portugal)

In this work, the design and development of an alternative three-dimensional array is presented. This arrangement aims to improve some Wireless Power Transmission (WPT) systems and to provide advantages when integrated into a Wireless Sensor Network (WSN) architecture. The conceived 3D antenna array consists of eight antenna elements operating at 5.65 GHz that are attached in a 3D printed heptagonal prism. With this structure, it is intended to achieve as close as possible to an omnidirectional radiation pattern with considerable gain, avoiding power losses. The experimental measurements carried out are in line with the performed electromagnetic simulations and validate the array operation. A full azimuth coverage was ensured with an average realized gain of 6.7 dBi. For some azimuth directions, this gain can reach approximately 8.35 dBi. This array proves to be a reliable solution to fed multiple low-power sensors that are placed over the 360 azimuth angles.

17:00 *A Novel Duplexing Antenna for Feedback Wireless Power Transfer*

[Sumin David Joseph](#) and [Yi Huang](#) (University of Liverpool, United Kingdom (Great Britain)); [Shuohung Hsu](#) (National Tsinghua University, Taiwan); [Manoj Stanley](#) (National Physical Laboratory, Teddington, United Kingdom (Great Britain)); [Ahmed Alieldin](#) and [Chaoyun Song](#) (University of Liverpool, United Kingdom (Great Britain))

In this work, a novel duplexing antenna is proposed for feedback wireless power transfer (WPT) applications. The proposed antenna has the capability to receive RF power at fundamental frequency 0.915 GHz and transmit the second harmonic at 1.83 GHz as a feedback signal simultaneously. Fundamental and harmonic resonances of a dipole antenna are utilized to design the dual-band antenna. A 0.5λ microstrip line resonator is coupled to the feed of the antenna to realize the duplexing action of the proposed antenna. Port 1 is for 0.915 GHz frequency band and has a measured bandwidth of 60 MHz (from 0.895 to 0.955 GHz). Port 2 is for 1.83 GHz frequency band (from 1.815 to 1.905 GHz). The worst-case isolation between the two ports is better than 13 dB at both bands. The proposed duplexing antenna exhibit similar gains and radiation patterns with good isolation, making it suitable for feedback WPT applications.

17:20 *Electromagnetic Field Modeling for Wireless Power Transfer in Biological Tissue*

[Tom van Nunen](#) and [Rob Mestrom](#) (Eindhoven University of Technology, The Netherlands); [Mark Bentum](#) (Eindhoven University of Technology & ASTRON, The Netherlands); [Hubregt J. Visser](#) (imec The Netherlands, The Netherlands)

We present a mathematical model that can be used to model the electromagnetic fields generated by a vertically oriented magnetic dipole located above a conductive half-space, such as biological tissue. The model was compared to a full-wave simulation in CST. The difference is shown to be below 8.1% on average for frequencies ranging from 13 MHz to 5 GHz. It executes over 50 times faster than a full-wave solver, using more than 20 times less memory, and can be adapted to model more realistic magnetic sources without much extra effort. This model can improve the design process of inductive or radiative links significantly, enabling rapid design iteration. It is well suited for biomedical applications. Extension to magnetic sources with arbitrary orientation, as well as electric sources, is possible.

17:40 100 W 6.78 MHz Inductive Power Transfer System for Drones

Lingxin Lan, Christopher H Kwan, Juan Arteaga, David Christopher Yates and Paul Mitcheson (Imperial College London, United Kingdom (Great Britain))

This paper reports on the design and development of a wireless charging solution for a DJI Matrice 100 quadcopter drone. The developed system is capable of delivering power to the drone at the same rate as the cable charger over a wide range of misalignment and any orientation. The system has a typical end-to-end efficiency of 70% and allow the drone to operate with complete autonomy without human interference

18:00 Appliqué: A Computationally Efficient Modeling Tool for Multi-Layer Printed Inductors, for near Field Wireless Power Transfer Applications

Brody Mahoney and Joshua R. Smith (University of Washington, USA)

This paper presents Applique, a computationally efficient open source environment for wireless power transfer coil design. The system allows designers to rapidly design and simulate coils. Applique extracts coil parameters and back-annotates the extracted values into a SPICE netlist model of the wireless power transfer coil. Applique then automatically executes SPICE and combines extracted inductances, capacitances, and resistances to provide the user with narrow or wide-band impedance analysis, as well as component values for a functionally meaningful simplified circuit model. Final designs may then be exported to common PCB CAD software.

IW01: Key Advantages of Combining Measurements and Simulations for Antenna Applications (MVG)

T12 Scientific / Industrial Workshops

Room: B3

Lucia Scialacqua, Microwave Vision Group (MVG)

Tuesday, 17 March

Tuesday, 17 March 8:30 - 10:10

EurAAP 5: WG Active Array Antennas (8:30-10:10, Room: 17)

Time: 8:30 - 10:10 Room: 17

Tuesday, 17 March 8:30 - 12:20

T02-A04/2: Millimetre-wave Arrays for Mobile Terminals

T02 Millimetre wave 5G / Regular Session / Antennas

Room: A2

Chairs: Anu Lehtovuori (Aalto University, Finland), Shuai Zhang (Aalborg University, Denmark)

8:30 Embedded 5G Wideband Dual-Polarized mm-Wave Antennas in Non-mm-Wave Antennas Integrating a Package (AiAiP) for a Metal-Framed Cell Phone

Zhimin Zhu (vivo Mobile Communication Co., Ltd, China); Huan-Chu Huang (vivo Mobile Communication Co., Ltd, Taiwan); Yijin Wang, Xianjing Jian and Rongjie Ma (vivo Mobile Communication Co., Ltd, China)

4 embedded wideband dual-polarized mm-Wave antennas as a linear array in a non-mm-Wave antenna integrating a package (AiAiP) for 5G cell phone with a metal frame as an LTE antenna and a high display A.A.-to-body ratio beyond 91.7% is presented. For simulated $|S_{nn}| \leq -10$ dB, bandwidths of the ports in the 5G mm-Wave antenna array for both the dual polarizations at $\varphi = 45^\circ$ and $\varphi = -45^\circ$ range from 24.19 GHz to 29.62 GHz and from 35.67 GHz to 40.24 GHz. All 5G mm-Wave bands n258, n257, n260 and n261 in 3GPP can be covered. Bandwidths for $|S_{nn}| \leq -6$ dB of the LTE antenna range from 878 MHz to 971 MHz and from 2258 MHz to 2763 MHz so Band 8, Band 40, and Band 41 are supported with efficiencies higher than -3.03 dB in Band 8 and higher than -1.30 dB in Bands 40 and 41.

8:50 Embedded 60-GHz mm-Wave Antennas in Non-mm-Wave Antennas Integrating a Package (AiAiP) for Motion Recognition in a Full-Screen Metal-Framed Cell Phone

Huan-Chu Huang (vivo Mobile Communication Co., Ltd, Taiwan); Heng Zha and Yijin Wang (vivo Mobile Communication Co., Ltd, China)

4 embedded 60-GHz mm-Wave antennas in a non-mm-Wave antenna integrating a package (AiAiP) for motion (e.g., gesture) recognition in a full-screen phone with a metal frame as an LTE antenna, 100% front glass coverage, and a high display-to-body ratio beyond 91.7% is presented. For $|S_{nn}| \leq -6$ dB, simulated bandwidths of the 4 antennas range from 56.91 to 64.30 GHz so the 60-GHz band is supported. In-band peak gains of 3 antennas as a receiving array are higher than 6.68 dBi with the peak of 9.17 dBi. Simulated bandwidths for $|S_{nn}| \leq -6$ dB of the LTE antenna range from 879 to 963 MHz and from 2281 to 2751 MHz to cover Band 8, Band 40, and Band 41 with efficiencies higher than -3.91 dB in Band 8 and higher than -1.85 dB in Bands 40 and 41. The design is promising to compatibility of motion recognition and full-screen features.

9:10 Dual-Polarized mm-Wave Antenna Solution for Mobile Phone

Resti Montoya and Juha Ala-Laurinaho (Aalto University, Finland); Ville Viikari (Aalto University & School of Electrical Engineering, Finland)

This article describes a novel dual-polarized mm-wave antenna for mobile phone devices. The mm-wave antenna module consists of a 4-layer PCB, an extra metallic piece acting as a reflector, and four metallic pins. The four metallic pins are placed on the top layer of the PCB acting as an array of vertically polarized monopoles. On the bottom layer an array of horizontally polarized dipoles are fed using microstrip lines. The two middle layers act as ground. Simulations show very good performance in the 27 to 29.5 GHz range. In this frequency range, the horizontally and vertically polarized arrays provide better than -1.5 dB efficiency, and higher than 11.5 dBi realized gain. Also, the reflection coefficient is mostly below -10 dB in the 27 to 29.5 GHz range for each individual antenna element. Beam-steering is possible up to 35 degrees for both polarizations with a scan loss below 3 dB.

9:30 Dual-Band Dual-Polarized mm-Wave Slot Antenna Array for Mobile Handsets

Joni Kurvinen (Aalto University School of Electrical Engineering, Finland); Anu Lehtovuori (Aalto University, Finland); Ville Viikari (Aalto University & School of Electrical Engineering, Finland)

Fifth generation (5G) mobile networks utilize millimeter-waves (mm-waves) to achieve higher data rates. This paper presents a dual-polarized antenna array that operates at 28 GHz (27.5-29.5 GHz) and 38 GHz (37-39 GHz) bands and is usable in mobile handsets. The array is based on slot antennas with separate feeds for each polarization and band. The multi-feed structure allows us to improve isolation between bands. The dual-polarized array has a peak realized gain of 10-13 dBi and it is capable of beam-steering for up to $\pm 35^\circ$ or $\pm 50^\circ$ at 28 GHz and 38 GHz bands, respectively. The performance of the array in the presence of a smartphone chassis is also studied.

9:50 A Novel Lens Antenna Design Based on a Bed of Nails Metasurface for New Generation Mobile Devices

Carla Di Paola (Aalborg University, Denmark); Kun Zhao (Sony Research Center Lund, Sweden & Aalborg University, Denmark); Shuai Zhang and Gert Pedersen (Aalborg University, Denmark)

This paper presents a lens antenna concept with multibeam performance in the mm-wave band for the next generation mobile devices. The lens consists of metallic vias, etched in the substrate with different height, to obtain different permittivity. The goal is to correct the phase distribution of the incoming electromagnetic wave, to radiate towards the desired direction with high gain. The -10 dB impedance bandwidth of 4 GHz is achieved around the central frequency of 38 GHz. Three beams pointing different directions allow to cover the angle range of 68° in azimuth with realized gain higher than 5 dBi. Simulations of the lens antenna placed on the top left corner of a mobile phone PCB confirm the performance of the prototype. Moreover, the total scan pattern (TSP) highlights wide coverage of 110° in elevation, where the gain is overall more than 6 dBi, reaching peak values of 9.4 dBi.

10:10 Coffee Break

10:40 *Frequency Reconfigurable Endfire Vertical Polarized Array for 5G Handset Applications*

[Jin Zhang](#), [Shuai Zhang](#) and [Gert Pedersen](#) (Aalborg University, Denmark)

This paper proposes a frequency reconfigurable phased array with endfire vertical polarized radiation pattern for 5G handset applications. The array element consists of a magnetic dipole and two reconfigurable strips, which are controlled independently by two PIN diodes. By combining the two PIN diodes, three resonating frequencies are achieved from 24 GHz to 27 GHz. An eight-element array is then constructed based on the proposed antenna. The scanning angle is from 130 deg to 220 deg with realized gain ranging from 7 dBi to 9 dBi. Moreover, the array has low profile of 0.508 mm and small clearance of 3.35 mm. The performances of the proposed antenna and array are verified by simulations.

11:00 *A Beam-Steerable Antenna Array with Radiation Beam Reconfigurability for 5G Smartphones*

[Naser Ojaroudi Parchin](#) (University of Bradford, United Kingdom, United Kingdom (Great Britain)); [Raed A Abd-Alhameed](#) (University of Bradford, United Kingdom (Great Britain)); [Ming Shen](#) (Aalborg University, Denmark)

A radiation-beam switchable phased array antenna is proposed for 5G mobile terminals. The design consists of eight discrete-fed slot radiators placed at the top edge of the mobile phone PCB. The configuration of the antenna element is composed of an I-shaped slot radiator with a single director. By implementing and biasing RF switches (D1&D2) across the I-shaped slot radiators of the main design, the radiation beams of the phased array can be switched from end-fire to broad-side radiation modes. The proposed design can provide a 2 GHz impedance-bandwidth with $S_{11} \leq -10$ dB at 28 GHz (5G candidate band) and generates high-gain radiation beams in both end-fire and broad-side modes. Fundamental characteristics of the design in terms of S-parameters, radiation patterns, efficiency, and antenna gain are investigated. The obtained results showed promising performance of the array under different states of the switches.

11:20 *A Millimeter-Wave Dual Band Antenna with Circular Polarization*

[Samaneh Sadeghi-Marasht](#) (University College Dublin, Ireland); [Mohammad S. Sharawi](#) (Polytechnique Montreal, Canada); [Anding Zhu](#) (University College Dublin, Ireland)

This paper presents a high efficiency dual band single layer antenna structure for MIMO array applications. The e-shape patch that is surrounded by two conductive walls is designed on an R05880 substrate with thickness of 0.508 mm. The operating frequencies of this antenna are 28 GHz and 38 GHz. Circular polarization is achieved by designing the specific shape of the inner patch and cutting the edge of the outer ring. The reflection coefficient is less than -10 dB at 25.9-28.6 GHz and 36-58.5 GHz with maximum gain and efficiency of 6.31 dB and 92% at 28 GHz and 5.2 dB and 71% at 38 GHz. This low-profile and lightweight antenna can be used in many 5G communication systems.

11:40 *Substrate Integrated Dual Linearly Polarized End-Fire Antenna Array Operating at 28GHz*

[Halim Boutayeb](#) (Huawei Technologies, Canada); [Wen Tong](#) (Huawei Technologies Canada Co., Ltd., Canada); [Fayez Hyjazie](#) (Huawei Technologies Co. Ltd., Canada); [Wenyao Zhai](#) (Huawei Technologies Canada Research Center, Canada); [Xin Feng](#) (Huawei Technologies Co., Ltd., Canada)

We present a new cost-effective technique for designing mm wave dual linearly polarized end-fire antennas and antenna arrays using multi-layer printed circuit boards. For vertical polarization (VP) we propose a modified inverted F antenna with plated through holes. Horizontal polarization (HP) is obtained with quasi Yagi-Uda printed dipole. VP and HP elements cross each other to ensure low coupling and size reduction. A conformal dual polarized array is fed by using a parallel plate horn feeding circuit. Transition from exciting ports to parallel plate horn and from horn to radiating elements were designed by using metallic vias. For cost reduction, no buried vias are used in the design. Based on this design methodology, an optimized dual polarized beam steering antenna operating at 28 GHz is presented. Applications of this work include the design of beam-steering antennas with wide scanning angle.

12:00 *Wideband Dual-Polarized Patch Antenna with Capacitive Coupling for mm-Wave Bands*

[Marko Sonkki](#) (University of Oulu, Finland); [Danping He](#) (Beijing Jiaotong University, China); [Zeeshan Siddiqui](#) (University of Oulu & Centre for Wireless Communications, Finland); [Marko E Leinonen](#) (University of Oulu, Finland); [Ke Guan](#) (Beijing Jiaotong University, China)

This paper presents a planar wideband dual-polarized antenna structure integrated on PCB. The patch itself is fed by capacitive coupling with smaller patches. Whereas the simulations predicts 24-40 GHz 10 dB impedance bandwidth, the measured ones shows 24.75-42.75 GHz bandwidth. The results are corresponding to 50% relative -10 dB impedance bandwidth. The patch antenna is on the ground plane of size 4.7 mm x 4.7 mm, and the corners of the ground plane are cut to gain better XPD. The manufactured prototype antenna is measured and simulated with a 50 Ω coaxial feed. Simulated total efficiency and XPD are presented as a function of frequency. The total efficiency shows better than 0.8 dB (83%) efficiency, whereas the simulated XPD is better than 14 dB. The simulated 3D radiation patterns are presented at 24 GHz, 32 GHz, and 40 GHz with gains of 2.8 dBi, 5.0 dBi, and 4.3 dBi, respectively.

CS35: IET/IRACON Session: Propagation Measurements and Modelling for 5G and Beyond

T02 Millimetre wave 5G / Convened Session / Propagation

Room: A3

Chairs: [Mark Beach](#) (University of Bristol, United Kingdom (Great Britain)), [Sana Salous](#) (Durham University, United Kingdom (Great Britain))

8:30 *Investigation of Resonance Based Propagation Loss Modeling for THz Chip-to-Chip Wireless Communications*

[Jinbang Fu](#), [Prateek Juyal](#), [Baki B Yilmaz](#) and [Alenka Zajic](#) (Georgia Institute of Technology, USA)

This paper proposes a path loss model for THz chip-to-chip wireless communication in desktop size metal enclosures with respect to transceivers positions. This path loss model accounts for the attenuation due to the signal spreading, resonant modes inside the cavity, and the radiation pattern of the antenna. Measurements were performed in LoS and 2-D and 3-D misalignment propagation scenarios. The model prediction shows a good agreement with measured results, which proves the validity of the model.

8:50 *A Hardware-in-the-Loop Evaluation of the Impact of the V2X Channel on the Traffic-Safety Versus Efficiency Trade-offs*

[Alessandro Bazzi](#) (University of Bologna, Italy); [Thomas Blazek](#) (TU Wien, Austria); [Michele Menarini](#) (CNR-IEIIT, Italy); [Barbara M Masini](#) (CNR - IEIIT & University of Bologna, Italy); [Alberto Zanella](#) (Istituto di Elettronica e di Ingegneria dell'Inform. e delle Telecomunicazioni, Italy); [Christoph F Mecklenbräuker](#) (TU Wien, Austria); [Golsa Ghiaasi](#) (Norwegian University of Science and Technology, Norway)

Vehicles are increasingly becoming connected and short-range wireless communications promise to introduce a radical change in the drivers' behaviors. Among the main use cases, the intersection management is surely one of those that could mostly impact on both traffic safety and efficiency. In this work, we consider an intersection collision warning application and exploit an hardware-in-the-loop (HIL) platform to verify the impact on the risk of accidents as well as the average time to travel a given distance. Besides including real ITS-G5 compliant message exchanges, the platform also includes a channel emulator with real signals. Results show that the risk of collisions can be drastically reduced, with an overall trade-off between safety and traffic efficiency. At the same time, it is shown that the presence of real channel conditions cannot guarantee the same condition of zero-risk as with ideal channel propagation, remarking the importance of channel conditions and signal processing.

9:10 *Multipath Characteristics of Outdoor-To-Indoor Propagation Based on 32-GHz Measurements*

[Juyul Lee](#), [Kyung-Won Kim](#), [Myung-Don Kim](#) and [Jae-Joon Park](#) (ETRI, Korea (South))

This paper investigates measurement-based multipath characteristics of millimeter-wave (mmWave) outdoor-to-indoor (O2I) propagation. The measurement campaigns were conducted in a typical office building with a 500-MHz bandwidth channel sounder operating at frequency 32 GHz. The multipath propagation characteristics are analyzed in spectrum-based approaches in temporal (delay) and spatial (angular) domains. In our measurement, we considered the effect of the transmit incidence angles on the multipath characteristics. In the perpendicular incidences, we observed regularly recurring multipath components reflecting from the back-side and the front-side windows. However, in non-perpendicular incidences, it was hard to identify the sources of multipath reflections from the spectrum-based approach. From the measurement data analysis, we also observed that the delay spread and the angular spread do not have any meaningful dependency on the incidence angles; these are more relevant to the surrounding indoor environments near the RX.

9:30 *Penetration Loss at 60 GHz for Indoor-to-Indoor and Outdoor-to-Indoor Mobile Scenarios*

[Sung Yun Jun](#) (National Institute of Standards and Technology, USA); [Derek Caudill](#) and [Jack Chuang](#) (NIST, USA); [Peter Papazian](#) (NIST Division 673, USA); [Anuraag Bodi](#) (National Institute of Standards and Technology, USA); [Camillo Gentile](#), [Jelena Senic](#) and [Nada Golmie](#) (NIST, USA)

This paper investigates the penetration loss of an office building in indoor-to-indoor and outdoor-to-indoor mobile scenarios. The measurements were collected using our 60-GHz double-directional switched-antenna channel sounder. During measurement, the transmitter, mounted on a tripod, was placed in an office and outside of the building, while the receiver, mounted on a mobile robot, moved along an interior hallway. The penetration loss for a variety of building materials was predicted versus incident angle by electromagnetic propagation theory using the ITU-R Recommendation P.2040 model parameters and compared with the measurement results. The wooden door, plasterboard wall, and interior glass were observed to have penetration losses ranging from 26 dB to 41 dB, 12 dB to 32 dB, and 8 dB to 18 dB, respectively, while the exterior building materials exhibited even larger penetration losses, ranging from 30 dB to 67 dB.

9:50 *Hybrid Channel Modeling for Intra-Wagon Communication in Millimeter-Wave Band*

[Xiping Wang](#), [Danping He](#), [Ke Guan](#) and [Bo Ai](#) (Beijing Jiaotong University, China); [Juan Moreno](#) (Universidad Politécnica de Madrid, Spain); [Cesar Briso](#) (Universidad Politécnica de Madrid & ETSIS Telecomunicacion, Spain)

Millimeter-wave (mmWave) wideband communication is considered as a potential candidate to meet the increasing data rate demands of the onboard passengers in the metro. Channel modeling is important for the system design and evaluation in such environment. Ray-tracing (RT) modeling can accurately trace propagation paths, and has been proven successful in many works. However, it is complicated and time-consuming to work in harsh environments, where dense multi-path components exist and the reverberation effects can happen. To tackle this problem, an hybrid channel modeling approach, which combines the RT method and the propagation graph (PG) method, is proposed and introduced in this work. According to the evaluation results, the proposed method performs better than either the RT or the PG alone model in terms of accuracy and efficiency.

10:10 Coffee Break

10:40 *Experimental Characterization of the Underframe Area of a Passenger Train with an UWB Channel Sounder: Preliminary Results*

[César Calvo Ramírez](#) (Universidad Politécnica de Madrid, Spain); [Juan Moreno](#) (Metro de Madrid S.A. & Universidad Politécnica de Madrid, Spain); [Cesar Briso](#) (Universidad Politecnica de Madrid & ETSIS Telecomunicacion, Spain)

In this paper we present a testbed for Ultra-Wide Band (UWB) measurements of the radio channel plus some early results taken on a very singular scenario: the underframe area of a passenger train. This area is heavily populated with heavy mechanical elements key for the safe movement of the train (axles, wheels, brakes, suspensions, etc.) which are prone to the installation of sensors in order to know the condition of these mechanical elements. The channel sounder is based on a commercial module (Decawave DWM1001) intended for indoor location but with some tinkering could be used to obtain channel measurements.

11:00 *Irregular MultiFocal Reflector for Efficient mmWave Propagation in Indoor Enviroments*

[J. Samuel Romero-Peña](#) (Universitat Politècnica de València, Spain)

In future implementations of 5G systems , it is essential the use of the spectrum in the range of mm-Waves frequencies , in order to offer to the users the bandwidth proposed in the standard. However , using this frequency range lead to many technical difficulties in which the most important challenge is the critical attenuation of the signal in non-line-of-sight (NLOS) environments in indoor environments. Therefore is essential to plan strategies that allow us to mitigate the problem of signal attenuation in this kind of complex environments and ensure the viability of using this technology in short term. Then the objective of this research is the design of a passive reflector that allow us to redirect the energy of the transmitting antenna efficiently in order to avoid the obstacles of the environment ,and therefore avoid excessive losses .

11:20 *Measurement and Characterization of an Indoor Industrial Environment at 3.7 and 28 GHz*

[Mathis Schmieder](#) (Fraunhofer Heinrich Hertz Institute, Germany); [Taro Eichler](#) (Rohde & Schwarz, Germany); [Sven Wittig](#) (Fraunhofer Heinrich Hertz Institute, Germany); [Michael Peter](#) (Fraunhofer Institute for Telecommunications, Heinrich Hertz Institute, Germany); [Wilhelm Keusgen](#) (Fraunhofer Heinrich Hertz Institute, Germany)

Fifth generation (5G) mobile networks are expected to play an increasing role in industrial communication with private mobile communication networks deployed on company premises. For planning, standardization and product development, it is crucial to to thoroughly understand the radio channel characteristics of such environments. Frequencies around 3.7 GHz were already reserved by regulation authorities and to meet the increasing demand for higher bandwidths, spectrum in the millimeter wave range around 28 GHz is targeted. This paper presents a wideband channel measurement campaign at both 3.7 and 28 GHz with direction-of-arrival information at 28 GHz. The results are compared to the 3GPP TR 38.901 Indoor Factory model and to two other recent papers. Evaluation of path loss and RMS delay and angle spread show the unique nature of industrial indoor environments.

11:40 *Channel Modelling Based on Game Engines Light Physics for mmW in Indoor Scenarios*

[Saúl Inca](#), [Danaisy Prado](#), [David Martín-Sacristán](#) and [Jose F Monserrat](#) (iTEAM Research Institute, Universitat Politècnica de València, Spain)

The importance of Millimeter Waves (mmW) band for the Fifth Generation (5G) of mobile and wireless communications has motivated a lot of work in mmW channel modeling. In this paper, we assess the use of the light physics modeling of a game engine to calculate the propagation losses at mmW band in an indoor scenario. With that aim, we propose a model that we refer to as Light Intensity Model (LIM), in which a detailed 3D scenario is created in a game engine, radio transmitters and receivers are replaced by light sources and detectors, and the received light intensities are translated to received radio signal power through a translation function which is the key of the model. The results obtained corroborate the validity of the assessed approach to model propagation losses in indoor scenarios.

12:00 *Path Loss Models and Delay Spread Parameters for the Millimetre Wave Channel in Indoor Environments*

[Sana Salous](#) and [Saied El-Faitori](#) (Durham University, United Kingdom (Great Britain))

This paper presents results of path loss and r.m.s. delay spread in two indoor environments based on measurements in three bands from 12 GHz to 73 GHz using the multiband custom designed channel sounder developed at Durham University. Results are presented for a corridor environment and for a factory environment both in line of sight and non-line of sight set ups.

CS38: ISAP Session: Recent Advances in Asian Antennas and Propagation Research

T02 Millimetre wave 5G / Convened Session / Antennas

Room: B1

Chair: [Mauro Ettorre](#) (University of Rennes 1 & UMR CNRS 6164, France)

8:30 *Reconfigurable Terahertz Reflectarray Based on Graphene Radiating Patches*

[Tiaoming Niu](#), [Jingwei Zhang](#), [Lin Cheng](#), [Pengfei Cao](#), [Ruoyu Cui](#) and [Zhonglei Mei](#) (Lanzhou University, China)

A reflectarray antenna based on graphene radiating patches is proposed for reconfigurable radiation patterns at 1 THz. The all radiating elements of the reflectarray are geometrically identical, and the graphene patches in the same row are connected in series to a particular bias electrode. The phase response of the radiating elements can be controlled by changing the value of the bias voltage due to the property of graphene. For the TE polarization, the simulated phase curve shows that a cycle phase range of 360 degree is obtained, while the magnitude of the reflected field is above 5.6 dB. Based on the phase response, each electrode biasing is accurately programmed to build up the required progressive phase distribution for a particular beam pattern. The numerically simulated results demonstrate that the designed reflectarray can reconfigure the deflection direction of the normal TE incident plane waves with excellent performance.

8:50 *Achieving Wider Impedance Bandwidth Using Full-Wavelength Dipoles*

[Can Ding](#) (University of Technology Sydney (UTS), Australia); [Haihan Sun](#) (University of Technology, Sydney, Australia); [He Zhu](#) and [Y. Jay Guo](#) (University of Technology Sydney, Australia)

This paper investigates the use of full-wavelength dipoles (FWD) to achieve wider bandwidth than half-wavelength dipoles (HWD). Two dual-polarized antennas are built based on FWDs for base station applications as examples. The first antenna is an isolated cross-dipole employing two FWDs with simple configuration. It is able to cover the lower band for cellular communication from 698 to 960 MHz. The second antenna has four FWDs arranged in a square loop array form and tightly coupled with each other. The employed full-wavelength dipoles are bent upward to maintain a small aperture size, so that the realized element still fits in traditional base station antenna (BSA) array. The antenna can be matched across the band from 1.65 to 3.7 GHz, which can cover both the 3G/4G band from 1.7 to 2.7 GHz and the 5G (sub-6 GHz) band from 3.3 to 3.6 GHz simultaneously.

9:10 *Single and Dual Beam Waveguide Slotted Antenna Using 3D Printing Technique for 5G Application*

[Muataz Watheq Almeshebe](#) (Faculty of Electrical Engineeri, Universiti Teknologi Malaysia, Malaysia); [Noor Asniza Murad](#) (University Technology Malaysia, Malaysia); [Mohamad Kamal A. Rahim](#) (Universiti Teknologi Malaysia, Malaysia); [Farid Zubir](#) (Universiti Teknologi Malaysia & Faculty of Electrical Engineering, Malaysia); [Osman Bin Ayop](#) and [Mohd Fairus Mohd Yusoff](#) (Universiti Teknologi Malaysia, Malaysia); [Huda A. Majid](#) (Universiti Tun Hussein Onn Malaysia, Malaysia); [Mohamed Nasrun Osman](#) (Universiti Malaysia Perlis, Malaysia); [Mohamad Zoinol Abidin Bin Abd Aziz](#) (Universiti Teknikal Malaysia Melaka & Hang Tuah Jaya, Malaysia)

This paper compares between four 3D metal printed antennas at Ka-band. The four antennas are two horns and two slotted antennas. The horn and slotted antenna are well known for their high gain characteristic. The antennas are designed based on WR-28 waveguide standard. The proposed antennas are 3D metal printed using direct metal laser melting printing technique. The performances of the 3D printed antennas are investigated in terms of reflection coefficient, gain, efficiency, and radiation pattern. The printed antennas are validated using standard VNA. The measured performance of the antennas prototypes are agreed well with the simulation results with reflection coefficient of less than -10 dB for all antennas. The measured gain of ranging 7-14 dB for all the prototypes are obtained with more than 90 % of antennas efficiency. These 3D metal antennas are suitable for Ka-bands applications such as 5G cellular network.

9:30 *Microwave Metasurface-based Lens Antennas for 5G and Beyond*

[Zhi Ning Chen](#) (National University of Singapore, Singapore); [Teng Li](#) (Southeast University, China); [Wei E. I. Liu](#) (National University of Singapore, Singapore)

Lens antennas have long been used at millimeter-wave bands and above because of their excellent power focusing performance, aperture sharing, and simple feeding structures. However, the conventional high-gain dielectric lens at microwave bands usually are too bulky. With the development of metasurfaces, the lens design has been replaced by single or multiple layered planar structures such as patterned PCB boards. This paper first briefs the mechanism of metasurfaces in the design of a planar lens. Then microwave lens antennas recently developed by our team from National University of Singapore are summarized to show the progress in this field. After that, one design for 5G NR (the fifth-generation new radio) demonstrates the feasibility of metasurface-based lens in multibeam antenna design. The progress of microwave metasurface lens antennas shows us the huge potential of metamaterial-based antennas (metantennas in short) in advanced wireless systems.

9:50 Coffee Break

10:20 *Modified Binomial Power Distribution Beamformer for Switched-Beam Circular Array*

[Sheng-Wei Wu](#), [Kun-You Lin](#) and [Shih-Yuan Chen](#) (National Taiwan University, Taiwan)

In this paper, we proposed a modified binomial power distribution circular beamforming network (BFN) with a single input port at the center and 12 antenna ports uniformly located along the outer rim of the BFN for full 360° azimuth coverage switched-beam circular antenna array. By combining and interleaving three modified binomial power distribution circuits (PDCs) with three two-way power combining circuits, a compact full horizontal plane coverage beam-switching beamformer is formed. While six switches are needed in the proposed BFN, a simplified prototype BFN without the switches is fabricated and tested for preliminary verification. Measured results agree well with those simulated. The proposed 1×12 modified binomial power distribution circular beamformer possesses several advantages over conventional circular BFN designs, including compact size, single-layered structure, and a wide bandwidth up to 11.4% centered at 5.6 GHz.

10:40 *Metal Stamped Antenna-in-Package for Millimeter-wave Large-scale Phased-array Applications Using Multiphysics Analysis*

[Junho Park](#) (Pohang University of Science & Technology, Korea (South)); [Wonbin Hong](#) (Pohang University of Science and Technology (POSTECH), Korea (South))

This paper presents a metal stamped AiP concept for enhanced cooling in millimeter-wave phased array systems. To verify the proposed AiP concept, the POC model is designed and fabricated using standard PCB and metal stamping process. The fabricated POC model achieves impedance bandwidth of 0.7 GHz with a center frequency of 28.5 GHz. Good agreement is achieved between the measured and simulated radiation patterns with the measured gain of 14.01 dBi. The effect of the fabrication error on EM properties is discussed to explain the difference between the simulated and measured results of the gain. The two-dimensional array is demonstrated to verify the feasibility for a practical application of mmWave Massive MIMO systems with main beam scanning range of $\pm 30^\circ$ in both elevation and azimuth planes. Computational fluid dynamics simulation confirms that the proposed AiP reduces the maximum surface temperature of the package by more than 11 °C.

11:00 *Antennas and Propagation Technologies of V2V Communications for Platooning*

[Kazuma Tomimoto](#) and [Koichi Serizawa](#) (Softbank Corp., Japan); [Masayuki Miyashita](#) (SoftBank Corp., Japan); [Ryo Yamaguchi](#) (SOFTBANK Corp., Japan); [Takeshi Fukusako](#) (Kumamoto University, Japan)

As a use case that takes advantage of the high reliability and low delay characteristics of 5G mobile communications (5G), its utilization for platooning (V2V direct communication) is being studied. Accordingly, we need to clarify propagation characteristics and study antenna configurations. This paper shows that the propagation loss characteristics in V2V application differ from those of conventional mobile communication. An antenna configuration suitable for V2V propagation loss characteristics is studied.

11:20 *Novel Millimeter-Wave Phased Array Antenna for 5G Wireless Communications*

[Fan Yang](#), [Shenheng Xu](#), [Yezhen Li](#) and [Yongli Ren](#) (Tsinghua University, China)

A novel phased electromagnetic surface antenna (PEMSA) is presented and experimentally verified for 5G millimeter-wave wireless communications. The PEMSAs integrated with a high-efficiency feed and a wave control circuit can perform real-time beam scanning by reconfiguring the phase of each electromagnetic surface unit. A prototype of the PEMSAs is fabricated and measured to demonstrate the feasibility of this approach. The measurement results indicate that the PEMSAs achieve high gain and fast-beam-steering. Compared to the conventional phased array antenna, the proposed PEMSAs have the advantages of low power consumption, low cost, and conformal geometry. Due to these characteristics, the PEMSAs are promising for wide applications in 5G millimeter-wave communication systems.

11:40 *Highly-Integrated Dual-Band mmWave Antenna Array for 5G Mobile Phone Application*

[Wei-Yu Li](#) and [Wei Chung](#) (Industrial Technology Research Institute, Taiwan); [Kin-Lu Wong](#) (National Sun Yat-Sen University, Taiwan)

A highly-integrated 28 GHz and 39 GHz array antennas for 5G mobile phone applications is presented. The 28 GHz array consists of dual open-slots antennas as array elements and the 39 GHz array consists of folded loop antennas as array elements. This article demonstrates that 0.25 wavelength slot mode of the open-slots antenna and 1.5 wavelength loop mode of the folded loop antenna are promising candidates for generating directional radiation patterns fulfilling beam-scanning applications. And by properly designing the 0.25 wavelength slot mode to cover 28 GHz band and the 1.5 wavelength loop mode to cover the 39 GHz band, the proposed 28 GHz and 39 GHz array antennas can be compatible and coexisted at a limited side space of a mobile phone with keeping independent beam scanning operations for a higher space utilization rate. This will be useful and attractive for future multiband and multimode millimeter wave mobile phones.

CS16: Antennas in IoT Wireless Devices: Modelling and Industrial Considerations

T04 IoT and M2M / Convened Session / Antennas

Room: B2

Chairs: [Jaume Anguera](#) (Fractus Antennas & Universitat Ramon Llull, Spain), [Miloslav Capek](#) (Czech Technical University in Prague, Czech Republic)

8:30 *A Small Metamaterial Dual-Band Dipole Antenna Fed by Small Metamaterial Balanced-Feed*

[Changhyeong Lee](#), [Heejun Park](#) and [Gwang-Gyun Namgung](#) (Incheon National University, Korea (South)); [Yejune Seo](#) (Incheon National University, Korea (South)); [Sungtek Kahng](#) (University of Incheon, Korea (South))

In this paper, a new design method is introduced to make a planar metamaterial dual-band dipole antenna fed by a small metamaterial balanced feed, which is adoptable to compact multi-function devices. Firstly, the balanced feed is made as a Composite Right and Left-Handed (CRLH) dual-band balun. Its operation frequencies are 2.4 GHz and 5.2 GHz. Secondly, while it is hard to make a dipole resonate at two frequencies not in harmonic relations, we let the dipole radiate at 2.4 GHz and 5.2 GHz as a metamaterial which avoids growth in size. match at the two frequencies The antenna gain above -1dB and radiation patterns almost equal to all directions are obtained as a very compact structure and though to be proper for wireless communication.

8:50 *Design of a Quad Band CPW - Fed Compact Flexible Patch Antenna for Wearable Applications*

[Bashar Bahaa Qas Elias](#) (Universiti Malaysia Perlis (UniMAP), Malaysia); [Ping Jack Soh](#) (Universiti Malaysia Perlis (UniMAP) & Katholieke Universiteit Leuven, Malaysia); [Azremi Abdullah Al-Hadi](#) (University Malaysia Perlis, Malaysia); [Rahil Joshi](#) and [Yuepei Li](#) (Heriot Watt University, United Kingdom (Great Britain)); [Symon K. Podilchak](#) (Heriot-Watt University, United Kingdom (Great Britain))

A compact and flexible coplanar waveguide-fed (CPW) monopole antenna designed to operate in four different wireless bands is presented. The patch is designed based on a simple rectangular patch which is then integrated with multiple L-slots to enable multiband operation at 1.22, 1.56, 2.45 and 3.42 GHz offering a reflection coefficient of -10 dB. Modeling is performed using FEKO, a commercial software, based on two approaches: the method of moments (MoM) and characteristic mode analysis (CMA). Results show that satisfactory agreements in terms of predicted resonant frequencies. In addition, results of the radiation efficiency, gain, bandwidth and current distribution of the proposed model are discussed. Finally, a systematic investigation of the bending effects for the proposed wearable antenna is also presented.

9:10 *From Optimal to Industrial Antenna: The Designer Dilemma for Compact NB-IoT Terminal*

[Fabien Ferrero](#) (University Nice Sophia Antipolis, CNRS, LEAT & CREMANT, France); [Lars Jonsson](#) (KTH Royal Institute of Technology, Sweden); [Leonardo Lizzi](#) (University Côte d'Azur, CNRS, LEAT, France)

This work will present the design of a NB-IoT integrated antenna on a compact 50*30mm² terminal. The study will start from the Q factor limitation study and finish with an simulated prototype considering the different constraints that a designer need to overpass.

9:30 *Implementation and Use of Physical Bounds for Antenna Optimization*

[Mats Gustafsson](#) (Lund University, Sweden); [Miloslav Capek](#) (Czech Technical University in Prague, Czech Republic)

Here, we present an overview of physical bounds on antennas with a focus towards their use for antenna design and implementation. The developed bounds are based on optimization over the antenna currents and can be considered application oriented in the meaning that they are easily adapted to practical design constraints in shape, size, and materials. Electromagnetic simulation codes based on the method of moments are easily adapted to compute the matrices used in the optimization problems. We also illustrate how the optimization problems can be implemented and that their solutions in many cases has a computational cost of similar order as solving one antenna problem.

9:50 *Design Concerns for In-body Antennas Based on Frequency Analysis of Fundamental Radiation Limitations*

[Zvonimir Sipus](#) and [Marko Bosiljevac](#) (University of Zagreb, Croatia); [Denys Nikolayev](#) (Institut d'Électronique et de Télécommunications de Rennes (UMR CNRS 6164), France); [Anja K. Skrivervik](#) (EPFL, Switzerland)

Fundamental radiation limitations of in-body or implantable antennas should give us an estimate on the feasibility of some desired system. It was shown that near-field effects and distance to the body - free space boundary are critical aspects, while the shape does not play a major role in the achievable power. Through the frequency analysis of these limitations in this paper we provide another perspective and show how rigorous and approximate approach to near-field and reflection losses manifest in the results. This is demonstrated on a spherical body example which contains a small spherical implant which can be placed at different positions within the body in order to simulate different implant depths. The results reveal that reasonably accurate description of in-body loss mechanisms can be achieved using our previously defined fundamental radiation limitations for power density, however, depending on the frequency different loss aspects must be treated with special care.

10:10 Coffee Break

10:40 *Requirements for Accurate Design of Matching Circuits at 5 GHz*

[Jussi Rahola](#) and [Joni Lappalainen](#) (Optenni Ltd, Finland); [Jaakko Juntunen](#) (Optenni Ltd., Finland)

There are many factors which make the design of matching circuits much more challenging at the 5 GHz frequency range than at lower frequencies. The starting point of the design is the measurement of the antenna input impedance at the correct reference plane, which must be determined using sub-millimeter accuracy. The measurement result also depends on the availability of a nearby ground reference, which is not always guaranteed. At higher frequencies, the effect of the layout (i.e. transmission lines between the matching components and parasitic reactances to the ground) becomes larger and must be taken into account in the design. Realistic and accurate component models of inductors and capacitors need to be used, capturing the effects of component losses and parasitic reactances. Finally, a proper measurement-based matching circuit design flow is not possible if the matching circuit layout interacts with the electromagnetic operation of the antenna.

11:00 *3D EM Simulation Environment for Development, Testing, and Functioning of Internet of Things*

[Branko Kolundzija](#) (University of Belgrade, Serbia); [Tomislav Milosevic](#) (WIPL-D, Serbia); [Milos Pavlovic](#) (WIPL-D DOO, Serbia); [Branko Mrdakovic](#) (WIPL-D, Serbia)

The exponential growth of IoT imposes increased needs for understanding and exploitation of EM phenomena. Consequently, there are growing demands for more flexible, accurate, and efficient 3D EM simulation, easy accessible to many engineers, many of them lacking deep knowledge of applied electromagnetics. To meet such needs it is necessary to adjust existing tools to create friendly 3D simulation environment, not only for development and testing of IoT, but even for inclusion of these tools into functioning of IoT. In this paper we propose the concept/structure of such environment. For the base of such environment we propose WIPL-D software. In addition we added libraries of EM models of electrical and environmental elements, and templates that combine them into IoT-scenarios. Special tools are included to enable easy creation of new libraries' components and their composition into complex scenarios, as well as for effective processing of EM field data obtained by simulation.

11:20 *Embedded Antennas in Cellular IoT Platforms*

[Jaume Anguera](#) (Fractus Antennas & Universitat Ramon Llull, Spain); [Aurora Andújar](#) (Fractus, Spain); [José Leiva](#) (Fractus Antennas, Spain); [Rosa Mateos](#) (Fractus, Spain)

The continuous increase of wireless devices boosts RF/microwave and wireless engineers to design in a simple, quick and effective way. For this purpose, a method for designing multiband antenna systems from a very simple antenna element is proposed. This results in a procedure where the antenna is seen as an impedance box where the number of bands is fixed exclusively by the design of a multi-band matching network with lumped elements. The design of said multiband matching network is addressed by a computerized procedure giving as a result the matching network topology and the values of each lumped element. To validate the procedure, a multiband antenna system operating at 824MHz-960MMHz and 1710-2690MHz is built. The matching network has been obtained using a fully automated method without human intervention and without any adjustment. This procedure opens the window to facilitate the design of multiband antenna system to IoT designers.

11:40 *Radiative Loss in Small Inverted-F Antenna Transmission Line Model*

[Rana Berro](#) (Grenoble Alpes University & CEA LETI, France); [Serge Bories](#) (CEA, France); [Christophe Delaveaud](#) (CEA-LETI, France)

An improved transmission line model of a lossy inverted-F antenna is presented, this model takes into account all losses in the antenna structure. So, complementary to ohmic losses, the radiative losses are introduced to improve the antenna input impedance model. This "extended" transmission line model proves to be accurate enough to allow the study of the antenna characteristics as function of its geometry and conductive material properties.

Tuesday, 17 March 8:30 - 10:10

T11-M02: Radar Scattering Measurement and Calibration Techniques

T11 Fundamental research and emerging technologies / Regular Session / Measurements

Room: B4

Chairs: [Veronica Santalla del Rio](#) (University of Vigo, Spain), [Pax S. P. Wei](#) (The Boeing Company, (retired), USA)

8:30 *Radar Cross Section Measurement Within Reverberation Chamber: Stirrer Position Issues*

[Ariston Reis](#) (Université Paris-Est Marne-la-Vallée, France); [Francois Sarrazin](#) (University of Paris-Est-Marne-la-Vallée & ESYCOM, France); [Pouliguen Philippe](#) (DGA, France); [Jérôme Sol](#) (INSA Rennes, France); [Philippe Besnier](#) (IETR, France); [Elodie Richalot](#) (Université Paris-Est (Marne-la-Vallée), France)

This paper presents the evaluation of the Radar Cross Section (RCS) of a metallic object by measurements accomplished within the diffuse-field environment produced by a Reverberation Chamber (RC). The method is based on the extraction of the ballistic wave between the antenna and the target that is mixed with the backscattering response of the RC. A good agreement is obtained when compared with classical RCS measurement inside an anechoic chamber. This communication also highlights the potential stirrer positioning issues and their impact on the retrieved RCS accuracy.

8:50 *Measurements on Extended Vertical Objects for Radar Field Probes*

[Pax S. P. Wei](#) (The Boeing Company, (retired), USA)

As a novel field probe concept, RCS measurements are reported on long rigid objects rotated within a small angular range about the broadside condition (called a glint). The rotation was maintained either in a horizontal (H) plane or in a vertical (V) plane containing the center of the quiet-zone (QZ). Processing the RCS data by DFT yields a spectrum which is recognized as the field distribution along that object. Such spectrum compares extremely well to traditional field probes taken earlier by translating a sphere across the QZ in the H- or V-direction. Preliminary results at several S-band frequencies are presented and discussed.

9:10 *Effects of the Antenna Measurement Uncertainties on the Estimation of the Differential Reflectivity*

[Brais Sánchez-Rama](#), [Veronica Santalla del Rio](#), [Rubén Nocelo López](#) and [María Vera-Isasa](#) (University of Vigo, Spain)

The parameters of interest in polarimetric weather radars, defined in terms of the scattering coefficients of the target, are affected by non-ideal radiation systems. The effect of the cross-polar radiation has been studied and the requirements that radiation patterns must verify in order to maintain the error of the estimates below a predefined value have been established. Unfortunately, these requirements are strict and difficult to achieve with phased array antennas. Recently, it was shown that the effect caused by antenna systems can be separated from the scattering parameters and, consequently, corrected. Hence, this technique could be used to make the transition to phased array polarimetric radar systems feasible. However, this correction requires knowing the antenna radiation patterns, so they must be measured. The aim of this work is to study the effect of the uncertainties introduced by the antenna measurement procedure in the correction of the differential reflectivity factor.

9:30 *Analysis of the Cross-polar Radiation Effects on Differential Reflectivity Calibration*

[Veronica Santalla del Rio](#), [Rubén Nocelo López](#) and [Brais Sánchez-Rama](#) (University of Vigo, Spain)

This paper discusses the effects of cross-polar radiation on the calibration methods usually employed for the calibration of the differential reflectivity. It is shown that cross-polar radiation has significant effects when simultaneous transmission and reception of horizontal and vertical polarizations are used to obtain polarimetric measurements. Additionally, it is shown that propagation through a transpolarizing medium considerably affects the results.

9:50 *On Models and Approaches for Human Vital Signs Extraction from Short Range Radar Signals*

[Mikolaj Wojciech Czerkawski](#), [Christos V. Ilioudis](#), [Carmine Clemente](#), [Craig Michie](#), [Ivan Andonovic](#) and [Christos Tachtatzis](#) (University of Strathclyde, United Kingdom (Great Britain))

The paper centres on an assessment of the modelling approaches for the processing of signals in CW and FMCW radar-based systems for the detection of vital signs. It is shown that the use of the widely adopted phase extraction method, which relies on the approximation of the target as a single point scatterer, has limitations in respect of the simultaneous estimation of both respiratory and heart rates. A method based on a velocity spectrum is proposed as an alternative with the ability to treat a wider range of application scenarios.

Tuesday, 17 March 8:30 - 12:20

CS01: Active Antennas for Onboard Space Applications

T09 Space (incl. cubesat) / Convened Session / Antennas

Room: B5

Chairs: [Baptiste Palacin](#) (CNES, France), [Giovanni Toso](#) (European Space Agency, ESA ESTEC, The Netherlands)

8:30 *Active Antenna Developments, Challenges and the Future*

[Sonya Amos](#), [Glyn Thomas](#), [Carolina Tienda](#) and [David Dupuy](#) (Airbus Defence and Space, United Kingdom (Great Britain))

Active Antennas are fast becoming the go-to antenna design as more complex solutions answer more flexible, adaptable, increased functionality cost effective solutions. Airbus Defence and Space are developing Product Lines that answer key market demands, benefit from state of the art equipment and techniques but harmonized in a definitive Product solution in which design, industrialization, validation and cost synergies are considered. This paper will highlight some of the key developments, technologies, challenges and asks some questions on where the future will take this active market.

8:50 *Front End Radiating Module for Advanced Active Antenna*

[Benoit Lejay](#) (Thales Alenia Space, France)

This paper presents the current development of a Front end radiating module in Ka band for advanced active antennas dedicated to Medium Earth Orbit mission at Thales Alenia Space France.

9:10 *Active Antennas Radiated Spurious*

[Jonathan Hill](#) (MDA Corporation, Canada); [Michel Bellemare](#) (MDA, Canada); [Yves Demers](#) (MDA Corporation, Canada); [Nicholas Boudreau](#), [Jean-Daniel Dea](#) and [Eric Amyotte](#) (MDA, Canada)

This paper describes the analysis of radiated spurious performance of active antennas. It outlines an analysis methodology and presents radiated spurious performance of selected beam layouts for Direct Radiating Array (DRA) and Array Fed Reflector (AFR) active antennas.

9:30 **Additive Manufacturing: Enabling Technology for Active Antennas in LEO and GEO Satellites**

[Esteban Menargues](#) and [Santiago Capdevila](#) (SWISSto12, Switzerland); [Tomislav Debogovic](#) (SWISSto12 SA, Switzerland); [María García-Vigueras](#) (IETR-INSA Rennes, France); [Emile de Rijk](#) (SWISSto12 SA, Switzerland)

Active antennas are one of the key elements in the upcoming flexible payloads for LEO constellations and GEO satellites. This paper describes the advantages in terms of mass, assembly, integration, test and RF performance of using the additive manufacturing process developed by SWISSto12 in the development of direct radiating arrays. Such advantages are highlighted through the design of two examples. The paper reviews SWISSto12 manufacturing process, includes measured RF performance of relevant active antenna hardware and presents innovative components to enable DRAs for LEO constellations.

9:50 **Potential Applications of Active Antenna Technologies for Emerging NASA Space Communications Scenarios**

[Felix Miranda](#) (NASA John H. Glenn Research Center, USA)

NASA is implementing far-reaching changes within the framework of both space and aeronautics communications architectures. Near earth relays are looking to transition from few large geostationary satellites to constellations of thousands of small LEO satellites while lunar space communications will require the need to relay data from many assets on the lunar surface back to earth. In aeronautics, satellite communications for BLOS links are being investigated in tandem with the proliferation of UAS systems within the UAM environment. Thus, future communications architectures will need to connect and quickly transition between many nodes for large data volume transport. NASA GRC is exploring 5G-based beamformer technologies to leverage commercial timescale and volume production cycles, heretofore not existent within frequencies used by NASA. An overview of future applications of phased arrays being envisioned by NASA are discussed, along with technology feasibility demonstrations being conducted by GRC implementing low cost, 5G based beamformer technologies.

10:10 Coffee Break

10:40 **Active Antennas for Earth Observation Missions in Thales Alenia Space Italia**

[Pasquale Capece](#) (Thales Alenia Space Italia, Italy); [Giovanni Gasparro](#) (THALES ALENIA SPACE ITALIA, Italy); [Roberto Giordani](#) and [Roberto Mizzoni](#) (Thales Alenia Space Italia, Italy); [Alberto Meschini](#) (ThalesAleniaSpace-Italia, Italy); [Giovanni Mannocchi](#) (THALES ALENIA SPACE ITALIA, Italy); [Andrea Suriani](#) (THALES ALENIA SPACE, Italy); [Salvatore Contu](#) (Thales Alenia Space, Italy)

The paper provides an overview of the most significant active phased array products for Earth Observation developed by Thales Alenia Space-Italia (TAS-I) over last two decades. In the first section the X band active antennas are presented while in the second part the electronics for phased array antennas working in L, C and X bands, developed also in the frame of international collaboration, are described. Finally on going studied for next generation SAR systems in C, X and Ka band are briefly reported.

11:00 **AIRBUS DS SPAIN Active Antennas for Earth Observation, Telecom, and Deep Space: Past and Future Challenges**

[Antonio Montesano](#) (AIRBUS DS, Spain)

This paper presents some key heritage projects in AIRBUS DS in Madrid- Barajas, and current challenges facing the future in RADAR, Telecom, Earth Observation and Science.

11:20 **Rigid-Flexible Antenna Array (RFAA) for Lightweight Deployable Apertures**

[William F. Moulder](#), [Rabindra N. Das](#), [Andrew C. Maccabe](#), [Landen A. Bowen](#), [Erik M Thompson](#) and [Patrick J Bell](#) (MIT Lincoln Laboratory, USA)

this paper presents the Rigid-Flexible Antenna Array (RFAA), a concept for realizing ultra-light flexible antenna arrays that can readily integrate active components. This enables realization of phased arrays that can be compactly stowed in small satellites, where mass and volume for antenna payloads are extremely limited. The RFAA is constructed with a very thin, physically flexible material and minimal rigid material, allowing it to be realized with an area density as low as 1.1 kg/m². It employs a compact novel capacitive antenna feed, which simplifies its construction. The concept is validated through simulation of two RFAA element designs, and measurements of two prototype arrays.

11:40 **NISAR Flight Feed Passive Antenna Measurements**

[Paolo Focardi](#) (Jet Propulsion Laboratory & California Institute of Technology, USA); [Jefferson Harrell](#) (Jet Propulsion Laboratory, USA)

NISAR (NASA ISRO SAR, National Aeronautics and Space Administration, Indian Space Research Organization, Synthetic Aperture Radar) is an Earth science project currently in its final development phase at NASA Jet Propulsion Laboratory (JPL) and at ISRO. Due for launch in 2022 it will assess how our planet changes over time by measuring differences in the Earth's solid surface due to factors like climate change, movement and melting of glaciers, earthquakes, land-slides, deforestation, agriculture and others. The enabling instrument for this mission is a dual band radar (L-band and S-band) that feeds a 12m deployable mesh reflector. This paper describes the measurement campaign of the L-band flight feed in its passive configuration. Further measurements will be done using the antenna with the active radar components but they are not part of this paper.

12:00 **Multibeam Array Antennas Based on Evanescent-Mode Ridge-Waveguide Radiating Filters**

[Daniel Sanchez](#) (Universidad de Valencia, Spain); [Mariano Baquero-Escudero](#), [Pablo Soto](#) and [Vicente Boria](#) (Universidad Politécnica de Valencia, Spain); [Giovanni Toso](#) (European Space Agency, ESA ESTEC, The Netherlands); [Piero Angeletti](#) (European Space Agency, The Netherlands); [Marco Guglielmi](#) (University of Valencia, Spain)

Possible applications of completely metallic radiating elements based on below-cutoff apertures are presented. The four below-cutoff sub-apertures are associated to two different linear polarizations and two different frequencies. The four elements are physically interleaved but behave as completely overlapped elements permitting to reuse four times the entire physical aperture of the radiating element. Possible applications in passive and active array antennas for multibeam applications are discussed.

CS60: Sensors and Systems for Microwave Biomedical Imaging and Sensing

T05 Biomedical and health / Convened Session / Antennas

Room: B6

Chairs: [Sandra Costanzo](#) (University of Calabria, Italy), [Natalia Nikolova](#) (McMaster University, Canada)

8:30 **Microwave Radar Breast Screening: System Interaction with the Post-Biopsy Clip**

[Lena Kranold](#) and [Milica Popović](#) (McGill University, Canada)

This work reports on recent progress in our feasibility assessment of the microwave radar prototype aimed at tumor detection through frequent breast screening. The previously reported time-domain system has 16 antenna-sensors in a multistatic arrangement. The phantoms used in our study are stable and carbon-based. With updated hardware, we now test the prototype to address an issue vital for our long-term clinical trials. Using phantoms in a controlled laboratory environment, we assess the influence of the miniature clip, typically left in the tissue as a marker after a biopsy, on the overall ability of our system to screen the patient frequently post-biopsy. This line of investigation is essential for the population of women with dense breast tissue, where the mammograms struggle to give reliable results and hence the biopsy is used as a follow-up procedure.

8:50 **Breast Cancer Imaging Using a 24 GHz Ultra-Wideband MIMO FMCW Radar: System Considerations and First Imaging Results**

[Maria Virginia Prati](#) (Politecnico di Milano, Italy); [Jochen Moll](#) (Goethe University Frankfurt am Main, Germany); [Christian Kexel](#) and [Duy Hai Nguyen](#) (Goethe University Frankfurt, Germany); [Avik Santra](#) (Infineon Technologies AG, Germany); [Andrea Aliverti](#) (Politecnico di Milano, Italy); [Viktor Krozer](#) (Goethe University of Frankfurt am Main, Germany); [Vadim Issakov](#) (Infineon Technologies AG, Germany)

Microwave imaging for breast cancer detection has been widely studied as an alternative technique to the conventional X-ray mammography. The systems developed until now operate at frequencies of a few gigahertz. This limits the achievable image quality. Higher operational frequencies are advantageous for achieving a better resolution, at the expense of a lower penetration depth. The downscaling of components together with an integrated radar transceiver would lead to the development of a compact and cost-effective radar imaging system. This paper investigates the possibility of using an integrated ultra-wideband frequency-modulated continuous-wave (FMCW) radar system operating at a center frequency of 20 GHz and bandwidth of 8 GHz for breast cancer imaging. System considerations are developed and first imaging results based on numerical data are presented.

9:10 **Phaseless Approach to Microwave Biomedical Imaging: System Requirements Towards Clinical Applications**

[Sandra Costanzo](#) and [Giuseppe Lopez](#) (University of Calabria, Italy)

A preliminary study on the implementation of a microwave imaging system for biomedical applications is outlined in this work. A low-cost, portable and easy implementable measurement setup for dielectric characterization of biomedical scenario, specifically in the field of breast imaging, is discussed. It is combined with the use of a phaseless reconstruction strategy for the solution of the related non-linear inverse scattering problem.

9:30 **Head and Neck Numerical Phantom Development for Cervical Lymph Node Microwave Imaging**

[Ana Catarina Pelicano](#) (Faculdade de Ciências, Universidade de Lisboa, Portugal); [Raquel C. Conceição](#) (Instituto de Biofísica e Engenharia Biomédica, Faculdade de Ciências, Universidade de Lisboa, Portugal)

In this paper, we present a methodology to build a numerical phantom for the head and neck regions, which can be used to develop a cervical lymph node microwave imaging device. We have shown a pipeline of data processing steps which can be applied to Magnetic Resonance Images (MRI) of the head and neck. Such models will be the starting point to start developing a microwave imaging device suitable to detect metastasised cervical lymph nodes and as a result contribute to the correct staging of head and neck cancer.

9:50 Integrating Nodal Adjoint Jacobian Method in the Discrete Dipole Approximation-based Image Reconstruction Algorithm

[Samar Hosseinzadegan](#), [Andreas Fhager](#) and [Mikael Persson](#) (Chalmers University of Technology, Sweden); [Paul M Meaney](#) (Dartmouth College, USA)

This paper focuses on the computational complexity of microwave image reconstruction algorithms. In microwave tomography, computing the forward solutions during the iterative reconstruction process directly impacts the accuracy and computational efficiency. Towards this end, we have applied the discrete dipole approximation for the forward solutions with significant time savings. However, while we have discovered that the imaging problem configuration can dramatically impact the computation time required for the forward solver, it can be equally beneficial in constructing the Jacobian matrix required in the iterative image reconstruction algorithms. Key to this implementation, we propose to use the same simulation grid for both the forward and inverse domain discretizations. In this way, the nodal adjoint method for computing the Jacobian matrix reduces to an Order N computation for each row of the matrix which is a dramatic improvement over previous implementations.

10:10 Coffee Break

10:40 A Tomographic Multistatic System for Biomedical Microwave Sensing

[Igor Bisio](#), [Claudio Estatico](#), [Alessandro Fedeli](#), [Fabio Lavagetto](#), [Matteo Pastorino](#), [Andrea Randazzo](#) and [Andrea Sciarrone](#) (University of Genoa, Italy)

The use of microwave techniques for biomedical sensing and imaging is in continuous evolution, and the realization of accurate and efficient system prototypes is fundamental in bridging the gap between the algorithm development and its practical application. In this paper, a prototype of multistatic imaging system, mainly designed for the quantitative reconstruction of the dielectric properties of the human head for brain stroke detection, is presented and some experimental results, obtained by processing the acquired data with a nonlinear inverse scattering technique, are shown.

11:00 Pilot Patient Study with the Wavelia Microwave Breast Imaging System for Breast Cancer Detection: Clinical Feasibility and Identified Technical Challenges

[Angie Fasoula](#) and [Luc Duchesne](#) (Microwave Vision (MVG)); [Brian M. Moloney](#) (Lambe Institute for Translational Research); [Julio Daniel Gil Cano](#) and [Cecile Chenot](#) (Microwave Vision (MVG), France); [Barbara L. Oliveira](#) (HRB Clinical Research Facility Galway, Ireland); [Jean-Gaël Bernard](#) (Microwave Vision (MVG)); [Sami M. Abd Elwahab](#) and [Michael Kerin](#) (Lambe Institute for Translational Research, Ireland)

In this paper, preliminary results of the first-in-human clinical investigation with the Wavelia Microwave Breast Imaging (MBI) system prototype are presented. The clinical feasibility of the system, in terms of potential to detect both malignant and benign palpable breast lesions, is illustrated with the MBI results of two patient scans. Some identified technical challenges, related to the patient positioning and breast deformation, are also discussed.

11:20 Coverage Estimation for Microwave Imaging Using Full Multistatic Radar Imaging Algorithms with Restricted Opening

[Hamza Benchakroun](#) (National University of Ireland Galway, Ireland); [Angie Fasoula](#) (Microwave Vision Group, France); [Luc Duchesne](#) (MVG Industries, France); [Martin O'Halloran](#) (National University of Ireland, Galway, Ireland); [Declan O'Loughlin](#) (National University of Ireland Galway, Ireland)

Many clinical investigations of microwave breast imaging systems are ongoing. However, few studies have investigated the optimal antenna design to maximise imaging performance. In this paper, the impact of the radial behaviour of the antenna on coverage area is investigated. A simplified antenna model in a homogeneous medium is used to estimate the power density and hence the coverage within the antenna array. Results from different antenna array configurations are compared, showing coverage can vary depending on the number of antennas used for multistatic imaging. The analysis is repeated for a lossy medium and highlights that losses increase the coverage estimation, although higher power and better signal-to-noise ratio would be required. In summary, this paper shows that the antenna radial behaviour can influence the coverage. In summary, this paper identifies preliminary limits on antenna design parameters to maximise coverage.

11:40 Investigation of Influences on the Detectability of Magnetic Nanoparticles by Means of Microwaves for Biomedical Applications

[Sebastian Ley](#) (Technische Universität Ilmenau, Germany); [Bernd Faenger](#) (University Hospital Jena & Institute of Diagnostic and Interventional Radiology, Germany); [Jürgen Sachs](#) (Ilmenau University of Technology, Germany); [Ingrid Hilger](#) (University Hospital Jena, Germany); [Marko Helbig](#) (Technische Universität Ilmenau, Germany)

This paper deals with the detection of magnetic modulated nanoparticles by means of ultra-wideband sensing. Magnetic nanoparticles are modulated by an external magnetic field. The resulting scattering changes of the magnetic nanoparticles are analyzed depending on the mass, the magnetic field strength and the surrounding medium in which the particles are embedded. The experiments are carried out on phantom measurements and the results show a linear behavior of the measured radar signal depending on the mass. Furthermore, the experiments show that the optimal choice of the magnetic field strength can increase the detectability of the magnetic nanoparticles. This applies both to particles that are diluted in distilled water and to particles that are embedded in a solid surrounding medium.

12:00 Qualitative Techniques for Generating Spatial Prior Information for Biomedical Microwave Imaging

[Martina Teresa Bevacqua](#) (Università Mediterranea di Reggio Calabria, Italy); [Nasim Abdollahi](#) and [Ian Jeffrey](#) (University of Manitoba, Canada); [Tommaso Isernia](#) (University of Reggio Calabria, Italy); [Joe LoVetri](#) (University of Manitoba, Canada)

The use of quantitative microwave imaging for biomedical applications represents one of its most relevant application areas due to the specificity of the complex-valued permittivity with regard to differentiating normal and diseased anatomical tissues. The success of such quantitative methods relies on improving their reconstruction accuracy and resolution. In the following we propose the use of two qualitative imaging methods, the linear sampling and the orthogonality sampling methods, to generate spatial priors that are used as a numerical inhomogeneous background medium within the (quantitative) contrast source inversion scheme. Both qualitative imaging methods are able to create morphological maps, in almost real-time, from the same microwave scattered-field data. The resulting quantitative reconstructions show improvements in both accuracy and resolution, compared to blind reconstruction, and thus the combined technique represents a significant contribution towards the design of simpler and low-cost imaging systems.

SW02: COST Session CA17115 (MyWAVE): Developments in Electromagnetic-Based Medical Technologies



T05 Biomedical and Health / Convened Session / Electromagnetics

Room: B7

Chairs: [Gennaro G. Bellizzi](#) (Erasmus University Medical Center, Italy), [Laura Farina](#) (National University of Ireland Galway & CURAM, Ireland)

8:30 Loco-regional Hyperthermia Delivery: Patient-specific Set-Up Procedures for Treatment Optimisation

[Johannes Crezee](#), [Remko Zweije](#) and [Petra Kok](#) (Academic Medical Center / University of Amsterdam, The Netherlands)

Locoregional hyperthermia (heating of deep-seated tumours to 40-43°C) increases effectivity of chemotherapy and radiotherapy. Phased arrays of antennas are positioned around the patient, using phase steering to focus energy deposition onto the tumour. This paper describes patient-specific set-up procedures for treatment optimisation for locoregional hyperthermia devices using an E-Field probe at or near the tumour location. A phase-sweep is performed for each individual antenna w.r.t. a reference antenna to determine the optimal phase-setting, yielding a maximum E-Field signal. A phase-shift is applied when the probe cannot be positioned at the tumour location. Correctness of phase settings thus found is verified using temperature rise measurements after a 60 sec power pulse for three different phase settings. Effectivity of the method is demonstrated by numerical simulations and clinically for patients with a cervical and bladder tumour. Results show this is a robust patient-specific method for clinical phase optimisation during locoregional hyperthermia.

8:50 Hyperthermia Treatment Planning: Clinical Application and Ongoing Research

[Petra Kok](#) and [Johannes Crezee](#) (Academic Medical Center / University of Amsterdam, The Netherlands)

Hyperthermia, i.e. heating tumour tissue to 40-43°C, is applied clinically to enhance the effectiveness of chemotherapy and radiotherapy. Treatment planning can be a very valuable tool to improve clinical treatment quality. Initially, hyperthermia treatment planning started as a research tool, but developments over the past decade have resulted in more advanced simulation tools and integration of treatment planning in clinical work flow is emerging. This paper discusses the most important clinical applications of hyperthermia treatment planning and ongoing research.

9:10 Influence of the BSD-2000 3D/MR Hyperthermia Applicator on MR Image Quality: A Quantitative Assessment

[Kemal Sumser](#) (Erasmus MC Cancer Institute, The Netherlands); [Margarethus M. Paulides](#) (Eindhoven University of Technology, The Netherlands); [Gennaro G. Bellizzi](#) (Erasmus University Medical Center, Italy); [Gerard C. van Rhoon](#) (Erasmus MC Cancer Institute, The Netherlands); [Juan Hernandez-Tamames](#) and [Sergio Curto](#) (Erasmus University Medical Center, The Netherlands)

MR compatible hyperthermia devices exploit MR thermometry capabilities for non-invasive treatment monitoring. These devices, which have been tested to be MR safe, can potentially influence the MR image quality. One such device is the Pyrexar BSD-2000 3D/MR applicator. In this study, we quantitatively evaluated the impact of the applicator for different setups on MR imaging by B1+ and signal-to-noise (SNR) measurements. Our results show 30% decrease in the B1+ transmit efficiency and 20% decrease in the SNR. We have found the biggest impact was caused by the device's water bolus. This effect can be overcome by increasing the B1 transmit gain or using a thinner water bolus in the device design.

9:30 The Required Patient Modeling Realism in Radiofrequency Heating Simulation Studies

[Gennaro G. Bellizzi](#) (Erasmus University Medical Center, Italy); [Kemal Sumser](#) (Erasmus MC Cancer Institute, The Netherlands); [Margarethus M. Paulides](#) (Eindhoven University of Technology, The Netherlands)

Clinical effectiveness of hyperthermia would benefit from a more controlled and target conformal heating of the tumor. Over the years, dosimetry using electromagnetic simulators has become a potent tool to study improvements in the application of hyperthermia. Literature suggests that simulation accuracy is dependent on the realism of the patient models. In this work, we compare the results for a detailed head and neck patient model to those for models with an approximated shape, a reduced tissue number and/or a spherical target volume. Our comparison shows a relative difference above 25% in the administered power absorption pattern. This large difference calls upon 1) follow-up research to establish the true impact using a larger set of patient models and 2) the development of a reference set of patient models to facilitate bench marking of novel devices, methods and treatment approaches.

9:50 Monitoring Microwave Thermal Ablation Using Electrical Impedance Tomography: An Experimental Feasibility Study

[Anna Bottiglieri](#) (Translational Medical Device Lab & National University of Ireland, Galway, Ireland); [Eoghan Dunne](#) (National University of Ireland & Translational Medical Device Lab, Ireland); [Barry McDermott](#) (Translational Medical Device Lab, National University of Ireland Galway, Ireland); [Marta Cavagnaro](#) (Sapienza University of Rome, Italy); [Emily Porter](#) (University of Texas at Austin, USA); [Laura Farina](#) (National University of Ireland Galway & CURAM, Ireland)

Low-cost and reliable methods for monitoring the size of the ablation zone during microwave thermal ablation (MTA) are crucial in the oncological clinical practice. The aim of this work is to test the performance of electrical impedance tomography (EIT) for the real-time monitoring of the ablation area where relevant temperature increases occur. In this work, two experimental studies were performed with a 16-electrode EIT system using a liver-mimicking agar phantom. First, an EIT system was tested to monitor the cooling of the phantom from an initial temperature of about 72°C. Secondly, the heating and the consequent cooling of the phantom were monitored. The heating was performed using a MTA applicator operating at 30W for 10 minutes at 2.45GHz. The results reporting the voltage and temperature data acquired, as well as the reconstructed time series images, confirm the feasibility of EIT to monitor the changes of the electrical conductivity with temperature.

10:10 Coffee Break

10:40 Effects of Choke in Minimally-Invasive Small-Profile Microwave Ablation Applicators

[Giuseppe Ruvio](#) (National University of Ireland, Galway, Ireland); [Marta Cavagnaro](#) (Sapienza University of Rome, Italy)

Microwave ablation is a fast-growing hyperthermic treatment option for unresectable malignancies. From pioneering percutaneous microwave procedures to treat liver lesions, nowadays several new clinical indications are emerging. The spread of microwave ablation in clinical practice is growing alongside with the requirement for minimally-invasive procedures and, consequently, minimally invasive microwave applicators. Tri-axial structures and chokes have been proposed in the literature as techniques to improve the ablation performance of needle-shaped antennas. In this paper, those techniques are compared in terms of electric field distribution, return currents on the feed cable and specific absorption rate when integrated into an 18-gauge applicator.

11:00 Characterization of Esophageal Temperature Profiles During Cardiac Radiofrequency Ablation

[Jan Sebek](#) (Kansas State University & Czech Technical University, USA); [Faraz Chamani](#) (Kansas State University, USA); [Jie Cheng](#) (Texas Heart Institute, USA); [Dhanunjaya Lakkireddy](#) (Kansas City Heart Rhythm Institute and Research Foundation, USA); [Punit Prakash](#) (Kansas State University, USA)

Radiofrequency ablation is a widely used approach for treatment of symptomatic atrial fibrillation by achieving pulmonary vein isolation. A rare, but severe, complication associated with ablation is perforation of the esophageal wall, due to unintended passive heating, leading to esophageal fistulas. Several strategies for managing esophageal luminal temperatures during ablation have been proposed, with the objective of limiting thermal damage and preventing perforation. However, there remains a limited understanding of the relationship between esophageal luminal temperatures and temperatures on the serosal surface. Here, we report on measured temperature profiles in a custom ex vivo layered tissue preparation during radiofrequency ablation. Over n=82 ablations, temperatures on the mucosal surface of the esophagus ranged between 37-38.1 °C as serosal surface thermal doses ranged between 0-80 CEM43. These findings may contribute to the identification of safety thresholds for esophageal temperatures, which may preclude the incidence of esophageal perforation during cardiac ablation.

11:20 Potentialities of Inverse Scattering Techniques for Breast Cancer Imaging at Millimeter-Waves Frequencies

[Martina Teresa Bevacqua](#) (Università Mediterranea di Reggio Calabria, Italy); [Simona Di Meo](#) (University of Pavia, Italy); [Lorenzo Crocco](#) (CNR - National Research Council of Italy, Italy); [Tommaso Isernia](#) (University of Reggio Calabria, Italy); [Giulia Matrone](#) and [Marco Pasian](#) (University of Pavia, Italy)

Breast cancer is one of the leading causes of cancer death among women in industrialized countries. Several microwave imaging systems have been proposed for the diagnosis of breast cancer, based on both the tomographic and radar approach, being tested in some cases even on real patients. However, the low working frequency of all these systems, which allows to reach non superficial targets, has been in some cases the main cause of a non-optimal resolution. Based both on the results of recent dielectric characterization campaigns on ex-vivo tissues of the human breast up to 50 GHz and on the promising achievements about the feasibility studies of mm-wave imaging systems, in this article, the tomographic approach to manipulate the simulated results of a linear radar scenario at the frequency of 30 GHz is proposed. In particular, two image reconstruction techniques, the Linear Sampling Method and the Born Approximation, are proposed and compared.

T09-P08: Satellite Propagation

T09 Space (incl. cubesat) / Regular Session / Propagation

Room: B8

Chairs: [Marco Pasian](#) (University of Pavia, Italy), [Martin Rytir](#) (Norwegian Defence Research Establishment (FFI), Norway)

8:30 First and Second Order Statistics of Two Years Alphasat Ka/Q Band Satellite Propagation Measurements in Budapest

[Bernard Adjei-Frimpong](#) and [László Csurgai-Horváth](#) (Budapest University of Technology and Economics, Hungary)

In the experimental campaign using the Alphasat Aldo Paraboni satellite payload at Budapest University of Technology and Economics, we contribute to characterizing the Ka/Q propagation channels. The satellite transmits unmodulated carrier signals on both frequencies in support of propagation experiments across Europe. Using data collected from Alphasat measurement, we investigate the atmospheric effects, mainly rain attenuation. In this paper we provide the analysis of our measured and pre-processed data relating to the first and second order statistics by presenting their long term cumulative distributions. Relevant recommendations from the ITU-R rain attenuation prediction models are compared with the measurements to classify the measured time series, which will be used to assess performance of the Ka/Q band satellite propagation channel in Budapest. We also demonstrate different data processing techniques showing how they influence the goodness of fit with the ITU-R model.

8:50 A Physical-Statistical Hybrid Model for Land Mobile Satellite Propagation Channel at Ku/Ka Band

[Sebastien Rougerie](#) (CNES, France); [Jonathan Israel](#) (ONERA - The French Aerospace Lab, France)

This paper presents an optimized Land Mobile Satellite (LMS) propagation channel model for Ku/Ka band. Here, a physical-statistical hybrid approach is proposed in order to simplify as much as possible the synthetic environment and the electromagnetic model, while keeping a good representation of the satellite propagation channel. This approach is complementary of full statistical approach [1] as a specific environment can now be tackled instead of a mixture of different propagation conditions. An original validation of the model is presented here, with an innovative method based on 360° panoramic images analysis in order to rebuild a simple synthetic environment. [1] Recommendation ITU-R P.681-11, "Propagation data required for design systems in the land mobile-satellite service", 08/2019.

9:10 Fade Slope Analysis with Q-band Alphasat Satellite Measurements in Madrid

[Domingo Pimienta-del-Valle](#) (Universidad Politécnica de Madrid, Spain); [Pedro Garcia-del-Pino](#) (Universidad Politecnica de Madrid, Spain); [Jose M Riera](#) (Universidad Politécnica de Madrid, Spain)

One of the second order statistics used to assess the adverse propagation effects of meteorological events in the signal propagation trough the atmosphere is the distribution of fade slope. In order to characterize properly this statistic, long data periods are needed. The Universidad Politécnica de Madrid (UPM) is receiving the 40-GHz signal coming from the Q-band Alphasat satellite beacon, with five years of measurements processed up to now. With the available excess attenuation data, fade slope distributions can be derived. Annual and period excess attenuation distributions and fade slope results are presented, together with the comparison of fade slope results with the Rec. ITU-R P.1623-1 model. The predictions of the ITU-R model follow adequately the experimental results, with most of the differences being obtained for the higher analyzed time intervals (from 60 to 180 s) and attenuations (higher than 15 dB and of up to 25 dB).

9:30 Heights of the 0°C Isotherm and the Bright Band in Madrid: Comparison and Variability

[Ana Benarroch](#) (Universidad Politécnica de Madrid, Spain); [Gustavo Siles](#) (Universidad Privada Boliviana, Bolivia); [Jose M Riera](#) and [Santiago Pérez-Peña](#) (Universidad Politécnica de Madrid, Spain)

Rain attenuation prediction models may require rain height data that can be obtained from the 0°C isotherm height as proposed in ITU-R Recommendations and also from radiosonde measurements. Statistical results on the variability of the 0°C isotherm in all conditions and in rainy conditions are presented in this paper for ten years of radiosonde data. Concurrent with these data, nine years of rainfall measurements performed with a vertical Doppler radar (MRR-2) have allowed comparing the height of the 0°C isotherm with the height of the bottom of the bright band considering simultaneous events. The variability of both heights and of their difference has been investigated as well.

9:50 An Empirical Model for Time Diversity Statistics at Ka- And Q-band

[Armando Rocha](#) (University of Aveiro & Instituto de Telecomunicações, Portugal); [Susana Mota](#) (University of Aveiro & Institute of Telecommunications, Portugal)

Time diversity is a diversity scheme to mitigate rain attenuation in Earth-Satellite links operating above 10 GHz. Here we derive an empirical model to obtain time diversity statistics using two years of statistical data obtained at Ka and Q-bands.

10:10 Coffee Break

10:40 *Statistical Analysis of Satellite Communication Experimental Time Diversity in Slovenia*

[Arsim Kelmendi](#) and [Ales Svigelj](#) (Jozef Stefan Institute, Slovenia); [Andrej Hrovat](#) (Jožef Stefan Institute, Slovenia)

In order to achieve larger capacities needed for modern multimedia services, satellite communications are using high frequencies, such as the Ka/Q bands and above. However, due to several atmospheric factors, in particular rain along the propagation path, communication at these high frequencies are subject to signal attenuation, which limits the availability and reliability of links. To mitigate signal attenuation, several fade mitigation techniques exist. Diversity techniques, such as site diversity, orbital diversity and time diversity, represent one such group. In this paper the performance of time diversity is investigated based on one-year measurement data statistical analyses of rain attenuation from Alphasat satellite at 19.7GHz and 39.4 GHz in Ljubljana. Moreover, the performance of time diversity in two-site diversity system is investigated based on two years experimental signal data from Astra 3B satellite at 20.2GHz measured at three locations in Slovenia.

11:00 *Cloud Free LOS Probability Estimation for MEO Optical Satellite Systems and Optical Satellite Network Dimensioning*

[Christos N. Efrem](#) and [Nikolaos Lyras](#) (National Technical University of Athens, Greece); [Charilaos Kourogiorgas](#) (Science and Technology Facilities Council\RAL Space, United Kingdom (Great Britain)); [Athanasios D. Panagopoulos](#) (National Technical University of Athens, Greece); [Pantelis-Daniel Arapoglou](#) (European Space Agency, The Netherlands)

Optical satellite networks have been recently proposed as an alternative solution of backhaul satellite networks. This paper studies the Medium Earth Orbit (MEO) optical satellite communication systems More specifically, simple algorithms for the optimum selection of the locations of the optical ground stations (OGSs) for a MEO optical satellite system are presented. The objective is to satisfy an availability threshold for each month for each orbital position of the MEO satellite. The algorithms take into account the monthly variability of cloud coverage, take advantage of locations in different hemispheres and select OGSs which are within the visibility area of the satellite for longer time. Additionally, an engineering methodology for the estimation of single and joint CFLOS statistics for MEO satellite communication systems based on Integrated Liquid Water Content (ILWC) monthly statistical parameters is presented. Finally using the proposed methodologies useful numerical results are presented.

11:20 *Variability of Gaseous Attenuation at Very Low Elevation Angle Slant Paths; Measurements and Modelling*

[Erik W Alsaker](#) (University of Bergen, Norway); [Martin Rytir](#) (Norwegian Defence Research Establishment (FFI), Norway)

Gaseous attenuation variability for a 3.2° elevation angle satellite link operating at 20 GHz in the Norwegian Arctic is analyzed and compared with different models. At a very low elevation link like this one, gaseous attenuation reaches high values and has significant temporal variation over short periods of time. 5 months of measured data are compared with a model based on measured ground meteorological data and two different numerical weather prediction (NWP) models. The simplified model based on ground data gives lower values than the measured levels and is unable to model the observed fast variations. Both the NWP model based on predictions and the one based on re-analysis of past data are able to model most of the fast variations. When cloud attenuation is included in the NWP models both show excellent agreement with the measured data, without a clear difference in accuracy between them.

11:40 *Potentialities of the Numerical Weather Prediction Model WRF to Produce Attenuation Statistics in Tropical Regions*

[Valentin Le Mire](#) (ONERA, France); [Xavier Boulanger](#) (CNES, France); [Laurent Castanet](#) (ONERA, France); [Bouchra Benammar](#) (Centre National d'Etudes Spatiales (CNES), France); [Laurent Féral](#) (Laboratoire LAPLACE, France)

This paper presents the use of a Numerical Weather Prediction model (WRF) coupled with an electromagnetic module to create rain attenuation time series and statistical results in a tropical region. Simulated results are compared with experimental data collected within a CNES/ONERA sponsored propagation experiment near Kourou, in French Guiana. Both simulated and experimental Complementary Cumulative Distribution Functions of rain attenuation (CCDF) are presented in an annual and monthly basis. Finally, a brief granulometric study is detailed to better understand the impact of the rain drop size distribution (DSD) on the obtained results.

12:00 *Performance Trends at 26 GHz for a Receiving Ground Station at Polar Latitudes: The SNOWBEAR Project*

[Matteo Marchetti](#) and [Donato Lospalluto](#) (University of Pavia, Italy); [Filippo Concaro](#) (European Space Agency, Germany); [Filomena Romano](#) and [Domenico Cimini](#) (CNR-IMAA, Italy); [Marco Pasian](#) (University of Pavia, Italy)

Radio links at around 26 GHz for space communications between Earth observation satellites and ground stations at Polar latitudes are being considered in recent year to increase the downlink performance. However, the precise link budget modelling and the experimental validation of such links is still open, partially due to large propagation losses at these frequencies and partially because of the effect of the harsh Polar environment (e.g., snow) on the antenna structure (e.g., the antenna radome). This paper presents the link budget model implemented in the framework of a dedicated project (SNOWBEAR) under European Space Agency coordination and examples of validation of such a model against experimental data, including cases either in clear sky condition or during a snowstorm. In addition, possible upgrades for the model, based on the use of the ERA5 database, are outlined.

CS09: Analytical and Numerical Methods for Metasurface Analysis and Design

T10 EM modelling and simulation tools / Convened Session / Electromagnetics

Room: B9

Chairs: [Christophe Craeye](#) (Université Catholique de Louvain, Belgium), [Oscar Quevedo-Teruel](#) (KTH Royal Institute of Technology, Sweden)

8:30 *Metasurface for Dense Dipole Array Decoupling in Ultra-High Field MRI*

[Marc Dubois](#) (Institut Fresnel, France); [Anna Hurshkainen](#) (ITMO University, Russia); [Masoud S. M. Mollaei](#) (Aalto University, Finland); [Sergei Kurdjumov](#) (ITMO University, Russia); [Redha Abdeddaim](#) (Aix Marseille University, France); [Stefan Enoch](#) (CNRS & Institut Fresnel, France); [Stanislav Glybovski](#) (ITMO University, Russia); [Constantin Simovski](#) (Aalto University, Finland)

Transmit phased array are developed in order to gain control over the radiofrequency magnetic field and reduce the inhomogeneities observed with ultra-high field MRI (>3T for clinical applications). Dipole antennas close to the subject body are often used because of their efficiency for deep targets. However, arranging dense array of such elements leads to strong mutual coupling that is detrimental to the MRI acquisition mainly because of the distortion of RF-fields and safety issues for the subject. In this work, we review previous decoupling technique mostly based on single scatterer and study the use of a metasurface, by means of impedance matrix theory, in order to decouple active dipole antennas separated by $\lambda/30$.

8:50 *Elliptical Glide-Symmetric Holey Metasurfaces for Wideband Anisotropy*

[Antonio Alex-Amor](#) (Technical University of Madrid, Spain); [Fateme Ghasemifard](#) (KTH Royal Institute of Technology, Sweden); [Guido Valerio](#) (Sorbonne Université, France); [Pablo Padilla](#) (University of Granada, Spain); [Jose Manuel Fernández González](#) (Universidad Politécnica de Madrid, Spain); [Oscar Quevedo-Teruel](#) (KTH Royal Institute of Technology, Sweden)

This paper presents a mode-matching technique to study the dispersive features of periodic structures composed of glide-symmetric elliptical holes. As a difference from purely numerical methods, our formulation provides physical insight on the Floquet harmonics. At the same time, the computational cost is reduced compared to general purpose commercial software. The fields inside the holes are described by means of Mathieu functions and subsequently used to compute the full 2-D dispersion diagrams. With the presented analysis, we demonstrate that glide-symmetric periodic structures with elliptical holes offer anisotropic refractive indexes over a wide range of frequencies.

9:10 *Derivation of Circuit Models Based on an Eigenvalue Problem for Periodic Surfaces with Multiple Resonances*

[Raúl Rodríguez-Berral](#) (Universidad de Sevilla, Spain); [Francisco Mesa](#) (University of Seville, Spain); [Francisco Medina](#) (University of Sevilla, Spain)

This work presents an eigenvalue problem to characterize the resonances of a 2-D periodic surface. The corresponding eigenvalues are related to the resonance frequencies and the eigenfunctions are the corresponding surface current resonant profiles on the metalized portion of the unit cell. Furthermore, the orthogonality properties of the resonant profiles lead to the derivation of simple circuit models with canonical topology (Foster's second form). The numerical results will show that, within the non-diffraction regime, the resonant profiles are a convenient set of macrobasis functions and also that the circuit model provides reasonably accurate results.

9:30 *Analysis of Curved Metasurfaces Based on Method of Moments*

[Dominik Barbaric](#) (Ericsson Nikola Tesla dd, Croatia); [Marko Bosiljevac](#) and [Zvonimir Sipus](#) (University of Zagreb, Croatia)

With research of curved metasurfaces gaining more attention, adequate analysis methods are needed to allow for an efficient design of such structures. Previous works dealt with specific canonical problems, such as those with cylindrical geometry, which were mostly analyzed using Mode Matching approach. In this paper we present an analysis based on Method of Moments which can be used for any generally-curved metasurface structure situated in free-space, or for metasurfaces embedded in canonical multilayer supporting structures (e.g. spherical or cylindrical). We implement a solver for this method and verify the results against other computational approaches, as well as against measurements of a developed antenna pattern-shaping metasurface.

9:50 *Coffee Break*

10:20 *Multifunctional Nonreciprocal Metasurfaces Based on Spatiotemporal Modulation*

[Xuchen Wang](#) and [Ana Diaz-Rubio](#) (Aalto University, Finland); [Huanan Li](#) (City University of New York, USA); [Sergei Tretyakov](#) (Aalto University, Finland); [Andrea Alù](#) (The University of Texas at Austin, USA)

In this talk, we put forward the concept of multifunctional nonreciprocal metasurfaces realized on an universal hardware platform. The proposed prototype is based on a spatiotemporally modulated impedance surface. We show that using appropriate traveling wave modulations it is possible to realize various nonreciprocal properties controlling the response for illuminating plane waves. Based on this principle, we find proper modulation functions for different application purposes, which allows us to switch the device functionality among isolators, phase shifters, circulators, and potentially even more functionalities.

10:40 *An Artificial Shield for MRI Birdcage Coil with Constructive Interference*

[Ksenia Lezhennikova](#) and [Anna Hurshkainen](#) (ITMO University, Russia); [Marc Dubois](#) and [Djamel Berrahou](#) (Institut Fresnel, France); [Constantin Simovski](#) (Aalto University, Finland); [Alexander Raaijmakers](#) (University Medical Center Utrecht, The Netherlands); [Irina Melchakova](#) (ITMO

University, Russia); [Stefan Enoch](#) (CNRS & Institut Fresnel, France); [Redha Abdeddaim](#) (Aix Marseille University, France); [Stanislav Glybovski](#) (ITMO University, Russia)

In this contribution, an artificial shield for an MRI birdcage coil based on a cylindrical miniaturized corrugated structure is proposed. The presence of a conventional metallic shield around the birdcage resonator leads to a destructive interference of the primary magnetic field of the coil and the reflected field inside the coil (in the region of an investigated sample). At the same time, the fields constructively interfere in the region between the coil and the shield. As a result, the efficiency of the coil may be limited. The proposed artificial shield has a miniaturized corrugated structure, which demonstrates the property of a constructive interference inside the coil. It has been shown that the proposed structure placed around the birdcage coil can increase the efficiency at its resonance similarly to an ideal cylindrical magnetic wall of the same diameter.

11:00 **Robust Homogenized Impedance Model for Periodically Modulated Metasurfaces**

[Enrica Martini](#) (University of Siena, Italy); [Francesco Caminita](#) (Wave-Up SRL, Italy); [Stefano Maci](#) (University of Siena, Italy)

This paper presents an investigation of the accuracy of the homogenized impedance model for the description of patch-type periodically modulated metasurfaces. Different method of analyses are implemented to this end: a rigorous full wave analysis based on a spectral MoM is used as reference solution, while the procedure introduced by Oliner for the analysis of scalar impenetrable impedance is generalized to tensor and/or penetrable impedance to analyze the homogenized structure. It is shown that the penetrable impedance model can provide very accurate results in the prediction of both the complex propagation constant and the current distribution.

11:20 **Dual-Band Beams Generation with Metasurface Based on the EFIE**

[Modeste Bodehou](#) (Université Catholique de Louvain, Belgium); [David González-Ovejero](#) (Centre National de la Recherche Scientifique - CNRS, France); [Christophe Craeye](#) (Université Catholique de Louvain, Belgium); [Isabelle Huynen](#) (Université catholique de Louvain, Belgium)

This paper investigates the generation of dual-band beams by modulated metasurface antennas. The developed technique combines a semi-separable model dependence of the sheet impedance (with respect to frequency and patch parameters) with the resolution of the electric field integral equation (EFIE). This allows us to express the impedance modulation at one frequency as a function of the modulation at the second frequency. Then, we can formulate the EFIE at both frequencies while referring to the surface impedance at a single frequency, still fully taking into account the frequency dispersion of the substrate. The method is illustrated through the synthesis of a circularly polarized conical beam and a broadside pencil beam at two different frequencies. Numerical validation with two different Method of Moments (MoM) codes is provided.

CS39: Machine Learning in Antennas

T11 Fundamental research and emerging technologies / Convened Session / Antennas

Room: B10

Chairs: [Bo Liu](#) (University of Glasgow, United Kingdom (Great Britain)), [Lei Wang](#) (Heriot-Watt University, United Kingdom (Great Britain))

8:30 **Machine Learning-assisted Antenna Design Optimization: A Review and the State-of-the-art**

[Mobayode Akinsolu](#) (Glyndwr University, United Kingdom (Great Britain)); [Keyur Mistry](#) (University of Huddersfield, United Kingdom (Great Britain)); [Bo Liu](#) (University of Glasgow, United Kingdom (Great Britain)); [Pavlos Lazaridis](#) (University of Huddersfield, United Kingdom (Great Britain)); [Peter S Excell](#) (Glyndwr University, United Kingdom (Great Britain))

Antenna design optimization continues to attract a lot of interest. This is mainly because traditional antenna design methodologies are exhaustive and have no guarantee of yielding successful outcomes due to the complexity of contemporary antennas in terms of topology and performance requirements. Though design automation via optimization complements conventional antenna design approaches, antenna design optimization still presents a number of challenges. The major challenges in antenna design optimization include the efficiency and optimization capability of available methods to address a broad scope of antenna design problems considering the growing stringent specifications of modern antennas. This paper presents a review of the most recent progress in antenna design optimization with a focus on methods which address the challenges of efficiency and optimization capability via machine learning techniques. The methods highlighted in this paper will likely have an impact on the future development of antennas for a multiplicity of applications.

8:50 **Machine Learning-Based Hybrid Random-Fuzzy Modeling Framework for Antenna Design**

[Duygu Kan](#) (Ghent University & IMEC, Belgium); [Simon De Ridder](#) (Ghent University, Belgium); [Domenico Spina](#) (Ghent University - imec, Belgium); [Ivo Couckuyt](#) (Ghent University, Belgium); [Flavia Grassi](#) (Politecnico di Milano, Italy); [Tom Dhaene](#) (Ghent University & IMEC, Belgium); [Hendrik Rogier](#) and [Dries Vande Ginste](#) (Ghent University, Belgium)

A machine learning-based framework is proposed to evaluate the effect of design parameters, affected by both aleatory and epistemic uncertainty, on the performance of antennas. In particular, possibility theory is leveraged to define aleatory and epistemic uncertainty in a common framework. Then, a method combining Bayesian optimization and Polynomial Chaos expansion is applied to accurately and efficiently propagate both uncertainties throughout the system under study. A suitable application example validates the proposed method.

9:10 **Compact Millimeter-Wave MIMO Antenna for 5G Applications**

[Issa Elfergani](#) and [Jonathan Rodriguez](#) (Instituto de Telecomunicações, Portugal); [Amjad Iqbal](#) (Multimedia University, Malaysia); [Maryam Sajedin](#) (University of Aveiro, Portugal); [Chemseddine Zebiri](#) (Ferhat Abbas University of Setif, Algeria); [Raed A Abd-Alhameed](#) (University of Bradford, United Kingdom (Great Britain))

An efficient four-elements mmWave multiple-input multiple output (MIMO) antenna is proposed for use in 5G system The proposed MIMO mmWave design operates at 35GHz and occupies an overall volume of 12.5 mm × 12.5 mm × 0.8 mm3. This antenna exhibits a good matching impedance at the operating frequency of 35GHz mmWave band, where an isolation greater than 25 dB, envelope correlation coefficient (ECC) less than 0.02, and diversity gain (DG) of around 10dB are obtained. The 4-elements MIMO mmWave antenna also shows a peak gain of 6 dB with 87% of peak radiation efficiency. The obtained results along with size miniaturization signify that the proposed MIMO antenna is deemed as an appropriate candidate for millimeter wave based wireless applications.

9:30 **A Dual-Polarized 5G Base Station Antenna Using Machine-Learning Based Optimization Method**

[Qiang Hua](#), [Yi Huang](#), [Chaoyun Song](#) and [Tianyuan Jia](#) (University of Liverpool, United Kingdom (Great Britain)); [Xu Zhu](#) (University of Liverpool, United Kingdom (Great Britain) & Harbin Institute of Technology, Shenzhen, China)

A broadband dual-polarized 5G base station antenna using a machine-learning based optimization method is presented, which covers 3.3 - 5.0 GHz and has a compact size with an overall dimension of 60 × 60 × 18 mm3. The antenna includes two double-oval-shaped dipoles, two F-shaped feeding lines and one reflector. The double-oval-shaped dipoles and F-shaped feeding lines can generate a broadband performance and high port-to-port isolation. The parallel surrogate model-assisted hybrid differential evolution for antenna optimization (PSADEA) is employed to optimize the overall antenna performance. An optimization procedure is also introduced in the paper. The proposed antenna has a high port-to-port isolation (better than 20 dB), a stable radiation pattern, and a flat gain (about 7.3 dBi). Meanwhile, the half-power beamwidth of the proposed antenna is within 65° ± 5°, which meets the industry requirement. Therefore, the proposed antenna is a good candidate for 5G base station applications.

9:50 **A Doherty Power Amplifier Based on the Harmonic Generating Mechanism**

[Maryam Sajedin](#) (University of Aveiro, Portugal); [Issa Elfergani](#) and [Jonathan Rodriguez](#) (Instituto de Telecomunicações, Portugal); [Raed A Abd-Alhameed](#) (University of Bradford, United Kingdom (Great Britain)); [Ahmed Maan Abdulkhaleq](#) (University of Bradford & SARAS Technology, United Kingdom (Great Britain)); [Naser Ojaroudi Parchin](#) (University of Bradford, United Kingdom, United Kingdom (Great Britain)); [Yasir Ismael Abdulaheem Al-Yasir](#) (University of Bradford, United Kingdom (Great Britain))

This Paper presents an energy-efficient asymmetrical Doherty amplifier based on the harmonic-tuned Class-F and inverse Class-F mode of operations. In addition, the design procedure of multi-resonant circuits tuned for second and third harmonics at the devise input/output are explored. The saturated Doherty architecture is designed by 10W GaN HEMT device from CREE at 3.6GHz and power added efficiency of 50% at 8dB back-off and 55% at maximum output power of 43dBm have been achieved. This superposition performance has been confirmed by comparing the simulated results with that of conventional one.

10:10 **Coffee Break**

10:40 **Machine Learning-Driven Design Optimization for a Multi-Layer Metasurface Antenna**

[Despoina Kampouridou](#) and [Alexandros Feresidis](#) (University of Birmingham, United Kingdom (Great Britain))

In this paper, the design of a five layer Fabry-Perot cavity leaky wave antenna is proposed via an optimization method. The antenna uses a triple-resonant slot feeding technique with a microstrip line for a broadband matching performance. Each antenna layer is a partially reflective surface which consists of 7 × 7 patch elements, where the outer two layers of elements serve for wave impedance matching to the free space impedance. Preliminary results demonstrate a high gain performance of 19.6 dBi at 14.3 GHz and a very good input matching.

11:00 **Wearable 5-Gigahertz Wi-Fi Antenna Design Using Whale Optimization Algorithm**

[Achilles D. Boursianis](#) (Aristotle University of Thessaloniki, Greece); [Stavros Koulouridis](#) (University of Patras, Greece); [Dimitrios Georgoulas](#) and [Sotirios Goudos](#) (Aristotle University of Thessaloniki, Greece)

In this paper, we design an antenna for wearable wireless applications. The proposed antenna is a planar inverted-F antenna (PIFA) for operation at 5GHz. The antenna design procedure is accomplished using a new nature inspired algorithm, the Whale Optimization Algorithm. Numerical results exhibit the applicability and validity of the proposed design framework.

11:20 **A Compact Frequency Reconfigurable DRA for GSM, LTE, and 5G Applications Services**

[Chemseddine Zebiri](#) (Ferhat Abbas University of Setif, Algeria); [Djamel Sayad](#) (University of 20 Aout, United Kingdom (Great Britain)); [Jamal Kosha](#) and [Widad Mshwat](#) (University of Bradford, United Kingdom (Great Britain)); [Issa Elfergani](#) and [Jonathan Rodriguez](#) (Instituto de

Telecomunicações, Portugal); [Raed A Abd-Alhameed](#) (University of Bradford, United Kingdom (Great Britain))

A compact PIN diode frequency reconfigurable dielectric resonator antenna (DRA) for GSM, LTE and 5G applications is studied and presented. The proposed antenna provides operating frequencies between 1.80 GHz, 2.6 GHz, 3.6 GHz and the lower 5G bands (3.4-3.8 GHz and 3.4-3.7 GHz) which makes it suitable for mobile communication devices. The antenna structure consists of three rectangular Dielectric Resonators DR1, DR2, and DR3 with permittivities 12.85 for RD1 and RD3 and 1.96 for RD2, of different dimensions. Two PIN diode switches are adequately placed on the microstrip line between the two dielectric resonators to assure the reconfiguration function. The proposed antenna size is 20×36×4.8 mm³. Simulation results are presented and discussed. For the antenna structure validation and to highlight its performances, the results are compared with data published in the literature. The proposed antenna, offering suitable performance, provides three modes of operation with bandwidths of 19%, 11%, and 9%

11:40 A New Broadband MIMO Antenna System for Sub 6 GHz 5G Cellular Communications

[Naser Ojaroudi Parchin](#) (University of Bradford, United Kingdom, United Kingdom (Great Britain)); [Yasir Ismael Abdurraheem Al-Yasir](#) (University of Bradford, United Kingdom (Great Britain)); [Ahmed Maan Abdulkhaleq](#) (University of Bradford & SARAS Technology, United Kingdom (Great Britain)); [Haleh Jahanbakhsh Basherlou](#) (Bradford College, United Kingdom (Great Britain)); [Atta Ullah](#) and [Raed A Abd-Alhameed](#) (University of Bradford, United Kingdom (Great Britain))

A new MIMO antenna system with broadband antenna radiators is introduced for sub 6 GHz fifth-generation (5G) mobile communications. The proposed design contains four pairs of compact coplanar-waveguide (CPW)-fed antennas with polarization diversity that are symmetrically placed at four corners of the smartphone printed circuit board (PCB). Therefore, the proposed 5G antenna design contains four horizontally polarized and four vertically-polarized antenna elements in total. A low-cost FR-4 substrate ($\epsilon= 4.4$, $\delta= 0.02$) with a dimension of 75×150 mm² is employed as the mainboard substrate. The proposed design offers good isolation, dual-polarized full radiation coverage, and sufficient efficiencies. In addition, a wide impedance bandwidth ($S_{11} \leq -10$ dB) of 3.3 to 6 GHz has been obtained for each antenna radiator. Moreover, the proposed design exhibits sufficient performance in the presence of the human-hand.

12:00 Mutual Coupling Effect on Three-Way Doherty Amplifier for Green Compact Mobile Communications

[Ahmed Maan Abdulkhaleq](#) (University of Bradford & SARAS Technology, United Kingdom (Great Britain)); [Maan Yahya](#) (Northern Technical University, Iraq); [Naser Ojaroudi Parchin](#) (University of Bradford, United Kingdom, United Kingdom (Great Britain)); [Yasir Ismael Abdurraheem Al-Yasir](#) (University of Bradford, United Kingdom (Great Britain)); [Maryam Sajedin](#) (University of Aveiro, Portugal); [Issa Elfergani](#) (Instituto de Telecomunicações, Portugal); [Raed A Abd-Alhameed](#) (University of Bradford, United Kingdom (Great Britain)); [Ashwain Rayit](#) (SARAS Technology Ltd. (SARAS), United Kingdom (Great Britain)); [Jonathan Rodriguez](#) (Instituto de Telecomunicações, Portugal)

Mutual coupling effect on three-way Doherty power amplifier is studied, where the amplifier is targeting 3.4-3.8 GHz for 5G applications using three GaN HEMT transistors (6W, 25W and 45W) to achieve a 76W peak power. A new impedance modulation configuration is used, where a gain of 12.5 dB was achieved over the design band. Changing the location of the peaking amplifier or changing the operation sequence of the peaking amplifier can achieve good efficiency at the back-off region. In addition, the performance variation of the designed amplifier was tested for different Voltage Standing Wave Ratio (VSWRs) considering the antenna impedance changing due to mutual coupling. There was an average of 3 dBm output power variation and $\pm 11\%$ efficiency variation at the peaking power and fewer variations in the performance for both factors at the back-off region for different VSWRs.

Tuesday, 17 March 8:30 - 10:10

BC/1: History of Electromagnetism 1 TOP

T13 Bicentennial Session / Electromagnetics

Room: B11

Chairs: [Ari Sihvola](#) (Aalto University, Finland), [Arthur D Yaghjian](#) (Electromagnetics Research Consultant, USA)

8:30 *The Road to Electromagnetism*

[Andrew D Jackson](#) (University of Copenhagen, Denmark)

The electromagnetic revolution began with Hans Christian Ørsted's observation of the effect of an electric current on a compass needle. The events that led to this discovery will be reviewed.

8:50 *The Discovery of Electromagnetism by Hans Christian Ørsted 200 Years Ago*

[Olav Breinbjerg](#) (Technical University of Denmark, Denmark)

In 1820 Hans Christian Ørsted (1777 - 1851), then a professor of natural philosophy at the University of Copenhagen and later a founder and the first president of the Technical University of Denmark, observed from systematic experiments that electricity and magnetism are related. He thus discovered an entirely new natural science that he termed electromagnetism; a science that became of paramount importance for the understanding of Nature and for technologies developing the modern society. This paper reviews Ørsted's epoch-making discovery through his own writings published between 1820 and 1830.

9:10 *Electromagnetism Before Maxwell: From Ørsted to Weber*

[Ovidio Mario Bucci](#) (University of Naples, Italy)

This paper summarizes the main stages of the development of Electromagnetism before Maxwell, from Ørsted's discovery of the magnetic effect of currents, through the Ampere's development of electrodynamics and Faraday's discovery of electromagnetic induction, until the development of Weber's electrodynamics. The emphasis is on the conceptual evolution that led, from one side, to the unification under a coherent, mathematically sound theory of all known electromagnetic phenomena within the Newtonian paradigm of instantaneous action at distance, from the other side to lay the foundation for the Maxwell's revolution, which definitely changed such paradigm.

9:30 *After Ørsted's Discovery: Johan Jacob Nervander and the Quantification of Electric Current*

[Ari Sihvola](#) (Aalto University, Finland)

This article focuses on the developments in electromagnetism after Ørsted's discovery in 1820. In particular, the principles to measure and quantify the electric current are given attention. Schweigger, Poggendorff, Nobili, and Pouillet contributed to the development of the galvanometer. The article puts special emphasis on the researches of Johan Jacob Nervander, whose "tangent bussol", presented to L'institute de France in Spring 1834, and later published in Annales de Chimie et de Physique, was an important development in the nstrumentation of electrical engineering.

9:50 *Oliver Heaviside, Maxwell's Apostle of Eccentric Elegance*

[Ismo V Lindell](#) (Aalto University, School of Electrical Engineering, Finland)

Oliver Heaviside has been known as the first one to express Maxwell's set of electromagnetic equations in elegant vector form. His life consisting of three quarter-century parts as telegraph engineer, innovative scientist and eccentric hermit, is briefly covered in this presentation.

Tuesday, 17 March 8:30 - 12:20

SW08: Challenges of Modern Material Measurements TOP

T12 Scientific / Industrial Workshops

Room: B3

Tuesday, 17 March 10:40 - 12:20

EurAAP 3: WG Software and modelling (10:40-12:20, Room: 17) TOP

EurAAP

T10-M10: General Antenna Measurements

T10 EM modelling and simulation tools / Regular Session / Measurements

Room: B4

Chairs: Benjamin Fuchs (University of Rennes 1 - IETR, France), Giorgio Giordanengo (LINKS Foundation & Politecnico di Torino, Italy)

10:40 Fast Antenna Array Characterization with Numerical Basis Functions

Marco Righero and Andrea Scarabosio (LINKS Foundation, Italy); Giorgio Giordanengo (LINKS Foundation & Politecnico di Torino, Italy); Giuseppe Vecchi (Politecnico di Torino, Italy)

A technique to exploit a priori information about an array antenna to reduce the number of Near Field samples needed for its characterization in Far Field is shown. Custom basis functions are built, considering the pattern of the isolated element, the elements position within the array, and additional auxiliary sources to account for coupling phenomena. Synthetic experiments show a four-fold reduction factor with respect to standard Near Field to Far Field techniques.

11:00 Near-to-Near- And Near-to-Far-Field Transformation for Millimeter-Wave Frequencies

Serge Pfeifer (Foundation for Research on Information Technologies in Society (ITIS Foundation), Switzerland); Jingtian Xi (The Foundation for Research on Information Technologies in Society (IT'IS), ETH Zurich, Switzerland); Sven Kuhn (IT'IS Foundation, Switzerland); Beyhan Kochali (Schmid&Partner Engineering AG, Switzerland); Niels Kuster (IT'IS Foundation, Switzerland)

With the advent of 5G mobile communications at millimeter-wave frequencies, exposure assessment by means of power density evaluation will become important; this, in turn, requires knowledge about the electric and magnetic field. To avoid measuring these quantities in the full volume of interest, this paper presents a method to reconstruct these quantities from measurements at very close distances, i.e., at a fraction of the wavelength, from the antenna. It is based on field integral equations and measurements with SPEAG's EUMMWVx probe. The method is evaluated in simulations with emulated measurement data. A successful reconstruction in the near and far-field is achieved both qualitatively and quantitatively. The deviation of reconstruction from simulation reference is less than 0.4 dB for the peak spatial-average power density. Therefore, this method is very promising for compliance assessment, and may reduce test time tremendously.

11:20 Fast Antenna Measurement via Model Order Reduction

Benjamin Fuchs (University of Rennes 1 - IETR, France); Athanasios Polimeridis (Q bio, USA)

A general procedure to characterize antennas from a reduced number of field samples is proposed. It relies on the construction and the fast evaluation of the reduced order model (ROM) of the antenna measurement problem. The ROM is built by computing the singular value decomposition (SVD) of the radiation operator that maps the equivalent currents surrounding the antenna under test (AUT) to the radiated near- or far- field. The SVD yields orthonormal basis for both sets and enables to compress the matrix of the discretized integral equation. The evaluation of the so-constructed reduced order model is expedited by using the discrete interpolation method (DEIM) that selects a small number of field sampling points. Experimental results of antenna prototypes for both near- and far- field radiation demonstrate the accuracy and the reduction of the measurement duration of the proposed approach.

11:40 Singularity Extraction of Electric-Field Integral Equations in Spherical Near-Field Antenna Measurement

Rezvan Rafiee Alavi, Rashid Mirzavand and Pedram Mousavi (University of Alberta, Canada)

In the solution of electric-field integral equation (EFIE) by the method of moment (MOM) on discretized planar triangles, singularities emerge in the inner integrals on the basis functions. In this paper, formulas for the singularity extraction of EFIE in the application of near-field measurement of antennas are systematically developed and presented. The simulations and measurements are performed to compare the results with and without singularity extraction. The results confirm the validity and accuracy of the proposed method.

12:00 Revisiting the Poincaré Sphere as a Representation of Polarization State

Brett Walkenhorst and Steven R Nichols (NSI-MI Technologies, USA)

Graphical representations of the polarization state of an antenna or an electromagnetic wave propagating through space are useful tools to supplement rigorous mathematical analyses. One such example, the polarization ellipse, is frequently used in combination with the mathematical development of polarization theory. The Poincaré sphere is another graphical representation but is much less widely used. Since each possible polarization state appears as a point on the surface of the sphere, it has limited value in representing a single polarization state. However, it can be quite useful for visualizing the relationships between multiple polarization states. In this paper, we show a different way of presenting the Poincaré sphere using a Mercator projection and elliptical parameters. We also describe a tool that implements this technique and provides a real-time display of polarization state as a function of frequency.

T10-E03/1: Computational and Numerical Techniques 1

T10 EM modelling and simulation tools / Regular Session / Electromagnetics

Room: B11

Chairs: Matthys M. Botha (Stellenbosch University, South Africa), Anders Karlsson (Lund University, Sweden)

10:40 An Iterative Method for the Analysis of Large Disjoint Antenna Arrays

Matthews Chose (Stellenbosch University & University of Stellenbosch, South Africa); Matthys M. Botha (Stellenbosch University, South Africa)

A new iterative method is presented, for the efficient method of moments (MoM) analysis of large antenna arrays with identical, disjoint elements. The method is an extension of the domain Green's function method (DGM). At each iteration, a local domain radius is used to identify sub-problems of closely-coupled elements centred around each antenna element. Rigorous MoM analysis is used on these local domains to account for strong mutual coupling, with an iteratively-refined current scaling assumption used to account for the influence of currents on the rest of the array elements. Numerical results demonstrate that the technique can converge rapidly for arrays with closely spaced elements.

11:00 Directional Method to Compute Reduced Matrix System in MBF Solvers

Keshav Sewraj and Matthys M. Botha (Stellenbosch University, South Africa)

Computation of reaction terms in macro basis function (MBF) solvers is computationally very expensive. A directional cross approximation technique is used in this paper to compute the reaction terms, which is a multilevel low-rank compression technique. The motivation to use a directional method is to keep the compression rank bounded irrespective of subdomain size, so as a fast algorithm can be ensured. Apart from the computational efficiency, a controlled and very good accuracy can be obtained with the directional method. The application focus of this work is large antenna arrays.

11:20 An Efficient Parallelization Strategy for the Adaptive Integral Method Based on Graph Partitioning

Damian Marek, Shashwat Sharma and Piero Triverio (University of Toronto, Canada)

The adaptive integral method (AIM) is frequently used to efficiently solve scattering problems involving conducting objects immersed in a uniform or stratified medium. We propose an efficient parallelization strategy for AIM suitable for distributed-memory computers. In the proposed approach, a weighted graph is associated to the given mesh, and partitioned in a way that results in an efficient distribution of computations across different processes. Numerical tests show that the proposed algorithm compares favorably to existing techniques to parallelize the AIM.

11:40 A False-Resonance-Free Integral Equation Formulation for the Electromagnetic Transmission Problem

Anders Karlsson and Johan Helsing (Lund University, Sweden)

We present a boundary integral equation formulation of the transmission problem where an incident electromagnetic wave is scattered from a bounded dielectric object. The formulation provides unique solutions for all combinations of wavenumbers with non-negative imaginary parts for which the Maxwell equations have unique solutions. This includes the combination of an imaginary wavenumber in the object and a real wavenumber in the outer region. Numerical examples involve field evaluations for smooth as well as non-smooth objects

12:00 An Explicit Time Domain Finite Element Boundary Integral Method with Element Level Domain Decomposition for Electromagnetic Scattering Analysis

Ming Dong (King Abdullah University of Science and Technology (KAUST), Saudi Arabia); Ping Li (The University of Hong Kong, Hong Kong); Hakan Bagci (King Abdullah University of Science and Technology (KAUST), Saudi Arabia)

A numerical scheme, which hybridizes the element level dual field time domain finite element domain decomposition method (ELDFDD/TDFEM) and time domain boundary integral (TDBI) method to accurately and efficiently analyze open-region transient electromagnetic scattering problems, is proposed. The element level decomposition permits an

Tuesday, 17 March 13:20 - 14:50

EurAAP 1: WG Measurements + AMTA Europe (12:50-14:50, Room: 5)

EurAAP

12:50 - 14:50 Room: 5

EurAAP 2: WG Small Antennas (12:40-14:00, Room: 17)

EurAAP

12:40 - 14:00 Room: 17

Convened Poster 1-CS08: Analysis, Design and Use of Microwave Techniques, Models, Systems, and Antennas for Snowpack Avalanches Monitoring

T08 Positioning, localization & tracking / Convened Session / Propagation

Room: [A2 \(Poster Area\)](#)

Chairs: [Guido Luzi](#) (Centre Tecnològic de Telecomunicacions de Catalunya (CTTC/CERCA), Spain), [Marco Pasian](#) (University of Pavia, Italy)

CP1.01 Complex Dielectric Constant of Wet Snow Using Bi-Static Synthetic Aperture Radar

[Jon Håvard H Eriksrød](#), [Kristian G Kjelgård](#) and [Tor Sverre Lande](#) (University of Oslo, Norway)

This paper presents a feasible method for measurements of the complex dielectric constant for snow assessment using a coherent Bistatic Synthetic Aperture Radar. The complex dielectric constant may be measured directly for both wet and dry snow. Since signal delay as well as signal loss is measured, the complex permittivity can be constructed as a closed form expressions. The radar system performance is validated on a characterized snow phantom with good results even for high water content indicating adequate measurements for wet snowpacks.

CP1.02 A Low Cost Active Corner Reflector to Assist Snow Monitoring Through Sentinel/1 Images

[Guido Luzi](#) and [Enric Fernandez](#) (Centre Tecnològic de Telecomunicacions de Catalunya (CTTC/CERCA), Spain); [Fermin Mira Perez](#) (Centre Tecnològic de Telecomunicacions de Catalunya, Spain); [Michele Crosetto](#) (Centre Tecnològic de Telecomunicacions de Catalunya (CTTC/CERCA), Spain)

The use of Sentinel-1 SAR images for snow behavior monitoring is one of the most studied applications, but due to the high temporal and spatial heterogeneity of this media, is quite challenging. The presence of reference targets in the observed areas is of main concern both for amplitude and interferometric based techniques, but in a typical scenario as snow covered slopes or glaciers there is a lack of stable natural targets; this can demand the installation of Corner Reflectors. In this study, the design and the first test of an active corner reflector (ACR) operating at 5.405 GHz \pm 50 MHz band, designed to be used in support to ESA Sentinel-1 spaceborne SAR images analysis and processing, is reported. The system here described was designed aiming at a tradeoff among low cost, simple functioning, easy and rugged hardware, to be deployed also in sites, as snow covered areas and glaciers.

CP1.03 Analysis of Snow Water Equivalent (SWE) of Snowpack by an Ultra Wide Band Step Frequency Continuous Wave Radar (SFCW)

[Rafael Alonso](#), [José María García del Pozo](#) and [Ismael Peruga](#) (University of Zaragoza, Spain); [Samuel Buisán](#) (Territorial Delegation of AEMET (Spanish State Meteorological Agency) in Aragón); [José Adolfo Álvarez](#) (Ebro River Basin Authority (CHE))

A ground-based step frequency continuous wave radar (SFCW), based in a software defined radio (SDR), in the range from 150MHz to 6GHz has been designed, fabricated and tested under real conditions. The radar has been applied to measure the snow water equivalent (SWE) of snowpack in the Spanish Pyrenees. A matrix method is applied to solve the electromagnetic reflectance of multilayer cover snow including frequency and wetness dependence of complex relative dielectric permittivity of snow layers. An approximated method to obtain SWE is presented. The method is based on the comparison of measured reflected signal vs distance plot with the calculated with an "equivalent" snow layer. Preliminary results are presented and compared with those provided by a cosmic-ray neutron SWE gauge over the 2019 winter. These results suggest the viability of the proposed method.

CP1.04 Identification of Multi-Temporal Snow Melting Patterns with Microwave Radars

[Marco Pasian](#) and [Pedro Fidel Espin Lopez](#) (University of Pavia, Italy); [Valentina Premier](#) (Eurac Research, Italy); [Claudia Notarnicola](#) (EURAC, Italy); [Carlo Marin](#) (Eurac Research, Italy)

Not available

Convened Poster 1-CS10: Antenna Array and Integrated Systems for 5G Communication Applications

T02 Millimetre wave 5G / Convened Session / Antennas

Room: [A2 \(Poster Area\)](#)

Chairs: [Darwin Blanco](#) (Ericsson, Sweden), [Christos Kolitsidas](#) (Ericsson, Sweden)

CP1.05 Antenna-Amplifier Co-design: On a Method to Shape the Antenna Impedance

[Lars Jonsson](#) and [Ahmad Emadeddin](#) (KTH Royal Institute of Technology, Sweden)

In this paper we examine a particular type of shape optimization to improve the antenna input impedance. In a co-integration application, the impedance goal for an antenna design is to approach an optimal load for the power amplifier, while maintaining low losses and good radiation properties. This is of increasing importance at above 20GHz, since commercially available, high efficient amplifiers tend to have a strong frequency variation in their optimal load-pull impedance. A classical approach to matching is a matching network, however at these higher frequencies such networks are associated with losses from radiation, conduction and dielectrics. Here we instead study how antenna shaping can be perturbed to exhibit the desired frequency response. This is a initial study focusing on only the antenna impedance at a given frequency and for a few generic antenna shapes.

CP1.06 5G Wideband Magneto-Electric Dipole Antenna Fed by a Single-Layer Corporate-Feed Network Based on Ridge Gap Waveguide

[Wai Yan Yong](#) (University of Twente, The Netherlands); [Thomas Emanuelsson](#) (Gapwaves AB, Sweden); [Andrés Alayón Glazunov](#) (University of Twente, The Netherlands & Chalmers University of Technology, Sweden)

This paper proposes a wideband magneto-electric (ME) dipole fed by a single-layer corporate-feed network based on the ridge gap waveguide (RGW) for 5G backhauling applications. The proposed antenna is composed of two layers. The top layer is the radiating layer that is composed of the 2x2 ME-dipole antenna element. The bottom layer is the corporate-feed network designed based on RGW. Our design allows for a smaller antenna volume as it excited the antenna directly by the RGW without the need of cavity layer. In addition, with the use of the ME-dipole, the bandwidth performance supported by the proposed design is larger as compared to the conventional designs. From the obtained simulation results, the proposed antenna produces S11 -10dB over 24 - 30 GHz resulting in a 22% fractional bandwidth. The maximum directivity over the operating bandwidth of the simulated 2x2 ME-dipole antenna element is approximately 15.4 dBi.

CP1.07 Design of Millimeter Wave True-Time-Delay Beam-formers for 5G Wireless Systems

[Dimitrios I. Lialios](#), [Konstantinos D. Paschaloudis](#), [Anastasios G. Koutinos](#), [Empliouk Tzihat](#) and [Nikolaos Ntetsikas](#) (Democritus University of Thrace, Greece); [Vasilis Kassouras](#) (Center for Security Studies (KEMEA), Greece); [Konstantinos Kardaras](#) and [Dimitrios S. Kritharidis](#) (Intracom

Telecom, Greece); [Christos Kolitsidas](#) (Ericsson, Sweden); [George A. Kyriacou](#) (Kimmeria Campus, Greece & Democritus University of Thrace, unknown)

The exploitation of the millimeter wave (mmW) spectrum is determinate in the upcoming fifth generation (5G) wireless communications, as it meets the requirements for high capacity links, large data-rates and small latency. However, the growing complexity of the 5G mobile communication systems requires the existence of antenna arrays with multiple-beam capability. To this scope, the current work presents two novel designs of millimeter wave beamforming networks. The first one refers to a "tree diagram topology", while the other architecture employs a Blass matrix, which is a known beamforming network at the microwave regime.

CP1.08 Circularly and Linearly Polarized Planar Reconfigurable Active Array Antennas in Ka Band

[Alfonso T. Muriel Barrado](#), [Jorge Calatayud Maeso](#), [Antonio Rodríguez Gallego](#), [Jose Manuel Fernández González](#) and [Manuel Sierra-Pérez](#) (Universidad Politécnica de Madrid, Spain); [Pablo Sanchez-Olivares](#) (Universidad Politecnica de Madrid, Spain)

This paper presents an evaluation procedure of a commercial integrated circuit (IC) for phased array antenna beam steering within mobile satellite communication applications at Ka Band (28-30 GHz). It allows to control amplitude and phase delivery from one common port to 8 independent channels. Therefore, only the transmission system is evaluated. Two different passive arrays are proposed to evaluate IC performance: a 2x2 planar array with switchable circular polarization (CP) capabilities and a 8x8 planar array for feeding in columns for azimuth beam steering with linear polarization (LP). Thus, since the first array is not as big enough for evaluate beam steering performance, it is only used for CP performance evaluation. A second bigger array, which is bigger but not circularly polarized, allow beam steering evaluation. Measurements of the proposed full integrated system will be presented at the conference.

CP1.09 Broadband CTS Array in PCB Technology

[Michele Del Mastro](#) (University of Rennes 1, France); [Adham Mahmoud](#) (Institut d'Électronique et de Télécommunications de Rennes, France); [Thomas Potelon](#) (IETR - University of Rennes 1, France); [Ronan Sauleau](#) (University of Rennes 1, France); [Mauro Ettore](#) (University of Rennes 1 & UMR CNRS 6164, France)

In this paper, a very low-profile wideband long-slot array is presented. The antenna system is realized using standard printed-circuit board (PCB) technology. Its architecture consists of radiating long slots, etched on the upper face of a PCB panel. The slots are parallel-fed by a corporate feeding network made in parallel-plate waveguide technology. An embedded pillbox coupler is employed to feed the structure. The antenna module is low-cost and presents a very low-form factor. The proposed solution covers the full Ka-band for Satcom applications (i.e., 47% of relative bandwidth). Very clear radiation patterns are shown in the H-plane. The maximum gain is about 18 dBi at 25 GHz. Moreover, the antenna efficiency is about 85% in the Ka-band.

CP1.10 A Simplified Extended SIW Supporting TE_{01} Integrated with a Feeding Structure

[Christos Kolitsidas](#) and [Darwin Blanco](#) (Ericsson, Sweden)

A TE_{01} substrate integrated waveguide is presented in this work. To avoid the propagation of this typically unsupported mode the SIW is integrated with an electromagnetic band gap EBG structure that confines the field within the waveguide structure. The EBG is simply stacked top and bottom of the proposed structure allowing manufacturing ease. The overall proposed structure is simulated and the results indicate very low insertion loss in the pass-band of the waveguide.

Convened Poster 1-CS17: Antennas with Multi-Port/Distributed Feeding and On-Antenna Power-Combining for Efficient Integration and Reconfigurability

T02 Millimetre wave 5G / Convened Session / Antennas

Room: [A2 \(Poster Area\)](#)

Chairs: [Marianna Ivashina](#) (Chalmers University of Technology, Sweden), [Ville Viikari](#) (Aalto University & School of Electrical Engineering, Finland)

CP1.11 Efficient Waveguide Power Combiners at mm-Wave Frequencies

[Ralph van Schelven](#), [Marco Spirito](#) and [Daniele Cavallo](#) (Delft University of Technology, The Netherlands)

In this work, an efficient power combiner for mm-wave frequency transmitters is investigated. The combiner is based on a parallel plate waveguide (PPW) excited with multiple parallel feeds and can be realized using standard PCB technology. The Doherty power combiner scheme can be also integrated in the proposed concept, to increase the efficiency of the amplifiers for implementing amplitude modulation. The advantage of the proposed PPW combiner with respect to other concepts, e.g. the ones based on substrate integrated waveguide (SIW), is the wider bandwidth and the scalability to arbitrarily large number of inputs.

CP1.12 Reducing User Effect on Mobile Antenna Systems with Antenna Cluster Technique

[Rasmus Luomaniemi](#), [Albert Salmi](#) and [Anu Lehtovuori](#) (Aalto University, Finland); [Ville Viikari](#) (Aalto University & School of Electrical Engineering, Finland)

This paper studies the use of antenna cluster technique in mobile antenna systems and especially its use in reducing the user effect. The study is conducted with measurements of two different antenna designs using a hand phantom to represent the user holding the device. The results show that antenna designs based on the antenna cluster technique can retain good performance in the presence of a user. Furthermore, the cluster technique can also be used to reduce the user effect by adapting the cluster operation for different environments.

CP1.13 Theory, Design and Validation of a Tunable, Injection-Matched, 2-Port Antenna

[Long Shen](#), [Peter Mgyaya Kihogo](#), [Peter Gardner](#) and [Costas Constantinou](#) (University of Birmingham, United Kingdom (Great Britain))

The wideband frequency tunability of a two-port microstrip-fed patch antenna is achieved using injection matching. It is demonstrated that controlling the relative amplitude and phase shift between the excitation signals at port one and port two of the microstrip-fed patch antenna can tune its operating band to a lower wideband frequency range compared to the fundamental intrinsic resonance frequency of the corresponding one-port antenna. The resulting two-port antenna has an overall efficiency in excess of 80% with fairly stable radiation pattern in the E-plane. The antenna is suitable for use in wireless communication applications in the C-band.

CP1.14 Filter Design Considerations for an Integrated Doherty Power Amplifier - Antenna for Telecommunication Applications

[Petrie Meyer](#) (Stellenbosch University, South Africa)

A systems solution is proposed for incorporating filtering in integrated Doherty Power Amplifier - Antenna Element subsystems. It is shown that such topologies do not allow for filters in front of the antenna element, as the impedance matrix terminating the amplifiers has to conform to very stringent requirements. In the proposed system, the filtering function is split into pre- and post-filtering functions, with the latter only used for harmonic suppression, thus leaving the terminating impedance matrix unchanged at the design frequency. A case study is presented at 2.14GHz.

CP1.15 High Power mm-Wave Spatial Power Combiner Employing On-Chip Isolation Resistors

[Artem Roev](#) (Chalmers University of Technology, Sweden); [Rob Maaskant](#) (CHALMERS, Sweden); [Marion Matters-Kammerer](#) (Eindhoven University of Technology, The Netherlands); [Marianna Ivashina](#) (Chalmers University of Technology, Sweden)

A spatial power combiner interfacing four power amplifiers (PAs) with isolation load resistors to a single substrate integrated waveguide (SIW) is presented. The isolation load resistors are envisioned on-chip and have been optimized to provide both the optimal active load impedance for the interconnected PAs as well as to mitigate undesired power combiner coupling effects due to non-equal excitations between PA channels. The proposed solution is compared to an ideal Wilkinson combiner in the presence of non-ideal PAs. The main performance targets are the combined output power, gain, and power efficiency at the 1-dB compression point. Simulation results demonstrate that introducing isolation load resistors allows to significantly reduce the impact of a non-uniform excitation on the combiner performance metrics.

CP1.16 In-Antenna Power Combining for Highly-Integrated Millimeter-Wave Transmitters

[Benjamin Göttel](#) (Wellenzahl Radar- und Sensortechnik GmbH & Co KG, Germany); [Akanksha Bhutani](#) (Karlsruhe Institute of Technology, Germany); [Sören Marahrens](#) and [Thomas Zwick](#) (Karlsruhe Institute of Technology (KIT), Germany)

In this paper an in-antenna power-combining approach based on a circularly-polarized primary radiator is investigated. The radiation is based on the principle of an integrated lens antenna, where the primary radiator consists of a slot antenna with eight excitation elements. The output power of parallel amplifiers can be directly combined in the primary radiator itself without an additional power combiner network. The bandwidth, efficiency and axial ratio of the proposed primary radiator is investigated through simulations and wherever possible verified by measurements. In this work, the passive antenna, the connected amplifiers and the active antenna are investigated in detail and are finally compared with each other.

CP1.17 Circuit-antenna Interactions in Multi-port Active Antennas

[Peter Gardner](#), [Yi Wang](#), [Costas Constantinou](#), [Long Shen](#) and [Peter Mgyaya Kihogo](#) (University of Birmingham, United Kingdom (Great Britain))

This paper presents a review of research in which multiple port antennas have been used to absorb circuit or system functions into the antenna structure. Examples reviewed include image reject mixers, LINC modulators and push-pull amplifiers. In the context of a convened conference session on multi-port antennas, the review provides discussion points for further developments in this area.

CP1.18 Phase Distribution Optimization for 1-Bit Transmitarrays with Near-Field Coupling Feeding Technique

[Artem Vilenskiy](#) and [Mikhail Makurin](#) (Samsung Research Institute Russia, Russia); [Chongmin Lee](#) (Samsung Electronics Co., Ltd, Korea (South))

The paper presents a consideration of the optimum initial phase distribution for 1-bit transmitarrays with near-field coupling feeding technique. The study is based on the array factor decomposition into a series of continuous aperture distributions, which naturally includes the phase quantization errors. The previously proposed virtual focus approach is compared with the optimum quadratic initial phase distribution. Both methods are found to be very similar for specific values of distribution parameters in terms of far-field performance. Some further sidelobes level improvement is proposed.

CP1.19 Outspacing Phased Arrays for Mm-Wave 5G Base Stations

[B. G. M. \(Bart\) Van Ark](#), A. B. (Bart) Smolders and [Peter Smulders](#) (Eindhoven University of Technology, The Netherlands)

Emerging applications such as next generation wireless communications at mm-waves require active array antenna systems for meeting the high performance demands. This calls for new power-efficient and linear phased-array concepts. The combination of in-space outphasing of constant-envelope phasemodulated signals and a beamforming array is a promising architecture. In this paper, the influence of the outphasing configuration on the array factor and Error Vector Magnitude (EVM) is investigated. A prototype at 2.4 GHz was realized and characterized which shows good agreement with the theory. The outspacing array achieves an Error Vector Magnitude (EVM) of 5% without calibration.

Convened Poster 1-CS18: Applications of mm-Wave Gap Waveguide Technology-I

T02 Millimetre wave 5G / Convened Session / Antennas

Room: [A2 \(Poster Area\)](#)

Chairs: [Ahmed Kishk](#) (Concordia University, Canada), [Ashraf Uz Zaman](#) (Chalmers University of Technology, Sweden)

CP1.20 Microstrip to Ridge Gap Waveguide Transition for 28 GHz Steerable Slot Array Antennas

[Alireza Bagheri](#) (Gapwaves AB, Sweden & University of Twente, The Netherlands); [Hanna Karlsson](#), [Carlo Bencivenni](#), [Abolfazl Haddadi](#) and [Thomas Emanuelsson](#) (Gapwaves AB, Sweden); [Andrés Alayón Glazunov](#) (University of Twente, The Netherlands & Chalmers University of Technology, Sweden)

In this paper three types of contactless vertical transitions from microstrip to double ridge waveguide are presented. The designs are compact in size and robust, with improved isolation by employing a pin structure, making them ideal for 5G mmWave phased arrays. All transitions cover the 26.5–29.5 GHz band, their dimensions are less than half a wavelength in pitch and have insertion losses less than 0.6 dB. The three designs apply different matching strategies and offer a trade-off between bandwidth and PCB areas. Finally, the behavior within an array configuration is analyzed.

CP1.21 Groove Gap Waveguide Slot Array Based on Glide-Symmetric Holes

[Qingbi Liao](#) (KTH Royal Institute of Technology, Sweden); [Eva Rajo-Iglesias](#) (University Carlos III of Madrid, Spain); [Oscar Quevedo-Teruel](#) (KTH Royal Institute of Technology, Sweden)

Gap waveguide technology enables a cost-effective and low-loss manufacturing of high frequency fully metallic components. With this technology, the microwave components can be made in two pieces that are assembled together after-wards. Between these two pieces, an undesired air gap due to surface roughness or manufacturing tolerances may cause energy leakage. To prevent this leakage, periodic structures that produce electromagnetic bandgaps (EBGs) are used. Here, we compare the performances of two holey EBG surfaces, which are a conventional holey periodic metasurface and a metasurface with glide symmetry. The glide-symmetric structure has a wider EBG and a similar leakage prevention with less number of hole rows. Using glide-symmetric holes, a 4x4 slot array antenna is designed. This slot array is excited with the TE₄₀ mode and has a rotationally symmetric radiation pattern

CP1.22 Packaging Technique of Highly Integrated Circuits Based on EBG Structure for +100 GHz Applications

[Ahmed Hassona](#), [Vessen Vassilev](#), [Ashraf Uz Zaman](#) and [Herbert Zirath](#) (Chalmers University of Technology, Sweden)

This work presents an on-chip packaging concept suitable for monolithic microwave integrated circuits (MMIC) operating above 100 GHz. The concept relies on using an on-chip transition that couples the signal to a standard air-filled waveguide. The proposed solution utilizes an electromagnetic band-gap (EBG) structure realized using bed of nails to prevent the propagation of parallel plate modes and improve the coupling between the MMIC and the waveguide. The technique shows an average insertion loss of only 0.6 dB across the frequency range 110 - 155 GHz. Moreover, the concept is demonstrated in a D-band amplifier circuitry that is fabricated in an indium phosphide (InP) double heterojunction bipolar transistor (DHBT) technology. Experimental results show that the amplifier exhibits a maximum gain of 18.5 dB with no sign of propagation of any parallel plate modes. This work presents a high-frequency packaging solution which paves the way towards system integration above 100 GHz.

Convened Poster 1-CS19: Applications of mm-Wave Gap Waveguide Technology-II

T02 Millimetre wave 5G / Convened Session / Antennas

Room: [A2 \(Poster Area\)](#)

Chairs: [Eva Rajo-Iglesias](#) (University Carlos III of Madrid, Spain), [Jian Yang](#) (Chalmers University of Technology, Sweden)

CP1.23 A Compact Double-Layer Groove Gap Waveguide Power Divider with High Isolation

[Enlin Wang](#) (National Key Laboratory of Antennas and Microwave Technology, Xidian University, China); [Tianling Zhang](#) and [Lei Chen](#) (Xidian University, China); [Ashraf Uz Zaman](#) and [Jian Yang](#) (Chalmers University of Technology, Sweden)

A compact double-layer power divider with high isolation between output ports based on the groove gap waveguide (GGW) is presented in this paper. A five-port 1-to-2 power divider is designed base on the gap waveguide technology. Then a 1-to-8 power divider is built up by connecting seven 1-to-2 five-port power dividers. To achieve a compact size, the 1-to-8 power divider adopts a double-layer structure. The top layer is the feeding structure of the power divider, and the bottom layer contains the loads. The simulated results show that the proposed power divider exhibits the impedance matching bandwidth for the reflection coefficient below -15 dB is from 23.7 GHz to 30 GHz, and isolations between the output ports is more than 18 dB.

CP1.24 Mechanical Phase Shifter in Gap-Waveguide Technology

[Daniel Sánchez-Escuderos](#) (Universitat Politècnica de València, Spain); [José Ignacio Herranz-Herruzo](#) (Universidad Politècnica de Valencia, Spain); [Miguel Ferrando-Rocher](#) (Universitat Politècnica de València, Spain); [Alejandro Valero-Nogueira](#) (Universidad Politècnica de Valencia, Spain)

This contribution presents a low-loss mechanical phase shifter in gap-waveguide technology. The phase shifter is aimed at ground terminals for Ka-band satellite on-the-move applications. The use of the gap-waveguide technology allows to divide the device into two main blocks distributed in two levels: a lower-movable block, in charge of the power distribution and the phase shifting; and an upper-fixed block with the output waveguides. In this paper, the lower and upper blocks are designed using Groove-gap waveguides (GGW), and Ridge-gap waveguides, respectively. In order to couple the energy between the two levels, a slot on the metallic plane between the two layers is used. Results show a good performance in terms of phase shift between consecutive output ports, and return loss level at the input port, within the operating frequency band.

CP1.25 Considerations in Designing Inverted Microstrip Gap Waveguide Components

[Francisco Pizarro](#) (Pontificia Universidad Católica de Valparaíso, Chile); [Carlos Sanchez-Cabello](#) (Universidad Carlos III de Madrid, Spain); [Jose-Luis Vazquez-Roy](#) and [Eva Rajo-Iglesias](#) (University Carlos III of Madrid, Spain)

This article presents a parametric study of the properties of the inverted microstrip gap waveguide with respect to the effects that the characteristics of the substrate and the bed of nails employed in its design have on the transmission line behavior. The work will focus on the line impedance sensitivity and the losses. To this aim, a methodology based on simulations is described and we include as well some experimental verification. The results are of great interest for designers of circuits in this technology.

Convened Poster 1-CS27: Electromagnetics in MRI Applications

T05 Biomedical and health / Convened Session / Electromagnetics

Room: [A2 \(Poster Area\)](#)

Chairs: [Theodore Anderson](#) (Haleakala Research and Development, USA), [Vitaliy Zhurbenko](#) (Technical University of Denmark, Denmark)

CP1.26 Design of Distributed Spiral Resonators for the Decoupling of MRI Array Coils

[Danilo Brizi](#), [Nunzia Fontana](#), [Filippo Costa](#) and [Rocco Matera](#) (University of Pisa, Italy); [Gianluigi Tiberi](#) (London South Bank University, London, UK); [Angelo Galante](#) (University of L'Aquila, Italy); [Marcello Alecci](#) (University of L'Aquila and INFN-LNGS L'Aquila, Italy); [Agostino Monorchio](#) (University of Pisa & CNIT, Italy)

This paper describes a distributed filter layout for the decoupling of 7T Radio Frequency (RF) Magnetic Resonance Imaging (MRI) 1H planar array coils based on miniaturized spiral resonators as unit-cells. The spirals, opportunely designed in terms of resonant frequency and with an optimized layout to minimize their number, are placed on the same dielectric substrate of the RF coils. We demonstrated through numerical simulations the decoupling effectiveness of the distributed filter, observing a decoupling greater than -20 dB and satisfying matching levels (-30 dB) for the RF coils. The possibility to print on the same substrate both the coils and the filter results in practical advantages like excellent mechanical robustness and less sensibility to potential fabrication tolerances.

CP1.27 Hybridized Electric Dipoles Applications in Ultra-High Field MRI

[Marc Dubois](#) (Institut Fresnel, France); [Tania Vergara Gomez](#) and [Frank Kober](#) (Aix Marseille Univ, CRMBM, France); [Luisa Ciobanu](#) (DRF/I2BM/Neurospin/UNIRS, France); [Alexandre Vignaud](#) (Commissariat à l'Energie Atomique & NeuroSpin, France); [Redha Abdeddaim](#) (Aix Marseille University, France); [Stefan Enoch](#) (CNRS & Institut Fresnel, France)

In this work, we demonstrate how a set of hybridized resonators can be used to achieve efficient and tunable electromagnetic field control in the radiofrequency range. We show that near field coupling between multiple electric dipoles yields multiple eigenmodes whose response can be exploited to improve different canonical scenarios of magnetic resonance imaging (MRI) acquisitions. Two main examples will be covered: the metamaterial will be i) inserted in a human head coil at 7 Tesla and ii) coupled to a surface coil for small animal MRI at 17.2 Tesla.

CP1.28 A Nesting Approach for the Numerical Analysis of MRI Birdcage Antennas in the Presence of the Human Head

[Farzad Jabbari gargari](#) (Université Catholique de Louvain, Belgium); [Chan-Sun Park](#) (Yonsei University, Korea (South)); [Donia Oueslati](#) (ICTEAM Institute, Université Catholique de Louvain, Belgium); [Denis Tihon](#) (University of Cambridge, Belgium); [Clément Durochat](#) (Multiwave Imaging SAS, Marseille, Belgium); [Thibaut Letertre](#) (Aix Marseille University, CNRS, Centrale Marseille, Institut Fresnel, France); [Pierre Sabouroux Pierre Sabouroux](#) (Institut Fresnel, France); [Christophe Craeye](#) (Université Catholique de Louvain, Belgium)

Integral-equation approaches are among the solvers that can be used to analyse RF fields in MRI scanners, in particular when the human body is divided into a collection of homogeneous objects. This solver can be relatively intensive in terms of computation time and memory if the full solution is rerun everytime minor changes are considered in the MRI antennas. In this work, an efficient solving tool based on a nesting approach is proposed. The idea consists of avoiding re-computation of all the equivalent currents inside the body. A validation is provided for a simple structure with a commercial solver (CST); then by using a developed in-house code, the magnetic field inside the brain is shown when a birdcage antenna is used around the human head.

CP1.29 Experimental Validation of the Concept of an Opencage Head Coil for Ultra-High Field MRI

[Anton Nikulin](#) (PSL Research University, France); [Marc Dubois](#) (Institut Fresnel, France); [Tania Vergara Gomez](#) (Aix Marseille Univ, CRMBM, France); [Djamel Berrahou](#) (Multiwave Innovation SAS, France); [Alexandre Vignaud](#) (Commissariat à l'Energie Atomique & NeuroSpin, France); [Redha Abdeddaim](#) (Aix Marseille University, France); [Julien de Rosny](#) (CNRS, ESPCI Paris, PSL Research University, France); [Abdelwaheb Ourir](#) (Institut Langevin ESPCI Paris CNRS, France)

At 7T, birdcage coil is used as a transmit radiofrequency coil for head imaging. However for some applications sufficiently wide opening is required. Here, we propose to replace the shielded birdcage coil by an original volume coil that provides an access to the sample under examination while maintaining the desired homogeneous magnetic field distribution. The designed coil, called Opencage, is a non-periodic cylindrical cage. An approach based on transmission line modeling is developed to optimize it in order to provide homogeneous magnetic field. The result has been validated with a full wave numerical simulation. An experimental demonstration of such an opencage is shown. The magnetic field that is generated is close to the one of a conventional birdcage coil.

CP1.30 Matching and Decoupling Networks for Receive-only MRI Arrays

[Wenjun Wang](#), [Vitaliy Zhurbenko](#), [Juan Diego Sánchez-Heredia](#) and [Jan Henrik Ardenkjær-Larsen](#) (Technical University of Denmark, Denmark)

Mutual inductive coupling between elements of an MRI detector array greatly complicates the process of impedance matching of the array. This problem is even more severe in flexible arrays, where coupling matrix will change with the shape of the array. To overcome this problem a low noise amplifier can be integrated in each element with a network providing simultaneous noise matching and power mismatching for decoupling. This work describes the design of such impedance transforming networks that allow minimizing the influence of the inductive coupling and, at the same time, to ensure minimum noise figure of the connected low noise preamplifier. Different circuit topologies are analyzed. Their performance with regard to bandwidth and noise figure are compared. The networks ensure minimum noise figure and decoupling level to about 28 dB. The presented analysis would be useful for MRI and antenna array designs where element coupling presents a practical problem.


CP1.31 Enhanced Low Frequency MRI Using Flexible Shape Arrays Made of Standard Wire

[Juan Diego Sánchez-Heredia](#), [Wenjun Wang](#), [Rie Beck Olin](#), [Vitaliy Zhurbenko](#) and [Jan Henrik Ardenkjær-Larsen](#) (Technical University of Denmark, Denmark)

Flexible coil arrays are increasingly popular in magnetic resonance imaging (MRI), due to their superior anatomical fitting and patient comfort. Several coil concepts have been proposed, using self-resonant structures for the implementation of the detecting coils. In this work, we show that flexible coil arrays can be implemented in a simpler way, using standard flexible copper wire, as long as the decoupling between elements is kept high. The design approach proposed here can be extended to any frequency, and an example of a 7-channel array for 13C at 3T (32 MHz) is shown, where an SNR increase is obtained for a human head phantom, compared to state-of-the-art traditional coils.

CP1.32 Design and Implementation of Solenoid and Alderman-Grant Coils for Magnetic Resonance Microscopy at 7T

[Marios Masouridis](#), [Tim Dyrby](#) and [Vitaliy Zhurbenko](#) (Technical University of Denmark, Denmark)

Magnetic resonance microscopy is an advanced type of magnetic resonance imaging (MRI) where the image resolution goes beyond of conventional clinical MRI to image very small tissue samples.. The image resolution directly depends on the sensitivity of the detector coil, which is responsible for sensing weak magnetic fields from small samples in an MRI scanner. This paper describes the design and comparison of two magnetic field detection coils based on a solenoid and Alderman-Grant shapes. The coils are designed to provide over 90 field homogeneity in a 125 mm[^]  3 to image 1 mm IDD tissue punctured sample. . The performance of the two coils are evaluated theoretically, using electromagnetic simulations, and experimentally in a 7 tesla preclinical MRI scanner.

CP1.33 Design of a Quadrature Coil for MRI of Carbon in Human Liver at 7T

[Alajdin Rustemi](#) (Technical University of Denmark, DTU, Copenhagen, Denmark); [Vincent Boer](#) (Danish Research Centre for Magnetic Resonance, Denmark); [Vitaliy Zhurbenko](#) (Technical University of Denmark, Denmark)

Magnetic Resonance Imaging (MRI) is a method of generating images of soft tissues inside the human body by means of magnetic fields. The method is widely used for medical diagnosis as well as healthcare research. A crucial component of an MRI system is the radio frequency (RF) coil, which should efficiently generate and detect alternating magnetic fields. While typically hydrogen nucleus is used for imaging purposes, imaging other nuclei can vastly extend the capability of MRI. In this work, the design of a coil for carbon-13 high field MRI is presented. The coil is specifically designed for human liver imaging and provides 2 to 3 times better SNR which will result in higher image resolution, or 4 to 9 times faster scan time.

Convened Poster 1-CS57: Recent Research on Wind Turbines: EM Modelling and Measurements TOP

T11 Fundamental research and emerging technologies / Convened Session / Electromagnetics

Room: [A2 \(Poster Area\)](#)

Chairs: [Alexandre Chabory](#) (ENAC, France), [Frank Weinmann](#) (Fraunhofer FHR, Germany)

CP1.34 Wind Turbine Blade Deflection Sensing Using Blade-Mounted Ultrawideband Antennas

[Ondřej Franek](#) (Aalborg University & APMS Section, Denmark); [Shuai Zhang](#), [Kim Olesen](#) and [Patrick Eggers](#) (Aalborg University, Denmark); [Claus Byskov](#) (LM Wind Power, Denmark); [Gert Pedersen](#) (Aalborg University, Denmark)

Wind turbine blade deflection sensing system using ultrawideband radio links propagating along the blade is presented. Special focus is given to the challenges related to the multipath propagation along the blade. Results of electromagnetic modeling of the wireless link budget for deflected blades are presented. Some aspects of the sensing system that are different from a typical wireless communication link are discussed.

CP1.35 An Improved Forecast Method for the Interaction of Wind Turbines with Doppler VOR

[Thorsten Schrader](#) (Physikalisch-Technische Bundesanstalt, Germany); [Jochen Bredemeyer](#) (FCS Flight Calibration Services GmbH, Germany); [Thomas Kleine-Ostmann](#) and [Marius Mihalachi](#) (Physikalisch-Technische Bundesanstalt, Germany)

The installation of wind turbines leads to bearing errors of Doppler Very High Frequency Omni-Directional Ranges used for terrestrial navigation. The German air navigation service provider uses a simple model to calculate bearing errors. Here, the results of an improved forecast tool are compared to the results from the original tool, full wave simulations and measurements for a distinct trajectory close to the DVOR Hehlingen.

CP1.36 Validity Domain of the Odunaiya Expression for Computing the Conventional VOR Multipath Error

[Seif Ben-Hassine](#), [Alexandre Chabory](#), [Christophe Morlaas](#) and [Rémi Douvenot](#) (ENAC, France)

This work presents a method to determine the validity domain of the static Odunaiya expression for computing the VOR multipath error in the presence of wind turbines. The Odunaiya formula is considered valid when it gives the consistent response compared to a dynamic receiver model. This validity domain is then expressed in terms of the Doppler shift of the multipath with respect to the direct path. This leads to a geometric criterion that is illustrated.

CP1.37 An Overview of Wind Turbine Interference Research Activities at Fraunhofer FHR

[Frank Weinmann](#) (Fraunhofer FHR, Germany)

This paper provides an overview of research activities at the Fraunhofer Institute for High Frequency Physics and Radar Techniques FHR in Germany, with respect to possible interferences from wind turbines against radar systems. Starting from phenomenological effects observed in measurements behind a wind farm, various types of electromagnetic

simulations have been performed in order to investigate the principal scattering mechanisms.

CP1.38 Acceleration of Physical Optics Interactions Using Inhomogeneous Plane Waves

[Oumaima Mhadhbi](#) (Icteam, Universite Catholique de Louvain, Belgium); [Jean Cavillot](#) (Université Catholique de Louvain (UCL), Belgium); [Thomas Pairon](#) (Université Catholique de Louvain, Belgium); [Christophe Craeye](#) (UCL, Belgium)

The physical optics (PO) approximation is used for scattering analysis of electrically large conducting objects. The main object is to efficiently evaluate fields generated by a given domain on another domain that do not necessarily lie in each-others far fields, in a multiple-scattering context. Assuming a triangular discretization of the surfaces, a reference solution is computed by considering every pair of triangles. Two solutions are evaluated against that reference. One of them makes use of the far-field radiation pattern of the transmitting domain, and the other one is based on a limited number of Inhomogeneous Plane Waves (IPWs). Based on an example involving two cylinders, it is shown that the IPW approach is quite efficient and quite accurate in the near field.

Poster1-A07: Dielectric Resonator Antennas TOP

Antennas

Room: Exhibition Hall

P1.001 On-Chip Micromachined Dielectric Resonator Antennas Loaded with Parasitic Circular/Crescent Patch for mm-Wave Applications

[Mai Sallam](#) (The American University in Cairo & Katholieke Universteit Leuven, Egypt); [Mohamed Serry](#) (The American University in Cairo, Egypt); [Sherif Sedky](#) (AUC, Egypt); [Atif Shamim](#) (King Abdullah University of Science and Technology, Saudi Arabia); [Guy Vandebosch](#) (Katholieke Universiteit Leuven (KU Leuven), Belgium); [Ezzeldin Soliman](#) (The American University in Cairo, Egypt)

In this paper, two designs of micromachined dielectric resonator antennas operating at 60 GHz are presented. The antennas are fabricated using a single silicon wafer in which the dielectric resonator is located at one side of the wafer while the feeding network is located on the other side. The feeding lines are terminated by magnetic dipole which excite the dielectric resonator and causes its radiation. In order to enhance the bandwidth of the antenna, the dielectric resonator is loaded with circular/crescent patch antenna. Both designs are characterized by their fabrication simplicity, and high radiation performance. Additionally, the proposed antennas have wide impedance bandwidth reaching more than 10% (21%) of the central frequency for the circular/crescent patch loaded dielectric resonator antennas.

P1.002 Filtering Dielectric Resonator Antenna Using Terminal-Loaded Resonators

[Yan-Ting Liu](#) and [Kwok Wa Leung](#) (City University of Hong Kong, Hong Kong)

A new filtering dielectric resonator (DR) antenna (DRA) is presented in this paper. The DRA and its feedline provide a bandpass response. The antenna feedline consists of two terminal-loaded microstrip resonators (MRs), which gives two independently tuned nulls with an improved selectivity. For the DRA, it is excited in the HEM113 mode, serving not only as a radiator but also as the last-stage resonator of bandpass filter (BPF).

P1.003 An Asymmetric Star Design for the Dynamic Control of Quantum-Emitter-Coupled Plasmonic Nanoantenna Emission

[Hisham Ashraf Amer](#) and [Tamer Ali](#) (Zewail University of Science and Technology, Egypt); [Ashraf Badawi](#) (Zewail City of Science and Technology, Egypt)

Plasmonic single nanoantennas and meta-surfaces can both enhance and manipulate emission from potential quantum emitters while their layer-like nano thick structure renders them integrable into quantum and nano-devices. Here we proposed an Isotoxal Star Nanoantenna design, which when coupled to a single quantum dot emitter, offered unique resonant enhancements in both single and array arrangements. This enhancement was most established with the array, where 3 main polarization tunable behavioral states were identified, ones we described as double, single and steady mode patterns. This polarization driven functionality could offer a much-needed means of control over quantum emitters.

P1.004 Reconfigurable All-dielectric Transmission Lens for Vortex Beam Generation

[Jianjia Yi](#) and [Menglan Lin](#) (Key Laboratory of Integrated Services Networks, Xidian University, China); [Lina Zhu](#) (Xidian University, China); [Caijie Dong](#) (Key Laboratory of Integrated Services Networks, Xidian University, China); [Hailin Zhang](#) (Xidian University, China)

In this paper, a novel design for vortex beam generation is proposed by utilizing phase-gradient all-dielectric metamaterials. The pluggable element of proposed design is able to provide a full transmission-phase covering the range of 2π together with a high transmission efficiency. The elements corresponding to each value of phase are encoded to 360 modules. Thus, designed phase modules can be judiciously arranged to generate vortex beams carrying orbital angular momentum with different modes. Full-wave simulations validate the spiral-shaped phase fronts of the vortex beam. The proposed lens paves the way for the applications of vortex beam.

P1.005 Impedance Bandwidth Performance of TM106 Mode in Equilateral Triangular DRA

[Anoop P](#) (Indian Institute of Technology Guwahati, India); [Ratnajit Bhattacharjee](#) (Indian Institute of Technology, Guwahati, India)

In this paper a method for calculating the impedance bandwidth around the resonance frequency of TM106 mode excited inside an Equilateral Triangular Dielectric Resonator Antenna (ETDRA) is reported. The method utilizes the expression of quality factor (Q-factor) of TM106 mode, which is obtained through curve fitting approximation technique. Q-factor is a function of aspect ratio (a/h) and the material dielectric constant (ϵ_r). The bandwidth performances of such modes around the resonance frequencies for different degrees of impedance matching are discussed. The proposed method for calculating the impedance bandwidth is also validated by comparing with the practical bandwidth of the ETDRA reported in the literature.

Poster1-A09: Lens Antennas TOP

Antennas

Room: Exhibition Hall

P1.006 2-D Wide-Scanning Flat Luneburg Lens Antenna for 5G Communication

[Kunning Liu](#) (University of Electronic Science and Technology of China, China); [Shi Wen Yang](#) (University of Electronic Science and Technology of china, China); [Shi-Wei Qu](#), [Yikai Chen](#) and [Jun Hu](#) (University of Electronic Science and Technology of China, China)

This paper presents the design of a two-dimensional (2-D) wide-scanning flat Luneburg lens antenna operating at Ka-band. Based on the transformation optics (TO) theory, the conventional Luneburg lens is compressed to the flat form while keeping its beam focus characteristics unchanged. The 2-D flat Luneburg lens consists of six discretized lens layers made of all-dielectric materials. A 15-element linear patch antenna array is employed to feed the lens between the metallic parallel plates. Experimental results show that the 1-D beam-scanning lens antenna has a scanning coverage of $-50^\circ \sim 48^\circ$ in the azimuth plane, which can be obtained by switching the feed array elements. The 3 dB beamwidth in the elevation plane is 79° at 28 GHz due to the low profile of proposed lens antenna. With the advantages of low profile, wide-scanning and low cost, the proposed 2-D flat Luneburg lens antenna is attractive for 5G communication.

P1.007 Ka-band Multi-beam Planar Lens Antenna for 5G Applications

[Eduardo Garcia-Marin](#) (Universidad Autonoma de Madrid, Spain); [Dejan Filipovic](#) (University of Colorado at Boulder, USA); [Jose Luis Masa-Campos](#) (Universidad Autonoma de Madrid, Spain); [Pablo Sanchez-Olivares](#) (Universidad Politecnica de Madrid, Spain)

A low-cost solution for multi-beam antenna systems is explored for 5G applications in the 26-GHz band. A 4-port stacked-patch microstrip antenna is used as feeder of a perforated flat lens. Each feeder is placed in a different position with respect to the lens, yielding four high-directivity independent beams. The beams cover an angular range from broadside to a 30-degree steering with a gain over 18 dB. The antenna has been implemented by low-cost processes, employing Printed Circuit Board fabrication for the feeder and 3D printing for the lens.

P1.008 H-band Quartz-Cavity Leaky-Wave Lens Feeder with Novel Chip Interconnect

[Marta Arias Campo](#) (IMST GmbH, Germany & Delft University of Technology, The Netherlands); [Katarzyna Holc](#) (Fraunhofer Institute for Applied Solid Physics IAF, Freiburg, Germany); [Arnulf Leuther](#) (Fraunhofer Institute for Applied Solid State Physics, Germany); [Rainer Weber](#) (Fraunhofer IAF, Germany); [Simona Bruni](#) (IMST GmbH, Germany); [Nuria LLombart](#) (Delft University of Technology, The Netherlands)

Thanks to the large bandwidth availability, millimeter and sub-millimeter wave systems are getting more and more attractive to be used in a wide range of applications, such as high-resolution radar or high-speed communications. In this contribution, a wideband H-band (220-320GHz) integrated lens antenna concept fed by a quartz-cavity leaky-wave antenna is presented, to be used in a Frequency-Modulated Continuous Wave (FMCW) radar system. A novel chip interconnect technology, based on spray coating of dielectric materials with low dielectric permittivity, is introduced. This transition acts as a wideband, low loss transition between the GaAs front-end and the quartz antenna, avoiding the use of expensive waveguide split-blocks. Simulation results for the antenna with interconnect show good impedance matching and aperture efficiency higher than 78% over 100GHz of bandwidth. A prototype is currently under fabrication.

P1.009 Highly Integrable High Gain Substrate-integrated Planar Lens for Wide D-band Applications

[Loic Marnat](#) (CEA, LETI, Minatec, France); [Kossaila Medrar](#) (CEA Leti, France); [Laurent Dussopt](#) (CEA, LETI, Minatec, France)

We present for the first time a 3-bit linearly-polarized substrate-integrated planar lens with focal source antenna monolithically fabricated with a low cost PCB technology operating in D band. The effective volume occupied by this compact antenna is $10.5 \times 10.5 \times 4.52$ mm³. An experimental gain of 21.1 dBi at 153 GHz, an aperture efficiency of 22.3%, a

3-dB gain bandwidth greater than 19% and a cross-polarization level lower than 23 dB are demonstrated.

P1.010 Waveguide Switch Based on Ferrite Circulator for Antenna Beam Steering Applications

[Stephanie Smith](#) (CSIRO & Astronomy and Space Science, Australia); [Andrew Weily](#) (Antenna Engineer, Australia); [Ken Smart](#), [Nick Carter](#) and [Santiago Castillo](#) (CSIRO Astronomy and Space Science, Australia)

A low loss waveguide switch based on the ferrite circulator concept has been designed, analyzed with coupled electromagnetic and magnetostatic solvers, manufactured and tested for operation at 20GHz. A prototype single-pole three-throw switch is presented here. This switch will form part of a larger switch network for antenna beam steering applications.

P1.011 Zero Index Metamaterial for High Gain Array

[Jiang Tingyong](#) (EPFL, Switzerland); [Ning Hui](#) and [Zhou Heng](#) (Northwest Institute of Nuclear Technology, Switzerland)

Traditional metamaterial including metal wire grid was adopted to enhance the radiation performance of the antenna, especially for the gain, a critical parameter of antenna array. In this study, a novel zero index metamaterial (ZIM) is proposed, consisting of double metal layers with periodic circular perforation cells for horn antenna loading. Full-wave simulations are used to simulate the characteristics of horn array loaded with the proposed ZIM, and thus a significant enhanced performance is demonstrated due to zero refractive index. Experiments are performed to verify the effects of antenna array loaded with ZIM. The results show that the gain of the loaded array increases by nearly 2.3 dB, the maximum aperture efficiency of horn array increase from 0.50 to 0.88 at the resonant frequency while the tapering length is half of the optimum horn and the aperture dimension remains the same. Thus, the loaded horn array shows a promising application

P1.012 Ray-Tracing Analysis of the near and Far Fields of Focusing Geodesic Lens Antennas

[Germán León](#) and [Omar Orgeira](#) (Universidad de Oviedo, Spain); [Nelson Fonseca](#) (European Space Agency, The Netherlands); [Oscar Quevedo-Teruel](#) (KTH Royal Institute of Technology, Sweden)

Geodesic lenses are a class of rotational-symmetric lenses that recently regained interest for the design of multiple beam antennas. Key features of these lenses include mechanical simplicity, wide scanning range and high efficiency. In this paper, a hybrid model to analyze focusing geodesic lens antennas is described. The method combines a ray tracing analysis and a point source array model. This model allows to calculate the near and far fields of a geodesic lens antenna in few seconds. Some results of a lens antenna in the Ka-band are compared with full-wave simulations, validating the model despite small differences in the main beam. This paper also discusses the ability of geodesic lenses to focus the energy in the near field which could be of interest for some applications.

Poster1-A17: Array Antennas, Antenna Systems and Architectures (incl. Radomes)

Antennas

Room: Exhibition Hall

P1.013 Effect of Element Number Reduction on Inter-User Interference and Chip Temperatures in Passively-Cooled Integrated Antenna Arrays for 5G

[Yanki Aslan](#) and [Jan Puskely](#) (Delft University of Technology, The Netherlands); [Antoine Roederer](#) (Technical University of Delft, The Netherlands); [Alexander Yarovoy](#) (TU Delft, The Netherlands)

The impact of reducing the total number of elements in passively-cooled, chip-integrated and space-tapered 5G base station antenna arrays on inter-beam interferences and chip temperatures is investigated for multi-user space-division-multiple-access applications. A convex element position optimization algorithm is used to synthesize the array layouts with minimized side lobes within a pre-defined cell sector. The multi-beam radiation patterns are computed to study the average trend of the maximum side lobe level with the element number. Thermal simulations are also performed by considering the same EIRP for all the arrays. The results indicate that, after an optimal number of elements, adding more elements to an array does not help reduce the inter-user interference further or provide significant advantage on decreasing the chip temperatures.

P1.014 An Irregular Tightly Coupled Dipole Array with Wide Scanning Angles

[Yankai Ma](#) (University of Electronic Science and Technology of China, China); [Shi Wen Yang](#) (University of Electronic Science and Technology of china, China); [Yikai Chen](#), [Shi-Wei Qu](#) and [Jun Hu](#) (University of Electronic Science and Technology of China, China)

An innovative architecture is proposed for tightly coupled dipole arrays partitioned irregularly by domino-shaped tiles. A 192-port finite array operating at 8-12GHz has been implemented, where the port spacing is 0.576 wavelength at the highest frequency. In order to achieve large elevation angle scanning, differential evolution (DE) algorithm is used to synthesize active radiation patterns and suppress the port active reflection coefficients simultaneously. Simulation results show that the finite array is able to achieve almost no reduction in gain for scanning to broadside and only less than 2dB for scanning up to 60° as compared to fully populated arrays.

P1.015 Tiled Arrays: Low Cost Solutions for Next Generation Communication and Sensing Systems

[Nicola Anselmi](#) (ELEDIA Research Center, Italy); [Paolo Rocca](#) and [Andrea Massa](#) (University of Trento, Italy)

Array tiling is a promising architectural solution for next generation communication and sensing antennas. This work reports a review of the array tiling synthesis methodologies developed at the ELEDIA Research Center, assuring exact tiled array designs by exploiting analytic tiling theorems and optimization-based techniques. Single-shape tiling methods, as well as recent developed multi- shape tiling approaches are reviewed and discussed. An illustrative numerical example is reported, showing the effectiveness of the proposed approaches when considering square shaped tiles of different sizes.

P1.016 From "Hostile" to "Nice" Environment in Communication and Sensing

[Marco Salucci](#) (ELEDIA Research Center, Italy); [Giorgio Gottardi](#) (ELEDIA Research Center, University of Trento, Italy); [Paolo Rocca](#) and [Andrea Massa](#) (University of Trento, Italy)

Innovative concepts and ideas are presented for addressing paramount challenges in the design of future wireless systems. According to the "smart electromagnetic (EM) environment" paradigm, multi-path scattering phenomena arising in complex propagation scenarios must not be regarded as an obstacle (as done in classical antenna designs), but rather as a key-asset for realizing innovative and unconventional systems in order to meet the ever-growing demand of link quality and mobile data traffic. Within this context, a proof-of- concept is shown to provide an illustrative example of how the surrounding complex environment can be opportunistically exploited to yield a desired field distribution radiated by an antenna.

P1.017 An 8×8 Cavity Backed Waveguide Antenna Array for D-Band Backhauling Communications

[Sherif R. Zahran](#) and [Luigi Boccia](#) (University of Calabria, Italy); [Giandomenico Amendola](#) (IEEE, USA); [Stefano Moscato](#) (SIAE Microelettronica, Italy); [Matteo Oldoni](#) (SIAE Microelettronica S.p.A., Italy); [Dario Tresoldi](#) (SIAE Microelettronica, Italy)

This work proposes a novel design of two-layered antenna array targeting the D-Band region of the spectrum, likely to become the next commercial battleground for millimeter-wave communications. The design is basically an 8×8 cavity backed antenna array exhibits a thin planar footprint with volume of (30.1×26.4×1.235 mm³) and is capable of covering the 153-161GHz about 5%. Radiation characteristics are investigated for both 2×2 and 8×8 antenna arrays where the obtained peak gain values are 12.4 dB and 22.4 dB, respectively. Sharp beam, required for point to point communication, has been confirmed for 8×8 antenna array where the largest value of the half power beam width is 3.5°.

P1.018 Compact and Low Cost Linear Antenna Array for Millimeter Wave Automotive Radar Applications

[Imran Aziz](#) (Uppsala University & Mirpur University of Science and Technology, Mirpur Azad Jammu and Kashmir, Sweden); [Wan-Chun Liao](#) (Chalmers University of Technology, Sweden); [Hanieh Aliakbari](#) (Lund University, Sweden); [Winfried Simon](#) (IMST GmbH, Germany)

A low-cost microstrip patch antenna array is proposed in this paper for automotive radar applications in ISM24 GHz band. The elements of the center-fed array are connected in series to make a compact design with low complexity by obviating Wilkinson power divider. This approach also helps to reduce the dielectric losses of the array. A full-wave electromagnetics (EM) software EMPIRE XPU is used in the design process. The measurement results show 25 percent fractional bandwidth in terms of antenna impedance (23.75-30 GHz), 8.5 dBi maximum gain, 6 degrees half power beam width (HPBW), -12 dB side lobe level (SLL), and more than 50 dB isolation between TX/RX in the desired frequency range.

P1.019 A Novel Probabilistic Interval Arithmetic Method for Tolerance Analysis of Phased Arrays Beamforming Networks

[Nicola Anselmi](#) (ELEDIA Research Center, Italy); [Alessandro Polo](#) (ELEDIA Research Center, University of Trento, Italy); [Paolo Rocca](#) and [Andrea Massa](#) (University of Trento, Italy)

This work presents a novel Interval Arithmetic (IA) methodology for the probabilistic tolerance analysis of linear phased array beamforming networks. Efficient IA-based antenna array tolerance techniques are used to compute accurate and reliable power pattern bounds, and extended to provide a probabilistic analysis of the possible random patterns within the computed intervals. The computation of the probabilities is performed analytically, without executing time-consuming random simulations. Eventually, a preliminary result is reported to assess the effectiveness of the proposed technique, showing its advantage in yielding a more informative tolerance analysis with respect to IA-based state-of-art methods.

P1.020 Optimization of Modular Multi-Function Radar Architectures for Two-Way Pattern Sidelobe Minimization

[Nicola Anselmi](#) (ELEDIA Research Center, Italy); [Alessandro Polo](#) (ELEDIA Research Center, University of Trento, Italy); [Paolo Rocca](#) (University of Trento, Italy)

This contribution proposes a modular phased array architecture for simultaneous transmit/receive functionalities. Rectangular antenna apertures are partitioned into domino shaped tiles, arranged according to irregular layouts fully covering the available physical aperture area. The multi-functionality is obtained assigning to each module a single function (i.e., transmission or reception) with the aim of synthesize a two-way radiation pattern having the lowest possible sidelobe level. Towards this end, an innovative hybrid GA-based method is proposed for the joint optimization of the clustering scheme and the membership of each module to one of the two functions. A simple preliminary example is reported showing the effectiveness of the proposed irregular tiled architecture for multi-function radar systems.

P1.021 Improving Physical Layer Security Technique Based on 4-D Antenna Arrays with Pre-Modulation

[Kejin Chen](#) (University of Electronic Science and Technology of China, China); [Shi Wen Yang](#) (University of Electronic Science and Technology of china, China); [Yikai Chen](#), [Shi-Wei Qu](#) and [Jun Hu](#) (University of Electronic Science and Technology of China, China)

Four-dimensional (4-D) antenna arrays formed by introducing time as the forth controlling variable are able to be used to regulate the radiation fields in space, time and frequency domains. Thus, 4-D antenna arrays are actually the excellent platform for achieving physical layer secure transmission. However, traditional direction modulation technique of 4-D antenna arrays always inevitably leads to higher sidelobe level of radiation pattern or less randomness. Regarding to the problem, this paper proposed a physical layer secure transmission technique based on 4-D antenna arrays, which combine the advantages of traditional phased arrays, and 4-D arrays for improving the physical layer security in wireless networks. This technique is able to reduce the radiated power at sidelobe region by optimizing the time sequences. Moreover, the signal distortion caused by time modulation can be compensated in the desired direction by pre-modulating transmitted signals.

P1.022 On the Use of Symmetry for Shaped-Beam Antennas Installed onto 8-U CubeSats

[Eduardo Yoshimoto](#) and [Marcos V. T. Heckler](#) (Universidade Federal do Pampa, Brazil)

This work describes the application of symmetry schemes and the Firefly Algorithm (FA) for the optimization of planar antenna arrays. The method is applied to non-uniformly spaced arrays composed of isotropic antennas operating in S-Band (2.26 GHz) and installed onto an 8-U CubeSat. In order to demonstrate the potential of this technique, radiation patterns with isoflux distribution were synthesized, so as to allow illuminating the Earth surface with uniform power density. Good agreement with the desired masks has been obtained.

P1.023 Design of TCDA Avoiding Half-wavelength Limitation Using PC

[Seoungjung Kim](#) (Seoul National University, Korea (South))

Low-profile array antennas are important in many defense and commercial communication systems. Although tightly coupled dipole arrays (TCDAs) have several advantages, their bandwidth is limited by their ground plane. The use of resistive frequency-selective surfaces to overcome this limitation generates ohmic losses which then deteriorate the radiation efficiency of the array antenna. In this paper, we propose a 4x4 TCDA with no ohmic loss. The proposed array employs a polarization convertor to overcome bandwidth limitation when antenna height is half the wavelength (λ). The impedance bandwidth for VSWR < 3 covers 0.43-8.06 GHz to broadside radiation (18.7:1), and antenna height is 0.07 λ low at the lowest operating frequency.

P1.024 Global Optimization of Pencil Beams with Constrained Dynamic Range Ratio

[Maja Jurisic Bellotti](#) and [Mladen Vucic](#) (University of Zagreb, Faculty of Electrical Engineering and Computing, Croatia)

The synthesis of array patterns with reduced dynamic range ratio (DRR) of excitation coefficients is important because it enables better control of mutual coupling between antennas and simplifies the design of the feeding networks. In this paper, a method for global optimization of linear pencil beams with constrained DRR is presented. The optimization problem is formed which minimizes the sidelobe level for a given beamwidth and DRR. This problem is solved by using branch and cut algorithm. The proposed method supports positive and negative coefficients including the values of 1 and -1. The design is fast, enabling interactive experimenting with various numbers of antenna elements and DRRs.

P1.025 New Hexagonal CORPS-BFN for Multibeam Antenna Applications

[Carlos Biurrun-Quel](#) (Universidad Publica de Navarra & Institute of Smart Cities, Spain); [Antonio Montesano](#) (AIRBUS DS, Spain); [Iñigo Ederra](#) (Universidad Pública de Navarra & Institute of Smart Cities, Universidad Pública de Navarra, Spain); [JuanCarlos Iriarte](#) (Public University of Navarra & Antenna Group, Spain); [Carlos del-Rio](#) (Universidad Publica de Navarra & Institute of Smart Cities, Spain)

This work presents a new topology of a Coherently Radiating Periodic Structure - Beam Forming Network (CORPS-BFN) and its application for multibeam systems. A unit cell, consisting of a transition from a coaxial input to an intersection of three striplines with an angular span of 120 degrees, is proposed and analysed. A periodical replication of the cell gives rise to a uniform layer, allowing a proper matching of the ports of the network. Stacked layers allow in-phase propagation and distribution of the energy through the structure, increasing the number of output ports with each layer.

P1.026 Window-to-Polynomial Transform and Its Application in Antenna Array Design

[Goran Molnar](#) and [Marko Matijaščić](#) (Ericsson Nikola Tesla d. d. & Research and Development Centre, Croatia)

Windowing is a common method in signal analysis and in digital and spatial filter design. In many cases, adjustable windows are preferable since they offer a tradeoff between requirements, usually sidelobe level and mainlobe width. In this paper, we present a straightforward method for the design of windows with prescribed sidelobe level or mainlobe width. The method is based on the transform of a given window into the polynomial, thus enabling the use of polynomial approximation in the window design. Consequently, the method introduces an additional degree of freedom into the design process. The features of the method are illustrated with the design of linear antenna arrays having low dynamic range ratio and high beam efficiency. In particular, the adjustment of Taylor-Kaiser arrays, the design of arrays with minimum dynamic range ratio based on the transformed Gaussian windows, and the combined array design incorporating rectangular and Gaussian window.

P1.027 Design of a Dual-Circularly-Polarized Stacked Patch Antenna for SOTM Application at Ka-band

[Salvatore Liberto](#) and [George Goussetis](#) (Heriot-Watt University, United Kingdom (Great Britain)); [Andrew Christie](#) (Sofant Technologies Ltd, United Kingdom (Great Britain))

A dual-circularly-polarized stacked patch antenna subarray block for satellite on the move (SOTM) applications at Ka-band is presented. The proposed multilayer antenna is designed for the downlink band operating in the region of 18 to 20 GHz with compliant scan performance up to $\pm 40^\circ$ in both E- and H- planes. The subarray includes a highly integrated miniaturised 90o hybrid such that the antenna can operate in switchable circular polarisation. It also includes an integrated power splitting network based on Wilkinson. The antenna element size is 8.0 mm x 8.0 mm x 2 mm and achieves an impedance bandwidth and circular polarization bandwidth (3-dB axial ratio) of 2 GHz (18 - 20) GHz. Index Terms- Dual-Circularly-polarized stacked patch, phased array, SOTM, surface wave, highly-integrated, WPD, Branch-Line Coupler, Phased Arrays.

P1.028 Reflectarray Antenna Changing Beam Direction by Polarization

[Mei Fukaya](#) and [Shigeru Makino](#) (Kanazawa Institute of Technology, Japan); [Michio Takikawa](#) and [Hiromasa Nakajima](#) (Mitsubishi Electric Corporation, Japan)

In this report, the design of an element to realise a reflectarray, which emits beams in different directions, is discussed. The emission in different directions depends on the polarisation, radiation pattern, and gain when the element is applied to a mirror surface. As for the elements, independent phase control is realised by separating the elements into two layers for each polarisation, and a gradual phase change is obtained by varying the element length of the three line elements without using the line length ratio. As a result, when applied to a reflectarray, beams could be swayed in different directions for the H and V polarisations; however, the difference from the desired angle was 0.1 ° for the H polarisation and 0.3 ° for the V polarisation.

P1.029 Compact and Modular Ka-Band Front-end Concept for SATCOM and 5G

[Winfried Simon](#) (IMST GmbH, Germany); [David Schaefer](#) (IMST & Antennas & EM Modelling, Germany); [Simona Bruni](#) (IMST GmbH, Germany); [Marta Arias Campo](#) (IMST GmbH, Germany & Delft University of Technology, The Netherlands); [Simon Otto](#) and [Sybille Holzwarth](#) (IMST GmbH, Germany)

In this paper a modular and compact Ka-band front-end module based on PCB technology is presented. The integration and packaging techniques combine multi-layer PCB technology with waveguide RF feeding and antennas. Metallic waveguide and backplane act also as heatsink for the active circuitry. The modular concept can be applied to large antenna arrays to fulfill the application specific link budget requirements. Depending on the chosen core chips this design concept can be used for SATCOM or for 5G.

P1.030 Exploiting Real Far Field Patterns into the Multiplicity of Solutions for Linear Array Pattern Synthesis: Bandwidth Studies

[Aaron A Salas-Sanchez](#) (University of Trento, Italy & University of Santiago de Compostela, Spain); [Paolo Rocca](#) (University of Trento, Italy); [Juan Rodríguez-González](#) and [Francisco Ares-Pena](#) (University of Santiago de Compostela, Spain)

On the basis of equispaced linear array synthesis, bandwidth studies of performance for different type of distributions were developed in this communication. Antenna array pattern quality parameters such as maximum Directivity, Half-Power Beamwidth, Side-Lobe Level and ripple level were evaluated. Also, active impedance terms were studied: maximum absolute value, maximum real part, and absolute value of edge and central elements. To develop all these studies, embedded impedance terms -which can manage different lengths of the elements- were calculated by means of standard formulation. The key innovation of these studies is the inclusion of pure real pattern distributions into the discussion about bandwidth performance. Accordingly, the multiplicity of equivalent pure real and complex pattern distributions in presence and absence of ground plane have been analyzed.

P1.031 Optimized Polarization for Rotationally Tiled, Wideband, Dual-Polarized Vivaldi Arrays

[Elizabeth Bekker](#), [Johann W Odendaal](#) and [Johan Joubert](#) (University of Pretoria, South Africa)

Grating lobe mitigation was achieved for planar, wideband dual-polarized Vivaldi arrays through the rotation and translation of equilateral pentagonally shaped subarrays that form an approximately circular array. The subarray outlines can be adjusted in order to included fewer elements per subarray, but this will result in less grating lobe reduction. By using dual-polarized elements optimized polarization in the main beam can be achieved. The array patterns were determined with both measured and simulated single element patterns of the dual-polarized Vivaldi element. The mutual coupling between the elements in the array was shown to be negligible.

P1.032 On the Development of a Scanning Lens Phased Array at 550GHz

[Nuria LLombart](#) and [Sjoerd Bosma](#) (Delft University of Technology, The Netherlands); [Maria Alonso-delPino](#) (Jet Propulsion Laboratory, USA); [Cecile Jung-Kubiak](#) (NASA-JPL, Caltech, USA)

Recently, we have proposed a hybrid electro-mechanical scanning antenna array architecture suitable for highly directive phased arrays at submillimeter wavelengths with field-of-views (FoV) of +/-30 degrees. The concept relies on combining electrical phase shifting of a sparse array with a mechanical translation of an array of lenses. The use of a sparse phased array significantly simplifies the RF front-end, while the translation of a fly's eye lens array steers the element patterns to angles off-broadside, reducing the impact of grating lobes over a wide FoV. The mechanical movement of the lens array can be done using a low-weight, low-power piezo-actuators. In this contribution, we present the current progress in the development of a 550 GHz prototype.

P1.033 Minimization Techniques of Q in Circular Taylor-like Distributions

[Aaron A Salas-Sanchez](#) (University of Trento, Italy & University of Santiago de Compostela, Spain); [Paolo Rocca](#) (University of Trento, Italy); [Juan Rodríguez-González](#) and [Francisco Ares-Pena](#) (University of Santiago de Compostela, Spain)

On the basis of far field pattern distributions, a robust analytical approach for the determination of the Q value -linked to the classical concept of superdirectivity- has been developed. Circular Taylor distributions were used for showing the performance of the method in high efficiency distributions. In this sense, a minimization of this Q value is interesting

for avoiding power losses in the invisible region of the pattern. Accordingly, several numerical optimizations were performed and results of improving this Q -by allowing different relaxation levels in the requirements in efficiency- have been developed and their results are here discussed.

P1.034 Design and Simulation of a Dual Horn Antenna with Low Sidelobes and High Gain

[Ely Levine](#) (AFEKA, Academic College of Engineering, Israel); [Haim Matzner](#) (HIT-Holon Institute of Technology, Israel)

A dual horn antenna with low sidelobes and high gain was designed and simulated. The antenna is matched to SWR = 1.8 in the frequency range 6 - 9 GHz. The height of the antenna is 89.5 mm, the directivity is between 15.8 to 18.6 dBi, and the sidelobe level ranges are between -26.9 dB to -18.5 dB in the E-plane and between -36.4 to - 21.7 dB in the H-plane. It is shown that the directivity of the proposed antenna is higher by 4.7 dB than the directivity of a conventional horn having similar sidelobe level in the E-plane and same height, in the center frequency.

P1.035 Optimization of Excitation and Geometry of Linear Dipole Array Above PEC Ground Plane for Directivity Maximization

[Tomas Lonsky](#) (Czech Technical University, Czech Republic); [Jan Kracek](#) and [Pavel Hazdra](#) (Czech Technical University in Prague, Czech Republic)

The modal approach was used to maximize the directivity of the linear dipole array above a perfect electric conductor ground plane. The directivity was maximized for the direction perpendicular to the ground in which this array can produce maximal directivity from all directions by a proper excitation. The modal approach was also connected with the optimization of geometrical parameters of the array to obtain not only optimal excitation currents for the array with fixed geometry but also optimal geometry of the array. It was observed that, thanks to the presence of the ground, the currents are equiphase and can be set to be real.

P1.036 A Recursive Calibration Approach for Smart Antenna Beamforming Frontend

[Moh Chuan Tan](#) (University of Glasgow & RFNet Technologies Pte Ltd, Singapore); [Minghui Li](#), [Qammer H Abbasi](#) and [Muhammad Ali Imran](#) (University of Glasgow, United Kingdom (Great Britain))

In this work, a simple iteration-based approach is proposed for calibration and characterization of the frequency, phase and transmit power relationship in a smart antenna Radio Frequency (RF) beamforming frontend, which has a very low computational complexity. The RF frontend has been experimentally calibrated, and the beamforming results are verified with the 4 x 4 phase array. The RF frontend has been built using off-the-shelf components for easy realization. The proposed architecture with the closed-loop monitoring and control such as the power control (Pctrl), power detection (Pdet), in addition to the phase control allows an automatic calibration of the beamforming weights, which forms a necessary process to ensure the accuracy of the antenna array beamforming.

P1.037 Modeling of a Realistic Hybrid Metal-Plasma Transmit-array with Beam-scanning Capabilities

[Giulia Mansutti](#) (Università degli Studi di Padova, Italy); [Mohammad Hannan](#) (ELEDIA Research Center, University of Trento, Italy); [Federico Boulos](#) (ELEDIA@UniTN - DISI, University of Trento, Italy); [Paolo Rocca](#) (University of Trento, Italy); [Paola De Carlo](#) and [Antonio-D. Capobianco](#) (University of Padova, Italy); [Alberto Tuozi](#) (ASI - Italian Space Agency, Italy)

This paper presents the design of a realistic hybrid metal-plasma transmit-array antenna with beam- scanning capabilities. The antenna operates at 1.07 GHz and consists of an active metallic dipole, a metallic ground plane, and a set of cylindrical plasma discharges arranged in a 2D lattice. The main lobe of the antenna can be tilted towards different directions simply by turning on/off specific subsets of plasma discharges. Towards this aim, a two-steps optimization strategy based on the combination of a particle swarm optimization and of a genetic algorithm is adopted. The antenna has been modeled in CST Microwave Studio using realistic design parameters for the plasma discharges. In particular, each plasma bar includes not only the plasma material, but also the glass envelope and the metallic electrodes used to confine and generate the plasma respectively.

P1.038 Direction of Arrival Estimation Using Hybrid Spatial Cross-Cumulants and Root-MUSIC

[Murdifi Muhammad](#) (University of Glasgow, Singapore); [Minghui Li](#) and [Qammer H Abbasi](#) (University of Glasgow, United Kingdom (Great Britain)); [Cindy Goh](#) (University of Glasgow, Singapore); [Muhammad Ali Imran](#) (University of Glasgow, United Kingdom (Great Britain))

This paper presents a novel Direction of Arrival (DOA) estimation technique called Cross Cumulant-MUSIC (CC-MUSIC) which jointly employs higher order cumulant statistics and the root-MUSIC algorithm to perform high-resolution DOA estimation in low Signal-to-Noise Ratio (SNR) scenarios. From the simulation results based out of a 4 element uniform linear array and a far-field narrowband signal source, CC-MUSIC outperforms second-order DOA estimation techniques such as root-MUSIC and ESPRIT with a minimum average of 10.99% to 46.33% depending on the snapshot values at SNR of <15dB for a single signal source scenario and 39.1% to 83.8% for a multi-signal source scenario respectively when contaminated with an Additive White Gaussian Noise (AWGN). The work presented here has implications of future studies for optimization and real-world application where SNR environment is noisy while requiring accurate DOA estimation.

Poster1-A18: Reflector, Feed Systems, and Components

Antennas

Room: Exhibition Hall

P1.039 64 Element Active Phased Array as Focal Plane Array Feed for Reflector Antennas for mm-Wave Wireless Communications

[Antonius Johannes van den Biggelaar](#), [Ali Al-Rawi](#), [Ulf Johannsen](#) and A. B. (Bart) Smolders (Eindhoven University of Technology, The Netherlands)

Reflector antennas are utilized in a lot of applications that require a high gain antenna system. Conventionally, the reflector antenna is fed by a single radiating element, making the direction of the beam fixed. Using a focal plane array (FPA) as feeding mechanism, the magnitude and direction of the resulting beam can be controlled electronically. Using an in-house developed tool, the amplitude and phase settings for a 28 GHz active phased array antenna are determined in order to mimic the ideal feeding pattern for a certain reflector. The far-field of the FPA in combination with the reflector antenna is determined for a scan angle of 0 degrees and 3 degrees.

P1.040 On the Magnification Factor of Ring Focus Imaging Systems

[Giuseppe Orlando](#) (ThalesAleniaSpace Italia, Italy)

A closed formula that well approximates the magnification factor of centered dual reflector ring focus imaging systems is proposed. Numerical verifications carried out on specific optics geometries provide a good correlation to the analytical formula.

P1.041 K-band Feed and Transceiver with Compact Monopulse Tracking Coupler for Deep Space Applications

[Ignacio Montesinos-Ortego](#), [Zoran Golubicic](#) and [Beatriz Bedia](#) (TTI, Spain); [Fabio Pelorossi](#) (ESOC, ESA, Germany); [Filippo Concaro](#) (European Space Agency, Germany)

This paper firstly describes the global architecture of a complete transceiver working from 22.5GHz to 27GHz devised to illuminate the beam waveguiding (BWG) section of ESA deep space antennas (DSAs). Then it individually reviews each of the devices that compose it. From the corrugated horn to the diplexer, the choosing of their architecture is justified and their main simulated figures of merit are shown.

P1.042 Improving Modal Purity in Quadaxially Fed Quadruple-Ridged Flared Horn Antennas

[Jacobus M Kotzé](#) and [Petrie Meyer](#) (Stellenbosch University, South Africa)

This paper presents an improvement of a quadaxial feed designed for quadruple-ridged flared horn antennas. Selective laser melting (SLM) 3-D printing allows for complex structures to be realised as one unibody component. The integration of complex structures into the quadruple-ridged waveguide suppresses all higher order modes by more than 25 dB relative to the fundamental TE11 mode, thereby achieving pure-mode excitation over a 8.5:1 bandwidth. The impedance match is also significantly improved due to the relaxation of design constraints from previous manufacturing techniques. The quadaxial feed presented in this paper presents an ideal candidate for the integration with differential amplifiers and a quadruple-ridged flared horn for next generation radio astronomy reflector antennas.

P1.043 C Band Self Diplexed Tx/Rx Feed System for Telecom

[Rodolfo Ravanelli](#) (Thales Alenia Space Italy SpA, Italy); [Giuseppe Addamo](#) (Istituto di Eletr. e di Ingegneria dell'Inform. e delle Telecom. (IEIIT-CNR), Italy); [Roberto Mizzoni](#) (Thales Alenia Space Italia, Italy); [Oscar A. Peverini](#) (Istituto di Eletr. e di Ingegneria dell'Inform. e delle Telecom. (IEIIT- CNR), Italy); [Marcello Zolesi](#) (Thales Alenia Space, Italy); [Giuseppe Virone](#) (Consiglio Nazionale delle Ricerche, Italy); [Franco Perrini](#) (Thales Alenia Space-Italia S.p.a., Italy); [Fabio Paonessa](#) (National Research Council of Italy (CNR - IEIIT), Italy)

A reverse coupled self-diplexing feed-system operating in the extended C-band is addressed in this paper. Strict requirements in terms of electromagnetic performances, power handling and mass/envelope have driven the selected configuration. The design, validated through the measurement over a flight H/W, demonstrates the validity of the solution, making this product appealing for telecom reflector shaped space antennas.

P1.044 Multi-frequency Dual-polarization Spaceborne Microwave Radiometer Antennas

[Hongjian Wang](#) (National Space Science Center, China)

As part of the overall Haiyang2C (HY2C) ocean dynamic satellite research, atmospheric correction microwave radiometer (ACMR) used to correct atmospheric path delay in the radar altimeter has recently been developed. Observing antenna of ACMR with three frequency bands and dual polarizations is realized by an offset deployable dish fed by a common corrugated horn. The deployable reflector is made of carbon fiber composite (CFRP) supported by a CFRP frame that connect to the satellite deck, and the deployment of the dish is implemented by two hinges. The feeding subsystem has a loaded rings corrugated horn, an ultra wideband orthomode transducer (OMT) that covers almost 2:1 bandwidth ratio followed by bandpass filters. Measured results show that the VSWRs are lower than 1.5 throughout all three working bands (18.7 GHz, 23.8 GHz and 37 GHz), the cross-polarization levels (CPs) are below -20 dB.

P1.045 Upgrade to the K-band Uplink Channel for the ESA Deep Space Antennas: Analysis of the Optics and Preliminary Dichroic Mirror Design

[Matteo Marchetti](#) (University of Pavia, Italy); [Filippo Concaro](#) (European Space Agency, Germany); [Fabio Pelorossi](#) (ESOC, ESA, Germany); [Luca Perregrini](#) and [Marco Pasian](#) (University of Pavia, Italy)

Not available

P1.046 Full-wave Scattering from Reflector Antennas on Electrically Large Platforms Using low-Memory Computers

[Oscar Borries](#), [Peter Demeyer](#) and [Erik Jørgensen](#) (TICRA, Denmark)

We consider the use of full-wave integral equation techniques on scattering problems involving electrically large structures, and consider how an implementation of such techniques could use an inexpensive solid-state drive (SSD) rather than costly random access memory (RAM). We begin by showing how a Multi-level Fast Multipole Method (MLFMM) code based on Higher-Order (HO) basis functions has fundamental properties that make it feasible to use disk storage for the less frequently used algorithm data. Then, we show how the use of the SSD allows us to solve larger problems than the RAM of the computing platform makes room for. Finally we consider how this implementation has only a modest impact on the computational time, particularly when compared to the reduction in financial cost of SSD storage rather than RAM.

P1.047 Circularly Polarized Axially Corrugated Feed Horn for CubeSat Reflectarray Applications

[Miroslav J. Veljovic](#) and [Anja K. Skrivervik](#) (EPFL, Switzerland)

Reflectarray (RA) and transmitarray (TA) antennas that use the element-rotation technique require the radiation from the feeding antenna to be circularly polarized (CP). A CP axially corrugated horn antenna is developed as a feeding element for CubeSat RA and TA antennas. The CP operation is enabled using a septum polarizer. The all-metal geometry is attractive for space applications and allows the horn to be 3D printed in aluminum in a single piece. A prototype of the feed chain was fabricated using the Direct Metal Laser Sintering (DMLS) technique. The results of 3D simulations and VNA/far-field measurements of the feed chain are presented in this paper.

P1.048 Tunable Dichroic Cell for Multi-band Reflector Antenna System

[Miguel Salas-Natera](#) and [Roberto Garrote Moreno](#) (Universidad Politécnica de Madrid, Spain); [Eduardo Carrasco](#) and [Jose A. Encinar](#) (Universidad Politecnica de Madrid, Spain); [Ramón Martínez Rodríguez-Osorio](#) (Universidad Politécnica de Madrid, Spain)

This work presents a novel dichroic cell for multi-band reflector antenna systems that has two different configurations using a novel resonant element formed by rings connected with tuning stubs. The case study presented shows the design of a symmetrical cell using two resonant elements in both faces of the dichroic cell and the design of a non-symmetrical cell using one novel resonant element in one face of the cell and a single ring in the other face. These two configuration allows performing different topologies of dual band feeds.

P1.049 Contingency Mitigation Aspects for Reflector Based Satellite SAR Systems

[Patrick T.P. Klenk](#), [Jens Reimann](#), [Sigurd Huber](#) and [Marco Schwerdt](#) (German Aerospace Center (DLR), Germany)

Contingency mitigation, especially with respect to potential failures of Transmit-Receive Modules (TRMs) is a critical issue for SAR system concepts based upon planar phased array antenna fed large-deployable reflector (LDR) instruments. One promising approach is defocusing the LDR from the usually employed paraboloid shape. This opens a trade-space which has to be carefully investigated. Based on the current instrument and spacecraft geometry of Tandem-L we here assess the potential of reflector shaping to mitigate potential TRM failures. In particular we discuss the potential for re-optimization of the transmit pattern in such a contingency case. We find that for the defocused reflector, the impact of a potential TRM failure on the transmit pattern can be largely mitigated with acceptable impacts on nominal operations.

P1.050 Design and Measurement of Possible Wide-band 67-116 GHz ALMA Vacuum Window Anti-reflection Layers

[Peter J Speirs](#) (University of Bern, Switzerland); [Rocío Molina](#) (Universidad de Chile, Chile); [Elena Saenz](#) (European Space Agency, The Netherlands); [Paul Moseley](#) (European Space Agency, Switzerland); [Pavel Yagoubov](#) (European Southern Observatory, Germany); [Axel Murk](#) (IAP, Switzerland)

A new broad-band vacuum lens/window design is required for the new Atacama Large Millimeter/submillimeter Array (ALMA) band 2 receiver, intended to cover 67-116 GHz. A suitable anti-reflection coating (ARC) for this will be necessary. This paper presents the optimization of a candidate ARC design in ultra-high molecular weight polyethylene (UHMWPE), alongside simulations and measurements of candidate designs in silicon. Machined triangular grooves are used as the ARC for the UHMWPE candidates, and stacked cuboids for the silicon candidate design.

P1.051 Electromagnetic Analysis of the ngVLA Reference Design Antenna

[Sivasankaran Srikanth](#) (National Radio Astronomy Observatory & Associated Universities Incorporated, USA)

This paper presents computed efficiency, efficiency loss and increase in crosspolarization due to feed positioning errors on the Next Generation Very Large Array antenna. The rationale behind the choice of configuration of the antenna is explained. The design of the proposed feed is shown.

P1.052 Compact Quasi-Optical Power Combiner with Single Shaped Reflector

[Dong Xia](#) and [Liao Ma](#) (Beihang University, China); [Ming Jin](#) (Beijing University of Chemical Technology, China); [Ming Bai](#) (Beihang University, China)

In this paper, a compact and efficient quasi-optical power combiner configuration is presented. A single shaped reflector is utilized to directly convert the radiated beam from a planar feedhorn antenna array with arbitrary elements into single output beam. An efficient shaping technique based on reflector Poynting vector tracing is employed to synthesize the reflector, which shows obvious advantage over existing iterative wave-front shaping approaches. For validation, two shaped reflectors dedicated for a 3x3 as well as a 5x5 feedhorn array are designed. Satisfying power combining results are obtained through full-wave electromagnetic simulation.

P1.053 4-40 GHz In-Phase/180° Out-of-Phase Power Dividers with Enhanced Isolation

[Hadi Hijazi](#) (Lab-STICC/ENSTA Bretagne, France); [Marc Le Roy](#) (Lab-STICC, France); [Raafat Lababidi](#) (Ensta Bretagne, France); [Denis Le Jeune](#) (ENSTA Bretagne, France); [Andre Perennec](#) (Lab-STICC, France)

This paper demonstrates a single topology to implement ultra-wideband in-phase and 180° out-of-phase power dividers which will be dedicated for ultra-wideband frontends and balanced antenna systems that require a decent amount of isolation between ports. Both power dividers are formed of two couples of microstrip-to-slotline transitions terminated with radial stubs and then cascaded with a multisection Wilkinson power divider. A parametric study of the microstrip-to-slotline transition is performed to identify the main parameters' influence on its frequency response, followed by a full-wave optimization. Both power dividers are designed on RO4003C substrates and both have the same size of 22x38 mm2. Simulation results show that the power dividers can operate between 4 and 40 GHz with less than 6 dB insertion loss and with small amplitude and phase imbalances between output ports. And most importantly, both devices have at least 20 dB of isolation between output ports over the entire bandwidth.

P1.054 Broadband Beam-Steering with Focused Connected Arrays in Quasi-Optical Systems

[Alejandro Pascual Laguna](#) (Delft University of Technology & SRON, The Netherlands); [Daniele Cavallo](#) (Delft University of Technology, The Netherlands); [Jochem Baselmans](#) (SRON, The Netherlands); [Nuria LLombart](#) (Delft University of Technology, The Netherlands)

In this paper we propose an efficient integrated antenna solution based on a near-field focused connected array of slots on a membrane. The focused aperture provides (1) with broadband and highly efficient illumination of subsequent quasi-optical systems and (2) with the scanning capability inside a focusing system. The connected array antenna in turn allows for a fully planar solution that can synthesize a focused aperture whilst providing with broadband matching performance and low levels of cross-polarization.

Poster1-A19: Reflectarrays and Transmitarrays

Antennas

Room: Exhibition Hall

P1.055 A Millimeter-Wave Low-Profile and Metal-Only Transmitarray Antennas at 28 GHz

[Seyedeh Zahra Mousavirazi](#) (Institut National de la Recherche Scientifique (INRS), Canada); [Seyed Ramazannia Tuloti](#) (Electrical and Computer Engineering Faculty, Semnan University, Iran); [Tayeb A. Denidni](#) (INRS-EMT, Canada)

A novel high-gain and low-profile transmitarray antenna, operating at 28 GHz, is presented in this paper. A four-layer metal-only element is used to achieve a full transmission phase range of 360° for a transmission magnitude equal to or better than -1.2 dB. A transmitarray with a main beam at the broadside direction is simulated via CST software. The achieved simulation results show that the designed antenna with an aperture size of 95.25 cm2 at 28 GHz, has 26 dBi maximum gain. In addition, the proposed transmitarray antenna achieves a 17.3% 1-dB gain bandwidth and 38.2% efficiency.

P1.056 Dual-Polarized Dual-Frequency Ka-band Transmitarray Lens

[Enrique G. Plaza](#) and [Germán León](#) (Universidad de Oviedo, Spain); [Susana Loredo](#) and [Luis Fernando Herran](#) (University of Oviedo, Spain)

In this contribution, a new dual-frequency unit cell for transmitarrays is presented. This cell is based on a rectangular structure consisting of 4-stacked rectangular patches coupled 2-by-2 using a cross slot. One of the polarization is optimized to be transparent at 28 GHz, and the perpendicular one at 38 GHz. The cell provides a phase delay up to 300 degrees for each polarization at both frequencies. Furthermore, it allows to develop different radiation patterns for each frequency independently. In order to show the potential applications of this cell, a transmitarray antenna has been designed and simulated. The antenna can focus the energy on a near-field spot at 28 GHz using one polarization and it can also steer a beam to the broadside direction with the other polarization at 38 GHz.

P1.057 Transmitarray Antenna for Converged Vortex Beam Generation and Steering

[Irina Munina](#) and [Pavel A. Turalchuk](#) (St. Petesburg Electrotechnical University LETI, Russia); [Dmitry E Zelenchuk](#) (Queen's University of Belfast, United Kingdom (Great Britain))

This paper proposes a 1-bit transmitarray antenna excited by planar patch array in C band. The patch array generates a vortex beam, which is further compressed by the transmitarray. It has been demonstrated that by changing the phase distribution across the transmitarray one can change the vortex beam direction whilst preserving the orbital angular momentum properties.

P1.058 Design and Operation of a Smart Graphene-Metal Hybrid Reflectarray at THz Frequencies

[Arjun Singh](#) (Northeastern Univierstiy, USA); [Michael Andreollo](#) (AFRL, USA); [Erik Einarsson](#) (University at Buffalo, USA); [Ngwe Thawdar](#) (Air Force Research Laboratory, USA); [Josep M Jornet](#) (Northeastern University, USA)

Terahertz (THz)-band (0.1 - 10 THz) communication is envisioned as a key wireless technology to fulfill the demand for dense networks and higher data rates. To overcome the complex THz communication channel, smart reflecting surfaces can be utilized to facilitate Non-Line of Sight (NLOS) communication and increase efficiency. In this light, the use of new 2D nanomaterials, such as graphene, to design reprogrammable reflectarrays is being explored. This paper presents a novel graphene-metal hybrid reflectarray for THz communications. The radiating element of the reflectarray is designed to have strong reflection efficiency and high tunability. The trade-offs in the design of the hybrid element are exhaustively studied. The ability to perform continuous dynamic beamforming is presented. Extensive numerical results are provided to demonstrate the functionality of the reflectarray to engineer NLOS paths for communication.

P1.059 Low-profile TM Incident Retrodirective Metasurface Using AMC Surface

[Sun-Gyu Lee](#) and [Jeong Hae Lee](#) (Hongik University, Korea (South))

This paper presents a low-profile TM incident retrodirective metasurface (RMS). The unitcell is modeled by equivalent circuit to derive the impedance condition of RMS for full reflection phase coverage (FRPC). A PMC ground is required for a low-profile unitcell. The surface impedance of a slot layer is calculated from metasurface Generalized sheet transition conditions (GSTCs) and Babinet's principle. The resultant unitcell includes the artificial magnetic conductor (AMC), and the total height of the RMS with AMC ground is reduced by 50% compared with PEC ground. The RMSs composed of 10x7 supercells are designed using generalized Snell's law. The measured bistatic pattern and efficiency show good agreement with those of the simulation.

P1.060 Ultrawideband Transmitarray Employing Connected Slot-Bowtie Dipole Elements

[Lizhao Song](#) (University of Technology Sydney, Australia); [Peiyuan Qin](#) (University of Technology, Sydney, Australia); [Stefano Maci](#) (University of Siena, Italy); [Y Jay Guo](#) (University of Technology Sydney, Australia)

In contrast to using elements based on multi-layer frequency selective structures (FSS) with either true time delay lines or orthogonal modes, a novel technique to achieve ultrawideband transmitarray with consistent radiation patterns using connected antenna elements is presented in this paper. The element consists of a horizontally connected slot-bowtie dipole and vertical meander slot-lines. It can realize a 360o phase variation range at the highest frequency 17GHz, with transmission loss less than 3dB from 2GHz to 17GHz. The element is employed for an ultrawideband transmitarray design, realizing consistent boresight radiation patterns from 7GHz to 17GHz with antenna efficiencies from 38% to 60%. A prototype is fabricated and measured, and good agreements between simulation and measurement are obtained.

P1.061 A Triple-layer Wideband Transmitarray Antenna Using Finger-Type Slot Elements

[Guang Liu](#) and [Hongjian Wang](#) (National Space Science Center, China); [Yang Liu](#) (National Space Science Center & University of Chinese Academy of Sciences, China)

A novel triple-layer wideband transmitarray antenna using finger-type slot elements is presented in this paper. The unit-cell contains five longitudinal slots and a transverse slot on every thin metal layer, the simulated transmission coefficients of the unit-cell indicate that low loss and wideband properties are achieved at Ku-band. A wideband TA with diameter of 7.1 wavelengths using the proposed unit-cell is designed and simulated by commercial software Ansys 18.0. Simulated gain of 21.2 dBi at the center working frequency of 13.58 GHz and -1 dB gain bandwidth of 24.3% are achieved at Ku band. The simulated radiation patterns of TA show that low side lobe level and low cross polarization level are reached in broadband range.

P1.062 An Ultra-wideband Reflectarray Antenna Using Connected Dipoles for Multifunctional Systems

[Junxun Zhang](#) and [Long Zhang](#) (Shenzhen University, China); [Wenting Li](#) (Kent, China); [Yejun He](#) and [Sai-Wai Wong](#) (Shenzhen University, China); [Steven Gao](#) (University of Kent, United Kingdom (Great Britain))

A novel ultra-wideband reflectarray antenna using connected dipoles for multifunctional systems is proposed in this paper. The reflectarray element is composed of an elliptical dipole and a slot line which are printed on a single substrate. Neighboring elements are connected to achieve the ultra-wide bandwidths for both the impedance and the radiation pattern bandwidths simultaneously. By combining the advantages of conventional reflectarray antennas and connected array antennas, the proposed reflectarray antenna achieves ultra-wide bandwidth with greatly reduced feeding complexity and fabrication cost. As a proof of concept, a 354-element reflectarray antenna is designed. The presented reflectarray antenna maintains undistorted beams and high antenna gain over a bandwidth of 100%, i.e., from 10 to 30 GHz.

P1.063 Equivalent Dielectric Description of Transmit-arrays as an Efficient and Accurate Method of Analysis

[Sergio Matos](#) (Instituto Universitário de Lisboa, Portugal); [Jorge R. Costa](#) (Instituto de Telecomunicações / ISCTE-IUL, Portugal); [Parinaz Naseri](#) (University of Toronto, Canada); [Eduardo B. Lima](#) (Instituto de Telecomunicações & Instituto Superior Técnico, Portugal); [Carlos A.](#)

[Fernandes](#) (Instituto de Telecomunicacoes, Instituto Superior Tecnico, Portugal); [Nelson Fonseca](#) (European Space Agency, The Netherlands)

Transmit-arrays (TAs) provide cost effective solutions for various antenna applications, including satellite and terrestrial communications. Usually, these antennas have electrically large apertures, comprising thousands of fine-tuned subwavelength unit-cells. This makes full-wave simulations demanding in terms of computational resources, constraining the antenna design and optimization. Herein, we present an efficient method for the reduction of the TAs computational complexity that still provides accurate results for the main figures of merit of the antenna. For the chosen example, the simulation was 3 times faster and required 50% less memory. Yet, as the complexity of the problem is further scaled, this method is expected to become even more effective.

Poster1-A22: MIMO, Diversity, Smart Antennas & Signal Processing

Antennas

Room: Exhibition Hall

P1.064 Enhanced Low Band MIMO Terminal Antenna Based on Selective Feeding of Chassis Modes

[Hanieh Aliakbari](#) (Lund University, Sweden); [Qiuyan Liang](#) (Lund University, Sweden & Xidian University, China); [Buon Kiong Lau](#) (Lund University, Sweden)

Multiple-input multiple-out (MIMO) is a mature technology in modern wireless communications. However, it is challenging to implement multi-antennas for MIMO operation in compact mobile terminals, due to high mutual coupling and correlation among closely spaced antenna elements. Moreover, a conventional terminal chassis only offers one resonant mode below 1 GHz, complicating multi-antenna design. Recently, it has been shown that the chassis can be modified to facilitate a few resonant modes below 1 GHz. However, attempts to excite these modes selectively using a single feed per antenna port result in limited bandwidth and isolation. In this work, we propose dual-feed antenna ports to improve selective feeding of the resonant modes of an existing two-port MIMO terminal antenna below 1 GHz. Simulation results reveal significantly enhanced bandwidths of 30% and 15% for the two ports, as well as high isolation of over 32 dB.

P1.065 Yagi-Uda-Inspired Pattern Reconfigurable MIMO Antenna with Suppressed Harmonics and Minimum Parasitic Presence for WLAN Applications

[Phalguni Mathur](#) (Bharathiar University, India)

In this paper, a dual port multiple-input-multiple-output (MIMO) antenna with pattern diversity, integrated with a low pass filter to eliminate higher order harmonics is presented. The operating principle of the prototype is similar to that of Yagi-Uda antennas where multiple parasitic elements loaded with single or multiple switches are utilized to achieve the desired radiation characteristics. In the present design, however, only a single parasitic element loaded with just one switch is used to obtain six different H-plane radiation patterns within 2.4GHz WLAN band (2.4GHz-2.48GHz). Since the proposed antenna has less parasitic involvement, spurious ohmic losses are also minimized. The low pass filter, integrated with the microstrip feedline of the radiator, can suppress the higher order harmonics (atleast upto 11GHz) as well as simplifies the back-end circuitry of the whole MIMO antenna system itself. The prototype is fabricated on FR4 glass epoxy substrate with 1.6mm thickness.

P1.066 Convergence of OAM Beams Using Time-Modulated Concentric Circular Arrays

[Yang Wang](#), [Jie Liu](#), [Tao Hu](#), [Wenjun Jie](#) and [Donghua Yang](#) (Chongqing University of Posts and Telecommunications, China); [Alan Tennant](#) (University of Sheffield, United Kingdom (Great Britain))

In this paper, time modulation technique is applied to concentric circular arrays for synthesizing orbital angular momentum (OAM) beams with lower sidelobe levels. Compared with traditional concentric circular arrays, time-modulated concentric circular arrays (TMCCAs) add a high-speed RF switch to each array element. TMCCAs can simultaneously generate multiple OAM beams by periodically controlling the working state of elements. Furthermore, the genetic algorithm (GA) is exploited to optimize the switch-on duration of each element. Results show that under the condition of equal amplitude excitation, TMCCAs can successfully synthesize lower sidelobe OAM beams.

P1.067 Printed Dipole MIMO Antenna for Wireless Handheld Terminals

[Ahmad Abdelgwad](#) and [Mohammad Ali](#) (University of South Carolina, USA)

This paper introduces a pattern diversity dipole multiple-input multiple-output (MIMO) antenna for wireless handheld devices. With the help of three driven dipoles and two parasitic dipoles disposed of on the dielectric housing of a device, the proposed antenna achieves beam pointing along 30°, 180°, and 330° in the azimuth plane with 4-6 dBi gain. MIMO system analyses in free-space and next to user scenarios indicate excellent performance.

P1.068 Non-Gaussian Colored Noise Generation for Wireless Channel Simulation with Particle Swarm Optimizer

[Shaowei Dai](#) (University of Glasgow, Singapore); [Minghui Li](#), [Qammer H Abbasi](#) and [Muhammad Ali Imran](#) (University of Glasgow, United Kingdom (Great Britain))

Random Variable with different Probability Density Function (PDF) and Power Spectral Density (PSD) is a critical component for simulation of different wireless channel fading profile. To get a specific PSD for simulation of different multi-path scenario, the usual method is to pass a white noise through a filter with the required shape. But the filtering process will cause the change of random variable's PDF unless the input noise follows Gaussian Distribution. In this paper, a Particle Swarm Optimization (PSO) based method to generate Non-Gaussian noise by a pre-distortion filter and Inverse Transform Sampling (ITS) that meets both the requirement of PSD and PDF is described. As the solution is based on filtering, after the filter weight is found using PSO, the simulation could be carried out in a real-time manner compared to block-based methods. The numerical simulation confirms its effectiveness

P1.069 Dynamic Short-Range Sensing Approach Using MIMO Radar for Brain Activities Monitoring

[Mohammad Ojaroudi](#) (University of Limoges/CNRS, France); [Stéphane Bila](#) (XLIM UMR 7252 Université de Limoges/CNRS, France)

This paper presents a new concept of functional microwave imaging using m-sequence multiple-input multiple-output (MIMO) radar as a non-ionizing application of functional brain imaging. The underlying hypothesis is that, if we can detect local changes in blood volume inside the brain precisely enough, we can infer which parts of the brain are activated when performing various tasks. In this point of view, the main challenge in terms of MIMO radar framework is multi-target localization based on time of arrival (TOA) results. For this purpose, we present a multi-lateral localization approach in collocated MIMO-radar to detect a target inside brain medium. A system concept is introduced, and results from simulations using a simplified physical model are presented. To validate this, we focus on the waveform diversity and signaling strategies options for short range sensing. Simulated results validate the effectiveness of the proposed methods for precisely calculating the time-dependent location of target.

P1.070 A Three-Antenna Compact Micro-Diversity Module for Automotive Satellite Radio Reception

[Simon Senega](#) and [Sebastian Matthie](#) (Universität der Bundeswehr München, Germany); [Stefan Lindenmeier](#) (Universität der Bundeswehr, Germany)

A new compact micro-diversity module is presented which integrates three antenna elements with a scan-phase diversity circuit for satellite radio services at 2.3325 GHz. The module has a size of 55 mm by 55 mm by 26 mm, or 75 mm by 75 mm by 26 mm with a small additional ground plane brim. Two ring antenna structures working in different modes are combined with a monopole with roof capacitance in the center. The new module is tested in a strong fading environment near Detroit (USA) showing a significant reduction of audio mutes compared to a single antenna. On the dashboard as well as on the roof edge with a strong tilting angle, the micro-diversity achieves acceptable mute ratios while a single antenna would fail. The diversity module offers new mounting positions as well as new regions of reception due to additional gain and fast antenna diversity in fading environments.

P1.071 Maximum Ratio Transmission for OAM Mode Multiplexing Using Multiple UCAs

[Ayano Yamamoto](#), [Toshihiko Nishimura](#) and [Takeo Ohgane](#) (Hokkaido University, Japan); [Tomoya Tandai](#) and [Daisuke Uchida](#) (Toshiba Corporation, Japan)

In recent years, a new spatial multiplexing transmission scheme using the orthogonality of OAM modes has attracted attention with growth of the millimeter wave technology and demands for further high-speed large capacity transmission. A UCA is one of the candidates for generating multiple OAM modes. However, each mode's quality changes with distance when a single UCA of fixed diameter is used due to a property of Laguerre-Gaussian beam. In this paper, we propose maximum ratio transmission method by using multiple UCAs at the transmitter side for improving the quality and stability of each mode. Adjusting the amplitude and phase for each mode of all UCA, we can increase the received power and reduce the fluctuation depending on the transmission distance. The simulation results assuming free-space propagation show that high throughput is maintained over a wide transmission range even if radii of UCAs at transmitting and receiving sides are fixed.

Poster1-M01: Material Characterisation and Non-destructive Testing

Measurements

Room: Exhibition Hall

P1.072 A Numerical Study on Tomographic Imaging Using Guided Electromagnetic Waves

[Jochen Moll](#) (Goethe University Frankfurt am Main, Germany); [Duy Hai Nguyen](#) (Goethe University Frankfurt, Germany); [Viktor Krozer](#) (Goethe University of Frankfurt am Main, Germany)

Guided electromagnetic waves (GEW) have many interesting properties for structural health monitoring of technical structures. In this work, we study the tomographic imaging capabilities of GEW for a metallic plate using a sparse and distributed sensor array. Therefore, we have developed a 2-dimensional numerical model in CST Microwave Studio with flat bottom holes at different spatial locations. The resulting simulated data have been processed for tomographic damage imaging. In addition, we included a description of the signals in the pristine and damaged structure as well as an analysis of the signal difference coefficient (SDC).

P1.073 Advanced Calibration Method for Accurate Microwave Absorber Reflectivity Measurements at Oblique Illumination Angles

[Willi Hofmann](#), [Andreas Schwind](#) and [Christian Bornkessel](#) (Technische Universität Ilmenau, Germany); [Matthias Hein](#) (Ilmenau University of Technology, Germany)

The increasing complexity of new radio systems requires a change of measurement sites towards more sophisticated virtual electromagnetic environments. RF absorbers are essential elements of these environments to achieve the propagation conditions desired by obtaining well-defined measurement conditions and suppressing interfering signals. Optimal propagation conditions can only be achieved by sufficient knowledge of the frequency- and angle-dependent reflectivity of RF absorbers. For this purpose, an advanced calibration procedure for reflectivity measurements at oblique illumination angles based on a combination of the established RCS- and NRL-arch methods is proposed. Measurement results obtained by the new technique show good consistency with the NRL-arch but with the advantage of accessing the angle-dependent behavior of the RF absorbers. The proposed calibration procedure will not only help manufacturers to characterize their absorbers more effectively, but additional knowledge of the off-normal reflectivity will also contribute to the optimization of measurement sites such as virtual electromagnetic environments.

Poster1-M03: Near-field, Far-field, Compact and RCS Range Measurement Techniques

Measurements

Room: Exhibition Hall

P1.074 Off-the-shelf Optical Antenna Feed System

[Christopher G Hynes](#) and [Rodney Vaughan](#) (Simon Fraser University, Canada)

An optical antenna feed system reduces or eliminates conducting feed cable effects and provides much more accurate antenna far-field pattern measurements. Optical feed systems can be expensive and require custom design. We present a simple optical feed system for antenna pattern measurement systems, using low-cost off-the-shelf components. We describe the performance-limiting factors of the optical system, and compare measurement results from an MVG Stargate 64 using a standard coaxial cable feed system with those from the optical feed system. The pattern accuracy improvement is significant, demonstrating that this type of system offers a simple and low-cost upgrade for antenna measurement.

P1.075 Height Profiles of Typical Automotive Landmarks Using Tomographic Compact-Range Measurements

[Roland Moch](#) and [Dirk Heberling](#) (RWTH Aachen University, Germany)

Height estimation of radar targets is of particular importance for self-localization and autonomous driving. It is an essential part of the risk assessment and makes it possible to assess whether certain obstacles can be traversed or an evasive maneuver must be initiated. In order to evaluate such situations as reliably as possible, high demands are placed on the classification of radar targets. New possibilities are opened up by determining not only the total height, but an intensity distribution resolved by the height. To prove the advantages, typical landmarks, namely two signs and a guide post, were measured in a compact antenna test range in the E-band frequency range. It is shown that besides the total height also the most important features of the landmarks can be identified in the height profile. This improves the overall perception of the environment as well as the detection of additional indicators for self-localization.

P1.076 A Novel Indoor and Outdoor Drone-Based Antenna and RCS Measurement Facility

[Pierre Massaloux](#) (CESTA, France)

Indoor RCS measurement facilities are usually dedicated to the characterization of only one azimuth cut and one elevation cut of the full spherical RCS target pattern. In order to perform more complete characterizations, a new experimental layout has been developed at CEA. The use of multi-rotor UAVs for antenna or RCS measurements opens up breathtaking possibilities in indoor or outdoor measurements. Industrial purpose multi-rotor UAVs provide an excellent ground for research and development activities and for proof-of-concept measurements. This paper presents the new measurement system and the different results obtained on RCS measurements.

P1.077 On the Influence of the Transformation Matrix in Compressed Spherical Near-Field Measurements

[Cosme Culotta-Lopez](#) and [Dirk Heberling](#) (RWTH Aachen University, Germany)

The radiation characteristics of an object are represented by the coefficients vector of a Wigner-D expansion. For most physical antennas and with appropriate choice of the expansion's center, the coefficients vector, also called the Spherical Mode Coefficients (SMCs) vector, is proven sparse. The sparsity of the vector allows the undersampling of the system and the reconstruction of the SMCs vector by application of l1-minimization methods. However, the reconstructed results, for equivalent analytical formulations of the problem, change depending on the used transformation matrix. In this work, the SMCs of two antennas calculated from measurement data are used to simulate compressed spherical near-field measurements. The sampling schemes used for the compressed measurements are calculated based on the minimum coherence of the sampling matrix for the basis functions. The reconstruction error is assessed for a different formulation of the problem, using a different transformation matrix and highlighting the performance difference.

Poster1-M04: Data Acquisition, Imaging Algorithms and Processing Methods

Measurements

Room: Exhibition Hall

P1.078 An Improved Receiver for Harmonic Motion Microwave Doppler Imaging

[Damla Alptekin Soydan](#) and [Ümit İrgin](#) (Middle East Technical University, Turkey); [Can Baris Top](#) (Aselsan Inc., Turkey); [Nevzat Gençer](#) (Middle East Technical University, Turkey)

Harmonic motion microwave Doppler imaging is a novel imaging method that combines focused ultrasound and radar techniques to obtain data based on mechanical and electrical properties of the tissue. In previous experimental studies, scanning time was high, the signal-to-noise ratio was low, and the multi-frequency operation was limited. In this study, we improved the receiving system with a low noise amplifier which led to an increase in signal-to-noise ratio. A breast phantom containing a cylindrical tumor of size 3 mm × 3 mm inside a homogeneous fat was built. An area of 40 mm × 40 mm is scanned in 45 minutes which is 50 % of the previous scanning time. The vibration frequencies which are higher than 35 Hz are employed for the first time to create 2D images. The increase in the vibration frequency resulted in the improvement of resolution; however, the signal-to-noise ratio of the images deteriorated.

P1.079 Interpretation of the Physical Layer Measurements of Smartphones as Measures of Exposure to Electromagnetic Fields

[Sascha Schießl](#), [Thomas Kopacz](#) and [Dirk Heberling](#) (RWTH Aachen University, Germany)

The monitoring of exposure to electromagnetic fields emitted by mobile radio networks is necessary for a responsible operation of these networks. A possible alternative to classical exposure assessment methods for a time-continuous and area-wide exposure monitoring is a crowdsourcing-based approach that relies on the use of ordinary smartphones. This paper discusses the interpretation of signal strength indicators measured by mobile phones in LTE networks and explains how instantaneous or maximum exposure is related to them. Long-term measurements of a smartphone and a field strength meter are presented in comparison, which show the time-dependent variation of the utilization of the cell. In addition, it is demonstrated how the measurement data of the smartphone have to be adjusted due to the measurement characteristics resulting from the considered signal components in order to correspond correctly with the exposure. The results show that RSSI is suitable for tracing variations in exposure over the day.

P1.080 Processing Azimuth-Time Domain Aliasing in Spaceborne Sliding-Spotlight SAR Imaging

[Yunxia Wang](#), [ShunSheng Zhang](#) and [Yuming Jia](#) (University of Electronic Science and Technology of China, China)

This paper proposes a modified two-step processing approach to deal with the problem of azimuth time domain aliasing in processing high resolution spaceborne sliding spotlight synthetic aperture radar (SAR) data. The signal model of spaceborne SAR is formulated, which includes the geometric model, echo model and Doppler bandwidth. This paper proposes a modified approach through parameter design to avoid azimuth-time domain aliasing. The sliding factor has a critical value for the azimuth-time aliasing, which meet the requirement of azimuth resolution and large imaging scene. The effectiveness of the proposed approach for sliding-spotlight SAR imaging is verified with simulation data for multi-point targets.

Poster1-P02: Propagation Modelling and Simulation

Propagation

Room: Exhibition Hall

P1.081 Wall Parameters Sensitivity for Indoor Radio Waves Attenuation

[Eran Greenberg](#) (RAFAEL, Israel); [Gil Segal](#) (Rafael, Israel)

In this contribution we investigate the propagation through walls and the loss sensitivity to a variety of parameters including permittivity, conductivity, wall width, incident field angle, frequency and polarization. The wall is modeled as a finite depth homogeneous slab and its influence is calculated using the effective Fresnel transmission coefficient. A statistical investigation reveals that as increasing the wall conductivity or width the loss is increased, the general influence of the frequency and permittivity is almost negligible, and the loss for perpendicular polarization is higher than for parallel polarization. Sensitivity analysis shows that the incidence angle, conductivity and wall width are the most important medium parameters and the knowledge of only these input variables values is sufficient to estimate the loss variance.

P1.082 Assessment of sub-THz Mesh Backhaul Capabilities from Realistic Modelling at the PHY Layer

[Grégory Gougeon](#), [Yoann Corre](#) and [Mohammed Zahid Aslam](#) (SIRADEL, France); [Simon Bicaïs](#) and [Jean-Baptiste Doré](#) (CEA, France)

Spectrum above 90 GHz is a key promising investigation domain to offer future wireless networks with performance beyond IMT 2020 such as 100+ Gbit/s data rate or sub-ms latency. As the propagation is strongly constrained at those frequencies, the short-range connectivity is a relevant target application. However, the huge available bandwidth can also serve the backhaul transport network in the perspective of future ultra-dense deployments, and massive fronthaul data streams. This paper investigates the feasibility and characteristics of the sub-THz mesh backhauling either installed in the streets or inside a large venue. The study relies on the highly realistic simulation of the physical layer performance, based on detailed geographical representation, ray-based propagation modelling, RF phase noise impairment, and a new robust polar modulation. It is shown that each link of a dense mesh backhaul network can reliably deliver several Gbit/s per 1-GHz carrier bandwidth.

P1.083 Joint Statistical Modeling of Received Power, Mean Delay, and Delay Spread for Indoor Wideband Radio Channels

[Ayush Bharti](#) (Aalborg University, Denmark); [Laurent Clavier](#) (Institut Mines-Telecom, Telecom Lille & IEMN / IRCICA, France); [Troels Pedersen](#) (Aalborg University, Denmark)

We propose a joint statistical model for the received power, mean delay, and rms delay spread, which are derived from the temporal moments of the radio channel responses. We begin by analyzing indoor wideband measurements from two different data sets. It appears that the temporal moments are strongly correlated random variables with skewed marginals. Based on the observations, we propose a multivariate log-normal model for the temporal moments, and validate it using the experimental data sets. The proposed model is found to be flexible, as it fits different data sets well. The model can be used to jointly simulate the received power, mean delay, and rms delay spread. We conclude that independent fitting and simulation of these statistical properties is insufficient in capturing the dependencies we observe in the data.

P1.084 A Bandwidth Scalable Millimetre Wave Over-The-Air Test System with Low Complexity

[Erich Zöchmann](#) (PIDSO - Propagation Ideas & Solutions GmbH); [Terje Mathiesen](#) (Norwegian University of Science and Technology, Norway); [Thomas Blazek](#) and [Herbert Groll](#) (TU Wien, Austria); [Golsa Ghiaasi](#) (Norwegian University of Science and Technology, Norway)

In this work, we show the design and validation of a testbed for over-the-air testing millimetre waves equipments. We have extended the frequency capabilities of a baseband channel emulator which is capable of emulating non-stationary channels, to higher frequencies. To assure that the propagation between devices-under-test and the RF-frontend of the emulator is only a line-of-sight link, we have isolated the devices-under-test in two anechoic chambers. We characterize the testbed at 57 GHz by means of frequency sweeps for two artificial cases: when the emulator is replicating a one-tap channel and a two-tap channel. Finally we demonstrate the system functionality through reproduction of channels which were acquired during a vehicular millimetre wave measurement campaign conducted in Vienna in 2018.

P1.085 Achievable Synchronisation Gain in Uncalibrated Large Scale Antenna Systems

[Jens Abraham](#) and [Torbjörn Ekman](#) (Norwegian University of Science and Technology, Norway)

Large scale antenna systems are used to exploit spatial multiplexing gains in massive MIMO systems. To realise those gains, channel state information has to be acquired at a base station. However, an initial control channel has to be provided to synchronise time and frequency at the user. This control channel should be undirected to cover the base stations operational area and can therefore not exploit the coherent array gain without additional strategies. Beam sweeping has been proposed to provide increased spatial coverage. Its performance for large scale antenna systems in Rayleigh and Rician fading environments is analysed. Even an orthogonal basis of antenna weights for full spatial coverage can not provide the full array gain. The results quantify the gap between achievable synchronisation and full array gain for uncorrelated antennas. Closed form solutions for the distribution of the gain gap under Rayleigh fading conditions are derived.

P1.086 Electromagnetic Pipeline Coating Communication for IoT Condition Monitoring of Subsea O&G Pipelines

[Knut Grythe](#) (SINTEF, Norway); [Irene Jensen](#) (SINTEF ICT, Norway); [Ole Knudsen](#) (SINTEF Industry, Norway)

A near real time situation awareness of an O&G pipeline enhances the response time in case of failure and supports a digital twin. We present results from a project on a pipeline IoT based upon electromagnetic (EM) field multi hop communication in the pipeline coating. A transverse electromagnetic (TEM) mode is excited in the coating via an inner semi-ring and an outer full-ring, where the example pipe supports frequencies from 1 MHz to 70 MHz with power loss below 2 dB/meter. A 50 mm long sacrificial anode adds losses from 2 dB at 50 MHz to 11 dB at 1 MHz. Measurements at 3.8 MHz on a 216 meters long pipeline gave an attenuation of 0.22 dB/m compared to simulated 0.35 dB/m, confirming the applicability of the simulations for designing the IoT solution. The results illustrate the multi hop capabilities covering nodes beyond the neighbor of the EM transmitting node.

P1.087 Combined Antenna-Channel Characterization for Wireless Communication from Horse Hoof to Base Station

[Jasper Goethals](#) (Ghent University & IMEC, Belgium); [Gunter Vermeeren](#) (Ghent University, Belgium); [Denys Nikolayev](#) (Institut d'Électronique et de Télécommunications de Rennes (UMR CNRS 6164), France); [Margot Deruyck](#) (Ghent University - IMEC, Belgium); [Luc Martens](#) (Ghent University-IMEC, Belgium); [Wout Joseph](#) (Ghent University/IMEC, Belgium)

This paper presents a design of an antenna in the complex environment of the horse hoof for sub-gigahertz (868 MHz) communication. The influence of the leg and the ground on the performance were examined by means of finite- difference time-domain simulations. Furthermore, an adaptation was presented to increase the efficiency of the antenna. Adding the ground to the model results in the ground absorbing most of the radiations which leads to a total efficiency drop of 50%. When the horseshoe is connected to the device, the antenna is not tuned anymore, yet the the total efficiency stays the same. This shows that connecting the device to the horseshoe leads to better radiation efficiency. When using LoRa technology, this setup can reach 1631 m if the hoof is in the air. When the hoof is on the ground, only a range of 115 m is estimated

P1.088 Remote Monitoring and Propagation Modeling of EM Side-Channel Signals for IoT Device Security

[Seun Sangodoyin](#), [Frank Werner](#) and [Baki B Yilmaz](#) (Georgia Institute of Technology, USA); [Chia-Lin Cheng](#) (Georgia Tech, USA); [Elvan Ugurlu](#), [Nader Sehatbakhsh](#), [Milos Prvulovic](#) and [Alenka Zajic](#) (Georgia Institute of Technology, USA)

This paper presents results from an investigation into long-range detection and monitoring of Electromagnetic (EM) side-channel signals leaked from Internet-of-Things (IoT) and Field Programmable Gate Array (FPGA) devices. Our work shows that operational information and program activities of the IoT and FPGA modules can be garnered at distances

excess of 25 m in an indoor Line-Of-Sight (LOS) environment, while at about 10 m in an indoor (through the wall) Non-Line-Of-Sight (NLOS) scenario. We provide a propagation model that can be used to predict the received power (and corresponding variation i.e., shadowing gain) of leaked EM side-channel signals at various distances and scenarios. A standard benchmark program bitcount used in the performance evaluation of ARM-based microprocessors and a microbenchmark SAVAT running on an IoT device were detected and monitored remotely in our work.

P1.089 Analysis of Delay Characteristics at 4.9 GHz and 28 GHz in an Indoor Industrial Scenario

[Zuolong Ying](#), [Tao Jiang](#), [Pan Tang](#) and [Jianhua Zhang](#) (Beijing University of Posts and Telecommunications, China); [Lei Tian](#) (Beijing University of Posts and Telecommunications & Wireless Technology Innovation Institute, China)

In this paper, we present measurements that were conducted at 4.9 GHz and 28 GHz. Based on the measured data, it can be found that the root mean square (RMS) delay spread (DS) is well fitted by a lognormal distribution. Besides, the mean RMS DS at 28 GHz is much smaller than that at 4.9 GHz. Compared with 3GPP standard, the mean RMS DS in the indoor industrial scenario is much larger than that in the traditional indoor office scenario. At last, the effects of the TX-RX distance and antenna heights on RMS DS are investigated. By modeling DS as a function of the TX-RX distance, it is found that in the line-of-sight (LOS) scenario, RMS DS increases linearly with the TX-RX distance. Finally, it is found that in non-line-of-sight (NLOS), the mean RMS DS in the clutter-elevated scenario is 12 ns smaller than that in the clutter-embedded scenario.

P1.090 Analysis of Phase Evolution Impact in SIMO Operation in Distributed Transceiver Systems

[Luis Lenin Trigueros](#) (Universidad Publica de Navarra and Institute of Smart Cities, Spain); [Peio Lopez Iturri](#) (Universidad Publica de Navarra and Institute for Smart Cities, Spain); [Leyre Azpilicueta](#) (Tecnologico de Monterrey, Mexico); [Carlos del-Río](#) (Universidad Publica de Navarra & Institute of Smart Cities, Spain); [Francisco Falcone](#) (Universidad Publica de Navarra and Institute for Smart Cities, Spain)

In order to enable context aware environments within the Internet of Things paradigm, distributed transceiver systems capable of providing low cost, low latency capabilities are required. Single Input Multiple Output systems provide an adequate solution by enabling non-coherent energy based detection. Phase distributions play a key role in transceiver location and hence overall system operation. In this work, SIMO operation based on volumetric phase analysis is performed on indoor scenarios, employing deterministic 3D Ray Launching channel estimation. The proposed methodology enables the estimation of system performance as a function of distributed transceiver location, aiding in network planning and deployment tasks

P1.091 Propagation Analysis of Terahertz OAM Waves in Atmospheric Turbulent Environment

[Jian Cui](#) and [Yang Wang](#) (Chongqing University of Posts and Telecommunications, China); [Yanli Tu](#) (China Mobile Group Design Institute Co., Ltd, China); [Guangyang Liu](#) (Chongqing University of Posts and Telecommunications, China); [Jie Zhang](#) (University of Sheffield, Dept. of Electronic and Electrical Engineering, United Kingdom (Great Britain))

The orbital angular momentum (OAM) wireless communication technology is widely studied in recent literature, and the propagation characteristics in the atmosphere turbulent environment have attracted the attention of scholars. OAM can be affected by atmosphere turbulence during space transmission, causing energy diffusion and phase profile distortion, which makes it difficult to analyze the information at the receiving end. Radio waves in different frequency bands have various performance when transmitting in space. This paper study the propagation of OAM waves in terahertz frequency bands. Power spectrum inversion method is employed to simulate phase distortion caused by atmosphere turbulence. A full study of distortions on vortex beam intensity and phase profiles in air environment is given along with OAM mode spectrum analysis in the visible and terahertz bands in atmosphere turbulence. Results suggest terahertz OAM waves can resist more air turbulence than visible-light OAM beams which have great potential in air/space communications.

P1.092 Analysis of Safe Ultrawideband Human-Robot Communication in Automated Collaborative Warehouse

[Branimir Ivšić](#) (Ericsson Nikola Tesla d. d. & University of Zagreb, Faculty of Electrical Engineering and Computing, Croatia); [Zvonimir Sipus](#) and [Juraj Bartolić](#) (University of Zagreb, Croatia); [Josip Babić](#) (Končar–Electrical Engineering Institute Inc., Croatia)

The paper presents the propagation analysis of ultrawideband Gaussian signal in an automated collaborative warehouse environment where human and robots communicate to ensure that mutual collisions do not occur. The warehouse racks are principally modeled as clusters of metallic (PEC) parallelepipeds, with dimensions chosen to approximate the realistic warehouse. The signal propagation is analyzed using a ray tracing software, with the goal to calculate the path loss profile for different representative scenarios and antenna polarizations. The influence of the rack surface roughness onto propagation is also analyzed. The guidelines for optimum antenna positions on humans and robots for safe communication are proposed according to the simulations results.

P1.093 Propagation Model for UCA-based OAM Communications in Six-Ray Canyon Channels

[Wenjun Jie](#), [Yang Wang](#), [Tao Hu](#), [Jie Liu](#) and [Donghua Yang](#) (Chongqing University of Posts and Telecommunications, China); [Jie Zhang](#) (University of Sheffield, Dept. of Electronic and Electrical Engineering, United Kingdom (Great Britain))

Orbital angular momentum (OAM) has attracted considerable attention as a novel solution for ultra-high spectrum efficiency wireless communications. However, researches have focused on the line-of-sight (LOS) scenario and the two-ray non-LOS model. In addition, the two-ray model cannot be applied to certain scenarios e.g. streets, valleys, tunnels, etc. To address this problem, we derive the propagation model of uniform-circular-array-based OAM communications in six-ray canyon channels. This paper gives a full investigation of the multi-path effects, including phase-front distortion, mode spectrum, and receiving power weighting. Numerical results show that the low-order OAM signal can obtain a better transmission gain than high-order OAM signal in multi-path environments. The proposed model can help research and application of OAM in future communication systems.

P1.094 Modified Two-Ray Model with UTD and Atmospheric Effects

[Andres Navarro](#) (Universidad Icesi, Colombia); [Diego Parada](#) (Federal University of Minas Gerais, Brazil); [Dinael Guevara](#) (Francisco de Paula Santander University, Colombia); [Cássio Rego](#) (Federal University of Minas Gerais, Brazil); [Roger Alexander Badillo](#) (Francisco de Paula Santander University, Colombia)

In this paper, we show a propagation model that combines the modified two-ray with a ray tracing (RT) technique based on uniform theory of diffraction (UTD) techniques, as well as refractive effects of the standard atmosphere. The proposed model improves some results of the Two Ray model, in a canonical scenario, and is compared with a Standard Parabolic Equation (SPE) model, implemented by some of the authors. The proposed model pretends to improve the results obtained in the design of point to point links in mountainous terrain, typical of andean countries.

P1.095 Analysis of Radiowave Propagation in Forest Media Using the Parabolic Equation

[Glaucio L. Ramos](#) and [Paulo Tibúrcio Pereira](#) (Federal University of São João Del-Rei, Brazil); [Nuno R. Leonor](#) (Instituto de Telecomunicações, Portugal); [Rafael F. S. Caldeirinha](#) (Polytechnic Institute of Leiria & Instituto de Telecomunicações, Portugal)

This paper presents preliminary results about path loss prediction in vegetation using the parabolic equation technique. The trees were modelled in a flat and a triangular format and their effect in the path loss was analysed. A real measurement scenario with trees was also modelled and compared with the PE simulation. The use of the parabolic equation method to study the path loss attenuation in forest environments seems to be very promise.

P1.096 Construction of Gaussian and Isotropic Channels Based on Electrically Small Dipole Arrays

[Assane Ngom](#) (ESIGELEC, IRSEEM, France); [Constant M. A. Niamien](#) (Normandie Univ, UNIROUEN, ESIGELEC/IRSEEM, Rouen, France)

This work presents methodology to construction the gaussian and isotropic channel. It consists to provide the spherical wave on the area surround the antenna under test (AUT). The wave incident source excitation can be modeling with the infinitesimal dipole model (IDM). theoretically, the electric far field of this model is determined by using the translation and rotation addition theorem in the origin coordinate system. By analyzing this expression, the ratio between the distance the observation point-AUT by the distance IDM-AUT is studied

P1.097 Reduction Technique of Differential Propagation Delay with Negative Group Delay Function

[Fayu Wan](#) and [Ningdong Li](#) (Nanjing University of Information Science and Technology, China); [Wenceslas Rahajandraibe](#) (IM2NP, France); [Blaise Ravelo](#) (NUIST, China)

This paper deals with an innovative technique of propagation delay reduction. The technique is based on the use of bandpass negative group delay (NGD) function. The principle of the propagation delay reduction is introduced by considering a simple scenario of Tx multi-wireless sensors communicating with a single Rx sensor. With the consideration of bandpass NGD function, it is shown that the differential between the propagation delay can be reduced considerably. The feasibility of the technique is confirmed with group delay diagram by considering microstrip NGD prototype measured S-parameters.

P1.098 On Separation of Wet Antenna Effects from Rain Attenuation Measurements

[Pavel Valtr](#) (Faculty of Electrical Engineering, Czech Technical University in Prague, Czech Republic); [Martin Fencl](#), [Vojtech Bares](#) and [Pavel Pechac](#) (Czech Technical University in Prague, Czech Republic)

Possibility of determination of attenuation caused by rain effects is examined here by separating attenuation by wet antenna radome from total measured loss of a microwave link. Measurement of signal strength of two commercial microwave links operating at 32 GHz frequency is analyzed. Measured attenuation is compared with theoretically predicted rain attenuation calculated using rain gauge measurements of rain rate. From this comparison, the empirical model of wet antenna effect as a function of measured attenuation is calibrated and analysed.

P1.099 Mode Modulation Based Multi-Mode Transmitter for Line-of-Sight Propagation

[Tao Hu](#) and [Yang Wang](#) (Chongqing University of Posts and Telecommunications, China); [Jie Zhang](#) (University of Sheffield, Dept. of Electronic and Electrical Engineering, United Kingdom (Great Britain))

As an emerging solution for line-of-sight (LOS) wireless communications, recently, mode division multiplexing (MDM) based orbit angular momentum (OAM) has attracted considerable attention due to its high spectral efficiency (SE). Since the high complexity in OAM modulations and the request for great radio frequency (RF) chains, the implementation of a mode division multiplexing-multiple-input multiple-output (MDM-MIMO) system is confusing. To address this problem, we proposed a low complexity mode modulation based multi-mode (4M) wireless communication system by utilising the positional information of none-zero source symbols to transmit additional data symbols. Numerical results demonstrate that the proposed 4M system outperforms conventional MDM-MIMO systems. Furthermore, the 4M scheme possesses higher robustness than MDM-MIMO systems in long-range transmissions.

P1.100 Detection Probability Calculations for Fluctuating Targets Under Clutter

[Ido Finkelman](#) (Elta Systems Ltd., Israel); [Nimrod Teneh](#) (Elta Systems Ltd, Israel); [Gregory Lukovsky](#) (Elta Systems Ltd., Israel)

Recent computational advantages in EM modeling, along with the growing demand to detect low observable moving targets, have brought about a renewed interest in the field of target detection. Real-life applications, such as flight path optimization, motivate a dynamical approach where the RCS is not only stochastic by nature, but also significantly

influenced by the target aspect angle. The classic techniques that modeled target RCS fluctuations as a random variable are generally found unsuitable for such tasks and make way to aspect-dependent RCS models produced by advanced EM softwares. The random nature of the echo target signals can then be simulated by introducing variations in aspect angle between detections. This paper describes a method for generating single-pulse detection probabilities of aspect-dependent RCS models in the presence of clutter. As an example, we compare various Weibull clutter models to emphasize the importance of clutter parameters selection.

Poster1-P03: Channel Sounding and Parameter Estimation Techniques

Propagation

Room: Exhibition Hall

P1.101 Mobile Measurements at 3.7 GHz Using a Massive MIMO Antenna Array in Outdoor Environments

[Nada Bel-Haj-Maati](#) (IMT Atlantique & Orange Labs, France); [Nadine Malhouroux](#) (France Telecom Research & Development, France); [Patrice Pajusco](#) and [Michel Ney](#) (IMT Atlantique, France)

Massive MIMO technology offers higher capacity, faster throughput and improved spectral and energy efficiency, thanks to the use of large-scale antenna arrays at the base station (BS), which enable beamforming and exploit the multipath richness. In this paper, we experimentally investigate massive MIMO propagation channel in several propagation environments. For this purpose, we have developed a new sounding experimentation using a large-scale planar array with about one thousand elements. Channel measurements were carried out at 3.7 GHz. We used a Virtual Planar Array (VPA) composed by an actual Uniform Linear Array (ULA) with 36 elements on the top of a moving vehicle to exploit its displacement to generate the second dimension of the VPA. A wideband channel sounder was used to record propagation channel transfer functions and to compute wideband characteristics. A new approach to estimate 3D direction of arrival (DoA) using a rectangular planar array is presented.

P1.102 A Novel 3D Beam Training Strategy for mmWave UAV Communications

[Weizhi Zhong](#), [Yong Gu](#), [Qiuming Zhu](#), [Xiaomin Chen](#), [Lei Wang](#) and [Kai Mao](#) (Nanjing University of Aeronautics and Astronautics, China)

The beam training technology which can overcome the easily-occurred beam misalignments is required urgently in unmanned aerial vehicles (UAVs) based millimeter wave (mmWave) communication systems. In this paper, a novel three-dimensional (3D) beam training strategy for UAV-assisted mmWave communications is proposed. The inverse discrete-space Fourier transform is introduced to construct the training beam with flat-topped characteristic. In addition, the hybrid beamforming (BF) system is taken into account and the greedy geometric (GG) algorithm is adopted to obtain the optimal beam. Numerical simulations are conducted to evaluate the performance and the simulation results demonstrate that our proposed 3D training strategy can provide both precise beams and high training efficiency for the 3D mmWave UAV communications.

P1.103 Measured Millimeter-Wave Channels in Corridor Scenarios with Large-Scale Antenna Arrays

[Allan Mbugua](#) (Huawei Technologies Duesseldorf GmbH, Munich Research Center, Germany); [Wei Fan](#) and [Fengchun Zhang](#) (Aalborg University, Denmark); [Yun Chen](#) (Huawei Technologies Duesseldorf GmbH, Munich Research Center, Germany); [Gert Pedersen](#) (Aalborg University, Denmark)

In this paper, measured millimeter-wave (mm-wave) channels with two large-scale antenna arrays in a corridor scenario are presented. The measurements were carried out using a radio-over-fiber (RoF) based vector network analyzer (VNA) channel sounder with a virtual uniform circular array (UCA) and a uniform rectangular array (URA) in a line-of-sight (LoS) scenario. The spatial-temporal characteristics of the channel are then obtained using the Bartlett beamformer and frequency invariant beamforming (FIBF) algorithms for the URA and UCA, respectively. The high dynamic range of the channel sounder coupled with the high spatial resolution of the large scale arrays enable the extraction of weak multipath components (MPC)s as well as MPCs arriving with a long delay.

P1.104 Propagation Channel Characterization for Ka Mobile Communication Systems

[Jonathan Israel](#) (ONERA - The French Aerospace Lab, France); [Sebastien Rougerie](#) (CNES, France)

The statistical characterization of the propagation channel is of paramount importance in the design of future mobile satellite communication systems. At Ka band, the propagation channel can be strongly impacted by tropospheric events but also by the receiver local environment. Buildings, poles or trees can lead to partial or even total shadowing effects. In this paper, we present an extensive characterization of the local propagation effects in various environments such as urban, rural, highway or railway environments. The statistical analysis of measurements made in Ka band confirms and extends observations that have been made previously in comparable or lower frequency bands.

P1.105 Complex Sounding of the Ionosphere During the Intense Magnetic Substorm

[Donat Blagoveshchensky](#) (Saint-Petersburg State University of Aerospace Instrumentation, Russia); [Alexey S Kalishin](#) (Arctic and Antarctic Research Institute, Russia); [Maria A Sergeeva](#) (CONACYT, SCiESMEX, LANCE, UNAM, Mexico)

The magnetic substorm effects on the ionosphere and radio propagation conditions are discussed. The vertical and oblique ionospheric sounding data were used for the study. The characteristic features at high latitudes were revealed: the Es oblique layers appearance, their multilayer structure and diffuse F-formations as well as the EsMOF changes and multi-hop Es reflections. The processes in the ionosphere were qualitatively similar within 400 km distance southward from Sodankyla. The difference of the processes much more southward (2250 km far) where the reflection point of the mid-latitude radio path lies was revealed.

Poster1-P04: Propagation Experimental Methods and Campaigns

Propagation

Room: Exhibition Hall

P1.106 Multiple Screen Diffraction Analysis Using the Parabolic Equation Technique

[Glaucio L. Ramos](#), [Paulo Tibúrcio Pereira](#) and [Pablo Andrade](#) (Federal University of São João Del-Rei, Brazil); [Diego Tami](#) (Federal University of Minas Gerais, Brazil); [Sandro Trindade Mordente Gonçalves](#) (CEFETMG, Brazil); [Elson Silva](#) (UFMG, Brazil)

This paper presents preliminary results about multiple screen diffraction loss obtained using the parabolic equation technique. The numerical simulation is compared with a measurement campaign performed at microwave frequencies. The main contribution is the characterization of diffraction effects in the frequency band from 1 to 8.5 GHz, which has the potential to be used in future wireless mobile communications.

P1.107 Measurements of a Dynamic 60 GHz Radio Channel in an Open-Space Office

[Marwan El Hajj](#) and [Gheorghe Zaharia](#) (IETR-INSA de Rennes, France); [Ghais El Zein](#) (IETR-INSA Rennes, France); [Hanna Farhat](#) (Lebanese University & University Institute of Technology, Lebanon); [Sawsan Sadek](#) (Lebanese University, Lebanon)

In this work, we study the dynamic 60 GHz radio propagation channel conducted by measurements in an open-space office. These measurements quantify the effect of natural people movements on the path loss before and during working hours. Thus, it's possible to compare the effect produced by these movements with the static case when the office is empty of people. Measurements were performed using a VNA operating on 2 GHz bandwidth. Five receiver positions were considered to study three cases of receiver positions type: LOS, OLOS and NLOS. The obtained results allow to compute successively the channel path loss, its probability density function and its cumulative distribution function. Finally we compare the evolution of the dynamic channel in the presence of people at 5.8 GHz and at 60 GHz in the same environment. The dynamic channel propagation measurements provide a statistical characterization for the power loss into a realistic environment.

P1.108 60 GHz Path Loss Modelling Inside Ships

[Brecht De Beelde](#) (Ghent University & IMEC, Belgium); [Emmeric Tanghe](#) and [Marwan Yusuf](#) (Ghent University, Belgium); [David Plets](#) (Ghent University - imec, Belgium); [Eli De Poorter](#) (Ghent University & Imec, Belgium); [Wout Joseph](#) (Ghent University/IMEC, Belgium)

This paper presents the results of a mmWave channel sounding campaign in a bulk carrier vessel. Using the Terragraph channel sounder, we measured path loss at 60.48 GHz for different separations between the transmit and receiving nodes in the engine room and steering control room of the vessel. The path loss at reference distance 1.5 m is 74.6 dB, which is higher than the free space path loss, whereas the path loss exponent of 1.7 is lower than in free space. The one-slope path loss model is used to estimate throughput via link budget calculations, which shows that 60 GHz propagation realizes high data rate communication in the engine room of a vessel if the Line-of-Sight path is not obstructed. Due to the highly metallic nature of the propagation environment, reflections make communication possible in an obstructed Line-of-Sight configuration, but there is no clear distance relationship.

P1.109 Problems While Setting the Reference Level in a Satellite Beacon Receiver Propagation Experiment at Ka-band

[Vicente Pastoriza-Santos](#) and [Fernando Machado](#) (University of Vigo, Spain); [Dalia \(Das\) Nandi](#) (Indian Institute of Information Technology, India); [Fernando Pérez-Fontán](#) (University of Vigo, Spain)

Satellite tropospheric propagation studies strongly rely on beacon receiver measurements. Two kinds of attenuations are normally studied: total attenuation and excess attenuation. Excess rain attenuation is the variation of the received signal level due to atmospheric effects with respect to a level with initial stable conditions characterized only by gaseous attenuation. When we want to measure rain attenuation events we have to decide where the reference signal level is at. If we observe such variations on a clear sky day, we should be getting a constant reading, however diurnal variations repeating themselves from day to day can be observed when using affordable receivers employed by many experimenters. Most probably, these diurnal variations are mostly due to thermal effects on the external unit's electronics. In experimental data pre-processing, one of the procedures involved is estimating the so-called "template", which is time-varying throughout the day. We illustrate example recordings during non-rainy days.

P1.110 ITALSAT Ka, Q and V Band Cross Polar Discrimination Statistics Measured in Spino d'Adda, Italy

[Eric Regonesi](#), [Carlo Riva](#) and [Lorenzo Luini](#) (Politecnico di Milano, Italy); [Antonio Martellucci](#) (European Space Agency, The Netherlands)

Cross polar discrimination (XPD) is a widespread parameter used to measure the disturbance introduced on electromagnetic signals by the loss of polarisation, when dual polarisation links are employed. Rain precipitations and ice clouds contribute to the increase of XPD in the atmosphere. The current ITU-R Recommendation P.618 links the prediction of the XPD to the excess attenuation probability of a specific site. The statistical analysis of the XPD reported in this contribution is a basic step towards an improved model for next generation dual polarisation links design.

P1.111 Cloud Detection Models and Their Effect on the Calculation of Cloud Attenuation: Assessment at Ka- And Q-band at 4065 Meters of Altitude

[Gustavo Siles](#) (Universidad Privada Boliviana, Bolivia); [Miguel Heredia](#) (Agencia Boliviana Espacial, Bolivia); [Rodrigo Harriague](#) (Universidad Privada Boliviana, Bolivia)

This contribution presents a comparative study of methods to calculate cloud attenuation in satellite communications at 20 GHz and 40 GHz. A set of 3 years of radiosonde observations, collected at 4065 meters of altitude in the southern hemisphere, are used as input to four different cloud detection models, in order to retrieve integrated liquid water content, then calculate the attenuation due to clouds. The results are compared with those calculated using the ITU-R method based on ERA-40 NWP data. Based on the analysis performed at this particular site, located in an extensive high altitude Andean region in Bolivia, the results given by the ITU-R ERA-40 model seems to approximate better to the estimates obtained with cloud detection models other than the Salonen model, which is commonly accepted in temperate and lower altitude regions. However, in absolute values, the differences are less noticeable at 20 GHz than at 40 GHz.

P1.112 Satellite Link-Budget Statistical Prediction from Weather Forecast Models: Verification with Hayabusa-2 Ka-band Data

[Marianna Biscarini](#) and [Andrea Vittimberga](#) (Sapienza University of Rome, Italy); [Klaide De Sanctis](#) (HIMET, Italy); [Saverio Di Fabio](#) (CETEMPS, Italy); [Luca Milani](#) (Sapienza University of Rome, Italy); [Maria Montagna](#) (SciSys @ ESA, Germany); [Frank S. Marzano](#) (Sapienza University of Rome, Italy)

This work aims to provide a weather-forecast-based technique (named RadioMetOP) for the stochastic optimization of Ka-band satellite links. The stochastic approach is realized by resorting to a space-time ensemble obtained exploiting the temporal and spatial evolution of the weather-forecast model. Such approach allows to minimize the double-penalty error typically connected to weather-forecast models and to take into account for the forecast uncertainty directly related to the multiplicity of possible meteorological scenarios. For the first time, this RadioMetOP technique can be verified thanks to the availability of Ka-band data from the Hayabusa-2 deep-space mission directed by the Japan aerospace exploration agency and supported by the European space agency. Such verification has proofed the strong advantage of the RadioMetOP model (with signal-to-noise ratio gain even higher than 8 dB) and its accuracy (with validation results showing mean values of correlation, bias and error standard deviation of 0.88, 0.17 dB and 0.65, respectively).

P1.113 Experimental Study of Dispersion/Attenuation by Trees from 1 to 40 GHz

[Maria-Teresa Martinez-Ingles](#) (University Centre of Defence at the Spanish Air Force Academy, MDE-UPCT, Spain); [Jose-Maria Molina-Garcia-Pardo](#), [Leandro Juan-Llacer](#), [Juan Pascual-García](#) and [José-Víctor Rodríguez](#) (Universidad Politécnica de Cartagena, Spain)

With the aim of analyzing radiowave propagation in agriculture applications, this work presents experimental results regarding dispersion/attenuation caused when waves from 1 GHz to 40 GHz propagate through trees (bonsais). Depending on the position of the transmitter antenna, different dispersion patterns were measured. In this sense, the power delay profile (PDP) obtained with the presence of the tree is delayed and attenuated with respect to the PDP without the tree. Specifically, the tree dispersion/attenuation (TDA) due to the presence of the tree can be increased with frequency up to 9.8 dB. If the transmitter height is half the tree height, a difference of 7.4 dB has been observed in the maximum TDA. On the contrary, for a transmitter height double than the tree height, the difference is 2.2 dB.

P1.114 Nine Years of Excess Attenuation Statistics of Earth-Space Propagation Experiments at Ka-Band in Toulouse, France

[Charles-Antoine L'Hour](#) (Onera, France); [Jean-Pascal Monvoisin](#) and [Laurent Castanet](#) (ONERA, France); [Xavier Boulanger](#) (CNES, France); [Valentin Le Mire](#) (ONERA, France)

Since 2009, ONERA has been running a Ka-band propagation experiment in Toulouse (south of France). A rain gauge, a microwave profiling radiometer and a beacon receiver able to record the 19.7 GHz signal from Hot Bird 6 satellite and the 20.2 GHz signal from Astra-3B satellite have been deployed. This paper gathers nine years of results from the still ongoing experiment. The annual, monthly and seasonal complementary cumulative distribution functions of rain attenuation are presented. A comparison is made with the annual rain attenuation prediction method of Recommendation ITU-R P.618-13 and its dispersion given by recommendation ITU-R P.678-3. Fade slope and fade duration statistics are studied for different attenuation thresholds.

P1.115 Transmission Loss Evaluation for Fabry-Perot Materials' Characterization

[Leonardo Possenti](#) (University of Bologna, Italy); [Juan Pascual-García](#) (Universidad Politécnica de Cartagena, Spain); [Vittorio Degli-Esposti](#) (University of Bologna, Italy); [Antonio Jose Lozano-Guerrero](#) (Universidad Politécnica de Cartagena, Spain); [Marina Barbiroli](#) (University of Bologna, Italy); [Maria-Teresa Martinez-Ingles](#) (University Centre of Defence at the Spanish Air Force Academy, MDE-UPCT, Spain); [Franco Fuschini](#) (Viale del Risorgimento 2, Italy); [José-Víctor Rodríguez](#) (Universidad Politécnica de Cartagena, Spain); [Enrico M. Vitucci](#) (University of Bologna, Italy); [Jose-Maria Molina-Garcia-Pardo](#) (Universidad Politécnica de Cartagena, Spain)

The knowledge of the electromagnetic properties of construction materials is crucial for the design of future wireless systems and for the practical use of deterministic ray-based propagation prediction tools. More specifically, with the allocation of several new frequency bands for 5G and beyond systems, the understanding of the electromagnetic properties of materials at those frequencies is needed to determine attenuation and reflectivity of walls and objects. In this work, a wideband method for the characterization of the imaginary part of the complex permittivity is presented; the method is intended to be combined with the recently proposed Fabry-Perot method to measure the permittivity's real part. Paraffin is selected as a reference material since it has long been used to assess methods in the literature.

P1.116 Antenna Design for RF Ion Heating of Anisotropic Magnetized Plasma

[Giuseppe Torrisi](#), [Giorgio Sebastiano Mauro](#) and [David Mascali](#) (INFN-LNS, Italy); [Alessio Galatà](#) (Istituto Nazionale di Fisica Nucleare, Italy); [Luigi Celona](#) (INFN-LNS, Italy); [Gino Sorbello](#) (University of Catania, Italy); [Santo Gammino](#) (INFN-LNS, Italy)

In this paper, we present and validate a 3D full-wave numerical model for solving the wave propagation in the anisotropic magnetoplasma of Electron Cyclotron Resonance (ECR) ion sources, with the aim to analyze and design radiofrequency antennas which could produce Ion Cyclotron Resonance Heating (ICRH). Our tool is based on the coupling between COMSOL FEM solution of Maxwell equations and the MATLAB-computed non-homogeneous plasma dielectric tensor. This approach allows the evaluation of RF absorbed power by the plasma as well as the antenna input impedance which represents a crucial parameter for the design of the feeding and matching circuits usually adopted in ICRH setup. A numerical study has been performed by varying antenna geometry and plasma parameters: results are reported and cross-validated against other models.

Tuesday, 17 March 14:50 - 15:30

IS-Tue 1/1: Invited Speaker Session TOP

Antennas

Room: A2

Chair: [Michael Jensen](#) (Brigham Young University, USA)

14:50 CubeSat Antennas: An Amazing Opportunity for Developing Out-of-the-Box Antennas

[Yahya Rahmat-Samii](#) (University of California Los Angeles (UCLA) & UCLA, USA)

CubeSats represent a remarkable revolution in the arena of satellites. Their small size and low cost have enabled space missions which seemed impossible with conventional satellites. A key element in furthering the potential of CubeSats is the development of antenna systems that can meet the data-rate and spatial resolution requirements for future space missions. This plenary talk describes the challenges and opportunities that CubeSats provide antenna engineers, and some innovative concepts that have been recently developed to facilitate advanced space missions. In particular, the talk focuses on the design of deployable high gain aperture antennas that can meet the demands of remote sensing, deep space missions and Internet of Space (IoS) with particular importance to the design tradeoffs engineers must account for while designing high gain CubeSat antennas.

IS-Tue 2/1: Invited Speaker Session TOP

Propagation

Room: A3

Chair: [Claude Oestges](#) (Université Catholique de Louvain, Belgium)

14:50 Antennas and Over-The-Air Testing for Millimeter-Wave Systems

[Gert Pedersen](#) (Aalborg University, Denmark)

Over-the-air (OTA) testing, where radio waves (rather than coaxial cables) are used to connect the device under test (DUT) and testing instruments, has been used to evaluate the true radio performance of antenna systems. OTA testing of single-antenna mobile handsets was proposed at Aalborg University (AAU) around 20 years ago, and has later become international standards. OTA testing for sub-6 GHz LTE multiple-input multiple-output (MIMO) handsets has been developed in recent years, where AAU was deeply involved in research and development of two standardized methods, namely the multi-probe anechoic chamber method and wireless cable method, together with industrial partners. Recently, OTA testing solutions are seen inevitable for more complicated and advanced antenna systems applied in automotive applications and 5G antenna systems. This plenary talk will discuss the history and research activities on OTA testing in recent years in antenna, propagation and millimeter-wave systems (APMS) group at AAU. Furthermore, the group has recently invested heavily in antenna measurement facilities, which include a world-class and unique anechoic chamber for antenna testing. The design and functionality of this anechoic chamber will be detailed in the talk. The APMS group has also been heavily involved in antenna design for millimeter-wave terminals and nano-satellites.

Tuesday, 17 March 15:30 - 16:10

IS-Tue 1/2: Invited Speaker Session

Antennas

Room: A2

Chair: [A. B. \(Bart\) Smolders](#) (Eindhoven University of Technology, The Netherlands)

15:30 *Antenna-in-Package Technology*

[Yue Ping Zhang](#) (Nanyang Technological University, Singapore)

Antenna-in-package (AiP) technology integrates an antenna or antennas with a radio or radar transceiver die (or dies) into a standard surface mount package. AiP technology well balances performance, size, and cost. Hence, it has been widely adopted by chip makers for radios and radars. It is believed that AiP technology will also provide elegant antenna and packaging solutions to the fifth generation cellular networks and beyond operating in the lower millimetre-wave (mmWave) bands. This paper will provide an overview of the development of AiP technology.

Tuesday, 17 March 16:40 - 18:20

T04-A20: Wireless Power Transfer and Inductive Coupling

T04 IoT and M2M / Regular Session / Antennas

Room: A2

Chairs: [Wei Lin](#) (University of Technology Sydney, Australia), [Debasis Mitra](#) (Indian Institute of Engineering Science & Technology, Shibpur, India)

16:40 *Efficient Two-layer Loop Array for Selective Magnetic Resonance Wireless Power Transfer*

[Yonghyun Nam](#) and [Jeong Hae Lee](#) (Hongik University, Korea (South))

This paper presents an efficient two-layer planar loop array resonator for selective magnetic resonance wireless power transfer (MR WPT). This two-layer structure provides two important functions with improved efficiency by adjusting the lumped capacitance of each loop: selective MR WPT, the ability of position- and alignment-free with the receiver. The optimal capacitance of each loop can be found using a genetic algorithm (GA). The two-layer array of 2x2 and 4x4 is designed at an operating frequency of 6.78MHz. This two-layer loop array has improved the measured power transfer efficiency (PTE) by ~10 % at distance of 500mm, compared with that of the previous single-layer 4x4 loop array.

17:00 *Wireless Power Transfer System Design in Reactive Near-Field for Implantable Devices*

[Tarakeswar Shaw](#) (Indian Institute of Engineering Science and Technology, Shibpur, Howrah, West Bengal, India); [Bappaditya Mandal](#) (Uppsala University, Uppsala, Sweden); [Debasis Mitra](#) (Indian Institute of Engineering Science & Technology, Shibpur, India); [Robin Augustine](#) (Uppsala University, Sweden)

In this paper, a wireless power transfer (WPT) system design for charging the bio-implantable devices in the reactive near-field of the antenna is presented. The proposed system is designed to operate in the industrial, scientific, and medical (ISM) of 2:40-2:48 GHz band. The WPT link is constructed with dual-ring slot antenna implanted in a single layer skin tissue model is used as a receiving (Rx) element and a simple patch antenna considered as transmitting (Tx) element. The patch antenna is designed to operate at the ISM of 2:45 GHz, whereas the dual-ring slot is used to obtain wideband characteristics that cover the entire ISM band. The strong mutual coupling between the Tx and Rx elements in the reactive nearfield provide high power transfer efficiency for the proposed WPT system.

17:20 *Headband Antenna for Wireless Power Transfer to Millimeter-Sized Neural Implants with Minimal Misalignment Effects*

[Shahbaz Ahmed](#) and [Lauri Sydänheimo](#) (Tampere University, Finland); [Leena Ukkonen](#) (Tampere University of Technology, Finland); [Toni Björninen](#) (Tampere University, Finland)

We present a headband loop antenna for wireless power transfer to multiple IMDs located in the cranial cavity at the depth of 10 mm from the skin. We characterize the wireless power transfer link in terms of the power gain and the power delivered to the IMD, when maximum SAR compliant transmission power is fed to the headband antenna at the frequency of 5 MHz. We also consider two types of misalignments i.e. lateral and angular, between the IMD antenna and the headband antenna and discuss their impact on the transducer gain, impedance matching and on the power delivered to the IMD.

17:40 *Sub-1 GHz Flexible Concealed Rectenna Yarn for High-Efficiency Wireless-Powered Electronic Textiles*

[Mahmoud Wagih](#), [Alex S Weddell](#) and [Stephen Beeby](#) (University of Southampton, United Kingdom (Great Britain))

Electronic textiles and seamlessly integrated flexible wearable electronics are an emerging platform for sensing and computing. Batteries and energy harvesters relying on specific materials and transducers are not fully compatible with e-textiles fabrication and large-scale manufacturing. This work proposes a radio frequency energy harvesting rectenna, operating in the sub- 1 GHz license-free band, packaged in the form of a rectenna yarn which can be concealed in standard textile weaves. The rectenna yarn is fabricated using thin polyimide copper laminates using photolithography. The rectenna is composed of a 50Ω meander-line coplanar waveguide monopole antenna and a voltage doubler rectifier, with a lumped matching network. The rectenna achieves 65.8% RF-DC efficiency and a 8.0-V DC output at 6 and 11 dBm input power, respectively. This is the highest voltage output of a textile wearable rectenna, while maintaining high efficiency down to -20 dBm and a -7 dBm 1-V sensitivity.

18:00 *A Dual-Polarized Rectenna with High Efficiency at Low Input Power Density*

[Jun-Hui Ou](#) and [Junyu Pan](#) (South China University of Technology, China); [Shi-Wei Dong](#) (National Key Laboratory of Space Microwave Technology, China); [Xiuyin Zhang](#) (South China University of Technology, China)

This paper presents a new 2.45-GHz rectenna with $\pm 45^\circ$ dual polarization for low-power-input microwave power transmission. By utilizing a $\pm 45^\circ$ dual-linearly-polarized antenna element, the rectenna is available for receiving incident power with arbitrary polarization angle, while avoiding 3-dB CP-to-LP polarization loss. In this way, the requirement of the receiving end to the placement angle is greatly liberated. Differential rectifier structure is utilized. The effect of cross connected load of two branches, which create DC voltage with opposite polarities, are studied. An integrated rectenna design is formed, fabricated and measured. Peak power conversion efficiency of 74.76% is found at input power density of 106.19 $\mu\text{W}/\text{cm}^2$ in the measurement. The power conversion efficiency of the rectenna stays higher than 58.4% regardless of the incident angle under the input power density of 67 $\mu\text{W}/\text{cm}^2$.

CS56: Recent Advances on Electronically Steerable Antenna Arrays at mm-Wave Frequencies

T02 Millimetre wave 5G / Convened Session / Antennas

Room: A3

Chair: [Antonio Clemente](#) (CEA-LETI Minatoc, France)

16:40 *Design of Wideband Wide-Scanning Dual-Polarized Phased Array Covering Simultaneously Both the Ku- And the Ka-Satcom Bands*

[Alexander J van Katwijk](#) and [Andrea Neto](#) (Delft University of Technology, The Netherlands); [Giovanni Toso](#) (European Space Agency, ESA ESTEC, The Netherlands); [Daniele Cavallo](#) (Delft University of Technology, The Netherlands)

We present the unit cell design of a wideband wide-scanning phased array operating in both Ku- and Ka-bands, for satellite communication applications. The radiating elements are dual-polarized connected slots loaded with an artificial dielectric superstrate, acting as a wide angle impedance matching (WAIM) structure. The design of the multi-layer artificial dielectric is based on analytical formulas describing the equivalent reactance of each layer, valid for geometries that are not periodic in the vertical direction. This allows to minimize the total number of metal layers composing the artificial dielectric. The predicted matching performance is investigated by means of simulations based on infinite array approximation.

17:00 *Towards the Realization of the E-Wall Concept at Mm-Waves*

[Marzieh SalarRahimi](#) (KU Leuven, Belgium); [Marcel Geurts](#) and [Tonny Kamphuis](#) (NXP Semiconductors, The Netherlands); [Guy Vandenbosch](#) (Katholieke Universiteit Leuven (KU Leuven), Belgium)

The so-called e-wall is a recently introduced concept with the implementation goal of making a flexible and cost-efficient infrastructure for next generation wireless communication systems in indoor environments. This paper is in line with our former paper, discussing the most recent steps toward the realization of the e-wall concept. An active beam-forming array based on tile sub-arrays has been fabricated and successfully measured. In addition, to improve the technical performance an antenna array has been designed to be integrated inside the packaging of a four-channel analog beam-former flip chip.

17:20 *Phased Array at Mm-Waves Based on Filter-Integrated Antenna Elements*

[Darwin Blanco](#) and [Christos Kolitsidas](#) (Ericsson, Sweden)

This paper presents a broadband phase array antenna based on the integration of a compact combline filter and a broadband tightly-coupled-dipole antenna. The presented approach can be easily scaled to any other application in the millimeter wave ranges keeping the low-cost and low-profile of a PCB structure. The methodology is based in a modular approach where first the broadband and large-scan angle antenna is introduced. Then a multi-layer combline filter is used as the input of the broadband antenna at the array element level. The designed combline filter use cross-coupling to make it more compact and to create a pseudo-elliptical response. Full wave simulations show an outstanding performance compared to the conventional planar filters with an insertion loss of less than 0.6dB in the transmission band from 23.5 GHz to 25.5 GHz.

17:40 *Review of W-band Reconfigurable Reflectarray and Transmitarray Antennas at Tsinghua University*

[Xiaotian Pan](#), [Fan Yang](#), [Shenheng Xu](#) and [Maokun Li](#) (Tsinghua University, China)

This paper reviews the recent research progress on the designs of w-band reconfigurable reflectarray (RRA) and reconfigurable transmitarray (RTA) at Tsinghua University. Several antenna designs are presented, including PCB-based RRA, PCB-based RTA, and chip-based RRA. These designs of RRAs and RTAs show promising potential in the w-band fast-beam-steering applications, especially for high-resolution imaging systems.

18:00 *Liquid Crystal-based Reconfigurable Metasurface for Beam Scanning at Millimeter Wave Frequencies*

[Enrica Martini](#) (University of Siena, Italy); [Gabriele Minatti](#) (Wave Up S. r. l., Italy); [Francesco Caminita](#) (Wave-Up SRL, Italy); [Giorgio Giordanengo](#) (LINKS Foundation & Politecnico di Torino, Italy); [Giovanni Toso](#) (European Space Agency, ESA ESTEC, The Netherlands); [Stefano Maci](#) (University of Siena, Italy); [Giuseppe Vecchi](#) (Politecnico di Torino, Italy)

This paper investigates the feasibility of an electronically scanning antenna based on a reconfigurable MTS. MTS reconfigurability is obtained by embedding small cavities filled with liquid crystals in the constituent unit cells. This approach can provide a low profile solution with the possibility of continuous beam scanning with low bias voltage and power consumption.

CS58: Reconfigurable Antennas for Compact Devices

T04 IoT and M2M / Convened Session / Antennas

Room: B1

Chairs: [Joseph Costantine](#) (American University of Beirut, Lebanon), [Leonardo Lizzi](#) (University Côte d'Azur, CNRS, LEAT, France)

16:40 *Electrically Small Antenna with Broadside and Monopole-Like Beam Reconfigurability*

[Ming-Chun Tang](#), [Yingjie Chen](#) and [Xiaoming Chen](#) (Chongqing University, China); [Richard Ziolkowski](#) (University of Technology Sydney, Australia & University of Arizona, USA)

An electrically small antenna (ESA) with broadside and monopole-like beam reconfigurability is presented. It consists of an electric monopole radiator and a magnetic radiator which are systematically placed orthogonal to the ground. By controlling the PIN diodes integrated into the feed structure, broadside and monopole-like beams can be switched dynamically. The broadside beam is generated by the capacitively loaded loop (CLL) near-field resonant parasitic (NFRP) element and the monopole-like beam is formed by the electric monopole. The simulated results indicate that the antenna is impedance matched within an overlapping operational fractional bandwidth of 2.5% even though it is electrically small with $ka=0.69$. The realized gain value at boresight is 7.1 dBi for the broadside beam and the null depth is over -30 dBi for the monopole-like beam, respectively. The proposed antenna is ideal for application to GPS systems that require anti-interference performance characteristics.

17:00 *Frequency Reconfigurable Antenna Loaded with Magneto Dielectric Materials at VHF Band*

[Lotfi Batel](#) (CEA-Leti, France); [Christophe Delaveaud](#) and [Jean-François Pintos](#) (CEA-LETI, France); [Jean-Luc Mattei](#) (Université de Bretagne Occidentale, LabSTICC, France); [Vincent Laur](#) (Lab-STICC / University of Brest, France); [Alexis Chevalier](#) (University of Brest & Lab-STICC UMR CNRS 3192, France)

This article describes a frequency agility technique of an electrically small Inverted-F Antenna loaded with tunable magneto-dielectric materials. A specific material developed for VHF applications is used to load the antenna and leads to a miniaturization factor of 20 % and a potential of frequency agility of 6 % in VHF band close to 70 MHz.

17:20 *Four-Element Beam Switching Antenna for Compact IoT Devices*

[Marios Patriotis](#) (The University of New Mexico, USA); [Firas Ayoub](#) (University of New Mexico & COSMIAC - University of New Mexico, USA); [Christos Christodoulou](#) (The University of New Mexico, USA)

This work presents a pattern reconfigurable antenna system at X-band for the Internet of Thing (IoT) devices. The system is composed of a printed circular array composed of four Yagi-Uda elements and an electrically controlled feeding network. The feeding network incorporates PIN diode RF switches that provide independent activation of each antenna element while maintaining overall system matching stability. The suggested technique results in pattern reconfigurability between 16 modes. The isolation between the elements is improved by incorporating a reflector between them. Simulation results reveal that such a pattern flexible antenna is a strong candidate for IoT devices in a multipath environment.

17:40 *Compact 4-Element Radiation Pattern Agile Antenna for Spatial Filtering in IoT Networks*

[Luca Santamaria](#) and [Leonardo Lizzi](#) (University Côte d'Azur, CNRS, LEAT, France); [Fabien Ferrero](#) (University Nice Sophia Antipolis, CNRS, LEAT & CREMANT, France); [Robert Staraj](#) (University Cote d'Azur, CNRS, LEAT, France)

This paper presents a compact radiation pattern agile antenna for spatial filtering in IoT networks. The antenna is constituted by 4 wire-patch elements mounted on the same ground plane. The antenna enables 4 radiation patterns rotated by 90 degrees and characterized by 4.2 dBi realized gain and 9.8 dB front-to-back ratio in the horizontal plane. The reconfiguration of the pattern can be digitally controlled thanks to the use of a SP4T switch.

18:00 *Reconfigurable Filtenna for 5G/LEO Constellations Mobile Terminals*

[Luís Carlos Rodrigues](#) (University of Aveiro & Instituto de Telecomunicações, Portugal); [Tiago Varum](#) and [João Matos](#) (Instituto de Telecomunicações, Universidade de Aveiro, Portugal)

A reconfigurable microstrip filtenna capable of working at two different frequencies is presented in this paper to integrate mobile terminals communicating with low orbit satellites constellations. The electrical size of the antenna can be changed with a PIN diode, allowing the antenna to commute between the 20GHz and 29GHz frequency bands. A Hairpin filter was integrated with the antenna to eliminate undesired frequencies. Its reduced size and cost, combined with its performance in two different bands make this antenna a good solution for integrating mobile terminals, communicating with satellite or 5G communication systems.

T04-A15: RFID and Backscattering Antennas

T04 IoT and M2M / Regular Session / Antennas

Room: B2

Chair: [Ignacio Gil](#) (Universitat Politècnica de Catalunya, Spain)

16:40 *Tag Design for RFID AC Current Sensing System*

[Irfan Ullah](#) (University of Kent, United Kingdom (Great Britain)); [Robert J Horne](#) (University of kent, United Kingdom (Great Britain)); [Benito Sanz-Izquierdo](#) and [John Batchelor](#) (University of Kent, United Kingdom (Great Britain))

This study describes the development of an RFID tag system and antenna for real-time ac current sensing of individual appliances in smart homes. The operating principle of the tag system is based on the tag antenna tuning via a tuning circuit. The auto-tuning chip is embedded to compensate the antenna matching and stores the impedance tuning in the form of a 5-bit sensor code. The tag wirelessly streams the 5-bit sensor code that represents the ac current drawn by the electrical load, to the dedicated RFID reader in the range of 3 m at 868 MHz. The tag device is an energy harvester and a cost-effective ac current sensing solution compared to commercial smart meters in smart power metering systems. The antenna is designed to fit around the housing of the current sensor.

17:00 *Design of a Resistant Circularly Polarized Tag Antenna with High Performances in the EU UHF RFID Band*

[Khodor Jebbawi](#) (IM2NP, France); [Amal Afyf](#) (IM2NP, Aix-Marseille Univerity, France); [Matthieu Egels](#) and [Philippe Pannier](#) (IM2NP, France)

In this study, a novel resistant RFID tag with high performances is presented. The proposed tag consists of two antennas. The first one is an inductive antenna used for matching the imaginary part of the chip impedance at the target frequency. The second antenna is coupled with the first one in order to increase the gain and improve the tag performances. The tag antennas are designed to operate in the EU-UHF-RFID band. The crossed dipole antennas technique is used to achieve the CP in the operating band. Many prototypes have been manufactured, and good agreement between simulations and measurements has been achieved. The band covered for an AR < 3dB is from 863 to 869MHz. The Read Range (RR) of the tag has been measured in a standard anechoic chamber. From the measured results in EU-RFID band, the tag has a maximum RR of about 16.35m at 868MHz.

17:20 *Effect of Bending on a Textile UHF-RFID Tag Antenna*

[Mohamed El Bakkali](#) (Abdelmalek Essaâdi University, Spain); [Marc Martinez](#) and [Raul Fernandez-Garcia](#) (Universitat Politècnica de Catalunya, Spain); [Ignacio Gil](#) (Universitat Politècnica de Catalunya, Spain); [Otman El Mrabet](#) (Abdelmalek Essaadi University, Morocco)

In this paper, a textile UHF-RFID Tag antenna at 915 MHz based on a T-match dipole loaded with circular patch on a felt fabric substrate is presented and discussed. In addition, the bending impact on the read range is analyzed by means of full 3D electromagnetic simulations. The bending analysis results indicate that the proposed textile Tag can be used under both, concave and convex bending with a reduction of read range lower than 10 % in all cases. These results confirm that the proposed UHF-RFID Tag is a useful design in application where the devices can be deformed, such as wearable applications

17:40 *Performances of a 3.6 GHz Epidermal Loop for Future 5G-RFID Communications*

[Francesco Amato](#) (University of Roma Tor Vergata, Italy); [Cecilia Occhiuzzi](#) (University of Roma Tor Vergata & DICII, Italy); [Gaetano Marrocco](#) (University of Rome Tor Vergata, Italy)

This paper explores, through simulations and preliminary experiments, the feasibility of a 5G-RFID link for a backscattering epidermal sensing architecture integrated within the 5G network. It demonstrates how a 3.6 GHz loop tag could provide the same read distance (one meter) of three-times larger UHF counterparts. The proposed loop is compliant with regulations on electromagnetic exposure and can theoretically achieve data rates up to 0.9 Gbps.

18:00 *Monolithic Antenna Array for Epidermal 5G Backscattering Communications*

[Cecilia Occhiuzzi](#) (University of Roma Tor Vergata & DICII, Italy); [Gaetano Marrocco](#) (University of Rome Tor Vergata, Italy)

5G network is expected to sensibly boost the diffusion of personal area networks for health and wellness monitoring purposes, especially with regard to battery-less devices and backscattering based communications. To overcome the power path-loss, however, high efficiency radiating elements are mandatory, especially for the highest frequencies. Here, the feasibility of adopting monolithic grid antenna arrays directly adhering onto the human skin is investigated. Numerical parametric analysis are performed to evaluate the backscattering link budget of the proposed epidermal devices and to derive their upper-bound performances. Early results demonstrate the rationality of the approach and the possibility to reach communication distances ranging from 20cm to 1m in case of sub-grid structures are adopted.

CS67: Water-Based Microwave Devices

T11 Fundamental research and emerging technologies / Convened Session / Electromagnetics

Room: B4

Chairs: [Sameel Arslanagić](#) (Technical University of Denmark, Denmark), [Andrei Lavrinenko](#) (Technical University of Denmark, Denmark)

16:40 *Water-Based Microwave Absorber*

[Patrick Bradley](#) (DCU, Ireland); [Max Munoz](#) (Queen Mary, University of London, United Kingdom (Great Britain)); [Conor Brennan](#) (Dublin City University, Ireland); [Yang Hao](#) (Queen Mary University, United Kingdom (Great Britain))

In this paper, we develop a novel design methodology that enables the design of all-dielectric 3d printable microstructures which can replicate the functionality of a resonant metallic metamaterial. Central to this capability is the inclusion of water within a 3d printable dielectric matrix to capture the benefit of this high contrast fluid. By judiciously distributing water within this internal architecture, which is governed by a solid isotropic material technique formulated as a nonlinear optimisation problem, we can obtain a robust magnetic and electric resonance. The capability of water as a design material and the success of our optimisation framework is illustrated in simulations and validated by experiential results through the creation of an all-dielectric 3d printable wideband perfect absorber.

17:00 *Water-Based Microwave Reflectarrays*

[Jonas Nielsen](#), [Rasmus Elkjaer Jacobsen](#), [Andrei Lavrinenko](#) and [Sameel Arslanagić](#) (Technical University of Denmark, Denmark)

Control of transmission/reflection of waves continues to be a task of great importance. Especially, 2-D structures such as metasurfaces, with imprinted spatial phase variation coming from arrays of small metallic/dielectric scatterers, are of increasing interest for microwave as well as optical frequencies. In this work, we demonstrate alternative and simple metasurface reflectarrays based on distilled water. The reflectarrays are composed of water-filled cylinders which are operated around their magnetic dipole resonance. The cylinders reside in a Rohacell 51HF host, and their size varies in order to span a 360o interval in the reflection phase. They reflect a normally incident plane wave at an angle of 51.34°. The numerical results predict a total reflected power of 36.9% with the reflection in the desired direction being more than 13 times larger than the reflections in other directions. A prototype was fabricated, with the measurements being in excellent agreement with the numerical results.

17:20 *Water-assisted Metasurface for Wireless Power Transfer*

[Polina Kapitanova](#), [Mingzhao Song](#), [Ksenia Rudneva](#), [Aleksandr Markvart](#) and [Stanislav Glybovski](#) (ITMO University, Russia); [Constantin Simovski](#) (Aalto University, Finland); [Pavel Belov](#) (ITMO University, Russia)

Metasurface which can be potentially used as a transmitter for wireless charging of multiple devices is proposed and studied numerically. The metasurface consists of two orthogonal wire layers separated by a short distance immersed in high permittivity dielectric. The currents excited in the metasurface generate the quasi-uniform magnetic field distribution over its area, while the electric field is confined inside of the structure. Here we demonstrate that distilled water can be used as dielectric providing high dielectric constant and low loss factor at radio frequencies. The wireless power transfer efficiency greater than 70% from the water-assisted metasurface to a rectangular loop receiver is numerically demonstrated at the frequency of 19.5 MHz over the 50cm×50 cm area.

17:40 *Towards Efficient EM Wave Manipulation Using a Discrete Dielectric Huygens' Metasurface*

[Abhishek Sharma](#) and [Alex Wong](#) (City University of Hong Kong, Hong Kong)

This paper presents a spatially varying discrete dielectric Huygens' metasurface (DDHMS) that achieves beam splitting. The proposed structure consists of two elements per grating period and the phase difference between neighbouring elements is 180 deg. The resultant bipartite Huygens' metasurface leads to a simplified, robust and cost-effective design as compared to finely discretized metasurfaces. A 2D full-wave Floquet simulation demonstrates that the proposed metasurface splits the normal incident plane wave into different directions according to the generalized Snell's law, and contains over 80% of the transmitted power.

18:00 *Dynamically Reconfigurable Metamaterial-Based Scatterer*

[Dmitry A Dobrykh](#) (ITMO University, Russia); [Dmitry Filonov](#) (Moscow Institute of Physics and Technology, Russia); [Anna Mikhailovskaya](#) (ITMO University, Russia); [Pavel Ginzburg](#) (Tel Aviv University, Israel)

Reconfigurable metamaterials can further enlarge those capabilities by time variable as an additional controllable parameter. In this work we demonstrate the first of a kind reconfigurable volumetric metamaterial-based scatterer, which electromagnetic properties are controlled dynamically with light. In particular, hybridized resonances in arrays of split ring resonators give rise to a collective mode, which poses properties of artificial high-frequency magnetism. Resonant behavior of each individual ring is controlled with a photocurrent, which allows obtaining fast of macroscopic effective permeability. As the result, artificial RF magnon resonant excitation within a subwavelength spherical scatterer is governed by light intensity. Four-dimensional control (both space and time) over electromagnetic scattering open new venues for modern applications, including wireless communications and automotive radars to name just few.

CS28: EuMA/EurAAP Session: From Radiating Section to Digital Interface - Research and Design Trends for an End-To-End Approach of Highly Integrated Active Antenna Systems

T02 Millimetre wave 5G / Convened Session / Antennas

Room: B5

Chairs: [Roberto Flamini](#) (Huawei Technologies, Italy), [Renato Lombardi](#) (Milan Microwave Competence Center, Italy)

16:40 *Active Antenna Architectures for Enhanced 5G System Performance*

[Bruno Biscontini](#), [Alejandro Murillo](#), [Juan Segador](#) and [Ignacio Gonzalez](#) (Huawei Technologies, Germany)

In this paper, we present a Massive MIMO antenna architecture whose system performance is higher in comparison with the traditional aperture geometry. Its advantage is explained in terms of an improved exploitation of the antenna Degrees of Freedom.

17:00 *Machine Learning-aided Design of Thinned Antenna Arrays for Optimized Network Level Performance*

[Mattia Lecci](#) and [Paolo Testolina](#) (University of Padova, Italy); [Mattia Rebato](#) (Università degli Studi di Padova, Italy); [Alberto Testolin](#) (University of Padova, Italy); [Michele Zorzi](#) (Università degli Studi di Padova, Italy)

With the advent of millimeter wave (mmWave) communication, the combination of a detailed 5G network simulator with an accurate antenna radiation model is required to analyze the realistic performance of complex cellular scenarios. However, due to the complexity of both the electromagnetic and network models, the design and optimization of antenna arrays is generally infeasible due to the required computational resources and simulation time. In this paper, we propose a Machine Learning framework that enables a simulation-based optimization of the antenna design. We show how learning methods are able to emulate a complex simulator with a modest dataset obtained from it, enabling a global numerical optimization over a vast multi-dimensional parameter space in a reasonable amount of time. Overall, our results show that the proposed methodology can be successfully applied to the optimization of thinned antenna arrays.

17:20 *Reconfigurable Metasurface Antenna for 5G Base Stations*

[Cristian Della Giovampaola](#) (Wave Up srl, Italy); [Francesco Caminita](#) (Wave-Up SRL, Italy); [Giuseppe Labate](#) (Wave Up S. R. L., Italy); [Enrica Martini](#) and [Stefano Maci](#) (University of Siena, Italy)

This work describes the operation principle and implementation of an electronically reconfigurable leaky-wave antenna based on an array of periodically modulated metasurface channels for 5G applications. While the scan angle along the channels is dictated by the bias voltage of PIN diodes distributed along the channels, the beam angle on the transverse plane is controlled by a digital network feeding the channels. Numerical results show good performance in terms of beam shape, beam direction control, and field of view coverage.

17:40 *ML Based Fully Digital UWB Antenna for Direction Finding Systems*

[Antonio Manna](#) (Elettronica SpA, Italy)

A new generation UWB Radio Frequency Direction Finding System is presented. The architecture of such system is based on phase interferometry and it exploits leading edge technologies such as, Radio Frequency direct sampling and Artificial Intelligence for the processing of incoming RF signal. Thanks to these new solutions, a minimum number of antennas are needed to cover a multi-octave band capable to operate in the so-called "folded mode": folding the RF band in the first Nyquist Sone, the instantaneous observation band is than identical to the entire operating band. The presented solution is based on four full band interferometer antenna array. The same signal collected from each antenna is digitized with different sampling frequencies to get the diversity needed to solve the frequency ambiguity problem. Machine Learning approach is adopted to face this issue and for the estimation of Direction of Arrival. Comparison between standard processing and ML is presented.

18:00 *A 5G Active Antenna Tile and Its Characterization in a Reverberation Chamber*

[Eduardo Anjos](#) and [Marzieh SalarRahimi](#) (KU Leuven, Belgium); [Robert Rehammar](#) (Bluetest AB & Chalmers University of Technology, Sweden); [Dominique Schreurs](#) (KU Leuven, Belgium); [Guy Vandenbosch](#) (Katholieke Universiteit Leuven (KU Leuven), Belgium); [Marcel Geurts](#) (NXP Semiconductors, The Netherlands)

This work presents a 5G active antenna tile system, enabling the flexible construction of hybrid beamforming (HBF) arrays. The proposed tile was fabricated using a standard PCB manufacturing process and to validate its performance. Using a Reverberation Chamber (RC), the tile was measured in both Tx and Rx mode, achieving up to 1.6 GHz in bandwidth around a central frequency of 27.8 GHz.

SW01: COST Session CA15104 (IRACON): Measurements and Simulations in Channel Modelling in Wireless Body Area Networks

T05 Biomedical and health / Convened Session / Propagation

Room: B6

Chairs: [Sławomir J. Ambroziak](#) (Gdańsk University of Technology, Poland), [Kenan Turbic](#) (INESC-ID / IST, University of Lisbon, Portugal)

16:40 *Human Body Modelling for Wireless Body Area Network Optimization*

[Lukasz Januszkiewicz](#) (Lodz University of Technology, Institute of Electronics, Poland); [Sławomir Hausman](#) (Lodz University of Technology, Poland); [Paolo Di Barba](#) (University of Pavia, Italy)

In the paper two simplified models of human body dedicated for the automated optimization of wireless body area networks are presented. First model maps the fragment of the body and allows to simulate impedance mismatch of wearable antennas. This model was used in the optimization process of a wearable antenna to reduce the simulation time in each iteration which significantly shortens the time needed for design. The second model uses cylindrical elements to reproduce the entire body. It has exact physical equivalent that can be easily fabricated. In addition, it can also be quickly generated automatically in the program for electromagnetic simulations during automated optimization of WBAN. Such model represents both the figure of a standing and sitting person, so the change of body position can be taken into account in the process of system optimization.

17:00 *Preliminary Empirical Validation of a Polarized Off-Body Channel Model with Dynamic Users*

[Kenan Turbic](#) (INESC-ID / IST, University of Lisbon, Portugal); [Sławomir J. Ambroziak](#) (Gdańsk University of Technology, Poland); [Luis M. Correia](#) (IST/INESC-ID - University of Lisbon & INESC, Portugal)

This paper presents an empirical validation of a polarized channel model for off-body communications with dynamic users, based on wideband indoor measurements at 5.8 GHz with a 500 MHz bandwidth. The model is based on geometrical optics, and takes the signal depolarization and influence of user dynamics into account. By considering a scenario with the user walking towards an access point with co-located vertical and horizontal dipole antennas, the simulated receiver (Rx) power is compared against measurements for wearable antenna placements on the chest, wrist and lower leg. The obtained root mean square error is found to be within 2.8 dB for the vertical off-body antenna polarization, and within 3.2 dB for the horizontal one. Fairly matching Rx power values are obtained even when only free space propagation is considered in the simulator, with the error being below 3.4 dB in most cases.

17:20 *Real-Time Demonstration of Antenna Effects on Emulated Wireless Capsule Endoscope Links*

[Rytis Stasiunas](#) and [Pasi Koivumäki](#) (Aalto University, Finland); [Md Miah](#) (Aalto University & School of Electrical Engineering, Finland); [Mikko Heino](#) and [Katsuyuki Haneda](#) (Aalto University, Finland); [Clemens Icheln](#) (Aalto University & School of Electrical Engineering, Finland)

Real-time over-the-air video transfer platform is developed for a wireless capsule endoscope scenario. The use of the platform for demonstration of video transfer aims at intuitive and instant understanding of antenna effects on quantitative and qualitative radio link performance, e.g., video image quality, bit error rate (BER) and constellation patterns of digital modulation. The platform consists of a host computer and a universal software defined peripheral as general video source and radio transceivers, complemented with capsule and on-body antennas and liquid body phantom to emulate an inbody-to-onbody radio link. The antennas operate at 433MHz, while the liquid mimics the complex permittivity of a colon tissue.

17:40 *Human Posture Effects of WBAN Measurement in a Reverberation Chamber*

[Takahiro Aoyagi](#) (Tokyo Institute of Technology, Japan)

In this paper, the effect of human movement in a wireless body area network (WBAN) measurements in a reverberation chamber is investigated by numerical simulations. A rotating stirrer and a walking human posture model are assumed in a small size reverberation chamber. Electric field amplitudes at observation points are calculated and the distributions of them are analyzed. As a result of the dispersion analyses, it is found that the human posture has a comparative effect on the electric field distribution than that of the stirrer. Also, it is found out that the effect of the observation points become large when conducting the measurement with a human model inside the chamber. To perform simulations and analyses with other conditions, to compare the results with measurements are left for further studies.

18:00 *Experimental Parameter Optimization for Adaptive LoRa Modulation in Body-Centric Applications*

[Thomas Ameloot](#) (Ghent University - imec, Belgium); [Patrick Van Torre](#) and [Hendrik Rogier](#) (Ghent University, Belgium)

The relentless expansion of the Internet of Things is fueled by constant innovations in low-power wide-area network technologies. Industry forerunners such as LoRa, SigFox and NB-IoT continuously seek to achieve larger communication ranges. These efforts facilitate performance increases in a range of related application areas, such as body-centric communication. For example, recently, LoRa modules have been integrated onto wearable textile antennas, greatly extending the range of the body-centric networks these nodes can be used in. However, as the resulting communication links need to accommodate mobile users, many nodes will regularly be communicating using suboptimal LoRa modulation parameters as these users move around. Adaptive LoRa modulation aims to solve this by optimizing these parameters in real-time based on the location of the user and the actual performance of the wireless link. In this contribution, the optimal settings for one of the key LoRa modulation parameters, the spreading factor, are experimentally determined.

CS03: Advanced Radar Measurements, Modelling and System Solutions for Vehicular Applications

T06 Aircraft (incl. UAV, UAS, RPAS) and automotive / Convened Session / Measurements

Room: B7

Chairs: [Vittorio Degli-Esposti](#) (University of Bologna, Italy), [Matthias Hein](#) (Ilmenau University of Technology, Germany), [Andreas Schwind](#) (Technische Universität Ilmenau, Germany)

16:40 *Bi-static Nearfield Calibration for RCS Measurements in the C-V2X Frequency Range*

[Andreas Schwind](#), [Willi Hofmann](#) and [Ralf Stephan](#) (Technische Universität Ilmenau, Germany); [Reiner S. Thomä](#) and [Matthias Hein](#) (Ilmenau University of Technology, Germany)

Distributed multi-static radar systems using communication signals, provide additional options to augment the radar visibility of road users. Due to electrically large targets and small distances between the radar systems and the crossing road users, these are usually detected under nearfield conditions. This paper describes two bi-static RCS calibration methods, using a reference object or the radar range equation. Accordingly, a further calibration approach is presented which takes the nearfield effects of the antennas into account. The bi-static electromagnetic scattering of a bicycle at 5.9 GHz was measured under nearfield conditions and calibrated with these different calibration approaches. Compared with numerical simulations of the far-field RCS, the calibrated measurements result significant, angle-dependent differences which indicate nearfield effects. The comparison between the different calibration methods shows differences up to 8 dB depending on the bi-static angles and demonstrates the importance of the consideration of nearfield effects during the RCS calibration.

17:00 Extraction of Scattering Centers Using a Greedy Algorithm for Traffic Participant

[Sevda Abadpour](#), [Axel Diewald](#), [Benjamin Nuss](#) and [Mario Pauli](#) (Karlsruhe Institute of Technology, Germany); [Thomas Zwick](#) (Karlsruhe Institute of Technology (KIT), Germany)

The multiplicity scattering points should be reduced to a few significant scattering centers to minimize computational effort. In the following step, the extracted scattering centers can be used for the simulation of the millimeter-wave automotive radar channel in realistic scenarios. Also, as in many cases, a precise CAD model of relevant traffic participants is not accessible, therefore presenting the simplified scattering model based on the relevant scattering centers will be very helpful. The scope of this work is to present a technique to generate a significantly simplified RCS model of the traffic objects with a limited number of virtual scattering centers, each with its scattering characteristic, and how to group these scattering centers in a cluster database. The work is based on ray-tracing simulations of complex traffic object models. The scattering centers may not be physically existing strong scattering centers, but virtual scattering centers representing a certain scattering behaviour.

17:20 A Ray Optical Diffraction Model for Car Chassis in V2X Communication

[Lennart Thielecke](#) (Technische Universität Braunschweig, Germany); [Nils Dreyer](#) (TU Braunschweig, Germany); [Johannes M. Eckhardt](#) and [Thomas Kürner](#) (Technische Universität Braunschweig, Germany)

In this paper, diffraction models are investigated in the context of V2X scenarios. First the physical effects which are needed to describe a propagating wave are summarized. Afterwards, an analytical diffraction model for simple geometric objects is derived from a full wave optical analysis. Using an equivalence principle, it is possible to apply this model to the calculation of diffraction effects from car chassis in V2X scenarios. Based on key geometric parameters, a ray optical diffraction model is derived from the full wave optical analysis. Scaled measurements with a 60GHz channel sounder are carried out, validating the presented model.

17:40 Dynamic Ray Tracing: Introduction and Concept

[Denis Bilibashi](#), [Enrico M. Vitucci](#) and [Vittorio Degli-Esposti](#) (University of Bologna, Italy)

Radio applications in vehicular environment are becoming popular due to the development of autonomous driving and safety enforcement technologies that make use of vehicle-to-vehicle, vehicle-to-infrastructure as well as of radar solutions. Due the large variety of possible environment configurations, and to the highly dynamic characteristics of the environment, specific deterministic radio propagation models must be developed to assist the design and simulation of such vehicular applications. In the present work we present a dynamic ray tracing model that can provide a multidimensional channel prediction, including Doppler's shifts, with a single run on the base of a suitable "dynamic environment database" that describes a scene with moving objects and terminals. The proposed approach applied to a reference street canyon scenario with a large moving object representing a bus is shown to yield realistic estimates of the channel's power-Doppler profiles.

18:00 Physics Based Target Scenario Simulation Using Asymptotic Solver Techniques for Automotive Applications

[Markus Laudien](#) (Ansoft Germany, Germany)

Simulation of traffic scenarios for radar applications has gained high attendance during the past years as this can significantly reduce the time for validation. Electromagnetic models of auto-radar scenarios require models of the TX- and RX-antennas that radiate towards the reflecting targets embedded within a model of the whole environment. While small antenna modules can be simulated using full-wave methods like FEM, IE or FD-TD geometrical large geometries with an extension of thousands of wavelengths mainly get addressed using asymptotic methods like shooting and Bouncing Rays. The need for validation of radar systems in critical scenarios points out the importance of sufficient high accuracy also for large and complex scenario geometries. After a short introduction to the SBR method some simple validation cases will be shown for different post processing purposes and finally some cases of traffic scenarios

CS15: Antennas for Radio Astronomy TOP

T09 Space (incl. cubesat) / Convened Session / Antennas

Room: B8

Chairs: [Quentin Gueuning](#) (University of Cambridge, United Kingdom (Great Britain)), [David S Prinsloo](#) (ASTRON & Netherlands Institute for Radio Astronomy, The Netherlands)

16:40 Characteristic Mode Analysis of Multi-Octave Asymmetric Dipoles

[Alberto Tibaldi](#) (Politecnico di Torino, Italy); [Giuseppe Virone](#) (Consiglio Nazionale delle Ricerche, Italy); [Pietro Bolli](#) (INAF - Osservatorio Astrofisico di Arcetri, Italy); [Fabio Paonessa](#) (National Research Council of Italy (CNR - IEIT), Italy); [Giuseppe Addamo](#) (Istituto di Elett. e di Ingegneria dell'Inform. e delle Telecom. (IEIT-CNR), Italy); [Oscar A. Peverini](#) (Istituto di Elett. e di Ingegneria dell'Inform. e delle Telecom. (IEIT- CNR), Italy); [Mauro Lumia](#) (CNR, Italy); [Lorenzo Ciorba](#) (Institute of Electronics, Computer and Telecommunication Engineering (IEIT-CNR), Torino & Politecnico di Torino, Torino, Italy)

This paper discusses the impedance and front-to-back ratio performance of asymmetric dipoles. These parameters are very important when the antennas are placed over a conductive ground plane and should operate over multi-octave frequency bands. The operation of these antennas is usually described relying on analogies with more classical structures such as symmetric dipoles and tapered slot antennas. To provide a solid theoretical background to this intuition, this work presents the application of characteristic mode analysis to multi-octave dipole antennas. Firstly, a brief review of the main characteristic mode content is presented. Then, characteristic mode analysis is applied to three antenna concepts to emphasize how their geometry impacts on the relevant figures of merit. This allows to draw some conclusions on the achievable performance by different designs.

17:00 Analysis of the Loading Effect of Faulty LNAs on Embedded Element Patterns in the Murchison Widefield Array

[Maria Kovaleva](#) (Curtin University & Macquarie University, Australia); [Daniel Ung](#), [Adrian Sutinjo](#) and [Budi Juswardy](#) (Curtin University, Australia); [David B Davidson](#) (Curtin University, Australia & Stellenbosch University, South Africa); [Randall Wayth](#) (International Centre for Radio Astronomy Research (ICRAR), Australia)

A number of natural phenomena occurring at the Western Australian site of the Square Kilometre Array (SKA), such as lightning or whirlwinds, can cause damage to electronic parts of antenna array elements. We consider an SKA precursor, the Murchison Widefield Array (MWA), in order to evaluate the consequences of faulty low-noise amplifiers in an array. Using network analysis methods, we predict exactly the field patterns of each array element under changing loading conditions. The values of load impedances used for MWA field calculations were based on measured data. It was observed that the tile pattern of MWA is robust to occasional low-noise amplifier damage. The ability to predict the embedded element patterns without the need to repeat numerical simulations is especially useful for such large-scale projects as the SKA.

17:20 A Beamforming Approach to the Self-Calibration of Phased Arrays

[Quentin Gueuning](#) (University of Cambridge, United Kingdom (Great Britain)); [Anthony Keith Brown](#) (University of Manchester, United Kingdom (Great Britain)); [Christophe Craeye](#) (Université Catholique de Louvain, Belgium); [Eloy de Lera Acedo](#) (University of Cambridge, United Kingdom (Great Britain))

In this paper, we propose a beamforming method for the calibration of the direction-independent gain of the analog chains of aperture arrays. The gain estimates are obtained by cross-correlating the output voltage of each antenna with a voltage beamformed using the other antennas of the array. When the beamforming weights are equal to the average cross-correlated power, a relation is drawn with the StEFCal algorithm. An example illustrates this approach for few point sources and a 256-element array.

17:40 Parallel Plate Waveguide Simulator of a Dense Connected Dipole Array

[Rene A.C. Baelemans](#) (International Centre for Radio Astronomy Research, Curtin University & Eindhoven University of Technology, Australia); [David S Prinsloo](#) (ASTRON & Netherlands Institute for Radio Astronomy, The Netherlands); [A. B. \(Bart\) Smolders](#) (Eindhoven University of Technology, The Netherlands); [Adrian Sutinjo](#) (Curtin University, Australia); [David B Davidson](#) (Curtin University, Australia & Stellenbosch University, South Africa); [Randall Wayth](#) (International Centre for Radio Astronomy Research (ICRAR), Australia)

In this paper we propose the use of a parallel-plate waveguide simulator as a useful design verification step of very large phased-array systems. We base the derivation of the theoretical concept upon the wideband capacitively connected-dipole array. It is shown to be key to correctly terminate the cavity to the free-space boundary with the use of electromagnetic absorbers to minimize reflections.

18:00 Investigations of Quadruple-Ridge Flared Horn Performance for ngVLA Band 2

[Dirk de Villiers](#) (Stellenbosch University, South Africa); [Robert Lehmsiek](#) (EMSS Antennas, South Africa); [Fahmi Mokhupuki](#) (Stellenbosch University, South Africa)

The design of an all-metal quadruple-ridge flared horn (QRFH) feed antenna for the current nominal ngVLA optics is presented. The antenna is required to operate over the 3.5 GHz - 12.3 GHz band with a reflection coefficient of better than 15 dB, while maximizing the receiving sensitivity over the band. Analytical profiles for the horn and ridges are employed to reduce the design space dimensionality (over that of spline profiled antennas). Simulated results suggest sensitivity performance to within 10% of that achievable with octave band corrugated horn antennas.

CS32: High-Frequency Methods and Applications

T10 EM modelling and simulation tools / Convened Session / Electromagnetics

Room: B9

Chairs: [Ludger Klinkenbusch](#) (Christian-Albrechts-Universitaet zu Kiel, Germany), [Giuliano Manara](#) (University of Pisa, Italy)

16:40 *Asymptotic Expansion of the Reciprocity Integral in a Bidirectional Ray-Tracing Approach*

[Mehmet Mert Taygur](#) (Technical University of Munich, Germany); [Thomas F. Eibert](#) (Technical University of Munich (TUM) & Chair of High-Frequency Engineering (HFT), Germany)

Bidirectional ray-tracing launches rays from both the transmitter and the receiver sites, where the transfer function between the antennas can be computed by evaluating a reciprocity interaction integral. In this work, an asymptotic expansion approach for the evaluation of this interaction integral is introduced and discussed. By using an oscillatory integral representation and high-frequency assumptions, it is shown that the stationary phase approximation yields a simple algebraic expression for the result of the integral. Thus, the evaluation of the reciprocity integral becomes much more straightforward without any significant decline in terms of accuracy. The strong dependency between computation time and operating frequency is mostly avoided, in contrast to the traditional integration approaches. As a result, substantial speed-up factors can be achieved. Numerical results demonstrate the merits of this approach.

17:00 *A Uniform Theory of Diffraction for a Curved PEC Wedge Excited by an Obliquely Incident Astigmatic Electromagnetic Gaussian Beam*

[Prabhakar H. Pathak](#) (The Ohio State University, USA); [Hsi-Tseng Chou](#) (National Taiwan University, Taiwan)

This paper presents a uniform theory of diffraction for a beam (UTDB) when it illuminates a general curved edge in an otherwise smooth PEC surface. The solution obtained is utilized for analyzing large reflector antennas in a very rapid fashion.

17:20 *Radiation Shaping by Using Lattice Modes in a Dual-feed Dielectric Structure*

[Silvio Ceccuzzi](#), [Ludovica Tognolatti](#) and [Paolo Baccarelli](#) (Roma Tre University, Italy); [Vakhtang Jandieri](#) (General and Theoretical Electrical Engineering (ATE), Faculty of Engineering, Germany); [Cristina Ponti](#) and [Giuseppe Schettini](#) (Roma Tre University, Italy)

Electromagnetic Band-Gap (EBG) media, working right above the band-gap can shape the radiation of a simple emitter embedded in their periodic structures. In this region of the dispersion diagram, degenerate lattice modes can be selectively excited with a proper positioning of the primary sources. This paper presents the design of an antenna that exploits such physical mechanism, which is potentially attractive at mm-waves since it relies on dielectric structures. An antenna fed by two sources and based on a square lattice of dielectric cylinders is presented. For the first time, the dependencies of radiation properties on some geometrical parameters are investigated before moving to a final realistic design.

17:40 *3D Diffraction of a Complex Source Beam by a PEC Wedge*

[Ludger Klinkenbusch](#) (Christian-Albrechts-Universitaet zu Kiel, Germany); [Giuliano Manara](#) and [Sergio Terranova](#) (University of Pisa, Italy)

The scattering and diffraction of a 3D Complex-Source Beam by a wedge made from a perfect electric conductor is analyzed in this paper. The analytic solution is based on the corresponding scalar (acoustic) fields where both soft and hard boundary conditions have to be considered at the wedge faces. In particular, a new spherical-multipole solution is presented for an incident uniform CSB which consist of both diverging and converging parts. First numerical results include the scattering and diffraction of a scalar 3D uniform CSB by both acoustically soft and hard wedges.

18:00 *Wiener-Hopf Analysis of the Scattering from an Abruptly Ended Dielectric Slab Waveguide*

[Vito Daniele](#) (Polytechnic of Turin, Italy); [Guido Lombardi](#) (Politecnico di Torino, Italy); [Rodolfo Zich](#) (Politecnico di Torino & ISMB, Italy)

Abruptly ended dielectric slabs are important components in several areas of applied electromagnetism. For the study of these geometries, a variety of analytical methods have been proposed in the past. In this paper we formulate the problem in terms of Wiener-Hopf equations and we apply the novel and effective semi-analytical solution technique known as Fredholm factorization.

T11-P02/1: Channel Modelling for Massive MIMO and Near-Field Communication Systems

T11 Fundamental research and emerging technologies / Regular Session / Propagation

Room: B10

Chair: [Said Mikki](#) (University of New Haven, USA)

16:40 *Measurement Based Millimeter Wave Massive MIMO Channel Parameter Comparison*

[Heng Zhang](#), [Yu Shao](#) and [Xi Liao](#) (Chongqing University of Posts and Telecommunications, China); [Jiliang Zhang](#) (The University of Sheffield, United Kingdom (Great Britain)); [Jie Zhang](#) (University of Sheffield, Dept. of Electronic and Electrical Engineering, United Kingdom (Great Britain))

Massive multiple-input multiple-output (MIMO) plays a key role in millimeter wave (mmWave) communications. In this paper, a measurement campaign based on virtual antenna arrays is proposed to characterize indoor massive MIMO channel in mmWave band. Measurements are taken place in an empty hall environment and a rich scattering environment. Measurements are conducted using a virtual uniform rectangular array (URA) whose total elements are set to be 5 by 5, 10 by 10 and 20 by 20 respectively at 28 GHz and 38 GHz with bandwidth of 4 GHz. The power angle delay profiles in each scenario are presented and channel characteristics are analyzed. MIMO performances such as beam width, side lobe level and spatial resolution are compared with different array sizes and frequencies. Measurement results show that the beamwidth of the main lobe decreases with array size and central frequency, and therefore the resolution of multipath becomes higher.

17:00 *Massive MIMO Channel Measurement and Characterization for Manufacturing Scenario*

[Zhimeng Zhong](#) (Huawei Technologies Co., Ltd., China); [Yuntian Pan](#) (Huawei Technologies CO., Ltd., China); [Jianyao Zhao](#) (Huawei Technologies Co., Ltd., China)

One of the main differences between 5G and previous generations of cellular networks is that 5G supports not only mobile broadband enhancement, but also unprecedented reliability and very low latencies. This is beneficial to new applications in manufacturing scenario. In order to design a feasible wireless solution for manufacturing scenario, the particular characteristics of manufacturing environments need to be considered. In this paper, the massive MIMO channel measurement in factory was conducted, and the channel propagation in the spatial and frequency domains were analyzed and compared with a general indoor scenarios. Due to more metal reflections and big machine deployment, it was found that there were dense multipath so that the delay and angular spreads are larger than the ones in office scenario. Moreover, the effect of particular channel characteristics on communication system in a manufacturing scenario, was investigated in terms of Cyclic Prefix length and MIMO rank.

17:20 *Study on Beamforming V2I Scenarios for Sub-6 GHz and mmWave Channels*

[Christian Ballesteros](#) (Universitat Politecnica de Catalunya, Spain); [German Ramirez Arroyave](#) (Universidad Nacional de Colombia, Colombia); [Luca Montero Bayo](#) (Universitat Politecnica de Catalunya, Spain); [Jordi Romeu](#) (Universitat Politècnica de Catalunya, Spain); [Luis Jofre](#) (Universitat Politecnica de Catalunya, Spain)

The study of the wireless channel between a hybrid massive MIMO Base Station (BS) and a vehicular platform is proposed. Several multi-antenna geometries and MIMO architectures in both vehicle and BS are numerically modeled and compared. Different metrics are used for the assessment of the system performance, including channel capacity, in two frequency bands, sub-6 GHz (5.9 GHz) and millimeter-wave (mmWave) (26 GHz), under different propagation conditions. The use of beamforming techniques on the vehicle side is compared to conventional SISO and MIMO solutions. In the urban scenario used in the study, a 45° beamwidth circular array is able to enhance the single monopole performance up to 157% in capacity, and outperform MIMO 4x4 in most situations.

17:40 *An Electromagnetic Framework for the Deployment of Reconfigurable Intelligent Surfaces to Control Massive MIMO Channel Characteristics*

[Debdeep Sarkar](#) (Royal Military College Canada, Canada); [Said Mikki](#) (University of New Haven, USA); [Yahia Antar](#) (Royal Military College of Canada, Canada)

In this paper, we deploy a full-wave FDTD paradigm to investigate the effect of reconfigurable intelligent surface (RIS) - switchable frequency-selective surfaces (FSS) - on generic massive MIMO uplink channel's eigenspace structure. We place an RIS based on two switchable FSS layers in the vicinity of a 64-element massive MIMO base-station (BS) array, serving a cluster of four fixed user equipment (UE) units. Utilizing an electromagnetic tool based on time-averaged Poynting flow developed recently by the authors, we demonstrate how the illumination of BS-array aperture can be controlled by the intentional deployment of various switching states in the RIS placed near the BS. We show that such supplementary RIS structures may assist the wireless link engineer in deterministically "customizing" the uplink channel behaviour by selectively enhancing/suppressing certain channel eigenvalues.

18:00 *WBAN Channel Modeling on Electromagnetic Interaction in Biological Tissues for Estimating Path Loss Characteristics*

[Prapti Ganguly](#) (A. K. Choudhury School of Information Technology, University of Calcutta, India); [Ananya Dey](#) and [Debarati Ganguly](#) (Institute of Radio Physics and Electronics, University of Calcutta, India); [Chinmoy Saha](#) (Indian Institute of Space Science and Technology, India & Royal Military College of Canada, Canada); [Jawad Y Siddiqui](#) (University of Calcutta, India & Royal Military College of Canada, Canada)

The increasing use of miniaturized non-invasive health monitoring devices have facilitated the growth and development of WBANs (Wireless Body Area Networks). Antennas used for this kind of applications are designed taking into account the properties of the biological medium on which they are to be placed. This paper presents results for deploying a

T10-E03/2: Computational and Numerical Techniques 2

T10 EM modelling and simulation tools / Regular Session / Electromagnetics

Room: B11

Chair: Abdelrahman Abdallah Ijeh (Université Cote d'Azur, France)

16:40 Floquet Mode Analysis on Groove Gap Waveguide

Jiro Hirokawa, Keisuke Ejiri and Takashi Tomura (Tokyo Institute of Technology, Japan)

This paper presents the Floquet mode analysis on a groove gap waveguide by considering the structural periodicity in the propagation direction. The Floquet modes are categorized into not only regular propagating and attenuating modes but also modes having the complex propagation constant reflecting the existence of the pins. The expansion of generalized scattering matrix using the Floquet modes gives difference from that using conventional cross-sectional modes in an example of a converter between a regular rectangular waveguide and the groove gap waveguide.

17:00 Modeling of Quantum-Dot Elliptical Nanowire Single-Photon Sources

Uğur Meriç Gür, Niels Gregersen, Samel Arslanagić and Michael Mattes (Technical University of Denmark, Denmark)

True monomode operation and polarization control capability of elliptical nanowires leads to the need of efficient solvers for open elliptical nanophotonic structures. In this contribution, a full-wave vectorial modal method for open boundary elliptical geometries is presented for designing quantum-dot elliptical nanowire structures. The method exploits symmetry properties, provides insight into the physical behavior of the system giving direct access to propagation constants and mode profiles, which will be used in the efficiency calculations of the single-photon sources.

17:20 Mapping Between Complex Eigenmodes and Complex Propagation Constant for Uniform Rectangular Metallic Waveguides

Joao Guilherme Nizer Rahmeier, Ville Tiukuvaara and Shulabh Gupta (Carleton University, Canada)

This paper presents a rigorous mathematical mapping between the complex eigenmodes and the complex propagation constant for a homogeneous lossy waveguide structure. We validate the results for a rectangular waveguide, comparing the analytical mapping with the results from a FEM-EM solver. It has been found that a precise mapping between $\Omega(\beta)$ and $\gamma(\omega)$ exists, which enables predicting the driven mode solution from the eigenmode analysis. While valid for a simple canonical case of a dispersive waveguide, such mapping establishes the underlying principles of how the complex eigenmodes are formulated inside typical commercial simulators.

17:40 Time-Domain Modeling and Simulation of EM-Fields Propagation in Anisotropic Dispersive Media with Non-Conformal Meshing

Abdelrahman Abdallah Ijeh (Université Cote d'Azur, France); Marylène Cueille (University of Nice Sophia Antipolis CNRS, France); Jean-Lou Dubard (Université de Nice - Sophia Antipolis, CNRS, France); Michel Ney (IMT Atlantique, France)

This article presents a time-domain numerical scheme for simulating EM-computational problems that include complex media and fine geometrical details in critical regions. These problems are common in engineering and applied physics. To name a few, microwave and optical devices that contain complex media, antennas characterization in presence of complex media, such as biological tissues, biomedical technology...etc. Modeling such scenarios requires the ability to handle two types of complexities, namely material at geometrical ones. Material complexity is taken in consideration using a convolution process with a matrix of time-domain filters; this models the dispersive and anisotropic nature of such media. On the other hand, non-conformal local mesh refinement approach is adopted to accurately discretize important fine details without exploding the computational resources. Numerical simulations are presented to show the efficiency, the accuracy and the stability of the proposed approach, with comparisons to FEM method and TLM method with regular fine meshing.

18:00 Perturbational Method for Modeling Electromagnetic Propagation Through Non-axisymmetric Geophysical Formations

Lisseth Saavedra (Pontifical Catholic University of Rio de Janeiro & Center for Telecommunications Studies, CETUC, Brazil); Guilherme Simon da Rosa (Pontifical Catholic University of Rio de Janeiro, PUC-Rio, Brazil); Jose R Bergmann (PUC-Rio, Brazil)

This work presents a new technique for modeling electromagnetic sensors used in well prospecting. These sensors are usually immersed in complex (asymmetric, inhomogeneous, and dissipative) geophysical formations, resulting in a challenging problem for traditional computation electromagnetic techniques. We analyzed this propagation problem by using a perturbational method based on the Born approximation for solving a Fredholm integral equation. Numerical results are presented for evidencing the effects of non-symmetric geophysical formations in the response of electromagnetic well-logging tools.

IW04: CTG Workshop on Advances in Antenna Measurements (Antenna Systems Solutions S.L.)

T12 Scientific / Industrial Workshops

Room: B3

Dr. Sergiy Pivnenko, Antenna Systems Solutions S.L.

IW10: Sophisticated Antenna Development for Modern Hearing Aids (WS Audiology)

T12 Scientific / Industrial Workshops

Room 6

Wednesday, 18 March

Wednesday, 18 March 8:30 - 12:20

T09-A19: Reflectarrays and Transmitarrays

T09 Space (incl. cubesat) / Regular Session / Antennas

Room: A2

Chairs: Jose A. Encinar (Universidad Politecnica de Madrid, Spain), Michael F. Palvig (TICRA, Denmark)

8:30 Multifocus Reflectarray Concept: Preliminary Design and Possible Applications

Christophe Granet (Lyrebird Antenna Research Pty Ltd, Australia); Michael F. Palvig, Min Zhou and Stig Sørensen (TICRA, Denmark)

The concept of a multifocus reflectarray is introduced along with a preliminary design at Ka-band and an explanation of the possible applications this new concept can be applied to. The realized reflectarray provided both Rx and Tx main beams in a single direction even though the feeds were separated.

8:50 Design of Ka-band Reflectarray Antennas for High Resolution SAR Instrument

Min Zhou, Michael F. Palvig, Stig Sørensen and Jakob Rosenkrantz de Lasson (TICRA, Denmark); David Marote Alvarez (Airbus/CASA, Spain); Michael Notter (Airbus DS Ltd, United Kingdom (Great Britain)); Dennis T. Schobert (European Space Agency, The Netherlands)

The design of polarization selective reflectarrays for high resolution and wide swath SAR instrument in Ka-band is presented. The antenna system consists of nine dual-offset reflectarray panels, each with the size of 1.5m×0.55m. The reflectarrays operate in two modes, a high-resolution mode with a directive beam in one polarization, and a low-resolution

mode with a broader beam in the orthogonal polarization. Two designs are presented, a single-layer design and a multilayer design. Both designs provide a gain >46.7dBi for the high-resolution mode and a gain >45.2 dBi for the low-resolution mode.

9:10 Preliminary Simulations of a 1.8-M Parabolic Reflectarray in a Geostationary Satellite to Generate a Complete Multi-Spot Coverage for Tx

[Daniel Martinez-de-Rioja](#) (Universidad Politécnica de Madrid, Spain); [Jose A. Encinar](#) (Universidad Politecnica de Madrid, Spain); [Yolanda Rodriguez-Vaqueiro](#) and [Antonio Pino](#) (University of Vigo, Spain)

A parabolic reflectarray antenna has been proposed to generate a complete cellular coverage in transmission to provide broadband services from a communication satellite in Ka-band. Two different approaches have been evaluated to design a parabolic reflectarray able to generate four spaced beams per feed in four different combinations of frequency and polarization. A 1.8 m parabolic reflectarray has been simulated when it is illuminated by a feed block of 27 horns. The results show the capacity to generate 108 spot beams in good agreement with the requirements imposed in satellite communications. The proposed concept could be used to reduce the number of on-board antennas and feed chains required to generate a multi-spot coverage in Ka-band.

9:30 A Wideband Reflectarray Using Slotted Patch with Concave Arms

[Ming Min](#), [Lu Guo](#) and [Wenjie Feng](#) (Nanjing University of Science and Technology, China)

In this paper, a wideband reflectarray antenna using dented patch with concave arms is presented. The broadband behavior is the result of combination of two bandwidth improvement approaches, i.e. employing multi-resonance element and slotted patch element. By varying the lengths of the slots together with the concave arms, the phase range can reach 360° with a rather linear slope. Based on this novel element, an offset-fed 23*23 reflectarray antenna is designed and simulated. The simulated 1-dB gain bandwidth is 40% with a peak aperture efficiency of 67%, while the side-lobe and cross-polarization levels are also satisfactory.

9:50 Band Enhancement in Reflectarrays for Space Communications Based on Multi-Frequency Synthesis Procedure

[Daniel R. Prado](#) (Universidad de Oviedo & Signal Theory and Communications, Spain); [Manuel Arrebola](#) and [Marcos R. Pino](#) (Universidad de Oviedo, Spain); [George Goussetis](#) (Heriot-Watt University, United Kingdom (Great Britain))

This paper describes a multi-frequency wideband optimization procedure and performance results of a very large spaceborne reflectarray for Direct-to-home (DTH) application in a 10% bandwidth. The proposed design methodology is based on the generalized intersection approach and the use of a multi-resonant unit cell with multiple degrees of freedom (DoF). The procedure is divided into three stages to facilitate convergence towards a wideband performance. First, a initial narrowband design at central frequency is obtained. Then, a broadband optimization including XPD requirements is carried out with a limited number of DoF. Finally, more DoF are included in the last stage optimization to obtain a wideband reflectarray with improved cross-polarization performance. A minimum improvement of 4.8 dB is achieved in the crosspolarization performance for both XPD and XPI in a 10% bandwidth, while ensuring that the copolar pattern complies with the specifications in the whole band.

10:10 Coffee Break

10:40 Bandwidth Improvement of Reflectarray Cells Using Variable Rotation Technique at Two Frequencies for Dual Circular Polarization

[Daniel Martinez-de-Rioja](#) (Universidad Politécnica de Madrid, Spain); [Eduardo Martinez-de-Rioja](#) (Universidad Rey Juan Carlos, Spain); [Jose A. Encinar](#) (Universidad Politecnica de Madrid, Spain); [Rafael Florencio](#) (University of Alcalá, Spain); [Rafael R. Boix](#) (University of Seville, Spain)

The bandwidth behavior has been studied and improved for a reflectarray cell formed by two symmetric arcs and dipoles printed in two layers, which uses Variable Rotation Technique at two frequencies for dual circular polarization. First, the appropriate thickness of the dielectric layers have been selected to improve the bandwidth. Then, an optimization routine has been applied to minimize the phase errors in a frequency band from 29.25-2.75 GHz. As a result of this optimization, the phase errors have been drastically reduced from ±40 to ±3 degree.

11:00 Design of a Wideband Linear-to-Circular Polarizing Reflector for Ka-band Satellite Applications

[Eduardo Martinez-de-Rioja](#) (Universidad Rey Juan Carlos, Spain); [Jose A. Encinar](#) (Universidad Politecnica de Madrid, Spain)

This contribution presents a low-profile linear-to-circular polarizing reflector with wideband operation in Ka-band. The polarizing cell consists of three parallel dipoles placed with 45° slant with respect to the direction of the incident linearly polarized field. The lengths of the dipoles are adjusted cell by cell through a dual-frequency optimization process, which accounts for the real incidence angles on the cell. A 25 x 25 cm flat polarizing reflector prototype has been manufactured and tested to validate the concept. The measurements show an axial ratio lower than 1.8 dB within the 19 - 30 GHz band, and good matching with the simulations. The proposed polarizing reflector has applications in novel multibeam antenna configurations for Ka-band satellites.

11:20 A Low-Profile and Efficient Front-End Antenna for Point-to-Point Wireless Communication Links

[Mst Nishat Yasmin Koli](#) and [Muhammad Usman Afzal](#) (Macquarie University, Australia); [Karu Esselle](#) (University of Technology Sydney, Australia); [Raheel Maqsood Hashmi](#) (Macquarie University & IEEE, Australia); [Md Zahidul Islam](#) (Teleaus: Serveno Australia Pty Ltd, Australia)

This paper investigates the design and performance of an efficient, medium-gain, front-end antenna of the type of radial line slot array (RLSA), for wireless communication systems. The antenna consists of two conducting metal plates forming a radial waveguide. A single coaxial connector is used to feed the electromagnetic energy from the bottom of the radial waveguide. The antenna has a radius of 0.15 m and operating at a frequency of 12 GHz. It was simulated using CST Microwave Studio 2019 and the results show that the antenna has an acceptable level of impedance matching in the frequency range from 11 GHz to 13 GHz, with a peak directivity of 25.6 dBi and a peak realized gain of 25 dBic at 12 GHz. The antenna has 3-dB gain bandwidth of 13.9% from 11.4 GHz to 13.1 GHz. Its radiation efficiency is 96% and a total efficiency is 85.3% at 12 GHz.

11:40 Perforated Dielectric Reflectarray in Ka-band

[Andrea Massaccesi](#), [Michele Beccaria](#) and [Paola Pirinoli](#) (Politecnico di Torino, Italy)

This paper proposes a single-layer perforated dielectric reflectarray antenna that operates in Ka-band. The unit-cell is made up of a dielectric element perforated by a centered square hole, whose size is used to control the phase of the reflection coefficient. This cell has been used to design a 52x52 offset reflectarray working at 30 GHz, whose numerical analysis proves that it has good radiation features. The proposed configuration is particularly convenient since Additive Manufacturing processes can be exploited for its fabrication.

12:00 A Reconfigurable Origami Reflectarray

[Abdul sattar Kaddour](#) (Florida International University, USA); [Constantinos L. Zekios](#) (Florida International University, ECE & FIU, USA); [Stavros Georgakopoulos](#) (Florida International University, USA)

This paper presents a novel Miura-Ori origami reflectarray unit-cell. This origami inspired unit-cell allows efficient folding/unfolding, high packing efficiency, easy deployment and frequency reconfigurable behavior. The unit-cell is composed of 4 parallelogram patches that can achieve 560° phase shift. To synthesize the radiation pattern and the directivity of a deployable 25 by 25 element reflectarray, for different folding states, a procedure based on the conventional array summation with proper element excitation is proposed. A maximum directivity of 32 dBi is obtained with a 2 dB bandwidth from 8.2 GHz to 9.4 GHz (13%). The proposed origami antenna can adjust its operational frequency band by changing its folding angle; therefore, it is physically reconfigurable. The main advantage of this antenna is that the size at its maximum folded state is approximately 6 times smaller than its volume when it is fully deployed thereby offering a significant advantage for small satellites applications.

CS06: AMTA/IRACON Session: Over-The-Air Testing of 5G Radios

T02 Millimetre wave 5G / Convened Session / Measurements

Room: A3

Chairs: [Wei Fan](#) (Aalborg University, Denmark), [Pekka Kyösti](#) (Keysight Technologies & University of Oulu, Finland)

8:30 Examining and Optimising Far-Field Multi-Probe Anechoic Chambers for 5G NR OTA Testing of Massive MIMO Systems

[Stuart F Gregson](#) (Queen Mary, University of London, United Kingdom (Great Britain)); [Clive Parini](#) (QMUL, United Kingdom (Great Britain))

Direct far-field (DFF) testing has become the de facto standard for sub-six GHz over the air (OTA) testing of the physical layer of radio access networks with the far-field multi-probe anechoic chamber (FF-MPAC) being especially widely deployed for the verification of massive multiple input multiple output (Massive MIMO) antennas in the presence of several users. The adoption of mm-wave bands within the fifth generation new radio (5G NR) specification has meant that, as these systems require the user equipment be placed in the far-field of the base transceiver station (BTS) antenna, either excessively large FF-MPAC test systems are required or, the user equipment is paced at range-lengths very much shorter than that suggested by the classical Rayleigh criteria. This paper explores range length effects on several communication system figures of merit and examines the consequences of testing within smaller enclosures. Results are presented and discussed.

8:50 Mid-field OTA RF Test Method: New Developments and Performance Comparison with the Compact Antenna Test Range (CATR)

[Hongwei Kong](#) (Keysight Technologies (China) Co., Ltd., China); [Ya Jing](#) (Keysight Technologies, China); [Zhu Wen](#) (Keysight Technologies Co. Ltd, China); [Li Cao](#) (Keysight Technologies (China) Co., Ltd., China)

In this paper, new mid-field developments, including the gray box approach and a mid-field prototype system covering both frequency range one and two, are presented to address challenges in 5G massive MIMO (mMIMO) base station (BS) OTA RF test. Simulations and measurements prove the effectiveness of the new developments. Further analysis of 3GPP BS OTA RF measurement metrics and performance requirements indicate that the mid-field system can measure most of those required metrics with enough dynamic range. Comparative test results with a CATR system using a commercial 5G BS prove that the mid-field system can achieve comparable test results as the CATR system. The comparability with the CATR system, the broad coverage of 3GPP measurement metrics, and the compact size show that the mid-field system is an effective system for 5G mMIMO BS OTA RF test in both frequency range one and two.

9:10 On Noise and Interference Modeling for Over-the-air Testing of MIMO Terminals

[Wei Fan](#) (Aalborg University, Denmark); [Pekka Kyösti](#) (Keysight Technologies & University of Oulu, Finland); [Yilin Ji](#) and [Gert Pedersen](#) (Aalborg University, Denmark)

As the fifth generation (5G) ecosystem matures, the time for large-scale 5G radio commercialization is now. Over-the-air (OTA) radiated testing is seen to replace currently dominantly adopted cable conducted testing for upcoming radio systems due to integrated antenna designs. To properly evaluate performance of radio systems in fading channel

conditions, it is typically needed to model the realistic signal, interference and noise conditions in the testing environment. However, interference and noise modeling is largely overlooked in the literature in OTA testing, since the discussion is typically focused on the signal alone. In this paper, interference and noise modeling in three OTA setups, including the multi-probe anechoic chamber (MPAC), radiated two stage (RTS) and reverberation chamber (RC) is discussed and summarized.

9:30 *The Study of 5G Massive MIMO End-to-End MPAC Test Solution*

[Xiang Zhang](#) (University of Posts and Telecommunications, China); [Xiaolong Liu](#) (Beijing University of Post Telecommunications, China); [Guiming Wei](#) (China Academy of Information and Communications Technology, China); [Yichen Zhao](#) (China Mobile Group Device Co., Ltd, China); [Yuhang Guo](#) (Beijing University of Posts and Telecommunications & Intel China Lab, China)

Due to the large demand of high data rate and low latency in mobile service, 5G network has been commercially deployed in the many countries, e. g., China, US, Korea and etc.. Massive multiple input multiple output (MIMO) and hybrid beamforming techniques are observed as the key enhancement in the physical layer, and therefore, how to accurately measure the data throughput between massive MIMO gNB and user equipment (UE) under channel fading conditions has drawn much attentions in recent years. This paper introduces a novel simplified bidirectional 3D channel reproducing method for multi-probe anechoic chamber, in which the channel parameters are co-generated by the phase shift box and channel emulator. The simulation and test results show that the proposed method achieves similar performance compared with the whole channel emulator solution and meanwhile significantly reduces the cost of instruments.

9:50 *Chamber Array Antenna Layout for Compact OTA Measurements*

[Mohammad Poordaraee](#) (University of Twente, The Netherlands); [Andrés Alayón Glazunov](#) (University of Twente, The Netherlands & Chalmers University of Technology, Sweden)

An optimized irregular planar array antenna layout with uniform excitation of antenna elements is presented for Random-LOS OTA (Random Line-Of-Sight Over-The-Air) characterization setups. A plane wave is synthesized within a cylindrical 3D test zone at 2.7 GHz. The obtained thinned array achieves a 52% reduction of the number of elements and a 45% aperture size as compared to a uniform fully populated planar array with an inter-element distance of 0.93λ , which is the optimum distance through $[\lambda/2, \lambda]$ based on the presented cost function at this paper. The obtained maximum phase deviation and the maximum field amplitude deviation from the average field distribution in the 3D test zone of the proposed optimized chamber array antenna layout are approximately 6.4 degrees and 3.9 dB, respectively. The numerical computation of the radiation pattern of a 10×10 element uniform planar array antenna as AUT placed within the test zone was performed too.

10:10 Coffee Break

10:40 *Measurement Characterization of Aperture Correction Technique for EMF*

[Johan Lundgren](#), [Jakob Helander](#) and [Mats Gustafsson](#) (Lund University, Sweden)

Techniques for accurate, robust and efficient over-the-air testing for devices in the next generation communication system are important. This work aims at presenting the use of an aperture calibration technique, through which field values and power density values are reconstructed at an arbitrary plane in the near-field from a measurement of a separate plane for devices operating in 28-60 GHz. The technique calibrates for the probe interaction, and for the measured position, providing promising results. Power density levels is important for electromagnetic field (EMF) compliance assessment of 5G. In this work the technique is utilized to reconstruct the power densities, as close as $\lambda/5$, for three different radiating devices. The results are compared with simulations. An investigation into how the technique performs – for different frequencies, using synthetic input data, various grid sampling, noise and choice of numerical parameters - is carried out, showing the regions of applicability.

11:00 *OTA Testing of Antennas & Devices Using Plane Wave Generator or Synthesizer*

[Francesco Scattone](#) (Microwave Vision Group (MVG), Italy); [Darko Sekuljica](#) (MVG, Italy); [Andrea Giacomini](#), [Francesco Saccardi](#), [Alessandro Scannavini](#) and [Lars Foged](#) (Microwave Vision Italy, Italy); [Evgeni Kaverine](#) and [Nicolas Gross](#) (MVG Industries, France); [Per Iversen](#) (Orbit/FR, USA)

The Plane Wave Synthesizer (PWS) approximates the plane-wave condition and, thus, the Far-Field condition over a finite volume at a reduced distance called the Quiet Zone (QZ). It consists of an array of elements with suitably optimized complex excitation coefficients. The concept of a high performance, dual polarized PWS supporting up to 1:10 bandwidth was presented. A demonstrator of a dual polarized PWS has been designed, manufactured and tested in the 600MHz to 6GHz frequency range. In this paper, we report on the measured QZ performance of different implementations of the PWS demonstrator. QZ fields are determined within a volume by spherical NF measurements and back-propagation. It is shown experimentally that the QZ field uniformity can be trade-off with size. Results of the verification testing and comparison to spherical near field measurements are reported using electrically small devices.

11:20 *Quiet Zone Verification of Plane Wave Synthesizer Using Polar Near-Field Scanner*

[Adam Tankielun](#), [Anes Belkacem](#), [Mustafa Akinci](#) and [Mert Celik](#) (Rohde & Schwarz GmbH & Co. KG, Germany); [Hendrik Bartko](#) (Rohde & Schwarz, Germany); [Benoit Derat](#) (Rohde & Schwarz, Spain)

5G active antenna system base stations operating in frequencies below 7.125 GHz (FR1) need to be tested using a cost-effective OTA measurement solution since traditional farfield antenna ranges are too large. Plane wave synthesizer (PWS) allows testing with far-field conditions at the near-field distance with the minimum system dimensions. Uniformity of the synthesized plane wave field in the quiet zone (QZ) is a key performance parameter of PWS. QZ verification setup using a polar near-field scanner and a vector network analyzer is presented with description of the main hardware components, instrument settings and correction techniques for raw measurement data. Various field uniformity metrics are defined and calculated for one measurement example. Measurement repeatability is also verified to evaluate stochastic errors in the verification.

11:40 *3D Calibration of an Over-the-Air Testbed for GNSS CRPA Antenna Testing*

[Renato Zea](#) (Fraunhofer IIS, Germany); [Ramona Brochloss-Gerner](#) (Fraunhofer Institute for Integrated Circuits IIS, Germany); [Mario Lorenz](#) (Technische Universität Ilmenau, Germany); [Markus Landmann](#) (Fraunhofer Institute for Integrated Circuits IIS, Germany); [Alexander Rügamer](#) (Fraunhofer IIS, Germany); [Giovanni Del Galdo](#) (Fraunhofer Institute for Integrated Circuits IIS & Technische Universität Ilmenau, Germany)

This paper presents an approach to calibrate an OTA testbed to perform 3D full polarimetric wave field synthesis (WFS) to test controlled reception pattern antennas for global navigation satellite systems (GNSS). So far 2D and 2.5D WFS has been mostly used for single polarization OTA testing, nevertheless the level of accuracy on representing real-world scenarios becomes always a challenge, specially for GNSS testing, since the azimuth and elevation angles of the satellites with relation to the device under test can be accurately represented only in a 3D environment. Instead of using three electromagnetic (EM) field probes to perform the calibration of the three orthogonal field vectors (XYZ) for emulation of arbitrary polarized wave fields, this approach uses only one EM field probe to perform the entire calibration process. The limitations and accuracy of the proposed calibration procedure for full polarimetric WFS is shown and demonstrated in this contribution.

12:00 *Comparing Options for 5G MIMO OTA Testing for Frequency Range One*

[Doug Reed](#) and [Alfonso Rodriguez-Herrera](#) (Spirent Communications, USA); [Jukka-Pekka Nuutinen](#) (Spirent Communications, Finland)

MIMO OTA is the well-established and predominant method to test mobile devices with multiple antennas. The MIMO OTA approach subjects the device under test to challenging channel conditions (Multipath, Doppler, Interference, Correlation, Cross-Polarization), and the mobile device is tested in a wholistic way, i.e. chipset, antenna design, and enclosure. Additionally, multiple antenna connectors make standard conductive tests complicated and impractical. As new 5G NR devices enter the market, it becomes necessary to create a test methodology that can assess their performance in a standardized way using a MIMO OTA test.

CS45: New Perspectives and Applications of Characteristic Mode Analysis in Antenna Design

T11 Fundamental research and emerging technologies / Convened Session / Antennas

Room: B1

Chairs: [Ozlem Aydin Civi](#) (Middle East Technical University, Turkey), [Hui Li](#) (Dalian University of Technology, China), [Philipp Gentner](#) (Ericsson Antenna Technology Germany GmbH, Germany)

8:30 *Characteristic Mode Analysis for the Design of Nanosatellite Reconfigurable Antennas*

[Simone Genovesi](#) (University of Pisa, Italy); [Francesco Alessio Dicandia](#) (GreenWaves, Italy)

A novel S-band antenna concept hosted on a 1U form factor CubeSat platform is designed by exploiting the Characteristic Modes Theory (CMT). The innovative strategy provides useful design guidelines to transform the external platform into an efficient radiator by stimulating an optimal current distribution on its conductive surface. The effect of the satellite platform on the radiated performances (efficiency, band, gain) is intrinsically taken into account and profitably exploited to realize an efficient radiation system. The minimally invasive radiators, strategically collocated on the platform thanks the CMT, allow achieving a great saving of space and an optimal modal current excitation able to provide excellent radiation performance.

8:50 *Antenna Positioning for Bandwidth Optimization Using Characteristic Mode Analysis*

[Peter William Futter](#) (Altair Development S.A. (Pty) Ltd, South Africa); [Ulrich Jakobus](#) (Altair Engineering GmbH, Germany)

Characteristic mode analysis is used to understand the modal behavior of antennas, and how they interact with the structure they are mounted on. While this insight can be applied in various ways to improve the design, one of the biggest challenges is often how to place the antenna on the structure to excite specific mode(s). Previous work describes a good approach but imposed certain limitations - multiple antennas were used, and a narrow frequency band was considered. For many applications an approach is needed to position a single antenna that operates in a wider frequency band. This paper will attempt to broaden the understanding of those limitations and proposes a design approach which surpasses the limitations, albeit at the cost of exciting additional modes. The approach covers positioning a single wider band antenna to excite specific modes while optimizing the antenna bandwidth. It is applied to two antenna examples.

9:10 *Use of Characteristic Modes in the CBFM for the Analysis of Large Arrays*

[Yigit Haykir](#) and [Ozlem Aydin Civi](#) (Middle East Technical University, Turkey)

In this work, the characteristic basis function method (CBFM) is presented in junction with the characteristic modes (CMs). In this approach, characteristic modes are defined as primary basis functions on each array element. In order to take into account mutual couplings, secondary basis functions are introduced as in conventional CBFM. Since characteristic modes are excitation-free, the basis functions and consequently the reduced matrix obtained by the CBFM are also independent of the excitation.

9:30 *Reducing User Effects on Mobile Handset Antennas Using Mode Mapping*

[Miao Wu](#), [BaoYi Wang](#) and [Hui Li](#) (Dalian University of Technology, China)

In this work, we investigate how different radiation patterns are influenced by the user's hand, based on which we design handset antennas that are robust to the hand effect. Handset antenna working at dual bands is firstly simulated numerically, with its eigenvalues, characteristic currents and farfields calculated. Afterwards, the total pattern of the antenna is mapped to its characteristic patterns using weighting coefficients. To study the influence of the hand on each modal pattern, the pattern for the antenna with hand is then obtained. Comparing the weighting coefficients of each mode in free space and with hand, the radiation pattern with null at the boresight is less affected by the hand. According to the observation, a handset antenna, which radiates little power towards the boresight, is designed. It is proved that the radiation efficiency of the proposed antenna with hand is 2.4 dB higher than that of the reference antenna.

9:50 *Influence of p-Refinement on Accuracy of Mode Tracking Based on Correlation of Characteristic Currents*

[Ana Djurdjevic](#) and [Branko Mrdakovic](#) (WIPL-D, Serbia); [Branko Kolundzija](#) (University of Belgrade, Serbia)

Characteristic mode analysis (CMA) is a useful tool that enables a deep insight into the physical behavior of the analyzed structure. In majority of cases of practical interest wide band CMA is required. Mode tracking is then very important, but also very challenging task. In this paper we are focused on mode tracking based on correlation of the modal currents over frequency, and possibility to improve the tracking by increasing accuracy of MoM matrix calculation by using p refinement method. Results obtained from mode tracking based on correlation of characteristic fields are used as a reference. It is shown that p-refinement can bring some limited improvement of mode tracking, but the main problems related to mode tracking based on correlating the modal currents still remain.

10:10 Coffee Break

10:40 *Systematic Design Method for Asymmetric Multiport Antennas Based on Characteristic Modes*

[Nikolai Peitzmeier](#) (Leibniz University Hannover, Germany); [Dirk Manteuffel](#) (University of Hannover, Germany)

A systematic design procedure for placing ports with low correlation on an asymmetric antenna geometry is presented. By applying the mathematical description of symmetry based on group theory and group representations to the theory of characteristic modes, it is shown that it is in general not possible to realize uncorrelated antenna ports on an asymmetric antenna. Therefore, a port placement procedure based on characteristic modes is proposed for such geometries in order to realize ports with low correlation. The design procedure is based on modal parameters alone. Thus, only one full simulation run is needed in order to perform the modal analysis. The proposed procedure is illustrated by means of numerical examples.

11:00 *Systematic Approach to Design a Circularly Polarized Antenna Using the Characteristic Modes Theory*

[Hussein Jaafar](#) (The French Alternative Energies and Atomic Energy Commission, France); [Ala Sharaiha](#) (Université de Rennes 1 & IETR, France); [Sylvain Collardey](#) (University of Rennes 1, France)

This paper presents a systematic approach to design a circularly polarized antenna by taking advantage of the physical insights provided by the characteristic modes theory (CMT). A non-conventional structure is considered (celtic triskle) . The characteristic modes supported by this structure are studied and various modifications are accordingly applied to generate the desired polarization.

11:20 *Flexible Antenna Design with Characteristic Modes*

[Eva Antonino-Daviu](#) (Universitat Politècnica de València, Spain); [Aline Eid](#), [Ryan Bahr](#) and [Manos M. Tentzeris](#) (Georgia Institute of Technology, USA)

A dual-band flexible antenna on a 3-D printed support is proposed for wrist worn applications. The antenna is aimed to work at 860 MHz and 2.4 GHz. A spatial diversity technique is used to overcome the blocking of the radiation by the arm. Characteristic Mode Analysis is used as a first step of the design process, analyzing different structures.

11:40 *Broadband Metasurface-Based Antenna Using Hexagonal Loop Elements*

[Wenzhang Zhang](#), [Yi Huang](#) and [Jiafeng Zhou](#) (University of Liverpool, United Kingdom (Great Britain))

A broadband metasurface-based antenna with hexagonal loop radiating elements is presented. To achieve a broadband response, an array of hexagonal loop elements is taken as the main metasurface-based radiator. The antenna is fed by a microstrip line through a coupling slot. To reveal the underlying modal behaviors, the characteristic mode analysis was used for modeling, analyzing, and optimizing the antenna structure. The proposed broadband hexagonal loop-based antenna with an overall size of $1.1 \lambda_0 \times 1.1 \lambda_0 \times 0.06 \lambda_0$ can achieve 56% fractional bandwidth and a relatively stable gain of 7-11 dBi over the operating band.

12:00 *On the Use of Characteristic Mode Analysis for the Design of Antenna Arrays*

[Philipp Gentner](#) (Ericsson Antenna Technology Germany GmbH, Germany)

For antenna array design used in base station antennas a high polarization purity is required. Therefore this paper exploits the use of characteristic mode analysis (CMA) \cite{Harrington1971} for the design of antenna arrays. The classical antenna array description is extended with the results from a modal analysis. With this method in hand, the modes can be differentiated and selected for the application in mind; additionally the potential bandwidth and the current distribution on the elements can be explored.

CS62: Small Antenna in a Human Body Environment

T04 IoT and M2M / Convened Session / Antennas

Room: B2

Chairs: [Eva Antonino-Daviu](#) (Universitat Politècnica de València, Spain), [Ala Sharaiha](#) (Université de Rennes 1 & IETR, France)

8:30 *Small New Wearable Metamaterials Antennas for IOT, Medical and 5G Applications*

[Albert Sabban](#) (Kinneret and ORT BRAUDE COLLEGE, Israel)

Efficient small antennas are crucial in the development of wearable wireless communications systems. Low efficiency is the major disadvantage of small antennas. Meta materials technology and active components are used to improve the efficiency of small antennas. Moreover, the dynamic range and the efficiency of communication system may be improved by using active antennas. Amplifiers may be connected to the wearable antenna feed line to increase the system dynamic range. Novel wideband passive and active efficient wearable metamaterial antennas for BAN and 5G applications are presented in this paper. The gain of antennas with Split-ring resonators, SRR, is higher by 2.5dB than the antennas without SRR. The resonant frequency of the antennas with SRR is lower by 4% to 11% than the antennas without SRR. Active small wearable antennas may be used in communication systems. For example, the active metamaterial antenna gain is 13+3dB for frequencies from

8:50 *Design and Optimization of a Flexible CPW-Fed Slotted Planar Monopole for WLAN/WBAN and 5G*

[Bashar Bahaa Qas Elias](#) (Universiti Malaysia Perlis (UniMAP), Malaysia); [Ping Jack Soh](#) (Universiti Malaysia Perlis (UniMAP) & Katholieke Universiteit Leuven, Malaysia); [Azremi Abdullah Al-Hadi](#) (University Malaysia Perlis, Malaysia); [Hadi Aliakbarian](#) (University of Tehran, Iran); [Sen Yan](#) (Xi'an Jiaotong University, China)

A flexible Kapton-based coplanar waveguide-fed (CPW) patch antenna has been designed in this work to operate in different wireless applications. The wideband operation and compact size of the antenna is enabled using a simple rhombic-shaped integrated onto the monopole which was designed using a rectangular patch. The proposed broadband antenna model operated below -10 dB at 2.45 GHz and 3.5 GHz for the WLAN/WBAN and 5G band, respectively. The antenna optimization process is explained when varying the ground structure, patch dimensions, feed width, and substrate thickness using FEKO software. The performance of the antenna is studied in terms of radiation efficiency, gain, bandwidth and current distributions. Results indicate that the proposed antenna operates throughout the 2.45 and 3.5 GHz bands, with a bandwidth of 1710 MHz.

9:10 *User Body Effects on Mobile Antennas and Wireless Systems of 5G Communication*

[Kun Zhao](#) (Sony Research Center Lund, Sweden & Aalborg University, Denmark); [Zhinong Ying](#) (Sony Coporation, Sweden); [Shuai Zhang](#) and [Gert Pedersen](#) (Aalborg University, Denmark)

User body effects on mobile antennas and wireless systems for the fifth-generation (5G) mobile network is analyzed in this paper. User body effects on different antenna technologies in mobile handsets include single antenna systems, multiple antenna systems, and the antenna arrays are discussed with simulation and measurement results. The corresponding impacts on the wireless networks are studied with raytracing simulations. Several technologies on mitigating user body effects have also been provided.

9:30 *An Ultrawideband Conformal Antenna for Implantable Drug Delivery Device*

[Ahsan Noor Khan](#) and [Dingliang Wen](#) (Queen Mary University of London, United Kingdom (Great Britain)); [Yujie Liu](#) (Queen Mary University of London & Antenna Group, United Kingdom (Great Britain)); [Gleb Sukhorukov](#) (Queen Mary University of London, United Kingdom (Great Britain)); [Yang Hao](#) (Queen Mary University, United Kingdom (Great Britain))

Therapeutic treatment has been revolutionized in recent past with the advent of implantable drug delivery devices. These devices hold immense potential to treat chronic ailments, such as cancer tumours that require high drug concentration. A wireless system is an integral part of the device to regulate drug release according to prescribed dosing schedule. An antenna is important facet of a wireless system for data telemetry and receiving triggering signal from external transmitter that actuates the drug release mechanism. In this paper, we propose an ultrawideband conformal loop antenna around the capsule shaped device. The flexible layer of microchambers is also conformed around the inner shell of the capsule. The CST Gustav voxel human body model was used to perform numerical study of the antenna. According to the simulation results, the proposed capsule antenna has shown reflection coefficient of -11.83 dB at the desired frequency of 900 MHz.

9:50 ***A Multi-Functional Compact Button Antenna for Wearable Applications***

[Jiahao Zhang](#) (KU Leuven, Belgium); [Sen Yan](#) (Xi'an Jiaotong University, China); [Xiaomu Hu](#) (KU Leuven, Belgium); [Tomislav Marinovic](#) (Katholieke Universiteit Leuven & Chalmers University of Technology, Belgium); [Guy Vandenbosch](#) (Katholieke Universiteit Leuven (KU Leuven), Belgium)

A multi-functional button antenna is designed, with dual-band and dual-polarization characteristics. This antenna is a dedicated design for wearable applications. A compact size button is achieved with a diameter of only 19.5 mm (0.29 λ), which optimizes the users' comfort. The proposed antenna works in the 4.5-4.6 unlicensed future 5G communication band, and the 5.1-5.5 GHz WLAN band. Two radiation patterns with orthogonal linear polarizations are obtained in each band. The mutual coupling between the two patterns is below -20 dB. The antenna is prototyped. Simulations and experiments confirm the validity of this novel concept.

10:10 **Coffee Break**

10:40 ***Small Implanted Antennas for Wireless Communication and Energy Harvesting***

[Stavros Koulouridis](#) (University of Patras, Greece)

In this work we visit implanted antenna designs that have focused on data telemetry and they occupy tiny volumes or antennas that can support both data telemetry and wireless harvesting without dramatic size increase. Emphasis is placed on Sub-gigahertz region since it can support deep implantation and is more applicable for minimizing dissipation losses inside the human body

11:00 ***Removable Finger Nail Antenna***

[Peter Njogu](#) and [Benito Sanz-Izquierdo](#) (University of Kent, United Kingdom (Great Britain))

An antenna on a removable fingernail for on-body communication applications is proposed. The antenna consist of patch design that is shaped around the curvature of an artificial nail. Two fabrication procedures are tested. The first uses copper layers that are attached to the nail. The second is a more realistic scenario where the patch is painted by hand onto the inexpensive polymer material. The antennas operate at the 10GHz band and are intended for future on-body wireless communications systems. Tests were conducted on the antenna, first in free space and then on human body. The tests results from the brush-painted antenna compare well with those of the design on copper and the simulations. The antennas performance in terms of reflection coefficient and radiation pattern are satisfactory. CST Microwave StudioTM was used for the simulations. This work aims to demonstrate a new concept of low-cost body-attached antenna using finger nails.

11:20 ***Antenna for a Cranial Implant: Simulation Issues and Design Strategies***

[Alberto Jose Moreno Montes](#) and [Ismael Vico Trivino](#) (EPFL, Switzerland); [Marko Bosiljevac](#) (University of Zagreb, Croatia); [Miroslav J. Veljovic](#) (EPFL, Switzerland); [Zvonimir Sipus](#) (University of Zagreb, Croatia); [Anja K. Skrivervik](#) (EPFL, Switzerland)

The design of a specific antenna for a cranial implant is used to illustrate design and simulation issues linked to implantable antennas. After a brief introduction, we will review the requirements for the antenna, and go through the design process, discussing the tools used and the issues encountered. The final design will then be presented and discussed

11:40 ***Penta-band Dual-fed Smart Glasses IoT Antenna***

[Bing Xiao](#) (The University of Hong Kong, Hong Kong); [Hang Wong](#) (City University of Hong Kong, Hong Kong); [Kwan L Yeung](#) (The University of Hong Kong, Hong Kong)

The method of designing multiband dual-fed smart glasses antennas is introduced in this paper. By utilizing the frame of glasses and applying the theory of characteristic mode (TCM), two ports with inductive coupler element (ICE) and capacitive coupler element (CCE) respectively are assigned that all characteristic modes on the wire antenna could be excited theoretically. Then by impedance matchings to the two ports respectively, the antenna could cover four ISM bands: 433 MHz, 915 MHz, 2450 MHz, and 5800 MHz. They are for the applications of Internet of Things (IoT): the low-power wide-area network (LPWAN) such as Lora, Zigbee, and Sigfox, and RFID. Besides, in consideration of the function of positioning for smart glasses, GPS L1 band (1575 MHz) is also covered. This research facilitates smart glasses to serve as an IoT hub.

CS26: Education in Electromagnetics, Antennas, and Microwaves

T11 Fundamental research and emerging technologies / Convened Session / Electromagnetics

Room: B4

Chairs: [Ari Sihvola](#) (Aalto University, Finland), [Henrik Wallén](#) (Aalto University, Finland)

8:30 ***Federated Non-Traditional Practical Work for Engineering Education***

[Timothy D Drysdale](#) (The University of Edinburgh, United Kingdom (Great Britain))

Non-traditional practical work is conducted primarily with digital technologies, such as remote-, simulated- and virtual-laboratories, and is optimally used as a complement to, or extension of, existing traditional practical work. The increasing desire for more active learning in the higher education sector, coupled with increasing student numbers, means that it is impossible to meet the outstanding demand for practical work by using only traditional laboratory facilities alone. This paper gives a brief overview of the educational case for non-traditional practical work, before going to give an outline for a software architecture that would allow the federation of remote laboratory experiments between different institutions, which would be a valuable education tool in areas such as antennas and propagation where test and measurement equipment and test devices can be expensive, fragile, and difficult or problematic to access.

8:50 ***Teaching Wireless Communications Courses: An Experiential Learning Approach***

[Hugo G Espinosa](#) (Griffith University, Australia); [Thomas Fickenscher](#) (Helmut Schmidt University, Germany); [Nickolas Littman](#) and [David V Thiel](#) (Griffith University, Australia)

Student engagement continues to be a major challenge, particularly in electromagnetics courses. This is independent of whether courses are compulsory or elective. This paper presents an approach to assessing students that provides them with an opportunity for experiential learning, following Kolb's learning cycle. Final year students are required to develop and complete two experimental projects over the 12-week trimester. At the outset of each project, pairs of students choose a three-line project outline; projects are unique to each two-person group with an obscure but practical industrial outcome designed to complement the lecture material. To succeed, students must continue to discuss their project strategies, measurements and final applications with the teaching team throughout the trimester. Students have rated the course experience very highly, and in some cases, their projects have enhanced their post-graduation employment opportunities in the field directly related to one of their projects.

9:10 ***A Modern Approach to Teaching and Learning Electromagnetics at DTU***

[Samel Arslanagić](#) (Technical University of Denmark, Denmark)

We describe the implementation of a B. Sc. course in electromagnetics at the Technical University of Denmark which over a number of years has received very positive student evaluations. The student perceptions of what makes the course good are first outlined. Unsurprisingly, they emphasize a clear organization and structure of the course, as well as the professional skills and personality of its teachers, as the main assets of the course. No specific teaching methods or a desire towards sophisticated e-learning tools are mentioned. Nevertheless, appropriate e-learning tools can supplement the course activities and enhance the students learning outcome significantly. In our course, we have recently implemented e-learning tools in terms of video problem tutorials of huge benefit to the students. Following their perceptions, the course structure is reviewed, with an emphasis on lectures, laboratory exercises, and particularly the successful video problem tutorials which are so tightly bound to the lectures.

9:30 ***Teaching Radar Systems: Wave Propagation, Scattering, Antennas, and Electronics***

[Daniel Sjöberg](#) (Lund University, Sweden)

We present the outline of a course on Radar and Remote Sensing recently introduced at Lund University in Sweden. The lecture topics are briefly reviewed, as well as the labs and final examination in terms of a radar system design task. From this course, the students get an overview of typical radar systems requirements and trade-offs, as well as an insight into different subsystems and physical phenomena like wave propagation in a layered atmosphere and scattering from complex targets.

9:50 ***Grading Written Exams in Electromagnetic Theory: Depth Versus Width***

[Martin Norgren](#) (KTH Royal Institute of Technology, Sweden)

In grading of written exams, the requirement that the passing grade reflects satisfactory performance in all intended learning outcomes has been handled in the calculation of the exam score. Without changing the structure of the exam itself, the score is calculated using a simple formula which emphasises width over many tasks, instead of depth in a few tasks. Grading results using the new approach have been compared against results from an earlier used summation approach. Somewhat unexpectedly, the new approach has resulted in an improved passing rate and a substantial increase of the highest grade. A possible explanation is that the students are aware of the sharpened requirements, right from the start.

10:10 **Coffee Break**

10:40 *Modern Challenges for EE Students Pursuing Fundamental Research in Metamaterials*

[Ashwin K. Iyer](#) (University of Alberta, Canada)

Electrical-engineering students considering fundamental research in metamaterials today may perceive challenges, ranging from the overwhelming diversity and breadth of the field following 20+ years of growth to questions about the applicability of their work and their own employability. This article provides some observations on these and other topics with the hopes of assuring young students that the field of metamaterials remains full with opportunity and, with a good amount of hard work, one can derive a satisfying and productive research career from it.

11:00 *Advanced Teaching in Electromagnetics at the ELEDIA Research Center*

[Nicola Anselmi](#) (ELEDIA Research Center, Italy); [Renzo Azaro](#) (Eledia Research Center, Italy); [Federico Boulos](#) (ELEDIA@UniTN - DISI, University of Trento, Italy); Luca Dall'Asta (ELEDIA Research Center, Italy); [Giorgio Gottardi](#) and [Mohammad Hannan](#) (ELEDIA Research Center, University of Trento, Italy); [Baozu Li](#) (Nanjing Normal University, Italy); [Giulia Mansutti](#) (Università degli Studi di Padova, Italy); [Davide Marcantonio](#) (ELEDIA Research Center, Italy); [Giacomo Oliveri](#) (University of Trento & ELEDIA Research Center, Italy); [Lorenzo Poli](#) and [Alessandro Polo](#) (ELEDIA Research Center, University of Trento, Italy); [Paolo Rocca](#) (University of Trento, Italy); [Marco Salucci](#) (ELEDIA Research Center, Italy); [Andrea Massa](#) (University of Trento, Italy)

An entire long-term educational framework has been designed and implemented by the ELEDIA Research Center to (i) renew the way of teaching electromagnetics (EM) to future engineers and (ii) increase students' self-confidence and admiration of the applicative and technological aspects of Maxwell's equations. According to authors' expectations and received students' feedback, such a training ecosystem will help a computer-naive generation in developing a more natural engineer-oriented thinking mechanism and attitude for continuously adapting to technological advances in EM leading-edge research and industry.

11:20 *Brewster Angle and Vanishing Polarization of Wave Reflected by Conductor-Backed Water Slab*

[Hsinju Chen](#) and [Shih-Yuan Chen](#) (National Taiwan University, Taiwan)

For ease of visualization of Brewster angle, we set up a simple experiment with copper-backed water slab to show near-full transmission of parallel polarization. Using a circularly polarized microstrip patch antenna connected to a portable USB signal generator as the transmitter and a linearly polarized patch with a portable USB spectrum analyzer as the receiver, the low parallel polarization reflection level is observable at the pseudo-Brewster angle, calculated with undergraduate-level electromagnetic theory. With the help of the experiment, the effect is intuitively understood and easily reproduced by students in classrooms.

11:40 *Teaching Applied Mathematics for Electromagnetics by Means of a Simple Scattering Problem*

[Nikolaos L. Tsitsas](#) (Aristotle University of Thessaloniki, Greece); [George Fikioris](#) (National Technical University of Athens, Greece)

In this paper, combined techniques from Complex Analysis, Fourier Transforms and Compact Operators are applied to investigate convergence properties of the solutions of a simple two-dimensional scattering problem. It is shown how basic tools of Applied Mathematics can aid the understanding and the gain of physical insight on the behavior of the scattered fields.

12:00 *In Favor of Re-Introducing and/or Expanding Rectangular Waveguides in Bachelor's and Master's Level Electromagnetic Courses*

[Mariangela Baggio](#) and [Zachary D Taylor](#) (Aalto University, Finland)

This paper makes a case for the continuing inclusions of rectangular waveguides in bachelors and masters level electromagnetics education. Modern training in electromagnetics, especially in preparation for industry careers, often excludes Rectangular waveguide theory. We believe that this theory is a concise and efficient way to teach broader wave propagation concepts and thus should be included in most curricula despite its continued drop in popularity

CS47: Non-Magnetic Nonreciprocity

T11 Fundamental research and emerging technologies / Convened Session / Electromagnetics

Room: B5

Chairs: [Andrea Alù](#) (CUNY Advanced Science Research Center, USA), [Dimitrios Sounas](#) (Wayne State University, USA)

8:30 *Nonreciprocal Metasurfaces Through Circular Polarization Biasing*

[Dimitrios Sounas](#) (Wayne State University, USA)

A new type of nonreciprocal metasurface is presented that is biased by two incident circular polarized waves and as a result does not require a complicated biasing network. The pumps are selected to have opposite polarizations and slightly detuned frequencies. The metasurface is designed to exhibit a third-order nonlinear response and nonreciprocity is the result of a four-wave mixing mechanism between the pumps and an incident signal. The metasurface exhibits nonreciprocal polarization rotation and it can be the building block of free space circulators and isolators.

8:50 *Quad Magnet-free Micro-acoustic RF Circulator with Intermodulation Suppression*

[Yao Yu](#) (Northeastern University, Boston, US, USA); [Matteo Rinaldi](#) (Northeastern University, USA)

In this paper, a micro-acoustic RF circulator with novel "quad" configuration is reported. Four micro-acoustic filters are periodically modulated by RF switches to break the reciprocity. The use of high-Q micro-acoustic filters significantly reduces the modulation frequency compared to previous demonstrations based on transmission lines. The low modulation frequency translates to an ultra-low power consumption (202uW, 3600 times smaller than [1]) and one of the highest linearity reported for magnet-free circulators. Furthermore, compared to the more conventional differential configuration, this quad configuration shows advantages in terms of intermodulation products (IMPs) suppression for all the in-band IMPs, guaranteeing a pseudo-linear-time-invariant (pseudo-LTI) operation.

9:10 *Low Loss, CMOS Integrated, Magnetic-Free Non-Reciprocal Components Operating from Radio Frequencies to Millimeter-Waves*

[Aravind Nagulu](#) and [Harish Krishnaswamy](#) (Columbia University, USA)

Magnetic-free non-reciprocity using time-variance has gained a lot of attention in recent years. Some initial approaches use permittivity-modulation along a transmission line or in a resonant ring structure. However, small modulation contrasts of permittivity imply high loss and a large form-factor or narrow transmission bandwidths. More recently, we leveraged the much larger conductivity modulation contrasts available in CMOS to achieve drastically smaller form-factors, wide-bandwidths and low-loss non-reciprocity across a wide range of operating frequencies. Here we review recent progress on spatio-temporal conductivity-modulation, which enabled non-reciprocal components operating from radio frequencies to millimeter-waves in a CMOS platform.

9:30 *Space-Time Modulated Loaded-Wire Metagratings for Magnetless Nonreciprocity*

[Yakir Hadad](#) (Tel-Aviv University, Israel)

We show that spatiotemporally modulated metagratings can lead to strong nonreciprocal responses, despite the fact that they are based on electrically-large unit cells and use only three modulation domains. We specifically focus on wire metagratings loaded with time-modulated capacitances. We use the discrete-dipole-approximation and an ad-hoc generalization of the theory of polarizability for time-modulated particles, and demonstrate an effective nonreciprocal anomalous reflection (diffraction) with an efficient frequency conversion.

9:50 *Nonreciprocal Antennas Based on Time-Modulation: Challenges and Opportunities*

[Alejandro Alvarez-Melcon](#) (Technical University of Cartagena, Spain); [Juan Sebastián Gomez-Diaz](#) (University of California, Davis, USA)

We explore the possibility to realize nonreciprocal antennas based on combining time-modulated resonators with high-Q structures. Upon an adequate low-frequency modulation scheme, such configuration enables very efficient frequency conversion between only two frequencies (one related to guided signals and another to waves in free-space) and empowers nonreciprocal phase control of the generated waves through the photonic Aharonov-Bohm effect. This approach is applied to demonstrate nonreciprocal and reconfigurable antenna configurations, including phased arrays able to independently control transmission and reception radiation patterns at the same operation frequency, reflectarrays antennas, and planar Yagi-Uda filter-antennas. We discuss the exciting functionalities and benefits enabled by this technology and provide a critical assessment of challenges that remain to be addressed in real-life applications. We envision that this paradigm will pave the way to a magnetic-free, fully integrated, and CMOS-compatible technology with profound implications in communication and wireless systems, sensing, imaging, and on-chip networks.

10:10 Coffee Break

10:40 *A Spatio-Temporally Modulated Metasurface as a Free-Space N-Path System*

[Zhanni Wu](#) (the University of Michigan, USA); [Cody Scarborough](#) (University of Michigan, USA); [Anthony Grbic](#) (University of Michigan, Ann Arbor, USA)

A spatio-temporally modulated metasurface, that functions as a free-space N-path system, is reported at X-band frequencies. The reflection phase of the rows of the metasurface can be independently time-modulated for two orthogonal polarizations. A space-time bias is applied to the metasurface, enabling directionally dependent electromagnetic responses. When the modulation wavenumber is larger than that in free space, the metasurface suppresses certain harmonic mixing products in the far field, allowing subharmonic mixing. The metasurface was experimentally validated for 2-path configuration, where the fabricated metasurface suppresses odd harmonic mixing products. With proper design of the space-time bias waveform, Doppler-like frequency translation is demonstrated at twice the modulation frequency.

11:00 *Temporal Modulation of Bianisotropic Metasurfaces for Unidirectional Wave Amplification*

[Xuchen Wang](#), [Ana Diaz-Rubio](#), [Viktar Asadchy](#), [Grigorii Ptitsyn](#), [Mohammad Sajjad Mirmoosa](#) and [Sergei Tretyakov](#) (Aalto University, Finland)

Nonreciprocity in time-modulated metasurfaces is normally achieved only when it is combined with space modulation, using at least two time-varying elements located at different positions in space. In this talk, we present the idea of time-modulated bianisotropic metasurfaces where nonreciprocal wave propagation is realized with time modulation of only a single element. The results show that by uniformly modulating a capacitive sheet mounted on a sub-wavelength dielectric layer, one can obtain strong nonreciprocity and achieve unidirectional wave amplification.

11:20 *First Principles Calculation of Topological Invariants by Means of the Photonic Green's Function*

[Filipa Prudencio](#) (Instituto Superior Técnico-Instituto de Telecomunicações, Portugal); [Mario Silveirinha](#) (Universidade de Lisboa - Instituto de Telecomunicações, Portugal)

The Chern topological numbers of a material platform are usually written in terms of the Berry curvature which depends on the normal modes of the system. Here, we use a gauge invariant Green's function method to determine from "first principles" the topological invariants of photonic crystals. The proposed formalism does not require the calculation of the photonic band-structure, and can be easily implemented using the operators obtained with a standard plane-wave expansion.

11:40 *Doppler Cloak: Concept and Realistic Implementation Through Space-Time Modulated Metamaterials and Time-Modulated Metasurfaces*

[Davide Ramaccia](#) (RomaTre University, Italy); [Andrea Alù](#) (The University of Texas at Austin, USA); [Alessandro Toscano](#) (University Roma Tre (IT), Italy); [Filiberto Bilotti](#) (University Roma Tre, Italy)

A Doppler cloak consists of a non-reciprocal space-time modulated metastructure that allows manipulating the apparent velocity of a moving object by inducing an artificial frequency shift in the reflected signals. In this contribution, we present two Doppler cloaks: one implemented through a spatio-temporal (ST-) metamaterial cover wrapped around or just in front of the object, and one implemented through a time-varying metasurface. We show that, by properly choosing the modulation scheme and frequency of the space-time modulated metastructure, it is possible achieving a full compensation of the Doppler frequency shift, making the composite system appearing to an external observer as stationary, even though it is actually moving. The Doppler cloak may have large impact also in other applications, such as restoration of electromagnetic invisibility and antenna matching in moving systems, just to name a few.

SW03: COST Session CA17115 (MyWAVE): Supporting Medical Device Development via Dielectric and Thermal Tissue Characterization

T05 Biomedical and health / Convened Session / Measurements

Room: B6

Chairs: [Raquel C. Conceição](#) (Instituto de Biofísica e Engenharia Biomédica, Faculdade de Ciências, Universidade de Lisboa, Portugal), [Martin O'Halloran](#) (National University of Ireland, Galway, Ireland)

8:30 *Fast Measurements of Dielectric Properties with Small Size Microwave Transceiver*

[Niko Ištuk](#) (National University of Ireland, Galway & Translational Medical Device Lab, Ireland); [Ferry Kienberger](#) (Keysight Technologies, Austria); [Emily Porter](#) (University of Texas at Austin, USA); [Martin O'Halloran](#) (National University of Ireland, Galway, Ireland); [Adam Santorelli](#) (National University of Ireland, Galway & Translational Medical Device Lab, Ireland); [Ivan Alic](#), [Mykolas Ragulskis](#), [Amin Moradpour](#) and [Manuel Kasper](#) (Keysight Technologies, Austria)

The dielectric properties of biological tissues are fundamental for the design of electromagnetic medical devices as well as in non-ionizing radiation dosimetry studies. In recent studies, dielectric data has been typically collected using the open ended coaxial probe and the vector network analyzer setup. In this work, we replace the traditional VNA from this setup with a more compact microwave transceiver. The microwave transceiver uses a novel broadband, multi-tone source and broadband receivers to capture the instantaneous S-parameters at multiple tones simultaneously. We conducted dielectric properties measurements on standard liquids which have known dielectric properties using our modified setup and compared the results with the theoretical values. We also conducted the same measurements with the typical setup with the swept frequency VNA and compared the performances of the measurement setups. We concluded that the microwave transceiver can provide faster measurement speeds than the conventional VNA without sacrificing precision and accuracy.

8:50 *Investigation on Temperature-Dependent Changes of Tissue Thermal Properties on Microwave Ablation Treatments*

[Marta Cavagnaro](#) (Sapienza University of Rome, Italy); [Rosanna Pinto](#) (ENEA, Italy); [Vanni Lopresto](#) (ENEA, Italian National Agency for New Technologies, Energy and Sustainable Economic Development, Italy)

Microwave thermal ablation treatments induce coagulation necrosis of diseased tissue through the absorption of an electromagnetic field at microwave frequencies. In particular, the electromagnetic field absorbed by the tissue induces a temperature increase that, in turn, produces an almost instantaneous cell death. The electromagnetic field is radiated by a minimally invasive antenna located in the centre of the diseased area. Temperatures close to 60 °C are needed to induce thermal ablation, so that very high temperatures values (up to 100°C or higher) can be achieved close to the radiating antenna. To develop reliable interventional protocols, numerical tools able to correctly predict the temperature increase are needed. In this work, values recently measured of the thermal conductivity as a function of the temperature have been introduced into the numerical model to evaluate their influence on the calculated data.

9:10 *Thermal Properties of Ex Vivo Biological Tissue at Room and Body Temperature*

[Nuno P. Silva](#) (National University of Ireland Galway & Faculdade de Ciências da Universidade de Lisboa, Ireland); [Anna Bottiglieri](#) (Translational Medical Device Lab & National University of Ireland, Galway, Ireland); [Raquel C. Conceição](#) (Instituto de Biofísica e Engenharia Biomédica, Faculdade de Ciências, Universidade de Lisboa, Portugal); [Martin O'Halloran](#) (National University of Ireland, Galway, Ireland); [Laura Farina](#) (National University of Ireland Galway & CURAM, Ireland)

In electromagnetic hyperthermic applications, the thermal properties of the biological tissue under treatment, as well as its dielectric properties, influence the deposition of the electromagnetic energy and the heat distribution into the tissue. Thus, their knowledge can allow to accurately model the therapeutic results. The induced heat distribution and the consequent temperature increase rate are ruled by the thermal properties of the biological tissues. The aim of this work is to experimentally investigate the thermal properties of ex vivo liver, lung, kidney, muscle and bone marrow at room (N = 66) and body (N = 45) temperatures; and to correlate these properties with the density and water content of the tissue.

9:30 *Advanced Temperature Dielectric Spectroscopy of Muscle Phantom at Microwave Frequencies*

[Ondrej Fiser, Jr.](#) (Czech Technical University in Prague & Faculty of Biomedical Engineering, Czech Republic); [Michaela Kantova](#) (CTU in Prague, Czech Republic); [Sebastian Ley](#), [Alexandra Prokhorova](#) and [Marko Helbig](#) (Technische Universität Ilmenau, Germany); [Jan Vrba](#) (Czech Technical University, Czech Republic)

The temperature dependency of the dielectric properties of tissues is very important for the development of novel microwave systems intended for non-invasive temperature monitoring. This paper deals with the measurement and optimization of the temperature dependence of the dielectric parameters of a muscle tissue mimicking phantom. The measurements were performed in the frequency band 0.1 - 3 GHz and in the temperature range 25 - 45 °C. The differences in the dielectric parameters caused by temperature change were analyzed and compared with the reference.

9:50 *Dielectric Properties of Biological Tissues at Frequencies Below 1 MHz: Development of an Improved Measurement Technique*

[Azadeh Peyman](#) (Public Health England, United Kingdom (Great Britain)); [Nishtha Chopra](#) (UK Government, United Kingdom (Great Britain))

At low frequencies, the dielectric values for biological tissues are difficult to determine due, at least partly, to the dependency of the dielectric properties on the physiological state of the tissues and changes occurring after death. In practice chemical interaction between the measuring probe and lossy material can cause several errors and uncertainties in the results. In an attempt to develop an advance black-platinum four-point electrode probe technology to measure impedance values of low concentration saline solutions, we have identified at least one major source of error namely, electrode polarisation and some other high-frequency effects as measurement artefacts that made the capacitive part of the dielectric data unreliable.

10:10 Coffee Break

10:40 *On the Dielectric/Thermal Characterization and Calibration of Solutions and Materials for Biomedical Applications*

[Simona Di Meo](#) (University of Pavia, Italy); [Julian Bonello](#) (University of Malta, Malta); [Matteo Lodi](#) (University of Cagliari, Italy); [Iman Farhat](#) and [Lourdes Farrugia](#) (University of Malta, Malta); [Alessandro Fanti](#) (University of Cagliari, Italy); [Marco Pasian](#) (University of Pavia, Italy); [Francesco Desogus](#) (University of Cagliari, Italy); [Charles Sammut](#) (University of Malta, Malta)

The exact and unambiguous knowledge of the dielectric and thermal properties of biological tissues is of fundamental importance for the design of all types of microwave systems for both diagnostic and therapeutic purposes that have been taking place in recent years. Several research groups around the world have been studying the dielectric and thermal properties of biological tissues for several years and numerous databases have been proposed. This paper presents some preliminary results about a cross study on the dielectric and thermal properties of known solutions. As an example of the possible set of measurements intended for such a study, two different setups are discussed. The impact on dielectric measurements of the system calibration temperature (23 °C and 80 °C), for a 0.1M NaCl solution, is outlined up to 30 GHz. Then, the thermal properties of sunflower oil are characterized in a temperature range from 35 °C to 45 °C.

11:00 *Extracting Dielectric Properties for MRI-based Phantoms for Axillary Microwave Imaging Device*

[Daniela M. Godinho](#) (Instituto de Biofísica e Engenharia Biomédica, Faculdade de Ciências, Universidade de Lisboa, Portugal); [Joao M. Felicio](#) (Instituto de Telecomunicações, Portugal); [Tiago Castela](#) (Departamento de Radiologia, Hospital da Luz Lisboa, Luz Saúde, Lisbon, Portugal); [Nuno Silva](#) (Hospital da Luz Learning Health, Luz Saúde, Portugal); [M Lurdes Orvalho](#) (Departamento de Radiologia, Hospital da Luz Lisboa, Luz Saúde, Lisbon, Portugal); [Carlos A. Fernandes](#) (Instituto de Telecomunicacoes, Instituto Superior Tecnico, Portugal); [Raquel C. Conceição](#) (Instituto de Biofísica e Engenharia Biomédica, Faculdade de Ciências, Universidade de Lisboa, Portugal)

Microwave Imaging (MWI) is an emerging medical imaging technique, which has been studied to aid breast cancer diagnosis. The information about the dielectric properties of each tissue is essential to assess the viability of this type of systems. However, accurate measurements of heterogeneous tissues can be very challenging, and the current available information is still very limited. In this paper, we present a methodology for extracting dielectric properties to create anatomical models of the axillary region. These models will be used in a MWI device to aid breast cancer diagnosis through the detection of metastasised axillary lymph nodes. We apply segmentation tools to Magnetic Resonance Images of the breast and assign dielectric properties to each tissue, extracting preliminary information about the properties of axillary lymph nodes. This study may open a way to more quickly extract dielectric properties of tissues and/or validate measurements, accelerating the development of microwave-based medical devices.

11:20 **Broadband Dielectric Measurements of Ex-Vivo Uterine Fibroid Tissues over the Ablative Temperature Range**

[Ghina Zia](#) (Kansas State University, USA); [Jan Sebek](#) (Kansas State University & Czech Technical University, USA); [Punit Prakash](#) (Kansas State University, USA)

Microwave ablation is under consideration as an energy modality for minimally-invasive treatment of uterine fibroids. Computational models of microwave ablation are useful for guiding the design of new devices and systems, but require tissue dielectric properties, including their variation at elevated temperatures, for accurate prediction of ablation profiles. This study reports on preliminary results of a study on experimental characterization of the broadband (0.5 - 6 GHz) dielectric properties of surgically excised uterine fibroids, with measurements taken at temperatures up to 155 °C. The measured dielectric properties at elevated temperatures dropped considerably, likely due to the effects of tissue desiccation and water vaporization, similar to reports of dielectric property measurements for other tissues.

11:40 **Microwave Calcaneus Phantom for Bone Imaging Applications**

[Bilal Amin](#) (National University of Ireland, Galway & Translational Medical Device Lab, Ireland); [Daniel Kelly](#) (School of Medicine, National University of Ireland Galway, Ireland); [Atif Shahzad](#), Martin O'Halloran and [Muhammad Adnan Elahi](#) (National University of Ireland, Galway, Ireland)

Microwave imaging can be used as an alternate modality for monitoring bone health. Dielectrically accurate, anthropomorphic phantoms play vital role in testing of imaging prototype prior to clinical applications. This paper presents multilayered 3D-printed human calcaneus structure. Further, we have proposed liquid based tissue phantoms that mimic the dielectric properties of skin, muscle, cortical bone and trabecular bone. Tissue phantoms are composed of Triton X-100, water and salt. The dielectric properties were measured across 0.5 - 8.5 GHz. Each layer of the 3D-printed structure was filled with corresponding tissue phantom. The combined average percentage difference between dielectric properties of reference data and proposed tissue phantoms was found to be 2.9% for trabecular bone, 7.3% for cortical bone, 7.1% for muscle, and 8.7% for skin over the full measured frequency band. These tissue phantoms and 3D printed human calcaneus structure can be used as valuable test platform for microwave diagnostic studies.

12:00 **Dielectric Properties of Tissues Historical Aspects and Measurement Challenges**

[Azadeh Peyman](#) (Public Health England, United Kingdom (Great Britain))

This paper reviews and summarises the state of knowledge on dielectric properties of tissues. Effect of ageing and pathological state of tissues on the dielectric properties are discussed as well as the impact of variation in dielectric data on the outcome of dosimetric studies. A critical analysis of the existing measurement techniques and uncertainty evaluation on the measured data are also presented. Finally, some unpublished data on dielectric properties of porcine abdominal tissues will be presented in light of rise in popularity of diagnostic imaging techniques utilising RF signals, and increase in demand for accurate in-vivo dielectric properties of abdominal tissues.

T06-A17: Automotive Antennas

T06 Aircraft (incl. UAV, UAS, RPAS) and automotive / Regular Session / Antennas

Room: B7

Chairs: [Jihun Choi](#) (Army Research Lab & Booz Allen Hamilton, USA), [Johan Wettergren](#) (Qamcom Research and Technology, Sweden)

8:30 **Transparent Glass Antenna for 28 GHz and Its Signal Reception Characteristics in Urban Environment**

[Minoru Inomata](#) (NTT DOCOMO, INC., Japan); [Toshiki Sayama](#) and [Takeshi Motegi](#) (AGC Inc., Japan); [Osamu Kagaya](#) (ASAHI GLASS CO., LTD., Japan); [Hideaki Shoji](#) (AGC Asahi Glass, Japan); [Shoichi Takeuchi](#) (AGC Inc., Japan); [Kiyoshi Nobuoka](#) (AGC Inc, Japan)

This paper proposes a transparent glass antenna for the 28-GHz band for 5G connected vehicles and clarifies the signal reception characteristics when distributing the glass antennas to vehicle windows in an urban environment. Comparison results between the distributed transparent glass antennas and an omni-directional antenna show that the relative received power for the glass antenna is higher than that for the omni-directional antenna. In addition, results show that the relative received power when using a vertically and horizontally polarized antenna are approximately the same. Therefore, we actualize a transparent antenna that maintains the high antenna gain and omni-directional antenna pattern using vertical and horizontal polarization when installed on the windows.

8:50 **Optically Transparent Antenna Integrated Inside a Headlamp for Automotive Radar Application**

[Sofian Hamid](#) and [Dirk Heberling](#) (RWTH Aachen University, Germany); [Manuela Junghähnel](#) and [Thomas Preussner](#) (Fraunhofer Institute for Organic Electronics, Electron Beam and Plasma Technology, Germany); [Patrick Gretzki](#), [Ludwig Pongratz](#), [Christian Hördemann](#) and [Arnold Gillner](#) (Fraunhofer Institute for Laser Technology, Germany)

A concept for integrating antenna inside a headlamp for automotive radar application is presented. The antenna comprises the primary (feed), which is embedded within the electronic unit, and the secondary one, which is made of transparent materials. The primary antenna can be the conventional one (e.g., patch, slot, sectoral horn), which is optically non-transparent. It is hidden from the optical path of the headlight. The secondary antenna is realized as a planar offset reflector, which is designed to collimate or shape the wave from the primary antenna. It is inserted in the space between the headlamp cover and the light unit. An antenna demonstrator has been fabricated, and together with the headlamp cover, the radiation pattern and realized gain are measured. We reported here the measurement results for several configurations and concluded that the headlamp cover gives minimal influence on the antenna performance.

9:10 **A Capacitively Coupled Patch Antenna Array for an Enlarged Bandwidth at 77 GHz**

[Jonathan Mayer](#) (Karlsruhe Institute of Technology, Germany); [Manuel Martina](#) (Schweizer Electronic AG, Germany); [Jerzy Kowalewski](#) (Karlsruhe Institute of Technology, Germany); [Jue Chen](#) (Schweizer Electronic AG, Germany); [Thomas Zwick](#) (Karlsruhe Institute of Technology (KIT), Germany)

Today's automotive radar systems are commonly equipped with serial-fed patch antennas. However, they lack on a too low bandwidth for the whole available bandwidth of 5 GHz. This paper introduces a new antenna principle using capacitively fed patches besides the feeding line with different resonance frequencies. This allows an enlarged bandwidth compared to serial-fed patch antennas without the need for additional layers in the printed circuit board (PCB). The antenna in this work has 12 patch elements and a gain of 10 dBi over more than 3 GHz bandwidth while the sidelobe suppression is at least 15 dB. For the manufacturing of the antenna an embedded technology with a high resolution was used.

9:30 **Broadband Frequency Reconfigurable Antenna Using Capacitive Loading for K-band Applications**

[Muhammad S. Anwar](#) and [Axel Bangert](#) (University of Kassel, Germany)

A novel reconfigurable antenna in K-band frequency is presented. The antenna employs a simple capacitive loading technique to increase the -10 dB bandwidth by 2.5 times (+150%). The proposed antenna is designed at the frequency of the unloaded state operating at 24.2 GHz (1.8GHz bandwidth) and the loaded state at 24.5 GHz (4GHz bandwidth). Antenna gain of 12 dBi and 9 dBi for unloaded and loaded configuration, respectively, are recorded. The directivity of the antenna is optimized by using reflectors and directors. Radiation pattern distortion caused by capacitive loading is corrected by using a dielectric lens. The designed frequencies are used in automotive radar. A narrow band centered at 24.2 GHz is used for Adaptive Cruise Control (ACC) and Lane Change Radar (LCR). A broad bandwidth centered at 24.5 GHz is used for Short Range Radars (SRR). The proposed design shows an excellent agreement between the simulated and measured results.

9:50 **An Efficient Low-Profile Low-VHF Antenna for Small Unmanned Ground Vehicles**

[Jihun Choi](#) (Army Research Lab & Booz Allen Hamilton, USA); [Fikadu Dagefu](#) (US Army Research Laboratory, USA); [Brian Sadler](#) (Army Research Laboratory, USA)

A compact, low-profile, efficient, low-VHF antenna designed for small UGV systems is presented. In order to achieve further gain enhancement from a recent development in an electrically small efficient monopole antenna, a new design approach is proposed. A single 180-degree phase shifter comprising a common capacitive top loading and multiple high-Q air-core coils connected to each corresponding short vertical element is designed to produce in-phase radiating fields from the multiple vertical elements at resonance, thereby considerably enhancing the antenna gain. Under practical considerations, performances of the antenna before and after integrating it on a small UGV are carefully characterized via simulations and measurements. The results show that a peak gain of the antenna integrated on the UGV with omnidirectional radiation pattern is 0.7 dBi which is comparable to that of a miniature dipole whose height is 7.5 times larger, facilitating low-power wireless compact UGV communications and networking at low VHF.

10:10 **Coffee Break**

10:40 **A Triband Wire Antenna for All Radio and TV Bands**

[Johan Wettergren](#) and [Robert Petersson](#) (Qamcom Research and Technology, Sweden); [Roman Iustin](#) (Volvo Technology, Sweden)

A triband rod antenna is presented. It is intended for reception of AM, FM, DAB and TV in vehicles. The antenna uses coil traps to facilitate multiple resonant lengths in order to be matched to 50 Ohms for frequency bands centred at 97, 204 and 571 MHz. In fact, it features a double resonance in the quite broad 470-694 MHz TV band. Difficulties in computer simulations of antenna match are discussed, a design methodology is suggested and measurements on a breadboard model are presented.

11:00 **Ka-Band Planar Magic-T Based on E-plane Groove Gap Waveguide for Monopulse Antenna System**

[Arefeh Kalantari Khandani](#) (Intelligent Boards Electronic Company, Iran); [Ali Farahbakhsh](#) (Graduate University of Advanced Technology, Iran)

A planar Magic-T is proposed based on E-plane groove gap waveguide for Ka-band applications. All four ports of the Magic-T are coplanar and E-plane groove gap waveguide. The frequency bandwidth of the proposed Magic-T is about 43% covering the whole Ka-band from 26 GHz to 40 GHz. The Magic-T isolation is better than 42 dB in the whole

bandwidth while its insertion loss is about 0.1 dB.

11:20 ***Harness Connection and Immediate Environment Impact on RF Automotive Receivers Antenna BW***

[Ahmadreza Jafari](#) (Renault S.A.S, France); [Gregory Siguier](#) (Continental Automitive S.A.S, France); [Clément Prince](#) (Continental Automotive S.A.S, I BS RD RF, France); [Philippe Boutier](#) (Renault sas, France); [Imene Elfeki](#) (Expleo, France); [Xavier Bunlon](#) (Renault sas, France)

Numerical simulations are used more and more to investigate the behavior of RF antennas and wireless systems in automotive industry and to assure their optimum functionality on the early stages of the vehicle development. This paper shows how 3D simulations help evaluate the impact of the immediate environment of the RF access receiver and its harness connections on the antenna performance, reflection coefficient and bandwidth.

11:40 ***Three Port Circular Patch Antenna with Pattern and Polarisation Agility***

[Peter J James](#) (University of Bristol, United Kingdom (Great Britain))

A three port circular patch antenna has been designed to provide pattern and polarisation agility at an operating frequency of 2.4 GHz. Independent excitation of the antenna modes TM00, TM01 and TM10 has been demonstrated and, by combining these modes, beamsteering has been achieved. The improved directivity of this antenna design at low elevation angles has been confirmed through these simulations. A directivity of 2.2 dB has been achieved at the horizon through this beamsteering method compared to -8.2 dB for the TM01 and TM10 modes and -0.7 dB for the TM00 mode at the same angle. A discussion of the active impedance and its implications for impedance matching is also included.

12:00 ***Wide-Angular Scanning Performance Enhancement in Linear Arrays via Combining Integrated In-line Subarrays and Amplitude Tapering***

[Fannush Shofi Akbar](#) and [Gamantyo Hendratoro](#) (Institut Teknologi Sepuluh Nopember, Indonesia); Leo P. Ligthart (em. prof. Delft University of Technology & Universitas Indonesia, Beijing Institute of Technology, ITS Surabaya, The Netherlands); [Ioan E. Lager](#) (Delft University of Technology, The Netherlands)

An advanced design, adding a significant first sidelobes level (FSL) improvement to a previously introduced wide-angular-scanning, linear array prototype with demonstrated scan-loss compensation (SLC) and sidelobes suppression features is discussed. The linear array makes use of in-line subarrays for SLC and an additional amplitude taper in its central, uniform region for lowering the FSL with as much as 4dB at $\pm 60^\circ$ scanning (13dB at $\pm 20^\circ$ scanning). Several Taylor-type amplitudes tapers are compared, the best overall performance improvement being observed for a -18dB prototype taper. The advocated solution is highly suitable to high-sensitivity radars requiring a fast-scanning, fan-shaped beam.

CS55: Recent Advances in Terahertz Antennas for Radio-Astronomy and Space Exploration

T09 Space (incl. cubesat) / Convened Session / Antennas

Room: B8

Chairs: [Luis-Enrique Garcia-Muñoz](#) (University Carlos III of Madrid, Spain), [David González-Ovejero](#) (Centre National de la Recherche Scientifique - CNRS, France)

8:30 ***Towards a Si/GaAs Based Flat-Panel Quasi-Optical Metasurface Antenna with Switchable Beam Characteristics***

[Okan Yurduseven](#) (Queen's University Belfast & Duke University, United Kingdom (Great Britain)); [Choonsup Lee](#) (JPL, USA); [David González-Ovejero](#) (Centre National de la Recherche Scientifique - CNRS, France); [Mauro Ettore](#) (University of Rennes 1 & UMR CNRS 6164, France); [Ronan Sauleau](#) (University of Rennes 1, France); [Vincent Fusco](#) (Queen's University Belfast, United Kingdom (Great Britain)); [Goutam Chattopadhyay](#) (NASA-JPL/Caltech, USA); [Nacer Chahat](#) (NASA-JPL, Caltech, USA)

This paper presents a silicon (Si) and gallium arsenide (GaAs) metasurface antenna to achieve beam-forming at 94 GHz. The metasurface antenna consists of a flat-panel system architecture and works in a holographic manner. The guided mode launched into the Si layer is converted to a planar wave-front using a quasi-optical pillbox feeding architecture, significantly simplifying the design process of the metasurface antenna. It is demonstrated that the developed metasurface can switch its radiation pattern in the azimuth plane by selectively activating between multiple input ports while beam forming in the elevation plane can be achieved by actively tuning the metamaterial elements forming the metasurface aperture. The simulated reflection coefficient patterns suggest an impedance matching better than -15 dB at all input ports is achieved at 94 GHz. The radiation patterns of the antenna clearly demonstrate the 3D beam scanning capability of the presented metasurface antenna ($\theta=0^\circ/15^\circ$, $\varphi=0^\circ/\pm 90^\circ$) at millimeter-wave frequencies.

8:50 ***Analysis Methods for Multimoded Horns for Future THz Missions (SAFARI Instrument for SPICA)***

[Neil Trappe](#) (NUI Maynooth, Ireland); [Gert de Lange](#) (SRON Netherlands Organization for Space Research, The Netherlands); [Creidhe O'Sullivan](#) (National University of Ireland Maynooth, Ireland); [Maarten van der Vorst](#) (European Space Agency, The Netherlands); [Marcin Gradziel](#) (National University of Ireland, Maynooth, Ireland); [Michael Audley](#) (SRON Netherlands Organization for Space Research, The Netherlands); [Peter Ade](#) (Cardiff University, United Kingdom (Great Britain))

We present an analytical technique of large waveguide antenna structures as used for a future proposed spectrometer instrument called SAFARI part of the ESA/JAXA proposed mission SPICA (SPace Infrared telescope for Cosmology and Astrophysics) mission [1], a collaboration between Europe and Japan. The SAFARI (SPICA FAR Infrared Instrument) instrument is an imaging grating spectrometer optimized to operate between 1.5 to 10 THz. SAFARI (high resolution spectrometer) will use Transition Edge Sensors (TES)s to detect this weak THz signal and uses large multimoded waveguide antennas and integrating cavities to maximize optical coupling from the optics to these sensitive detectors. We present a modal analysis outline of these focal plane antennas. Measurement campaigns of these waveguide structures at the Space Research Organization of the Netherlands, SRON Groningen and at Cardiff University will ultimately be used to verify this simulation technique outlined here.

9:10 ***Antennas, Arrays, and Systems for Submillimeter-Wave Radio Astronomy***

[Goutam Chattopadhyay](#) (NASA-JPL/Caltech, USA); [Maria Alonso-delPino](#) (Jet Propulsion Laboratory, USA); [Jacob Kooi](#) (USA)

In this paper we present the design and development of a 16-pixel submillimeter-wave array instrument using SIS technology. We show that this instrument concept demonstration and component development dramatically simplifies the fabrication, assembly, and integration of large focal plane arrays at these frequencies. This advancement is enabled by the innovative array architecture with silicon microlens based antenna arrays, highly sensitive SIS mixers at these frequencies, integrated SiGe BiCMOS based low-noise intermediate frequency (IF) amplifiers, and silicon micromachined packaging.

9:30 ***Effect of Metal Resistive Losses on the Gain of a THz Planar Spiral Antenna***

[Elliott R Brown](#) (2565 Vayview Drive, USA); [Kerlos Atia Abdalmalak](#) (Universidad Carlos III de Madrid, Spain); [Weidong Zhang](#) (Wright State University, USA)

Full-wave finite-element antenna simulations are carried out between 100 and 700 GHz for a planar square spiral antenna, investigating the effect on the antenna gain of resistive losses in the metal arms. It is found that a large degradation of the gain occurs relative to the same antenna with arms of pure gold. However, the degradation is greatest at low frequencies where the skin depth in the lossy metal is significantly greater than the thickness of the metal arms. As the skin depth approaches the thickness of the arms, the lossy-metal antenna gain approaches the gold-arm antenna gain asymptotically.

9:50 ***Compact Millimeter and Submillimeter-Wave Photonic Radiometer for Cubesats***

[Michal Grzegorz Wasiak](#) (Carlos III University of Madrid, Spain); [Gabriel Santamaria Botello](#) and [Kerlos Atia Abdalmalak](#) (Universidad Carlos III de Madrid, Spain); [Florian Sedlmeir](#) and [Alfredo Rueda](#) (Max Planck Institute for the Science of Light, Germany); [Daniel Segovia-Vargas](#) (Universidad Carlos III de Madrid, Spain); [Harald Schwefel](#) (Max Planck Institute for the Science of Light, Germany); [Luis Enrique García Muñoz](#) (Universidad Carlos III de Madrid, Spain)

In this paper we present a room temperature radiometer that can eliminate the need of using cryostats in satellite payload reducing its weight and improving reliability. The proposed radiometer is based on an electro-optic upconverter that boosts up microwave photons energy by upconverting them into an optical domain what makes them immune to thermal noise even if operating at room temperature. The converter uses a high-quality factor whispering gallery mode (WGM) resonator providing naturally narrow bandwidth and therefore might be useful for applications like microwave hyperspectral sensing. The upconversion process is explained by providing essential information about photon conversion efficiency and sensitivity. To prove the concept, we describe an experiment which shows state-of-the-art photon conversion efficiency 10^{-5} per mW of pump power at the frequency of 80 GHz.

10:10 **Coffee Break**

10:40 ***Comparison of Modified Soret Lenses for Dual Band Integrated Detectors***

[Alicia E. Torres-García](#) (Public University of Navarra, Spain); [Jose M. Perez](#) (Universidad Publica de Navarra, Spain); [Ramon Gonzalo](#) (Public University of Navarra, Spain); [Iñigo Ederra](#) (Universidad Pública de Navarra & Institute of Smart Cities, Universidad Pública de Navarra, Spain)

This paper presents the comparison of different modified Soret lenses suitable for a millimeter and submillimeter-wave dual-band integrated pixel detectors. The approach is based on the modification of a printed planar Soret lens, designed to operate in the sub-mm range, to obtain an antenna at the millimeter region. Three modifications of a transmission-mode Soret Lens at 850 GHz based on spiral, logarithmic and meander antennas geometries have been analyzed with a combination of Kirchhoff's Diffraction and full-wave simulation methods. The performance of the designs has been experimentally demonstrated in the submillimeter-wave band, showing good agreement with simulation results.

11:00 ***The Optical Combiner of QUBIC: The Q & U Bolometric Interferometer for Cosmology***

[Creidhe O'Sullivan](#) (National University of Ireland Maynooth, Ireland); [David Burke](#), [Donnacha Gayer](#) and [James Murphy](#) (National University of Ireland, Maynooth, Ireland); [Stephen Scully](#) (Institute of Technology Carlow, Ireland); [Michele De Leo](#) (Università di Roma – La Sapienza, Italy); [Marco De Petris](#) (Università di Roma – La Sapienza, Ireland); [Massimo Gervasi](#) and [Mario Zannoni](#) (Università di Milano – Bicocca and INFN Milano-Bicocca, Italy); [Peter Ade](#) (Cardiff University, United Kingdom (Great Britain)); [Jose Alberro](#) (GEMA Universidad Nacional de La Plata,

Ireland); [Alejandro Almela](#) (Instituto de Tecnologías en Detección y Astropartículas, Argentina); [Giorgio Amico](#) (Università di Roma – La Sapienza, Italy); [L Arnaldi](#) (Centro Atómico Bariloche and Instituto Balseiro (CNEA), Argentina); [Didier Auguste](#) (Laboratoire de L'Accelérateur Linéaire, Orsay CNRS-IN2P3, France); [Jonathan Aumont](#) (Institut de Recherche en Astrophysique et Planétologie, Toulouse (CNRS-INSU), France); [Susanna Azzoni](#) (University of Manchester, United Kingdom (Great Britain)); [Stefano Banfi](#) (Università di Milano – Bicocca and INFN Milano-Bicocca, Italy); [Elia Battistelli](#) (Università di Roma – La Sapienza, Italy); [Alessandro Bau](#) (Università di Milano – Bicocca and INFN Milano-Bicocca, Italy); [Benoît Belier](#) (Paris Sud University, France); [Laurent Berge](#) (Centre de Spectrométrie Nucléaire et de Spectrométrie de Masse, Orsay, Ireland); [Jean-Philippe Bernard](#) (Centre de Spectrométrie Nucléaire et de Spectrométrie de Masse, Orsay, France); [Marco Bersanelli](#) (Università degli Studi di Milano, Italy); [N Bleurvaq](#) (Astroparticule et Cosmologie, Paris, France); [J Bonaparte](#) (Centro Atomico Constituyentes, France); [J Bonis](#) (Laboratoire de L'Accelérateur Linéaire, Orsay CNRS-IN2P3, France); [A Bottani](#) (GEMA Universidad Nacional de La Plata, Argentina); [Emory Bunn](#) (University of Richmond, USA); [Alberto Etchegoyen](#) (Instituto de Tecnologías en Detección y Astropartículas, Argentina); [Yannick Giraud-Heraud](#) (Astroparticule et Cosmologie, Paris, France); [Marcin Gradziel](#) (National University of Ireland, Maynooth, Ireland); [John Anthony Murphy](#) (National University of Ireland Maynooth, Ireland); [Laurent Grandsire](#) and [Jean-Christophe Hamilton](#) (Astroparticule et Cosmologie, Paris, France); [Aniello Mennella](#) (Università degli Studi di Milano, Italy); [Michel Piat](#) (Astroparticule et Cosmologie, Paris, France); [Lucio Picirillo](#) (University of Manchester, United Kingdom (Great Britain)); [Andrea Tartari](#) (INFN - Pisa Section, Italy); [Stephen Torchinsky](#) (Astroparticule et Cosmologie, Paris, France); [Sophie Henrot-Versille](#) (Laboratoire de L'Accelérateur Linéaire, Orsay CNRS-IN2P3, France); [Paolo De Bernardis](#) (Università di Roma – La Sapienza, Italy); [Diego Harari](#) (Centro Atómico Bariloche and Instituto Balseiro (CNEA), Argentina); [Jean Kaplan](#) (Astroparticule et Cosmologie, Paris, France)

In this paper we briefly describe QUBIC, the Q & U Bolometric Interferometer for Cosmology, a novel ground-based instrument designed to measure the extremely faint polarization anisotropy of the cosmic microwave background at intermediate angular scales. A Technical Demonstrator of the instrument has been built, is being currently tested, and we plan to start observations from Argentina in 2020. Here we will concentrate in particular on simulations of the input feedhorn array, the optical combiner (an off-axis Gregorian imager) and early laboratory calibration measurements.

11:20 *Optics for the Submillimeter Wave Instrument on Jupiter Mission JUICE*

[Mikko Kotiranta](#), [Karl Jacob](#) and [Tobias Plüss](#) (University of Bern, Switzerland); [Paul Hartogh](#) (Max Planck Institute for Solar System Research, Germany); [Axel Murk](#) (University of Bern, Switzerland)

The Submillimeter Wave Instrument is a passive heterodyne radiometer/spectrometer for the JUperiter Icy moons Explorer (JUICE) mission of the European Space Agency. It consists of a 29-cm off-axis Cassegrain antenna and passively cooled Schottky-mixer receivers tunable in the frequency ranges of 530-625 and 1080-1275 GHz. This paper gives an overview of the instrument optics and describes the results of Monte Carlo simulations that have been performed to determine the adverse effect of mounting tolerance of relay optics to the instrument far-field performance. Further, instrument thermal contraction based on predicted mission temperatures has been included in the optical model and its effect on the half power beam width has been evaluated. Finally, the electromagnetic reflection loss of several coating materials has been assessed. A coating protects the mirrors made of AlBeMet from corrosion and potentially reduces the reflection loss by providing a lower surface resistance than the base material.

11:40 *Jupiter Icy Moon Explorer, Submillimeter Wave Instrument: Status and Performances of the 1200 GHz High Spectral Resolution Receiver Front End*

[Jeanne Treuttel](#) (Observatoire de Paris, France)

The Jupiter Icy Moons Explorer (JUICE) [1] is a mission chosen in the framework of the Cosmic Vision 2015-2025 program of the Science and Robotic Exploration Directorate of the European Space Agency. The Submillimeter Wave Instrument (SWI) is a spectrometer/radiometer instrument operating in two submillimeter channels between 530 - 625 GHz and 1080 - 1275 GHz to study the dynamics of Jupiter's stratosphere, vertical profiles of wind speed, temperature, composition and structure of exospheres of Ganymede, Europa and Callisto. LERMA is responsible for the delivery of critical sub-systems of the two channel front-ends, including its 1200GHz mixer and last frequency stage local oscillator. In this paper will describe the SWI radiometer front-end system and address the different procurement steps of the flight hardware. We will present some of the test structures used, the tests conditions as well as some of the failure criterias and allowable drifts.

12:00 *Design and Characterization of 275-500 GHz Corrugated Horns and Optics for a Wideband Radio Astronomy Receiver*

[Bangwon Lee](#) (Korea Astronomy and Space Science Institute, Korea (South)); [Alvaro Gonzalez](#), [Keiko Kaneko](#) and [Ryo Sakai](#) (National Astronomical Observatory of Japan, Japan); [Jung-Won Lee](#) (Korea Astronomy and Space Science Institute, Korea (South))

As a technical demonstration of an astronomical receiver working in a frequency range of 275-500 GHz, we are developing such a wide-band one, called as band 7+8 receiver. The splined corrugated horn and corresponding quasi-optics in the receiver designed for ASTE telescope in Chile are described. The fabricated horn has < -20 dB of return loss and < -23 dB of cross-polarization over the frequency range. Based on the measured beam field propagating through the fabricated optics illuminated by the horn, aperture efficiency is estimated to be > 80 % at all frequencies.

CS66: Unconventional Techniques and Applications for Inverse Scattering Problems

T11 Fundamental research and emerging technologies / Convened Session / Electromagnetics

Room: B9

Chairs: [Martina Teresa Bevacqua](#) (Università Mediterranea di Reggio Calabria, Italy), [Rosa Scapatizzi](#) (CNR-National Research Council of Italy, Italy)

8:30 *Limited-view Prototype Design for Radar-based Fruit Imaging*

[Navid Ghavami](#), [Ioannis Sotiriou](#) and [Panagiotis Kosmas](#) (King's College London, United Kingdom (Great Britain))

The need for non-destructive food testing has received increasing attention with the rapid global growth in food demand and consumption over the past decades. Current limitations in assessing fruits' internal quality motivates the requirements of enhancing existing quality assessment procedures to decrease product wastage and increase the safety of the consumers. Microwave imaging is an emerging non-ionizing and non-invasive technology for various applications. This paper investigates and presents the effects of reducing the number of views on the capability of a Huygens-based algorithm to detect and locate seeds inside the fruits. The results show that limiting the number of receiving views to 180 degrees does not affect the resolution of detected target while further reduction of the views to 90 degrees only causes minor offset in localization. This reduction in the number of receiving positions makes way for the design of a faster, cheaper and less complex food imaging prototype.

8:50 *Inverse Scattering in the Framework of Unconventional Lebesgue Spaces: A Case Study*

[Claudio Estatico](#), [Alessandro Fedeli](#), [Matteo Pastorino](#) and [Andrea Randazzo](#) (University of Genoa, Italy)

An inverse scattering procedure working in the unconventional Lebesgue spaces with variable exponent is considered in this paper. In this method, instead of adopting a single and constant value of the exponent, a variable function is adaptively defined based on the evolution of the inverse scattering problem solution during inexact-Newton iterations. In particular, the effects of the choice of the range of admissible values for the exponent function used in the definition of the involved Luxemburg norm are analyzed. To this end, an experimental case study involving a dielectric cylindrical target is considered as reference scenario.

9:10 *A Phaseless Gauss-Newton Inversion Algorithm for Imaging and Design*

[Chaitanya Narendra](#) and [Puyan Mojabi](#) (University of Manitoba, Canada)

A novel phaseless Gauss-Newton inversion inverse scattering algorithm is presented and extended with three forms of multiplicative regularization schemes: weighted L2 norm total variation, shape and location, and spatial prior regularization. It is shown that the presented algorithm, along with regularization, can invert experimental data, and can be used to design dielectric objects that produce a desired magnitude pattern when illuminated by a known source.

9:30 *Recent Advances and Current Trends in Compressive Processing as Applied to Inverse Scattering*

[Lorenzo Poli](#) and [Alessandro Polo](#) (ELEDIA Research Center, University of Trento, Italy); [Marco Salucci](#) and [Nicola Anselmi](#) (ELEDIA Research Center, Italy); [Giacomo Oliveri](#) (University of Trento & ELEDIA Research Center, Italy)

A novel Compressive Processing (CP) method is presented for an effective solution of inverse scattering problems jointly addressing the sampling problem of the scattering field data and the sensing problem related to the retrieval of the unknowns scatterers within a contrast source framework. Representative numerical results are presented in a comparative fashion with those obtained with a conventional compressive sensing (CSE) approaches.

9:50 *Comparison Between MR, CT, and Quantitative Microwave Holography Images of a Compressed Breast Phantom*

[Daniel Tajik](#), [Natalia Nikolova](#) and [Michael Noseworthy](#) (McMaster University, Canada)

Microwave imaging has been explored for use in medical diagnostics for over 40 years. While advantages related to the use of non-ionizing radiation and low-cost hardware make the technology very promising, it has yet to be deployed clinically, possibly due to low resolution and extensive computational costs. Here, we present images of breast-tissue phantoms obtained with a recently developed real-time imaging method, quantitative microwave holography (QMH), with a microwave scanning prototype. The images are compared with those obtained with two conventional diagnostic methods, X-ray Computed Tomography (CT) and Magnetic Resonance Imaging (MRI). The results highlight the differences between microwave imaging, CT, and MRI. They demonstrate that, although the QMH resolution is inferior to CT and MR, it is more than sufficient to detect tumors of sub-centimeter size. The ability of QMH to generate 2 quantitative images per object, one for the permittivity and one for the conductivity, adds diagnostic value.

10:10 Coffee Break

10:40 *Machine Learning for Microwave Imaging*

[Michele Ambrosanio](#) (Università di Napoli Parthenope, Italy); [Stefano Franceschini](#) (University of Naples Parthenope, Italy); [Fabio Baselice](#) (Università degi Studi di Napoli Parthenope, Italy); [Vito Pascazio](#) (Università di Napoli Parthenope, Italy)

This paper proposes a fully-connected artificial neural network (ANN) approach for addressing the full-wave inverse scattering problem in a quantitative fashion. The proposed scheme processes the scattered field samples collected at receivers locations and provides as output an estimate of the unknown complex permittivity in strongly non-linear scenarios. The proposed approach requires a proper training step, which is also addressed via an automatic randomly-shaped complex profile generator inspired by the statistical distribution of breast biological tissues, and is almost real-time in the recovery step. Several representative numerical tests were carried out to evaluate the performance of the

proposed method and to validate the use of ANN for quantitative imaging purposes in biological-inspired scenarios.

11:00 *Warping Method for Probe Location in near/far Field Transformation*

[Maria Antonia Maisto](#) and [Raffaele Solimene](#) (Università degli studi della Campania Luigi Vanvitelli, Italy); [Rocco Pierri](#) (Università della Campania Luigi Vanvitelli, Italy)

In this paper, planar near field measurement techniques are addressed. In particular, a strategy to collect the near field data which allows to decrease the number of measurements and to foresee the plane wave spectrum within the valid angular region recently introduced in [10] is illustrated.

11:20 *Microwave Imaging Device for In-Line Food Inspection*

[Marco Ricci](#) (Politecnico di Torino, Italy); [Lorenzo Crocco](#) (CNR - National Research Council of Italy, Italy); [Francesca Vipiana](#) (Politecnico di Torino, Italy)

Foreign body contamination is a key issue in food production and packaging industries. The constant increase of mechanized process chain, the variety of materials employed during the production and the growing consumer awareness about food quality arose the number of complaints in the recent years. Several technologies are applied to ensure that products are free from contaminations, but they may fail in detecting low-density plastic or glass fragments contaminants accidentally present inside food/beverage products. To address this issue, a system exploiting microwave imaging is proposed and assessed in this work. To this end, we designed a system which is capable of monitoring of packaged food along the production line, taking into account the specific and challenging constraints arising in such a scenario. Its design and full characterization with full-wave simulation are reported in the paper. The obtained results set the ground for the realization of the prototype of the system.

11:40 *On the Use of Spherical Harmonics in Sparse Microwave Imaging*

[Nebojsa Vojnovic](#) and [Marija Stevanovic](#) (University of Belgrade, Serbia); [Lorenzo Crocco](#) (CNR - National Research Council of Italy, Italy)

In this paper, we introduce a novel microwave imaging method using spherical harmonics and sparse processing. As the sources of the spherical harmonics, we use multipoles of different orders. Based on theoretical considerations and as shown by numerical examples this approach is capable of retrieving concave shapes, which is particularly interesting when imaging complex-shaped targets. In this paper, we limit ourselves to the utilization of the multipoles parallel to the z-axis. We implement rigorous analytical expressions describing the first three multipole orders to improve the method's accuracy. As a test bed we analyze a centered and an offset star-shaped object in the presence of noise. For such a meaningful case, satisfying results have been obtained.

12:00 *Microwave Imaging Profilmetry for Plasma Diagnostics*

[Karunakaran Shruthi](#) (SSN Institutions, India); [Giuseppe Torrisi](#) and [David Mascali](#) (INFN-LNS, Italy); [Nagaradjane Prabagarane](#) (SSNCE, India); [Gino Sorbello](#) and [Loreto Di Donato](#) (University of Catania, Italy)

Microwave imaging can provide effective means for non invasive electromagnetic diagnostics of plasma showing several advantages with respect to traditional techniques. Although microwave imaging entails solution of a full wave inverse scattering problem, it can be addresses in a less complex (but not simpler) way considering the one-dimensional inverse scattering problem for microwave imaging profilometry (MIP). In this contribution we describe a frequency difference domain approach for MIP and provide a possible 3D full wave experimental setup in order to make a step forward application of MIP against laboratory experimental data.

Wednesday, 18 March 8:30 - 10:10

T11-P02/2: Machine Learning in Radio Propagation

T11 Fundamental research and emerging technologies / Regular Session / Propagation

Room: B10

Chair: [Mohammad Ojaroudi](#) (University of Limoges/CNRS, France)

8:30 *VoglerNet: Multiple Knife-Edge Diffraction Using Deep Neural Network*

[Viet-Dung Nguyen](#) (ENSTA Bretagne, France); [Huy Phan](#) (University of Kent, United Kingdom (Great Britain)); [Ali Mansour](#) and [Arnaud Coatanhay](#) (ENSTA Bretagne, France)

Multiple knife-edge diffraction estimation is a fundamental problem in wireless communication. One of the most well-known algorithm for predicting diffraction is Vogler algorithm which has been shown to reach the state-of-the-art results in both simulation and measurement experiments. However, it can not be easily used in practice due to its high computational complexity. In this paper, we propose VoglerNet, a data-driven diffraction estimator, by converting the Vogler algorithm into a deep neural network based system. To train VoglerNet, we propose to minimize a regularized loss function using Levenberg-Marquardt backpropagation in conjunction with a Bayesian regularization. Our numerical experiments show that VoglerNet provides fast solution in order of milliseconds while its performance is very close to that of the classical Vogler algorithm.

8:50 *Study on Radio Propagation Prediction by Machine Learning Using Urban Structure Maps*

[Tatsuya Nagao](#) and [Takahiro Hayashi](#) (KDDI Research, Inc., Japan)

In recent years, mobile data traffic has been increasing, and high-quality mobile communication services are required. Therefore, it is essential to understand the complex radio propagation characteristics in an actual environment. In this paper, we propose a method of predicting radio propagation characteristics by machine learning called gradient boosting, in which the feature is the building information around a transmission point and a receive point, which affects radio propagation characteristics. Gradient boosting is a method of constructing a prediction model using a plurality of weak learners, and it is possible to output the importance of the input feature. That is, it is possible to quantify which feature had a large impact on the radio propagation prediction, and to verify the validity of the model. We evaluated the prediction accuracy using the measured data in an urban area, and clarified the effect of the difference of the feature on the accuracy.

9:10 *A Novel Machine Learning Approach of Hemorrhage Stroke Detection in Differential Microwave Head Imaging System*

[Mohammad Ojaroudi](#) (University of Limoges/CNRS, France); [Stéphane Bila](#) (XLIM UMR 7252 Université de Limoges/CNRS, France); [Mahdi Salimitorkamani](#) (Bio-Electromagnetic Group, Microwave Technology Company (MWT), Tehran, Turkey)

In this paper, brain hemorrhage stroke detection approach using microwave-imaging system with a novel machine-learning based post-processing method is presented. In order to create a circular array based microwave imaging system sixteen elements of the modified bowtie antennas are simulated in CST medium around the full head phantom. In order to radiate in desired band from 0.5-5 GHz an appropriate matching medium is designed. In addition, a hierarchical preprocessing method is employed to calibrate the reflected signals. In the processing section, a confocal image-reconstructing algorithm based is used. Finally, a new machine learning technique including discrete wavelet transform (DWT) and principle component analysis (PCA) for feature extraction and reduction, respectively. In addition, support vector machine (SVM) is used for segmentation and clustering of hemorrhage stroke detection from reconstructed image is employed. Simulated results are presented to validate the effectiveness of the proposed method for precisely localizing and classifying bleeding targets.

9:30 *A Study on the Variety and Size of Input Data for Radio Propagation Prediction Using a Deep Neural Network*

[Takahiro Hayashi](#), [Tatsuya Nagao](#) and [Satoshi Ito](#) (KDDI Research, Inc., Japan)

Not only has the volume of mobile traffic been increasing exponentially, making various services available, such as IoT and connected cars, has also become necessary; moreover, the quality of these services has to be extremely high. As a result, it is necessary to clarify the complicated characteristic of radio propagation. In this paper, we describe radio propagation prediction using a deep neural network (DNN) that can regress to non-linear functions without having to derive complex functions. DNN can learn the features needed for problem solving from input data, in other words, in radio propagation prediction, it is able to learn the environment parameters required for propagation prediction from spatial information that is input such as map data. Based on the evaluation results of propagation prediction with DNN using measurement data in an urban area, we clarify the relationship between the variety and size of input data from the viewpoint of estimation accuracy and computational complexity.

9:50 *Microwave Tomography for Estimating Moisture Content Distribution in Porous Foam Using Neural Networks*

[Rahul Yadav](#) and [Marko Vauhkonen](#) (University of Eastern Finland, Finland); [Guido Link](#) (Karlsruhe Institute of Technology, Germany); [Stefan Betz](#) (Vötsch Industrietechnik GmbH, Reiskirchen, Germany); [Timo Lähivaara](#) (University of Eastern Finland, Finland)

Selective heating in industrial microwave drying could be more efficiently addressed by intelligent control of distributed microwave sources. As a result, increasing system efficiency and reducing thermal runaway while processing low loss dielectric samples. However, applying such a precise microwave control requires non-invasive in-situ measurement of the unknown distribution of moisture inside the material. In this work, the feasibility of integrating a microwave tomography (MWT) with the drying system is demonstrated. The studied imaging modality is applied to estimate the moisture content distribution in a polymer foam. To solve the estimation problem in a fast way, a neural network based approach is proposed in this work. Promising estimation results are shown using synthetic measurement data.

BC/2: History of Electromagnetism 2

T13 Bicentennial Session / Electromagnetics

Room: B11

Chairs: [Ari Sihvola](#) (Aalto University, Finland), [Arthur D Yaghjian](#) (Electromagnetics Research Consultant, USA)

8:30 History of URSI Commission B and the Young Scientist Program

[Edward V. Jull](#) (University of British Columbia, Canada)

This presentation reviews the history of the Commission B (Fields and waves) of the international union of radio science (URSI), and in particular its program to involve young researchers into the community, during the times of the the Cold War up to the breakup of Soviet Union.

8:50 EM Modeling of Stratified Media: From Radio Propagation over Ground to THz Graphene Antennas

[Juan R Mosig](#) (Ecole Polytechnique Federale de Lausanne, Switzerland); [Krzysztof Michalski](#) (Texas A&M University, USA)

In this paper we sketch the history of the development of electromagnetic Green's functions for stratified media, in the frame of the Sommerfeld integral formulation. Two classic, almost canonical, problems are discussed in detail: the Sommerfeld half-space problem and the microstrip antenna problem. The paper concludes with some remarks about numerical techniques and with hints about the extension of the theory to recent topics, like graphene antennas and metasurface based structures.

9:10 A Brief History of Ray Methods from Ancient to Modern Times and Their Impact on Electromagnetic Engineering Applications

[Prabhakar H. Pathak](#) (The Ohio State University, USA); [Hsi-Tseng Chou](#) (National Taiwan University, Taiwan)

This paper briefly reviews a few of the major steps in the evolution of ray concepts and methods from about 700 B.C. to the present. Some applications of the modern ray methods to solving complex high frequency (or electrically large) problems are later summarized; they clearly illustrate the distinct advantages of ray methods not available in other methods.

9:30 Beam Frame Representations: New Alternatives to the Plane Wave and Green Function Representations in the Frequency and Time Domains

[Ehud Heyman](#) (Tel Aviv University, Israel)

Beam summation methods have long been utilized for modeling wave propagation in complex environments due to their unique properties, combining local resolution of the source distributions; asymptotically uniform spectral representation; and algorithmic ray-based structure. So far, beam summation methods were mainly a source-based approach: The beams were used only for spectral expansion of the source, and thereby as propagators. The beam frame is a new concept where a properly constructed phase-space set of beam waves constitutes a frame everywhere in the propagation domain and thus can be used for local expansion not only of the sources but also of the medium. This transforms the problem of tracking waves in complicated media into a local-spectrum diagrammatic formulation where the same beam-set is used to expand both the source, the medium, and the local interaction of the field with the medium.

9:50 Maxwell's Derivation of the Lorentz Force from Faraday's Law

[Arthur D Yaghjian](#) (Electromagnetics Research Consultant, USA)

In a brief but brilliant derivation that can be found in Maxwell's 1861 and 1865 papers as well as in his Treatise, he derives the force on a moving electric charge subject to electric and magnetic fields from his mathematical expression of Faraday's law for a moving circuit. The derivation of this force, which is usually referred to today as the Lorentz force, is given in detail in the present paper using modern notation.

IW06: Active Impedance Assessment and Beamforming Optimization for mm-Wave Antenna Arrays (Optenni Ltd)

T12 Scientific / Industrial Workshops

Room: B3

Jaakko Juntunen, Optenni Ltd

IW09: 5G Antenna Array Design and Integration Simulation (ANSYS)

T12 Scientific / Industrial Workshops

Room 6

David Prestaux, ANSYS

Wednesday, 18 March 10:40 - 12:20

T11-P04: Experimental Methods and Campaigns

T11 Fundamental research and emerging technologies / Regular Session / Propagation

Room: B10

Chairs: [Maria A Sergeeva](#) (CONACYT, SCiESMEX, LANCE, UNAM, Mexico), [Elizabeth Verdugo](#) (PUC RIO, Brazil)

10:40 Possibility of Signal Reflection from the Northern Crest of EIA: Case Study

[Maria A Sergeeva](#) (CONACYT, SCiESMEX, LANCE, UNAM, Mexico); [Alexey S Kalishin](#) (Arctic and Antarctic Research Institute, Russia); [Olga Maltseva](#) (Institute for Physics & Southern Federal University, Russia); [Donat Blagoveshchensky](#) (Saint-Petersburg State University of Aerospace Instrumentation, Russia); [Juan Americo Gonzalez-Esparza](#) (Universidad Nacional Autonoma de Mexico, Mexico); [Pedro Corona-Romero](#) (Instituto de Geofisica, Universidad Nacional Autonoma de Mexico, Mexico); [Victor Jose Gatica-Acevedo](#) (Instituto Politecnico Nacional, Mexico)

The case of the anomalous signal propagation in the low-latitude American sector was studied. The possibility of the signal reflection from the electron density gradient caused by the northern crest of the equatorial ionization anomaly at the background of geomagnetic activity increase was considered. In the absence of other probable causes, it seems that the short-time anomalous signal reflection from the density gradient is possible when the local geomagnetic index K_{mex} is more or equal to 5 during the evening hours.

11:00 Measured Activity in 860 MHz Channels

[Jesper Ø Nielsen](#) (Aalborg University, Denmark); [Maria Fresia](#) (Intel Deutschland, Germany); [Gert Pedersen](#) (Aalborg University, Denmark)

This work investigates the channel activity in the European license free 863-870 MHz band via measurements in 7 widely different urban and sub-urban areas. The data is analyzed in 8 different sub-bands. The measured 1 ms sweeps are used to characterize the random activity, where the estimated complementary cumulative distribution functions (CCDFs) are found to be highly dependent on both location and sub-band. In addition, the probability of observing an unused channel for varying lengths of time is estimated.

11:20 Signal Reception Measurements Using Mobile HD Radio and DRM Systems in Two Urban Regions in Brazil

[Elizabeth Verdugo](#) (PUC RIO, Brazil); [Luiz da Silva Mello](#) (CETUC-PUC-Rio & Inmetro, Brazil); [Marta Pudwell Chaves de Almeida](#) (Inmetro, Brazil)

This paper present mobile measurements of digital radio made in dense urban regions of Brazil. Measurements at medium wave were carried out in São Paulo and Minas Gerais using the two standards available for this frequency range DRM and HD Radio. Comparison of electrical field strength with predictions from ITU recommendation are presented. Large- and small-scale fading probability distribution functions of the received signals were estimated for each measurements route.

11:40 Aircraft Measurements of the Marine Surface Layer Refractive Index During the TAPS Campaign

[Andrew Kulesa](#) (Airborne Research Australia, Australia); [Jorg Hacker](#) (Airborne Research Australia & Flinders University, Australia); [Hedley J Hansen](#) (Defence Science Technology, Australia); [Marion Kermann](#) (Airborne Research South Australia, Australia); [Alex Vanderklugt](#) (DST,

Australia); [Jacques Claverie](#) (CREC St-Cyr & IETR, France)

This paper describes some of the airborne atmospheric measurements, within the atmospheric surface layer, undertaken during the TAPS field campaign. A hybrid (flux - Bulk) model for refractivity is outlined which makes suitable use of the aircraft data. The model provides the evaporation duct structure over the regions where the aircraft was flown, providing a 3D spatial and temporal description of surface layer refractivity.

12:00 *Observations and Modelling of Propagation Loss in the Turbulent Sea Surface Environment*

[Hedley J Hansen](#) (Defence Science Technology, Australia); [Alex Vanderklugt](#) (DST, Australia); [Andrew Kulesa](#) (Airborne Research Australia, Australia); [Jorg Hacker](#) (Airborne Research Australia & Flinders University, Australia); [Stephen Salamon](#) (University of Adelaide & Telstra Corporation, Australia); [Martin Veasey](#) (MET Office, United Kingdom (Great Britain))

The paper presents a case study investigating the effect of turbulence on microwave X-band reception. Path loss estimates for the X-band link operated during the Tropical Air- Sea Propagation Study (TAPS) in the Coral Sea in November- December 2013 have been modelled with refractivity profiles derived from a bulk parameterization based on Monin-Obukov similarity theory using near surface data that was co-recorded on a suitably located open sea jetty site. The results reported show that including stochastic effects in the environmental propagator of the Parabolic Equation Method (PEM), appropriate to the sea surface environment at the time of the RF reception measurements, improves on the predictive modelling of the path loss measurements.

T06-M10: UAV-Based Antenna Measurements (AMTA)

T06 Aircraft (incl. UAV, UAS, RPAS) and automotive / Regular Session / Measurements

Room: B11

Chair: [Giuseppe Virone](#) (Consiglio Nazionale delle Ricerche, Italy)

10:40 *Versatile Low-Cost and Light-Weight RF Equipment for Field Measurements*

[Jonas Kornprobst](#) (Technical University of Munich, Germany); [Raimund A. M. Mauermayer](#) (Independent Researcher, Germany); [Thomas F. Eibert](#) (Technical University of Munich, Germany)

We present a low-cost and light-weight measurement equipment based on a software-defined radio (SDR) and a radio-frequency over fiber (RToF) connection. The main purpose of the hardware are near-field antenna measurements, but possible use-cases also include imaging and other inverse-source scenarios. The two hardware features "low-cost" and "light-weight" are important for the use on an unmanned aerial vehicle (UAV): Crashes should not financially ruin the operator and the UAV payload is limited. Regarding the RF properties of the hardware, the RToF connection has the benefit of extremely low-loss as compared to coaxial cables, while the SDR offers great flexibility for measurement frequency, bandwidth, and signal filtering. One SDR transmit channel is employed to provide a coherent signal to an antenna and two receive channels capture two field components (linearly independent polarizations). As an important part of the RF circuitry, a drift compensation is a countermeasure against changing temperature conditions.

11:00 *RF-Signal Receiver for UAV-Based Characterisation of Aeronautical Navigation Systems*

[Alexander Weiß](#), [Robert Geise](#) and [Björn Neubauer](#) (Technische Universität Braunschweig, Germany); [Fabian T. Faul](#) (Technical University of Munich, Germany); [Thomas F. Eibert](#) (Technical University of Munich (TUM) & Chair of High-Frequency Engineering (HFT), Germany); [Torsten Fritzel](#), [Hans-Juergen Steiner](#) and [Rüdiger Strauß](#) (Aeroxess UG, Germany)

This contribution presents measurements with a self-built high frequency receiver architecture for nearfield measurements without synchronization between devices under test and the receiving stage that can be mounted on an unmanned aerial vehicle. It comprises a stationary monitor with a fixed location and a monitor, that can vary in space to measure the phase and amplitude dependency with respect to its location, as required for nearfield measurements and farfield transform. One application for that is the nearfield inspection of navigation systems. The measurement concept also applies laser tracking of the variable monitor and a sophisticated synchronization of the measured high frequency data and location data. In particular, real time capability of data acquisition is validated with this setup. First measurement results demonstrate the functionality of the architecture that allows an unsynchronized phase accuracy of better than 8° at 2 GHz.

11:20 *Comparison Between Measured and Simulated Antenna Patterns for a LOFAR LBA Array*

[Paola Di Ninni](#) (OAA - INAF, Italy); [Pietro Bolli](#) (INAF - Osservatorio Astrofisico di Arcetri, Italy); [Fabio Paonessa](#) (National Research Council of Italy (CNR - IEIIT), Italy); [Giuseppe Pupillo](#) (IRA - INAF, Italy); [Giuseppe Virone](#) (Consiglio Nazionale delle Ricerche, Italy); [Stefan J. Wijnholds](#) (ASTRON, The Netherlands)

A UAV-based system has been employed for a measurement campaign on a station of the radio telescope LOFAR to characterize the individual Low Band Antenna patterns. The experimental set-up has been then simulated with a full-wave software and numerical embedded element patterns have been compared to the measured results. A statistical analysis of the differences between the two data sets has been finally carried out to estimate the accuracy of the electromagnetic model.

11:40 *A Drone-Mounted Q-Band Test-Source for the Validation of the Large Scale Polarization Explorer*

[Fabio Paonessa](#) (National Research Council of Italy (CNR - IEIIT), Italy); [Giuseppe Virone](#) (Consiglio Nazionale delle Ricerche, Italy); [Lorenzo Ciorba](#) (Institute of Electronics, Computer and Telecommunication Engineering (IEIIT-CNR), Torino & Politecnico di Torino, Torino, Italy); [Oscar A. Peverini](#) (Istituto di Elett. e di Ingegneria dell'Inform. e delle Telecom. (IEIIT- CNR), Italy); [Giuseppe Addamo](#) (Istituto di Elett. e di Ingegneria dell'Inform. e delle Telecom. (IEIIT-CNR), Italy); [Mauro Lumia](#) (CNR, Italy); [Marco Bersanelli](#) and [Aniello Mennella](#) (Università degli Studi di Milano, Italy)

The Unmanned Aerial Vehicles (UAVs) technology represented a significant innovation for antenna measurements in the last years. So far, UAVs have been mainly exploited for the characterization of the radiation pattern of antennas and arrays up to C-band. An evolution of the system working in the Q-band is planned to be used for the validation of the future Survey TeneRife Polarimeter (STRIP) of the Large-Scale Polarization Explorer (LSPE), an Italian project. This contribution presents a payload solution and a preliminary test performed.

12:00 *Advanced Remote-Controlled Airborne Sensor Systems*

[Thorsten Schrader](#) (Physikalisch-Technische Bundesanstalt, Germany); [Jochen Bredemeyer](#) (FCS Flight Calibration Services GmbH, Germany); [Thomas Kleine-Ostmann](#) and [Marius Mihalachi](#) (Physikalisch-Technische Bundesanstalt, Germany)

Based on commercially available octocopters, PTB has developed flight measurement platforms with RF front-ends for various frequency bands. The remote-controlled measurement systems are designed for calibrated on-site measurements of the signals emitted by terrestrial navigation systems and radars. They are used to measure signal strengths quantitatively and to investigate the disturbance potential of wind turbines.

12:20 *Precise 6D RTK Positioning System for UAV-based Near-Field Antenna Measurements*

[Patrick Henkel](#), [Andreas Sperl](#) and [Ulrich Mittmann](#) (ANavS GmbH, Germany); [Torsten Fritzel](#), [Rüdiger Strauß](#) and [Hans-Juergen Steiner](#) (Aeroxess UG, Germany)

Near-field antenna measurements with an Unmanned Aerial Vehicle (UAV) require an accurate 3D position and 3D attitude information. In this paper, we estimate the position and velocity of the UAV, the quaternion that describes its attitude, the carrier phase integer ambiguities related to both the attitude and position, and the accelerometer bias with a Kalman filter. The raw measurements were obtained from the ANavS Multi-Sensor RTK module with its 3 Multi-frequency, Multi-GNSS receivers and a MEMS-based Inertial Measurement Unit (IMU). We used the UAV of AeroXess to validate our method and achieved a centimeter-level positioning accuracy in both static and kinematic conditions.

IW02: Analysis and Design of Advanced Antenna Systems using TICRA Tools (TICRA)

T12 Scientific / Industrial Workshops

Room: B3

Dr. Peter Meincke and Dr. Min Zhou, TICRA

IW07: State-of-the-art in Antenna System Simulation with CST Studio Suite (Dassault Systèmes)

T12 Scientific / Industrial Workshops

Room 6

Wednesday, 18 March 13:20 - 14:50

Convened Poster 2-CS14: Antennas for Harsh Environment

T11 Fundamental research and emerging technologies / Convened Session / Antennas

Room: [A2 \(Poster Area\)](#)

Chairs: [Loic Bernard \(ISL, France\)](#), [Nicolas Capet \(ANYWAVES FRANCE, France\)](#)

CP2.01 Optimal Frequency of Operation and Radiation Efficiency Limitations of Implantable Antennas

[Denys Nikolayev](#) (Institut d'Électronique et de Télécommunications de Rennes (UMR CNRS 6164), France); [Zvonimir Sipus](#) and [Marko Bosiljevac](#) (University of Zagreb, Croatia); [Wout Joseph](#) (Ghent University/IMEC, Belgium); [Maxim Zhadobov](#) (University of RENNES 1, France); [Ronan Sauleau](#) (University of Rennes 1, France); [Luc Martens](#) (Ghent University - imec, Belgium); [Anja K. Skrivervik](#) (EPFL, Switzerland)

Fundamental limits on radiation performance of implantable antennas serve as the design quality gauge, facilitate the choice of the antenna type, and provide simple design rules to maximize the radiation performance. This study obtains the limits using two formulations: 1) theoretical spherical-wave expansion using elementary magnetic and electric dipoles and 2) realistic full-wave 2D-axisymmetric models of TM₁₀ and TE₁₀ mode capsule antennas. Using both formulations, the optimal radiation conditions are investigated, the effects of antenna dimensions and its implantation depth are quantified. The results also demonstrate that an electric antenna operating close to the optimal frequency could achieve higher efficiency than a magnetic one. The latter, however, is more efficient below the optimal frequency range.

CP2.02 3D Printed Ceramic Antennas for Space Applications

[Gautier Mazingue](#) (Anywaves, France); [Benedikt Byrne](#) (ANYWAVES, France); [Maxime Romier](#) (Anywaves, France); [Nicolas Capet](#) (ANYWAVES FRANCE, France)

This paper is an application and an evolution of the new technology that has been already used for a GNSS L1 patch antenna. This technology allows the design of miniature antennas consisting of ceramic material manufactured with an additive process. Based on a patented technology, the dielectric material is structured with a 3D lattice design to obtain the desired effective permittivity. Two different lattices have been studied in this paper which are applied to a miniature circularly polarized dielectric resonator antenna (DRA). Simulated results are given and discussed.

CP2.03 Mechanical and Environmental Aspects of Antennas for a Novel Maritime Search and Rescue System

[Taher Badawy](#), [Alexander Kremring](#) and [Dawood Nulwalla](#) (Fraunhofer Institute for High Frequency Physics FHR, Germany); [Thomas Bertuch](#) (Fraunhofer FHR, Germany)

This paper presents the mechanical and environmental aspects of a novel dual-band harmonic radar antenna for maritime search and rescue system. These aspects are considered in the mechanical design of the proposed antenna. The dual-band radar antenna operates in the frequency range from 2.90 GHz to 2.95 GHz (S-band) and from 5.80 GHz to 5.90 GHz (C-band). The antenna configuration is based on two slotted waveguide antennas sharing the same housing and provides dual polarizations. One waveguide array employs edge slots with horizontal polarization, the other waveguide uses broadwall slots with vertical polarization. The mechanical design of the antenna is presented providing a low profile and lightweight structure that is compatible with the marine environmental conditions. A radome made of glass fiber reinforced plastic is used to protect the antenna against environmental influences. The radome structure is flexible enough to be easily integrated with the antenna.

CP2.04 Transmit-Arrays at Ka-band for Harsh Environment

[Trung Kien Pham](#) (International University, VNU-HCM, Ho Chi Minh City 70000, Vietnam); [Ronan Sauleau](#) (University of Rennes 1, France); [Erwan Fourn](#) (INSA of Rennes & IETR, France); [Antonio Clemente](#) (CEA-LETI Minatec, France)

This paper demonstrates a promising antenna solution for operation in harsh environment: it consists of a metal-only transmitarray antenna. The latter is based on a C-shaped slot unit-cell exhibiting a phase variation of 360 degrees with insertion loss below 1-dB at 29 GHz. Several antenna prototypes have been fabricated and their performance has been characterized in anechoic chamber. Here, two different antenna prototypes are presented demonstrating, respectively, beam pointing at 30 degree and 50 degree with good agreement between simulated and measured results. For beam pointing at boresight, the aperture efficiency is greater than 50% and the half power bandwidth is around 7.5% at 29 GHz.

CP2.05 Telemetry Antennas Withstanding Very High Accelerations and Centrifugal Forces

[Loic Bernard](#), [Hrvoje Covic](#), [Andreas Zeiner](#) and [Armin Schneider](#) (ISL, France)

This paper presents the design steps of a coaxial dipole antenna for telemetry applications under extreme conditions of accelerations and centrifugal forces. Both electromagnetic and mechanical designs are presented, as well as performance compromise that have to be made between both domains. The experimental results are given in the last part of the article.

Convened Poster 2-CS29: Exotic Antennas from Nano to Macro Scales

T11 Fundamental research and emerging technologies / Convened Session / Antennas

Room: [A2 \(Poster Area\)](#)

Chairs: [Samel Arslanagić \(Technical University of Denmark, Denmark\)](#), [Richard Ziolkowski \(University of Technology Sydney, Australia & University of Arizona, USA\)](#)

CP2.06 Metamaterial-inspired Near-Field Resonant Parasitic Dipole Antennas on High Permittivity Dielectrics

[Richard Ziolkowski](#) (University of Technology Sydney, Australia & University of Arizona, USA)

It is well-known that if a (horizontal) electric dipole antenna is placed on the interface between a high permittivity dielectric and air, it will radiate a majority of its power into the dielectric rather than into the air region. This basic physics effect is a significant roadblock to achieving efficient on-body and on-chip antennas. The future 5G outlook includes numerous Internet-of-Things (IoT) devices that involve both types of antenna systems. It will be described herein and in my presentation how one can use metamaterial-inspired Huygens dipole antennas to achieve systems that radiate primarily into the air region rather than into the dielectric.

CP2.07 Using Superdirectivity to Enhance the Performance of Different Scattering Processes

[Iñigo Liberal](#) (Public University of Navarre, Spain)

Superdirectivity is a thrilling theoretical concept that usually finds applications in antenna systems for communication and wireless power transfer applications. However, the concept of superdirectivity could be applied to enhance the performance of a large number of scattering configurations. Here, we show how superdirective end-fire arrays can enhance the performance of cross-polarization backscatterers located at a perfect electric conductor interface. In our talk, we will discuss the key role of an enhanced directivity for a wide range of scattering configurations.

CP2.08 A Concept of Flexible Non-Metallic Dielectric Resonator Antenna for Conformal Applications

[Shengjian Jammy Chen](#) (The University of Adelaide, Australia); [Christophe Fumeaux](#) (The University of Adelaide & School of Electrical and Electronic Engineering, Australia)

A concept of flexible dielectric resonator antenna based on non-metallic materials is presented in this paper for conformal applications. To attain mechanical flexibility, the dielectric resonator and the substrate of the antenna are realized using a flexible PDMS(Polydimethylsiloxane)-ceramic mixture, whereas the microstrip feed and the ground plane are based on a flexible and conductive carbon cloth. To validate the concept, an antenna prototype is designed, fabricated and experimentally characterized. The good agreement between simulation and measurement suggests that the antenna concept is promising for conformal applications.

CP2.09 Water-Based Microwave Antennas

[Rasmus Elkjaer Jacobsen](#), [Mads Vandborg](#), [Andrei Lavrinenko](#) and [Samel Arslanagić](#) (Technical University of Denmark, Denmark)

The interesting properties of water makes it an attractive material platform for many microwave applications including artificial material design, sensing, heating systems and dielectric resonator antennas. Presently, electrically small versions of the latter are considered. We present the numerical and experimental results for an antenna consisting of a short monopole fed against a large conducting ground plane and encapsulated by a water-filled cylindrical cavity. The resonant antenna is designed for 300 MHz operation and is successfully matched to a 50 Ohm transmission line and the surrounding air. The total efficiency is 33.4 % and the reflection coefficient is -28 dB. The reduced efficiency is due to water losses and the small antenna size. A prototype of the antenna was fabricated, and the measurements and numerical predictions exhibit good agreement. Additionally, frequency-tuning by extraction of water is investigated.

CP2.10 Design of a Tunable Subwavelength Plasma-Based Resonator for Electrically Small Antenna Applications in L-band

[Adrien Laffont](#) (CEA, DAM, CEA-Gramat, France); [Théo Delage](#), [Romain Pascaud](#), [Marjorie Grzeskowiak](#) and [Cyril Cailhol](#) (ISAE-SUPAERO, Université de Toulouse, France); [Thierry Callegari](#), [Laurent Liard](#) and [Olivier Pascal](#) (LAPLACE, CNRS, UPS, INP, Université de Toulouse, France); [Jean-Pierre Adam](#) (CEA, DAM, CEA-Gramat, France)

A preliminary study of the design of an electrically small plasma-based resonator using a localized surface plasmon resonance (LSPR) above 1 GHz is presented. Such a resonator is intended to be used to develop an electrically small antenna with frequency agility. This resonator consists of a plasma discharge confined in a hemispherical glass shell 3 cm in diameter on a ground plane. From 1 to 1.5 GHz, the plasma electron density required to achieve the LSPR must be between 0.5×10^{11} and 1.4×10^{11} cm⁻³. Plasma losses are taken into account in this study and provide information on the required gas pressure. Typically for neon gas, the working pressure must be around 50 mTorr. A practical implementation using a miniature inductively coupled plasma (mICP) source is finally discussed.

Convened Poster 2-CS36: Innovative Lens Antennas for Future Communication Systems

T02 Millimetre wave 5G / Convened Session / Antennas

Room: [A2 \(Poster Area\)](#)

Chair: [Oscar Quevedo-Teruel \(KTH Royal Institute of Technology, Sweden\)](#)

CP2.11 Parallel-Plate Waveguide Lens for Mechanical Beam Scanning Using Gap Waveguide Feed System

[Thomas Ströber](#) (Univ Rennes 1, IETR, France); [Ségolène Tubau](#) (Thales Alenia Space, France); [Hervé Legay](#) (Thalès Alenia Space, France); [Etienne Girard](#) (Thales Alenia Space, France); [George Goussetis](#) (Heriot-Watt University, United Kingdom (Great Britain)); [Mauro Ettore](#) (University of Rennes 1 & UMR CNRS 6164, France)

A parallel-plate waveguide lens with mechanically reconfigurable feed network for continuous beam scanning is presented. The quasi-optical system is designed using an optimization process based on previously developed ray-optical methods. The feed network relies on the non-contacting properties of groove gap waveguides which allows for a fixed input port and simple mechanical actuation. Numerical results are presented for a Ka-band lens design, demonstrating a high scanning performance over an angular range of +/-35° with scan losses lower than 2 dB; the simulated mismatch loss is lower than -15 dB between 27 and 31 GHz. The proposed all-metal beamformer is therefore a promising solution for next-generation Satcom applications.

CP2.12 Fully-Metallic Rinehart-Luneburg Lens at 60 GHz

[Martin Petek](#) and [Oskar Zetterstrom](#) (KTH Royal Institute of Technology, Sweden); [Elena Pucci](#) (Ericsson AB, Sweden); [Nelson Fonseca](#) (European Space Agency, The Netherlands); [Oscar Quevedo-Teruel](#) (KTH Royal Institute of Technology, Sweden)

In this paper, we present the design of a Rinehart-Luneburg lens antenna operating from 56 to 62 GHz. At these high frequencies, dielectric materials introduce high losses, so fully-metallic solutions are typically preferred. The required refractive index of the Luneburg lens is realized by deforming the parallel plate waveguide following the concept of geodesic surfaces. Despite the high frequency, the achieved radiation efficiency is roughly 90%. Thirteen antenna ports are angularly placed along the contour of the lens to enable an electronical beam switching of +/- 55 degrees with equally spaced steps and an interleaving dip loss of 6 dB.

CP2.13 3D-printed Wideband Hyperbolic Lens Antenna for Ka-band

[Jose M Poyanco](#) (Pontificia Universidad Catolica de Valparaiso, Chile); [Nelson Mario Castro](#) (Pontificia Universidad Catolica de Valparaiso, Chile); [Francisco Pizarro](#) (Pontificia Universidad Catolica de Valparaiso, Chile); [Eva Rajo-Iglesias](#) (University Carlos III of Madrid, Spain)

This article presents a 3D-printed wideband hyperbolic lens antenna covering the complete Ka-band. The design of the lens is totally flat as it is derived after an optic transformation. The lens was constructed using a 3D printer with ABS filaments that were characterized with respect its infill percentage. Different of strategies for the manufacturing will be evaluated.

CP2.14 On the Use of Dielectric Gratings for Enlarging the Field of View in Low Dielectric Permittivity Lenses

[Marta Arias Campo](#) (IMST GmbH, Germany & Delft University of Technology, The Netherlands); [Simona Bruni](#) (IMST GmbH, Germany); [Giorgio Carluccio](#) and [Nuria LLombart](#) (Delft University of Technology, The Netherlands)

Low relative permittivity plastic elliptical lenses are a promising solution to be used in the future mm- and sub-mm wave systems, due to the availability of materials with moderate loss, light weight and cost-effective manufacturing. However, the low permittivity implies a reduction in the field of view achieved when displacing the lens feeder within the focal plane. In this contribution, the use of dielectric gratings with modulated height integrated inside elliptical lenses with low permittivity is investigated, with the aim of enlarging the steering angle reached. The dielectric gratings synthesize a tilted feeder pattern inside the elliptical lens, reducing the reflection loss and spill-over when illuminating the lens off-focus. The analytical approach used to dimension the gratings is explained here. An example in G-band (140-220GHz) has been simulated as a first proof-of-concept, showing promising results.

CP2.15 Transmit-array Antenna Design for Broadband Backhaul 5G Communications at WiGiG Band

[Sergio Matos](#) (Instituto Universitário de Lisboa, Portugal); [Jorge R. Costa](#) (Instituto de Telecomunicações / ISCTE-IUL, Portugal); [Carlos A. Fernandes](#) (Instituto de Telecomunicações, Instituto Superior Técnico, Portugal); [Nour Nachabe](#) (University of Nice Sophia Antipolis, France); [Cyril Luxey](#) (University Nice Sophia-Antipolis, France); [Diane Titz](#) (University Nice Sophia Antipolis, France); [Frédéric Giancesello](#) (STMicroelectronics, France); [Carlos del-Río](#) (Universidad Publica de Navarra & Institute of Smart Cities, Spain); [Ana Arboleya](#) (Universidad Rey Juan Carlos, Spain); [Jorge Teixeira](#) (ISCTE-IUL, Instituto de Telecomunicações, Portugal); [Jean-Philippe Garnero](#) (Polytech'Lab, Université Nice Sophia Antipolis, France); [Jean-Francois Vizzari](#) (Polytech'Lab, Université Nice Sophia Antipolis, France)

A cost-effective transmit-array (TA) antenna design framework is presented and experimentally validated for a 5G backhaul application at the WiGiG band. The antenna is composed of a discrete dielectric lens (DDL) fed by a horn, specifically designed for this application. Both the TA and feed are fabricated using additive manufacturing. Metal coating and Fuse Deposition Modeling are employed for the horn and TA fabrication, respectively. Simple design rules are devised to quantify the bandwidth of this type of antennas as function of the aperture dimension and focal distance. Based on this framework a compact TA antenna (≠) than can comply with typical specifications for 5G backhaul links at WiGiG band (minimum gain of 30 dBi from 57 to 66 GHz) is designed.

Convened Poster 2-CS41: Metasurfaces for Mobile (5G and Beyond) and Satellite Communication Systems

T09 Space (incl. cubesat) / Convened Session / Antennas

Room: [A2 \(Poster Area\)](#)

Chair: [Alexandros Feresidis \(University of Birmingham, United Kingdom \(Great Britain\)\)](#)

CP2.16 Glide-Symmetric Luneburg Lens Using Substrate-Integrated-Holes for 5G Communications at Ka-Band

[Ramez Hamarneh](#) (KTH, France); [Oskar Zetterstrom](#) and [Oscar Quevedo-Teruel](#) (KTH Royal Institute of Technology, Sweden)

Here, we propose a cost-effective implementation of a planar metasurface Luneburg lens operating at Ka-band. The lens is implemented in a parallel plate structure. The required graded refractive index is realized through spatially varying the dimensions of an array of inclusions placed in both plates of the parallel plate waveguide. More specifically, the inclusions are square holes printed on a substrate which is attached to a ground plane. Each square is surrounded by metallic vias which are connected to the ground plane. The inclusions in both plates are arranged to possess glide symmetry. Waveguide feeds are integrated in the parallel plate waveguide. The lens is terminated with a flare to achieve an efficient radiation to free space.

CP2.17 Peripherally Excited Phased Arrays with Practical Active Huygens' Sources and Slot Elements

[Ayman H. Dorrah](#) and [George V. Eleftheriades](#) (University of Toronto, Canada)

Antenna phased arrays have become increasingly more important in recent years with the advent of technologies such as 5G communications, automotive radars, and satellite internet. These phased arrays are costly to design, fabricate and deploy. A main component of the cost of traditional phased arrays is that of the necessary feeding network and phase shifters or transceivers. A recently developed concept called the peripherally-excited (PEX) phased array has been proposed which is capable of generating electronically scanned pencil beams with a reduced number of phase shifters. The concept of the PEX phased array relies on peripheral active Huygens' sources that are solely used along the periphery of the cavity. This paper proposes a practical Huygens' source implementation which is compatible with printed-circuit-board technology, and exhibits low reflections and mutual coupling between adjacent sources. Furthermore, a specially-engineered slot arrangement is proposed which can achieve effective radiation at broadside and tilted angles.

CP2.18 An Ultra-thin Wide-Angle Scanned Planar Array Antenna for Satellite Communication

[Yujie Liu](#) (Queen Mary University of London & Antenna Group, United Kingdom (Great Britain)); [Ahsan Noor Khan](#) and [Qiao Cheng](#) (Queen Mary University of London, United Kingdom (Great Britain)); [Max Munoz](#) (Queen Mary, University of London, United Kingdom (Great Britain)); [Yang Hao](#) (Queen Mary University, United Kingdom (Great Britain))

The requirements of high data throughput nowadays for satellite communication are expediting for worldwide connectivity. The antenna features, such as low profile and lightweight are desirable for future satellite systems. In this paper, we propose a novel ultra-thin and easy-fabricated scanned array antenna operating in X band from 10.7 GHz to 12.7

GHz with S11≤ -10 dB. The antenna array offers advantage with beam steering capability of nearly 60 degree without utilizing any costly phase shifter. This is achieved by rotating the relative position of the upper radiated layer regarding the bottom feeding layer. The total height of this array antenna is about 0.23 λ_{highest} and the radiation efficiencies are all above 60% during the whole scanning range.

CP2.19 Quasi-Periodic Metasurfaces and Their Equivalent Dielectric Models

[Qiao Cheng](#) (Queen Mary University of London, United Kingdom (Great Britain)); [Shiyu Zhang](#) (Loughborough University, United Kingdom (Great Britain)); [Raj Mittra](#) (Penn State University, USA); [J \(Yiannis\) Vardaxoglou](#) (Loughborough University, United Kingdom (Great Britain)); [Yang Hao](#) (Queen Mary University, United Kingdom (Great Britain))

In this paper, we present an equivalent dielectric method to speed up simulation of quasi-periodic metasurfaces. The idea is to use homogeneous equivalent dielectric material to replace original metasurface unit cells for simulation. An X-band reflectarray antenna was used to demonstrate this approach. Simulated results show both good accuracy and reduced simulation time as compared to the original array.

CP2.20 Metasurface-Based Circularly-Polarized Multibeam Reflect-/Transmit-Arrays

[Zhi Hao Jiang](#), [Fan Wu](#) and [Xiaowei Zhu](#) (Southeast University, China); [Qiang Ren](#) (Beihang University, China); [Pingjuan Werner](#) and [Douglas H Werner](#) (Pennsylvania State University, USA)

In this paper, we present an overview of recent progress on metasurface-based circularly-polarized reflect and transmit-arrays for millimeter-wave applications. The reflect- and transmit-arrays are composed of sub-wavelength unit cells containing multiple cascaded layers of anisotropic impedance surfaces. By utilizing either the Berry phase and/or dynamic phase, highly-directive circularly-polarized multibeam can be generated with a single feed or a cluster of feeds. Three proof-of-concept examples are showcased, which are all validated by experimental measurements.

CP2.21 Recent Advances on Modulated Metasurface Antennas for SatCom

[Marco Faenzi](#) (Université de Rennes 1, France); [Gabriele Minatti](#) (Wave Up S. r. l., Italy); [David González-Ovejero](#) (Centre National de la Recherche Scientifique - CNRS, France); [Francesco Caminita](#) (Wave-Up SRL, Italy); [Enrica Martini](#) (University of Siena, Italy); [Cristian Della Giovampaola](#) (Wave Up srl, Italy); [Stefano Maci](#) (University of Siena, Italy)

In this paper, some of the newest antenna prototypes, based on modulated metasurface technology are presented. These devices show some interesting radiation features that have been implemented to comply with specific needs of satellite links, space-to-ground communications and deep space missions. Irrespectively of the challenging performances achieved by the modulated MTS apertures presented here, all the examples shown preserve some key features rendering these prototypes extremely appealing for space environment such as low mass and low envelope, low production costs and low profile, simple feeding systems that render them suitable to onboard satellites or spacecrafts usage; also, such devices can be easily mounted on flat platforms.

CP2.22 Electro-Mechanically Tunable Meta-Surfaces for Beam-Steered Antennas from mm-Wave to THz

[Muhammad S Rabbani](#), [James Churm](#) and [Alexandros Feresidis](#) (University of Birmingham, United Kingdom (Great Britain))

Electro-mechanically tunable meta-surfaces are presented for high gain, beam steerable Leaky-Wave Antennas (LWAs) at 37 GHz and 280 GHz bands. The proposed metasurfaces are: a tunable High Impedance Surface (HIS) in case of 37 GHz LWA, and tunable Partially Reflective Surface (PRS) in case of 280 GHz LWA. The proposed metasurfaces serve as a phase shifter in the beam steering antenna. The required phase shift is achieved by varying the mechanical separation between the HIS/PRS periodic array and ground layer using a piezoelectric actuator (PEA). The presented phase shifting technique offers an extremely low loss solution for antenna beam steering at mm-wave frequencies. The designed antenna at the selected frequency bands may find applications in broadband mobile communications in 5G and beyond. The presented antenna yields a wide S11 bandwidth (BW), high gain and wide beam scanning range as required for broadband mobile applications.

Convened Poster 2-CS50: Novel Wave Phenomena in Metamaterials and Metasurfaces Applied to Antennas and Propagation

T11 Fundamental research and emerging technologies / Convened Session / Antennas

Room: [A2 \(Poster Area\)](#)

CP2.23 Analytical Study of Dielectric-wall Conical Horn Antennas

[Anastasios Paraskevopoulos](#) (University of Siena, Italy); [Francesco Caminita](#) (Wave-Up SRL, Italy); [Roberto Giusto](#) (Huawei Technologies, Italy); [Matteo Albani](#) (University of Siena, Italy)

An analytical model of a dielectric-wall conical horn antenna is developed in order to characterise its radiation characteristics. An approximate model analysis is formulated in a semi infinite conical geometry in order to calculate the modes supported by the structure. It is proven that the desired hybrid HE11 mode is excited that allows the hollow dielectric cone to perform as an antenna with high directivity, low sidelobe levels, good polarisation purity and very stable phase center in a wide frequency range. This study will allow us to define the design criteria for conical dielectric-wall horn antennas which can effectively replace metallic corrugated horns as reflector feeds in the millimeter wave band. Numerical results and design examples will be shown during the conference.

CP2.24 Ray-tracing in Dielectric Inhomogeneous Metalenses

[Francesca Maggiorelli](#) and [Matteo Albani](#) (University of Siena, Italy); [Roberto Giusto](#) (Huawei Technologies, Italy); [Stefano Maci](#) (University of Siena, Italy)

We present a very fast and efficient analysis of inhomogeneous dielectric lenses based on Geometrical Optics (GO) ray-tracing. The ray-tracing algorithm has been implemented in a Matlab code in order to overcome time-consuming full-wave simulations in the analysis and synthesis of inhomogeneous lens-antennas. Phase and amplitude distributions at the output interface of a generic inhomogeneous dielectric lens can be obtained by solving the eikonal and the energy transport equations, respectively. Once the field distribution at the lens-antenna aperture has been achieved, the radiation pattern, is derived by aperture type radiation integral. The developed algorithm has been validated by full-wave analysis, after predetermining the feed source, the lens dimensions and the refractive index profile. Thus, the source incident field in absence of lens is supposed to be known by simulation or by measurements. Results achieved by the homemade algorithm and the full-wave analysis have shown to be in good agreement.

CP2.25 Dielectric Rectangular Lens for Antenna Array Scanloss Mitigation

[Giorgio Gottardi](#) and [Alessandro Polo](#) (ELEDIA Research Center, University of Trento, Italy); [Giacomo Oliveri](#) (University of Trento & ELEDIA Research Center, Italy); [Andrea Massa](#) (University of Trento, Italy)

Wide scan-angle antenna arrays are of fundamental importance for nowadays and future communications. In this paper, an innovative iterative procedure based on the System-by-Design paradigm is applied for designing rectangular-shaped lenses to be integrated in suitably weighted array structures to minimize the scan-loss of resulting radiating system so that the antenna scan-range turns out to be significantly extended. A preliminary numerical design example is reported to give some insights on the potentialities of the proposed approach.

CP2.26 Study of Printed Scattering Reflectors Based on Discretised Metasurface

[Michal Cerveny](#), [Kenneth Lee Ford](#) and [Alan Tennant](#) (University of Sheffield, United Kingdom (Great Britain))

In this paper, metasurface synthesis for plane wave to plane wave scattering was studied from the practical perspective. The study was focused on the design of discretised surfaces that do not conform to standard specular scattering behaviour as described by Snells law but allow to reflect wavefronts to prescribed directions. The results of the synthesis were compared with full-wave simulations and measurements. Furthermore, the design was adopted for testing of a textile metasurface manufactured by an electroplating process. The practical design requirements are presented.

CP2.27 Latest Developments on Non-linear and Time-varying Metasurfaces and Topological Antennas

[Davide Ramaccia](#) (RomaTre University, Italy); [Mirko Barbuto](#) and [Alessio Monti](#) (Niccolò Cusano University, Italy); [Stefano Vellucci](#) (Roma Tre University, Italy); [Angelica Viola Marini](#) (Università degli Studi Roma Tre, Italy); [Alessandro Toscano](#) (University Roma Tre (IT), Italy); [Filiberto Bilotti](#) (University Roma Tre, Italy)

In this contribution, we present the latest developments from our group on metasurfaces for antenna applications. In particular, we present the properties and a possible implementation of non-linear and time-varying metasurfaces: the first one have been used for conceiving power-dependent and waveform-dependent mantle cloaks for antennas, allowing them to become invisible/visible to an electromagnetic wave depending on the power level or waveform of the incident wave, respectively; the second one allows to realize Doppler mantle cloaking, which can vanish the Doppler frequency shift due to the motion of the antenna system. Finally, we present the design of patch antennas with reconfigurable radiation characteristics exploiting the position of the phase singularities of vortex fields.

Convened Poster 2-CS61: Signal Processing Techniques for Advanced Electromagnetics Synthesis, Analysis, and Measurements

T10 EM modelling and simulation tools / Convened Session / Antennas

Room: [A2 \(Poster Area\)](#)

Chairs: [Nicola Anselmi](#) (University of Trento, Italy), [Marco Donald Migliore](#) (University of Cassino, Italy)

CP2.28 Multiband Patch Antenna Design for RF Energy Harvesting Applications Using Coyote Optimization Algorithm

[Achilles D. Boursianis](#), [Dimitrios Georgoulas](#), [Maria Papadopoulou](#) and [Apostolia Karampatea](#) (Aristotle University of Thessaloniki, Greece); [Juliano Pierezan](#) (Universidade Federal do Paraná - UFPR, Brazil); [Leandro dos Santos Coelho](#) (Pontifical Catholic University of Parana & Federal University of Parana, Brazil); [Viviana Mariani](#) (Pontificia Universidade Católica do Paraná & Universidade Federal do Paraná, Brazil); [Katherine Siakavara](#) and [Sotirios Goudos](#) (Aristotle University of Thessaloniki, Greece)

Radio frequency energy harvesting is a relatively recent and quite interesting technique for delivering adequate amounts of energy in low power consumption wireless networks. This technique faces several challenges, with most of them are related to the antenna design of the harvesting system. In this paper, we address to these challenges by designing a multiband microstrip patch antenna with three slits. The proposed antenna operates in the LoRaWAN (Long Range Wide Area Network) and the cellular (GSM-1800 and UMTS) communication frequency bands. Numerical results demonstrate a satisfactory performance of the proposed patch antenna as an energy harvester in radio frequency environments.

CP2.29 Synthesis of Sparse Linear Arrays Including Directivity via a Hybrid L1 Minimization Algorithm

Feng Yang (University of Electronic Science and Technology of China & University of Electronic Science and Technology of China (UESTC), China); [Shiwen Yang](#) (University of Electronic Science and Technology of China (UESTC), China); [Yikai Chen](#) (University of Electronic Science and Technology of China, China); [Paolo Rocca](#) (University of Trento, Italy)

A hybrid l1 minimization algorithm with enhanced sparsity is proposed for the synthesis of sparse linear arrays. Moreover, the desired directivity as a constraint condition for a fixed scanning range is included in the hybrid algorithm in order to obtain a better pattern. In particular, the proposed hybrid algorithm can be divided into two steps. The first step is to iteratively solve a smooth-weighted l1 minimization problem. The obtained weight vector is then considered as the initial weight vector in the second step, where a weighted l1 minimization problem is solved. In comparison to other methods, simulation results show that the proposed method has an improved synthesis efficiency for sparse arrays.

CP2.30 Efficient and Effective Synthesis of Large Arrays for 5G and Beyond

[Daniele Pinchera](#) (University of Cassino, Italy); [Fulvio Schettino](#) (Università degli Studi di Cassino, Italy); [Mario Lucido](#) (University of Cassino and Southern Lazio, Italy); [Marco Donald Migliore](#) (University of Cassino, Italy)

In this contribution we will discuss the synthesis of very large arrays, that are going to become a key technology of 5G and beyond communication systems. By means of a slightly improved version of IDEA (Inflating Deflating Exploration Algorithm), we demonstrate the ability to synthesize very sparse arrays, with a strong reduction of the number of control points with respect to a classical equispaced array radiating a beam with the same specifications.

CP2.31 Shannon and Kolmogorov in Space Communication Channels

[Marco Donald Migliore](#) (University of Cassino, Italy)

The aim of this paper is to discuss an asymmetry between the space-channel and the time-channel in wireless space-time communication systems and its consequence when we use Shannon and Kolmogorov theory to evaluate the amount of information transmissible along a space channel. It is also shown that the use of unbounded "Massive Antenna" radiating systems restore, at least theoretically, the symmetry between space and time.

CP2.32 The Sparsity and Incoherence in Compressive Sensing as Applied to Field Reconstruction

[Baozhu Li](#) (Nanjing Normal University, China); [Marco Salucci](#) (ELEDIA Research Center, Italy); [Paolo Rocca](#) (University of Trento, Italy); [James Ben](#) and [Wanchun Tang](#) (Nanjing Normal University, China)

Compressive Sensing (CS) opens up new perspectives for field reconstruction. Electromagnetic far field can be reconstructed by CS from a reduced number of samples when no prior knowledge of the radiating source is available with large probability as long as two constraints are satisfied, that is sparsity and incoherence. A set of representative numerical examples considering different sampling strategy and different recover algorithms is reported and discussed to demonstrate that when CS condition holds true, a perfect reconstruction with large probability is guaranteed.

CP2.33 Tools for the Efficient Implementation of the DBIM Algorithm in Microwave Imaging Experiments

[Pan Lu](#) (King's College London, United Kingdom (Great Britain)); [Juan Córcoles](#) (Universidad Autónoma de Madrid, Spain); [Panagiotis Kosmas](#) (King's College London, United Kingdom (Great Britain))

We present two efficient tools to improve both the experimental data and the reconstruction results in microwave imaging. The time-gating technique can remove part of the unexpected reflections of the cables and tanks, thus improving the quality of the received signals obtained from the experiment system. We also apply the fast iterative shrinkage thresholding algorithm (FISTA) to the distorted Born iterative method (DBIM) as a linear inverse solver at each iteration of the DBIM, which shows better capabilities than the conventional conjugate gradient least squares (CGLS) method with experimental data. Results confirm that the two tools used in the DBIM can be efficient and accurate when employed in the microwave imaging system.

CP2.34 Direction of Clutter Estimation by Total-Variation Compressive Sensing

[Mohammad Hannan](#) and [Alessandro Polo](#) (ELEDIA Research Center, University of Trento, Italy); [Paolo Rocca](#) (University of Trento, Italy)

The problem of estimating the direction of clutter (DoC) is reformulated as a problem of estimating the directions of many closely spaced signals (DoAs). These signals may or may not be sparse in the discrete angular domain but they are exploited as sparse in the total-variation sense. Therefore, the sparseness is exploited in the gradient domain and the Total-Variation Compressive Sensing (TV-CS) is adopted to estimate efficiently the DoC or DoAs of many closely spaced signals. Selected results from an extensive analysis are reported in this paper, which suggests the potentialities of the proposed method at different noisy conditions for single snapshot data.

Poster2-A01: Antenna Theory

Antennas

Room: Exhibition Hall

P2.001 Three-Element End-Fire Linear Arrays (Super) Directivity and Gain Optimization

[Alexandre Debard](#) (University of Grenoble Alpes & CEA-LETI, France); [Antonio Clemente](#) (CEA-LETI Minatec, France); [Christophe Delaveaud](#) (CEA-LETI, France)

This paper presents the results of the optimization of two three-element end-fire linear arrays based on straight- and bent-electrical dipoles, respectively. To achieve a compact architecture, the inter-element distance is fixed to 0.12λ , while λ is the wavelength calculated at the operation frequency (850 MHz). The array complex excitation coefficients have been optimized to achieve maximum directivity or gain. The synthesis procedure is based on the optimization of the directivity and gain formulas considering the array factor and the active element patterns. The numerical results have been validated by 3D full-wave electromagnetic simulations. The maximum directivity is equal to 10.0 (gain 2.91 dBi) and 9.83 dBi (gain 3.67 dBi) in the case of straight- and bent-electrical-dipole based arrays, respectively. Instead, the maximum gain is equal to 6.81 (directivity 8.84 dBi) and 7.85 dBi (directivity 9.19 dBi), respectively.

P2.002 A Miniaturized Circularly Polarized Antenna Using a Meandered Folded-Shorted Patch Array for CubeSats

[Yuepei Li](#) (Heriot Watt University, United Kingdom (Great Britain)); [Symon K. Podilchak](#) (Heriot-Watt University, United Kingdom (Great Britain)); [Dimitris E. Anagnostou](#) (Heriot Watt University, United Kingdom (Great Britain))

The design and operation of a miniaturized antenna array offering circularly polarized (CP) radiation for CubeSats and other micro-satellites is presented. The proposed antenna array combines folded-shorter patches (FSPs) and meandering for antenna miniaturization. Both techniques enable a decrease of the quarter wavelength shorter patch while maintaining a quarter wavelength resonant length. Realization of CP is achieved by an ultra-compact and planar feed circuit consisting of a network of meander-shaped 90° and 180° hybrid couplers, providing quadrature feeding of the FSP elements and for integration onto the backside of the antenna ground plane whose physical dimension is only 9 cm x 9 cm. Good CP performances are observed for the developed UHF-band antenna and with an antenna size of $0.135\lambda \times 0.135\lambda$ considering the 450 MHz design frequency.

P2.003 A Broadband Transition from Microstrip to Groove Gap Waveguide for Ka-Band Applications

[Davood Zarifi](#) and [Atefe Ashrafi](#) (University of Kashan, Iran)

This paper describes a wideband and low-loss microstrip to groove gap waveguide transition for millimeter wave applications. The microstrip mode is effectively transformed into the groove gap waveguide (GGW) mode by means of a slot-line. The simulation results of the transition show an insertion loss of 0.3 dB and a return loss less than 20 dB over 42.5% relative bandwidth from 26 to 40 GHz.

P2.004 Closed Form Characterization of Mutual Coupling in Uniform Linear Arrays

[Grzegorz Wolosinski](#) (Huawei Munich Research Center, Germany); [Harsh Tataria](#) (Lund University, Sweden); [Vincent Fusco](#) (Queen's University Belfast, United Kingdom (Great Britain))

This paper proposes a pragmatic methodology to characterize mutual coupling in uniform linear arrays (ULAs). The classical coupling model used in the literature of multiple input multiple output (MIMO) antenna arrays is based on impedance parameters, resulting valid only for electromagnetically small antennas, e.g. short dipole. To test the robustness and accuracy of the proposed coupling model we consider ULAs with different antenna types and number of elements. We provide closed form expressions for the mutual coupling characterization of the studied ULAs, which are then used to evaluate the spectral efficiency performance of a MIMO cellular system. Our results show that the proposed method can provide more accurate characterization of the studied mutually coupled ULAs and hence better estimation of the spectral efficiency in comparison to the classical method.

P2.005 Approximating the Directivities of Antenna Elements and Arrays

[Maor Mordehai](#) (HIT-Holon Institute of Technology, Israel); [Maor Kadosh](#) (HIT, Israel); [Ely Levine](#) (AFEKA, Academic College of Engineering, Israel); [Haim Matzner](#) (HIT-Holon Institute of Technology, Israel)

The directivities of antenna elements and arrays (no mutual coupling included) is discussed. Replacing the directivity of the simulated or measured element pattern by a continuous function is needed here in order to improve the approximation of the directivity of the arrays. Two kinds of arrays are treated: a dipole array and a microstrip array. It is shown that the proposed method, based on the definition of the directivity, is more accurate than the simple formula based on the sum (in dB) of the directivity of the element and the directivity of the array factor (AF). Moreover, we show that the deviation of the directivity calculated by the proposed method from the simulated directivity is less than 0.5 dB.

P2.006 Double-Layer Machine Learning Assisted Optimization for Antenna Sensitivity Analysis

[Qi Wu](#), [Haiming Wang](#) and [Wei Hong](#) (Southeast University, China)

A double-layer machine-learning assisted optimization (DL-MLAO) method for antenna sensitivity analysis (SA) is proposed. The machine-learning (ML) method is introduced to largely alleviate the computation burden of both worst case searching (WCS) and maximum input tolerance searching (MITS) in antenna robust design. First, the MLAO is introduced in the fundamental layer to accelerate the WCS for given input antenna design tolerance. Then, based on the improved WCS process, another MLAO process is introduced to operate MITS for given output antenna design tolerance efficiently. The proposed DL-MLAO is compared with the previously reported antenna SA methods, which shows its superior in both robustness and accuracy.

P2.007 Exact Derivation of the Radiation Law of Antennas Embedded into Generic Nonlocal Metamaterials: A Momentum-Space Approach

[Said Mikki](#) (University of New Haven, USA)

We solve the problem of how antennas radiate into generic nonlocal metamaterials by using a momentum-space formalism to rigorously derive the general radiation formula. The energy per Hertz by unit solid angle is computed by first deriving the dyadic Green's function of nonlocal media in the momentum space. We show that due to causality only the antihermitian part of the dyad will contribute to the radiation field. We avoid any spectral integration or using the Poynting vector (the latter known to be already inadequate in nonlocal media) by working directly with momentum space formulation and derive analytically the exact expression. The final result depends only on the modal analysis of the metamaterial.

P2.008 A New Feed Network for the Communication Signal and Excitation of Surface-Wave-Driven Plasma Antennas

[Fateme Sadeghikia](#), [Ali K. Horestani](#), [Mohammad reza Dorbin](#) and [Mahmoud Talafi Noghani](#) (Aerospace Research Institute, Iran); [Hajar Ja'afar](#) (Universiti Teknologi MARA, Malaysia)

This paper proposes a novel structure for a surface-wave-driven plasma monopole antenna to simplify the antenna structure and also to improve the antenna performance. The proposed configuration allows both communication signal and excitation wave to be applied to a single coupling sleeve on the plasma column. As a result, the plasma conductivity at the communication signal point is maximized. On that bases, a plasma monopole antenna is designed to be excited by 1500 MHz RF signal source with a controllable power level between 1 and 100 watts to adjust the effective length of the antenna.

P2.009 Beamwidth Control of a Helical Antenna Using Truncated Conical Plasma Reflectors

[Mahsa Valipour](#), [Fateme Sadeghikia](#) and [Ali K. Horestani](#) (Aerospace Research Institute, Iran); [Mohamed Himdi](#) (Université de Rennes 1, France)

This paper presents an approach to simultaneous beamwidth and gain control in a circular polarization helical antenna using a truncated conical plasma reflector. Requirements and trade-offs regarding the feasible structure of this antenna are discussed. The antenna operation is confirmed by full-wave simulations. The results show that the proposed plasma reflector can be used to improve the radiation gain of the considered helical antenna up to around 17%.

Poster2-A02: Antenna Interactions and Coupling

Antennas

Room: Exhibition Hall

P2.010 Antenna Mutual Coupling Effects in Highly Integrated Transmitter Arrays

[Wan-Chun Liao](#) (Chalmers University of Technology, Sweden); [Rob Maaskant](#) (CHALMERS, Sweden); [Thomas Emanuelsson](#) (Gapwaves AB, Sweden); [Artem Vilenskiy](#) (Samsung Research Institute Russia, Russia); [Marianna Ivashina](#) (Chalmers University of Technology, Sweden)

An antenna S-parameter re-normalization procedure is proposed to obtain a new set of scattering parameters that directly quantifies the actual coupling and reflection coefficients of power waves in highly integrated antenna systems employing unequal port terminations. We examine both the inter-element coupling between the radiator and the active circuitry as well as the element-to-element coupling in an antenna array and discuss the important differences with the more customary 50-Ohm S-parameters.

P2.011 A Method of Reducing Mutual Coupling for a Finite Array

[Lei Chen](#) and [Tianling Zhang](#) (Xidian University, China); [Ashraf Uz Zaman](#) and [Jian Yang](#) (Chalmers University of Technology, Sweden)

A method of reducing mutual coupling for a finite array with the characteristics of wideband and beam steering is presented in this paper. By adding an extra decoupling network, the mutual coupling can be efficiently suppressed for the antenna array. To verify the validity of the proposed method, a 1 × 8 millimeter-wave array antenna based on the gap waveguide technology is used in this work. The simulation results show that the active reflection coefficients are improved from -6.98 dB to -8.29dB, and the mutual coupling between adjacent elements is reduced to below -16.73 dB covering 20-33 GHz with the beam steering angle range of ±70°.

P2.012 Antenna Adaptation Circuits for High Data Rate Magneto Inductive Underwater Communications

[Thierry Deschamps de Paillette](#) (University of La Rochelle, France); [Alain Gaugue](#) (La Rochelle University, France)

Environmental and aquaculture monitoring in seawater use standalone and robust underwater sensor networks to properly and regularly harvest useful data. The need of submarine images transmissions in real time require higher data rate. In this paper we introduce an innovative prototype of reliable magneto-induction based wireless submarine communication system adapted to a medium-range underwater telemetry application matching those requirements.

P2.013 Mechanically Influenced Antennas for Strain Sensing Applications Using Multiphysics Modelling

[Shaghayegh Soltani](#), [Paul Taylor](#) and [John Batchelor](#) (University of Kent, United Kingdom (Great Britain))

Here we report highly flexible 3D antennas which leverage nonlinear compressive buckling to tune their operating frequency through 0 to 30% uniaxial or biaxial stretch /release of their elastomeric substrate. The proposed 3D designs are straightforward to fabricate compared to the existing direct 3D fabrication routes which makes them promising for strain sensing applications. By utilizing a soft silicone substrate and structural design of the conventional metallic materials, we have demonstrated two designs of 3D stretchable antennas: "Popup convoluted loop antenna" and "Popup multilayer dipole antenna". Multiphysics simulation using FEA method is used to analyze the antenna models and the numerical results are in a good correlation with measurements.

P2.014 Wireless Link for Micro-scale Biomedical Implants Using Magnetolectric Antennas

[Fazel Rangriz](#) (NTNU, Norway); [Ali Khaleghi](#) (Norwegian University of Science and Technology (NTNU) & Oslo University Hospital, Norway); [Ilangko Balasingham](#) (NTNU, Norway)

Miniaturization of implant antennas without significant performance degradation is of great interest for future medical devices. Systems operating at low frequencies are preferred in wireless implant technology because the tissues' losses increase with frequency and the device's power consumption is lesser in the low-frequency range. The extremely small antennas face significant performance degradation in terms of efficiency, impedance matching and have a very high-quality factor that makes the antenna susceptible to the surrounded medium and electronics. Considering the impedance of a micro-scale antenna in sub-GHz frequency, the antenna performs like a short circuit or open circuit, and it is almost impossible to match the antenna to a standard source impedance for communication or wireless power transfer. To achieve a realistic micro-scale antenna, the magnetolectric (ME) antenna is a promising option.

P2.015 Multi-ring Circular Parasitic Antenna with Circularly Polarized Conical Beam and High Gain

[Niyonzima Laetitia](#) (Université Catholique de Louvain, Belgium); [Donia Oueslati](#) (ICTEAM Institute, Université Catholique de Louvain, Belgium); [Christophe Craeye](#) (Université Catholique de Louvain, Belgium)

The design of a 3D multi-ring circular parasitic antenna with circular polarization and conical patterns excited by a center monopole is presented. Such antennas are specifically well-suited to conical patterns with grazing angles. Two rings bearing respectively 8 and 16 parasitic elements are located at distances allowing minimal radiation from the vertical parts of the parasitic elements. The simulation results show that after limited optimization efforts, and for an elevation angle of 40°, we can reach a minimum gain of 7.7 dB against a maximum gain of 7.9 dB with 2 rings in circular polarization for an axial ratio below 3 dB.

P2.016 Antennas on CubeSat Platforms: Accurate RF Predictions

[Cecilia Cappellin](#), [Mustafa Murat Bilgic](#), [Jakob Rosenkrantz de Lasson](#) and [Oscar Borries](#) (TICRA, Denmark)

A typical 3U and 6U CubeSat hosting antennas ranging from the low UHF to the higher Ka band are modelled in the ESTEAM software package. The antennas are inspired by recent designs published in the literature. RF performances of the antennas installed on the CubeSats are computed with the MoM/MLFMM full wave analysis method and compared with the ones in the absence of the CubeSat platform. The results show that the RF performances of the antennas are substantially changed once these are installed on the CubeSats, indicating that platform scattering and coupling with the neighboring antennas must be included and accounted for already in the antenna design phase.

P2.017 Power Transfer Efficiency Analyzed Using Characteristic Mode Coupling Between Two Parallel Loops

[Ferdaous Abderrazak](#) (ITEAM-UPV, Spain); [Eva Antonino-Daviu](#) and [Miguel Ferrando-Bataller](#) (Universitat Politècnica de València, Spain)

Independently of any electrical contact, running electronic devices such as smartphones, smart watches, RFID tags etc., is now attainable over small and large distances through Wireless Power Transfer technology. Although, designing systems maintaining appreciable power transfer efficiency still not always achievable. Using two parallel loops, the Theory of Characteristic Modes provide physical insight into the power transfer efficiency. Furthermore, to reach straightforward maximization of the modal power transfer efficiency, the focus of this paper is analyzing the impact of the separation distance and the overlapping between the two antennas on the characteristic modes and their contribution in the total efficiency of the power. The study considers different positions and frequencies of the two parallel antennas.

P2.018 Preliminary Analysis of the Effects of the Ground Plane on the Element Patterns of SKA1-Low

[Pietro Bolli](#) (INAF - Osservatorio Astrofisico di Arcetri, Italy); [Mirko Bercigli](#) (IDS Ingegneria Dei Sistemi S. p. A, Italy); [Paola Di Ninni](#) (OAA - INAF, Italy); [Maria Grazia Labate](#) (SKA Organisation, United Kingdom (Great Britain)); [Giuseppe Virone](#) (Consiglio Nazionale delle Ricerche, Italy)

Each station of the SKA1-Low radio telescope is composed by 256 dual-polarized log-periodic antennas deployed over a metallic ground plane with 42 m diameter. This station is usually modelled in EM simulators by considering an infinite ground plane, which drastically reduces the computational time. This contribution shows that a finite ground plane can bring to quite significant differences in some embedded element patterns with respect to the infinite ground plane case. Furthermore, we show the impact on the antenna pattern of different dielectric media surrounding the finite ground plane. For instance, at 50 MHz the antenna gain decreases by 5% maximum due to the ohmic loss considered in the terrain.

Poster2-A04: Mm-, Sub-mm-wave, and Nano-optical Antennas

Antennas

Room: Exhibition Hall

P2.019 Uplink Design of Millimeter Wave Based Moving Network System

[Dae-Soon Cho](#) (ETRI, Korea (South))

In this paper, we introduce a millimeter wave band based Moving Network (MN) System. Especially, the structure, design and performance of MN system uplink channels are described. MN system is being developed with a view to support very high speed public Wi-Fi in public transportation, especially in a bus, which uses FACS frequency band (22~23.6GHz) that is supported by Korean government for the public purpose. Both V2I link and V2V link use this frequency band. Total data transmission rate of base station is maximum 6Gbps and the maximum 1Gbps level of data rate can be supported for one vehicle. Beam switching is one of main features and relay function is also major feature in MN system. Beam switching can be a good solution in case that a bus changes the lane, and relay function can be applied when the received mmWave signal is blocked by road sign or another vehicle.

P2.020 Characterizing 60 GHz Patch Antenna Segments for Fully Digital Transceiver

[Jaakko Haarla](#) (Aalto University School of Electrical Engineering, Finland); [Vasilii Semkin](#) (VTT Technical Research Centre of Finland, Finland); [Kai Zheng](#) and [Aditya Dhananjay](#) (NYU, USA); [Marco Mezzavilla](#) (NYU Tandon School of Engineering, USA); [Juha Ala-Laurinaho](#) (Aalto University, Finland); [Ville Viikari](#) (Aalto University & School of Electrical Engineering, Finland)

In this work, we present the simulation and measurement results of patch antenna elements operating at 60 GHz for future integration with fully digital transceiver. The antennas are fabricated on Rogers 4350B substrate of 168 μm thickness and their radiation patterns are measured both in the anechoic chamber and planar near-field range. In addition, different types of transmission lines are designed and fabricated. Results for both patch antennas and transmission lines show rather good agreement between simulation and measurements. The measured -10 dB bandwidth of single element is 1.76 GHz around center frequency of 60.3 GHz. In the future, 1x4 patch antenna array will be integrated with the four channel software-defined radio.

P2.021 High-gain Resonant Continuous Transverse Stub Array Using Ridge Gap-Waveguide Technology

[Javier Benavides-Vazquez](#), [Jose-Luis Vazquez-Roy](#) and [Eva Rajo-Iglesias](#) (University Carlos III of Madrid, Spain)

This work presents an 8 x 8 continuous transverse stub (CTS) planar array operating at Ka-band with a pencil broadside beam in a series-feed configuration. For the purpose of maximizing the directivity of the antenna, ridge gap-waveguide (GWG) and short CTS elements are used. The ridge waveguides excite the stubs placed above them and a proper selection of the geometry and the dielectric leads to a close-to-uniform field distribution in both main planes. A beamforming network implemented in ridge-GWG technology is also designed and described. A maximum gain of 26.3 dBi is obtained for an antenna whose radiating area is 6.87 x 7.67 (free-space wavelengths) keeping side lobes level below -13 dB in both main planes. Some other simulation results will be shown to prove the potential of the proposed design.

P2.022 A Gap Waveguide Fed Circular Polarization Antennas in the Millimeter Wave Range

[Dayan Pérez](#) (Public University of Navarra (UPNA) & Institute of Smart Cities (ISC), Spain); [Alicia E. Torres-García](#) (Public University of Navarra, Spain); [Iñigo Ederra](#) (Universidad Pública de Navarra & Institute of Smart Cities, Universidad Pública de Navarra, Spain); [Miguel Beruete](#) (Universidad Publica de Navarra, Spain)

In this work, a novel way to generate circular polarization (CP) using gap waveguide (GW) technology in an antenna, is studied. The antennas are fed from the bottom with a WR-15 waveguide (V-band), which couples the wave to the RGW system, working in the millimeter-wave band (60 GHz). CP is generated in a simple and effective way, by means of two orthogonal feeder arms that excite a CP in a diamond-shaped slot on top. Parametric simulation studies demonstrate that a difference between both arms length of approximately $\lambda/4$ leads to high-purity CP within a relatively broad bandwidth. A diamond-shaped slot antenna is manufactured and experimentally analyzed. A broadband matching with a reflection coefficient magnitude below -10 dB ($S_{11} < -10$ dB) is achieved from 60.5 to 69.3 GHz. Applying the axial ratio criterion ($AR < 3$ dB) the bandwidth in CP is 10.74 %, with respect to the central frequency.

P2.023 Design of Compact H-plane SIW Antenna at Ka Band

[Cleofás Segura-Gómez](#) and [Angel Palomares-Caballero](#) (Universidad de Granada, Spain); [Antonio Alex-Amor](#) (Technical University of Madrid, Spain); [Juan Valenzuela-Valdés](#) (Universidad de Granada, Spain); [Pablo Padilla](#) (University of Granada, Spain)

This paper presents the compact design of a substrate-integrated waveguide (SIW) antenna based on H-plane aperture structure. The antenna is composed by a coaxial feeding and an aperture. In this aperture inner metallic vias are introduced acting as partially detached walls in order to form 4 adjacent subapertures at the end of the aperture antenna. Thus, the field from the feeding is divided in different wavefronts that are composed at the antenna aperture to get an endfire radiation. In this manner, a flatter wavefront is generated to achieve high directivity. Additionally, some periodic parallel strips are printed after antenna aperture to improve the impedance matching with the air. The proposed antenna has impedance matching below -10 dB from 34 to 36 GHz with nearly constant gain between 13 and 15 dBi. A prototype is manufactured to validate the proposed antenna design.

P2.024 Trapped Microstrip-Ridge Gap Waveguide for Standalone Millimeter Wave Structures

[Amir Arayeshnia](#) (Imam Khomeini International University, Iran); [Ali Araghi](#) (University of Surrey, United Kingdom (Great Britain)); [Mohsen Khalily](#) (University of Surrey & 5G Innovation Centre, Institute for Communication Systems (ICS), United Kingdom (Great Britain)); [Pei Xiao](#) and [Rahim Tafazolli](#) (University of Surrey, United Kingdom (Great Britain))

This paper presents a novel design of trapped microstrip-ridge gap waveguide by using partially filled air gaps in a conventional microstrip-ridge gap waveguide. The proposed method offers an applicable solution to obviate frustrating assembly processes for standalone high-frequency circuits employing the low temperature co-fired ceramics technology which supports buried cavities. To show the practicality of the proposed approach, propagation characteristics of both trapped microstrip and microstrip-ridge gap waveguide are compared first. Then, a right-angle bend is introduced, followed by designing a power divider. These components are used to feed a linear 4-element array antenna. The bandwidth of the proposed array is 13 GHz from 64~76 GHz and provides the realized gain of over 10 dBi and the total efficiency of about 80% throughout the operational band. The antenna is an appropriate candidate for upper bands of WiGig (63.72~70.2) and FCC-approved 70 GHz band (71~76 GHz) applications.

P2.025 A Multiple-Feed Connected Leaky Slot Antenna for In-Antenna Power Combining in 0.13Um SiGe BiCMOS Technology

[Jiangcheng Chen](#) and [Shihai He](#) (University of Oulu, Finland); [Markus Berg](#) (University of Oulu & Excellant Ltd., Finland); [Aarno Pärssinen](#) (University of Oulu, Finland)

In this paper, a differentially-driven wideband multiple-feed on-chip antenna design in 0.13 μm SiGe technology is proposed for millimeter-wave power combining. The in-antenna power combining concept is achieved by combining parallel amplifiers in the multi-port radiator where each port corresponds directly to a differential power amplifier (PA) stage. Specifically, the radiator is composed of a leaky slot with multiple differential microstrip feed lines. In addition, the differential PA has a combined output power of 10 dBm and its output is directly connected with the balun. Consequently, the proposed multiple-feed antenna has four differential microstrip feed lines connected with four Marchand baluns driven by four parallel differential PAs respectively. Also, to compensate for the loss, pre-amplification PA stage is a necessity. An extended hemispherical silicon lens is used to suppress the substrate modes. Simulations results show that the antenna has over 50 % fractional bandwidth and calculated EIRP is 15dBm.

P2.026 Millimeter-Wave Wide Scan Beam Steering 5G MIMO Antenna Array in Mobile Terminals

[Mohammad Mehdi Samadi Taheri](#) and [Abdolali Abdipour](#) (Amirkabir University of Technology, Iran); [Shuai Zhang](#) and [Gert Pedersen](#) (Aalborg University, Denmark)

In this paper, multiple-input multiple-output (MIMO) millimeter-wave wide scan beam 5G antenna array for 28 GHz application in the mobile terminals is presented. The MIMO antennas operate in 25-30 GHz in the end-fire direction. The antenna array composed of eight-element tapered tilted dipole antennas. The proposed antenna array can scan the beam in a wide coverage region from ± 80 degrees in wide operating bandwidth with scan loss better than 3 dB. The antenna coverage efficiency is better than 94 %, 78%, and 52 % for minimum realized gain of 0, 5, and 8 dBi respectively. The antenna has a good impedance matching ($S_{11} < -10$ dB) and mutual coupling better than -28 dB in whole operating frequency bands from 25-30 GHz.

P2.027 Practical Low-Loss Substrate-Integrated-Waveguide Feed Network for mm-Wave PCB Antenna Designs

[James R Henderson](#) and [Marcus C Walden](#) (Plextek, United Kingdom (Great Britain))

This paper discusses a novel SIW feed network which demonstrates a substantial reduction in the insertion loss of SIW at V band (50-75 GHz). More than 30 dB improvement was achieved in the loss-per-unit length compared with that for same-width SIW on a thin substrate. This design technique targets multilayer PCBs that carry both mm-wave electronic devices and planar antennas and is particularly beneficial for designs that feature electrically-large, high-gain mm-wave antennas, including those with a corporate-feed network synthesized in SIW.

P2.028 A V-Band Low Sidelobe Cavity-Backed Slot Array Antenna Based on Gap Waveguide

[Davood Zarifi](#) (University of Kashan, Iran); [Ali Farahbakhsh](#) (Graduate University of Advanced Technology, Iran); [Ashraf Uz Zaman](#) (Chalmers University of Technology, Sweden)

A cavity-backed slot antenna array element is designed to operate in V-band with low sidelobe level (SLL). The 2×4 element array is fed by a groove gap waveguide (GGW) cavity in the bottom layer. Simulated results indicate that the array element can achieve a 7.4% bandwidth (59.7-64.3 GHz) with a gain of more than 16.5 dBi. Besides, the low SLL characteristic is achieved and the simulated first SLLs are below -20 dB across the desired working band.

P2.029 Polarization-Reconfigurable Patch Antenna-on-Package for Millimeter-Wave Operations with DC Bias Circuit Design

[Hsinju Chen](#) and [Shih-Yuan Chen](#) (National Taiwan University, Taiwan)

The proposed polarization-reconfigurable antenna is designed for implementation on IC packaging. For verification, we used Rogers R04003C boards which closely resembles the material of PCB with packaging. Our prototype swaps out the switchable PIN diode with copper strip and is measured using a styrofoam rotation platform. With DC block and RF choke present in the design, the measurement results show that the design achieves 3-dB axial ratio with sub-6 dB reflection coefficient at 30 GHz.

P2.030 Magneto-Electric Dipole Antenna for 5-G Applications

[Giuseppe Scalise](#) and [Luigi Boccia](#) (University of Calabria, Italy); [G. Amendola](#) (Universita della Calabria, Italy); [Mohadig Rousstia](#) and [Alireza Shamsafar](#) (Ampleon Netherlands BV, The Netherlands)

Magneto Electric (ME) dipoles have been widely studied over the last few years. They are becoming increasingly popular as they allow to generate a wide bandwidth in a printed circuit board (PCB). Nevertheless, their principle of operation requires the use of relatively thick substrates (i.e. about $0.25\lambda_0$, where λ_0 is the free-space wavelength) thus resulting in a bulky stack-up. This work tackles this problem by proposing a new type of low-profile ME dipole. The proposed configuration is fed using a slot-coupled microstrip line feed and it employs bandwidth enhancement solutions previously used in metal-only structures. As a result, an ultrathin antenna is achieved which operates over a 20% bandwidth at Ka-band while using an ultrathin dielectric layer being the antenna thickness equal to $0.082\lambda_0$. Moreover, the antenna has a gain of about 5.5 dBi across the entire bandwidth, which makes the proposed design suitable for next generation 5G base stations.

P2.031 High-gain and Low-profile Dielectric Cuboid Antenna at J-band

[Yuto Samura](#) and [Kazuki Yamada](#) (Gifu, Japan); [Oleg Vladilenovich Minin](#) (National Research Tomsk State University, Russia); [Atsushi Kanno](#) (National Institute of Information and Communications Technology, Japan); [Norihiro Sekine](#) (National Institute for Information and Communications Technology, Japan); [Junichi Nakajima](#) (Softbank, Japan); [Igor Vladilenovich Minin](#) (Siberian State Academy of Geodesy, Russia); [Shintaro Hisatake](#) (Gifu University, Japan)

We demonstrate a high-gain and low-profile dielectric cuboid antenna (DCA) at J-band for terahertz (THz) wireless communication applications. The developed DCA is made of polytetrafluoroethylene (PTFE) and can be connected to a standard waveguide (WR-3.4). The structure is very simple, and the size is in mesoscopic scale; $1.36\lambda \times 1.36\lambda \times 1.79\lambda$ (1.36 mm × 1.36 mm × 1.79 mm for 300 GHz). The simulated antenna gain of the DCA was 15.5 dBi. We characterized the DCA at 300 GHz based on the near-field electro-optic sensing technique and far-field transformation. The measured full width at half maximum were 23° and 24° for E-plane and H-plane, respectively, showing good agreement with simulated value.

P2.032 A Series-fed High-Gain Gap Waveguide Planar Array Antenna Fed by Quasi-TEM Wave

[Tianling Zhang](#) and [Lei Chen](#) (Xidian University, China); [Ashraf Uz Zaman](#) and [Jian Yang](#) (Chalmers University of Technology, Sweden)

A series-fed high-gain gap waveguide planar array antenna is presented in this paper. The element is a corporate-fed long slot pair which is series-fed by the quasi-TEM wave in the oversized rectangular gap waveguide. Using the methods of the quasi-TEM wave and series-fed concept, the proposed array antenna achieves a simple structure, low profile and high gain. The proposed array antenna is designed based on the gap waveguide technology, which makes it possible to simplify the assembly and fabrication tolerances. The simulated results show that the antenna achieves a good performance of high gain and high efficiency at Ka-band.

P2.033 A 16×16-Element Single-Layer Full-Corporate-Fed SIW Slot Array Antenna

[Miao Zhang](#) and [Baoquan Duan](#) (Xiamen University, China); [Jiro Hirokawa](#) (Tokyo Institute of Technology, Japan); [Qing Huo Liu](#) (Duke University, USA); [Guan-Long Huang](#) (Shenzhen University, China)

A single-layer corporate-fed substrate integrated waveguide slot array is newly proposed. Since every radiating slot is individually connected to one of the output ports of the corporate feeding circuit, the low-sidelobe antenna with a low profile can be easily realized without grating lobes. A 16×16-element slot array is designed by HFSS and is fabricated by the standard processes for the PCB and milling. Good agreement between the simulated and the measured directivity and radiation pattern has been observed. The aperture efficiency higher than 80% is achieved over the frequency ranging from 57 to 66 GHz. The antenna performance has been verified.

P2.034 Broadband Dual-Polarized Stacked Microstrip Antenna with Pin- And Edge-Fed for 5G Applications in Ka-Band

[Karina Schneider](#) (Karlsruhe Institute of Technology, Germany); [Sören Marahrens](#) (Karlsruhe Institute of Technology (KIT), Germany); [Joerg Eisenbeis](#) and [Jerzy Kowalewski](#) (Karlsruhe Institute of Technology, Germany); [Thomas Zwick](#) (Karlsruhe Institute of Technology (KIT), Germany)

This paper introduces concept, simulation and measurement results for a broadband dual-polarized stacked microstrip antenna with pin- and edge-feed for 5G applications in Ka-band. The design approaches take several requirements into account that are decisively for next generation 5G base stations. Dual-polarization for doubling link capacity, a large bandwidth for high data throughput as well as array compatibility are main issues. Especially the combination of these requirements makes the antenna design fastidiously. Techniques for bandwidth enhancement and dual-polarized feeding are elucidated. The realization is carried out in standard multilayer printed circuit board technology. The proof-of-concept shows that both antenna types reach measured -10 dB relative bandwidths between 12.8% and 16.4% with measured gains in mainbeam direction between 6.3 dBi and 7.1 dBi at 28 GHz.

P2.035 Switched Beam Lens Antennas Fed with Magneto-Electric Dipoles

[Qian Zhu](#) (Huawei Technologies Co., Ltd., China); [Jingjing Huang](#) (Huawei Technologies Co. Ltd., China); [Rui Ni](#) (Huawei Technologies Co Ltd, China); [Mengyao Ma](#) (Huawei Technologies Co., Ltd., China)

Two switched beam antennas fed with Magneto-Electric (ME) dipole elements are introduced. Depending on the arrangement of the feeding elements, beam steering in 1D or 2D can be realized. The ME dipole feed covers a wide bandwidth of 30.8%. Moreover, both lens antennas fully cover the 60 GHz frequency band, from 57 to 64 GHz. It can be used for AR/VR services that require high data rate and ultra-low latency.

P2.036 Design of Efficient Photomixer-based Terahertz Dielectric Resonator Antenna

[Xiaohang Li](#) (University of Sheffield, United Kingdom (Great Britain)); [Wenfei Yin](#) (The University of Sheffield, United Kingdom (Great Britain)); [Salam Khamas](#) (University of Sheffield, United Kingdom (Great Britain))

A dipole-fed photomixer based THz dielectric resonator antenna (DRA) has been truncated from an electrically Gallium Arsenide (GaAs) substrate. The photomixer is supported by a low temperature GaAs substrate with two dimensional photonic crystal (2D-PhC) and optical superstrate that maximize the optical power absorption. As a result, the optical-to-THz power conversion has been improved by a factor of 256. Additionally, a THz dielectric superstrate has been employed above the DRA, which results in an overall antenna gain of 10dBi and an input resistance of 436Ω. Consequently, the radiated THz power from the proposed DRA has improved substantially due to the improved optical-to-THz power conversion and enhanced matching and radiation efficiencies.

P2.037 Axicon-hyperbolic Lens for Reflectivity Measurements of Curved Surfaces

[Aleksi Tamminen](#), [Samu-Ville Pälli](#) and [Juha Ala-Laurinaho](#) (Aalto University, Finland); [Mika Salkola](#) (Icare Finland Oy, Finland); [Antti V. Räsänen](#) and [Zachary D Taylor](#) (Aalto University, Finland)

We present a quasioptical element design that transforms a diverging Gaussian beam to an approximate Bessel beam. The elements are designed to deliver millimeter waves to a curved surface in reflectivity measurements. Compared to canonical focused quasioptical designs, such as the Gaussian-beam telescope, diffraction from an axicon surface allows for significant relaxation in alignment requirements. This research is motivated by in vivo cornea measurements where achieving optimal optical alignment is difficult. Combined axicon-hyperbolic lenses were designed for 220-330 GHz and fabricated of TOPAS, a low-loss material at millimeter waves. The lens performance is evaluated with near-field measurements. Compared to the Gaussian beam, the in-range alignment requirement can be relaxed by an order of magnitude with the Bessel beam.

P2.038 Wideband Tapered Slot Antenna for D-Band Applications

[Yunfeng Dong](#), [Arsen Turhaner](#), [Vitaliy Zhurbenko](#) and [Tom Johansen](#) (Technical University of Denmark, Denmark)

This paper presents a wideband tapered slot antenna for D-band (110-170 GHz) applications. The antenna is fed by a substrate integrated waveguide (SIW) and achieves a simulated gain of 11.1 dBi at 170 GHz. The in-band gain variation is less than 3 dB. The designed SIW is based on a thin aluminium nitride (AlN) substrate with hollow plated vias working as the vertical conductor walls. The substrate is extended and inserted into a tapered slot antenna. The concept of designing SIW-fed tapered slot antenna is described in detail. The assembly structure is illustrated and the antenna radiation pattern is shown. The proposed SIW-fed tapered slot antenna also provides a wideband matching at D-band. The simulated return loss remains better than 18 dB from 110 GHz to 170 GHz which corresponds to a bandwidth of 43% at 140 GHz.

P2.039 Dual Circularly Polarized Waveguide Array Antenna Formed by Full-Metallic Bow-tie Radiating Cavities

[Eduardo Garcia-Marin](#) (Universidad Autonoma de Madrid, Spain); [Pablo Sanchez-Olivares](#) (Universidad Politecnica de Madrid, Spain); [Jose Luis Masa-Campos](#) (Universidad Autonoma de Madrid, Spain); [Jorge A Ruiz-Cruz](#) (Universidad Autonoma de Madrid & Escuela Politecnica Superior, Spain); [Javier Herranz-Alpanseque](#) (RFCAS, Spain)

A full-metallic dual circularly polarized antenna based on an array of bow-tie shaped radiating elements is presented in this contribution. The radiating element, formed by a bow-tie shaped cavity, can generate dual circular polarization. It is fed by a square waveguide path that supports the two degenerate modes TE10 and TE01. The excitation of the TE10 mode in the input port generates left-hand circular polarization while the TE01 mode generates right-hand circular polarization. Furthermore, a dual circularly polarized array antenna formed by bow-tie radiating elements has been designed. The two degenerate modes TE10 and TE01 are supported by a four-way feeding network implemented in square waveguide technology. Both the single radiating element and the dual circularly polarized array have been fabricated by CNC milling techniques. A pure circular polarization performance, high gain or high efficiency have been obtained, experimentally validating the dual circularly polarized bow-tie element in an array configuration.

P2.040 Circularly Polarized Conical Beam Antenna with Stable 3dB Axial Ratio Beamwidth

[Junxiang Yang](#) and [Shi-Shan Qi](#) (Nanjing University of Science and Technology, China); [Wen Wu](#) (Nanjing University of Science & Technology, China)

A new geometry is proposed for an antenna producing circularly polarized (CP) conical beam with wide 3 dB axial ratio (AR) beamwidth. A coaxial-line waveguide 8-way power divider has been employed to feed eight helices. The symmetrically placed helices around the sphere control the circular polarization purity. The locations, dimensions, and spin angles of the helices are tuned to achieve wide 3-dB AR beamwidth. The simulated results show that the proposed antenna achieves an impedance bandwidth of 16.6% from 32.1 GHz to 37.9 GHz with the gain no less than 6.36 dBi at 30°, and 3dB AR beamwidth steadily covers from 1° to 58° over the bandwidth. The proposed antenna has a compact

size of 11mm×11mm×8.2mm, which will be useful in satellite communication applications.

P2.041 Improved Equivalent Norton Circuit for Pulsed Photoconductive Antennas

[Andrea Degasperi](#), [Arturo Fiorellini Bernardis](#), [Andrea Neto](#) and [Nuria L.Lombart](#) (Delft University of Technology, The Netherlands)

A revised version of the Norton equivalent circuit proposed in [1] is presented in order to describe more accurately the saturation at high optical powers. The revised model relies on an improved characterization of the generator impedance, now approximately one order of magnitude lower than the previous one and comparable to the impedance of the bow-tie antenna. The model is validated with a full wave simulation of the photoconductive antenna (PCA) in CST MWS. The proposed simulations are discussed in details and are presented as a new tool in literature to model PCAs.

P2.042 Circular-Polarization Mushroom EBG Antenna Module for 122 GHz Monostatic Radar Sensor in LTCC Technology

[Akanksha Bhutani](#) (Karlsruhe Institute of Technology, Germany); [Sören Marahrens](#) (Karlsruhe Institute of Technology (KIT), Germany); [Benjamin Göttel](#) (Wellenzahl Radar- und Sensortechnik GmbH & Co KG, Germany); [Thomas Zwick](#) (Karlsruhe Institute of Technology (KIT), Germany)

This paper presents a circular-polarization Mushroom electromagnetic bandgap (EBG) antenna module for realizing a 122 GHz monostatic radar sensor. The module consists of an aperture-coupled Mushroom EBG antenna, a novel stripline patch quadrature hybrid and two stripline-to-grounded coplanar waveguide signal transitions. The quadrature hybrid provides two orthogonal stripline feeds to the Mushroom EBG antenna, thus generating circular-polarization radiation characteristics. The module is designed and fabricated in low temperature co-fired ceramic technology. Simulation results of the novel quadrature hybrid demonstrate an amplitude imbalance less than 1.5 dB and a phase imbalance less than +/- 5 degree over a broadband operating range of 110 to 155 GHz. Simulation and probe-based measurement results of the antenna module demonstrate that the reflection coefficients, isolation between the transmitter and receiver paths, the radiation patterns and the axial ratio are suitable for realizing a 122 GHz monostatic radar sensor.

Poster2-A08: Electrically Small Antennas

Antennas

Room: Exhibition Hall

P2.043 Miniaturized On-Chip Meandered Loop Antenna with Improved Gain Using Partially Shield Layer

[Harshavardhan Singh](#) and [Sujit Kumar Mandal](#) (National Institute of Technology, Durgapur, India)

This work presents the design of a miniaturized on-chip meandered loop antenna (OCMLA) with improved gain characteristics at 11 GHz. A standard CMOS technology with low resistive Si wafer ($\rho=10 \Omega \cdot \text{cm}$) is considered for simulation and fabrication of design. The meandered loop miniaturization technique applied for enhancing the electrical length of antenna and achieving a miniaturization up to $\lambda/15.11$ with dimension of $2.1 \times 2 \text{ mm}^2$. The introduction of partially shield layer (PSL) layer below the top radiating layer in between the SiO₂ in OCMLA provides the gain enhancement of +4 dBi by reducing EM wave propagation toward the substrate. The proposed antenna shows a gain and bandwidth of -29.2 dB and 250 MHz respectively. Also, the simulated and measured results of OCMLA are showing very good agreement and has been presented successfully. The characteristics proposed OCMLA makes it appropriate candidate for short and ultra-short range communication SoC devices.

P2.044 Remote Characterization of Small Antennas Using Waveguide

[Hamed Hasani](#) (Sivantos GmbH, Germany)

A new method is introduced for remote (i.e. cable-less, indirect) estimation of radiation efficiency and input impedance of electrically small antennas (ESA) by placing them inside a rectangular waveguide with dominant TE₁₀ mode. The estimation is carried out using the scattered field from ESA when it is terminated with three different impedances. Input impedance and radiation efficiency are then calculated using the obtained complex scattering values. In addition, the paper discusses the relationship between the obtained ESA parameters inside the waveguide to those in free-space. The method has been verified by simulations on two different ESAs in the frequency range of 2 to 3 GHz.

P2.045 Compact Circularly Polarized E-Shaped Crossed-Dipole Antenna

[Kam Kedze](#) (Ajou University, Korea (South)); [Youngwook Kim](#) (California State University, Fresno, USA); [Ikmo Park](#) (Ajou University, Korea (South))

This study proposes a circularly polarized (CP) compact E-shaped crossed-dipole antenna comprising two printed crossed-dipole arms and a pair of vacant quarter printed rings. The design goals are attained through the rotation and folding of the arms of the conventional crossed-dipole antenna to achieve a miniaturized CP antenna. A compact antenna is designed by rotating half of the crossed dipole by 90° and folding its arms to form a small E-shaped antenna that generates CP radiation with satisfactory performance. The performance of the proposed antenna is discussed and confirmed both numerically and experimentally. This antenna has overall dimensions of 26.8 mm × 30.6 mm × 0.508 mm ($0.28\lambda_0 \times 0.32\lambda_0 \times 0.0055\lambda_0$ at 3.22 GHz), a measured $|S_{11}| < -10 \text{ dB}$ impedance bandwidth of 2.75-3.6 GHz (26.77%), and a simulated 3-dB axial ratio bandwidth of 3.0-3.45 GHz (13.95%).

P2.046 Effect of the Ground Plane in UHF Chip Antenna Efficiency

[Jaime Molins-Benlliure](#) (Universitat Politècnica de València & ITEAM, Spain); [Marta Cabedo-Fabrés](#) (Universidad Politécnica de Valencia, Spain); [Eva Antonino-Daviu](#) and [Miguel Ferrando-Bataller](#) (Universitat Politècnica de València, Spain)

A study on the effect of the ground plane in a chip antenna efficiency is presented. For the experiment, a chip antenna has been designed to be fabricated in LTCC technology. The size of the ground plane, the clearance area where the antenna is placed and the position of the antenna has been analyzed obtaining their impact in the radiation properties of the antenna. Useful information has been obtained for the design and implementation of small antennas for sub-1GHz application such as ISM bands(868 MHz Eur, and 915 MHz USA) or the new licensed sub-1GHz 5G bands.

P2.047 A Very Compact Implantable Antenna for Wireless Biotelemetry Applications in the MedRadio Band

[Tomer Paley](#) (School of Electrical and Electronic Engineering, Israel); [Guy Lasri](#) (Faculty of Engineering, Holon Institute of Technology, Israel); [Benjamin Milgrom](#) (University of Connecticut, USA); [Motti Haridim](#) (Holon Institute of Technology, Israel)

A very compact implantable monopole using a nullifier is presented. The nullifier is a voltage zeroing circuit that can replace the monopole's ground plane without degrading its performances. Miniaturization is achieved by partial meandering of the antenna structure. Using this approach, an implantable monopole was designed to have a minimal size and cover the Medical Device Radio communications Service band (MedRadio, 401-406 MHz). The simulation and experimental results show that the proposed antenna can achieve a realized gain of approximately -20 dBi with a small volume of 12.6 mm³.

P2.048 Compact Circular Polarized Antenna for Multi-band Operation

[Sarrah Jemmel](#) (University of Limoges, France); [Laure Huitema](#) (Xlim Laboratory, France); [Thierry Monediere](#) (XLIM-University of Limoges, France)

In the present communication, we present a miniature, multi-band and circular polarized patch antenna based on ferrite material. The main properties of ferrites are presented with an highlight on their anisotropic behavior and their non-reciprocal character allowing the generation of circular polarized antenna operating over several frequency bands. A further challenge of downsizing the antenna's dimensions is also proposed. Good performances in terms of impedance matching, axial-ratio and radiation efficiency are demonstrated.

P2.049 Compact UHF Printed Antennas for Nano-Satellites

[Juner M. Vieira](#) (Aeronautics Institute of Technology, Brazil); [Rodrigo Facco](#) (Federal University of Pampa, Brazil); [Marcos V. T. Heckler](#) (Universidade Federal do Pampa, Brazil)

This paper presents the application of miniaturization techniques to UHF printed antennas designed for installation onto 8-U nano-satellites. The first structure studied is a rectangular dielectric resonator antenna and the second one is a compact reactive loaded slot antenna. Both radiators are used to compose four-element planar arrays. The analyzed topologies are compared, whereby the array composed of slot antennas yielded the lighter solution with good electromagnetic performance.

P2.050 Circularly Polarized Electrically Small Antenna Using Chiral Metamaterials and Based on Characteristic Modes Theory

[Nadia Kari](#) (Universite Paris Est, ESYCOM & FSTTAR, COSYS, LEOST, France); [Divitha Seetharamdoo](#) (IFSTTAR, LEOST & Univ Lille Nord de France, France); [Jean-Marc Laheurte](#) (Université Paris-Est-Marne-la-Vallée, France); [Francois Sarrazin](#) (University of Paris-Est-Marne-la-Vallée & ESYCOM, France)

This paper presents a novel circularly polarized electrically small antenna that has been designed thanks to the Characteristic Mode Analysis. It is based on the energy compensation between two elements: a non-resonant dipole antenna and a chiral Metamaterial in order to achieve a Circular Polarization. First, the two elements are analyzed separately using CMA to analyze the physical behavior of both structures. Then, the intermodal coupling between the dipole and the MTM is studied between the modes to propose a better understanding of the net stored energy compensation. The coupling between the two structures is through the magnetic and electric modes and it thus increases the overall efficiency. Circular polarization of the antenna is obtained through the chirality properties of the helix. The proposed antenna resonates at 2.35 GHz. The radiation pattern of the antenna is omnidirectional with a fair axial ratio for a circularly polarised antenna

P2.051 A Novel Design Methodology for Non-Foster Elements with Application in Broadband Self-oscillating Antennas

[Bair Buiantuev](#) (St. Petersburg Electrotechnical University LETI, Russia); [Leo Vincelj](#) (University of Zagreb, Croatia); [Dmitry Kholodnyak](#) (Saint Petersburg Electrotechnical University LETI, Russia); [Silvio Hrabar](#) (University of Zagreb, Croatia)

Non-Foster elements are electronic circuits with inverse dispersion properties comparing to ordinary reactive elements. The evolution of their design is mostly related to antenna matching applications. Moreover, recent introduction of self-oscillating non-Foster antenna has motivated the negation of a complex impedance via negative impedance converter (NIC). This negation is affected by NIC conversion error, which is dependent on both load Q-factor and NIC properties. Here, we propose a novel method for design of Linvill's NIC, based on its decomposition into passive and active building blocks. Proposed approach is verified by analysis of Linvill's NIC for recently investigated self-oscillating non-Foster antenna.

Poster2-A10: Slotted-waveguide and Leaky-wave Antennas

Antennas

Room: Exhibition Hall

P2.052 The Slotted Waveguide Array Antenna with Reflection Canceling Stairs in Millimeter Waveband

[Wenbo Liu](#) (Graduate School of Engineering, Takushoku University, Japan); [Yasuhiro Tsunemitsu](#) (Takushoku University, Japan)

We propose and design 38-GHz slotted waveguide antenna with reflection canceling stairs to improve aperture efficiency. The waveguide includes 10 linearly arranged slots and 9 stairs. From the Finite Element Method (FEM) calculation, length and offset of each slot are optimized to obtain uniform radiation intensity. Then the corresponding stair position and height are designed to suppress the reflection. The simulation of the full model confirms that aperture efficiency is improved to 64.9%.

P2.053 Electronic Beam Scanning Leaky-Wave Antenna Based on Delta Shape Half-Mode Substrate Integrated Waveguide

[Nima Javanbakht](#), [Barry Syrett](#) and [Rony E. Amaya](#) (Carleton University, Canada); [Jafar Shaker](#) (Communications Research Centre Canada, Canada)

A novel reconfigurable leaky-wave antenna is presented in this paper. The proposed antenna is based on a half-mode substrate integrated waveguide. The beam-steering is achieved using novel cells. The effective surface impedance can be changed by configuring the cells. Sweeping the bias voltage causes variation of the phase constant which leads to electronic beam-scanning. The operating frequency is chosen as 28.5 GHz in the support of upcoming 5G communications systems. The length, width, and height of the antenna are 67 mm, 45 mm, and 0.3 mm, respectively. To achieve an optimal response, cells are located in the delta configuration. Electronic beam-scanning capability, compactness, and high gain of the proposed antenna make it a suitable candidate for future 5G wireless networks.

P2.054 Quasi-Periodic Leaky-Wave Antenna Based on Substrate Integrated Waveguide and Liquid Crystal Technologies

[Anastasis C Polycarpou](#) (University of Nicosia, Cyprus)

A quasi-periodic leaky-wave antenna (LWA) based on substrate integrated waveguide (SIW) and liquid crystal (LC) technologies is presented in this paper for single-frequency dynamic beam steering. The antenna works based on the fundamental space harmonic ($n=0$) in the frequency band from 10.2~GHz to 12.5~GHz. A very thin layer of nematic LC cell is placed underneath the substrate, which is then biased with an external electric field. The dielectric properties of the LC are controlled by the strength of the bias electric field. As a result, the main beam of the antenna pattern is deflected by an angle which depends on the bias voltage. The angular scanning range depends on the dielectric anisotropy of the LC compound and the substrate-to-LC thickness ratio. Simulation results based on the ANSYS HFSS commercial software are used in order to numerically verify the design concept.

P2.055 Design of an Array of Stacked Groove Gap Waveguide Leaky-Wave Antennas in the Ka Band

[Nafsika Memeletzoglou](#) and [Eva Rajo-Iglesias](#) (University Carlos III of Madrid, Spain)

In this paper, the design of an array of leaky-wave antennas in groove gap waveguide technology is developed. The array is formed by stacking leaky-wave antennas one on top of the other. The design of the array consists on the investigation of the number of elements to be stacked, and the inter-element distance to avoid grating lobes and to obtain high directivity levels. The feeding of the array is done through the design of a vertical coupler. Phase shifters placed after the feeding network, ensure that all the elements radiate in-phase, aiming to achieve maximum directivity. The central frequency of the design is 28 GHz, and the array of four elements, achieves an enhancement of +5 dB, reaching 24.5 dB of directivity, in comparison to 19.6 dB of directivity of the single leaky-wave antenna made in this technology. The proposed design was validated experimentally with a prototype.

P2.056 A Novel Circularly-Polarized T-shaped Slot Array Antenna in Ka-band

[Miguel Ferrando-Rocher](#) (Universitat Politècnica de València, Spain); [José Ignacio Herranz-Herruzo](#) (Universidad Politècnica de Valencia, Spain); [Daniel Sánchez-Escuderos](#) (Universitat Politècnica de València, Spain); [Alejandro Valero-Nogueira](#) (Universidad Politècnica de Valencia, Spain)

A T-shaped slot-array antenna fed through a Groove Gap Waveguide (GGW) is presented in this paper. The array antenna operates at 30 GHz. The way the slots are excited, along with the T-shape on its lid allows a compact single-layer architecture. A uniform linear array of 12 elements is designed to demonstrate the viability of this concept for high-efficient single-layer slot-array antennas. Preliminary results show a frequency bandwidth of 1~GHz with an input reflection coefficient better than -12 dB. In addition, being a full-metal antenna, the expected efficiency is high. It is worth stressing the good polarization purity achieved, being below 1.5~dB within the band of interest.

P2.057 A Low-Profile Millimeter-Wave Circularly-Polarized Multilayer Waveguide Antenna Array for Satellite Communication Application

[Hong-Tao Zhang](#) (NO. 38 Research Institute of CETC, China); [Wei Wang](#) (No. 38 Research Institute of CETC, China); [Guan-Long Huang](#) (Shenzhen University, China); [Yongqing Zou](#) (East China Research Institute of Electronic Engineering (ECRIEE), China)

A low-profile circularly-polarized multilayer waveguide antenna array operating in Ka-band is proposed. The antenna array is also characterized for low axial ratio (AR), high-efficiency and wide operating bandwidth. To achieve a wide operating bandwidth from 29.4 GHz to 31.0 GHz and improve the AR, sequential rotation technique is utilized. The complete array is composed of five aluminum layers firmly brazed with each other. Each layer is manufactured by using the computer numerical control (CNC) milling machine. Experimental results demonstrate that a desired bandwidth with VSWR and AR less than 1.6 and 2 dB respectively have been realized with high radiation gain. The proposed antenna array is an excellent candidate for advanced satellite communication (Satcom).

P2.058 Practical Design of Radiating Part of Post-Wall Waveguide-Fed Parallel Plate Slot Array Antenna by Method of Moments

[Koh Hashimoto](#) and [Makoto Higaki](#) (Toshiba Corporation, Japan)

A practical design of a radiating part of a post-wall waveguide-fed parallel plate slot array antenna is presented. The radiating part of the antenna is a parallel plate waveguide with an array of radiating slot pairs. The slot pairs are designed by the method of moments (MoM). In the MoM analysis, unknown equivalent magnetic currents on slot apertures are expanded with entire-domain sinusoidal basis functions. The dependence of accuracy and computation time on the number of basis functions is evaluated. The MoM with an appropriate number of basis functions enables accurate and fast analyses. As an example, an efficient design of an array consisting of 21 slot pairs in the longitudinal direction of the parallel plate waveguide is demonstrated.

Poster2-E02: EM Theory and Analytical Techniques

Electromagnetics

Room: Exhibition Hall

P2.059 Target Feature Extraction in Narrowband Mode

[Xiaochuan Wu](#) (Harbin Institute of Technology, China)

Pole is an important feature of radar target recognition in resonance region, and it is not sensitive to attitude. However, the pole extraction requires time-domain late response or frequency-domain response (i.e. radar cross section, RCS) of the broadband signal, which is difficult to meet in the actual system. In this paper, a method of pole extraction based on sparse representation is proposed, which can obtain the pole characteristics of the target by fewer RCS in the narrowband mode. It is of great significance to the target classification and identification in resonant region.

P2.060 Proposal on Hybrid Propagation Analysis of Aperture Field Integration Method and Ray Tracing Method Suitable for Airport Surface in VHF Band

[Satoshi Kuroda](#) and [Ryosuke Suga](#) (Aoyama Gakuin University, Japan); [Atsushi Kezuka](#) (Electronic Navigation Research Institute, MPAT, National R&D Agency, Japan); [Osamu Hashimoto](#) (Aoyama Gakuin University, Japan)

A hybrid propagation analysis method of ray-tracing method and aperture-field-integration method for airport surface is proposed. Its effectiveness was evaluated by measurements using a 1/50 scaled model. As a result, the simulated power distribution by the proposed method agreed with the measured one.

P2.061 Volume Integral Equation Formulation for Electromagnetic Scattering by Highly Inhomogeneous Anisotropic Cylinders

[Konstantinos Katsinos](#), [Grigorios Zouros](#) and [John Roumeliotis](#) (National Technical University of Athens, Greece)

In this work we report a volume integral equation formulation for the electromagnetic scattering by highly inhomogeneous anisotropic circular cylinders under normal incidence. The development of the method is based on a vectorized formalism which exploits the cylindrical vector wave functions and allows for the simultaneous treatment of both transverse electric (TE) and transverse magnetic (TM) incidence. The cylindrical vector wave functions employed in this work form entire domain basis vector functions which are constructed so as to guarantee orthogonal relations in the circular domain of anisotropy. The method is validated with the exact solution for single and double layered isotropic cylinders, for both TE and TM incidence, as well as with the commercial HFSS software for anisotropic permittivity profiles. Numerical results are given for various values of the parameters.

P2.062 Evaluating the RCS Contribution of Geometrical Singularities: An Analytical Model

[Alexandre Corazza](#) and [Pascal Pagani](#) (CEA - CESTA, France); [Sylvain Morvan](#) (CEA-DAM & Centre des Etudes Scientifiques et Techniques Aquitaine, France)

In the context of radar detection, the assessment of Radar Cross Section (RCS) requires computing the scattered electromagnetic field using numerical solvers. In order to study the potential contribution of geometrical singularities to the object's RCS, we propose an analytical model, applicable to Perfect Electric Conductors (PEC) in the case of Bodies of

Revolution (BOR). The method based on physical optics is valid for small profile variations in the object's illuminated region. The proposed model is validated for a circumferential slot. Further, the proposed approach can be extended to a statistical description of the geometry variation. As an illustration, the RCS contribution of a random surface roughness is evaluated.

Poster2-E03: Computational and Numerical Techniques

Electromagnetics

Room: Exhibition Hall

P2.063 General Formulation of the Boundary Element Method (BEM) for Curvilinear Metasurfaces in the Presence of Multiple Scattering Objects

[Tom Smy](#), [Jacob Connor](#), [Scott Stewart](#) and [Shulabh Gupta](#) (Carleton University, Canada)

This paper presents a general formulation for determining the scattered Electromagnetic fields present for a multi-surface configuration of curvilinear interfaces comprised of metasurfaces, dielectrics and perfect conductors. The method uses a Boundary Element Method (BEM) formulation of the frequency domain version of Maxwell's equations, where the general metasurface boundaries are represented in terms of surface susceptibilities which are then integrated within the BEM using the Generalized Sheet Transition Conditions (GSTCs). These curvilinear surfaces are next described by parametric equations allowing for an elegant formulation for geometrically complex systems. The proposed method is then demonstrated using a numerical example.

P2.064 Gradient-induced Heating of a Metallic Hip Implant in Magnetic Resonance Imaging

[Alessandro Arduino](#), [Oriano Bottauscio](#), [Mario Chiampi](#) and [Luca Zilberti](#) (INRIM, Italy)

This work focuses on the evaluation, via numerical simulations, of the energy deposited by MRI switched gradient fields in bulky metallic implants and the consequent temperature increase in the surrounding tissues. An original computational strategy allows describing realistically the evolution of the phenomena produced by the gradient coils fed according to any imaging sequence. Pennes' bioheat equation is solved through a Douglas-Gunn time split scheme to compute the time-dependent temperature increase. The heating generated inside the body of a patient with a unilateral hip implant when undergoing an Echo Planar Imaging sequence is evaluated and the role of the parameters affecting the thermal results (body position, coil performing the frequency encoding, effects of thermoregulation) is discussed. The results show that the gradient coils can generate local increases of temperature up to some kelvin. Hence, their contribution in general should not be disregarded when evaluating patients' safety.

P2.065 Model Simplification and Validation of Virtual Prototypes for Vehicular Antenna Design

[Irfan Yousaf](#) (Lunds University & Volvo Cars Corporation, Sweden); [Kranti Kumar Katare](#) (IIT Kanpur, India); [Buon Kiong Lau](#) (Lund University, Sweden)

Wireless connectivity is becoming an important feature in cars, which together with recent developments in car design point to the need to accurately predict the performance of real antennas in simulation, to speed up the design cycle. However, it is challenging to accurately represent structurally complex real cars in simulation. This paper proposes a car model simplification approach for designing vehicular antennas, exemplified using three progressively simplified models of a hatchback car. For validation, a monopole and a PIFA operating at 800 MHz and 2.4 GHz, respectively, were mounted and simulated at two locations on these prototypes. The proposed scheme reduced the computational time to less than a third, while maintaining similar simulated antenna performance. Specifically, the antenna patterns of the simplest prototype and original one are correlated by 84% and 59% at 800 MHz and 2.4 GHz, respectively. Therefore, the proposed scheme is promising for real application.

P2.066 Integral Equation Formulation for Planar Plasmonic Nano Structures in Layered Media

[Esraa Mahdy](#) (Cairo University, Faculty of Engineering, Egypt); [Alaa Abdelmageed](#) (Cairo University, Egypt); [Ezzeldin Soliman](#) (The American University in Cairo, Egypt)

In this work, an integral equation formulation for planar plasmonic structures in layered media is developed. First, closed-form spatial domain Green's functions are obtained using the discrete complex images method. Then, the boundary conditions along the localized plasmonic structures are applied and written in the form of an integral equation. Finally, the Method of Moments (MoM) is applied where the integral equation is transformed into a matrix equation, which is solved using traditional matrix routines. The developed solver is applied on a square patch nano antenna fed with a plasmonic transmission line. Its accuracy is compared with CST microwave studio and a very good agreement between the results is observed. The proposed solver has a number of appealing features such as the small number of unknowns and the absence of truncation boundaries, which makes it suitable for nano antennas.

P2.067 Impact of Parameters Variability on the Performances of an Implanted Antenna for Biomedical Applications

[Shuoliang Ding](#) (GeePs & CentraleSupélec, France); [Yao Pei](#) (University Paris-sud, France); [Lionel Pichon](#) (Group of Electrical Engineering Paris, Université Paris-Saclay & GeePs Laboratory, France); [Stavros Koulouridis](#) (University of Patras, Greece)

In this work, non-intrusive stochastic techniques are combined with 3D modeling in order to build adequate surrogate models for the evaluation of performances of a transmission link for biomedical applications. A surrogate model is appropriate to deal with uncertainties and variabilities of parameters defining the electromagnetic problem. Numerical results obtained in case of a realistic configuration involving an external patch antenna and an embedded antenna illustrate the proposed methodology.

P2.068 Application of non-PEC Walled Mode-Matching Techniques to a Prototype SAFARI M-band Multi-Mode Receiver

[Joseph Brennan](#) (Maynooth University, Ireland); [Marcin Gradziel](#) (National University of Ireland, Maynooth, Ireland); [Neil Trappe](#) (NUI Maynooth, Ireland); [Peter Ade](#) (Cardiff University, United Kingdom (Great Britain))

An extension of the traditional mode-matching methods to consider non-PEC boundary walls is presented. These non-PEC boundary walls consider mechanisms for loss which are generally not included in the analysis of guide structures. In particular, these losses manifest themselves more significantly in multi-moded structures, as field distributions for increasing azimuthal order modes are localised to a greater extent at the boundary walls. This lossy mode-matching method is applied to a prototype M-band horn for the proposed SAFARI system. Here we attempt reconcile the measurement data with simulation results by considering the surface impedance of the guide walls due to the finite conductivity and surface roughness from the manufacturing process.

P2.069 Neural Network Approach for Dielectric Characterization of Tissues in Microwave Frequencies Using Coplanar Waveguide Transmission

[Viktor Mattsson](#) (Uppsala University, Sweden); [Mauricio D Perez](#) (Uppsala University, Sweden & National Technological University, Argentina); [Dario Dematties](#) (Universidad de Buenos Aires, Sweden); [Robin Augustine](#) (Uppsala University, Sweden)

This paper presents an extension to previous work, using neural networks to characterize materials in microwave frequencies, to extend the applicability of a deep learning model to be able to characterize the dielectric properties of biological tissues. A neural network model using convolutional and fully connected layers is designed to predict the permittivity and loss tangent using the scattering parameters from a coplanar waveguide transmission sensor. Simulated data from the sensor provide a large dataset, with a wide range of values for the permittivity and loss tangent, which is used to train and test the model. The trained network is validated by predicting the output parameters on the test set. Compared with previous work, by using convolutional layers the applicable parameter space is vastly extended while keeping satisfying levels of accuracy. A complete system with a trained network is proposed to be used in a lab or in clinics.

P2.070 Feeding Positions Providing the Lowest TARC of Uncorrelated Channels

[Michal Masek](#) (Czech Technical University in Prague & MECAS ESI s.r.o., Pilsen, Czech Republic); [Miloslav Capek](#) and [Lukas Jelinek](#) (Czech Technical University in Prague, Czech Republic)

In this paper, point group theory is utilized for the simultaneous block-diagonalization of all linear operators representing the underlying symmetrical structure. This procedure is utilized for designing orthogonal channels suitable, for example, for MIMO systems. Within these uncorrelated channels, the total active reflection coefficient is further formulated within the method of moments framework and is used to find position of feeders that provide orthogonal channels with maximum radiation.

P2.071 PML Effectiveness in the Transmission Line Modelling Method for Radiation and Scattering Applications

[Jomiloju Odeyemi](#), [Chris Smartt](#), [Ana Vukovic](#), [Trevor Benson](#) and [Phillip Sewell](#) (University of Nottingham, United Kingdom (Great Britain))

This paper demonstrates the effectiveness of the recently introduced, stable, perfectly matched layer (PML) for the Transmission Line Modelling (TLM) method. The superiority of the new PML over the TLM matched boundary is demonstrated by application to electromagnetic scattering and radiation simulations.

P2.072 Effects of Common Approximations in the Modeling of a Liquid-Crystal-Based Patch Antenna: A Numerical Investigation

[Nectarios Papanicolaou](#), [Anastasis C Polycarpou](#) and [Marios Christou](#) (University of Nicosia, Cyprus)

Liquid crystal compounds are increasingly used as tunable materials for a plethora of microwave and millimeter-wave devices. Liquid crystal modeling mandates the solution of the directors' field under an external electric field, governed by the Oseen-Frank free-energy functional. Its minimization results in a nonlinear partial differential equation which is often simplified by applying the one-constant approximation, where the splay and bend elastic constants are set equal to each other. The effects of this approximation on the radiation characteristics of a microstrip patch antenna built on top of a liquid-crystal substrate are not well-studied. Here, we adopt this approximation, along with neglecting the off-diagonal entries of the corresponding dielectric tensor, and compare the results with the original model. The reduced model results in a more computationally efficient algorithm for the characterization of liquid crystal materials; however, there are substantial discrepancies in the simulated antenna figures of merit for intermediate bias voltages.

P2.073 Hybrid MoM/T-Matrix Method for Analysis of Interaction Between Objects

[Vit Losenicky](#), [Miloslav Capek](#) and [Lukas Jelinek](#) (Czech Technical University in Prague, Czech Republic); [Mats Gustafsson](#) (Lund University, Sweden)

A hybrid method for analysis of an interaction between electromagnetic scatterers is introduced. The method connects the method of moments and T-matrix method and represents a promising candidate capable of solving problems associated with 5G or antennas close to the human body. Two specific cases of the mutual position of the objects are shown. Preliminary results are demonstrated on two examples. The advantages and limitations of the method are discussed.

P2.074 A Parallelized Fast Array Analysis Approach

[Danie Ludick](#) and [Tameez Ebrahim](#) (Stellenbosch University, South Africa)

In this work, a hybrid distributed/shared memory parallelization scheme is presented for the domain green's function method (DGFM). The DGFM is a domain decomposition based computational electromagnetics (CEM) method used for analyzing large disjoint antenna arrays. The array configurations considered consists of identical elements, with regular or irregular array layouts. The hybrid MPI/OpenMP parallelization strategy introduced in this work offers satisfactory speedup performance. This allows for the simulation of large array geometries in a distributed computing environment.

P2.075 Accuracy and Modeling Improvements for an Integral Equation Framework Applied to Thin Layer Microstrip and Substrate Integrated Waveguide (SIW) Structures

[Thomas Vaupel](#) (Fraunhofer FHR, Germany)

For the analysis and design of PCBs or antennas embedded in general layered media, commercial tools based on integral equation methods (IE) or finite elements (FEM) show sometimes a low efficiency leading to long meshing and solution runtimes or doubtful solutions. Furthermore the direct integration of lumped elements within (microstrip) circuit or antenna structures is not possible. Then an improved Legendre-Filon quadrature is introduced well suited for the computation of coupling integrals of our IE approach leading to a higher accuracy especially for circuits on thin layers which often lead to unreliable results with commercial solvers. Then we show the additional integration of lumped elements not possible with HFSS together with an interface for a co-simulation. Another application comprises the improved modelling of substrate integrated waveguides (SIW) and antennas based on a very accurate size dimensioning of equivalent quadratic vias for the improved design process of e.g. leaky-wave antennas.

P2.076 Electromagnetic Design of Beam Position Monitor Based on Diffraction Radiation from Twin Dielectric Nanowires

[Dariia O. Herasymova](#) (Institute of Radio-Physics and Electronics NASU, Ukraine)

The diffraction radiation of a modulated beam of charged particles, which flow between twin dielectric circular nanowires is considered. This nanowire configuration can be considered as a pair of optically coupled open resonators. The electron beam field is a slow wave, which decays exponentially from the beam trajectory and is anti-symmetric with respect to that trajectory. We use the Fourier expansions in local polar coordinates of each wire and the addition theorems for the cylindrical functions in order to reduce the wave-scattering problem to the discrete form. As soon as we cast the derived matrix equation to the Fredholm second-kind type, the convergence is guaranteed. The diffraction radiation power shows the peaks at the supermode wavelengths, some of which appear only if the beam trajectory has non-zero rotation angle from the symmetric position. This effect can be scaled to the other wavelength ranges and used in the beam position monitoring.

P2.077 Simulations and Measurements of Brick-Like Axial-Mode Helix Antenna Using CAD Tools

[Dragan I. Olcan](#) (University of Belgrade, Serbia); [Umut Bulus](#) (Antenom Antenna Technologies, Turkey)

We present an axial-mode uniform helix antenna made of brick-like elements. The antenna is modeled using a CAD tool and numerically analyzed using method of moments with higher order basis functions for the approximation of surface currents. The prototype of the antenna is built and measured. The simulated and measured radiation patterns match very well.

P2.078 Modelling of the Mechanical Antenna Using the Biot-Savart Law

[Ben I Jones](#) and [Theo Saunders](#) (Queen Mary University of London, United Kingdom (Great Britain)); [Yang Hao](#) (Queen Mary University, United Kingdom (Great Britain))

We introduce a Mechanical Antenna experiment which was performed by James Bickford and colleagues, and we present an alternative way of modelling the experiment. Our model is based on the Biot-Savart law for the magnetic field produced by a moving point charge. We outline our C++ simulation code and present the results, then discuss comparison with Bickford's model. Finally, we extend our model to asymmetric charge distributions.

Poster2-E04: Optimisation Methods in EM

Electromagnetics

Room: Exhibition Hall

P2.079 Antenna Design Exploration and Optimization Using Machine Learning

[Christoph Maeurer](#) (Germany, Germany); [Peter William Futter](#) (Altair Development S.A. (Pty) Ltd, South Africa); [Gopinath Gampala](#) (Altair Engineering Inc., USA)

Design exploration using numerical field simulation is a valuable approach to analyze antenna performance parameters. In such a process many data describing a mapping from design variables to response functions are generated. In this work different machine learning (ML) techniques are applied on these data to analyze and optimize antenna performance. This data driven simulation approach can speed up antenna optimization tremendously. Also, the benefit of dimensionality reduction algorithms and evolutionary learning in antenna performance analysis is described.

P2.080 Optimal Beamforming Using Clustered Evolutionary Teaching and Learning

[Amirashkan Darvish](#) and [Ahmed Kishk](#) (Concordia University, Canada); [Ataollah Ebrahimzadeh](#) (Babol Noshirvani University of Thecnology, Iran); [Samineh Sarbazi Golazari](#) (Concordia University, Canada)

An improved Teaching and Learning Based Optimization algorithm, C-TLBO, is employed to obtain user-defined shaped radiation patterns. An example of 70-element linear array with a specific asymmetric mask is considered. A novel redistribution mechanism is adopted in order to increase the convergence rate of the original optimizer. The mechanism uses the concept of multiple teachers to cluster the learner groups. It triggers an extra exploration with the same exploitation of the cost function to alter the distribution of the proposed solutions. The performance is validated using a set of standard objective functions. Comparisons to Gradient Descent (GD), Particle Swarm Optimization (PSO) and Genetic Algorithm (GA) illustrate a superior performance for designing such large dimensional beam-shaping problem.

P2.081 Fast Globalized Gradient-Based Optimization of Multi-Band Antennas by Means Smart Jacobian Updates and Response Features

[Slawomir Koziel](#) and [Anna Pietrenko-Dabrowska](#) (Gdansk University of Technology, Poland)

Fulfilling stringent performance requirements calls for a precise adjustment of the antenna dimensions in multi-parameter spaces. Solving such tasks is expensive when using conventional algorithms. Furthermore, global optimization is needed in many cases, which increases the level of design process difficulty. As a matter of fact, utilization of state-of-the-art population-based metaheuristics is prohibitive when the antenna is evaluated by means of full-wave EM analysis. This paper proposes a novel technique for globalized optimization of multi-band antennas. Our approach adopts the accelerated trust-region gradient search with Jacobian change monitoring and response feature technology. The latter permits reliable allocation of the antenna resonances even if the initial design is poor and traditional techniques fail to find a satisfactory design. The algorithm is demonstrated using a dual-band uniplanar dipole antenna. The numerical results indicate that optimization can be performed at the cost typical for local search routines while retaining global search capabilities.

P2.082 Low-Cost Design-Oriented Surrogate Modeling of Multi-Band Antennas by Nested Kriging and Response Features

[Slawomir Koziel](#) and [Anna Pietrenko-Dabrowska](#) (Gdansk University of Technology, Poland)

Electromagnetic (EM)-driven parameter tuning is an important stage of contemporary antenna design process. Its intrinsically high cost can be reduced by employing fast replacement models (or surrogates). Unfortunately, curse of dimensionality often renders construction of conventional surrogates computationally prohibitive. This paper proposes a novel approach to design-oriented modeling of narrow- and multi-band antennas. Our methodology involves a recently reported nested kriging framework as well as a response feature technology. The latter only focuses on the selected characteristic points of the antenna responses (e.g., frequency/level coordinates of antenna resonances) which are relevant from the standpoint of the assumed optimization goals. A combination of these techniques permits construction of reliable surrogates over wide ranges of geometry parameters and using extremely small numbers of training points as demonstrated through examples. Benchmarking against state-of-the-art modeling techniques as well as applications for antenna optimization are also discussed.

Poster2-E05: Imaging and Inverse Scattering

Electromagnetics

Room: Exhibition Hall

P2.083 Application of MRI, fMRI and Cognitive Data for Alzheimer's Disease Detection

[Chiara Dachena](#), [Sergio Casu](#), [Matteo Lodi](#), [Alessandro Fanti](#) and [Giuseppe Mazzarella](#) (University of Cagliari, Italy)

Magnetic resonance imaging has the clinical potential of helping diagnosis in providing to doctors structural and functional information of several neurological disorders. In this study, we proposed a new method based on the elaboration of MR-Images and fMR-Images, combined with the exploitation of Mini Mental Score Examination (MMSE) to discriminate Alzheimer's Disease by control subjects using SVM classification. 69 subjects from the ADNI open database, 33 AD patients and 36 healthy controls, were analyzed. The use of a unimodal approach led to unsatisfactory results, whereas the multimodal approach, i.e., the combination of MRI, fMRI, and MMSE features, resulted in an accuracy of 95.65%, a specificity of 97.22%, and a sensibility of 93.39%.

P2.084 A New Focused Hyperthermia Based on SpaceFrequency DORT

[Sajjad Sadeghi](#) (University of Tehran, Iran); [Alireza Madannejad](#) (Research Assistant, University of Tehran, Iran); [Faezeh Ravanbakhsh](#) (Student, University of Shahid Beheshti, Iran); [Javad Ebrahimzadeh](#) (University of Uppsala, Sweden); [Mauricio D Perez](#) (Uppsala University, Sweden &

National Technological University, Argentina); [Robin Augustine](#) (Uppsala University, Sweden)

Estimating the correct amplitude and phase of excitation for a phased array applicator in hyperthermia is crucial to focus the electromagnetic power only on the malignant biological tissue. The proposed algorithm is based on singular value decomposition to remove unwanted hot spots. Space Frequency DORT method is used to separate the main scattering field from second-order scattering. A complex voxel model is implemented for near to real scenario simulation

P2.085 Towards an Effective Inverse Design of Artificial Materials Based Devices Through the Scattering Matrix Method

[Roberta Palmeri](#) (Università Mediterranea di Reggio Calabria, Italy); [Tommaso Isernia](#) (University of Reggio Calabria, Italy)

In this contribution, the problem of designing artificial materials based devices is dealt with. In particular, a novel approach based on the Scattering Matrix Method is proposed as a potentially efficient and effective synthesis procedure.

Poster2-E06: Scattering and Diffraction

Electromagnetics

Room: Exhibition Hall

P2.086 Depolarization Due to Wedge Diffraction in Satellite Radiowave Communication

[Ankit Regmi, Md. Rafiqul Islam](#) and [Aarno Pärssinen](#) (University of Oulu, Finland); [Markus Berg](#) (University of Oulu & Excellant LTd., Finland)

In this paper, the depolarization effect due to the electromagnetic wave diffraction from the rooftop wedge of a building at 1.575 GHz frequency is presented. Diffraction measurement was performed using a dual circularly polarized (CP) antenna system. The Right Hand Circularly Polarized (RHCP) Global Positioning System (GPS) satellite transmission was utilized for measurement. The orbital motion of a single satellite enabled diffraction measurement as a function of the receiver depth in the shadow region, while the receiver was static. The experimental result of RHCP signal was compared with a theoretical knife-edge diffraction model, and they were in good agreement. In case of the deep shadow region, we found the levels of left- and right circular polarized signals to be equal, which indicates a strong depolarization of the incident RHCP wave. The observed depolarization for conductive wedge is explained by the geometrical theory of diffraction.

Poster2-E07: Frequency and Polarization Selective Surfaces

Electromagnetics

Room: Exhibition Hall

P2.087 Frequency Selective Surface with Polarization Staggered Bands

[Yan Zhang, Yifang Guo](#) and [Xiayuan Yao](#) (North China Electric Power University, China)

In this paper, a novel Frequency Selective Surface (FSS) with polarization staggered bands is proposed. The beams in orthogonal polarization of different frequency bands are divided into a group and transmitted the FSS. The rest are divided into another group and are reflected by the FSS. The FSS with polarization staggered bands is good at separation the bands with narrow transition zone, which realizes transmission and reflection of the incident waves in four different physical mechanisms. What is more, a new frequency separation scheme in quasi-optical feed system is discussed. The FSS with polarization staggered bands, which separate two bands near 90GHz and 108GHz, is fabricated and tested. The reflection coefficient of TM polarization is about 1dB, and the transmission and reflection coefficients in the other band or polarization are less than 0.6dB.

P2.088 Ultra-wideband Polarization-insensitive Thin Microwave Absorber Composed of Triple-layer Resistive Surfaces

[Yixian Fang](#) and [Zhirun Hu](#) (University of Manchester, United Kingdom (Great Britain))

An ultra-wideband and polarization-insensitive microwave absorber, which is composed of three layers of metasurfaces with different patterns and sheet resistances, is proposed in this paper. The bandwidth of effective absorptivity (over 90%) is from 6 GHz to 50 GHz, with relative absorption bandwidth of 157%. The equivalent circuit of the proposed absorber is investigated thoroughly. The circuit model analysis results agree quite well with the numerical simulation, which indicates the accuracy of the equivalent circuit model. The performances of this absorber under various polarizations and incident angles are also investigated. The results indicate the proposed absorber is polarization insensitive and has relatively good stability of wide incident angles.

P2.089 Millimeter-wave Bandpass Frequency Selective Structure Using Stacked Dielectric Slabs

[Joseph Botros, Mohamed K. Emara, Rony E. Amaya](#) and [Shulabh Gupta](#) (Carleton University, Canada)

A simple stacked dielectric structure is presented to achieve a broadband filtering response at millimeter-wave (mm-wave) frequencies. The structure consists of alternative slabs of different dielectric materials (non-periodic designs possible) to exhibit a bandpass response. The structure is designed using a transmission line model and confirmed with full-wave simulations. Compared to standard printed circuit board (PCB) fabrication, stacked dielectric structures are expected to exhibit better loss performance, due to absence of metallic patterns, and be easier to fabricate at mm-waves because of the absence of constraints from PCB line-width/gap dimension tolerances. An example structure was designed, fabricated, and measured with a center frequency 57 GHz consisting of three dielectric slabs and two air gaps. ANSYS FEM-HFSS simulations of this structure show well-matched bandpass performance, insertion loss of less than 1 dB, and a 3-dB bandwidth of 4.5 GHz. Measurement of the fabricated structure shows excellent performance and correlation with simulation.

P2.090 Three-Dimensional Frequency Selective Surface for Single-Polarized Filtering Applications with Angular Stability

[Paul Le Bihan](#) (Institut d'Electronique et de Télécommunications de Rennes & THALES Defence Mission Systems, France); [María García-Vigueras](#) (IETR-INSA Rennes, France); [Erwan Fourn](#) (INSA of Rennes & IETR, France); [Raphael Gillard](#) (IETR & INSA, France); [Isabelle LeRoy-Naneix](#) (THALES AIRBORNE SYSTEMS, France); [Stefan Varault](#) (THALES Defence Mission Systems, France); [Christian Renard](#) (Thales Systèmes Aéroportés, France)

This paper presents a new three-dimensional frequency selective structure for single linear polarization filtering applications. Full-wave simulations of the structure in an infinite periodic configuration exhibit a wide band-pass response reaching 60%, with out-of-band rejection of at least 10 dB. Dielectric loading ensures miniaturization of the unit cell, which prevents the onset of Floquet harmonics in the bandwidth of interest, making the structure's response stable up-to 60° degrees of incidence angle.

P2.091 A Wide-Angle Scanning Polarization Converter Based on Jerusalem-Cross Frequency Selective Surface

[Emilio Arnieri](#) (University of Calabria, Italy); [Francesco Greco](#) (Universita' delle Calabria, Italy); [Luigi Boccia](#) (University of Calabria, Italy); [G. Amendola](#) (Universita della Calabria, Italy)

A broadband and broad-angle linear-to-circular polarization converter based on a dual-layer substrate is presented. The elementary cell of the proposed converter is composed by a Jerusalem Cross (JC). The design procedure is based on transmission line circuit theory and on full-wave unit cell analysis in frequency domain. Simulated results demonstrate a 24% axial ratio bandwidth for an incidence angle $\theta = \pm 50^\circ$ in both x-z and y-z planes. The proposed converter provides a unique combination of wide bandwidth, thin profile, and stable response with respect to the angle of incidence. It can be integrated to any linearly polarized antenna to generate circular polarization without affecting the antenna performances.

P2.092 Dual-Band Band-Pass Frequency Selective Surface Based on the Matryoshka Geometry with Angular Stability and Polarization Independence

[Alfredo Neto](#) (Federal Institute of Paraíba & Grupo de Telecomunicações e Eletromagnetismo Aplicado - GTEMA, Brazil); [Jefferson Costa Silva](#) (Instituto Federal da Paraíba & IFPB, Brazil); [Alexandre Serres](#) (UFCG, Brazil); [Marina Alencar](#) (IFPB, Brazil); [Ianes Coutinho](#) (Instituto Federal da Paraíba, Brazil); [Thamyris da Silva Evangelista](#) (Instituto Federal de Educação Ciência e Tecnologia da Paraíba, Brazil)

This paper describes by the first time, at least of the authors' knowledge, a frequency selective surface, FSS, based on the Matryoshka geometry, with dual-band band-pass frequency response, keeping the interesting features previously outlined: angular stability and polarization independence. Moreover, it is a single layer FSS and the reduction of the resonant frequencies, a characteristic of the Matryoshka geometry, was maintained. Initial design equations are proposed, providing good results, making easy the design of the FSS for other resonant frequencies and specific applications. Two FSS were designed, fabricated and characterized, verifying a good agreement between numerical and experimental results. The resonant frequencies remain almost constant for different incident angles, from 0° to 45°, confirming the angular stability

P2.093 Microwave Polarization Converter with Multilayer Metasurface

[Fuheng Zhang, Guomin Yang](#) and [Ya-Qiu Jin](#) (Fudan University, China)

This paper introduces low profile linear-to-circular polarization and left hand circular polarization to right hand circular polarization converters based on third-order metasurface structure that operates at the X-band. The metasurface unit cell is composed of three metal layers and is separated by two dielectric substrates. The transmission coefficients at two orthogonal directions are equal, while a 90° or 180° transmission phase difference is introduced between them over a wide bandwidth. A horn antenna is employed as a linear source to verify the performance of the linear-to-circular polarization converter, while a helical antenna is designed as the left hand circular polarization to right hand circular polarization converter. The results show that the designed metasurface can effectively convert a linear polarized (LP) wave to a left-hand circular polarized (LHCP) wave or a left hand circular polarized wave to right hand circular polarized wave.

P2.094 Novel Dichroic Subreflector Design for Cassegrain Antennas

[Seymur Shukurov](#) (Yeditepe University & Profen Communication Technologies, Turkey)

Novel subreflector design for Dual Band Cassegrain Antenna systems was proposed in this paper. Proposed Frequency Selective subreflector, reflecting frequencies in X Band and transmitting in S Band was designed and manufactured using Selective Laser Synthering method. Tests were made both on the manufactured unit and on a complete antenna system using GEO satellite beacon signals. It was shown that total antenna efficiencies in both frequency bands using Frequency Selective Surface dichroic subreflector were more than 65 %.

P2.095 Retrieval of Effective Permittivity and Permeability of Periodic Structures on Dielectric and Magnetic Substrates

[Peng Mei](#) and [Shuai Zhang](#) (Aalborg University, Denmark); [XianQi Lin](#) (University of Electronic Science and Technology of China, China); [Gert Pedersen](#) (Aalborg University, Denmark)

This paper presents the retrieval of effective permittivity and permeability of periodic structure on dielectric and magnetic substrates. The retrieval approach is based on investigating the equivalent circuits. For demonstration, a single square loop-based periodic structure is served as an example to elaborate the retrieval process. Firstly, the equivalent circuit of the freestanding structure is modeled with inductor and capacitor, where the values of these components are determined by the simulated Z-matrix of the freestanding structure; the effects of supporting substrates are then considered, where the compensating principles are deduced from inductive grids and capacitive patches, to compensate the corresponding values in the former equivalent circuit on purpose. The compensating values are also determined from the simulated S-parameter of the structure with supporting substrates. The formulas of effective permittivity and permeability are readily deduced and obtained from the original and compensating values of components in the equivalent circuits.

Poster2-P05: Mm-wave and UWB Propagation

Propagation

Room: Exhibition Hall

P2.096 Channel Measurement and Analysis for Polarimetric Wideband Outdoor Scenarios at 26 GHz: Directional Vs Omni-Directional

[Sohail Payami](#) (University of Surrey, United Kingdom (Great Britain)); [Mohsen Khalily](#) (University of Surrey & 5G Innovation Centre, Institute for Communication Systems (ICS), United Kingdom (Great Britain)); [Sohail Taheri](#) (VIAMI Solutions, United Kingdom (Great Britain)); [Konstantinos Nikitopoulos](#) and [Rahim Tafazolli](#) (University of Surrey, United Kingdom (Great Britain))

This paper presents the measurement results and analysis for outdoor wireless propagation channels at 26 GHz over 2 GHz bandwidth for two receiver antenna polarization modes. The angular and wideband properties of directional and virtually omni-directional channels, such as angular spread, root-mean-square delay spread and coherence bandwidth, are analyzed. The results indicate that the reflections can have a significant contribution in some realistic scenarios and increase the angular and delay spreads, and reduce the coherence bandwidth of the channel. In addition, the analysis in this paper show that using a directional transmission can result in an almost frequency-flat channel over the measured 2 GHz bandwidth; which consequently has a major impact on the choice of system design choices such as beamforming and transmission numerology.

P2.097 Ray-tracing Based Channel Clustering and Analysis at 28 GHz in Conference Environment

[He Ding](#) (Beijing University of Posts and Telecommunications, China); [Lei Tian](#) (Beijing University of Posts and Telecommunications & Wireless Technology Innovation Institute, China); [Pan Tang](#), [Li Yu](#), [Wanpeng Zhang](#), [Tao Jiang](#) and [Jianhua Zhang](#) (Beijing University of Posts and Telecommunications, China)

The millimeter-wave (mm-wave) band will be a key component of fifth-generation (5G) wireless communication systems. Studies on millimeter-wave channels are of great importance to mm-wave wireless technologies. In this paper, we investigate the 3-D clustering phenomenon of mm-wave propagation at 28 GHz in a conference room. The results including cluster propagation mechanisms, the relationship between the clusters and physical environment, and intra-cluster statistics are presented. Results show that the cluster propagation mechanisms are influenced by the room geometry. Besides, cluster statistics including intra-cluster delay spread (DS), angle spread (AS), and sub-paths number are discussed. These results could help extend the current research on mm-wave channels. Moreover, a ray-tracing (RT) tool is used to emulate the measurements and similarity results are presented and analyzed. Excellent agreements between measurement and simulation verify the feasibility of RT for studying the cluster characteristics, especially when exploring the relationship between clusters and the physical environment.

P2.098 5G Millimeter-Wave NLOS Coverage Using Specular Building Reflections

[Robbert Schulpen](#), L. A. (Sander) Bronckers, A. B. (Bart) Smolders and [Ulf Johannsen](#) (Eindhoven University of Technology, The Netherlands)

Maximization of 5G millimeter-wave base station coverage and range is important to reduce the number of required base stations. Buildings could be used as reflectors to provide coverage in NLOS areas due to their high reflectivity at millimeter-waves. This paper presents the results of a measurement campaign investigating specular reflections from buildings at 24.00-24.25 GHz. The angle of minimum path loss for single-building reflections agrees well with the direction of the specular path. This agreement is less accurate in case of a double-building reflection, possibly due to obstructions in the specular path or multipath fading. In case of a single-building reflection, 1-9 dB excess loss compared to free-space path loss is measured. The excess loss is in the range of 9-20 dB for a double-building reflection. Although more research on this topic is required, these results are promising and indicate that buildings can be used as effective millimeter-wave reflectors.

P2.099 Availability of 7 Km-Long Parallel 18 GHz Band and E-band Links for Multi Band Solutions

[Christina Larsson](#) (Ericsson Research & Ericsson AB, Sweden); [Lei Bao](#) (Ericsson AB, Sweden)

E-band (70/80 GHz) backhaul links are nowadays available with multi-Gbs capacity. Unfortunately, the high attenuation due to rain is limiting the link lengths to about 2 km. One way to overcome this limitation is to set up the E-band link in some sort of carrier aggregation solution together with a conventional backhaul band, usually 18-23 GHz to guarantee availability of critical data transfer also during heavy rain. This study compares long term logging of 7 km-long parallel backhaul links with carrier frequency 18.6/19.6 GHz and 71.6/81.6 GHz. This summary includes a comparison with ITU recommendations and a discussion on which phenomena, more than precipitation, is influencing the availability of these links.

P2.100 Multi-band Characterization of Propagation in Industry Scenarios

[Diego Dupleich](#) (Ilmenau University of Technology, Germany); [Robert Müller](#) (TU Ilmenau, Germany); [Markus Landmann](#) (Fraunhofer Institute for Integrated Circuits IIS, Germany); [Jian Luo](#) (Huawei Technologies Duesseldorf GmbH, Germany); [Giovanni Del Galdo](#) (Fraunhofer Institute for Integrated Circuits IIS & Technische Universität Ilmenau, Germany); [Reiner S. Thomä](#) (Ilmenau University of Technology, Germany)

Industry 4.0 is the scenario in which the 5G and beyond networks are expected to show all their potential. However, while propagation at sub-6 GHz has been widely investigated in industry environments, mm-waves propagation and channel modelling in those scenarios is still under early research. Therefore, we introduce novel simultaneous multi-band ultra-wideband measurements at 6.75 GHz and 30 GHz in LOS and NLOS with RX below and above clutter level. This unique set-up allows a direct comparison between the sub-6 GHz and mm-wave channel. Results have shown larger specular to dense multi-path components power ratio and shorter large-scale parameters at mm-waves .

P2.101 Indoor mmWave Channel Characterization with Large Virtual Antenna Arrays

[Alfred Mudonhi](#) (CEA Leti and Universite Catholique de Louvain & Universite Grenoble-Alpes, France); [Raffaele D'Errico](#) (CEA, LETI, Minatec Campus & Univ\ Grenoble-Alpes, France); [Claude Oestges](#) (Université Catholique de Louvain, Belgium)

In this paper we present an indoor channel measurement campaign from 26 to 30 GHz, using a virtual antenna array. On the receiving side a 3x3 spatial grid, moving in the environment, was considered. On the transmitting side we considered a massive virtual array of 21x21 elements. Multi path components have been extracted by means of high resolution algorithm. The results obtained with the full massive array are compared with those obtained with a small sub-array, in order to investigate the effect of array size in channel modeling.

P2.102 Cluster Intensity and Spread Characteristics in Classroom Scenario at 10 and 28 GHz Bands

[Panawit Hanpinitsak](#) and [Kentaro Saito](#) (Tokyo Institute of Technology, Japan); [Wei Fan](#) (Aalborg University, Denmark); [Johannes Hejlsbæk](#) (Nokia Bell Labs, Denmark); [Jun-ichi Takada](#) (Tokyo Institute of Technology, Japan); [Gert Pedersen](#) (Aalborg University, Denmark)

This paper discusses the cluster spreads and scattering intensity (SI) characteristics at 10 and 28 GHz band in a typical classroom environment. The multi-path components (MPCs) were calculated from the measurement data using space alternating generalized expectation-maximization (SAGE) algorithm. Next, the scattering point-based KPowerMeans (SPKPM) algorithm was used to obtain the clusters based on interacting objects (IOs) in the environment. Lastly, the cluster delay spread (DS), angular spread (AS), and SI were computed and their characteristics were discussed. The results showed that the channels at both bands were almost equally directive. Moreover, cluster spreads depended on the number of layers and surfaces of IOs, whereas IO material and propagation mechanism influenced the cluster SI.

P2.103 A Comparative Study for Indoor Factory Environments at 4.9 and 28 GHz

[Yicheng Guan](#) (Beijing University of Posts and Telecommunications & Key Lab of Universal Wireless Communications, Ministry of Education, China); [Jianhua Zhang](#) (Beijing University of Posts and Telecommunications, China); [Lei Tian](#) (Beijing University of Posts and Telecommunications & Wireless Technology Innovation Institute, China); [Pan Tang](#) and [Tao Jiang](#) (Beijing University of Posts and Telecommunications, China)

The industrial Internet of Things (IIoT) has benefited from the fifth-generation (5G) wireless network and is providing much-needed impetus for economic growth. Because of a very wide frequency range of 5G wireless network, the microwave and millimeter wavebands will constitute hybrid wireless communication systems, thus it is essential to have a thorough knowledge of the propagation characteristics in industrial scenarios at different frequencies. In this paper, we provide a comparative study of channel characteristics, i.e., the path loss and Ricean K-factor, at 4.9 and 28 GHz in indoor factory environments based on channel measurements. The results consistently indicate that rich reflection paths occur in industrial scenarios, relative to indoor office environments. Also, severer attenuation and lower multipath richness occur at 28 GHz. Meanwhile, the impact of antenna height on the propagation channel is studied. These results are helpful for the frequency band selection and antenna height design of IIoT systems.

P2.104 Impact of UWB Antennas on Ranging Accuracy

David Veit, Michael Gadringer and Erich Leitgeb (Graz University of Technology, Austria)

This work deals with the impact of antennas on the ranging accuracy of an ultra-wideband system. For two different antennas we tried to relate multiple commonly used antenna characteristics with the ranging error produced by the ultra-wideband system. Our analysis showed that parameters which do not incorporate information about the used transmit signal deliver only limited information. In the conclusion we provide some advice for ultra-wideband antenna designers and system architects.

Poster2-P09: Propagation for Vehicular Communications

Propagation

Room: Exhibition Hall

P2.105 Clustering Performance Evaluation Algorithm for Vehicle-to-Vehicle Radio Channels

Chen Huang and Ruisi He (Beijing Jiaotong University, China); Bo Ai (Beijing Jiaotong University & State Key Lab of Rail Traffic Control and Safety, China); Mi Yang, Yangli-Ao Geng and Zhangdui Zhong (Beijing Jiaotong University, China)

Nowadays, propagation channels are mostly modeled based on the structure of the clusters of multipath components (MPCs). The clusters of the MPCs can be identified by using clustering algorithms. Most of the clustering algorithms are sensitive to the number of clusters, which however, is hard to be acquired from the channel measurement. In this case, most of the algorithms use clustering performance evaluating methods to determine the best number of clusters. Nevertheless, none of the current evaluating methods are able to properly evaluate the time-varying clustering results, where the evolution pattern in time dimension needs to be additionally considered. In this paper, we propose a novel clustering evaluation method for the clusters in time-varying channels, which considers the evolution pattern of the clusters during the evaluation. Based on the simulations, the new cluster evaluation can better assess the time-varying channels comparing to the existing evaluation methods.

P2.106 Measurements of Reflection and Penetration Losses in Low Terahertz Band Vehicular Communications

Vitaly Petrov (Tampere University, Finland); Johannes M. Eckhardt (Technische Universität Braunschweig, Germany); Dmitri Moltchanov and Yevgeni Koucheryav (Tampere University, Finland); Thomas Kürner (Technische Universität Braunschweig, Germany)

The beyond-5G vehicular communications are expected not only to utilize the already explored millimeter-wave band but also to start harnessing the higher frequencies above 100 GHz ultimately targeting the so-called low terahertz band, 300 GHz-1 THz. In this paper, we perform a set of propagation measurements at 300 GHz band in representative vehicular environments. Particularly, we report on the reflection losses from the front, rear, and side of a regular vehicle. In addition, the penetration losses when propagating through, over, and under the vehicle are presented. Our study reveals that the vehicle body is extremely heterogeneous in terms of the propagation losses: the attenuation heavily depends on the trajectory of the 300 GHz signal through the vehicle. The reported measurement data may be used as a reference when developing the vehicle-specific channel and interference models for future wireless communications in the low terahertz band.

P2.107 In-Stationary Tapped Delay Line Channel Modeling and Simulation

Nina Hassan and Reiner S. Thomä (Ilmenau University of Technology, Germany); David W Matolak (University of South Carolina, USA)

An essential tool in the performance analysis of communication systems is a tractable and accurate propagation channel model. The aim of this paper is to discuss the implementation of tapped delay line channel model for vehicle to infrastructure channels and devise a generator to produce a channel impulse response based on an already derived model parameters from measurement data. The root-mean square delay spread is used for a model validation between simulated and collected data on the basis of how well they agree. The analysis investigates correlation coefficient among taps persistence, as well as higher order Markov model. The results illustrate that only few taps are essential to regenerate accurately the delay spread.

Poster2-P10: Propagation in Biological Tissues and Body Area Propagation

Propagation

Room: Exhibition Hall

P2.108 Pathloss Calculation for Fat-Intra Body Communication Using Poynting Vector Theory

Javad Ebrahimzadeh (University of Uppsala, Sweden); Seyed Abbas Akbarzadeh Jahromi (University of Tehran, Sweden); Mauricio D Perez (Uppsala University, Sweden & National Technological University, Argentina); Robin Augustine (Uppsala University, Sweden)

Recently, Fat-based Intra-Body Communication (Fat-IBC) has been proposed and studied in terms of its reliability in simulation and laboratory settings. We, in this work, try to address another important aspect of communication, namely path loss, in the context of fat-IBC. This paper provides numerical and experimental modeling of path loss through the fat layer using the Poynting Vector theory and the multi-layer dielectric Green's function (MGF). To calculate the path loss based on the Poynting vector theory, the electromagnetic field distribution through the involved media should be known. This paper exploits the EM fields using MGF theory or commercial software CST Microwave Studio 2019. Finally, experimental measurement is done on ex-vivo tissue made of porcine skin, fat and muscle at the frequency range of 5 GHz - 6 GHz. The average measured path loss is around 5.5 dB/cm which has good compliance with the theoretical Poynting vector path loss estimation

P2.109 Verification of a Simplified Channel Modeling Technique for Ultra Wideband In-Body Communication with Simulations

Jan-Christoph Brumm and Gerhard Bauch (Hamburg University of Technology, Germany)

For wireless capsule endoscopes, high data rate communication is needed between a transmitter in the gastrointestinal tract and a receiver on the body surface. One widely considered technique to achieve this is ultra wideband transmission. To the best of our knowledge no comprehensible channel models exist for the scenario of in-body communication. To change that, we recently proposed a simplified layer modeling technique. The goal of this paper is to verify that the resulting channel characteristics derived with our proposed method are on average similar to those obtained from numerical wave simulations. Our results show that on average the transmission loss for both approaches is nearly the same. Moreover, the correlation between the transfer functions is very strong. Finally, the power delay profiles generated are almost identical. Hence, it is possible to create a channel model with the same characteristics using a much simpler and less computationally expensive approach.

P2.110 A Low Cost Stable Adipose Phantom for Microwave Breast Cancer Investigation

Akinola Eesuola (University of Kent)

In this paper, we present a low-cost and stable dielectric composite from non-toxic particulate, Marmite and Clover butter. These samples were mixed in the proportion of approximately 9:0.5 using Lichtenecker logarithmic mixture equation for particles with arbitrary shape, to produce a homogeneous fat phantom, which is the main constituent of the breast tissue. The composite is characterized experimentally at 22degrees Centigrade in the UWB frequency region in terms of its constitutive parameters, reflection and transmission coefficients. Cole-Cole parameters were extracted from experimental data. The permittivity of the fat phantom at zero, 4.5GHz and optical frequency are 48.13, 10.13 and 7.61 respectively. The relaxation time for this phantom is 19.23ps. The reflection and transmission coefficients are 0.48 and 0.52 respectively. These parameters are particularly useful in understanding the propagation of electromagnetic (EM) wave through glandular tissue where most cancers are known to be found.

P2.111 Compact Honey-Cell CSRR-based Microwave Biosensor for Monitoring Glucose Levels

Ala Eldin Omer (University of Waterloo, Canada); George Shaker (University of Waterloo & Spark Tech Labs, Canada); Safieddin Safavi Naeini (University of Waterloo, Canada); Hamid Kokabi (Laboratory of Electronics and Electromagnetism (L2E), Sorbonne University, Canada); Georges Alquié (UPMC, France); Frederique Frederique Deshours (Laboratory of Electronics and Electromagnetism (L2E), Sorbonne University, France)

In this article, we propose a planar microwave sensor that consists of four distinct hexagonal-shaped complementary split ring resonators (CSRRs) configured in the honey-cell pattern. The sensor element operating at 1.5 - 3.0 GHz is fabricated on an FR4 dielectric substrate and excited via the microstrip technology in the cm-wave band. The proposed sensor is used as a near-field probe to detect the glucose levels in the blood mimicking aqueous solutions via tracing the frequency shift responses for tested glucose concentrations in the range 70 - 120 mg/dL. The sensor exhibits an excellent resonant frequency sensitivity that excels others in the literature. The sensor sensitivity, reliability and repeatability are demonstrated by the in-lab measurements via a Vector Network Analyzer (VNA).

P2.112 Propagation Analysis for an Implanted Antenna Model at Pancreas

Konstantina Zarafeta and Stavros Koulouridis (University of Patras, Greece); Stavros Kotsopoulos (Wireless Telecommunications Laboratory, Greece)

This paper presents a numerical and experimental study and channel characterization for an implanted antenna located upon the tissue of pancreas. Implanted antenna will be transmitting to a receiver that is located at specific distances in an indoor environment, like a hospital room. The antenna could support wireless data telemetry and power transmission operation within the industrial, scientific, medical band (ISM, 902.8-928 MHz). Here the aim is to investigate the propagation pattern of the near and overall field of electromagnetic waves in an indoor environment and to determine if this behavior causes difficulties between the two devices. To address this problem, the signal propagation of a system that consists of two dipoles, over a sampled trajectory is carried out. We then extended our study using virtual human models. Simulation results are examined and depicted extensively.

P2.113 A Preliminary Analysis of User's Body Impact on Signal Polarization in WBANs

Kenan Turbic (INESC-ID / IST, University of Lisbon, Portugal); Mariella Särestöniemi (Erkki Koiso-Kanttilan katu 1 & Center for Wireless Communication, University of Oulu, Finland); Matti Hämäläinen and Timo Kumponiemi (University of Oulu, Finland); Luis M. Correia (IST/INESC-ID - University of Lisbon & INESC, Portugal)

This paper analyses the impact of the human body on antenna radiation characteristics, with a focus on the polarization aspect. The effect of the body tissues on a wrist-worn ultra-wideband double loop antenna radiation characteristics is investigated at 3, 4 and 5 GHz, based on numerical full-wave simulations complemented with a voxel model of a hand. Results show a strong influence of the body on the gain and polarization characteristics; the radiation in the direction towards the body is suppressed by 20 dB or more, and the antenna polarization changes from a linear to an elliptical one. By simulating an off-body communications scenario with the user walking at a fixed distance from the off-body antenna, up to 6.5 dB lower received power is obtained by using the wearable antenna radiation pattern simulated with the hand phantom, compared to the case when the antenna in free space.

P2.114 Automated Measurement Setup for the On-body Link of Wireless Body Area Networks

[Andreas Pfrommer](#) and [Martin Schmidt](#) (Sivantos GmbH, Germany)

In this work a new automated measurement setup for the on-body link of wireless body area networks is described. The setup consists of an array of eight field probes distributed around the chest of an anthropomorphic body phantom. The whole system is in an anechoic chamber. As an example, we characterize the on-body link of a hearing instrument and compare experimental data with simulation results.

P2.115 Procedure for Simulating the Direct Path Loss Between Body-Worn Antennas

[Oleksandr Rybalko](#), [Jens Troelsen](#), [Rune Sørensen](#) and [Morten Thouggaard](#) (Oticon A/S, Denmark)

An efficient procedure for simulating the direct path loss between body-worn antennas is presented. Nearfield sources are used to simplify the simulations and reduce the number of mesh cells. The procedure is validated with conventional full 2-port CST T-solver simulations. Next, the direct path loss between each of five different hearing solutions and a connectivity device placed on the chest are presented and discussed. Finally, it is reported that the simulation time for some of the hearing solutions is improved with up to a factor of 5.

Poster2-P12: Radar, Localisation, and Sensing

Propagation

Room: Exhibition Hall

P2.116 Evolution of the Image Quality over Time for a Freehand Monostatic mm-Wave Radar Imager

[Guillermo Alvarez Narciani](#) (University of Oviedo, Spain); [Jaime Laviada](#) (Universidad de Oviedo, Spain); [Fernando Las-Heras](#) (University of Oviedo, Spain)

In this paper the performance over time of a freehand, mm-wave imaging scanner is studied. The system comprises a FMCW on-chip-radar and a motion capture system used to estimate the position of the scanner during the acquisition process in order to coherently combine the measured data creating a synthetic aperture. The scanner is controlled by a conventional laptop, which is also in charge of processing the obtained data displaying real-time results. Specifically, four snapshots of the same scan comprising a target hidden under a hard cardboard box are analyzed. The obtained results show that only a few seconds can be enough to retrieve a rough estimation of the shape of the targets within the volume under test.

P2.117 Extracting the Features of the Shallowly Buried Objects Using LeNet Convolutional Network

[Mostafa Elsaadouny](#), [Jan Barowski](#) and [Ilona Rolfes](#) (Ruhr-Universität Bochum, Germany)

The convolutional neural networks are considered as the best artificial intelligence algorithms for image classification problems. Generally, a ConvNet requires a very large number of images to be trained well and to achieve the best results. This paper investigates the implementation of the LeNet convolutional network (ConvNet) for images classification using a small dataset. The dataset of interest comprises images of buried objects obtained by a ground penetrating radar (GPR), which is considered as an efficient tool for detecting and defining buried objects. One of the main problems facing this classification task is the limited available data. The LeNet has been deployed and trained on the Fashion-MNIST dataset, and the learned features have been transferred to our GPR dataset. The network performance has been monitored and the classification results show a high degree of precision and accuracy.

P2.118 Two-dimensional OAM Radar Imaging Using Uniform Circular Antenna Arrays

[Yanzhi Zeng](#), [Yang Wang](#) and [Zhihui Chen](#) (Chongqing University of Posts and Telecommunications, China); [Jiliang Zhang](#) (The University of Sheffield, United Kingdom (Great Britain)); [Jie Zhang](#) (University of Sheffield, Dept. of Electronic and Electrical Engineering, United Kingdom (Great Britain))

The vortex radio wave carrying orbital angular momentum (OAM) can potentially be exploited to achieve azimuthal super-resolution for target identification and radar imaging realms. A two-dimensional (2D) imaging method for OAM-based radar is presented in this paper. Based on the incrementally phased uniform circular antenna (UCA) arrays, the generation method and the echo signal model of OAM beams for radar imaging are established firstly. Subsequently, the modified multiple signal classification (MUSIC) algorithm is carried out to realize the 2D joint detection of the multi-target in the elevation and azimuth domain. Compared with the existing OAM-based radar target azimuth imaging, this proposed method can readily achieve 2D joint imaging of target's elevation and azimuth simultaneously without increasing the cost of hardware. The work and results provide suggestions to the design of OAM-based 2D radar systems.

P2.119 Super-Resolution DOA Estimation Using Dynamic Metasurface Antenna

[Shengyao Chen](#), [Boyu Sima](#) and [Feng Xi](#) (Nanjing University of Science and Technology, China); [Wen Wu](#) (Nanjing University of Science & Technology, China); [Zhong Liu](#) (NJUST, China)

Dynamic metasurface antenna (MSA) exploits radiation properties of its elements to generate a variety of desired beam-patterns, and unlike traditional antenna array it avoids controlling the gain and phase at each element. This inherent beamforming capability leads to a compact and low-cost antenna implementation. This paper investigates direction-of-arrival (DOA) estimation using dynamic MSA. MSA has only a single-port output, and thus traditional DOA estimation techniques with array data are not applicable. However, the outputs from the diverse patterns of dynamic MSA are similar to the data of traditional antenna array in beam-space. Then beam-space DOA estimation approaches can be utilized to process the dynamic MSA data. A MUSIC-based algorithm is suggested and the DOA estimation performance of dynamic MSA is simulated. It is found that the super-resolution DOA estimation can be achieved and the dynamic MSA for DOA estimation is an interesting alternative to the traditional antenna array.

P2.120 Intensity-only Imaging Using Broadband Correlations in Reverberation Chambers

[Philipp del Hougne](#) (Institut de Physique de Nice, France); [Philippe Besnier](#) (IETR, France); [Fabrice Mortessagne](#), [Ulrich Kuhl](#) and [Olivier Legrand](#) (Institut de Physique de Nice, France); [Matthieu Davy](#) (IETR, Université de Rennes 1, France)

In this article, we present a proof-of-concept of intensity-only passive imaging inside a reverberating environment in the microwave domain. The auto-correlation of the diffuse field generated by a single source makes it possible to reconstruct the impulse response of an antenna, as if the antennas was both transmitting and receiving. This impulse response includes the reflection on objects within the medium. We demonstrate in microwave measurements in a mode stirred-reverberation chamber (RC) that an object can thus be accurately detected and located from intensity measurements on an array of antennas. These results pave the way to indoor intensity-only passive imaging using illuminators of opportunity in the microwave regime.

P2.121 Experimental Results on Rain Detection at Ka-Band Based on Range-Doppler Signal Processing

[Ashkan Taremi Zadeh](#), [Moritz Mälzer](#) and [Jonas Simon](#) (Goethe University Frankfurt am Main, Germany); [Sebastian Beck](#) (Goethe-University Frankfurt, Germany); [Jochen Moll](#) (Goethe University Frankfurt am Main, Germany); [Viktor Krozer](#) (Goethe University of Frankfurt am Main, Germany)

Radar technology in the mm-wave frequency band is a promising approach for local rain detection and classification of precipitation. In this paper we present a Frequency Modulated Continuous Wave (FMCW) radar system with 1 Tx and 2 Rx operating in the Ka-band from 33.4 GHz to 36.0 GHz. This Radar is a low-cost, portable system that requires minimum supervision in the field. As such, we use this system for structural health monitoring of rotor blades on wind turbines, detection of flying animals e.g. birds and bats and rain detection. When analyzing rain data with Range-Doppler (RD) algorithm, we noticed characteristic patterns of rain, which we investigated more closely. To better understand these patterns we designed an experiment and implemented a numerical modelling framework. Experimental and numerical results for rain detection and classification are presented and discussed here.

P2.122 Estimation of the Number of Persons in a Reverberant Environment Using Bistatic Radar

[Marwan Yusuf](#) (Ghent University, Belgium); [Brecht De Beelde](#) (Ghent University & IMEC, Belgium); [Emmeric Tanghe](#) (Ghent University, Belgium); [Eli De Poorter](#) (Ghent University & Imec, Belgium); [Luc Martens](#) (Ghent University - imec, Belgium); [Pierre Laly](#), [Davy P Gaillot](#) and [Martine Liénard](#) (University of Lille, France); [Wout Joseph](#) (Ghent University/IMEC, Belgium)

The theory of room electromagnetics provides a simple characterization of indoor microwave propagation. By considering the indoor environment as a lossy cavity, the exponential decay rate of the power-delay profile is related to the total absorption inside the room. In this paper, we explore the possibility of estimating the number of people inside a below-deck ship compartment using only the decay time constant, also known as reverberation time. First, we verify the reverberating nature of the room. Then, we find the relation between reverberation time and the number of people inside the room. We show that it is possible to estimate the number of people with a good accuracy, depending on the number of antennas used. With a success rate of 88%, the estimation error is only 1 person when 16 spatially averaged antennas are used.

P2.123 Simulation Validation of High Resolution Indoor Terahertz Synthetic Aperture Radar Imaging

[Aman Batra](#) (University of Duisburg-Essen, Germany); [Michael Wiemeler](#) (Universität Duisburg-Essen, Germany); [Diana Goehringer](#) (Technische Universität Dresden, Germany); [Thomas Kaiser](#) (Universität Duisburg-Essen, Germany)

Indoor Terahertz Synthetic Aperture Radar (SAR) is an emerging technology for material characterization, high resolution imaging and localization. In comparison to optical technology, it provides benefits in hazardous scenarios such as fire in a building as objects inside the building can be characterized and localized. The principles of SAR are well established but the main challenge lies with extending this technology to high frequencies and indoor environment. To investigate this technology, imaging geometry and system parameters have to be evaluated respectively. This paper explains the signal processing of SAR and presents the imaging geometry for an indoor scenario. Further, it evaluates the parameters for high resolution imaging and localization. Based on these parameters, system design has been simulated and results of 2D high resolution indoor SAR imaging at 300 GHz are presented. Additionally, the proof of theoretical resolution across the range and azimuth is shown with the simulation results.

P2.124 Temporal-Range-Doppler Features Interpretation and Recognition of Hand Gestures Using mmW FMCW Radar Sensors

[Guiyuan Zhang](#), [Shengchang Lan](#), [Kang Zhang](#) and [Linting Ye](#) (Harbin Institute of Technology, China)

This paper introduced a comparative study of using deep neural networks in non-contact hand gesture recognition based on millimeter wave FMCW radar. Range-doppler maps are processed with a zero-filling strategy to boost the range and velocity information of gesture motions. Two optimal types of deep neural networks, 3D-CNN and CNN-LSTM are

respectively constructed to reveal the temporal gesture motion signatures encoded in multiple adjacent radar chirps. With the proposed networks, the recognition accuracy of six popular hand gestures reach to 95%. Meanwhile, this letter further explores the performance of the proposed networks in the impacts of training data size on the recognition accuracy. The proposed methods can be applied in the recognition of minor finger motions, providing some preliminary experimental results compared with other baseline methods.

P2.125 Human Motion Detection Using Planar Array FMCW Radar Through 3D Point Clouds

[Ibrahim Alnujaim](#) (California State University, Fresno, USA); [Ikmo Park](#) (Ajou University, Korea (South)); [Youngwook Kim](#) (California State University, Fresno, USA)

We propose to detect different human motions using planar phased-array FMCW radar through investigating 3D point clouds, which has not yet been presented. While human motion has been analyzed using micro-Doppler signatures, studies investigating an approach that employs point clouds are lacking. We measured 7 human motions including bowing, kicking, punching, walking, running, sitting down, and standing using a planar phased-array FMCW radar system operating at 77GHz. Next, 3D point clouds were extracted by calculating direction-of-arrival from point scatterers on the human body. As the point clouds contained human posture information, we classified the motions using convolutional neural networks. The classification accuracy was 80%.

P2.126 Data Transfer and Communication in Radar Networks

[Peter Müller](#), [Matthias Weiß](#), [Stephan Sandenbergh](#), [Daniel O Hagan](#) and [Peter Knott](#) (Fraunhofer FHR, Germany)

A robust architecture for the transfer and centralised storage of time stamped multi-sensor data of arbitrary types and sizes. It is aimed specifically at networks using physical infrastructure. The idea to observe the environment with the aid of multiple sensors of different types has existed for many decades. However, advances in synchronisation, localisation and networking technologies stimulated renewed interest in networked-centric sensing. Multistatic distributed sensors offer many advantages over single sensors. More target information can be extracted and it has increased sensitivity, detection, and classification abilities. Hence, there is a strong drive to further develop the underlying technologies of sensor networks. One such technology is the robust transfer of data between the network nodes and a central storage node. This paper proposes a communication architecture adapted to the requirements of sensor networks. This architecture can efficiently transfer and store arbitrary data types from multiple nodes to a central storage node.

Poster2-P13: Radio Science and Remote Sensing TOP

Propagation

Room: [Exhibition Hall](#)

P2.127 Wideband Superconducting Integrated Filter-bank for THz Astronomy

[Alejandro Pascual Laguna](#) (Delft University of Technology & SRON, The Netherlands); [Kenichi Karatsu](#) (SRON, The Netherlands); [David Thoen](#) (Kavli Institute of NanoScience, Delft University of Technology, The Netherlands); [Vignesh Murugesan](#) (SRON, The Netherlands); [Akira Endo](#) (Delft University of Technology, The Netherlands); [Jochem Baselmans](#) (SRON, The Netherlands)

A wideband band, terahertz, superconducting, integrated filter-bank for astronomy is presented. The dispersion mechanism is an array of shunted microstrip bandpass filters rendering a spectrometer implementation with 347 spectral channels sampling the band 220-440 GHz with a spectral resolution of 400 and coupling strength in-band of 40%. To efficiently read out all these channels with background-limited sensitivity, Microwave Kinetic Inductance Detectors (MKIDs) are employed to sense the filtered THz radiation. In this paper we derive a transmission line model for a bandpass filter that can be cascaded resorting to ABCD matrices to enable the study of large filter-banks. Fast and accurate predictions are thereby obtained for the frequency response of a filter-bank. With the insights obtained from the model, several prototype chips have been designed and are under fabrication.

P2.128 On the Use of Adjoint Methods for Refractivity Estimation in the Troposphere

[Uygar Karabaş](#) (ENAC & ISAE-SUPAERO, France); [Youssef Diouane](#) (ISAE-SUPAERO, France); [Rémi Douvenot](#) (ENAC, France)

This paper presents a preliminary study of a new inversion strategy combining the method of adjoint applied to the wide-angle parabolic equation and the method of split-step wavelet for tropospheric refractivity estimation. Our main motivation is to use a gradient based optimization method to infer atmosphere from radio-frequency data, in an effort towards a real-time accurate refractivity-from-clutter system. The proposed adjoint formulation is validated with the method of finite differences. The validation setup is developed for inversion using a tomographic approach.

P2.129 Monitoring the Greenland and Antarctica Ice Sheets Using Ultra-Low-Frequency Electromagnetic Resonances

[Alexander G. Voronovich](#) (325 Broadway & NOAA/Earth System Research Laboratory, USA)

Monitoring the total mass of the Greenland and Antarctica ice sheets, which currently show a tendency of rapid decline, would provide one measure of global climate change. Different techniques, including radio echo-sounding, gravimetry, satellite altimetry and others have been used for this purpose with varying degrees of success. A novel approach based on measurements of resonant frequencies of waveguides formed by the ice sheets with respect to electromagnetic waves of ultra-low-frequencies was recently suggested in [1]. This paper presents an extension of the earlier work to include a cylindrical slab dielectric model for the ice sheets. Estimates of resonant frequencies are presented, which confirm the feasibility of the suggested approach. Estimates of the sensitivity of the corresponding measurements are also provided.

Wednesday, 18 March 14:50 - 15:30

IS-Wed 1/1: Invited Speaker Session TOP

Electromagnetics

Room: [A2](#)

Chair: [Lars Jonsson](#) (KTH Royal Institute of Technology, Sweden)

14:50 A Holy Grail Quest: The Concept of Stored Electromagnetic Energy

[Guy Vandebosch](#) (Katholieke Universiteit Leuven (KU Leuven), Belgium)

The quest for the "final" expressions for the energy stored in a radiator is overviewed. First, the several forms of power and energy that have been defined in electromagnetics over the last 100 years are briefly summarized, and their most important characteristics are discussed. In a first step, frequency domain is considered. Starting from two power balance equations, a field based reactive energy is formally defined and compared to the numerous "definitions" already available in literature. Then the concept of recoverable energy is introduced. Moving to time domain, it is possible to write unifying expressions generalizing the concept of reactive energy. It is shown that recoverable energy is just a special case for a specific future current. Examples are given where these energies can be used to solve practical problems. The paper clearly illustrates that the concept of stored electromagnetic energy is still not well-understood when a radiator is involved.

IS-Wed 2/1: Invited Speaker Session TOP

Electromagnetics

Room: [A3](#)

Chair: [Giovanni Toso](#) (European Space Agency, ESA ESTEC, The Netherlands)

14:50 Computational Electromagnetics in Space

[Erik Jørgensen](#), [Oscar Borries](#), [Min Zhou](#), [Peter Meincke](#), [Stig Sørensen](#), [Niels Vesterdal](#) and [Michael F. Palvig](#) (TICRA, Denmark)

We review a number of CEM algorithms developed for space applications. The algorithms are tailored to the special needs of the space industry through a combination of several approaches, including application of higher-order methods, development of dedicated solvers for specific types of antennas, hybridisation of methods, as well as inclusion of advanced techniques for quantifying uncertainties on the input variables. Application examples will be presented to illustrate the capabilities of the algorithms.

Wednesday, 18 March 16:00 - 18:00

ESoA: ESoA Meeting (16:00-18:00, Room: 5)

16:00 - 18:00 Room: 5

Wednesday, 18 March 16:00 - 16:40

IS-Wed 1/2: Invited Speaker Session

Propagation

Room: A2

Chair: Vittorio Degli-Esposti (University of Bologna, Italy)

16:00 Recent ITU Propagation Models for Millimeter Waves

[Sana Salous](#) (Durham University, United Kingdom (Great Britain))

Fifth generation mobile radio systems are expected to use a variety of techniques and frequencies toward providing high data rates to the user. This has led to a concerted international effort towards characterizing the radio channel in the higher frequency bands particularly in the frequency range of 24-86 GHz following the World Radiocommunications Conference in November 2015 (WRC15) and the recent allocations in WRC19. This talk gives an overview of radio propagation measurements and models in these frequency bands that have been adopted in ITU recommendations and the international effort towards achieving such models.

IS-Wed 2/2: Invited Speaker Session

Antennas

Room: A3

Chair: Ahmed Kishk (Concordia University, Canada)

16:00 Submm-resolution Photoconductive Connected Array Radars

[Andrea Neto](#) (Delft University of Technology, The Netherlands)

A THz radar can realize images with fine lateral resolutions even with moderate antenna sizes. However, exploiting only limited absolute Bandwidth (BW), state of the art THz radars provide at most a moderate centi-metric range resolutions. Within this paper I will describe the strategy of the Tera Hertz Sensing group to break the mm range resolution limit, aimed at developing radar front ends, at a fraction of the complexity of existing THz radar architectures. This could be achieved by exploiting pulsed Optical-to-THz up/down conversions via Photoconductive Antennas (PCA). Recently the TS Group has demonstrated m-watt power sources in the THz spectrum. The remaining bottle necks are mostly associated to pulse conditioning.

Wednesday, 18 March 17:45 - 23:59

Conference Dinner (Wallmans)

Wallmans Cirkusbygningen, Jernbanegade 8, 1608 København V

17:45: Doors open and welcome drink 18:00 - 18:30: Seating 18:30 - 22:00: Dinner and show 22:00 - 24:00: Nightclub with DJ

Thursday, 19 March

Thursday, 19 March 8:30 - 10:10

T01-A11: Multiband and Wideband Antennas

T01 LTE and Sub-6GHz 5G / Regular Session / Antennas

Room: A2

Chairs: Shih-Yuan Chen (National Taiwan University, Taiwan), Mohammad S. Sharawi (Polytechnique Montreal, Canada)

8:30 Compact Eight-Band Monopole for LTE Mobile Phone

[Ying-Ning Li](#) and [Qing-Xin Chu](#) (South China University of Technology, China)

A compact eight-band monopole for LTE mobile phone is presented. The antenna is mainly composed of a T-shape monopole and a coupled parasitic ground strip which are excited to cover LTE800/GSM850/GSM900 bands. Moreover, three modes of parasitic ground strip contribute to covering the DCS/PCS/UMTS/LTE2300/LTE2500 bands. The merit of the proposed antenna is to cover eight bands in the 2G/3G/4G bands without any lumped-element matching circuit under the condition of $16 \times 46 \times 0.8$ mm³ nonground portion, which is suitable for the wideband LTE mobile phone applications. Good agreement is achieved between the measurement and simulation results.

8:50 Miniaturized Base-station Antenna Element with Sinuously Bent Arms

[Hailiang Zhu](#) and [Yuwei Qiu](#) (Northwestern Polytechnical University, China); [Jinliang Bai](#) (National Key Laboratory of Test Physics and Numerical Mathematics, China); [Pei Zheng](#) (National Key Laboratory of Science and Technology on Test Physics and Numerical Mathematics, China); [Gao Wei](#) (Northwestern Polytechnical University, China)

Miniaturized $\pm 45^\circ$ dual-polarized antenna element for cellular base-station application is proposed. The radiators of the antenna are sinuously folded, reducing the aperture size to $0.27\lambda_0 \times 0.27\lambda_0$, where λ_0 is the wavelength at the center frequency. Despite the compact size, simulated results show that stable radiation pattern, high port and cross-

polarization isolation are archived.

9:10 **Dual-Band Array of Cross-Polarized Vivaldi Antennas for 5G Applications**

[Paula Fernandez-Martinez](#) (University Carlos III de Madrid, Spain); [Sergio Martin-Anton](#) (University Carlos III of Madrid, Spain); [Daniel Segovia-Vargas](#) (Universidad Carlos III de Madrid, Spain)

In this work, a broadband dual-polarized base station array is designed. The 1400MHz-2700MHz band is covered by a single broadband Vivaldi antenna element. The 690MHz-960MHz band is covered by a conventional dipole-like element. The array synthesis has been carried out by time-domain full-wave simulations where excitation is applied to a unit cell embedded in an array. Then, array theory is applied to estimate the far-field of the entire structure. This is computationally efficient, which allows us to optimize the performance of the array with both analytical and numerical approaches.

9:30 **A Wideband Dual-Polarized Antenna with Enhanced Cross-Polarization Discrimination for Base Station Application**

[Jin Jiang](#) and [Qing-Xin Chu](#) (South China University of Technology, China)

A Wideband $\pm 45^\circ$ dual-polarized antenna for base station bands is proposed in this paper. By embedding a pentagonal ring in the square loop dipole and adopting Branch-shaped coupling feeding structure, a wideband impedance bandwidth was achieved. We can also enhance the cross-polarized discrimination (XPD) by adding four vertical parasitic elements. It is shown by simulation and experiment that bandwidth enhanced dual-polarized antenna achieves a wideband of 49.9% (1.64-2.73GHz) for reflection coefficients < -15 dB with an isolation of 28 dB. The enhanced XPD is greater than 20dB in the axial direction and greater than 10dB within $\pm 60^\circ$ at the horizontal plane. A stable gain of 8.34 ± 0.71 dBi over the operating bands and half-power beamwidth of $68.15^\circ \pm 2.75^\circ$, suitable for base station applications.

9:50 **A Broadband Dual-Polarized Dipole Antenna for LTE and 5G Base Station**

[Bingguang Zhong](#) (Shenzhen Sunway Communication Co., Ltd., China)

A novel broadband dual-polarized planar dipole antenna is proposed for LTE/5G base stations. The proposed antenna is composed of two perpendicularly crossed polygon dipoles. Each polygon dipole is excited by a dual T-shaped microstrip feedline that is directly fed by a coaxial cable, making the dual-polarized antenna a completely planar structure. Due to the strong coupling between feedline and dipole antenna, a broad impedance bandwidth can be achieved. It is shown that the dual-polarized antenna has a impedance bandwidth of 66.7% (2.5-5.0 GHz) with return loss >10 dB and an isolation of higher than 20 dB between two polarization input ports. The dual-polarized antenna has a stable antenna gain of 7.7 ± 1.1 dBi from 2.5 to 5.0 GHz for slant $\pm 45^\circ$ polarizations. Simulation results have a good agreement with measurement ones.

Thursday, 19 March 8:30 - 12:20

CS34: IET/AMTA Session: Test and Measurement Challenges for 5G and Beyond

T02 Millimetre wave 5G / Convened Session / Measurements

Room: A3

Chairs: [Tian Hong Loh](#) (UK, National Physical Laboratory, United Kingdom (Great Britain)), [Janet O'Neil](#) (ETS-Lindgren, USA)

8:30 **Antenna Simulation Accuracy vs. Measurement Results of Small Form Factor Device**

[Petri Mustonen](#) and [Olli Talvitie](#) (Radiantum Oy, Finland)

A three-band LTE Cat-M1 PCB antenna is simulated and measured and these results are compared in this paper. Antenna resonance frequency at 700 MHz is matching well with simulations. Above 1.5 GHz resonances have a difference of about 70 MHz. With tuned antenna measured efficiencies are 1 dB worse on average than simulated efficiencies when difference at reflection coefficient is taken into account. Active TRP measurements finally show maximum efficiency difference between simulation and measurement of 2.2 dB. As results show there are some differences between the measurements and simulations. However, these differences are small enough that new design round for the device is not needed and the device can be finished with tuning component changes only.

8:50 **Incident Power Density Assessment Study for 5G Millimeter-Wave Handset Based on Equivalent Currents Method**

[Wang He](#) (Zhejiang University, China); [Lucia Scialacqua](#) and [Alessandro Scannavini](#) (Microwave Vision Italy, Italy); [Zhinong Ying](#) (Sony Coporation, Sweden); [Kun Zhao](#) (Sony Research Center Lund, Sweden & Aalborg University, Denmark); [Bo Xu](#) (Ericsson AB, Sweden); [Carla Di Paola](#) and [Shuai Zhang](#) (Aalborg University, Denmark); [Sailing He](#) (Zhejiang University, China)

When placed on the market, mobile handsets are required to comply with relevant electromagnetic field (EMF) exposure limits. In the millimeter-wave (mmWave) frequency band, human exposure to EMF needs to be evaluated in terms of incident power density (IPD). In this work, the equivalent currents (EQC) method is applied to assess the IPD of a 5G mmWave mobile handset mock-up. The IPDs in the near field (NF) region are obtained using the field data measured in the intermediate field (IF) region with an MVG mmWave spherical measurement system. The results are compared with those obtained by simulations and also with those obtained by reference NF scanning measurements. The agreement between the methods indicates that the EQC method is a promising candidate for the IPD assessment of 5G mmWave handsets.

9:10 **What's in a Name? an Analysis of the True Meaning of MIMO and Beamforming**

[Michael D. Foegelle](#) (ETS-Lindgren, USA)

IEEE 802.11n and LTE made the term MIMO common place in technical literature. The 5G New Radio (NR) is doing the same for the concepts of phased arrays and beam forming. However, in both cases the terms are often used imprecisely at best. At a minimum, this can cause confusion between readers with different specializations, but can also result in arguments and frustration when specific terms are used loosely. This paper will investigate the meaning and background of these and other related terms and how they apply to today's emerging radio technologies.

9:30 **An Assessment of the Radio Frequency Electromagnetic Field Exposure from A Massive MIMO 5G Testbed**

[Tian Hong Loh](#) (UK, National Physical Laboratory, United Kingdom (Great Britain)); [Fabien Héliot](#) (University of Surrey, United Kingdom (Great Britain)); [David Cheadle](#) and [Tom Fielder](#) (National Physical Laboratory, United Kingdom (Great Britain))

Current radiofrequency electromagnetic field (RF-EMF) exposure limits have become a critical concern for fifth-generation (5G) mobile network deployment. Regulation is not harmonized and in certain countries and regions it goes beyond the guidelines set out by the International Commission on Non-Ionizing Radiation Protection (ICNIRP). Using a massive multiple-input-multiple-output (mMIMO) testbed with beamforming capabilities that is capable of mimicking realistic 5G base station (BS) performance, this paper presents an experimental and statistical assessment of its associated RF-EMF exposure within a real-world indoor environment. The mMIMO testbed has up to 128 channels with user-programmable software defined radio (SDR) capability. It could perform zero-forcing precoding after channel state information (CSI) acquisition for different beamforming scenarios with respect to the associated user terminal antenna setups and positions. With 64 active mMIMO transmit antennas, 8 beamforming scenarios have been considered for single-user (SU) and multi-user (MU) downlink communications at different locations. Using a calibrated triaxial isotropic field-probe, the received channel power heat map for each beamforming scenario was acquired and then converted into an RF-EMF heat map. The relevant RF-EMF statistics was evaluated based on the variations of beam profiles and number of users.

9:50 **Coffee Break**

10:20 **EMF Exposure Assessment of Massive MIMO Radio Base Stations Based on Traffic Beam Pattern Envelopes**

[Bo Xu](#), [Davide Colombi](#) and [Christer Törnevik](#) (Ericsson AB, Sweden)

This paper investigates the applicability of the far-field spherical formula to estimate EMF compliance boundaries (exclusion zones) for massive MIMO radio base stations characterized by a large number of antenna elements. Numerical and measurement-based methods were implemented and compared. The results show that knowledge of the traffic beam pattern envelope is sufficient to accurately assess the EMF exposure and determine the compliance boundary for a radio base station product at distances far smaller than the traditional far-field distance.

10:40 **Over-the-air Investigation of Transmitter and Receiver Nonlinear Distortion Using a Mm-Wave MIMO Testbed**

[Hamza Nachouane](#), [Thomas Eriksson](#) and [Koen Buisman](#) (Chalmers University of Technology, Sweden)

In this paper, we evaluate the nonlinear distortion of the transmitter (Tx) and receiver (Rx), separately, of the developed mm-wave testbed at Chalmers University of Technology, MATE, using Over-The-Air (OTA) measurement. The developed testbed has been designed to operate within 27 - 31 GHz frequency range, with 1 GHz analog bandwidth per Tx or Rx. An overview on the system configuration has been provided. In order to evaluate the limitations of the proposed testbed, we have conducted several experiments on nonlinear distortion effects of the constructed Tx and RF frontends.

11:00 **Design and Simulation of a 28 GHz Plane Wave Generator for NR Measurements**

[Sara Catteau](#) (Bluetest AB, Sweden); [Marianna Ivashina](#) (Chalmers University of Technology, Sweden); [Robert Rehammar](#) (Bluetest AB & Chalmers University of Technology, Sweden)

Design constraints for a plane wave generating array antenna at mm-wave frequencies are investigated. Focus is on how to realize the power distribution network and the amplitude tapering of the array element excitation in a cost-effective manner. These are key decisions that need to be made for a plane wave generator. In this paper, we specifically look at a few design solutions which are constrained by practically realizable tapering distributions. It is shown that the best tapering distribution, taking into account the design aspects of a realistic distribution network, is different from the best solution for an ideal radiating aperture. We also briefly discuss the impact of the radiating antenna element and

show that it has a minor impact on the end performance.

11:20 *Fading Channel Emulation for Massive MIMO Testing Using a Conductive Phase Matrix Setup*

[Pekka Kyösti](#) (Keysight Technologies & University of Oulu, Finland); [Petteri Heino](#) (Keysight Technologies Finland oy, Finland)

Functionalities, algorithms, and performances of massive MIMO base stations are should be tested in versatile fading radio channel conditions. Base stations of 5G "New radio" that operate on sub 6 GHz frequency bands typically provide antenna connectors enabling RF cable connection of test devices to the device under test (DUT). Furthermore, the number of DUT antennas is high and consequently the need of fading channel emulator (CE) resources becomes high. An approach can be taken to reduce the number of independent fading channels to be emulated. This can be done by using a phase shifting and combining unit (aka phase matrix unit) in between the DUT and CE. The phase matrix concept in fading emulation, together with its capabilities and limitations, is discussed in this paper.

11:40 *Throughput and Spherical Coverage Performance of mmWave Dual Polarized Antenna Arrays*

[Ali Hazmi](#) (Magister Oy & Huawei Technologies, Finland); [Ruiyuan Tian](#) (Huawei Technologies, Finland)

This paper studies the correspondence between two metrics namely the spherical coverage CDF of array Effective Isotropic Radiated Power (EIRP) and the link-level throughput when the same mmWave antenna arrays are considered at the user equipment. The CDF of array EIRP is a convenient metric to use when ordering the performance of two antenna array designs in the spherical coverage perspective. However, for the end user experience, the end-to-end throughput link-level metric taking into account the full base station, channel and user equipment is needed. This paper shows the correspondence of these two metrics in the case of diversity performance evaluation of different antennas array configurations. However for MIMO throughput, the CDF of array gain cannot be exclusively used to classify the performance of different antenna array designs and a full link-level evaluation is still required.

12:00 *5G Over-the-Air Conformance Testing*

[Jonas Fridén](#) and [Sam Agneessens](#) (Ericsson AB, Sweden); [Aidin Razavi](#) (Ericsson Research, Sweden); [Aurelian Bria](#) (Ericsson, Sweden); [Torbjörn Elfström](#) (Ericsson AB, Sweden)

5G base station conformance testing has recently been adopted in 3GPP specifications both in form of conducted and radiated requirements. The option of over-the-air testing of multi-standard active antenna systems (AAS) base stations over-the-air has come with a set of challenges and changes in the requirements definitions. Equivalent Isotropic Radiated Power (EIRP) and Total radiated Power (TRP) have become main figures of merit for a system that aims to combine radios and antenna elements into one enclosure, without access to any physical antenna ports. The evolution from conducted to radiated requirements is presented, together with challenges faced along the way.

Thursday, 19 March 8:30 - 10:10

T02-P02: Millimetre-wave Propagation Modelling TOP

T02 Millimetre wave 5G / Regular Session / Propagation

Room: B1

Chairs: [Marcelo S. Alencar](#) (Federal University of Campina Grande & Institute for Advanced Studies in Communications, Brazil), [Sajjad Hussain](#) (National University of Sciences and Technology, Pakistan)

8:30 *Performance Comparison of Single- And Multi-Lobe Antenna Arrays in 5G Urban Outdoor Environments at mm-Waves via Intelligent Ray Tracing*

[Yanki Aslan](#) and [Jan Puskely](#) (Delft University of Technology, The Netherlands); [Antoine Roederer](#) (Technical University of Delft, The Netherlands); [Alexander Yarovoy](#) (TU Delft, The Netherlands)

The effect of forming single and multi-lobe beam patterns at mm-wave base station antennas on the received signal strength and co-channel interference is studied for mm-wave urban outdoor environments. A sample, simplified urban city model is used with randomly selected user positions. Ray tracing simulations are performed to analyze the channel's directional characteristics towards the test users. Depending on the number of dominant paths, single or multiple main lobes are created in the appropriate directions. Through the simulations, it is observed that in comparison with the multi-lobe beam option, the single-lobe beam provides similar or better received power results (unless the ray phases are equalized at the transmitter or receiver with perfect channel information or there is an unexpected sudden blockage in the main path), while providing better interference cancellation capabilities towards other co-channel users.

8:50 *A Dynamic Visibility Algorithm for Ray Tracing in Outdoor Environments with Moving Transmitters and Scatterers*

[Sajjad Hussain](#) (National University of Sciences and Technology, Pakistan); [Conor Brennan](#) (Dublin City University, Ireland)

This paper presents an efficient technique to identify surfaces which are visible to a mobile transmitter in outdoor environments with moving scatterers. The presence of moving scatterers or a mobile transmitter in a propagation environment makes the radio channel modelling very challenging as visibility computations need to be repeatedly performed in a changing scenario. This makes the pre-processing overhead unfeasible for ray-tracing based propagation prediction models. The algorithm described in this paper first computes the static visibility table for the mobile transmitter assuming that the environment is static. Then the effects of moving scatterers are modelled to compute the so-called dynamic visibility table. Both the static and dynamic visibility tables are used along with information about the scatterers' location to validate the rays arriving at the receiver. Validation results show a considerable reduction in run times.

9:10 *Analysis of 60-GHz In-street Backhaul Channel Measurements and LiDAR Ray-based Simulations*

[Mohammed Zahid Aslam](#) and [Yoann Corre](#) (SIRADEL, France); [Jakob Belschner](#), [Gnana Soundari Arockiaraj](#) and [Monika Jäger](#) (Deutsche Telekom AG, Germany)

The large gains provided by millimeter-wave (mmWave) frequencies in terms of available bandwidth have made them a popular choice to be included in different standards like the 5G-NR and IEEE 802.11ay. Although mmWave frequencies offer an opportunity for large capacities, they face many challenges related to the propagation channel such as strong blockage or attenuation losses. In this paper, 60 GHz in-street backhaul propagation channel is measured and evaluated along with ray-based simulations in two different scenarios; urban canyoning and residential. The channel sounder allows for bi-directional path-loss measurements with highly-directive beamforming at both sides. And the simulator takes benefit from highly accurate LiDAR point cloud data in order to identify the obstacles and compute losses along the direct and indirect paths. Both the measurements and simulations show strong channel sparsity when antennas are located at 3 meters above the ground, caused by the many in-street obstacles.

9:30 *On a Fresnel-Integrals-Based Back-Scattering Model at Millimeter-Waves*

[Adrián Lahuerta-Lavieja](#) (KU Leuven, Belgium); [Martin Johansson](#) (Ericsson Research, Sweden); [Ulf Gustavsson](#) (Ericsson AB, Sweden); [Guy Vandenbosch](#) (Katholieke Universiteit Leuven (KU Leuven), Belgium)

Geometry-based stochastic channel models (GSCMs) are suitable models at millimeter-wave (mm-wave) frequencies. Proper forward-scattering and back-scattering modeling is needed in order to realize realistic channel assessments. In this paper, a recently-proposed back-scattering model, 3D Fresnel, goes through further investigations: first, the impact of frequency in the results of a single scenario is investigated and, second, the effect of multiple surfaces is studied. In both cases, the model shows good agreement with respect to the Physical Optics (PO) reference model.

9:50 *Cell-Free at Millimeter Wave Frequency Simulation Using the Ray Tracing Method*

[Higo Thaian Pereira da Silva](#) (Federal University of Campina Grande, Brazil); [Rafael M. Duarte](#) (Universidade Federal de Campina Grande, Brazil); [Marcelo S. Alencar](#) (Federal University of Campina Grande & Institute for Advanced Studies in Communications, Brazil); [Wamberto Queiroz](#) (Universidade Federal de Campina Grande, Brazil)

In cell-free (CF) networks, a large number of distributed access points (APs) provides communication to a small number of users using the same time-frequency resources. This work presents results related to a CF network at millimeter wave spectrum (mmWave), with carrier frequency of 26 GHz, using a 3D ray tracing simulation. The applied ray tracing simulation is based on the Shooting-and-Bouncing Rays (SBR) method. The propagation environment is based on the Bessa neighborhood in the João Pessoa city, Brazil. As results, are presented a path loss characterization of the considered sites and the computation of achievable rate in the simulated CF networks. The simulation results show that the CF architecture can provide a mean achievable rate of 2.8 bits/s/Hz and 50% of users experience rates greater than 2.6 bits/s/Hz.

Thursday, 19 March 8:30 - 12:20

CS46: New Trends in Leaky Wave Antennas TOP

T11 Fundamental research and emerging technologies / Convened Session / Antennas

Room: B2

Chairs: [Filippo Capolino](#) (University of California, Irvine, USA), [David R. Jackson](#) (University of Houston, USA)

8:30 *Broadside Radiation Equalization Through Mode Coupling Balancing in Periodic Leaky-Wave Antennas*

[Amar Al-Bassam](#) and [Dirk Heberling](#) (RWTH Aachen University, Germany); [Christophe Caloz](#) (Ecole Polytechnique de Montreal, Canada)

Periodic leaky-wave antennas (P-LWAs) may be optimized by equalizing the resonance frequencies of the two radiation modes and their quality factors, i.e., by full-filling the frequency-balancing and Q-balancing conditions. These conditions may be achieved by introducing a proper amount of asymmetry in the unit cell of the P-LWA. This paper extends the previously report circuital perspective to a full-wave electromagnetic perspective. Specifically, it shows that the required Q-balancing condition corresponds to complete coupling between the longitudinal and transverse modes, which leads to their perfect coalescence. Finally, it illustrates the theory by the numerical example of a series-fed patch (SFP) P-LWA.

8:50 *Open-Stopband Suppression in a Canonical 1-D Periodic 2-D Structure with Asymmetric Unit Cell*

[Paolo Baccarelli](#) (Roma Tre University, Italy); [Paolo Burghignoli](#), [Davide Comite](#), [Walter Fuscaldo](#) and [Alessandro Galli](#) (Sapienza University of Rome, Italy)

Periodic leaky-wave antennas are typically affected by the open-stopband (OSB) problem, i.e., the pattern degradation as the beam scans through broadside. Over the years, various techniques have been proposed to mitigate, or even suppress, this longstanding issue. However, most of these techniques cannot be easily applied to 1-D periodic 2-D structure. Recently, it has been theoretically and experimentally shown that the OSB can be suppressed by means of a very simple technique: it consists of designing a unit cell with two unequal discontinuities suitably spaced one another. In this work, we apply this novel technique to a canonical 1-D periodic 2-D structure, namely a grounded dielectric slab with a metal strip grating on top. To validate the concept, full-wave results are presented in the 17.5-20.5 GHz band considering an asymmetric unit-cell characterized by two narrow strips for the TM-polarized case.

9:10 *Reconfigurable Leaky-wave Antennas with Independent Control of the Leakage Constant and Radiation Angle*

[Minseok Kim](#) and [George V. Eleftheriades](#) (University of Toronto, Canada)

This work proposes a reconfigurable leaky-wave antenna that can dynamically and independently control (a) its radiation angle (including broadside) and (b) the leakage constant at the fixed operating frequency of 5 GHz. This is achieved by realizing a reconfigurable omega-bianisotropic Huygens' metasurface and integrating it to the design of a leaky-wave antenna in a waveguide environment. In particular, by synthesizing the Huygens' metasurface in terms of four cascaded tunable impedance layers, we realize a dynamic control over the constitutive parameters of the Huygens' metasurface. As a result, unwanted Floquet modes and any open-stopband are suppressed while dynamically controlling the leakage constant and the radiation angle. The proposed reconfigurable Huygens' metasurface consists of cascaded arrays of dual-loop unit cells which incorporate varactor diodes for obtaining the necessary tunability. The versatile scanning capability of the proposed reconfigurable leaky-wave antenna is numerically studied based on full-wave simulations.

9:30 *Latest Developments and New Design Approaches in Designing Leaky-wave Antennas Based on Substrate Integrated Waveguide Technology*

[Anirban Sarkar](#) (School of Electrical and Electronics Eng., Chung-Ang University, Korea (South)); [Sungjoon Lim](#) (Chung-Ang University, Korea (South))

In this paper, the new findings in designing high gain, compact, larger beam scanning range and highly efficient leaky-wave antennas based on substrate integrated waveguide (SIW) since last few years are proposed. The utilization of SIW in various ways not only eliminates the drawbacks of metallic waveguide but also found suitable for integrating with microwave or mm-wave circuitry with reduced fabrication cost and complexity. Initially, the structural advantages of SIW in designing high gain and polarization diversity LWAs are presented. Further, exploitation of 1D-asymmetric half-mode SIW, quarter-mode SIW and 2D-asymmetric eighth-mode SIW in the design results into significant improvement of gain and radiation efficiency keeping the geometry much compact. Several analysis and antenna parameters are optimized by validating the response of HFSS full-wave simulation with ADS circuit simulator.

9:50 *Recent Advances in Magnet-less Non-reciprocal Leaky Wave Antennas*

[Ohad Silbiger](#) and [Yakir Hadad](#) (Tel-Aviv University, Israel)

We explore nonreciprocal leaky modes and nonreciprocal leaky wave antennas that are based on spatiotemporal modulation of the guiding structure. Thus, enabling an isolation between transmit and receive channels by the antenna itself, and without the need for bulky magnetized materials. Since it involves only with modulation of the guiding structure, and does not require peculiar material properties such as gyrotropy, this approach is moreover applicable for nonreciprocal acoustic leaky wave antennas.

10:10 *2-D Planar Leaky-wave Antenna with Fixed Frequency Beam Steering Through Broadside*

[Victoria Gómez-Guillamón Buendía](#) (Heriot-Watt University, United Kingdom (Great Britain)); [Davide Comite](#) (Sapienza University of Rome, Italy); [Symon K. Podilchak](#) (Heriot-Watt University, United Kingdom (Great Britain)); [Maksim Kuznetsov](#) (Heriot Watt University, United Kingdom (Great Britain)); [Alois Freundorfer](#) (Queens University, Canada); [Yahia Antar](#) (Royal Military College of Canada, Canada)

A simple two-dimensional (2-D) leaky-wave antenna (LWA) system for continuous beam steering through broadside at a fixed frequency is presented. In particular, the implementation of a "bull-eye" LWA and by using the integrated and extremely tunable feed defined by four surface-wave launchers (SWLs), one can achieve limited gain degradation at broadside while also offering beam steering in elevation and azimuth planes in the farfield. Measurements results show beam scanning in both planes at 20 GHz with gain values of almost 10 dBi at broadside. Such a novel system, which offers low-cost fabrication with directive broadside radiation, may be useful for radar, satellite systems and other telecommunication applications.

10:30 Coffee Break

11:00 *Controlling Dual Polarization with Metasurface Leakage*

[Alice Benini](#) and [Enrica Martini](#) (University of Siena, Italy); [Charlotte Tripon-Canseliet](#) (Université Pierre et Marie Curie, France); [Jean-Maurice Chazelas](#) (Thales Aerospace Division, France); [Stefano Maci](#) (University of Siena, Italy)

This paper presents a low profile planar dual polarized metasurface (MTS) antenna consisting of alternating lines of dipoles and slots. This configuration allows for high polarization purity and excellent decoupling between adjacent channels. This makes the structure suitable for applications like 5G and Satcom with polarization diversity and beam scanning. A preliminary design in Ka band is presented to demonstrate the concept.

11:20 *Leaky-Wave Analysis of an Ultrathin Planar High Impedance Surface Antenna*

[Ahmad T. Almutawa](#) (PAAET, Kuwait); [Filippo Capolino](#) (University of California, Irvine, USA)

High impedance surfaces (HISs) have been used in the past to act like artificial magnetic conductors to improve the efficiency of a dipole parallel to a metallic surface. We demonstrate how such HISs can be directly used as antennas without the need for a dipole on top. The HIS is made of 2D periodic dogbone-shaped patches on top of an extremely thin grounded substrate with a thickness around 1/100 of a wavelength. The analysis of a unit cell of the HIS antenna in terms of its magnetic resonance (zero phase reflection) gives sufficient information on the radiation of the HIS operating as a leaky-wave antenna with large attenuation constant. We implement a fast and simple method based on Floquet-Bloch periodic boundary conditions (PBCs) to design and optimize the radiation properties of such an antenna. Despite being extremely flat, the HIS antenna provides a significantly large relative gain-bandwidth exceeding 15%.

11:40 *Electronically-Tunable Scanning Antennas by Using Slotted Rectangular Waveguides Loaded by Reconfigurable Surface Susceptances*

[Santi Concetto Pavone](#) (Università degli Studi di Catania, Italy); [Loreto Di Donato](#) and [Gino Sorbello](#) (University of Catania, Italy)

In this paper, we present a simple technique to achieve electronically-controlled beam scanning, by properly acting on the exhibited average surface susceptances placed in correspondence of the sidewalls of a slotted rectangular waveguide. Such an approach allows to avoid the surface susceptance spatial modulation, thus it inherently simplifies the active elements biasing-network design. The preliminary results in the case of a 1D traveling-wave array demonstrates the concept and paves the way for the full development of 2D scanning arrays and for surface reactance synthesis by means of active elements, such as PIN diodes.

12:00 *Cylindrical Aperture Synthesis with Metasurfaces*

[Faris Alsolamy](#) (University of Michigan Ann Arbor, USA); [Anthony Grbic](#) (University of Michigan, Ann Arbor, USA)

A general method to realize arbitrary, azimuthally-invariant aperture fields using a metasurface is presented. The metasurface, consisting of cascaded inhomogeneous electric sheet impedances, is placed within a cylindrical waveguide to generate specified aperture fields through mode conversion. The surface impedance profiles of the electric sheets are found using optimization. Rapid optimization is enabled by modal network theory, and the Discrete Hankel Transform (DHT). As an example, a radially polarized Gaussian beam launcher is designed.

12:20 *Holographic-Based mmW-Wideband Bidirectional Frequency Scanning Leaky Wave Antenna*

[Ali Araghi](#) (University of Surrey, United Kingdom (Great Britain)); [Mohsen Khalily](#) (University of Surrey & 5G Innovation Centre, Institute for Communication Systems (ICS), United Kingdom (Great Britain)); [Pei Xiao](#) and [Rahim Tafazolli](#) (University of Surrey, United Kingdom (Great Britain))

Utilizing the holography theory, a bidirectional wideband leaky wave antenna in the millimetre wave (mmW) band is presented. The antenna includes a printed pattern of continuous metallic strips on an Alumina 99.5% sheet, and a surface wave launcher (SWL) to produce the initial reference waves on the substrate. To achieve a bidirectional radiation pattern, the fundamental TE mode is excited by applying a Vivaldi antenna (as the SWL). The proposed holographic-based leaky wave antenna (HLWA) is fabricated and tested and the measured results are aligned with the simulated ones. The antenna has 22.6% fractional bandwidth with respect to the central frequency of 30 GHz. The interference pattern is designed to generate a 15 deg backward tilted bidirectional radiation pattern with respect to the normal of the hologram sheet. The frequency scanning property of the designed HLWA is also investigated.

CS44: Near-Field Focusing and Pulse Generation Through Localized Waves

T11 Fundamental research and emerging technologies / Convened Session / Antennas

Room: B4

Chairs: [Matteo Albani](#) (University of Siena, Italy), [Walter Fuscaldo](#) (Sapienza University of Rome, Italy), [Santi Concetto Pavone](#) (Università degli Studi di Catania, Italy)

8:30 *Engineering the Realizations of Localized Waves with Independently Addressable Pulse Driven Arrays*

[Richard Ziolkowski](#) (University of Technology Sydney, Australia & University of Arizona, USA)

The various descriptions of localized wave solutions of the wave equation and Maxwell's equations are briefly reviewed. The generation of these space-time coupled fields from independently addressable pulse driven arrays is discussed. Important aspects of pulse driven array elements and their impact on the overall performance of a pulse driven array is emphasized. It is further described that many of the exotic properties associated with launched localized waves can be realized with these arrays.

8:50 *Terahertz X-wave Launchers by Metallic Spline-Profiled Horns*

[Srđan Paković](#) (Université de Rennes 1, France); [Nicola Bartolomei](#) (University of Rennes 1, France); [Mauro Ettore](#) (University of Rennes 1 & UMR CNRS 6164, France); [Ronan Sauleau](#) (University of Rennes 1, France); [David González-Ovejero](#) (Centre National de la Recherche Scientifique - CNRS, France)

This paper describes the design of a novel X-wave launcher in the terahertz frequency range. The theoretical background of X-waves and the basic design rules for synthesizing X-wave launchers are presented. The proposed launcher consists of a spline profiled metal horn, it is solely made of metal and can thus be easily scaled for operation in different frequency bands. The performance of the launcher has been analyzed by an in-house mode-matching based tool and validated using full-wave simulations. Finally, the performance of the launcher are compared to other solutions present in the literature.

9:10 *An Overview of the Techniques to Generate Limited-diffractive Bessel Beams and Localized Pulses by Using RLSA and Leaky-Wave Antennas*

[Santi Concetto Pavone](#) (Università degli Studi di Catania, Italy); [Walter Fuscaldo](#) (Sapienza University of Rome, Italy); [Alessandro Galli](#) (Sapienza University of Rome 1, Italy); [Matteo Albani](#) (University of Siena, Italy)

In this paper, two different but complementary techniques developed to generate limited-diffractive electromagnetic (EM) beams and pulses by using radial line slot arrays (RLSA) and leaky-wave (LW) planar devices at microwaves/millimeter waves are presented. In the first part of the paper, two kinds of RLSA Bessel beam launchers are proposed, obtained by implementing an inward cylindrical traveling-wave aperture distribution in the longitudinal and transverse electric field components. Moreover, in the second part, two different LW launchers are presented, namely based on forward and backward leaky-waves.

9:30 *Multi-spot Adaptive Near-Field Focusing Through Transmitting Time-Modulated Arrays*

[Rafael González Ayestarán](#) and [Marcos R. Pino](#) (Universidad de Oviedo, Spain); [Paolo Nepa](#) (University of Pisa, Italy)

A novel approach for Near-Field Focusing is studied, which is based on the Time-Modulated Arrays concept. The latter exploits the adaptation of digital signals to control the radiating properties of an antenna array, hence simplifying the implementation of adaptive arrays with respect to more complex architectures based on high-frequency amplifiers and phase shifters. The price to pay is a strong reduction in the number of degrees of freedom available for synthesis purposes, and whose potential impact is here evaluated. It is especially intended for scenarios where multiple users are present and different frequency channels may be used, with devices to be wirelessly fed and requiring a fast adaptation of the radiating system, for example in applications such as Wireless Power Transfer, IoT or 5G scenarios. Some preliminary tests and results are presented to evaluate the potential of the proposed approach.

9:50 *Space-Fractional Bessel Beams with Self-Healing and Diffraction-Free Propagation Characteristics*

[Aqsa Ehsan](#) and [Muhammad Qasim Mehmood](#) (Information Technology University of the Punjab, Pakistan); [Yee Sin Ang](#) (Singapore University of Technology and Design, unknown); [Lay Kee Ang](#) (SUTD, Malaysia); [Muhammad Zubair](#) (Information Technology University of the Punjab, Pakistan & Singapore University of Technology and Design, Singapore)

In the recent years, fractional-dimensional approach has gained the attention of researchers due to its applications in modeling complex structures. In this paper, we introduce a new class of non-diffracting space-fractional Bessel beam using a new type of solution of the cylindrical wave equation in a fractional-dimensional space. It encompasses the limiting cases of both the ordinary integer-order Bessel beam and the fractional-order Bessel beam. In contrast to the ordinary Bessel beam, the space-fractional Bessel beam can have an arbitrary non-integer dimension that is less than or equal to three. This beam preserves the non-diffracting property of Bessel beam and is also self-healing in nature. The propagation features of this new class of solution are discussed in comparison with ordinary Bessel beams. Beams of these types have evident advantages in the near-field applications such as optical trapping and manipulation.

10:10 Coffee Break

10:40 *Towards 3-D Vector Intensity Focusing of near and Far Fields*

[Giada Battaglia](#) (Università Mediterranea di Reggio Calabria, Italy); [Andrea Francesco Morabito](#) (University Mediterranea of Reggio Calabria, Italy); [Roberta Palmeri](#) (Università Mediterranea of Reggio Calabria, Italy); [Tommaso Isernia](#) (University of Reggio Calabria, Italy)

A new approach to the problem of focusing the intensity of vector fields into a target point (subject to sidelobe constraints elsewhere) is proposed. While allowing the adoption of completely arbitrary array antennas as radiating systems, the method exploits a nested optimization procedure properly acting on both the field polarization on the target point and the array excitations. By so doing, it is able to improve the performances of existing procedures (that usually handle scalar fields) and to deal with both the near-field (NF) and the far-field (FF) focusing problems in complex inhomogeneous 3-D media.

11:00 *Field Focusing for Nanophotonic Engineering and Applications*

[Loreto Di Donato](#) (University of Catania, Italy); [Davide Rocco](#) (Università degli Studi di Brescia, Italy); [Gino Sorbello](#) (University of Catania, Italy); [Costantino De Angelis](#) (Università degli Studi di Brescia, Italy)

We propose a new strategy to deal with second harmonic generation (SHG) in dielectric bow-tie antennas by properly focusing the field inside the antenna's gap. This is conveniently done via convex optimization techniques which ensure global optimal solution for both scalar and vector fields. For the sake of simplicity we consider such a problem in 2D geometry dealing with parallel (TE) and orthogonal polarization (TM) of the electric field.

11:20 *Frequency-Scanned Focused Leaky-Wave Antennas for Direction-of-Arrival Detection in Proximity BLE Sensing Applications*

[Miguel Poveda-Garcia](#) (Technical University of Cartagena, Spain); [Alejandro Gil Martinez](#) (Technical University of Cartagena Cartagena, Spain); [Jose-Luis Gómez-Tornero](#) (Polytechnic University of Cartagena, Spain)

The synthesis of monopulse functions in the Fresnel region for Direction-of-Arrival (DoA) detection in proximity sensing applications, based in the use of near-field focused leaky-wave antennas (LWA), is presented in this work. It is demonstrated that, using the three advertising channels provided by the Bluetooth Low Energy (BLE) protocol: channel #37, #38 and #39 at the frequencies 2.402, 2.426 and 2.48 GHz, respectively, the focusing technique allows for obtaining well-defined radiation patterns in the vicinity of the antenna, which properly overlap to obtain monopulse functions. This is not possible with conventional far-field focused antennas, in which the radiation pattern is very distorted in the near-field region, as it is shown in the work. Also, the limits of this near-field focused antennas are discussed

11:40 *3-D Printed Terahertz Lens for Generation of Non-diffractive Bessel Beam Carrying OAM*

[Gengbo Wu](#), [Ka Fai Chan](#) and [Chi Hou Chan](#) (City University of Hong Kong, Hong Kong)

A novel 3-dimensional (3-D) printed lens for high-order Bessel beam generation operating at 300 GHz is proposed in this paper. The designed terahertz (THz) lens can transform the spherical wave-front from the feed horn into non-diffractive Bessel beam carrying orbital angular momentum (OAM). The lens consists of discrete dielectric posts, whose height can be tuned from pixel to pixel to realize the desired aperture phase distribution. Furthermore, 3-D printed technology is used to fabricate the lens with low cost. Measured results demonstrate that the designed 3-D printed lens can generate THz non-diffractive Bessel vortex beam carrying OAM.

CS25: Convergence of Mobile Radio and Radar

T08 Positioning, localization & tracking / Convened Session / Propagation

Room: B5

Chairs: [Thomas Dallmann](#) (Fraunhofer Institute for High Frequency Physics and Radar Techniques FHR, Germany), [Reiner S. Thomä](#) (Ilmenau University of Technology, Germany)

8:30 *Towards Joint Sensing and Communication for 5G and Beyond Systems*

[Andrea Massa](#) and [Paolo Rocca](#) (University of Trento, Italy); [Marco Salucci](#) and [Nicola Anselmi](#) (ELEDIA Research Center, Italy)

The acquisition of an accurate channel model through an high-resolution environmental sensing is of crucial importance for future multiple-input multiple-output (MIMO) systems. Nevertheless, nowadays MIMO beam-forming networks perform the channel sensing through pilot signal transmission, using sets of orthogonal beams, therefore a non optimal sensing of the channel is acquired. For this reason, a novel mobile communication paradigm is presented in this work as the joint synthesis of the sensing and communication beams, in order to enable (i) high channel capacity through capacity-driven synthesis of the communication beams, and (ii) high resolution modeling of the channel through dedicated beam patterns synthesized for optimal sensing performances.

8:50 *An OCDM Radar-Communication System*

[Lucas Giroto de Oliveira](#), [Mohamad Basim Alabd](#) and [Benjamin Nuss](#) (Karlsruhe Institute of Technology, Germany); [Thomas Zwick](#) (Karlsruhe Institute of Technology (KIT), Germany)

This study investigates a Radar-Communication (RadCom) system based on the orthogonal chirp-division multiplexing (OCDM) scheme, which is introduced as an alternative to its counterpart based on orthogonal frequency-division multiplexing (OFDM). In this context, a description of the system model addressing both communication data obtaining and radar image generation features is presented. Next, both the communication and radar aspects of the introduced OCDM RadCom system are compared with the ones of its OFDM counterpart. It is concluded that the introduced system yields lower bit error rate values, while demanding higher computational complexity and presenting higher sidelobe

level than OFDM RadCom.

9:10 ***IQ-Imbalance Compensation for Wideband OFDM-Radar***

[Benedikt Schweizer](#) and [Christina Knill](#) (Ulm University, Germany); [Daniel Schindler](#) (Robert Bosch GmbH, Germany); [Christian Waldschmidt](#) (University of Ulm, Germany)

Orthogonal frequency-division multiplexing is a promising modulation format for future automotive radar sensors. Although it benefits from a simple homodyne transceiver design, it requires quadrature signal generation and evaluation, which suffers from IQ imbalance in transmitter and receiver. This paper describes the effects of IQ-imbalance on OFDM radars in general and demonstrates how digital signal processing techniques can be adopted to mitigate this impairment based on adaptive filtering. The effectiveness of the approach is demonstrated with simulations.

9:30 ***A MIMO Joint Communication-Radar Measurement Platform at the Millimeter-Wave Band***

[Preeti Kumari](#) (UT Austin, USA); [Amine Mezghani](#) (Electrical and Computer Engineering & University of Manitoba, Canada); [Robert Heath](#) (The University of Texas at Austin, USA)

A fully-digital wideband joint communication-radar (JCR) at the millimeter-wave (mmWave) band will simultaneously enable high communication and radar performances with enhanced design flexibility. In this paper, we present a measurement platform with a software-defined architecture to evaluate and demonstrate the performance of these JCR systems using real channel measurements. We develop this platform by extending a mmWave communication set-up with an additional full-duplex radar receiver and by capturing the MIMO JCR channel using a moving antenna on a sliding rail. To characterize the JCR performance, we conduct indoor experiments and apply traditional/advanced processing algorithms on the measured data. The results demonstrate that our testbed at 73 GHz with 2 GHz bandwidth can capture the JCR channel with high range/direction estimation accuracy. The comparison between the communication and radar channel shows the potential for improving JCR performance by exploiting the antenna diversity due to widely-separated communication and radar receivers.

9:50 ***Mutual Over-The-Air Synchronization of Radar Sensors***

[Thomas Dallmann](#) (Fraunhofer Institute for High Frequency Physics and Radar Techniques FHR, Germany)

Over-the-air synchronization of radar waveforms can be used to achieve better interference suppression and enable radar-based communication. Within this initial study, a reformulation of the Kuramoto model is presented, which allows to synchronize the pulse repetition frequencies of two pulsed radar systems. To investigate the applicability of this approach, a simulation model was implemented and tested with various parameter sets. It can be shown that under certain circumstances, the pulse repetition frequencies converge to the same value and thus allow the radars to perceive their interferer as a single echo along range and Doppler.

10:10 **Coffee Break**

10:40 ***System Level Synchronization of Phase-Coded FMCW Automotive Radars for RadCom***

[Franz Lampel](#) (Eindhoven University of Technology, The Netherlands); [Faruk Uysal](#) (Delft University of Technology, The Netherlands); [Recep Firat Tigrek](#) (Eindhoven University of Technology, the Netherlands); [Simone Orru](#) (Delft University of Technology, The Netherlands); [Alex Alvarado](#) (Eindhoven University of Technology (TU/e), The Netherlands); [Frans MJ Willems](#) (Technical University Eindhoven, The Netherlands); [Alexander Yarovoy](#) (TU Delft, The Netherlands)

This paper describes an FMCW based radar and communication (RadCom) system and addresses the challenges in the synchronization of multiple units for communication functionality. We proposed a novel technique to detect the FMCW RadCom signal at the communication receiver and derive the detection and false alarm probabilities of it. Moreover, to achieve fine synchronization between transmit and receive devices, a novel approach based on FMCW RadCom signal time of arrival estimation is proposed. The potential capability of a RadCom system is experimentally demonstrated for the first time by a set of automotive-grade mmWave radars with GPS-based synchronization.

11:00 ***Performance of OFDMA Resource Scheduling in Joint Mobile Radio and Radar Networks***

[Steffen Schieler](#) (Ilmenau University of Technology, Germany); [Michael Döbereiner](#) (Technische Universität Ilmenau & Fraunhofer IIS, Germany); [Reiner S. Thomä](#) and [Christian Schneider](#) (Ilmenau University of Technology, Germany); [Giovanni Del Galdo](#) (Fraunhofer Institute for Integrated Circuits IIS & Technische Universität Ilmenau, Germany)

In this paper, we study the impact of time-frequency resource scheduling on the performance of an OFDM radar receiver for joint mobile radio and radar networks. Our results illustrate how the distribution of resources in the time-frequency grid, as used for OFDMA, affects the cost function of a maximum-likelihood estimator. Based on our results, we provide a simple set of rules for the design of resource scheduling schemes in joint networks. Furthermore, we reveal that an OFDM radar can benefit from multiple algorithms and procedures already employed in mobile communication standards, such as synchronization and error correction.

11:20 ***Stepped-Carrier OFDM V2V Resource Allocation for Sensing and Communication Convergence***

[Musa Furkan Keskin](#), [Canan Aydogdu](#) and [Henk Wymeersch](#) (Chalmers University of Technology, Sweden)

Stepped-carrier orthogonal frequency division multiplexing (OFDM) radar is a promising low-cost alternative to conventional OFDM radar for automotive applications due to its capability to provide high resolution with low-rate analog-to-digital converters (ADCs). In this paper, we investigate centralized time-frequency resource allocation strategies in vehicular networks for vehicle-to-vehicle (V2V) sidelinks employing stepped-carrier OFDM waveform for joint radar sensing and communications. To quantify radar-communication performance trade-offs, we formulate a nonlinear integer programming problem for weighted optimization of radar accuracy and communication spectral efficiency, and perform Boolean relaxation to obtain an efficiently solvable convex program. Simulation results demonstrate radar-optimal and communication-optimal operation regimes, providing insights into time-frequency weightings along the trade-off curve.

11:40 ***Accuracy Requirements for Cooperative Radar with Sensor Fusion***

[Mehdi Ashury](#) (TU Wien, Austria); [Christian Eliasch](#) (Vienna University of Technology, Austria); [Thomas Blazek](#) and [Christoph F Mecklenbräuer](#) (TU Wien, Austria)

Reliability and robustness are the essential requirements for automotive radar systems. However an automotive radar system suffers from environmental conditions and interference. Applying a proper radar data fusion algorithm can significantly increase the detection probability and robustness. This article investigates the accuracy requirements based on the geometric parameters for cooperative radar sensors with central sensor fusion. The results show that a radar sensor fusion for cooperative radar can increase the detection probability and therefore the system robustness by using at least two radar sensors. Furthermore, results show that three to four sensors at a minimum distance of ten meters are sufficient for high quality estimation. At the same time the system requirements regarding the accuracy for every single radar sensor can be relaxed to a range accuracy as low as one meter standard deviation.

12:00 ***Physical Modeling for Device-Free Localization Exploiting Multipath Propagation of Mobile Radio Signals***

[Martin Schmidhammer](#), [Michael Walter](#), [Christian Gentner](#) and [Stephan Sand](#) (German Aerospace Center (DLR), Germany)

This work proposes a model to describe the impact of a target on the received power of a multipath component (MPC). The physical propagation path of an MPC is decomposed geometrically and is described by direct propagation paths between physical and virtual nodes. Using the scalar theory of diffraction, the impact of a target on the electric field can be calculated for each component, individually. Thereby, the model relates alternations of the received power of MPCs to the location and orientation of the target, which allows device-free localization systems to exploit multipath propagation. The model is evaluated for a single link scenario of one specular reflection. A comparison of modeled attenuation results to wideband measurement data qualitatively confirms the applicability of the proposed model representing target-induced attenuation.

T05-A12/2: Point of Care Microwave Sensors

T05 Biomedical and health / Regular Session / Antennas

Room: B6

Chairs: [Robin Augustine](#) (Uppsala University, Sweden), [Joseph Costantine](#) (American University of Beirut, Lebanon)

8:30 ***Handheld, Broadband Transmission-Based Probe - The Next Star Trek Tri-Corder***

[Paul M Meaney](#) (Dartmouth College, USA); [Robin Augustine](#) (Uppsala University, Sweden); [Timothy Reynolds](#) (Dartmouth College, USA)

We have developed a portable, side-by-side transmission dielectric probe that could have substantial clinical applications. This invention builds on three novel concepts that allow deep signal penetration over a very broad bandwidth: the larger aperture coaxial aperture, transmission mode utilizing adjacent open-circuit coaxes, and narrowing of the apertures in the co-localized plane. These act to enhance penetration and focus the beam within a narrow plane. They are also dramatically unsusceptible to multipath signal corruption due to the close proximity of the transmitting and receiving apertures. The new design has been shown to operate from 100 MHz to 6 GHz, is not susceptible to motion of the connecting cables and can sense property aberrations at over 2 cm depth. These features are in stark contrast to the more ubiquitous and commercially available reflection-based dielectric probes. We have exploited 3D printing technology to develop geometries that can maximize performance and user convenience.

8:50 ***An NRW Extension for Dielectric Characterization of Arbitrary Length Low-Loss Materials***

[Hassan Shwaykani](#), [Joseph Costantine](#) and [Ali El-Hajj](#) (American University of Beirut, Lebanon); [Mohammed Al-Husseini](#) (Beirut Research and Innovation Center, Lebanon)

In this paper, we propose an extension for the Nicolson-Ross-Weir (NRW) method that enables the retrieval of the electrical parameters of low-loss materials that are thicker than one-half wavelength ($\lambda/2$). The proposed extension overcomes the NRW intrinsic limitation that causes a divergence of results at frequencies where the material thickness is an integer multiple of $\lambda/2$. The method is tested on different sample materials, and is proven to provide a stable permittivity estimation, with no divergence at frequencies corresponding to integer multiple of $\lambda/2$.

9:10 ***Clustering of Dielectric and Colour Profiles of an Ex-vivo Burnt Human Skin Sample***

[Pramod K B Rangaiah](#) (Researcher & Uppsala University, Sweden); [Javad Ebrahimizadeh](#) (University of Uppsala, Sweden); [Abhishek Honganally Nagaraju](#) (Uppsala University & Uppsala, Sweden); [Irina El-Ali](#) and [Mokhtar Kouki](#) (Datamatrix AG, Switzerland); [Bappaditya Mandal](#) (Uppsala University, Uppsala, Sweden); [Fredrik RM Huss](#) (Uppsala University Hospital & Uppsala University, Sweden); [Mauricio D Perez](#) (Uppsala University, Sweden & National Technological University, Argentina); [Robin Augustine](#) (Uppsala University, Sweden)

In this work we introduce two techniques to characterize human burnt skin based on dielectric and colour profiling. The first method is the sectorized measurement of permittivity by using an open-end coaxial probe technique. The second method is the analysis of color variation in the burnt skin sample through image processing. Statistical analysis is done using tools such as Analysis of Variance, k-means, in order to classify the data. As part of the classification, the experimental data are clustered into groups based on the distribution of means and centroids. The color image is converted into a gray image and resized to a one-dimensional array. Furthermore, the analysis is done based on the intensity range, various centroid values, and silhouette analysis. The clustering results we obtained with these two methods can be used for comparing the dielectric characteristics with the color variation of the burnt human skin to assess burn degree.

9:30 Non-Invasive Transmission Based Tumor Detection Using Anthropomorphic Breast Phantom at 2.45 GHz

[Laya Joseph](#) (FTE, Angstrom Laboratory, Lägerhyddsvägen 1 & Uppsala University, Sweden); [Noor Badariah Asan](#) (Uppsala University, Sweden & FKEKK, Universiti Teknikal Malaysia Melaka, Malaysia); [Javad Ebrahimizadeh](#) (University of Uppsala, Sweden); [Arvind Selvan Chezhan](#) (Uppsala University, Sweden); [Mauricio D Perez](#) (Uppsala University, Sweden & National Technological University, Argentina); [Thiemo Voigt](#) (Swedish Institute of Computer Science & Uppsala University, Sweden); [Robin Augustine](#) (Uppsala University, Sweden)

In this paper, we propose the development of semi-solid and stable breast phantom with skin, fat, muscle and spherical tumor models and a transmission-based sensing for tumor detection. The proposed breast phantom emulates the anatomical, physical and electrical properties as human breast tissues. The dielectric properties of the breast phantom tissues are measured using open ended coaxial slim probe from Keysight Technologies in the frequency range of 500 MHz-20GHz. The S21 scattering parameters are measured and studied for a normal breast phantom and breast phantom with tumor models representing its different growth stages using Topology Optimized Planar Antenna (TOPA) based probe. The study shows a detection an S21 amplitude variation of 2 - 12 dB for tumor inclusion models of size from 4mm - 16mm diameter with respect to normal breast model. This study indicates that with further development transmission-based methods can be used for preliminary screening of breast tumor.

9:50 On the Optimal Matching Medium and Working Frequency in EM-based Medical Devices

[Gennaro G. Bellizzi](#) (Erasmus University Medical Center, Italy); [Martina Teresa Bevacqua](#) (Università Mediterranea di Reggio Calabria, Italy)

From an engineering perspective, propagation theory is underlying all electromagnetic-based medical devices development. Optimally selecting the matching medium and the operating frequency has a pivotal role in terms of technical as well as clinical efficiency of such devices. However, sub-optimal, yet easy to realize, working conditions are usually adopted without taking into account some important aspects of propagation theory. In this contribution, we propose an innovative approach for optimally determining both the matching fluid and the working frequency in an optimal fashion. Even if application-independent, it is tested and assessed within the framework of hyperthermia: an adjuvant oncologic thermal therapy consisting in the deposition of electromagnetic power in the tumor to increase its temperature.

10:10 Coffee Break

10:40 Low Profile Implantable Antenna for Fat Intra-Body Communication

[Bappaditya Mandal](#) (Uppsala University, Uppsala, Sweden); [Laya Joseph](#) (FTE, Angstrom Laboratory, Lägerhyddsvägen 1 & Uppsala University, Sweden); [Javad Ebrahimizadeh](#) (University of Uppsala, Sweden); [Mauricio D Perez](#) (Uppsala University, Sweden & National Technological University, Argentina); [Debasis Mitra](#) (Indian Institute of Engineering Science & Technology, Shibpur, India); [Robin Augustine](#) (Uppsala University, Sweden)

A flexible low profile biocompatible implantable antenna for fat intra-body communication is presented. This article gives an idea of fat channel communication at different distances. The antenna is designed on 0.25 mm thick low loss taconic material. The antenna is cover by 0.1 mm thick PDMS (Polydimethylsiloxane) to ensure biocompatibility with human tissue. A coplanar wave (CPW) microstrip line is used to feed the antenna. This antenna has been optimized to operate at the 2.4 GHz ISM band frequency in the human three-layer tissue model. The simulation, as well as measurement, were done at a minimum distance of 10 mm, and the maximum distance of 70mm between of two implantable antennas. The measured path loss of the fat channel by using the proposed implantable antenna is estimated to be almost 2.5 dB per centimetre. The measured bandwidth of the proposed antenna found to be 660 MHz.

11:00 Optimal Probe Geometry for Microwave Monitoring During in-Lab Ex-Vivo Measurements

[Giselle González-López](#) (Universitat Politècnica de Catalunya, Spain); [Susana Amorós García de Valdecasas](#) (Predoctoral Researcher, Spain); [Luis Jofre](#) (Universitat Politècnica de Catalunya, Spain)

In this paper, a 3D printed geometry for optimal ex-vivo in-lab microwave monitoring applications is presented. This geometry is meant to be of use for mimicking the shape and dielectric properties of certain parts of the human body, and to recreate the conditions present during in-field measurements. This geometry is validated through analytic and experimental tests by monitoring an implanted device at different depths inside the set up, and the results are presented.

11:20 Metasurface Sensors for Healthcare Applications

[Antoine Durant](#) (Edinburgh Napier University, United Kingdom (Great Britain) & Université Grenoble Alpes, France); [Celia Lacoste](#) (INP-ENSEEIH University of Toulouse, United Kingdom (Great Britain)); [Erin Donnelly](#) and [Luigi La Spada](#) (Edinburgh Napier University, United Kingdom (Great Britain))

Electromagnetic sensors have received huge attention in the last few years, due to the rising demand of devices able to improve quality, performance and safety in different industrial sectors: both sensing and medical industries are outstanding examples. Despite reliable diagnostic technologies have been developed, some drawbacks are still present: bandwidth, large dimensions and limited response control. Metasurfaces, bi-dimensional engineered materials, represent an optimal solution to overcome such issues enhancing existing systems for an accurate diagnosis. Therefore, in this paper, metasurface-based sensors are proposed and realized by using new additive manufacturing processes. The structures are finally experimentally tested and verified in different medical diagnostic applications, namely: cancer stage recognition, glucose/sugar levels measurements and blood oxygen saturation detection. The high performances shown by such meta-sensors, in terms of selectivity and sensibility, pave a new way to realize advanced platforms for non-invasive, high quality and faster patient diagnosis.

11:40 Multiple-Pole CSRR-based Microwave Sensor for Glucose Levels Detection

[Ala Eldin Omer](#) (University of Waterloo, Canada); [George Shaker](#) (University of Waterloo & Spark Tech Labs, Canada); [Safieddin Safavi-Naeini](#) (University of Waterloo, Canada); [Hamid Kokabi](#) (Laboratory of Electronics and Electromagnetism (L2E), Sorbonne University, Canada); [Georges Alquié](#) (UPMC, France); [Frederique Frederique Deshours](#) (Laboratory of Electronics and Electromagnetism (L2E), Sorbonne University, France)

We propose a microwave biosensor that comprises a rectangular plexiglass channel integrated on a triple-pole complementary split ring resonator structure. The sensor operates in the centimeter-band 1 - 6 GHz and is fabricated on top of a thin FR4 dielectric substrate . The sensor element is excited via a coupled microstrip transmission-line etched on the bottom side of the substrate. The proposed CSRR-based sensor is used as a near-field probe to non-invasively monitor the changes in glucose concentrations in the blood mimicking fluid by tracking the amplitude variations of the harmonic transmission resonances at various concentrations. The fluids are loaded inside a channel representing roughly a blood vessel. The proposed sensor is shown to exhibit higher sensitivity performance compared to the conventional single-pole and other similar sensors in the literature. The sensitivity, reliability and repeatability of the proposed sensor are demonstrated by the in-lab measurements using a Vector Network Analyzer.

Thursday, 19 March 8:30 - 10:10

T06-P09: Propagation for Unmanned Aerial Vehicles (UAVs)

T06 Aircraft (incl. UAV, UAS, RPAS) and automotive / Regular Session / Propagation

Room: B7

Chairs: [Uwe-Carsten G. Fiebig](#) (German Aerospace Center (DLR), Germany), [Fernando Pérez-Fontán](#) (University of Vigo, Spain)

8:30 A USRP-based Channel Sounder for UAV Communications

[Guojin Zhang](#), [Xuesong Cai](#), [Wei Fan](#) and [Gert Pedersen](#) (Aalborg University, Denmark)

The unmanned-aerial-vehicle (UAV) has attracted great interest in both civil and military applications, due to its low cost, flexibility and the ability to establish seamless coverage. In this paper, a Universal Software-defined Radio Peripheral (USRP) based channel sounding system for characterizing the UAV communication channel is introduced, which can be applied in both active and passive measurement campaigns. To investigate the effect of the equipment in the UAV measurement system, measurements were conducted by connecting the two USRP devices directly with a cable. For calibrating the deviation of the crystal oscillator in the system, the post-processing method is proposed in case of the unavailable reference frequency.

8:50 Wideband Channel Measurements and First Findings for Low Altitude Drone-to-Drone Links in an Urban Scenario

[Dennis Becker](#), [Uwe-Carsten G. Fiebig](#) and [Lukas Marcel Schalk](#) (German Aerospace Center (DLR), Germany)

In order to prevent collisions between unmanned aerial vehicles (UAVs) , Drone-to-Drone communication is a promising technology for enabling reliable collision avoidance systems. For a reliable communication system accurate channel models, specifically designed for UAVs in typical environments, are needed. Especially, the urban environment for small UAVs in very low level airspace is challenging due to rich multipath propagation and non-line of sight conditions. In order to model the real world propagation behavior, channel measurements with small UAVs in different urban scenarios are mandatory. So far, no wideband channel model based on measurements for D2D communication has been proposed. Therefore we conducted wideband channel measurements in the C-band. In this paper, we present the scenarios of our campaign and show first findings. With a geometrical signal path simulation we identify where the physical signal paths come from. The measurements reveal that the D2D MPCs scenario is clearly three-dimensional.

9:10 On the Second Order Statistics of 3D Non-Stationary UAV Channels Allowing Velocity Variations

[Yawen Wang](#), [Neng Cheng](#) and [Xiaomin Chen](#) (Nanjing University of Aeronautics and Astronautics, China); [Wei Fan](#) (Aalborg University, Denmark); [Qiuming Zhu](#) and [Weizhi Zhong](#) (Nanjing University of Aeronautics and Astronautics, China)

The level crossing rate and average fading duration are two important statistical properties of channel fading envelope. In this paper, a geometry-based stochastic model for unmanned aerial vehicle (UAV) channel allowing three-dimensional trajectory of the UAV and ground station is proposed. On this basis, the theoretical expressions of level crossing rate and average fading duration are analyzed and derived. Under the UAV high-speed flight scenarios, numerical simulations show that the theoretical results of level crossing rate and average fading time agree well with the simulated and measured ones. The proposed model and derived expressions are very helpful for the design of block interleave and channel coding in UAV communication systems.

9:30 Performance of 5G Terrestrial Network Deployments for Serving UAV Communications

[Zeyu Huang](#) and [José Rodríguez-Piñeiro](#) (Tongji University, China); [Tomás Domínguez-Bolaño](#) (University of A Coruña, Spain); [Xuefeng Yin](#) (Tongji University, China); [Juyul Lee](#) (ETRI, Korea (South)); [David W Matolak](#) (University of South Carolina, USA)

With the recent decrease in their size and cost, the unmanned aerial vehicles (UAVs) have become more accessible for general-purpose applications. A natural way of providing network access to UAVs is to use terrestrial fifth generation (5G) deployments. In this paper, we assess 5G air-to-ground (A2G) links of low-height UAVs in suburban scenarios with system-level simulations. In order to obtain realistic results, we utilized a propagation channel model extracted from actual A2G measurements. We characterized the performance of the communications system by means of throughput results. We also showed the importance of the feedback delay optimization when the UAV flight speed is high, not only for the achievable throughput, but also for the end-to-end transmission delay, which may be crucial in critical communications (e.g., safety related ones).

9:50 Modeling and Simulation for UAV Air-to-Ground mmWave Channels

[Lele Cheng](#) and [Qiuming Zhu](#) (Nanjing University of Aeronautics and Astronautics, China); [Cheng-Xiang Wang](#) (Southeast University & Heriot-Watt University, China); [Weizhi Zhong](#), [Boyu Hua](#) and [Shan Jiang](#) (Nanjing University of Aeronautics and Astronautics, China)

In this paper, we propose a new three-dimensional (3D) channel model for the millimeter wave (mmWave) communication links between the Unmanned Aerial Vehicle (UAV) and vehicle. The new model applies the ray tracing (RT) theory in traditional geometry-based stochastic model (GBSM), and it also takes the specific features of mmWave propagation into account. Meanwhile, the time evolving algorithms of channel parameters, i.e., communication distance, propagation angles, path delays, and powers are analyzed and illustrated. On these basis, the mmWave channel simulations at 28 GHz are conducted under the campus scenario. Simulation results demonstrate that the proposed model can generate the non-stationary Air-to-Ground mmWave channels, of which statistical properties have a good agreement with the measured ones. Therefore, this model is valuable for the system design, performance optimization, and evaluation of UAV mmWave communication systems.

10:10 Micro-UAV Radar Imaging via DGPS and Microwave Tomography

[Giuseppe Esposito](#) (IREA-CNR, Italy); [Carlo Noviello](#) (IREA-CNR & University of Napoli Federico II, Italy); [Giovanni Ludeno](#) and [Gianluca Gennarelli](#) (IREA-CNR, Italy); [Giancarmine Fasano](#) and [Alfredo Renga](#) (University of Naples Federico II, Italy); [Francesco Soldovieri](#) (CNR, Italy); [Ilaria Catapano](#) (IREA-CNR, Italy)

Radar imaging from UAV is becoming a research theme attracting a huge interest for its practical fall-outs. This contribution deals with an ultra-light radar system mounted on a micro drone and presents the results of a proof of concept measurement campaign. Specifically, a Differential Global Position System, synchronized with the radar, is adopted to estimate the location of the measurement points, properly. Moreover, a data processing procedure involving a linear microwave tomographic approach is exploited to obtain a focused image providing an accurate localization of on surface targets.

10:30 Identifying low-RCS Targets Using micro-Doppler High-Resolution Radar in the Millimeter Waves

[Nezah Balal](#) and [Yair Richter](#) (Ariel University, Ariel, Israel); [Yosef Pinhasi](#) (Ariel University, Israel)

In recent years, the use of drones and unmanned aerial vehicles (UAV) have become popular. Delinquent and terrorist agents use these measures to harm the routine of life. Sufficient technology need for detecting and tracking drones in the airspace. The use of existing aircraft detection systems is not possible due to the physical differences between the targets, smaller physical size, lower speed, and lower flight altitude relative to approved aircraft. This paper introduces the characteristics of the unique micro-Doppler signature of drones. After analyzing the radar signal, one can deduce the speed and frequency of the propeller and from these find the length of the drone blade. The measurements were made using the CW radar operating in the W band at frequency 94 GHz. The results clearly show that a unique drone Doppler signature can be identified, and the geometric properties of the drone can be extracted and categorized accordingly.

Thursday, 19 March 8:30 - 12:20

CS30: Fundamental Challenges and Novel Methodologies in the Next-Generation Computational Electromagnetics

T10 EM modelling and simulation tools / Convened Session / Electromagnetics

Room: B8

Chairs: [Zhen Peng](#) (University of Illinois at Urbana-Champaign, USA), [Francesca Vipiana](#) (Politecnico di Torino, Italy)

8:30 Numerical Synthesis of Translation Operators for the Multi-Level Fast Multipole Method

[Arslan Azhar](#) and [Thomas F. Eibert](#) (Technical University of Munich (TUM) & Chair of High-Frequency Engineering (HFT), Germany)

A key operation in the fast multipole method is the translation of propagating plane waves from source groups to observation groups. For calculating the translation functions, the classical approach typically requires an exact knowledge of the system, such as given for the free-space Green's function. The resulting operators are commonly defined over all propagating plane-wave directions on the Ewald sphere. A relatively less explored alternative, however, is a numerical approach in which the translation operators are synthesized from known point to point interactions. This approach also provides an opportunity to reduce the matrix vector multiplication time. It is demonstrated that numerically synthesized translation operators are not only accurate enough but also greatly improve the performance of multi-level fast multipole method based electromagnetic solvers.

8:50 Characteristic Mode Equations for Non-Symmetric Surface Integral Operators

[Pasi Ylä-Oijala](#) and [Henrik Wallén](#) (Aalto University, Finland)

The magnetic field integral operator (MFIO) based characteristic mode formulation for closed perfect electric conductor is considered. Since the MFIO is non-symmetric, we need to consider the eigensolutions of both the MFIO and its transpose operator for a characteristic mode expansion. The eigenvectors of the transpose of the MFIO are shown to be in the dual of the range of the MFIO. Physically, these vectors can be interpreted as the tangential electric field on the surface.

9:10 Analytic Expressions for Matrix Elements of Integral Equation Operators and Aspects of Their Numerical Implementation

[Elizabeth Bleszynski](#) (Monopole Resesarch, USA); [Marek Bleszynski](#), Dr (Monopole Resaearch, USA); [Thomas Jaroszewicz](#) (Monopole Research, USA)

We present extensions of the method of evaluating matrix elements of integral equations with the help of suitably constructed Laplacian-type representations of singular kernels. Such representations allow to convert surface integrals to line integrals involving only non-singular, smoothly varying integrands amenable to numerical evaluation with low order numerical quadratures as well as to analytical evaluation. We present: (a) Construction of revised expressions for the auxiliary functions needed for the Laplacian representations of the tensor and vector Green functions for geometries located on parallel planes. The approach guarantees smoother behavior of these functions in the limit of small separations between the triangular facets. (b) An improved analytic evaluation of double line integrals resulting in analytic expressions significantly simpler and more compact than the ones previously reported. We also discuss the relative merits of the direct numerical and analytic evaluations of these line integrals.

9:30 Reducing the Dimensionality of 6-D MoM Integrals Applying Twice the Divergence Theorem

[Javier Rivero](#) and [Francesca Vipiana](#) (Politecnico di Torino, Italy); [Donald Wilton](#) (University of Houston, USA); [William Johnson](#) (Private Consultant, USA)

In this paper we propose a scheme for evaluating the 6-D interaction integrals appearing in volume integral equation solved with the Method of Moments and tetrahedral elements. We treat as a whole the double volume integral, applying the divergence theorem first on the source domain and then on the test domain. With the proper variable transformation and reordering, the 6-D integrals are expressed as two radial integrals plus four linear integrals over the source and observation domain planes.

9:50 Toward Extremely Scalable IE-DDM for Distributed Computing

[Víctor Martín](#) (Universidad de Extremadura, Spain); [Diego M Solís](#) (University of Pennsylvania, USA); [David Larios](#) (Universidad de Extremadura, Spain); [Luis Landesa](#) (University of Extremadura, Spain); [Fernando Obelleiro](#) (University of Vigo, Spain); [Jose M. Taboada](#) (University of Extremadura, Spain)

In this work, we describe a hybrid MPI/OpenMP parallel implementation of the surface integral equation - domain decomposition method (SIE-DDM) in distributed mixed memory computers for the simulation of extremely large scale and complex problems. The proposed approach greatly reduces the global network communications and memory burden, providing an extremely scalable implementation both in time and, especially, in memory.

10:10 Coffee Break

10:40 Overview of Surface-Volume-Surface Electric Field Integral Equation Formulations for 3-D Composite Metal-Dielectric Objects

[Reza Gholami](#) (University of Toronto & University of Manitoba, Canada); [Shucheng Zheng](#) and [Vladimir Okhmatovski](#) (University of Manitoba, Canada)

The Surface-Volume-Surface Electric Field Integral Equation (SVS-EFIE) has been recently generalized to solution of general scattering and radiation problems for 3D composite objects. These objects can be formed by multiple piece-wise homogeneous dielectric regions which do or do not share common boundaries. Generalization to the composite objects formed by metal and piece-wise homogeneous dielectric regions which share common boundaries has also been demonstrated. Since the SVS-EFIE formulation utilizes only the electric field dyadic Green's functions, it can be extended to the case of composite objects situated in non-magnetic planar multilayered media by casting its operators into the mixed-potential form using classical Michalski-Zheng's approach. Examples of the above SVS-EFIE formulations are summarized in the paper.

11:00 On the Information Entropy of Diffusive Multipath Scattering Environments

[Shen Lin](#) (University of Illinois at Urbana Champaign, USA); [Zhen Peng](#) (University of Illinois at Urbana-Champaign, USA)

We propose a novel mathematical/statistical model to analyze the information transmission in diffusive multipath scattering environments. The methodology is to first establish fundamental statistical representations of complex diffusive media, then integrate component-specific features of transmitters and receivers, and finally encode the governing physics into the mathematical information theory. The work qualitatively characterizes the correlated Rayleigh diffusive multipath, coherent specular direct-paths, and mutual coupling between antennas. The theoretical research is evaluated and validated through representative experiments.

11:20 Modal Characterization of Thermal Emitters Using the Method of Moments

[Denis Tihon](#) (University of Cambridge, Belgium); [Stafford Withington](#) (Cavendish Laboratory, United Kingdom (Great Britain)); [Christophe Craeye](#) (Université Catholique de Louvain, Belgium)

Electromagnetic sources relying on spontaneous emission are difficult to characterize without a proper framework due to the partial spatial coherence of the emitted fields. In this paper, we propose to characterize emitters of any shape through their natural emitting modes, a set of coherent modes that add up incoherently. The resulting framework is very intuitive since any emitter is regarded as a multimode antenna with zero correlation between modes. Moreover, for any finite emitter, the modes form a compact set that can be truncated. Each significant mode corresponds to one independent degree of freedom through which the emitter radiates power. The proposed formalism is implemented using the Method of Moments (MoM) and applied to a lossy sphere and a lossy ellipsoid. It is shown that electrically small structures can be characterized with a small number of modes, and that this number grows as the structure becomes electrically large.

11:40 A Numerically Efficient Technique for the Analysis of Metamaterial- And Metasurface-based Antennas

[Abdelkhalek Nasri](#) (Research Unit of Mechatronic Systems and Signals, National Engineering School of Carthage, Tunisia); [Raj Mittra](#) (Penn State University, USA)

Metasurface-based antennas have received considerable recent attention because they are not only useful for designing new antennas, but for improving the performance of legacy design as well. However, these antennas are usually multiscale in nature and they typically require an inordinately long time when simulated by using commercial solvers. In this work, we present a new approach for analyzing antennas that utilize Metasurfaces (MTSs) and Metamaterial (MTMs). The proposed method departs from the widely used technique based on an anisotropic impedance representation of the surface and relies on an equivalent medium approach instead. The principal advantage of this approach is that such an equivalent medium representation can be conveniently used in commercial EM solvers. Several illustrative examples are presented in the paper to demonstrate the efficacy of the present approach when simulating MTS- and MTM-based antennas.

12:00 Fast and Accurate Analysis of Multilayered Periodic Structures Used in the Design of Reflectarray and Metasurface Antennas

[Miguel Camacho](#) (University of Pennsylvania, USA); [Rafael R. Boix](#) (University of Seville, Spain); [Francisco Medina](#) (University of Sevilla, Spain)

The spectral domain Method of Moments (SD-MoM) is applied to the efficient analysis of multilayered structures containing periodic arrays of patches of many different geometries, and in particular, patches of the type that have been customarily used as elements of reflectarray and metasurfaces antennas. In the approximation of the electric current density on the patches we use basis functions accounting for edge singularities, which make it possible to obtain very accurate results while requiring small MoM matrices. Although the two dimensional Fourier transform (2-D FT) of the basis functions can not be analytically determined, the Nonuniform Fast Fourier Transform (NUFFT) algorithm is used to numerically compute these 2-D FT. The SD-MoM based on NUFFT turns out to be 80 times faster than commercial software CST, and only 15% slower than the conventional SD-MoM customarily used when the 2-D FT of the basis functions can be obtained in closed-form.

T10-E05/1: Electromagnetic Methods for Direct and Inverse Scattering Involving Stratified Media

T10 EM modelling and simulation tools / Regular Session / Electromagnetics

Room: B9

Chairs: [Alessandro Fedeli](#) (University of Genoa, Italy), [Cristina Ponti](#) (Roma Tre University, Italy)

8:30 Electromagnetic Excitation of a Layered Medium by N Magnetic Dipoles

[Andreas Kalogeropoulos](#) and [Nikolaos L. Tsitsas](#) (Aristotle University of Thessaloniki, Greece)

Excitation of a layered medium by N magnetic dipoles is considered. Scattering relations and physical bounds concerning the scattering cross sections and the number of dipoles are derived. Potential applications of such problems are pointed out. Numerical implementations of the derived relations for specific scattering geometries are included.

8:50 Cloaking and Magnifying Using Radial Anisotropy in Non-Integer Dimensional Space

[Sidra Batool](#), [Mehwish Nisar](#), [Fabio Mangini](#) and [Fabrizio Frezza](#) (Sapienza University of Rome, Italy)

This paper analyzes the electrostatic responses of polarly radially anisotropic (PRA) cylindrical shell and spherically radially anisotropic (SRA) spherical shell in presence of non-integer dimensional (NID) space. This is obtained by placing both of these geometries in space having non-integer dimensions. The influence of presence of NID space on cloaking and magnification using these geometries have been worked out. Observations have shown that PRA cylindrical shell can only yield cloaking by selecting certain anisotropy ratio in presence of NID space, whereas magnification cannot be achieved. Numerical simulations have been done to show the effectiveness of NID space and for difference of the presence of NID space and ordinary space. However, SRA spherical shell is independent of the presence of NID space for cloaking and magnification.

9:10 Reflected Wave Fields from a Fluctuating Earth Surface - a Phase-Space Approach

[Valon Blakaj](#) (Research Associate, United Kingdom (Great Britain)); [Gabriele Gradoni](#), [Stephen Creagh](#) and [Gregor Tanner](#) (University of Nottingham, United Kingdom (Great Britain)); [Manohar Deshpande](#) (NASA, USA)

In this paper we present a phase-space approach that models wave fields reflected from random surfaces. By using transformations based on the Wigner distribution function (WDF), we represent the diffuse wave fields in phase-space. This representation offers an efficient approach for modelling complex and noisy sources. We focus on the application of this approach to modelling of wave fields reflected from rough Earth, with potential applications in microwave remote sensing.

9:30 Towards Asteroid Tomography: Modellings and Measurements Using an Analogue Model

[Christelle Eyraud](#) (Institut Fresnel, Aix Marseille Université, CNRS, Centrale Marseille, France); [Lisa-Ida Sorsa](#) (Tampere University, France); [Alain Hérique](#) (Université Grenoble Alpes, CNRS, IPAG, France); [Jean-Michel Geffrin](#) (Institut Fresnel & Aix Marseille Univ, CNRS, Centrale Marseille, France); [Sampsa Pursiainen](#) (Tampere University, France); [Wlodek Kofman](#) (Université Grenoble Alpes, CNRS, IPAG/Space Research Centre, PAS, France)

The interior structures of the comets and asteroids, still poorly known, might hold a unique key to understand the early Solar System. Considering the interaction of an illuminated electromagnetic wave with this kind of targets, these "objects" are very large compared to the applicable wavelength. Consequently, tomographic imaging of such targets, i.e., reconstructing their interior structure via multiple measurements, constitutes a challenging inverse problem. To reach this objective and to develop and test inverse algorithms, we need to investigate electromagnetic fields that have interacted with structures analogous to real asteroids and comets. In this study, we focus on the acquisition of these fields considering three methods: calculated fields obtained with (1) time and (2) frequency domain methods and (3) microwave measurements performed for an analogue model, i.e., a small-scale asteroid model.

9:50 Modeling Cylindrical Slot Antenna for Borehole GPR

[Alexei Popov](#) (IZMIRAN); [Vladimir Garbatsevich](#) and [Pavel Morozov](#) (IZMIRAN, Russia); [Fedor Morozov](#) (JSC VNIISMI, Russia); [Igor Prokopovich](#) (IZMIRAN, Russia)

We discuss application of slot antennas in the problem of subsurface radar logging. Frequency dependence of radiation pattern is studied. Preliminary field tests are reported.

10:10 Coffee Break

10:40 GPR Probing of Smoothly Layered Subsurface Medium: 3D Analytical Model

[Alexei Popov](#) (Pushkov Institute of Terrestrial Magnetism, Ionosphere and Radio Wave Propagation, Russia); [Pavel Morozov](#) (IZMIRAN, Russia); [Marian Marciniak](#) (National Institute of Telecommunications, Poland); [Igor Prokopovich](#) (IZMIRAN, Russia)

An analytical approach to GPR probing of a horizontally layered subsurface medium is developed, based on the coupled-wave WKB approximation. An empirical model of current in dipole transmitter antenna is used.

11:00 Qualitative Imaging of Experimental Multistatic Ground Penetrating Radar Data

[Michele Ambrosanio](#) (Università di Napoli Parthenope, Italy); [Martina Teresa Bevacqua](#) (Università Mediterranea di Reggio Calabria, Italy); [Vito Pascazio](#) (Università di Napoli Parthenope, Italy); [Tommaso Isernia](#) (University of Reggio Calabria, Italy)

Subsurface imaging of unknown buried objects is of fundamental importance in several fields, spanning from civil engineering applications to safety and biomedical issues. The detection of objects located in an investigation domain in a nondestructive fashion can be faced via addressing an electromagnetic inverse scattering problem. In this paper, an experimental assessment of a simple, linear approach, known as linear sampling method (LSM), is proposed. The results show good recovery performance and robustness against model error, while keeping a low computational burden, which is very important for practical, almost real-time applications.

11:20 **Multi-Resolution Through-the-Wall Microwave Imaging of Strong Scatterers**

[Federico Boulos](#) (ELEDIA@UniTN - DISI, University of Trento, Italy); [Marco Salucci](#) (ELEDIA Research Center, Italy); [Kuiwen Xu](#) (Hangzhou Dianzi University, China); [Yu Zhong](#) (A*STAR IIPC, Singapore); [Andrea Massa](#) (University of Trento, Italy)

The solution of highly non-linear through-the-wall microwave imaging (TWMI) problems is addressed. An innovative inverse scattering (IS) methodology is proposed to retrieve strong scatterers embedded within a known inhomogeneous background. Towards this goal, the IS problem at hand is formulated in a differential imaging framework allowing the exploitation of a-priori information on the probed domain. Then, the linearization and regularization capabilities of the difference contraction integral equation (D-CIE) method are combined with those of a multi-resolution (MR) inversion scheme for yielding accurate and reliable quantitative reconstructions. Some preliminary numerical results are shown to verify the effectiveness of the MR-D-CIE approach, as well as to demonstrate its superior performance over a standard single-resolution (SR) solution strategy.

11:40 **Forward and Inverse Scattering Models Applied to Through-Wall Imaging**

[Alessandro Fedeli](#) and [Matteo Pastorino](#) (University of Genoa, Italy); [Cristina Ponti](#) (Roma Tre University, Italy); [Andrea Randazzo](#) (University of Genoa, Italy); [Giuseppe Schettini](#) (Roma Tre University, Italy)

Through-wall imaging is an application field in which microwaves play an important role, thanks to their ability of penetrating inside building materials. In this framework, the aim of this paper is twofold. On the one hand, it presents an analytical forward model able to effectively describe the scattering phenomena by fully taking into account all the reflection and transmission effects due to the wall. On the other hand, a new inversion procedure, able to address the full underlying non-linear inverse scattering problem, is introduced. Some numerical results aimed at validating the two approaches are shown.

12:00 **Image Radar Determining the Nominal Body Contour for Characterization of Concealed Person-Worn Explosives**

[Mohammad M. Tajdini](#), [Kurt Jaisle](#) and [Carey Rappaport](#) (Northeastern University, USA)

Accurate characterization of suspicious body-worn objects may speed up the passenger screening process by reducing the number of manual screenings while maintaining the ability to detect more complex threats. This improves passenger experience in the screening process while preserving strong security. This paper presents an innovative real-time method for millimeter wave nearfield radar reconstructing the nominal contours of human bodies without affixed foreign objects. This important step is required for characterizing unique aspects of concealed objects when they are affixed to the body. The method is verified experimentally when applied to the images of a recently developed laboratory prototype millimeter-wave scanning system. The method works well both when there is a weak dielectric object affixed to human body and when a portion of the body cross-section is not captured by the imaging system. The reconstructed contour can then be used to estimate the dielectric constant of the suspicious body-worn objects.

CS07: AMTA/EurAAP Session: Post Processing Techniques in Antenna Measurements

T11 Fundamental research and emerging technologies / Convened Session / Measurements

Room: B10

Chair: [Francesco Saccardi](#) (Microwave Vision Italy, Italy)

8:30 **Near-Field to Far-Field Transformation for Fast Linear Slide Measurements**

[Fernando Rodríguez Varela](#) (Universidad Politécnica de Madrid, Spain); [Ruben Tena Sanchez](#) (Technical University of Madrid, Spain); [Manuel José López-Morales](#) (Universidad Carlos III de Madrid, Spain); [Manuel Sierra-Castañer](#) (Universidad Politécnica de Madrid, Spain)

This paper presents an algorithm for the far-field transformation of fields measured over linear cuts (slides) in planar measurement scenarios. Instead of scanning the complete plane, only two perpendicular slide measurements are performed, which reduces drastically measurement times. From these two measurements, the radiation pattern in the main cuts can be obtained, and then, the full 3D pattern is derived. The algorithm is based on particularizing the planar near-field to far-field transformation theory to a one-dimensional space. The proposed technique is presented and tested using simulated and measured data, showing low transformation errors and promising capabilities for the fast testing of antennas.

8:50 **Fast Single-Cut Antenna Characterization by near Field Measurements**

[Amedeo Capozzoli](#), [Claudio Curcio](#) and [Angelo Liseno](#) (Università di Napoli Federico II, Italy)

A new approach for the partial reconstruction in near-field antenna characterization is presented. The goal of the partial reconstruction is to determine the optimal near-field sampling distribution required to provide a partial reconstruction of the antenna patter (along some cuts). The method is based on the formulation of the near-field characterization as a linear inverse problem and on the singular-value-optimization. It is aimed to reconstruct only that part of the unknown contributing to the far-field pattern along the desired cuts. A numerical analysis shows the performance of the method.

9:10 **Single-Cut Near-Field Far-Field Transformation and Implicit Plane-Wave Synthesis for RCS Prediction Including Multiple Scattering Effects**

[Shuntaro Omi](#) (National Institute of Advanced Industrial Science and Technology, Japan); [Michtaka Ameya](#) (NMIJ/AIST, Japan); [Masanobu Hirose](#) and [Satoru Kurokawa](#) (National Institute of Advanced Industrial Science and Technology, Japan)

A single-cut near-field (NF) radar cross-section (RCS) measurement method is proposed which is based on the full-wave formulation. The method enables the exact prediction of RCS including the multiple scattering effects and requires the NF sampling points are required only on a single-cut-plane. It is based on the single-cut near-field far-field transformation (NFFFT) for antenna measurements and consists of NFFFT and implicit plane-wave synthesis (IPWS) steps. The proposed method is formulated based on the scattering theory discussed and validated numerically and experimentally.

9:30 **Experimental Determination of the Total Radiated Power of Automotive Antennas in the Installed State**

[Muhammad Ehtisham Asghar](#) and [Christian Bornkessel](#) (Technische Universität Ilmenau, Germany); [Matthias Hein](#) (Ilmenau University of Technology, Germany)

Total radiated power (TRP) is a crucial figure-of-merit used to characterize the performance of automotive antennas, similar to hand-held user terminals. Presence of a truncated region in nearfield measurement facilities can induce errors in the data after nearfield-to-far-field transformation, resulting in inaccurate estimation of the TRP. To improve this, different extrapolation techniques are used in post-processing to reconstruct the data in the truncated region. Several measurements were conducted for an automotive antenna installed at different locations on a car in a facility with truncated measurement region. The measured data were extrapolated in the truncated region, and the impact of post-processing was analyzed by comparing the reconstructed pattern with the pattern obtained from a facility without truncation, and by calculating the TRP values. The results indicate that extrapolation techniques, in particular modal filtering, are capable of accurately extracting the TRP values, with a deviation of 0.1...1.1 dB compared to the reference.

9:50 **AUT Far-Field Pattern Reconstruction from a Reduced Set of Spherical Near-Field Data Collected in Presence of an Infinite Perfectly Conducting Ground Plane**

[Francesco D'Agostino](#), [Flaminio Ferrara](#), [Claudio Gennarelli](#), [Rocco Guerriero](#) and [Massimo Migliozi](#) (University of Salerno, Italy)

The non-redundant sampling representations of electromagnetic fields and the image principle are properly applied in this work to develop an effective probe-compensated spherical near-field to far-field (NFTFF) transformation, which makes use only of the NF data measured over the upper hemisphere, due to the presence of an infinite perfectly conducting ground plane. According to these representations, the considered antenna under test (AUT) and its image are assumed as enclosed in a surface consisting of a cylinder ended in two half-spheres. Then, an efficient 2-D optimal sampling interpolation scheme is used to reconstruct the NF data required by the standard spherical NFTFF transformation from the NF samples collected over the upper hemisphere and from those properly synthesized from these last over the lower one. Numerical examples are shown to assess the effectiveness of the developed non-redundant spherical NFTFF transformation.

10:10 **Coffee Break**

10:40 **Diagnostics on Electrically Large Structures by a Nested Skeletonization Scheme Enhancement of the Equivalent Current Technique**

[Lucia Scialacqua](#) (Microwave Vision Italy, Italy); [Francesca Mioc](#) (Consultant, Switzerland); [Lars Foged](#) (Microwave Vision Italy, Italy); [Giorgio Giordanengo](#) (LINKS Foundation & Politecnico di Torino, Italy); [Marco Righero](#) (LINKS Foundation, Italy); [Giuseppe Vecchi](#) (Politecnico di Torino, Italy)

The use of the Fast Multipole Method (FMM) in an equivalent current reconstruction technique, based on a dual-equation formulation, has been presented in the past for antenna design and diagnostics. The method was applied in design validation from measured data, demonstrating diagnostics feasibility of different large antennas up to an equivalent antenna volume of $2380 \lambda^3$. Despite the computational advantages coming from the FMM, the memory request and the run time constraints could be still crucial in the processing of electrically large antennas. An enhancement of the equivalent current reconstruction technique based on a Nested Skeletonization Scheme is here presented. The new technique leads to a further reduction of memory requirements and computational time, applicable to diagnostic investigation of electrically larger problems in a wider frequency band. In this paper the nested skeletonization scheme enhancement of the equivalent current technique is applied and demonstrated for diagnostics on electrically large structures.

11:00 **Suppressing Undesired Echoes by Sparsity Based Time Gating of Reconstructed Sources**

[Josef Knapp](#), [Jonas Kornprobst](#) and [Thomas F. Eibert](#) (Technical University of Munich, Germany)

The free-space radiation characteristic of an antenna under test (AUT) is determined from measurements in proximity of a scatterer by time gating reconstructed equivalent currents for the AUT and the scatterer. The presented approach effectively combines spatial filtering methods with time domain methods while mitigating their individual drawbacks. In contrast to conventional time-gating methods which usually work on the measured probe signals this approach allows to get rid of undesired echo perturbations even if measurement samples are located in the shadow region of the scatterer and the line of sight (LOS) contribution and the echo contribution are indistinguishable for the field probe. In contrast to conventional frequency domain methods, mutual coupling contributions of the AUT currents are identified and removed in the time domain. Numerical examples show that, due to the sparse reconstruction, the AUT radiation can be determined accurately even at the borders of the measured bandwidth.

11:20 **Portable, Freehand System for Antenna Diagnosis Using Amplitude-Only Data**

[Guillermo Alvarez Narciandi](#) (University of Oviedo, Spain); [Jaime Laviada](#) (Universidad de Oviedo, Spain); [Yuri Alvarez-Lopez](#) (University of Oviedo, Spain); [Guillaume Ducournau](#) (IEMN, University of Lille, France); [Cyril Luxey](#) (University Nice Sophia-Antipolis, France); [Frédéric Giancesello](#) (STMicroelectronics, France); [Fernando Las-Heras](#) (University of Oviedo, Spain)

A freehand portable system to perform antenna diagnosis using amplitude-only data is presented. It employs a handheld probe antenna, tracked by an easy-to-deploy motion capture system, a spectrum analyzer or a power detector to measure the amplitude of near-field samples, and a laptop to process the data. The system uses the phaseless Sources Reconstruction Method to retrieve an equivalent currents distribution on the AUT aperture, enabling antenna diagnosis. For that, near-field samples are acquired in two scanning zones parallel to the antenna aperture. The far-field pattern radiated by the AUT is computed by means of NF-FF transformation. The system was tested measuring a Ka band two-horn antenna array and the obtained outcomes were compared against reference results retrieved using both amplitude and phase information. Results show that the system can provide fast diagnosis of antennas, detecting malfunctioning elements and checking that the radiation pattern points at the expected directions.

11:40 **Characterisation of a Fibre-Optic Active Probe for Compensation of the Test-Zone Field**

[Thomas M Gemmer](#) (RWTH Aachen University, Germany); [Wieland Mann](#) (enprobe GmbH, Germany); [Dirk Heberling](#) (RWTH Aachen University, Germany)

Compensation of the non-ideal Test Zone Field (TZF) in which an antenna under test is characterised requires a precise determination of the incident electric field. In order to perform spherical measurements of the test zone, a probe is, thus, inevitable which interacts with the TZF as slightly as possible. Therefore, a fibre-optic probe is used which primarily consists of dielectric parts. To correct for the measuring test-zone probe, a thorough determination of its radiation pattern and polarisation ratio is mandatory. To this end, full-wave simulations are carried out on the probe model and compared to spherical near-field measurements, thereby ensuring an accurate probe characterisation. Subsequently, the probe is included to simulated TZF data via spherical wave expansion in order to demonstrate the suitability of this fibre-optic probe for measuring the incident field and the importance of test-zone probe correction.

12:00 **Locating Sources of Reflection Errors in an Anechoic Chamber by Creating an Error Surface Plot**

[Alo-Hélène Bester](#) (University of Stellenbosch, South Africa); [Petrie Meyer](#) (Stellenbosch University, South Africa)

A technique to locate sources of reflection errors in an anechoic chamber is presented in this article. This technique expands the NIST 18 term error analysis method and compares reflections over the whole sphere instead of using only cuts which are the proposed method of analysis. Reflection errors are consequently portrayed as an error surface. These error surfaces are displayed with surface plots and can be used as a tool to locate the origin of reflections.

Thursday, 19 March 8:30 - 10:10

BC/3: History of Electromagnetism 3 TOP

T13 Bicentennial Session / Electromagnetics

Room: B11

Chairs: [Ari Sihvola](#) (Aalto University, Finland), [Arthur D Yaghjian](#) (Electromagnetics Research Consultant, USA)

8:30 **The Amazing History of Reflector Antennas: From Hertz to Modern CubeSats and Beyond**

[Yahya Rahmat-Samii](#) (University of California Los Angeles (UCLA) & UCLA, USA); [Vignesh Manohar](#) (University of California, Los Angeles, USA)

Reflector antennas have evolved significantly over the years. Starting from its use in the form of mirrors in the optical domain, reflectors have found use in a significant number of modern day applications. In this review paper, we begin with the development of reflector antenna in the radio wave domain by Hertz, and then march through the evolution of reflector antennas in three major regimes: radars, radio astronomy and satellites. Due to page limitations, only representative examples can be covered. However, the authors have provided relevant references that covers a much wider scope.

8:50 **A View of Some Key Developments of Spacecraft Antennas, Their Modelling and Technologies**

[Antoine Roederer](#) (Technical University of Delft, The Netherlands)

This paper reviews the evolution of spacecraft antennas and related techniques and technologies from the bent wire antennas of Sputnik (1957) to the multiple beam array fed reflector antennas of tomorrow's Terabit communication satellites. Some key developments of antennas for telemetry, tracking & command, of reflector, lens and array antennas for communications, localization and remote sensing will be highlighted, as well as their associated modelling techniques and technologies.

9:10 **A Brief History of Frequency-Independent and Not-so-Frequency-Independent Antennas**

[Raj Mittra](#) (Penn State University, USA)

This paper briefly traces the history of the development of the so-called Frequency-independent antennas which provide a backdrop of the development of Log Spiral and Log-periodic Dipole Array antennas. The paper will reminisce some of the personal experiences the author had, during the course of development of these antennas, primarily at the Antenna Laboratory of the University of Illinois.

9:30 **The Phased Array Antenna: A History of Progress in Analysis and Technology**

[Robert Mailloux](#) (University of Trento, Italy)

This paper describes original contributions to the analysis and technology of phased array antennas, with particular emphasis on the rate of progression with time.

9:50 **History of Microstrip and Dielectric Resonator Antennas**

[David R. Jackson](#) and [Stuart A. Long](#) (University of Houston, USA)

The history of microstrip antennas (MSAs) and dielectric resonator antennas (DRAs) is reviewed. The early work is reviewed, including some interesting controversies. Some of the important developments in these areas are discussed, including methods for improving performance in terms of bandwidth, radiation efficiency, mutual coupling, and physical size.

Thursday, 19 March 8:30 - 12:20

SW07: H2020 Project ACASIAS (GA N° 723167) - Antennas for Integration into Aircraft Structure TOP

T12 Scientific / Industrial Workshops

Room: B3

Thursday, 19 March 8:30 - 10:10

IW03: Efficiently Simulating and Optimising Antenna Placement in Virtual Test Scenarios (Altair) TOP

T12 Scientific / Industrial Workshops

Room 6

Thursday, 19 March 10:40 - 12:20

T01-A02: Terminal Antennas and Interactions with Surroundings

T01 LTE and Sub-6GHz 5G / Regular Session / Antennas

Room: A2

Chairs: [Yen-Sheng Chen](#) (National Taipei University of Technology, Taiwan), [Zhinong Ying](#) (Sony Coporation, Sweden)

10:40 *Isolation Enhancement of Closely Spaced MIMO System Using Inverted Fork Shaped Decoupling Structure*

[Jogesh Chandra Dash](#) and [Nagalakshmaiah Kalva](#) (Indian Institute of Technology Bombay, India); [Shilpa Kharche](#) (Indian Institute of Technology, Bombay, India); [Jayanta Mukherjee](#) (Indian Institute of Technology Bombay, India)

A two element closely spaced microstrip MIMO antenna with improved isolation characteristics is proposed. An inverted fork-shaped decoupling (IFSD) structure is placed between two closely spaced radiating elements, having $0.03\lambda_0$ edge-to-edge spacing. Further, a rectangular slot is designed on each radiating element to fill the null in the antenna broadside radiation pattern. The isolation (S21 and S12) of more than 20 dB at 5.5 GHz is achieved using the proposed technique. Antenna elements provide a very good impedance matching (S11 < -15 dB) at 5.5 GHz. Implementation of IFSD structure and slot provide enhanced isolation of 65.39% compared to MIMO system without proposed technique. The proposed MIMO antenna structure having effective dimensions of $0.86\lambda_0 \times 0.64\lambda_0$ is simple to design and low in cost. The total-active-reflection coefficient (TARC) and envelope-correlation-coefficient (ECC) of the antenna are below 0.3 and 0.005 respectively. The proposed structure is fabricated and measured.

11:00 *Improvements of Multi-Antenna Specific Absorption Rate Using a Two-Stage Technique*

[Yuan-Hung Lin](#) and [Yen-Sheng Chen](#) (National Taipei University of Technology, Taiwan)

In this paper, we propose a two-stage optimization technique that reduces the multiple-input multiple-output (MIMO) specific absorption rate (SAR) for mobile terminals. In multi-antenna devices, the SAR value is affected by amplitude distributions and excitation phases of feed currents; therefore, various combinations of SAR need to be considered, and it is time-consuming to determine all the SAR results using full-wave simulation. The phase one of the proposed technique exploits a fast estimation model, which solves only few pre-planned simulations yet leads to predictions of SAR resulting from any combination of feed currents. Next, the prediction of SAR is cast into an optimization framework, and an optimization algorithm is applied to determine the current distribution that minimizes the peak MIMO SAR. A four-element antenna is validated to minimize the maximum SAR value of several situations. The optimization results demonstrate that the method exhibits an average improvement of 13.8%.

11:20 *Effect of Dielectric Properties of Human Hand Tissue on Mobile Terminal Antenna Performance*

[Stanislav Stefanov Zhekov](#) and [Gert Pedersen](#) (Aalborg University, Denmark)

A good approach when designing antennas for mobile terminals is to optimize them for operation in the vicinity of the user body. The presence of a lossy human tissue in the antenna's near field has an adverse effect on the radiator's performance. The focus of this paper is on studying the change in the antenna performance due to the change in the dielectric properties of the human hand holding the mobile terminal. The investigation is conducted by using an antenna array consisting of two identical and symmetrical PIFA antennas covering the frequency band from 5.8 GHz to 7.7 GHz. Several different values of the complex permittivity are assigned to a human hand phantom in the numerical simulations and it is found that the variation of the complex relative permittivity within a large range of values does not change largely the S-parameters and radiation efficiency of the antenna.

11:40 *A Single Port Orthogonally Polarized Antenna for Handsets, IoT Terminals and Vehicles*

[Mohamed Sanad](#) (Amant Antennas, Egypt); [Noha Hassan](#) (Faculty of Engineering, Cairo University, Egypt)

A broadband resonant antenna has been developed for handsets, vehicles and IoT terminals. It does not use any matching/tuning circuits or extended ground-planes. It can be bent/folded around the narrow sides of the terminal, which allows using efficient MIMO configurations with a high isolation. To significantly reduce the need for spatial diversity MIMO, a single port orthogonally polarized terminal antenna has been developed. It is equally sensitive to two perpendicular polarizations and it also has a good sensitivity to circular polarization, which is important for GPS and satellite phones. So, any two orthogonally polarized MIMO antennas can be replaced by a single port orthogonally polarized antenna. In some applications, such as vehicles, a good MIMO configuration can be obtained by combining a linearly polarized antenna with a single port orthogonally polarized antenna in 2x2 MIMO. It can efficiently receive signals from different directions with different polarization in any complicated environment.

12:00 *Comparison of Different Antenna Cluster Weighting Methods*

[Jari-Matti Hannula](#) (KTH Royal Institute of Technology, Sweden); [Anu Lehtovuori](#) (Aalto University, Finland); [Ville Viikari](#) (Aalto University & School of Electrical Engineering, Finland)

The antenna cluster concept utilizes multiple, simultaneously-fed radiating elements collaboratively as one antenna. We have previously presented several methods to obtaining feeding weights to realize certain impedance. In this work, we compare the previously documented methods and discuss their benefits and challenges. As a new method, we consider the case where the weighting is performed by measuring the antenna response using a receiver antenna.

T01-P02: Propagation Modelling and Simulation

T01 LTE and Sub-6GHz 5G / Regular Session / Propagation

Room: B1

Chair: [Nima Jamaly](#) (Swisscom, Switzerland)

10:40 *Penetration Loss into Train Wagons: Q-factor Measurements*

[Nima Jamaly](#) (Swisscom, Switzerland); [Reto Schoch](#) (Schoch Technik GmbH, Switzerland); [Daniel Wenger](#) (Swisscom, Switzerland); [Stefan Mauron](#) (Swisscom (Schweiz) AG, Switzerland)

The Q-factor of train wagon plays a significant role in calculation of EM penetration into the wagon. It also can be used as an alternative metric indicating richness of the multipath propagation inside a wagon. We present the results of Q-factor measurements for similar wagons equipped with two different RF-friendly windowpanes. The measurement results show that inside the wagons with RF-friendly windowpanes, we have a non-rich multipath environment not allowing to make best use of spatial multiplexing feature supported by modern wireless communication systems.

11:00 *Generation of Realistic Railway Based Mobility Scenarios*

[Christoph Herold](#), [Lennart Thielecke](#) and [Thomas Kürner](#) (Technische Universität Braunschweig, Germany)

Planning and operating cellular networks for railway coverage is a challenging task due to the trains high speeds, the number of users traveling and the surroundings. Simulations of the radio environment are a crucial part of the radio network planning process as they allow to test different network layouts and configurations. Accurate simulations however require appropriate input data. In this paper, we present a process for the generation of realistic railway based mobility scenarios from public domain environmental data. From clutter, building and height data, the train routes, the positions of base stations and their antennas as well as the user movement will be derived. Using these realistic scenarios will allow for detailed system-level simulations for specific locations and their characteristics.

11:20 *A Study on Vegetation Loss Model with Seasonal Characteristics*

[Daigo Ogata](#), [Akihiro Sato](#), [Sho Kimura](#) and [Hideki Omote](#) (Softbank Corp., Japan)

In mobile communications, it is necessary to accurately estimate and evaluate the influence of the environment between the BS and the MS, such as the terrain, clutter, vegetation, etc. Rural areas have few surrounding reflective objects, and so are not multipath-rich environments. Therefore, it is considered that the received power is reduced when direct waves are blocked by buildings, trees, etc. In such an environment, it is necessary to clarify the characteristics of diffracted waves, waves scattered by isolated buildings, vegetation. This paper focuses on the loss due to vegetation blockage. The vegetation loss has been standardized as ITU-R P.833-9, but the region and kinds of trees considered are limited. In this paper, we measure and analyze the vegetation loss of deciduous trees in different seasons in Japan. From the results, we propose a new vegetation loss model that can take frequency and seasonal characteristics into consideration.

11:40 *Channel Modeling for Wireless Sensor Networks Deployment in the Smart City*

[Eran Greenberg](#) (RAFAEL, Israel); [Amitay Bar](#) and [Edmund Klodzh](#) (Rafael, Israel); [Liat Peled-Eitan](#) (RAFAEL, Israel)

In the near future many objects in the urban environment will be able to communicate with each other as part of the smart city vision. Unattended wireless sensor networks, which will be deployed in the streets and on the buildings, will generate big data for the benefit of the city residents. In this contribution we investigate the wireless propagation channel for terminals located on/near ground/building level by using ray-tracing simulations. Taking advantage of using multi-core processors we have analyzed a large dataset of sensor locations for a statistical analysis. The behavior of the path loss, mean time of arrival, delay spread and mean direction of arrival are presented and modeled.

12:00 Analytic Propagation Approximation over Variable Terrain and Comparison to Data

[Dmitry Chizhik](#) (Nokia Bell Labs, USA); [Jani Moilanen](#) (Nokia Bell Labs, Finland); [Siegfried Klein](#) (Nokia Bell Labs, Germany); [Luis Maestro](#) and [Reinaldo Valenzuela](#) (Nokia Bell Labs, USA)

An analytical modeling methodology to rapidly predict signal strength over variable terrain has been developed. Methodology relies on approximating the intervening terrain by a constrained parabola, allowing the use of a modal sum solution. The model has been compared against an extensive data set of over 3000 links, measured in a desert environment of Fuerteventura, Spain, resulting in 8.5 dB RMS error, an improvement over a linear fit to data, which has 12.5 dB RMS deviation. The model is intended for use in future lunar missions where rapid coverage calculations are important for selection of optimal landing sites.

T11-P10: Propagation in Biological Tissues

T11 Fundamental research and emerging technologies / Regular Session / Propagation

Room: B7

Chairs: [Gennaro G. Bellizzi](#) (Erasmus University Medical Center, Italy), [Charles Sammut](#) (University of Malta, Malta)

10:40 EM-Thermal Co-Simulation of Microwave Ablation Applicator in Liver Tissue Phantom with Bowtie-Slot Surface Antenna

[Muhammad Saad Khan](#) (RheinMain University of Applied Sciences, Germany); [Georg Rose](#) (OVGU, Germany); [Bernd Schweizer](#) (RheinMain University of Applied Sciences, Germany); [Andreas Brensing](#) (Hochschule RheinMain, Germany)

In this paper, design and electromagnetic-thermal co-simulation of a microwave catheter and a bowtie-slot body matched antenna are discussed. The catheter is inserted into a liver tissue phantom to heat the tissue with 50 W power for 300 seconds in thermal simulation. The resultant temperature profile is fed back into the electromagnetic simulation with temperature-dependent material properties of a liver. Similarly, 50 W power is also stimulated in the catheter in electromagnetic simulation to observe the difference in received power at the surface bowtie-slot antenna during the heating process.

11:00 Characterization of an Integrated Radiofrequency System for MR-guided Hyperthermia

[Gennaro G. Bellizzi](#) (Erasmus University Medical Center, Italy); [Kemal Sumser](#) (Erasmus MC Cancer Institute, The Netherlands); [Ria Forner](#) (UMC Utrecht, The Netherlands); [Tomas Drizdal](#) (Czech Technical University in Prague, Czech Republic); [Margarethus M. Paulides](#) (Eindhoven University of Technology, The Netherlands)

Clinical studies have established the clinical benefit of adjuvant mild hyperthermia, but further improvements require magnetic resonance (MR) thermometry for accurate temperature dosimetry. In this work, we experimentally investigate the feasibility of our approach consisting of a receiver-only coil array, for accurate MR thermometry, integrated into a phased array for heating purposes. An experimental setup was constructed consisting of a 4-element heating array working at 434MHz and a 2-channel MR receive coil array working at 63.89MHz. In our approach, these arrays are oriented to exploit polarization decoupling. Vector network analyzer measurements showed satisfactory reflection and transmission characteristics for the heating (S_{ii}=-20dB, S_{ij}=-31dB) and imaging (S_{ii}=-21dB, S_{ij}=-12dB) arrays and the inter-array coupling was as low as -56dB. We conclude that this combined arrangement is highly suitable for a simultaneous operation.

11:20 An Open-Access Experimental Dataset for Breast Microwave Imaging

[Tyson Reimer](#), [Jordan Krenkevich](#) and [Stephen Pistorius](#) (University of Manitoba, Canada)

Microwave imaging has shown potential for breast cancer screening, but further evaluation of the clinical viability of breast microwave imaging (BMI) systems is required. Previous phantom studies have shown promise, but after decades of BMI research, simulation studies still dominate. This work addresses the challenges of small sample sizes and a lack of experimental data by providing an open-source experimental dataset, obtained using a pre-clinical BMI system. At time of submission, the University of Manitoba BMI Dataset (UM-BMID) contains data from 452 phantom scans and will be expanded to contain 1257 scans. UM-BMID is publicly available, and the community is encouraged to use it for large-scale BMI analysis. The application of logistic regression for tumor-detection on a subset of the dataset was studied to demonstrate one use of UM-BMID. The diagnostic accuracy of the classifier was (85 ± 4)%, demonstrating the promise of machine learning methods for tumor-detection in BMI.

11:40 Determining the Concentration of Red Blood Cells Using Dielectric Properties

[Jeantide Said Camilleri](#), [Lourdes Farrugia](#), [Julian Bonello](#) and [Nikolai Paul Pace](#) (University of Malta, Malta); [Adam Santorelli](#) (National University of Ireland, Galway & Translational Medical Device Lab, Ireland); [Emily Porter](#) (University of Texas at Austin, USA); [Martin O'Halloran](#) (National University of Ireland, Ireland); [Charles Sammut](#) (University of Malta, Malta)

This paper investigates an innovative method to determine the red and white blood cell concentrations in blood using their dielectric properties at microwave frequencies. The dielectric properties characterise the interaction of a time-varying electric field with the biological tissue. The concentrations of red blood cells (RBCs) and white blood cells in a sample of whole blood can vary due to illness or disease. This study is a proof-of-concept, where the dielectric properties of samples containing RBCs and plasma are investigated. The dielectric properties of samples of different concentration of RBCs in plasma are measured and used to train artificial neural networks which relate the measured properties to the known concentrations of RBCs. The results show that a trained neural network can predict the RBC concentrations in arbitrary samples not used to train the model with an average error of 1.37 % with respect to the actual concentration in the samples.

12:00 Temperature-Corrected SAR Focusing in Cancer Hyperthermia

[Rossella Gaffoglio](#) and [Marco Righero](#) (LINKS Foundation, Italy); [Giorgio Giordanengo](#) (LINKS Foundation & Politecnico di Torino, Italy); [Marcello Zucchi](#) and [Giuseppe Vecchi](#) (Politecnico di Torino, Italy)

In hyperthermia cancer treatments, the tumour mass temperature is selectively increased to a supra-physiological temperature (40 - 44 °C). In current state of the art, this is achieved with an array of antennas, backed by cooling system in contact with the skin of the patient. The antenna excitations are usually found with a SAR-based focusing optimization aimed at maximizing the energy deposition inside the tumour. However, it might happen that a good SAR focusing on the target volume does not lead to an equally satisfying temperature focusing, due to the thermal boundary conditions dictated by the cooling system. We propose a procedure to find the appropriate SAR focusing that maximizes the actual temperature coverage of the tumor. The procedure involves multiple solutions of the bioheat equations; it is found that a 2D version of the bioheat equation is enough for the current correction purposes.

T11-E01: EM Theory

T11 Fundamental research and emerging technologies / Regular Session / Electromagnetics

Room: B11

Chairs: [Daniel Sjöberg](#) (Lund University, Sweden), [Niklas Wellander](#) (Swedish Defence Research Agency, Sweden)

10:40 Multiple Scattering by a Collection of Randomly Located Obstacles Distributed in a Dielectric Slab

[Gerhard Kristensson](#) (Lund University, Sweden); [Niklas Wellander](#) (Swedish Defence Research Agency, Sweden)

Scattering of electromagnetic waves by discrete, randomly distributed objects inside a slab is addressed. The non-intersecting scattering objects can be of arbitrary form, material and shape with a number density of n_0 (number of scatterers per volume). The main aim of this paper is to calculate the coherent reflection and transmission characteristics for this configuration. Typical applications of the results are found at a wide range of frequencies (radar up to optics), such as attenuation of electromagnetic propagation in rain, fog, and clouds etc. The integral representation of the solution of the deterministic problem constitutes the underlying framework of the stochastic problem. Conditional averaging and the employment of the Quasi Crystalline Approximation lead to a system of integral equations in the unknown expansion coefficients. Explicit solutions for tenuous media and low frequency approximations can be obtained for spherical obstacles.

11:00 Radiation of Planar Dielectric Waveguide Eigenwaves Scattered by Graphene Strip Grating in THz Range

[Mstyslav Kaliberda](#) and [Sergey Pogarsky](#) (Karazin National University of Kharkiv, Ukraine); [Lubov Kaliberda](#) (Kharkiv Petro Vasylenko National Technical University of Agriculture, Ukraine)

Scattering of planar dielectric waveguide H-polarized eigenwaves by graphene strip grating in the THz range is considered. The grating is placed inside the waveguide. Our analysis is based on the method of singular integral equations. The scattering and absorption cross section, as well the radiation patterns, are presented. We concentrate our analysis on studying the characteristics near the plasmon resonances and the grating-mode resonances.

11:20 Analytical Modeling and Multiphysics Simulation of Acousto-Electromagnetic Interaction

[Niklas Wingren](#) and [Daniel Sjöberg](#) (Lund University, Sweden)

A model for interaction between acoustic and electromagnetic waves based on photoelasticity is presented. A radar equation based on physical, geometric and system parameters is shown, as well as a condition for maximizing interaction (equivalent to the Bragg condition in acousto-optics). The photoelastic model is used to implement a multiphysics simulation of the problem. The Bragg condition is shown to hold for the simulated case. Additionally, simulations are used to show how a contrast in material properties in a small inclusion affects the interaction.

11:40 Re-moving the Scattered Energy from Dielectric Objects in Spatial and Frequency Domain for Cloaking Techniques

[Giuseppe Labate](#) (Wave Up S. R. L., Italy); [Roberta Palmeri](#) (Università Mediterranea di Reggio Calabria, Italy); [Tommaso Isernia](#) (University of Reggio Calabria, Italy); [Andrea Alù](#) (CUNY Advanced Science Research Center, USA)

In this paper, we report two different techniques that show how it is possible to manipulate the scattered energy from dielectric objects in order to reduce the outgoing electromagnetic fields as sensed by external observers. The first method is based on a multi-harmonic scattering cancellation, as generalized for dielectric objects, able to suppress the

scattered waves for a fixed given direction of the incoming wave. While external fields are suppressed towards perfect zero cancellation, internal fields within the dielectric particle are demonstrated to increase due to energy conservation. The second technique exploits the relationship between the scattered field and the spectral content of the overall system (object plus cloak) under certain approximations to design coats able to shift the energy content outside the visible range.

12:00 On the Optical Theorem and Optimal Extinction, Scattering and Absorption in Lossy Media

[Sven Nordebo](#) (Linnaeus University, Sweden); [Mats Gustafsson](#) (Lund University, Sweden); [Yevhen Ivanenko](#) (Linnaeus University, Sweden)

This paper reformulates and extends some recent analytical results concerning a new optical theorem and the associated physical bounds on absorption in lossy media. The analysis is valid for any linear scatterer, consisting of arbitrary materials and arbitrary geometries, as long as the scatterer is circumscribed by a spherical volume embedded in a lossy background medium. The corresponding formulas are here reformulated and extended to encompass magnetic as well as dielectric background media. Explicit derivations, formulas and discussions are also given for the corresponding bounds on scattering and extinction. A numerical example concerning the optimal microwave absorption and scattering in atmospheric oxygen in the 60 GHz communication band is included to illustrate the theory.

Thursday, 19 March 13:20 - 14:50

Poster_Awards: Best Paper Awards Poster Sessions

Room: A2 (Poster Area)

Chair: [Marianna Ivashina](#) (Chalmers University of Technology, Sweden)

EuCAP Best Paper Award - Antennas

Nonreciprocal Antennas Based on Time-Modulation: Challenges and Opportunities

[Alejandro Alvarez-Melcon](#) (Technical University of Cartagena, Spain); [Juan Sebastián Gomez-Diaz](#) (University of California, Davis, USA)

We explore the possibility to realize nonreciprocal antennas based on combining time-modulated resonators with high-Q structures. Upon an adequate low-frequency modulation scheme, such configuration enables very efficient frequency conversion between only two frequencies (one related to guided signals and another to waves in free-space) and empowers nonreciprocal phase control of the generated waves through the photonic Aharonov-Bohm effect. This approach is applied to demonstrate nonreciprocal and reconfigurable antenna configurations, including phased arrays able to independently control transmission and reception radiation patterns at the same operation frequency, reflectarrays antennas, and planar Yagi-Uda filter-antennas. We discuss the exciting functionalities and benefits enabled by this technology and provide a critical assessment of challenges that remain to be addressed in real-life applications. We envision that this paradigm will pave the way to a magnetic-free, fully integrated, and CMOS-compatible technology with profound implications in communication and wireless systems, sensing, imaging, and on-chip networks.

P3.080 A Compact Mass-producible E-band Bandpass Filter Based on Multi-layer Waveguide Technology

[Abbas Vosoogh](#) (Metasum AB, Sweden); [Astrid Algaba Brazález](#) (Ericsson Research, Ericsson AB, Sweden); [Yinggang Li](#) (Ericsson AB, Sweden); [Zhongxia Simon He](#) (Chalmers University of Technology & Microwave Electronic Lab, Sweden)

This paper presents the design, implementation and experimental validation of a bandpass filter for high-data rate point-to-point link applications at E-band. The proposed design is developed in multilayer waveguide (MLW) technology, where an air-filled waveguide transmission line is formed by stacking several unconnected thin metal plates. Our MLW bandpass filter is designed by combining low-pass and high-pass filtering structures, and consists of 19 separate metal layers. An array of glide-symmetric holes, which act as an electromagnetic band gap (EBG) structure, are used to prevent any possible field leakage due to the air gaps between the layers. The fabricated filter provides a bandpass from 71.5 to 76 GHz with measured return loss better than 15 dB, and insertion loss better than 1.3 dB. These results confirm the advantages of MLW technology for implementing ultra-compact bandpass filters showing low loss and potential for being mass-produced at millimeter-wave frequencies.

A Method for Extending the Bandwidth of Modulated Metasurface Antennas

[Marco Faenzi](#) (Université de Rennes 1, France); [David González-Ovejero](#) (Centre National de la Recherche Scientifique - CNRS, France); [Stefano Maci](#) (University of Siena, Italy)

Modulated metasurface (MTS) antennas can provide a broadside pencil beam at the frequency where the cylindrical surface wave (SW) wavelength matches the period of the impedance modulation. The mismatch between the SW wavelength and the period of the modulation imposes a limitation on the product bandwidth-gain. Here, we overcome this limitation by acting on the function that provides the local period for a given radial distance. Doing so, we generate annular active regions on the antenna aperture. Such regions typically move from the antenna center to the circular rim as the frequency decreases. This paper shows that one can optimize the profile of the local periodicity function to obtain broadside pencil beams over large bandwidths, while preserving the flatness of the gain versus frequency response. The presented results prove that these antennas can provide high broadside gain over bandwidths difficult to reach by other flat antennas based on printed technology.

P1.029 Compact and Modular Ka-Band Front-end Concept for SATCOM and 5G

[Winfried Simon](#) (IMST GmbH, Germany); [David Schaefer](#) (IMST & Antennas & EM Modelling, Germany); [Simona Bruni](#) (IMST GmbH, Germany); [Marta Arias Campo](#) (IMST GmbH, Germany & IMST GmbH, Germany); [Simon Otto](#) (IMST GmbH, Germany); [Sybille Holzwarth](#) (IMST GmbH, Germany)

In this paper a modular and compact Ka-band front-end module based on PCB technology is presented. The integration and packaging techniques combine multi-layer PCB technology with waveguide RF feeding and antennas. Metallic waveguide and backplane act also as heatsink for the active circuitry. The modular concept can be applied to large antenna arrays to fulfill the application specific link budget requirements. Depending on the chosen core chips this design concept can be used for SATCOM or for 5G.

Design of a Wide-Scan Lens Based Focal Plane Array for Sub-millimeter Imaging Systems Using Coherent Fourier Optics

[Shahab Oddin Dabironezare](#) (Delft University of Technology, The Netherlands); [Muhan Zhang](#) (Delft University of Technology, The Netherlands); [Giorgio Carluccio](#) (Delft University of Technology, The Netherlands); [Angelo Freni](#) (University of Florence, Italy); [Andrea Neto](#) (Delft University of Technology, The Netherlands); [Nuria LLombart](#) (Delft University of Technology, The Netherlands)

Future sub-millimeter imagers will use large format focal plane arrays (FPAs) of lenses to increase their field of view and the imaging speed. This abstract employs a spectral technique based on Fourier Optics for analyzing lens based FPAs. Here, the method is applied to optimize the scanning performance of an imager with monolithically integratable lens feeds without employing any optimization algorithms, by doing a field match by a tunable leaky resonant antenna. The synthesized FPA achieved scan losses much lower than the ones predicted by standard formulas related to the direct field coming from the reflector. In particular, a FPA with scan loss below 1 dB while scanning up to +17.5° is presented with directivity of 52 dB. A prototype of the described design using realistic antenna feeders is also presented.

EuCAP Best Paper Award - Electromagnetics

On the Optical Theorem and Optimal Extinction, Scattering and Absorption in Lossy Media

[Sven Nordebo](#) (Linnaeus University, Sweden); [Mats Gustafsson](#) (Lund University, Sweden); [Yevhen Ivanenko](#) (Linnaeus University, Sweden)

This paper reformulates and extends some recent analytical results concerning a new optical theorem and the associated physical bounds on absorption in lossy media. The analysis is valid for any linear scatterer, consisting of arbitrary materials and arbitrary geometries, as long as the scatterer is circumscribed by a spherical volume embedded in a lossy background medium. The corresponding formulas are here reformulated and extended to encompass magnetic as well as dielectric background media. Explicit derivations, formulas and discussions are also given for the corresponding bounds on scattering and extinction. A numerical example concerning the optimal microwave absorption and scattering in atmospheric oxygen in the 60 GHz communication band is included to illustrate the theory.

Metasurface Modeling of Periodic Diffraction Gratings Based on Generalized Sheet Transition Conditions (GSTCs)

[Ville Tiukuvaara](#) (Carleton University, Canada); [Tom Smy](#) (Carleton University, Canada); [Shulabh Gupta](#) (Carleton University, Canada)

Space-modulated diffraction gratings are modelled and analyzed using a zero thickness metasurface grating approach, and demonstrated using numerical examples. The constitutive parameters of the grating are described using surface susceptibilities of the Lorentzian form, where their resonant frequencies are sinusoidally modulated. They are then solved self-consistently with the Generalized Sheet Transition Conditions (GSTCs) to determine the scattered fields from the metasurface for specified plane-wave incident fields, for various cases of modulation periodicities and depths.

Elliptical Glide-Symmetric Hole Metasurfaces for Wideband Anisotropy

[Antonio Alex-Amor](#) (Technical University of Madrid, Spain); [Fateme Ghasemifard](#) (KTH Royal Institute of Technology, Sweden); [Guido Valerio](#) (Sorbonne Université, France); [Pablo Padilla](#) (University of Granada, Spain); [Jose Manuel Fernández González](#) (Universidad Politécnica de Madrid, Spain); [Oscar Quevedo-Teruel](#) (KTH Royal Institute of Technology, Sweden)

This paper presents a mode-matching technique to study the dispersive features of periodic structures composed of glide-symmetric elliptical holes. As a difference from purely numerical methods, our formulation provides physical insight on the Floquet harmonics. At the same time, the computational cost is reduced compared to general purpose

commercial software. The fields inside the holes are described by means of Mathieufunctions and subsequently used to compute the full 2-D dispersion diagrams. With the presented analysis, we demonstrate that glide-symmetric periodic structures with elliptical holes offer anisotropic refractive indexes over a wide range of frequencies.

A Spatio-Temporally Modulated Metasurface as a Free-Space N-Path System

[Zhanni Wu](#) (the University of Michigan, USA); [Cody Scarborough](#) (University of Michigan, USA); [Anthony Grbic](#) (University of Michigan, Ann Arbor, USA)

A spatio-temporally modulated metasurface, that functions as a free-space N-path system, is reported at X-band frequencies. The reflection phase of the rows of the metasurface can be independently time-modulated for two orthogonal polarizations. A space-time bias is applied to the metasurface, enabling directionally dependent electromagnetic responses. When the modulation wavenumber is larger than that in free space, the metasurface suppresses certain harmonic mixing products in the far field, allowing subharmonic mixing. The metasurface was experimentally validated for 2-path configuration, where the fabricated metasurface suppresses odd harmonic mixing products. With proper design of the space-time bias waveform, Doppler-like frequency translation is demonstrated at twice the modulation frequency.

Near-Field Beamforming in Leaky-Wave Resonant Antennas

[Sjoerd Bosma](#) (Delft University of Technology, The Netherlands); [Huasheng Zhang](#) (Delft University of Technology, The Netherlands); [Andrea Neto](#) (Delft University of Technology, The Netherlands); [Nuria LLombart](#) (Delft University of Technology, The Netherlands)

There is a large interest in utilizing lens arrays for many applications in the mm- and submm- wavelength ranges. The efficiency of the excitation of dielectric lenses increases significantly when the feeding structures support leaky-wave radiation mechanisms. Leaky-wave feeding structures based on resonant cavities can generate very high directivity in a dense medium. Many scenarios require lenses of moderate size and typically the focusing surface needs to be in the near field of the radiators. In this contribution, we analyse the near-field radiation mechanism of such leaky-wave feeds and provide guidelines to design moderate size lenses.

EuCAP Best Paper Award - Propagation

The MEKaP Project: Measuring Tropospheric Impairments at Ka Band with MEO Satellites

[Lorenzo Luini](#) (Politecnico di Milano, Italy); [Carlo Riva](#) (Politecnico di Milano, Italy); [Alberto Panzeri](#) (Politecnico di Milano, Italy); [Armando Rocha](#) (University of Aveiro & Instituto de Telecomunicações, Portugal); [Susana Mota](#) (University of Aveiro & Instituto de Telecomunicações, Portugal); [Frank S. Marzano](#) (Sapienza University of Rome, Italy); [Augusto Marziani](#) (Sapienza University of Rome, Italy); [Marianna Biscarini](#) (Sapienza University of Rome, Italy); [Fernando Consalvi](#) (FUB, Italy); [Vincenzo Schena](#) (Thales Alenia Space Italia, Italy); [Antonio Martellucci](#) (European Space Agency, The Netherlands)

The design phase of an ESA-funded project (MEKaP - MEO Ka-band Propagation) is described. The study, involving Politecnico di Milano, Sapienza Università di Roma, Instituto de Telecomunicações-Aveiro Pole and Thales Alenia Space-Italia, aims at characterizing the main properties of the atmospheric radio channel of a MEO Ka-band SatCom system. The propagation campaign, lasting at least two years and including four ground receivers, will rely on the MEO O3b Ka-band satellite constellation, which provides key characteristics for propagation measurements, such as continuous observation time (always at least one satellite is visible) and global coverage up to mid-latitudes. The experimental data collected during the campaign will be used to test and improve the available propagation models for non-geostationary systems and to extend the experimental database of radio regulatory bodies such as the ITU-R.

P1.082 Assessment of sub-THz Mesh Backhaul Capabilities from Realistic Modelling at the PHY Layer

[Grégory Gougeon](#) (SIRADEL, France); [Yoann Corre](#) (SIRADEL, France); [Mohammed Zahid Aslam](#) (SIRADEL, France); [Simon Bicaïs](#) (CEA, France); [Jean-Baptiste Doré](#) (CEA, France)

Spectrum above 90 GHz is a key promising investigation domain to offer future wireless networks with performance beyond IMT 2020 such as 100+ Gbit/s data rate or sub-ms latency. As the propagation is strongly constrained at those frequencies, the short-range connectivity is a relevant target application. However, the huge available bandwidth can also serve the backhaul transport network in the perspective of future ultra-dense deployments, and massive fronthaul data streams. This paper investigates the feasibility and characteristics of the sub-THz mesh backhauling either installed in the streets or inside a large venue. The study relies on the highly realistic simulation of the physical layer performance, based on detailed geographical representation, ray-based propagation modelling, RF phase noise impairment, and a new robust polar modulation. It is shown that each link of a dense mesh backhaul network can reliably deliver several Gbit/s per 1-GHz carrier bandwidth.

Breast Cancer Imaging Using a 24 GHz Ultra-Wideband MIMO FMCW Radar: System Considerations and First Imaging Results

[Maria Virginia Prati](#) (Politecnico di Milano, Italy); [Jochen Moll](#) (Goethe University Frankfurt am Main, Germany); [Christian Kexel](#) (Goethe University Frankfurt, Germany); [Duy Hai Nguyen](#) (Goethe University Frankfurt, Germany); [Avik Santra](#) (Infineon Technologies AG, Germany); [Andrea Aliverti](#) (Politecnico di Milano, Italy); [Viktor Krozer](#) (Goethe University of Frankfurt am Main, Germany); [Vadim Issakov](#) (Infineon Technologies AG, Germany)

Microwave imaging for breast cancer detection has been widely studied as an alternative technique to the conventional X-ray mammography. The systems developed until now operate at frequencies of a few gigahertz. This limits the achievable image quality. Higher operational frequencies are advantageous for achieving a better resolution, at the expense of a lower penetration depth. The downscaling of components together with an integrated radar transceiver would lead to the development of a compact and cost-effective radar imaging system. This paper investigates the possibility of using an integrated ultra-wideband frequency-modulated continuous-wave (FMCW) radar system operating at a center frequency of 20 GHz and bandwidth of 8 GHz for breast cancer imaging. System considerations are developed and first imaging results based on numerical data are presented.

Physical Modeling for Device-Free Localization Exploiting Multipath Propagation of Mobile Radio Signals

[Martin Schmidhammer](#) (German Aerospace Center DLR, Germany); [Michael Walter](#) (German Aerospace Center DLR, Germany); [Christian Gentner](#) (German Aerospace Center DLR, Germany); [Stephan Sand](#) (German Aerospace Center DLR, Germany)

This work proposes a model to describe the impact of a target on the received power of a multipath component (MPC). The physical propagation path of an MPC is decomposed geometrically and is described by direct propagation paths between physical and virtual nodes. Using the scalar theory of diffraction, the impact of a target on the electric field can be calculated for each component, individually. Thereby, the model relates alternations of the received power of MPCs to the location and orientation of the target, which allows device-free localization systems to exploit multipath propagation. The model is evaluated for a single link scenario of one specular reflection. A comparison of modeled attenuation results to wideband measurement data qualitatively confirms the applicability of the proposed model representing target-induced attenuation.

Characterization of the Propagation Channel in Conference Room Scenario at 190 GHz

[Diego Dupleich](#) (Ilmenau University of Technology, Germany); [Robert Müller](#) (TU Ilmenau, Germany); [Sergii Skoblikov](#) (TU Ilmenau, Germany); [Markus Landmann](#) (Fraunhofer Institute for Integrated Circuits IIS, Germany); [Giovanni Del Galdo](#) (Fraunhofer Institute for Integrated Circuits IIS & Technische Universität Ilmenau, Germany); [Reiner S. Thomä](#) (Ilmenau University of Technology, Germany)

In the present paper we introduce unique double-directional dual-polarized measurements at 190 GHz in a conference room with the aim of characterizing propagation for channel modelling and beam-forming applications. Assisted by ray-tracing, multiple scatterers have been identified, showing a rich multi-path environment. Investigations have shown that polarization diversity increases spatial diversity and a more deterministic modelling approach in polarization is needed to avoid overestimating polarization diversity gains.

EuCAP Best Paper Award - Measurement

Examining and Optimising Far-Field Multi-Probe Anechoic Chambers for 5G NR OTA Testing of Massive MIMO Systems

[Stuart F Gregson](#) (Queen Mary, University of London, United Kingdom (Great Britain)); [Clive Parini](#) (Queen Mary, University of London, United Kingdom (Great Britain))

Direct far-field (DFF) testing has become the de facto standard for sub-six GHz over the air (OTA) testing of the physical layer of radio access networks with the far-field multi-probe anechoic chamber (FF-MPAC) being especially widely deployed for the verification of massive multiple input multiple output (Massive MIMO) antennas in the presence of several users. The adoption of mm-wave bands within the fifth generation new radio (5G NR) specification has meant that, as these systems require the user equipment be placed in the far-field of the base transceiver station (BTS) antenna, either excessively large FF-MPAC test systems are required or, the user equipment is placed at range-lengths very much shorter than that suggested by the classical Rayleigh criteria. This paper explores range length effects on several communication system figures of merit and examines the consequences of testing within smaller enclosures. Results are presented and discussed.

Real-Time Demonstration of Antenna Effects on Emulated Wireless Capsule Endoscope Links

[Rytis Stasiunas](#) (Aalto University, Finland); [Pasi Koivumäki](#) (Aalto University, Finland); [Md Miah](#) (Aalto University & School of Electrical Engineering, Finland); [Mikko Heino](#) (Aalto University, Finland); [Katsuyuki Haneda](#) (Aalto University, Finland); [Clemens Icheln](#) (Aalto University & School of Electrical Engineering, Finland)

Real-time over-the-air video transfer platform is developed for a wireless capsule endoscope scenario. The use of the platform for demonstration of video transfer aims at intuitive and instant understanding of antenna effects on quantitative and qualitative radio link performance, e.g., video image quality, bit error rate (BER) and constellation patterns of digital modulation. The platform consists of a host computer and a universal software defined peripheral as general video source and radio transceivers, complemented with capsule and on-body antennas and liquid body phantom to emulate an inbody-to-onbody radio link. The antennas operate at 433MHz, while the liquid mimics the complex permittivity of a colon tissue.

Suppressing Undesired Echoes by Sparsity Based Time Gating of Reconstructed Sources

[Josef Knapp](#) (Technical University of Munich, Germany); [Jonas Kornprobst](#) (Technical University of Munich, Germany); [Thomas F. Eibert](#) (Technical University of Munich, Germany)

The free-space radiation characteristic of an antenna under test (AUT) is determined from measurements in proximity of a scatterer by time gating reconstructed equivalent currents for the AUT and the scatterer. The presented approach effectively combines spatial filtering methods with time domain methods while mitigating their individual drawbacks. In contrast to conventional time-gating methods which usually work on the measured probe signals this approach allows to get rid of undesired echo perturbations even if measurement samples are located in the shadow region of the scatterer and the line of sight (LOS) contribution and the echo contribution are indistinguishable for the field probe. In contrast to conventional frequency domain methods, mutual coupling contributions of the AUT currents are identified and removed in the time domain. Numerical examples show that, due to the sparse reconstruction, the AUT radiation can be determined accurately even at the borders of the measured bandwidth.

P1.073 Advanced Calibration Method for Accurate Microwave Absorber Reflectivity Measurements at Oblique Illumination Angles

[Willi Hofmann](#) (Technische Universität Ilmenau, Germany); [Andreas Schwind](#) (Technische Universität Ilmenau, Germany); [Christian Bornkessel](#) (Technische Universität Ilmenau, Germany); [Matthias Hein](#) (Ilmenau University of Technology, Germany)

The increasing complexity of new radio systems requires a change of measurement sites towards more sophisticated virtual electromagnetic environments. RF absorbers are essential elements of these environments to achieve the propagation conditions desired by obtaining well-defined measurement conditions and suppressing interfering signals. Optimal propagation conditions can only be achieved by sufficient knowledge of the frequency- and angle-dependent reflectivity of RF absorbers. For this purpose, an advanced calibration procedure for reflectivity measurements at oblique illumination angles based on a combination of the established RCS- and NRL-arch methods is proposed. Measurement results obtained by the new technique show good consistency with the NRL-arch but with the advantage of accessing the angle-dependent behavior of the RF absorbers. The proposed calibration procedure will not only help manufacturers to characterize their absorbers more effectively, but additional knowledge of the off-normal reflectivity will also contribute to the optimization of measurement sites such as virtual electromagnetic environments.

P2.037 Axicon-hyperbolic Lens for Reflectivity Measurements of Curved Surfaces

[Aleksi Tamminen](#) (Aalto University, Finland); [Samu-Ville Pälli](#) (Aalto University, Finland); [Juha Ala-Laurinaho](#) (Aalto University, Finland); [Mika Salkola](#) (Icare Finland Oy, Finland); [Antti V. Räsänen](#) (Aalto University, Finland); [Zachary D Taylor](#) (Aalto University, Finland)

We present a quasioptical element design that transforms a diverging Gaussian beam to an approximate Bessel beam. The elements are designed to deliver millimeter waves to a curved surface in reflectivity measurements. Compared to canonical focused quasioptical designs, such as the Gaussian-beam telescope, diffraction from an axicon surface allows for significant relaxation in alignment requirements. This research is motivated by in vivo cornea measurements where achieving optimal optical alignment is difficult. Combined axicon-hyperbolic lenses were designed for 220-330 GHz and fabricated of TOPAS, a low-loss material at millimeter waves. The lens performance is evaluated with near-field measurements. Compared to the Gaussian beam, the in-range alignment requirement can be relaxed by an order of magnitude with the Bessel beam.

Best Student Paper Award

Metal Stamped Antenna-in-Package for Millimeter-wave Large-scale Phased-array Applications Using Multiphysics Analysis

[Junho Park](#) (Pohang University of Science & Technology, Korea South); [Wonbin Hong](#) (Pohang University of Science and Technology (POSTECH), Korea South)

This paper presents a metal stamped AiP concept for enhanced cooling in millimeter-wave phased array systems. To verify the proposed AiP concept, the POC model is designed and fabricated using standard PCB and metal stamping process. The fabricated POC model achieves impedance bandwidth of 0.7 GHz with a center frequency of 28.5 GHz. Good agreement is achieved between the measured and simulated radiation patterns with the measured gain of 14.01 dBi. The effect of the fabrication error on EM properties is discussed to explain the difference between the simulated and measured results of the gain. The two-dimensional array is demonstrated to verify the feasibility for a practical application of mmWave Massive MIMO systems with main beam scanning range of $\pm 30^\circ$ in both elevation and azimuth planes. Computational fluid dynamics simulation confirms that the proposed AiP reduces the maximum surface temperature of the package by more than 11 °C.

Terahertz MIMO Fading Analysis and Doppler Modeling in a Data Center Environment

[Chia-Lin Cheng](#) (Georgia Tech, USA); [Seun Sangodoyin](#) (Georgia Institute of Technology, USA); [Alenka Zajic](#) (Georgia Institute of Technology, USA)

In this paper, we present results from a Terahertz (THz) channel measurement campaign in a data center environment. We analyze propagation parameters, such as pathloss, shadowing gain, and RMS delay spread. Amplitude fading statistics in a 4×4 Multiple-Input-Multiple-Output (MIMO) channel are also investigated. Furthermore, Doppler shift in THz bands due to the effect of cooling airflow turbulence, which causes cables (lying in the wireless propagation path) to vibrate is also measured. A two-dimensional (2-D) geometrical propagation model that includes moving scatterers (cables) is introduced. From the 2-D model, a corresponding Doppler power spectrum (DPS) is derived and validated with measured data. This work is pertinent to THz wireless systems design for a data center environment.

A MIMO Joint Communication-Radar Measurement Platform at the Millimeter-Wave Band

[Preeti Kumari](#) (UT Austin, USA); [Amine Mezghani](#) (Electrical and Computer Engineering & University of Manitoba, Canada); [Robert Heath](#) (The University of Texas at Austin, USA)

A fully-digital wideband joint communication-radar (JCR) at the millimeter-wave (mmWave) band will simultaneously enable high communication and radar performances with enhanced design flexibility. In this paper, we present a measurement platform with a software-defined architecture to evaluate and demonstrate the performance of these JCR systems using real channel measurements. We develop this platform by extending a mmWave communication set-up with an additional full-duplex radar receiver and by capturing the MIMO JCR channel using a moving antenna on a sliding rail. To characterize the JCR performance, we conduct indoor experiments and apply traditional/advanced processing algorithms on the measured data. The results demonstrate that our testbed at 73 GHz with 2 GHz bandwidth can capture the JCR channel with high range/direction estimation accuracy. The comparison between the communication and radar channel shows the potential for improving JCR performance by exploiting the antenna diversity due to widely-separated communication and radar receivers.

Broadband Metasurface-Based Antenna Using Hexagonal Loop Elements

[Wenzhang Zhang](#) (University of Liverpool, United Kingdom (Great Britain)); [Yi Huang](#) (University of Liverpool, United Kingdom (Great Britain)); [Jiafeng Zhou](#) (University of Liverpool, United Kingdom (Great Britain))

A broadband metasurface-based antenna with hexagonal loop radiating elements is presented. To achieve a broadband response, an array of hexagonal loop elements is taken as the main metasurface-based radiator. The antenna is fed by a microstrip line through a coupling slot. To reveal the underlying modal behaviors, the characteristic mode analysis was used for modeling, analyzing, and optimizing the antenna structure. The proposed broadband hexagonal loop-based antenna with an overall size of $1.1 \lambda_0 \times 1.1 \lambda_0 \times 0.06 \lambda_0$ can achieve 56% fractional bandwidth and a relatively stable gain of 7-11 dBi over the operating band.

3-D Printed Terahertz Lens for Generation of Non-diffractive Bessel Beam Carrying OAM

[Gengbo Wu](#) (City University of Hong Kong, Hong Kong); [Ka Fai Chan](#) (City University of Hong Kong, Hong Kong); [Chi Hou Chan](#) (City University of Hong Kong, Hong Kong)

A novel 3-dimensional (3-D) printed lens for high-order Bessel beam generation operating at 300 GHz is proposed in this paper. The designed terahertz (THz) lens can transform the spherical wave-front from the feed horn into non-diffractive Bessel beam carrying orbital angular momentum (OAM). The lens consists of discrete dielectric posts, whose height can be tuned from pixel to pixel to realize the desired aperture phase distribution. Furthermore, 3-D printed technology is used to fabricate the lens with low cost. Measured results demonstrate that the designed 3-D printed lens can generate THz non-diffractive Bessel vortex beam carrying OAM.

Poster3-A06: Conformal Antennas

Antennas

Room: Exhibition Hall

P3.001 Green Coordinates for Generation of Conformal Antenna Geometries

[Ekrem Altinozen](#) (George Green Institute for Electromagnetics Research & Nottingham University, United Kingdom (Great Britain)); [Harrison Ian](#), [Ana Vukovic](#) and [Phillip Sewell](#) (University of Nottingham, United Kingdom (Great Britain))

Conformal antennas and antenna arrays have emerged as a powerful platform for a wide number of applications from mobile and stationary communication to aerospace. In many cases producing numerical models of conformal antennas is not trivial especially in cases of complex feed circuits. In this paper, we investigate the Green Coordinate method for space manipulation of three-dimensional objects and apply it to generating geometries of conformal antennas. By considering a special case of antenna bent over a developable cylindrical surface, the paper explores the impact of the Green Coordinate method on the object deformations and its impact on the electromagnetic simulations, i.e., on the accuracy of antenna parameters, namely the reflection coefficient and the far-field radiation patterns.

P3.002 Element Positioning Effect on the Performance of Conformal Arrays: Synthesis and Diagnostics

[Giovanni Leone](#), [Fortuna Munno](#) and [Rocco Pierri](#) (Università della Campania Luigi Vanvitelli, Italy)

The inverse source problem has a number of applications in antenna analysis and synthesis. The properties of the radiation operator, connecting the source current to the far zone field, depends on the source geometry and can be analyzed by its Singular Value Decomposition. In this paper we examine point source reconstructions by considering the Point Spread Function. An approximate closed form evaluation for limited observation domains reveals a space variant behavior. It turns out that for a conformal array a non-uniform elements spacing accommodates definite advantages both for diagnostic and synthesis purposes. Numerical results are shown for a semi-circumference source observed in far zone over a semi-circumference.

P3.003 Design and Evaluation of a Radio-Interferometry Antenna for the REXUS 25 Sounding Rocket

[Ivar Jansen](#), [Ronis T. Maximidis](#), [Mark Wijtvliet](#) and A. B. (Bart) Smolders (Eindhoven University of Technology, The Netherlands)

This paper presents the design and analysis of an on-rocket antenna used in a radio-interferometry experiment. The goal of the experiment is to accurately track a sounding rocket during flight. The antenna operates in the 70 cm band and is designed to work under tight constraints; a confined space, stable center frequency under large temperature variations and low budget. A microstrip patch antenna on PEEK450G903 substrate was identified as the most suitable solution, due to the relatively low cost and temperature stable dielectric properties of the PEEK material. This antenna design achieved a bandwidth of 2.5 MHz. Measurements were performed on the antenna before and after flight such that changes in performance due to vibrations, temperature and other environmental conditions can be evaluated.

P3.004 Power Allocation Optimization of A Conformal Antenna Array for Satellite Applications

[Yijun Zhou](#) (I2R, Singapore); [Xianming Qing](#), [N Nasimuddin](#) and [Terence S.P. See](#) (Institute for Infocomm Research, Singapore); [Chan Kuen Sim](#) (Institute for Microelectronics, A*Star, Singapore); [Yunjia Zeng](#) (Institute for Infocomm Research, Singapore); [Guan Seng Ngo](#) (Addvalue

Innovation Pte Ltd, Singapore)

A power allocation optimization method of a conformal antenna array is proposed for L-band low Earth orbit (LEO) satellite applications. For a required effective isotropic radiated power (EIRP), the power consumption of the RF payload with optimized power allocation for antenna elements is greatly reduced, namely, up to 52% reduction compared with the one with single antenna excitation.

P3.005 Spherical Harmonic Theory Investigations for Spherical Antenna Arrays

[Leonidas Marantis](#) (University of Piraeus, Greece); [Paul Brennan](#) (University College London, United Kingdom (Great Britain)); [Athanasios G. Kanatas](#) (University of Piraeus, Greece)

Low Earth Orbit satellite communications can be significantly improved by the omni-directional beam-scanning ability of the spherical antenna arrays. The signal processing of spherical antenna arrays is essentially enhanced by employing spherical harmonic theory. Spherical harmonics (or spherical modes) exploit sphere's perfect symmetry and demonstrate the feature to "reproduce" themselves in the far-field. First, this paper justifies the cost and performance superiority of the spherical arrays compared to the planar case. In addition, it presents several spherical array investigations that utilize spherical harmonic theory, offering substantial enhancement and simplifying the computational level of the array processing.

P3.006 Design of Multiband Conformal Antenna for Sounding Rocket

[Unai Beaskoetxea](#) (Anteral, Spain); [JuanCarlos Iriarte](#) (Public University of Navarra & Antenna Group, Spain); [Iñigo Ederra](#) (Universidad Pública de Navarra & Institute of Smart Cities, Universidad Pública de Navarra, Spain); [Itziar Maestrojuán](#) (Anteral, Spain)

In this paper, the design of a multiband low-profile conformal antenna for the first European suborbital launcher, MIURA-1 is presented. The antennas cover the telemetry and GNSS applications. Here, the antenna physical and RF characteristics are given. The proposed antennas-solution is not only interesting for the launcher's market, but also could find its application in space, aviation, or automotive, they can easily integrated in curved surfaces.

P3.007 Rapid Analysis of Arbitrary-Shaped Conformal Beam-Scanning Arrays

[Denys Nikolayev](#) (Institut d'Électronique et de Télécommunications de Rennes (UMR CNRS 6164), France); [Agnese Mazzinghi](#) (University of Florence, Italy); [Anja K. Skrivervik](#) (EPFL, Switzerland)

Conformal antenna arrays are able to fit seamlessly on curved 3D-shaped surfaces, which are found ubiquitously on vehicles, aircraft, a human body, etc. In addition, conformal structures can overcome the scan loss limitations of conventional planar arrays. Yet, only a few computational analysis methods have been proposed with either performance or applicability limitations. In this study, a rapid analysis methodology is developed for the analysis of arbitrary-shaped conformal beam-scanning arrays. The method requires only specifying the element position vectors and normals in space. Arbitrary individual antenna patterns could be specified. Finally, an example study is provided examining the beam-steering performance of half-cylinder conformal arrays vs a reference square planar array.

P3.008 Conformal 2.4 GHz Antenna with Room Temperature Vulcanized (RTV) Silicone Rubber Substrate

[Denis Le Goff](#), [Yuchan Song](#), [Ghilsain Riondet](#) and [Koen Mouthaan](#) (National University of Singapore, Singapore)

A flexible and conformal antenna for 2.4 GHz applications, using a commercial off-the-shelf (COTS) room temperature vulcanized (RTV) silicone rubber substrate and flexible polyimide printed circuit board (PCB) technology, is presented. Three different solutions for the ground plane are investigated. Antennas are tested on a flat surface and conformed to a cylindrical surface as well. The presented antennas greatly simplify the fabrication of highly conformal antennas and enable the practical implementation of flexible antennas with minimal performance degradation and at a relatively low cost.

Poster3-A11: Multiband and Wideband Antennas

Antennas

Room: Exhibition Hall

P3.009 A Dual-Element Folded Strip Monopole with SRR Loading for Multiband Handset MIMO Applications

[Saqer S Alja'afreh](#) (Mutah University, Jordan); [Qian Xu](#) (Nanjing University of Aeronautics and Astronautics, China); [Lei Xing](#) (Nanjing University of Aeronautics and Astronautics, United Kingdom (Great Britain)); [Yi Huang](#) (The University of Liverpool, United Kingdom (Great Britain)); [Chaoyun Song](#) (University of Liverpool, United Kingdom (Great Britain)); [E'qab Almajali](#) (University of Sharjah, United Arab Emirates)

A compact, low profile and multiband dual-element folded strip monopole is presented for mobile phone MIMO applications. Both the compactness and the multiband operation are achieved by loading the folded strip with a split ring resonator (SRR). The antenna elements are placed on the same mobile PCB arm in order to achieve angle diversity that enhances ports isolations, especially below 1 GHz. The proposed antenna achieves isolations of higher than 12 dB, enveloped correlation coefficients (ECC) of less than 0.1, apparent diversity gain around 10 dB and total efficiencies of greater than 60 within the frequency band of interest (GSM850, DCS1800, PCS1900, and LTE2500).

P3.010 Multi-Mode Smartphone Antenna Array for 5G Massive MIMO Applications

[Naser Ojaroudi Parchin](#) (University of Bradford, United Kingdom, United Kingdom (Great Britain)); [Haleh Jahanbakhsh Basherlou](#) (Bradford College, United Kingdom (Great Britain)); [Yasir Ismael Abdulaheem Al-Yasir](#) (University of Bradford, United Kingdom (Great Britain)); [Maryam Sajedin](#) (University of Aveiro, Portugal); [Jonathan Rodriguez](#) (Instituto de Telecomunicações, Portugal); [Raed A Abd-Alhameed](#) (University of Bradford, United Kingdom (Great Britain))

A multi-band antenna array is proposed for 5G massive MIMO systems. The presented antenna not only exhibit multi-band operation but also generates the polarization diversity characteristic which make it suitable for multi-mode operation. Its configuration contains eight modified planar-inverted F antenna (PIFA) elements located at different corners of the smartphone main board. For ease integration and design facilitation, the antenna elements and ground plane are etched on the same layer. For S11≤−10 dB, PIFA elements of the MIMO design operate at the frequency ranges of 2.5-2.7 GHz, 3.4-3.8 GHz, and 5.6-6 GHz covering the LTE 2600, 42/43, and 47 operation bands. Due to placement of the antenna elements, the proposed design can support both vertical and horizontal polarizations. It offers good S-parameters, acceptable isolation, dual-polarized radiation coverage, and sufficient efficiency. In addition, the calculated TARC and ECC results of modified PIFAs are low over the operation bands.

P3.011 Ultra-Wideband MIMO Diversity Antenna System for Future Handsets

[Naser Ojaroudi Parchin](#) (University of Bradford, United Kingdom, United Kingdom (Great Britain)); [Haleh Jahanbakhsh Basherlou](#) (Bradford College, United Kingdom (Great Britain)); [Yasir Ismael Abdulaheem Al-Yasir](#), [Ali A. S. AlAbdullah](#) and [Raed A Abd-Alhameed](#) (University of Bradford, United Kingdom (Great Britain))

A new design of UWB-MIMO antenna system is proposed for future smartphones. The design contains four pairs of compact microstrip-fed slot antennas with dual-polarized function that are placed symmetrically at different edge corners of the smartphone mainboard. Each antenna pair consists of a circular-ring slot radiator fed by two independently semi-arc-shaped microstrip feeding lines which can exhibit polarization diversity characteristic. The characteristics of the smartphone antenna are examined using both simulations and measurements and good results are achieved. An impedance bandwidth of 2.5-10.2 GHz with 121% fractional bandwidth (FBW) is achieved for S11 ≤ -10 dB. However, for S11 ≤ -6 dB, this value is more than 130% (2.2-11 GHz). In addition, the calculated diversity performances of the design in terms of ECC and TARC are very low over the entire operation band. Furthermore, sufficient values for the channel capacity and its loss are obtained.

P3.012 Multi-Band/Wide Band Printed Quad Helical Antenna

[Fayez Hyjazie](#) (Huawei Technologies Co. Ltd., Canada); [Halim Boutayeb](#) (Huawei Technologies, Canada)

A technique is proposed for designing multi-band and/or wide band printed quadrifilar helical antennas. This technique uses a microstrip line tuning section in the vicinity of the feeding ports. This section contains an elongated body and a tail member extending away from the body. A geometry of the tail member is selected for modifying an impedance of the radiating element and broadening the antenna resonance bandwidth. A four port antenna is designed for operating in wide band (24%, S11<-15dB) or in three frequency bands, with one of the frequency bands being more than 24% (S11<-10dB): 1.88-2.12GHz (E-UTRA 39), 2.3-2.4GHz (E-UTRA 40) and 3.4-3.8GHz (E-UTRA 42 and 43). Index Terms- quadrifilar, helical antenna, multi-band, wide band

P3.013 Design of Dual-band Coupled-fed Dipole Array Antenna Element for PCL Systems

[Sungsik Wang](#) (Hongik University, Korea (South)); [Junsik Park](#) (Hanwha Systems, Korea (South)); [Hosung Choo](#) (Hongik University, Korea (South))

This article proposes a dual-band coupled-fed dipole array antenna element for Passive Coherent Location (PCL) systems, which is operating in FM and T-DMB bands. The proposed coupled-fed antenna is composed of the internal and external dipoles that resonate in FM and DMB frequencies, respectively. To confirm the suitability of the proposed coupled-fed antenna, we construct an 8-element uniform circular array (UCA) with the proposed coupled-fed dipole element and examine the beamforming performance of the array. The results verify that the proposed antenna structure can achieve the required dual-band operation for PCL systems using the coupled-fed mechanism

P3.014 Validation Tests for the Application of a Circular PMA with Slotted Ground Plane for Partial Discharges Detection in Power Transformers

[Arthur Souza](#) (UFCEG, Brazil); [Luiz Nobrega](#) (Universidade Federal de Campina Grande, Brazil); [Alexandre Serres](#) (UFCEG, Brazil); [Edson G da Costa](#) (Federal University of Campina Grande, Brazil); [George Xavier](#) (Universidade Federal de Campina Grande, Brazil); [Ana Cruz](#) and [Matheus Gomes](#) (UFCEG, Brazil)

In this article, the applicability of an UHF circular printed monopole antenna with slotted ground plane was evaluated in order to detect partial discharges in power transformers. To verify the applicability of the antenna for this purpose, validation tests were performed: reflection coefficient (bandwidth) and gain in an anechoic chamber, to avoid external interferences; and PD sensitivity tests from the comparison with the conventional method of IEC 60270, using for this purpose an oil cell with immersed flat-tip electrodes. These analyzes were performed for the design of an antenna with optimized performance. The obtained values for the antenna's bandwidth, size, gain and PD detection sensitivity make it possible to classify the antenna as efficient in detecting partial discharges in power transformers.

P3.015 An Ultra-Wideband Stacked Spiral-Helix Composite Antenna

[Jiachun Jiang](#), [Long Zhang](#), [Ning Luo](#), [Yejun He](#), [Sai-Wai Wong](#) and [Xiao Zhang](#) (Shenzhen University, China); [Steven Gao](#) (University of Kent, United Kingdom (Great Britain))

This paper presents an ultra-wideband stacked spiral-helix antenna. The proposed antenna consists of two stacked Archimedean spirals and a pair of helix. By connecting the two stacked spirals through two helices, the effective electrical length is increased, and thus the low-end cutoff frequency of the proposed antenna can be greatly decreased. By reasonably designing the height and number of turns of the helix, the helical antenna can operate in the axial mode. Since the proposed antenna is mainly radiated by the spiral at high frequency and mainly radiated by the helix at low frequency, the proposed antenna can obtain bidirectional radiation at high frequency range and unidirectional radiation at low frequency range. Simulated results show that the proposed antenna can achieve a 3-dB axial ratio bandwidth from 1.5 GHz to 20 GHz

P3.016 Shared Aperture Dual S- And X-band Antenna for Nano-Satellite Applications

[Daniel E. Serup](#), [Robin Williams](#), [Shuai Zhang](#) and [Gert Pedersen](#) (Aalborg University, Denmark)

This paper presents the simulated performance of a dual S- and X-band shared aperture antenna design. The antenna is 82 by 82 mm and it has a total height of less than 4 mm. This size allows the antenna to fit within the parameters of a nano-satellite unit structure. The antenna is right hand circularly polarized in both bands. The Antenna is tuned to a S-band frequency range from 2.025 to 2.075 GHz and a X-band frequency range from 7.75 to 8.75 GHz. The design has a Realized right hand circularly polarized gain of more than 6 dB in the S-band and more than 12 dB in the X-band. The impedance bandwidth is very wide as it exceeds the selected frequency ranges. The cross-coupling is below -25 dB in the S-band and below -30 dB in the selected X-band frequency range.

P3.017 Low Attenuation Dichroic Sub-Reflector for Wide Incident Angles for Ka/Ku Band Satellite Antenna Systems: An ECA Analysis

[Chung-Chin Jian](#), [Yu-Lun Su](#), [Thomas Lohrey](#) and [Yu-Ling Lee](#) (Atom Element Matter B. V., The Netherlands); [Hsi-Sheng Goan](#) (National Taiwan University, Taiwan)

In this paper, we conduct an equivalent circuit approach (ECA) analysis to investigate the incident angle dependence on the performance of different frequency-selective-surface structures and arrangements in dichroic sub-reflectors (DSR's). We find a DSR with low-attenuation performance for a range of incident angles, capable of combining both Ku band TV and Ka band broadband interactive services with the LNB located beside the feedarm of a one-arm satellite antenna dish.

P3.018 Roof/Side Mount Combination Antenna for LTE and Satellite Communication Applications

[Liu Guifeng](#) (The 54th Research Institute of China Electronics Technology Group Corporation, China); [Biao Du](#) (JLRAT, China); [Chuanfeng Niu](#) (Joint Laboratory of Radio Astronomy Technology, China); [Yingran He](#) (The 54th Research Institute of CETC, China)

A roof/side mount combination antenna for Long Term Evolution (LTE) and satellite communication applications is presented. The proposed antenna includes 4G (The Fourth Generation Mobile Communication System) antenna and VHF (Very High Frequency) antenna. In order to realize a compact structure, some miniaturization and multiband techniques are employed, such as meandered structure, lumped element and multiple branch radiating elements. Finally, the antenna in this paper occupies a compact volume of 360mm×90mm×54mm. The 4G antenna produces two wide bands which can cover GSM850, GSM900, DCS1800, PCS1900, UMTS2100 and LTE2300/2500. The two bands yielded by VHF antenna can cover 135-138MHz and 145-149MHz. Besides, the two antennas in this paper are planar printed structures which can significantly reduce the cost.

P3.019 A Single-feed Compact Wideband Circularly Polarized Antenna for INMARSAT/GNSS Applications

[N Nasimuddin](#) and [Xianming Qing](#) (Institute for Infocomm Research, Singapore)

A single-feed low profile compact wideband circularly polarized (CP) stacked antenna is proposed for INMARSAT/GNSS applications. The antenna consists of a ring-slotted radiating patch with a grounded metallic-via, a slit-slotted parasitic patch, and a coaxial feeding probe. The wideband CP radiation is attributed to the stacked slit-/slotted-patches combination and ring-slot patch with grounded via. An antenna prototype at the L-band with an overall size of 0.381emdash0.381emdash0.0661emdash (lmda is the free space wavelength at 1.518 GHz) shows a measured 3-dB axial ratio (AR) bandwidth of 9.8% (1.50 GHz x 1.67 GHz), impedance bandwidth (-10dB reflection coefficient) of 12.9% (1.479 GHz x 1.683 GHz), and gain greater than 5.2 dBic across the AR bandwidth.

Poster3-A12: Wearable and Implantable Antennas

Antennas

Room: Exhibition Hall

P3.020 Graphene Printed Flexible and Conformal Array Antenna on Paper Substrate for 5.8GHz Wireless Communications

[Xinyao Zhou](#) and [Ting Leng](#) (University of Manchester, United Kingdom (Great Britain)); [Kewen Pan](#) (University of Manchester, United Kingdom (Great Britain)); [Mahmoud Abdelrahman Abdalla](#) (MTC, Cairo, Egypt); [Zhirun Hu](#) (University of Manchester, United Kingdom (Great Britain))

In this paper, a printed graphene compact, low-cost, disposal, flexible and conformal, coplanar waveguide (cpw) fed, linear array antenna has been proposed. It was designed for 5.8GHz radars, portable electronic devices, and commercial wireless LAN applications and manufactured by screen printing formulated highly conductive graphene ink on paper substrate. The array achieves 73% total radiation efficiency and a peak gain value of 4.5dBi at 5.8GHz, with its bandwidth ranges from 4.6GHz to 7.9GHz (52.8%). Over the operating frequency, the radiation of the antenna has been proved as a typical radiation pattern of a patch antenna array.

P3.021 Circularly Polarized Corner-Truncated and Slotted Microstrip Patch Antenna on Textile Substrate for Wearable Passive UHF RFID Tags

[Duc Viet Le](#) (University of Tampere, Finland); [Leena Ukkonen](#) (Tampere University of Technology, Finland); [Toni Björninen](#) (Tampere University, Finland)

We present a compact circularly polarized (CP) antenna for wearable passive UHF RFID tags. The antenna is a square-shaped microstrip patch antenna where we have applied corner truncation and slotting techniques in the top layer conductor for achieving the CP property and a shorting pin and loop structure for impedance matching. Despite using a low-permittivity textile as an antenna substrate, the antenna's footprint size is only 5-by-5 cm, which is approximately 15% of the operating wavelength. At the same time, the on-body measurements, the antenna's axial ratio is 0.9 dB and the measured attainable read range (reader's EIRP = 3.28 W) of the tag reaches 4.2 meters with a CP reader antenna and ranges from 2.9 meters to 3.4 meters for a linear reader antenna, depending on the rotation angle between the antennas.

P3.022 Antenna Packaging for In-body Applications

[Jordi Romeu](#), [Giselle González-López](#) and [Sebastian Blanch Boris](#) (Universitat Politècnica de Catalunya, Spain); [Luis Jofre](#) (Universitat Politècnica de Catalunya, Spain)

A cylindrical mode expansion of the fields produced by an embedded antenna is used to determine the dimensions of the antenna packaging in order to minimize antenna impedance changes when the antenna is immersed in a varying dielectric medium

P3.023 A 915 MHz Wristwatch-Integrated Antenna for Wireless Health Monitoring

[Sanjeev Kumar](#) (Tyndall National Institute, University College Cork, Ireland); [John Laurence Buckley](#) (Tyndall National Institute & University College Cork, Ireland); [John Barton](#) (Tyndall National Institute, Ireland); [Robert Newberry](#) (Sanmina Corporation, USA); [Gary Dunlop](#) (Sanmina Corporation, Ireland); [Matthew Rodencal](#) (Sanmina Corporation, USA); [Carlo Webster](#), [Mélusine Pigeon](#) and [William G. Scanlon](#) (Tyndall National Institute, Ireland); [Brendan O'Flynn](#) (Tyndall National Institute, Ireland)

A compact 915 MHz antenna integrated within a wristwatch wireless sensor device is presented. The antenna is a variant of a planar inverted-F antenna (PIFA) and uses a dual-resonator configuration. The results of simulation and measurement are shown to be in good agreement with the antenna exhibiting desirable impedance and radiation characteristics together with low Specific Absorption Rate (SAR) performance. The antenna is fabricated using a low cost flexible printed circuit and is fully integrated into the watch device. Measurements on the prototype antenna show a -10 dB impedance bandwidth of 30 MHz, a peak realized gain of -4.9 dBi and a peak radiation efficiency of 15.9 % at 915 MHz. The antenna also has a low specific absorption rate (SAR) value of 0.003 W/kg making it suitable for a wide range of wrist-worn wireless applications.

P3.024 E-Field Distribution in Ex-Vivo Porcine Skin Layer from a Subsurface UHF Transmitter

[Noor Albadri](#), [Yana Salchak](#), [David V Thiel](#) and [Hugo G Espinosa](#) (Griffith University, Australia)

A tuned small slot antenna has been used for radio communications with internal transceivers/transmitters for in-vivo medical applications. The 2.45 GHz properties (permittivity and conductivity) shows that porcine skin tissue can be used as a substitute for human skin tissue in medical applications. In this study, a measure of the E-field distribution on the skin surface of human and porcine tissue is presented. Ex vivo measurements on boneless layered pork belly-fat (45mm thick 300mm x 150 mm sample of skin, fat and muscle) were compared with numerical modelling for a subdermal PIFA tuned antenna. The surface electric field distribution is quite well matched to an analytical formula over a 70dB dynamic range. The conductivity and relative permittivity adjusted to fit the measurement profile aligned with previously reported values. These results support the strategy that field strength measurements can be used to locate an injects radio transmitter.

P3.025 A Novel Wearable RF Head Coil for High Resolution 7T Magnetic Resonance Imaging

[Pouya Goodarzi](#) and [Fateme Geran Gharakhili](#) (Shahid Rajae Teacher Training University, Iran); [Hamidreza Saligheh Rad](#) and [Mohammad Reza Nazem Zadeh](#) (Tehran University of Medical Sciences, Iran)

In this article, a new structure of 7T magnetic resonance imaging RF coil has been designed and presented. The flexibility of this coil distinguishes it from others traditional coils. The mentioned array coil consists of 8-channels, each made of two antenna elements. The results show that using compressed elements in designing this coil provides a desired recursive factor (isolation better than 35 dB), while coupling is kept less than 60 dB between non-adjacent elements. In this report, the structure coupling effects include mutual effects of coil elements, resources, and phantom. The obtained results of the magnetic field homogeneity, bandwidth, and specific absorption rate are also evaluated. The results show that the bandwidth, the SAR for the 1w input power, and the B₁⁻ homogeneity distribution are 1.1%, 0.07969 W/kg, and 84%, respectively. To present this coil for a brain imaging, elements miniaturization is done where the elements size has been decreased in design.

P3.026 Textile Antenna as Moisture Sensor

[Davor Bonefačić](#) (University of Zagreb, Faculty of Electrical Engineering and Computing, Croatia)

The paper proposes the application of a resonant textile antenna as moisture sensor. Two setups are discussed, the first considering the textile antenna used in transmission and the second considering only the reflection at the antenna input. Laboratory tests have been performed on both setups, showing that the second, reflection based, approach shows better sensitivity and accuracy for moisture measurement.

Poster3-A13: Adaptive and Reconfigurable Antennas

Antennas

Room: Exhibition Hall

P3.027 A Novel Frequency Reconfigurable Yagi-Like MIMO Antenna System

[Syed Jehangir](#) (United Arab Emirates University, United Arab Emirates); [Rifaqat Hussain](#) (KFUPM, Saudi Arabia); [Mohammad S. Sharawi](#) (Polytechnique Montreal, Canada)

A compact single layer frequency reconfigurable Yagi-like multiple-input-multiple-output (MIMO) antenna system is presented based on slot excitation. The traditional omnidirectional pattern of a slot antenna is made directional by using a common complementary slot reflector (CSR) element. The total size of the CSR is 9.5*70 mm². The proposed MIMO antenna system can cover the frequency bands from 2.5 - 4.5 GHz, with a minimum bandwidth of 200 MHz. The frequency reconfigurability is achieved using varactor diodes. The overall size of the proposed antenna system is 40*100*0.76 mm³, making it suitable for compact wireless handheld devices. The antenna system satisfies Yagi as well as MIMO performance metrics.

P3.028 A Beam Steerable Resonant Cavity Antenna Based on Tunable Partially Reflective Surface

[Shufeng Zheng](#), [Fan Di](#), [Na Zhou](#) and [Le Kang](#) (Xidian University, China); [Muhammad Wasif Niaz](#) (Northwestern Polytechnical University, China)

A beam steerable resonant cavity antenna (RCA) enabled by using tunable partially reflective surface (PRS) is proposed in this paper. Tunable PRS loaded with varactor diodes evolves from complementary frequency selective surface (FSS) which consists of square loop patch and slot arrays. The reflection phase of PRS unit cell can be tuned by adjusting the biasing status of varactors, while the reflection magnitude keep a relative high value within a frequency band of interest, owing to the complementary configuration. The reflection coefficients of PRS unit cells are independently controlled in rows so that a gradient phase distribution within the aperture can be achieved, leading to an 1D scannable directive beam. An implementation is demonstrated with simulated results, which exhibits maximum scanned angle of 13 degrees with a gain of 13.6 dB for a 2λ×2λ antenna aperture size.

P3.029 Mechanically Circular Polarization Reconfigurable Antenna

[Jeen-Sheen Row](#) and [Po-Kai Wang](#) (National Changhua University of Education, Taiwan)

A design for single-fed circularly-polarized (CP) antennas with broadband operation is first described. The antenna is mainly composed of a monopole slot, a dipole, and a metallic box. When the monopole slot is operated in its half-wavelength mode, the radiated fields of the slot and dipole have the same amplitudes and 90° phase differences; in addition, the two radiating elements are arranged in an orthogonal configuration. Consequently a CP radiation is obtained. To realize a polarization reconfigurable design, a pair of screws are used to act as the radiating arms of the dipole. By manually turning the two screws, the axial ratio and polarization sense of the antenna can be changed. For the proposed reconfigurable antenna, the analyses for key components are performed, and a prototype is constructed. Both measured and simulated results show that the CP reconfigurable antenna has a 3 dB-axial-ratio bandwidth of more than 22 %.

P3.030 A New Beam-Steering Antenna with Variable Gain

[Ghada Elzwawi](#) (EMT-INRS, Canada); [Rabeia Alwahishi](#) (INRS, Canada); [Tayeb A. Denidni](#) (INRS-EMT, Canada)

In this paper, a beam-steering antenna with variable gain based on frequency selective surfaces (AFSSs) is presented. The proposed design comprises of a dipole antenna as a source of the electromagnetic waves (EM waves) , two reconfigurable AFSS screens, and six metallic sheets placed around the source to increase the values of the proposed antenna gain. The AFSS screens are arranged around the dipole antenna in a hexagonal shape to steer the radiation pattern in six different directions. The transmission/ reflection characteristics of the proposed antenna are investigated in various combinations for diode ON/OFF states for both AFSS screen. The proposed antenna can switch its gain between 14dBi and 17dBi. The performance of the antenna is evaluated at 5.8 GHz.

P3.031 A Single-Layer Planar Antenna Unaffected by a Possibly Close-by Metal Surface

[Serafin Benedikt Fischer](#) and [Jan Hesselbarth](#) (University of Stuttgart, Germany)

A planar antenna on a single metal layer is proposed, whose feed remains matched at frequency of operation of 4.85GHz, no matter if there is a metal ground plane close-by, or at some distance, or far away. In free space, the proposed antenna acts like a slot antenna. Otherwise, if a metal plane is located close to the antenna, a current will flow in the ground and the antenna behaves like a coplanar waveguide patch antenna. For the first case, dipole-like omnidirectional radiation occurs, while for the second case, the typical patch-like radiation pattern is observed. In both cases, the complex feed impedance is about the same. If the metal ground is located at intermediate distance, the feed impedance variation remains small. Measurements of a prototype show that for the distance between antenna and metal ground ranging from 4mm to 250mm, feed match better than -12dB is achieved at 4.85GHz.

P3.032 Reconfigurable SRR Antenna

[Kammel Rachedi](#) (Institut Langevin ESPCI Paris CNRS, France); [Julien de Rosny](#) (CNRS, ESPCI Paris, PSL Research University, France); [Abdelwaheb Ourir](#) (Institut Langevin ESPCI Paris CNRS, France); [Dinh-Thuy Phan-Huy](#) (Orange-France Telecom, France); [Yvan Kokar](#) (IETR-INSA Rennes, France)

A new antenna based on reconfigurable Split Ring Resonators (SRR) is proposed. Based on numerical and experimental results, the SRR reconfigurable antenna can generate up to 8 different patterns with a good impedance-matching at 2.45 GHz. A semi-analytical model based on coupled electric and magnetic dipoles is proposed to describe the pattern diversity. Finally, the efficiency of this reconfigurable antenna is demonstrated with a new wireless MIMO communication scheme, called Spatial Modulation (SM-MIMO) dedicated to small devices.

P3.033 A Compact Pattern Reconfigurable Antenna for UHF Internet of Things Applications

[Saeed A. Haydhah](#) (King Fahad University of Petroleum and Minerals, Saudi Arabia); [Fabien Ferrero](#) (University Nice Sophia Antipolis, CNRS, LEAT & CREMANT, France); [Leonardo Lizzi](#) (University Côte d'Azur, CNRS, LEAT, France); [Azzedine Zerguine](#) (KFUPM, Saudi Arabia); [Mohammad S. Sharawi](#) (Polytechnique Montreal, Canada)

A compact pattern reconfigurable antenna is proposed for Internet of Things (IoT) applications. The resonant frequency of the antenna is 868 MHz with a -10 dB impedance bandwidth of 9 MHz. The size of the antenna is 80*55*0.72 mm³ (Credit Card Size). Three pattern configurations are obtained from this design with peak gains above -1.98 dB, and radiation efficiencies above 33.2%. Two patterns follow magnetic-dipole patterns along the azimuthal plane with maximum peak gains directed to phi=120 degrees and phi=-70 degrees, and one electrical-dipole pattern along the elevation plane phi=120 degrees. Pattern reconfigurability is achieved using PIN diodes. The used substrate is FR-4 with a dielectric constant of 4.4, and a loss tangent of 0.02.

P3.034 Miniaturization of ESPAR Antenna Using Low-Cost 3D Printing Process

[Mateusz Czelen](#) (Gdansk University of Technology, Poland); [Mateusz Rzymowski](#) (Gdansk University of Technology & WiComm Center of Excellence, Poland); [Krzysztof Nyka](#) (Gdansk University of Technology, Poland); [Lukasz Kulas](#) (Gdansk University of Technology, Faculty of Electronics, Telecommunications and Informatics, Poland)

In this paper, the miniaturized electronically steerable parasitic array radiator (ESPAR) antenna is presented. The size reduction was obtained by embedding its active and passive elements in polylactic acid (PLA) plastic material commonly used in low-cost 3D printing. The influence of 3D printing process imperfections on the ESPAR antenna design is investigated and a simple yet effective method to compensate them has been proposed. Designed antenna is characterized by 5.7 dBi peak gain and reflection coefficient of -33 dB. An antenna prototype was fabricated and measured, which showed that the experimental and simulated results are in good agreement. Base radius reduction of 23% and occupied area reduction of 40% were achieved.

P3.035 A Concept of Pattern-Reconfigurable Single-Element Antenna Based on Half-Mode Substrate-Integrated Cavity

[Feng-Xue Liu](#) (Jiangsu Normal University & Southeast University, China); [Wenbin Dou](#) (Southeast University & State Key Of MMW, Southeast University, China); [Jie Cui](#) (Jiangsu Vocational Institute of Architectural Technology, China); [Shengjian Jammy Chen](#) (The University of Adelaide, Australia); [Christophe Fumeaux](#) (The University of Adelaide & School of Electrical and Electronic Engineering, Australia)

A concept of pattern-reconfigurable single-element antenna operating at 2.45 GHz is proposed in this paper. The antenna consists of two back-to-back half-mode substrate-integrated cavities with switchable shortings at both radiation apertures. One of the cavities is fed by an SMA probe while the other cavity is excited by the coupling through an aperture on the shared sidewall. This leads to the excitation of an even and an odd mode in the coupled cavities. Changing the states of the two switchable shortings leads to the switching between the even and odd coupled modes, which reconfigures the radiation pattern, and changes the main beam direction. The measured results on a fabricated prototype where the switches are mimicked by retractable screws validate the concept and illustrate that the main beam can be steered in the direction of either $\theta = 12^\circ$ or 36° .

P3.036 A Sectoral Conformal Array Antenna with an Improved Circular Polarized Patch for UHF Radiosonde Receivers

[Farhad Ghorbani](#) and [Hadi Aliakbarian](#) (K. N. Toosi University of Technology, Iran); [Mehdi Shirichian](#) and [Gholamreza Moradi](#) (Amirkabir University of Technology, Iran)

In this paper, an easy-to-manufacture and relatively low profile sectoral antenna for receiving radiosonde signals is proposed, simulated and fabricated. Depending on the radiosonde motion in air, a patch antenna with circular polarization as the top antenna as well as six patch antennas with linear polarization as side antennas are designed. In the patch antenna with Circular Polarization (CP) a new method is proposed to eliminate the frequency shift between the Axial Ratio (AR) bandwidth (BW) and the reflection coefficient bandwidth. The side antennas have a trapezoidal geometry instead of a regular rectangular due to the antenna holder structure, which reduces the final volume of the structure. The final structure is fabricated and tested at frequency of 403 MHz and the results indicate good antenna performance.

P3.037 Microstrip Tunable Antenna Based on Commercial Graphene Nanoplatelets

[Muhammad Yasir](#) and [Patrizia Savi](#) (Politecnico di Torino, Italy)

This paper presents a tunable antenna with frequency reconfigurability caused by an external bias voltage. The antenna is composed of a patch with two stubs and commercial graphene nanoplatelets deposited in designated gaps between the antenna and the stubs. As the graphene nanoplatelets are biased with a dc voltage, their sheet resistance is varied causing a change in the reactance at the radiating edge of the patch antenna resulting in a variation of the resonant frequency. Even though commercial graphene nanoplatelets bearing higher sheet resistance are deployed yet the prototype is designed so as to provide comparable frequency shift to tunable antennas based on lab grown graphene flakes. Simulated values of return loss are compared to measured values. The resulting shift in the frequency is 370 MHz at a frequency of 5GHz.

Poster3-A14: Active and Integrated Antennas

Antennas

Room: Exhibition Hall

P3.038 Post-Manufacturing Calibration Procedure for Medium-Sized Silicon-Based Active Phased Arrays for mm-Wave Wireless Communications

[Antonius Johannes van den Biggelaar](#), [Niels Vertegaal](#) and [Ulf Johannsen](#) (Eindhoven University of Technology, The Netherlands); [Marcel Geurts](#) (NXP Semiconductors, The Netherlands); A. B. (Bart) Smolders (Eindhoven University of Technology, The Netherlands)

The next generation radio access networks (5G) will make use of active phased array antennas to enable beamforming. Calibration of the array is an essential step to maximize its performance. The calibration procedure of an active phased array can be divided into two different phases: post-manufacturing calibration and online calibration. In this paper, a post-manufacturing calibration procedure using over-the-air measurements is presented. This procedure is applied to an 8x8 active phased array containing low-cost silicon-based ICs. It is shown that with this procedure, it is possible to steer the main lobe of the array as far as +/-40 degrees, while maintaining a side lobe level of around -20 dB. The measurements were performed at a frequency of 29.5 GHz.

P3.039 A Hybrid Beamforming-Based Transceiver with Antenna in Package for Millimeter-Wave Small Cell

[Ruiheng Zhang](#) and [Guangli Yang](#) (Shanghai University, China)

a millimeter-wave hybrid beamforming-based (HBF) transceiver designed for small cell has been presented in this paper. A large-scale array for massive MIMO is divided into several subarrays. Every subarray has 16 active elements and adopts analog beamforming to save the number of digital processing channels. A dual-polarized antenna in package (AiP) architecture is constructed to implement each subarray, which operates from 23.2 to 28.3GHz in vertical polarization and from 23.4 to 27.5GHz in horizontally polarization. By using multiple AiP subarrays, the HBF transceiver has a maximum transmit linear power more than 33dBm and a receive sensitivity of -76dBm. The proposed transceiver can meet the need of small cell well, achieving miniaturization, large capacity and high-data rate.

P3.040 Frequency Reconfigurable Self-oscillating Active Integrated Antenna Using Metamaterial Resonators and Diode Switches

[Tzyh-Ghuang Ma](#), [Huy Nam Chu](#) and [You-Jiun Wang](#) (National Taiwan University of Science and Technology, Taiwan)

In this paper, a frequency reconfigurable self-oscillating active integrated antenna (AIA), realized by a metamaterial resonator, a feedback oscillator and a pair of PIN diodes, is proposed and experimentally demonstrated. By turning on and off the PIN diodes bridging the shunt inductance, the resonator can be operated as a composite right-/left-handed (CRLH) resonator or a mu-negative material (MNG) resonator, both operating in the +1 mode. The resonator functions as the frequency selective element of oscillator, thereby determining the oscillating frequency of the AIA in the two states. The design principle and experimental results will be discussed.

P3.041 A Compact and Broadband Four-Way Dual Polarization Waveguide Power Divider for Antenna Arrays

[Charalampos Stoumpos](#) (Thales Alenia Space & Heriot-Watt University, France); [Jean Philippe Fraysse](#) and [Ségolène Tubau](#) (Thales Alenia Space, France); [George Goussetis](#) (Heriot-Watt University, United Kingdom (Great Britain)); [Ronan Sauleau](#) (University of Rennes 1, France); [Hervé Legay](#) (Thalès Alenia Space, France)

A novel, compact and highly efficient waveguide power divider exhibiting dual-polarization in an in-phase 2x4 scheme (4-way) is presented. The component comprises Orthomode Transducers (OMTs) with a turnstile junction configuration accompanied by E-plane power dividers for the equiphasic excitation for each set of 4 output TE10 modes and H-plane power dividers in order to end up to two input ports. The presented passive component is fully metallic and can be used as a dual-polarized feeding network for a 2x2 antenna array or four-port radiating elements with aperture sizes above 2.4λ that are commonly targeted for focal array or direct radiating elements at GEO applications. Finally, a compact topology of a 2.5λ aperture size horn antenna array in a 2x2 scheme was designed and optimized where the level of aperture efficiency was the principal design goal. The array is after connected to the exciter to obtain the final feed system.

P3.042 AMOLED In-Display Antennas

[Senglee Foo](#) (Huawei Technologies Canada, Canada)

This article presents a novel concept of in-display antennas, which is a complex integration of millimeter-wave and sub-millimeter-wave antennas with organic light emission display (OLED) structure. The proposed structure is a flat-screen display that is almost transparent to both optical signals and high-frequency electromagnetic transmissions. The concept is achieved through direct integration of millimeter-wave and Terahertz antenna technologies with active matrix light emission display (AMOLED) using existing OLED Si/CMOS technology. The in-display antenna concept can potentially have great impact on future display technology and high speed wireless transmission using millimeter-wave and THz frequencies.

P3.043 Transmit and Receive Module with a Fully-Digital Interface

[Yasuaki Wada](#), [Koji Fujita](#), [Yoshinori Kuji](#), [Masaki Iwasaki](#) and [Tomohide Mizuno](#) (Toshiba Infrastructure Systems & Solutions Corporation & Komukai Complex, Japan); [Masahiro Tanabe](#) (Toshiba Infrastructure Systems & Solutions Corporation, Japan)

This paper presents a fully-digital transmitting and receiving module (FDTR-MOD) for a future active electrically scanned array (AESAs). The FDTR-MOD is composed of a fully-digital transmitting and receiving circuit (FDTR-circuit) mounted in a novel stack module package (SMP). The interface signal of the FDTR-MOD is digitized by operating analog-to-digital converters (ADCs), digital-to-analog converters (DACs) and phase lock loop (PLL) for each antenna element. The prototype of the SMP and FDTR-circuit are made and measured. It is found that the SMP has good RF characteristics. It is also found that the standard deviation is 0.21 degree in receiving circuits and 0.31 degree in transmitting and receiving circuits of the FDTR-circuit.

Poster3-A15: RFID Antennas/Sensors and Systems

Antennas

Room: Exhibition Hall

P3.044 Concept of Beam Steerable Transponder Based on Load Modulation

[Tauseef Ahmad Siddiqui](#) (School of Electrical Engineering, Aalto University, Finland); [Prabhat Khanal](#) (Chalmers University of Technology, Sweden); [Jari Holopainen](#) (Aalto University School of Electrical Engineering, Finland); [Ville Viikari](#) (Aalto University & School of Electrical Engineering, Finland)

The concept of beam steering transponder based on load modulation is proposed to enhance the received power of backscattered communication devices. The transponder consists of antenna array elements of equal length operates at the Wi-Fi frequency band of 2.4 GHz. By properly weighting the modulated signal in each port, the received power can be maximized in a particular direction depending on the direction of arrival (DoA) of the signal. The weighting is done differently for each direction. It provides up to approximately 11 dB improvement in received power with weighting compared to backscatter communication with a single antenna transponder. The concept is studied theoretically and by simulations.

P3.045 High PAPR Multi-Tone Waveforms as a Method of Boosting DC Voltage in RF Wireless Power Transfer Systems

[Kyriakos Neophytou](#) and [Marco A. Antoniadis](#) (University of Cyprus, Cyprus)

A DC voltage boosting technique in radio frequency (RF) wireless power transfer (WPT) systems is proposed. This technique utilizes high PAPR multi-tone waveforms. It is demonstrated that increased efficiencies and DC voltages can be achieved for conventional single- and multi-stage rectifiers. First, the use of multi-stage rectifiers in wireless power transfer as a method to increase the DC output voltage is investigated and it is shown that at low input powers the implementation of a large number of stages can reduce the efficiency dramatically. Then, high PAPR waveforms are presented as an alternative method to multi-stage rectifiers that can increase the DC output voltage without decreasing the efficiency at low input powers. Finally, it is shown that by incorporating high PAPR waveforms with multi-stage rectifiers can decrease the required number of rectifier stages, and hence increase the rectifier efficiency at extremely low input powers.

P3.046 A UHF RFID Reader Antenna with Tunable Axial Ratio and Fixed Beamwidth

[Rui Chen](#) and [Shuai Yang](#) (University of Cambridge, United Kingdom (Great Britain)); [Ajeck M Ndifon](#) (Cambridge University, United Kingdom (Great Britain)); [Ian White](#) (University of Cambridge, United Kingdom (Great Britain)); [Richard Penty](#) (Cambridge University, United Kingdom (Great Britain)); [Michael J Crisp](#) (University of Cambridge, United Kingdom (Great Britain))

A novel ultra-high-frequency (UHF) RFID reader antenna is proposed. The antenna has a unique property as being able to change its axial ratio (AR) without affecting its gain, beamwidth or impedance matching performance, enabling the isolated study of the effect of different axial ratios in RFID tag reading.

P3.047 On Complex Radar Cross Section and Backscatter Modulation Efficiency in RFID Systems

[Christoph Degen](#) (Hochschule Niederrhein University of Applied Sciences, Germany); [Patrick Bosselmann](#) (Bochum University of Applied Sciences, Germany)

The objective of this paper is to provide a throughout complex-valued treatment of different aspects in backscatter modulation. Such modulation is a key aspect in radio-frequency identification (RFID) communication. The main point in this paper is the introduction of a complex radar cross section that describes amplitude and phase effects of any reflecting object but especially of RFID tag antennas. Then, the efficiency of sideband modulation is derived based on switching between different complex radar cross section values. Finally, the modulation efficiency is illustrated in an example scenario with a tag antenna placed in front of a metal plate.

P3.048 Modified Yagi-Uda Reader Antenna for UHF RFID Smart-Glove

[Rajesh K Singh](#), [Andrea Michel](#) and [Paolo Nepa](#) (University of Pisa, Italy); [Alfredo Salvatore](#) (Sensor ID, Italy)

This paper introduces a modified Yagi-Uda antenna with the capability of focusing field in a particular direction. The antenna comprises of a rectangular shaped driven element with one parasitic element. Parasitic element is used as a director to focus the field in a particular direction and increased its strength compared to other directions. The antenna is analyzed in terms of the electric and magnetic field distribution in the near field to the structure. A prototype is developed by using copper tape on a stretchable fabric to validate the design. A good agreement between measured and simulated results in terms of input impedance matching and field distribution is obtained. The read range of 30 cm in front direction and 19cm in rear direction is achieved with the transmitted power of 45mW. The presented antenna is compact in size and it is suitable to be integrated into a UHF RFID Smart Glove.

P3.049 Reduced Size RFID Reader Antenna Based on Reconfigurable Feeding Network Realized with Artificial Transmission Lines

[Enrico Tolin](#) (Politecnico di Torino, Italy & IMST GmbH, Germany); [Achim Bahr](#) and [Simona Bruni](#) (IMST GmbH, Germany); [Francesca Vipiana](#) (Politecnico di Torino, Italy)

In this paper, a compact and low-cost solution for a frequency and polarization reconfigurable UHF RFID reader antenna is presented. The proposed reconfigurable concept is based on a switchable feeding network, which uses only four state-of-the-art CMOS switches for both covering the EU and US frequency bands and for selecting among four linear polarizations. Moreover, the reconfigurable feeding network concept is applied to a reduced size square patch antenna with 60 mm side length, mounted on an electrically small ground plane with dimensions 95 mm x 95 mm. This compact design can be easily integrated in standard RFID applications. Circuit and EM simulation have shown promising results. Being a compact and low-cost solution, the frequency and polarization reconfigurable feeding network is an alternative to standard aperture tuning and circular polarized antenna RFID reader antenna designs.

P3.050 An Enhanced Road Vehicle Positioning Method Using Roadside Furniture with Radio Frequency Identity Tags and the EPC Gen2 Standard

[Zhan Wang](#) and [Robert Michael Edwards](#) (Loughborough University, United Kingdom (Great Britain))

In this paper, a new method for augmenting current self-localization methods for autonomous based on Global Navigation Systems (GNSS) and Lidar is introduced as a backup system for primary equipment. The method uses Radio Frequency Identity Tags (RFID) running under a modified EPC Gen2 Standard. Simulated results are presented for a representative 6.5km circular track around Loughborough, UK town centre with a 911 items inventory of roadside furniture. The virtual test track as input for an RFID tag simulator that uses an interrogator/inventory protocol. The technique is shown to be a good candidate for improving safety in Autonomous Vehicles and position finding for vehicles in general.

P3.051 A Passive RFID Tag for Biomass Tracking

[Amjad Ali](#), [Roderick Mackenzie](#), [Edward Lester](#), [Orla Williams](#) and [Steve Greedy](#) (University of Nottingham, United Kingdom (Great Britain))

This paper presents the design for a low cost miniaturized chipless RFID tag for short-range biomass tracking and monitoring purposes. The concentric hexagonal geometry and angular stability, leading to higher data capacity are the novel aspects of the proposed design, which can encode four data bits within a compact size of a 1 cm radius. The designed is capable of encoding 2n unique IDs in a 4-to-9 GHz frequency band, where n is the number of etched slots. The angular stability makes this tag readable from any angle in biomass. Moreover, this chipless RFID tag has no hazard as compared to battery-based active tags during biomass combustion processes.

P3.052 A Compact Printed Wideband Circularly Polarized Slot Antenna for Universal UHF RFID Reader

[Nathapat Supreayatitikul](#), [Nonthapat Teerasuttakorn](#), [Phanuphong Boontamchay](#) and [Manurak Rattanasuttikan](#) (Civil Aviation Training Center of Thailand, Thailand)

A compact circularly polarized (CP) slot antenna is proposed in this research, which has a wideband operation bandwidth for universal ultrahigh-frequency (UHF) identification (RFID) reader applications. This antenna fed by a coplanar waveguide (CPW) with an L-shaped feeding line for achieving impedance matching wider bandwidth and wideband CP operation can be obtained by two rectangular-shaped stubs into the square slot of the ground plane. The measured 10-dB reflection coefficient (return loss) bandwidth is 790 MHz (620-1410 MHz, 87.7% centered at 900 MHz). The measured 3-dB axial ratio (AR) bandwidth is about 445 MHz (795-1240 MHz, 49.44% centered at 900 MHz). The maximum measured gain of the antenna about 3.7 dBi. The dimension of the proposed antenna is 120x120x1.6 mm3.

Poster3-A16: UWB Antennas and Time-domain Techniques

Antennas

Room: Exhibition Hall

P3.053 Single-Chip Impulse-Radar Integrated Circuits for Microwave-Imaging

[Takamaro Kikkawa](#) (Hiroshima University, Japan); [Akihiro Toya](#) (Kure National College of Technology, Japan); [Yoshihiro Masui](#) (Hiroshima Institute of Technology, Japan); [Hiroyuki Ito](#) (Tokyo Institute of Technology, Japan); [Takuichi Hirano](#) (Tokyo City University, Japan); [Mitsutoshi Sugawara](#) (Hiroshima University, Japan); [Tomoaki Maeda](#), [Masahiro Ono](#), [Yoshitaka Murasaka](#), [Toshifumi Imamura](#) and [Atsushi Iwata](#) (A-R-Tec Corporation, Japan); [Tsuyoshi Matsumaru](#) and [Michimasa Yamaguchi](#) (Syswave Corporation, Japan)

In order to develop a portable multi-static radar system for microwave imaging, a single chip impulse radar large scale integrated circuit (LSI) is developed by 65-nm complementary metal oxide semiconductor (CMOS) technology. Total area and power consumption are 1.7 mm x 0.74 mm and 90 mW, respectively. Gaussian mono-cycle pulses (GMP) having the pulse width of 250 ps and the repetition period of 10 ns are transmitted and received via ultrawideband (UWB) bowtie patch antennas with the size of 5 mm x 20 mm. Received signals are sampled by the effective time sampling with 9.77 ps shifting clock and converted to digital data by 8-bit successive approximation register analog to digital converter (SAR-ADC).

P3.054 A 2-18 GHz Semi-Omnidirectional Antenna

[Gokhan Ucuncu](#) and [Mustafa Kuloglu](#) (Aselsan Inc., Turkey)

A "semi-omnidirectional antenna" which operates in 2-18 GHz frequency band. A semi-omnidirectional antenna is a modified biconical antenna having a "blind" sector (i.e. a sector where gain is suppressed) and has H-plane 3dB beamwidths about 180 degrees or more. One sample antenna is designed, manufactured and measured. For more than 90 percent of the band, the antenna has over 10 dB gain suppression in the blind sector. Gain of the antenna is measured to be minimum -2.21 dBi and higher than 0 dBi for frequencies higher than 3.6 GHz. E-plane beamwidth of the antenna is greater than 15 degrees in the entire 2-18 GHz frequency range.

P3.055 Pulsed 2D ElectroMagnetic Field Propagation in a Rectangular Waveguide

[Martin Štumpf](#) (Brno University of Technology, Czech Republic); [Ioan E. Lager](#) (Delft University of Technology, The Netherlands); [Guy Vandenbosch](#) (Katholieke Universiteit Leuven (KU Leuven), Belgium)

Closed-form space-time expressions are derived for the two-dimensional electromagnetic (EM) field propagating in a rectangular waveguide. The pulsed EM field inside the waveguide is activated by an electric line current source applied across the rectangular cross section. This field is written as a superposition of time-domain (TD) constituents denoted as generalized rays, progressing along the waveguide via multiple reflections against its conducting walls. Illustrative numerical examples are presented. The thus constructed propagating field is compared against results available in literature, demonstrating the effectiveness and accuracy of the generalized-rays approach.

P3.056 Time-Domain Reflectometry for Measuring Scattering Parameters: Comparison of M-sequence Device and Step-generator TDR

[Shekoufeh Abdollahi](#) and [Somayyeh Chamaani](#) (K. N. Toosi University of Technology, Iran); [Jürgen Sachs](#) (Ilmenau University of Technology, Germany)

Scattering parameters of microwave networks and antennas could be measured in time domain to lower the measurement cost and time. Although time-domain data may include some errors and inaccuracies, they can be compensated by proper measurement systems and processing. In this study, we examined a comprehensive method for two measurement devices, a step-generator time-domain reflectometer and a maximum length sequence (M-sequence) sensor. The resulted scattering parameters are compared with frequency domain results measured by a vector network analyzer (VNA). Both measurements are in agreement with the frequency domain results, however, considering the effect of random errors in two devices, maximum length sequence shows significantly accurate results according to its higher signal-to-noise ratio. Index Terms-time domain reflectometry, scattering parameters, antenna measurements, microwave network measurements, maximum length sequence.

P3.057 A Novel Approach for Compact Antenna with Parasitic Elements Aimed at Ultra-Wideband Applications

[Sudeep Baudha](#) (BITS PILANI K K BIRLA GOA Campus, India); [Manish Varun Yadav](#) (BITS Pilani K K Birla Goa Campus & BITS PILANI, India); [Ishita Srivastava](#) (BITS PILANI K K BIRLA GOA CAMPUS, India)

A novel approach for compact antenna with parasitic elements is proposed and investigated for Ultra-wideband applications. The proposed structure consist of a multiple rectangular parasitic elements etched on flame retardant (FR-4) substrate with 50Ω feed line. Return loss (magnitude of S11 < -10dB) and the simulated bandwidth of the structure is 3.0 GHz to 12.89 GHz with the fractional bandwidth of 124%. The overall volume of the structure has a compact size of 14*18*1.5 mm3 and has a maximum gain and maximum radiation efficiency of 2.9 dB and 70% respectively. Measured and simulated Co-pol. and Cross-pol. are in relatively good agreement with the selected operating frequencies. The proposed antenna's properties make it suitable for UWB frequency range which includes 3.5-5.5 GHz (WiMAX), 5.2-5.8 GHz (WLAN), 8-12 GHz (X-band), data links to satellites along with various applications in the wireless communication field.

P3.058 Low Profile Absorber Backed Extremely Wideband Antennas

[Umair Naeem](#) (Centre for Wireless Innovation, ECIT Institute, Queen's University Belfast, United Kingdom (Great Britain)); [Vincent Fusco](#) (Queen's University Belfast, United Kingdom (Great Britain)); [Dmitry E Zelenchuk](#) (Queen's University of Belfast, United Kingdom (Great Britain)); [Robert Cahill](#) (Queens University Belfast, United Kingdom (Great Britain))

In this paper design and electromagnetic performance of a low profile and extremely wideband antenna which works from 10 to 40 GHz is presented. The differentially fed antenna benefits from suppressed back lobe radiation by exploiting the use of a resistively loaded low profile absorber. The proposed antenna uses both the reflection and absorption phenomenon in near field and exhibits two octaves of bandwidth.

Poster3-A20: Antennas for Wireless Power Transmission and Harvesting

Antennas

Room: Exhibition Hall

P3.059 Waveform Optimization for Efficiency Improvement of Traditional RF-to-dc Rectifiers Without Input Matching Network

[Viet-Duc Pham](#) (Universty Paris-Est Marne-la-Vallée, France); [Hakim Takhedmit](#) (Paris-Est Marne-la-Vallée University, France); [Laurent Cirio](#) (Université de Paris-Est Marne-la-Vallée, France)

This paper reports the waveform optimization, based on pulse-modulated signal, for efficiency improvement of three traditional rectifiers: series, shunt and voltage doubler rectifiers. The circuits do not contain input matching networks. The measurement results show that the optimization of the pulse waveforms, by varying the duty cycle, makes it possible to compensate for the decrease in efficiency due to the absence of a matching circuit and also to the load resistance that deviates from its optimum value. In this work, the effort of design and optimization is reported on the waveform. At -20 dBm input power level, the efficiency of RF pulse signal on un-optimized series-mounted diode rectifier is 58 % higher than that of 1-tone signal applied on optimized rectifier. Meanwhile, at different loads, the efficiency of RF pulse can be 3 times higher than 1-tone signal. Similar results are obtained with shunt-mounted diode and voltage doubler rectifiers.

P3.060 Impact of Multisine and RF Pulse Signals on the Efficiency of Different Rectifier Topologies for WPT

[Viet-Duc Pham](#) (Universty Paris-Est Marne-la-Vallée, France); [Hakim Takhedmit](#) (Paris-Est Marne-la-Vallée University, France); [Laurent Cirio](#) (Université de Paris-Est Marne-la-Vallée, France)

This paper presents the impact of Power Optimized Waveforms (POWs) such as RF Pulse and Multisine Signals (MS) on the efficiency of several rectifiers with different topologies such as voltage doubler, shunt and series, with and without input matching networks. The aim consists to demonstrate that instead of optimizing accurately the rectifiers, one can compensate the performance by optimizing the waveform. In this study, a comparison is made between optimized and non-optimized rectifiers, supplied by CW (Continuous Waves) and POW, respectively. The optimized circuits contain input matching networks. Measurement results show that the efficiency of multisine signals increases with respect to the number of subcarriers. Also, the performances of non-optimized rectifiers supplied by multisine signals becomes comparable and close to those of optimized rectifiers supplied with CW. RF pulse signal gives the highest output dc voltage over the frequency band of interest for duty cycle values less than 15%.

P3.061 A Dual-Port, Dual-Polarized and Wideband Slot Rectenna for Ambient RF Energy Harvesting

[Saqer S Alja'afreh](#) (Mutah University, Jordan); [Chaoyun Song](#) (University of Liverpool, United Kingdom (Great Britain)); [Yi Huang](#) (The University of Liverpool, United Kingdom (Great Britain)); [Lei Xing](#) (Nanjing University of Aeronautics and Astronautics, United Kingdom (Great Britain)); [Qian Xu](#) (Nanjing University of Aeronautics and Astronautics, China)

A dual-polarized rectangular slot rectenna is proposed for ambient RF energy harvesting. It is designed in a compact size of $55 \times 55 \times 1.0$ mm³ and operates in a wideband operation between 1.7 to 2.7 GHz. The antenna has a two-port structure, which is fed using perpendicular CPW and microstrip line, respectively. To maintain both the adaptive impedance tuning and the adaptive power flow capability, the rectenna utilizes a novel rectifier topology in which two shunt diodes are used between the DC block capacitor and the series diode. The simulation results show that RF-DC conversion efficiency is greater 40% within the frequency band of interested at -3.0 dBm received power.

Poster3-A21: Additive Manufacturing

Antennas

Room: Exhibition Hall

P3.062 3D Printed Helix Antenna for 77 GHz

[Konstantin Lomakin](#) and [Mark Sippel](#) (Friedrich-Alexander University, Germany); [Ingrid Ullmann](#) (Institute of Microwaves and Photonics, Germany); [Klaus Helmreich](#) (Universität Erlangen- Nürnberg, Germany); [Gerald Gold](#) (FAU Erlangen-Nürnberg, Germany)

In this work, an additively manufactured helix antenna for a center frequency of $f_c = 77$ GHz is presented. A novel feed concept is proposed including a transition from the helix coil to an E-band waveguide, which allows for tuning of antenna matching. Measurements suggest a -15 dB bandwidth of B15dB = 8 GHz and -10 dB bandwidth of B10dB = 16 GHz respectively with a fractional bandwidth of 20 %. An axial ratio below AR < 5 dB is achieved within the entire B10dB and even AR < 3 dB within B15dB in main lobe direction. The ≈ 11 dBi in linear polarization realized antenna gain ranges at G_z component yielding a circular polarization gain of G_{cp} ≈ 12 to 13 dBi. Hence, measurements suggest general feasibility of the proposed helix antenna for mmWave applications despite the relatively high structure complexity due to the miniaturized dimensions at the aimed frequencies.

P3.063 Direct-Write Dispenser Printing for Rapid Antenna Prototyping on Thin Flexible Substrates

[Mahmoud Wagih](#) (University of Southampton, United Kingdom (Great Britain))

Rapid prototyping of antennas is crucial to validation of simulation models when designing conformal antennas on unusual substrates such as polymers and textiles. This paper presents direct-write dispenser printing, using a commercial Printed Circuit Board (PCB) printer, as a simple mean of prototyping planar antennas on ultra-thin (25 μ m) flexible Polyimide substrates. Two Coplanar Waveguide (CPW) monopole antennas have been designed for the 2.4 GHz band and fabricated using dispenser printing and standard photolithography. The impedance bandwidth and gain of both antennas has been compared and the printed prototype was found to match the performance of the etched antenna within a 2.6% and 2.3% margin respectively, as well as matching the full-wave 3D simulation of the connectorized antennas. Based on the measured performance of the printed antenna, the potential of utilising commercial dispenser printers to prototype and manufacture low-volume antennas for low-cost unobtrusive Internet of Things applications is demonstrated.

P3.064 Self-Sustained Biconical Antenna Realized in Additive Manufacturing Technology

[Alessandro Calcaterra](#), [Domenico Gaetano](#), [Christian Canestri](#), [Pietro Bia](#) and [Cosmo Mitrano](#) (Elettronica Group)

This paper describes the design procedures and manufacturing processes of a self-sustained vertically polarized biconical antenna for ultra-wideband (UWB) applications. The proposed antenna has been designed for Additive Manufacturing (AM) fabrication to reduce the total weight, simplify the assembly operations and facilitate the installation on the platform. In particular it has been produced via Direct Metal Laser Sintering (DMLS) technique. The radiating element works from 1 GHz to 4 GHz with good impedance matching, high total efficiency and omnidirectional patterns on the azimuth plane (elevation = 0 deg.). The designed layout provides mechanical stability to the antenna through optimized supports (spiral wires and rings). The design has been validated throughout simulations (using different solvers) and measurements.

P3.065 Ultra-broadband Multilayer Microwave Absorber by Multimaterial 3D Printing

[Thi Quynh Van Hoang](#) and [Brigitte Loiseaux](#) (Thales Research & Technology, France)

In this paper, an ultra-broadband microwave absorber, covering the C-band, X-band and Ku-band, has been proposed and investigated. The innovative nature of this absorber is based on the combined use of multilayer structure and multimaterial 3D printing technology. The designed unit cell is a stack of 22 pairs of layers made of metal and dielectric square patches with a total thickness of 13.5mm (0.5 centre wavelength). Two dielectric materials with different relative permittivity (2.6 and 8.0) are used to obtain ultra-wideband behaviour. The simulation results show more than 93% absorptivity over an ultra-wideband from 3.5 to 18.5 GHz (fractional bandwidth of 1.36). The structure offers a good robustness under oblique incidence with more than 80% absorptivity from 4.0 to 18.5 GHz up to 45° in both TE and TM polarizations. The paper demonstrates a new way to design and manufacture promising low profile and ultra-wideband absorbers for microwave applications.

P3.066 Temperature Characterization of High-Q Resonators of Different Materials for mm-Wave Indoor Localization Tag Landmarks

[Alejandro Jiménez-Sáez](#) (Technische Universität Darmstadt, Germany); [Martin Schüßler](#) (TU Darmstadt, Germany); [Damian Pandel](#) (University of Duisburg-Essen, Germany); [Christopher Krause](#) (Fraunhofer IMS, Germany); [Yixiong Zhao](#) (Fraunhofer-Institut für Mikroelektronische Schaltungen und Systeme IMS, Germany); [Gerd vom Bögel](#) (Fraunhofer IMS, Germany); [Niels Benson](#) (Institute for Nanostructures and Technology (NST), University of Duisburg-Essen, Germany); [Rolf Jakoby](#) (Institute for Microwave Engineering and Photonics, Technische Universität Darmstadt, Germany)

This paper discusses a temperature-dependent characterization of deep reactive ion-etched high-resistive silicon (DRIE HR-Si), 3D printed alumina and milled Rogers RT/Duroid 6010.2LM. The characterization is performed by measuring high-Q photonic crystal resonator samples in W-band and the measurements are taken from 30 to 115 °C. HR-Si is the material with the lowest losses at room temperature. However, its losses increase with temperature and become higher than 3D printed alumina at 75°C, reducing the radar cross section and maximum readout range of chipless wireless RFID tags integrating several of these resonators. These results demonstrate that, while HR-Si performance is higher for the usual temperatures achieved in an indoor localization scenario, 3D printed alumina is more suitable if a temperature-stable response is needed or if the tags need to operate at high temperatures, such as in case of fire.

P3.067 A Conformal Spherical DRA for MEO Applications in Ka-band Realized with Additive Manufacturing

[Valerio Panaro](#) (Airbus Italia S.p.A., Italy); [Giovanni Toso](#) (European Space Agency, ESA ESTEC, The Netherlands); [Esteban Menargues](#) (SWISSto12, Switzerland); [Alfredo Catalani](#) (European Space Agency – ESTEC, Noordwijk, The Netherlands)

Active phased arrays have been widely studied for satellite applications and space hardware has been mainly developed in Europe for geostationary (GEO) defence applications, Low (LEO) and Medium Earth Orbit (MEO) constellations. This class of arrays allow generating multiple beams with a high degree of reconfigurability and flexibility. Considering a MEO application, a conformal spherical array operating in Rx Ka band (27.5 to 30 GHz), in dual circular polarization, has been designed and a small passive demonstrator has been manufactured with additive manufacturing and tested.

P3.068 Simulation of Effective Medium Theory for Additive Manufacturing of Dielectric Media

[Gregory A Mitchell](#) (Army Research Laboratory, USA); [Quang Nguyen](#) (United States CCDC Army Research Laboratory, USA); [Theodore K Anthony](#) (US Army Research Laboratory, USA)

We compare the Maxwell-Garnett effective medium theory to a full wave simulation utilizing the Nicolson-Ross-Weir method to predict effective permittivity in a representative additively manufactured medium. Three-dimensional anisotropy in the medium highlights differences between the two methods, and we discuss potential causes and solutions to the observed discrepancies.

Poster3-A23: Other Antenna Topics

Antennas

Room: Exhibition Hall

P3.069 A Differential-Fed Dual-Polarized High-Gain Filtering Antenna Based on SIW Technology for 5G Applications

[Yasir Ismael Abdurraheem Al-Yasir](#) (University of Bradford, United Kingdom (Great Britain)); [Naser Ojaroudi Parchin](#) (University of Bradford, United Kingdom (Great Britain)); [Mohammad Fares](#) (University of Basra, Iraq); [Ahmed Maan Abdulkhaleq](#) (University of Bradford & SARAS Technology, United Kingdom (Great Britain)); [Mustafa Bakr](#) (University of Leeds, United Kingdom (Great Britain)); [Mohammed Al-Sadoon](#) (Richmond Road, Bradford, BD7 1DP, United Kingdom (Great Britain) & University of Bradford, Iraq); [Jamal Kosha](#) and [Raed A Abd-Alhameed](#) (University of Bradford, United Kingdom (Great Britain))

A new differential-fed wideband dual-polarized microstrip filtering antenna exhibiting high gain, and high common-mode rejection is presented in this paper. The presented antenna is composed of a square patch radiator mounted on a substrate integrated waveguide (SIW) cavity. The structure is excited by two differential pairs of feeding probes providing differentially exciting signals. The filtering response is achieved by introducing symmetrical defected ground structures (DGS) in the ground layer surrounding the four excitation ports for dual-polarized antenna. The DGS is optimized to introduce nulls at the high and low edges of the passband transmission maintaining high gain and wide bandwidth. Good performance is obtained with wide bandwidth of 11%, realized gain of 8 dBi at the resonant frequency (3.5 GHz) and low cross-polarization level due to the differentially driven ports, and complete symmetry using SIW technology.

P3.070 Eco-Friendly Metamaterial Antenna for 2.4 GHz WLAN Applications

[Georgina Serres](#) (Federal University of Campina Grande, Brazil); [Raimundo Freire](#) (Universidade Federal de Campina Grande - PB, Brazil); [Samuel Morais](#), [Camila Caroline Rodrigues de Albuquerque](#) and [Jéssyca Araujo](#) (Federal University of Campina Grande, Brazil); [Alexandre Serres](#) and [Laura de Carvalho](#) (UFCG, Brazil); [Joabson Nogueira de Carvalho](#) (Instituto Federal de Educação, Ciência e Tecnologia da Paraíba, IFPB, Brazil)

In this paper, an eco-friendly metamaterial antenna for 2.4 GHz WLAN applications is presented. The rectangular patch antenna is composed of two copper tape layers, one as the radiating element and the other as the modified ground plane with Complementary Split Ring Resonators (CSRR). The substrate that separates these two layers is a mixture of polybutylene adipate-co-terephthalate (PBAT) and polyhydroxybutyrate (PHB) polymers, both biodegradable. The electrical characterizations of the mixture were performed using the probe method and the antenna simulations were performed using the commercial software ANSYS® Electronics Desktop. Convergent results were obtained with simulated and measured prototypes, with a measured resonant frequency in 2.44 GHz and bandwidth of 360 MHz, simulated gain of 4.01 dBi and half power beam width of 48.2°, which shows great potential for WLAN applications.

P3.071 Antenna Phase Center and Angular Dispersion Estimation Using Planar Acquisition Setup Applied to Microwave Breast Imaging

[Joao M. Felicio](#) (Instituto de Telecomunicações, Portugal); [Jose Bioucas](#) (Instituto de Telecomunicoes, Portugal); [Jorge R. Costa](#) (Instituto de Telecomunicações / ISCTE-IUL, Portugal); [Carlos A. Fernandes](#) (Instituto de Telecomunicacoes, Instituto Superior Tecnico, Portugal)

We propose a "near-field phase center" estimation technique based on planar acquisition setup. It requires a single antenna and an electrically small object to serve as target. The technique allows to estimate the phase center spatial coordinates, as well as its angular dispersion. This data is useful in microwave imaging applications where the antenna operate in near-field regime, such as medical applications (e.g. breast and head imaging). We demonstrate that for a commonly used Vivaldi antenna operating in the 2-5 GHz band, the angular dispersion of the pseudo phase center can be as high as 50 mm. Moreover, we show that incorporating this data in the signal processing algorithms improves the imaging results, by applying it to microwave breast imaging. We believe this type of antenna-characterization techniques will leverage the use of more informative imaging algorithms (e.g. truncated singular value decomposition), since they increase the accuracy of the distance calculations, thus improving the signal to noise ratio.

P3.072 Holographic Antenna Using Slotted Hologram Patterns for High Efficiency

[Sang Hyuck Han](#), [Seongjin Park](#) and [Young Joong Yoon](#) (Yonsei University, Korea (South))

This paper proposes the holographic antenna using slotted hologram patterns for high efficiency at 24 GHz. The 4 slotted quasi-Yagi antennas are arrayed as a surface-wave launcher. The proposed antenna using the slotted patterns provides the higher gain at the broadside direction and more compact size than conventional holographic antennas with metal line patterns. The proposed antenna has the maximum gain of 15.8 dBi at broadside direction and the aperture efficiency is 30.65%, which is higher than 9.25% compared to the conventional antenna.

P3.073 A Bird-Cage Coil for MRI Studies of Unsaturated Granular Materials

[Sina Marhbaie](#) (Laboratoire Navier (UMR 8205 CNRS, IFSTTAR, Ecole des Ponts ParisTech), France); [Hakim Takhedmit](#) (Paris-Est Marne-la-Vallée University, France); [Patrick Poulichet](#) (ESIEE, France); [Marjorie Grzeskowiak](#) (ISAE Supaero, France); [Abdoulaye Fall](#) (Université Paris-Est, France)

Magnetic Resonance Imaging (MRI) is a powerful and non-invasive technique that can be used to reveal useful information about different types of materials. During an MRI experiment a magnetic resonance signal is induced (according to Faraday's law of induction) in a device called "probe". MRI probes are simply near field antennas designed in a specific way in order to produce a homogeneous magnetic field at a specific frequency in the region of interest. MRI is a strong technique to study unsaturated granular materials. However, it suffers from a significant drawback, that is inherent small signal-to-noise ratio. To overcome this problem the probe used for a specific MRI experiment must be optimised. In this work a bird-cage probe operating at 21.3 MHz, optimised to study unsaturated granular materials under shear stress as well as some experimental results will be presented.

Poster3-E08: Metamaterials, Metasurfaces and EBG

Electromagnetics

Room: Exhibition Hall

P3.074 Miniaturization of Base-station Antenna Element Using Non-uniform Meta-surface

[Yuwei Qiu](#) and [Hailiang Zhu](#) (Northwestern Polytechnical University, China); [Jinliang Bai](#) (National Key Laboratory of Test Physics and Numerical Mathematics, China); [Pei Zheng](#) (National Key Laboratory of Science and Technology on Test Physics and Numerical Mathematics, China); [Gao Wei](#) (Northwestern Polytechnical University, China)

This work reports a novel $\pm 45^\circ$ dual-polarized base-station antenna element with small aperture and low profile utilizing non-uniform meta-surface. The whole size of the antenna element is 119.5*119.5*72mm³ (0.32 λ 0*0.32 λ 0*0.19 λ 0), making it competitive in terms of miniaturization. The antenna exhibits bandwidth from 0.69 to 0.96 GHz, which covers the lower operating band of base station. Simulated results show that stable radiation pattern and high port isolation are achieved over the operating frequency band.

P3.075 Mechanically Tunable MTM-EBG-based Bandstop Filter

[Jacob A Brown](#) and [Ashwin K. Iyer](#) (University of Alberta, Canada)

Tunable filters are increasingly popular components in telecommunication systems as they are flexible and adaptable to changing conditions. A tunable bandstop filter based on the recently proposed metamaterial-based electromagnetic bandgap structure (MTM-EBG) is demonstrated here that relies on a single mechanically tuned element. This structure, without any tuning mechanism attached, has a simulated 10-dB transmission absolute bandwidth (ABW) of 225 MHz centered at 4.18 GHz. It is then made tunable by placing a dielectric plate on the surface of the MTM-EBG and varying the position of the plate; this changes the reactive loading and subsequently shifts the response. Using a plate of RO4350B, a tuning range from 3.43 to 4.05 GHz with a 13.6% variation in ABW is demonstrated in simulation.

P3.076 Wideband Vertically Polarized Dual-Beam Antenna Using Modulated Metasurfaces

[Ali Mohammad Hakimi](#), [Homayoon Oraizi](#), [Ali Keivaan](#) and [Amrollah Amini](#) (Iran University of Science and Technology, Iran)

In this paper, a dual beam vertically polarized metasurface antenna with broad bandwidth and high polarization purity is designed. Its aim is to improve the antenna polarization all over the visible region. Furthermore, by implementing a surface-wave reflector and removing the destructive effects of backward modes, the operational bandwidth of antenna is significantly improved. The scanning bandwidth of antenna is achieved for the frequency band of 16-19.5 GHz with suitable levels of cross polarization. Also, the gain of two distinct beams are approximately equal all over the operational bandwidth. The Fourier technique is used in the aperture of antenna to synthesize the dual-beam pattern. Moreover,

there is a good agreement between this method and the full-wave simulations.

P3.077 Ultra Wideband Dual Polarization Metamaterial Absorber for 5G Frequency Spectrum

[Majid Amiri](#) (University of Technology Sydney, Sydney, Australia); [Farzad Tofigh](#) (University of Technology, Sydney, Australia); [Negin Shariati](#) (University of Technology Sydney, Australia); [Justin Lipman](#) (University of Technology, Sydney (UTS), Australia); [Mehran Abolhasan](#) (University of Technology Sydney, Australia)

Implementing 5G technology contribute to improve the communication quality and facilitate several interesting applications in daily life such as Internet of things. Despite outstanding features of 5G, the amount of ambient electromagnetic waves will be increased significantly in environment, which may be undesired. Ultra-wideband metamaterial perfect absorber is a promising solution to collect these undesired signals. Using lumped elements in absorber structure to increase the absorption bandwidth leads to design and fabrication process complexity. In this paper, a low profile polarization angle selective metamaterial absorber has been designed to absorb signals in the frequency range of 21.79 GHz to 53.23 GHz with more than 90% efficiency. The relative absorption bandwidth of the final structure is 83.81%. Moreover, the final structure is reasonably insensitive facing different incident angle up to 40 degree.

P3.078 Degenerate Band Edge Resonances in Air-filled Substrate Integrated Waveguide

[Tianyu Zheng](#) (Sorbonne University, France); [Massimiliano Casaletti](#) (Sorbonne Universités UPMC, France); [Ahmed F. Abdelshafy](#) and [Filippo Capolino](#) (University of California, Irvine, USA); [Zhuoxiang Ren](#) and [Guido Valerio](#) (Sorbonne Université, France)

The degenerate band edge (DBE) is a special fourth-order degenerate point in a dispersion diagram, where four eigenmodes coalesce to a single degenerate eigenmode. It leads to field enhancement of the Bloch mode and to high quality factors, which are useful for high-Q resonators and ultra-sensitive sensors. The air-filled substrate integrated waveguide (AFSIW) is a novel form of SIW which is low-cost and low-loss. We propose a design of an AFSIW supporting a degenerate band edge (DBE). We show the occurrence of the so-called "giant resonance" associated to the DBE and we study how losses influence the DBE.

P3.079 A Hybrid SSPPs-EBG Filter with Glide Symmetry for 5G Applications

[Marzieh SalarRahimi](#) (KU Leuven, Belgium); [Guy Vandebosch](#) (Katholieke Universiteit Leuven (KU Leuven), Belgium)

In this paper, we propose a metamaterial-based low-pass band-pass hybrid filter combining the low-pass features of a spoof surface plasmon polaritons transmission line and band-reject features of an edge via mushroom-like glide-symmetric EBG structure. The idea of the proposed hybrid filter is to increase the degrees of freedom to tune the performance. The filter has been designed for 5G applications, covering both the sub 6 GHz and millimeter-wave frequency ranges. A stopband suppression of more than 25 dB has been achieved.

P3.080 A Compact Mass-producible E-band Bandpass Filter Based on Multi-layer Waveguide Technology

[Abbas Vosough](#) (Metasum AB, Sweden); [Astrid Algaba Brazález](#) (Ericsson Research, Ericsson AB, Sweden); [Yinggang Li](#) (Ericsson AB, Sweden); [Zhongxia Simon He](#) (Chalmers University of Technology & Microwave Electronic Lab, Sweden)

This paper presents the design, implementation and experimental validation of a bandpass filter for high-data rate point-to-point link applications at E-band. The proposed design is developed in multilayer waveguide (MLW) technology, where an air-filled waveguide transmission line is formed by stacking several unconnected thin metal plates. Our MLW bandpass filter is designed by combining low-pass and high-pass filtering structures, and consists of 19 separate metal layers. An array of glide-symmetric holes, which act as an electromagnetic band gap (EBG) structure, are used to prevent any possible field leakage due to the air gaps between the layers. The fabricated filter provides a bandpass from 71.5 to 76 GHz with measured return loss better than 15 dB, and insertion loss better than 1.3 dB. These results confirm the advantages of MLW technology for implementing ultra-compact bandpass filters showing low loss and potential for being mass-produced at millimeter-wave frequencies.

P3.081 All-Dielectric Huygens' Metasurface Pair for mm-Wave Circularly-Polarized Beam-Forming

[Mohamed K. Emara](#) (Carleton University, Canada); [Takashi Tomura](#) and [Jiro Hirokawa](#) (Tokyo Institute of Technology, Japan); [Shulabh Gupta](#) (Carleton University, Canada)

A novel all-dielectric Huygens' metasurface pair capable of circularly-polarized beam-forming is proposed. The proposed structure consists of two layers of dielectric resonators separated by approximately one quarter-wavelength at the design frequency. Each dielectric resonator is symmetrical to allow for the transmission of circularly-polarized waves. In order to physically design the structure, each resonator is connected to neighboring resonators using four symmetrical bridges. The second dielectric layer is added to cancel reflections caused by the bridges, allowing for the achievement of perfect matching. Full-wave simulations are used to demonstrate the full phase range achieved by varying unit cell dimensions. The operation of the proposed metasurface is further demonstrated by obtaining refracted and difference-pattern beams from a circularly-polarized slot array antenna.

P3.082 THz Power Divider Based on Self-Complementary Metasurface

[Andrey Sayanskiy](#) and [Vladimir Lenets](#) (ITMO University, Russia); [Sergei A. Kuznetsov](#) (Rzhanov Institute of Semiconductor Physics SB RAS, Russia); [Stanislav Glybovski](#) (ITMO University, Russia); [Juan Domingo Baena](#) (Universidad Nacional de Colombia, Colombia)

In this work we present the results of numerical simulation of the self-complementary metasurface which is illuminated by circular polarized plane wave providing spatial separation of the co- and cross-polarized THz beams. We show that the metasurface will create the cross-polarized beam focusing in the certain focal point, while keeping the co-polarized beam transmitted in the broadside. It could be obtained by gradually altering the geometry of the unit cell along the metasurface to get different phase jumps for the cross-polar transmission coefficient.

P3.083 Wideband Substrate Integrated Luneburg Lens Using Glide-Symmetric Technology

[Lei Wang](#) (Heriot-Watt University, United Kingdom (Great Britain))

With a glide-symmetric mushroom unit cell, a wideband Luneburg lens is integrated into print circuit boards (PCBs). Due to the low dispersion of such a unit cell of the metallic via in glide-symmetric technology, the equivalent refraction index of the unit cell remains stable versus a wide frequency range, which is a good candidate for the design of wideband Luneburg lenses. Electric fields in simulation has validated the proposed technology in a wide frequency band. Such Luneburg lens can be easily integrated with other microwave components in PCB technology, promising for applications as beamforming network and multibeam antennas.

P3.084 Labyrinth Absorber Based on Metageometries Metasurface for Fungi Detection

[Irati Jáuregui-López](#) (Universidad Pública de Navarra, Spain); [Pablo Rodríguez-Ulbarri](#) (Asociación de Industria Navarra, Spain); [Sergei A. Kuznetsov](#) (Rzhanov Institute of Semiconductor Physics SB RAS, Russia); [Miguel Beruete](#) (Universidad Publica de Navarra, Spain)

In this paper a labyrinth metasurface based in the new paradigm of metageometries is designed to operate in the Terahertz (THz) band as a biosensor. First, a numerical study is carried out to study the performance of the metasurface as a refractometer when working in two different configurations: transmission and reflection. Then, its performance as a fungi detector is evaluated and a comparison with other devices is performed, showing that the sensitivity and Figure of Merit (FOM) can be enhanced by the use of these kind of devices, in comparison with the classical approach of metaatoms. Particularly, the designed structure is able to detect 5 fungi elements arbitrarily distributed on the unit cell, which is equivalent to a concentration of 0.004/ μm^2 , improving the results available in the literature by a factor of more than 4.

P3.085 Flat Meta-Reflector for Broadband Circularly Polarized Parabolic Antenna

[Vivien Taverny](#) (LEME, UPL, Univ Paris Nanterre, France); [Badreddine Ratni](#) (Univ Paris Nanterre, France); [Alexandre Piche](#) (Airbus Defence and Space, France); [Shah Nawaz Burokur](#) (LEME, France)

A broadband flattened parabolic antenna based on a metasurface reflector that operates in right-handed circular polarization is proposed. The high directive antenna is intended for frequencies spanning from 10.7 GHz to 12.7 GHz in the Ku-band. The designed metasurface is composed of two layers of square patches printed on a grounded low loss dielectric substrate. The metasurface is illuminated by a broadband circularly polarized patch antenna placed at the focal point. The proposed concept is first validated numerically and then experimentally by measurements performed on a fabricated prototype. A highly directive beam is obtained in both simulation and measurement.

P3.086 Study of Broadband/Dual-band Stack Prism Absorber

[Chao Gu](#) and [Vincent Fusco](#) (Queen's University Belfast, United Kingdom (Great Britain))

This paper presents the study of multilayered absorbers. Such structures can be designed to exhibit broadband absorption performance of 52% fractional bandwidth. We discuss the TE, TM incidence angle dependency characteristics of a doubly periodic arrangement of the square, conical and hexagonal truncated stacked lamination prism arrays. Then further geometry modification is made to achieve a dual-band operation with a low profile. The simulation results show that the frequency ratio can be tuned by controlling the metallic via location. The resultant dual-band design has stable absorption performance at different incident angles.

P3.087 A Highly Efficient Multifunctional Metasurface for C- And X-Band Applications

[Syed Muhammad Qasim Ali Shah](#) (National University of Sciences and Technology, Pakistan); [Fahad Ahmed](#) (Research Institute for Microwave and Millimeter-Wave Studies (RIMMS) & (NUST), Pakistan); [Nosherwan Shoaib](#) (Research Institute for Microwave and Millimeter-Wave Studies (RIMMS) & National University of Sciences and Technology (NUST), Pakistan)

A simultaneous linear and circular polarizer for C- and X-band applications is presented and analyzed. The proposed structure has the capability to attain linear to circular (LTC) polarization conversion in the complete X-band (fractional bandwidth 40%) with more than 90% efficiency. Moreover, structure also performing linear to linear (LTL) polarization conversion in the frequency range of 6.88-7.32 GHz with more than 90% efficiency. The structure gives same response against oblique incidence up to 300. The miniaturization in unit cell size, stability and multifunctional operation make this metasurface a strong candidate for C- and X-band applications.

P3.088 Towards Real-time Independent Control of Reflection Magnitude and Phase in Electromagnetic Metasurfaces

[Ahmed Ashoor](#) and [Shulabh Gupta](#) (Carleton University, Canada)

A novel configuration of a metasurface unit cell is proposed to independently control its reflection phase and magnitude at the specified frequency and is demonstrated using an equivalent circuit model. The unit cell of the proposed metasurface structure consists of two resonators with integrated resistive and capacitive loads in each resonator, which are respectively responsible for dynamically controlling the reflection magnitude and phase. An equivalent circuit model of such confirmation is developed to study the reflection response of the metasurface as a function of various lumped-element controls. It is shown that an arbitrary combination reflection amplitude and phase can be achieved by an appropriate combination of these lumped elements. Using commonly available tunable resistive and capacitive components, a real-time tunable metasurface is envisioned where the reflection amplitude and phase of the metasurface can be engineered with complete flexibility.

P3.089 Tailoring Fe80Co20 Composite Material for High Permeability at High RF Frequency for Antenna Applications

[Amir I Zaghoul](#) (US Army Research Laboratory & Virginia Tech, USA)

Snoek's law is a well-known theory used to describe relationship between ferromagnetic resonant frequency, f_{res} , and static permeability, μ_s , in magnetic materials. Within the limits imposed by Snoek's law, higher μ_s leads to lower f_{res} and vice versa. Recently, Rogers Corporation introduced magneto-dielectric material. It has permeability and permittivity of 6 and 6.5, respectively, along with low magnetic and dielectric loss below 500 MHz, which is also governed by Snoek's law. Extending f_{res} to higher frequencies while keeping the value of μ_s relatively high, is imperative for developing higher GHz-range magnetic devices for antenna substrates and other applications. This can be achieved by controlling dimensions and orientation of magnetic fine, thin flakes or nano-particles of Fe80Co20 in polymers. In this paper, we focus on fabricating low-loss Fe80Co20 composite materials using two different techniques: electrodeposition and sputtering processes. The prototype is measured using waveguide system to confirm its magnetic properties.

P3.090 Fano Resonance Based Multiple Angle Retrodirective Metasurface

[Mohammed Kalaagi, III](#) (Universite Lille 1 & The French Institute of Science and Technology for Transport, Spatial Planning, Development and Networks, France); [Divitha Seetharamdoo](#) (IFSTTAR, LEOST & Univ Lille Nord de France, France)

In this paper, a Fano resonance based multi-angle retrodirective metasurface is introduced. The aim is to investigate the potential of Fano-resonating structures, to suppress the losses and complexity of metasurface designs with high super-cell periodicities. A dolmen structure is given in this case which is well known for its Fano-resonating characteristics. It consists of two sub-radiant modes and one super-radiant mode. The design is given following the generalized phase law of reflection and surface impedance modulation for higher efficiency. The super-cell design has been given with a periodicity of 5.74λ , and frequency of 24 GHz. This is to achieve numerous retro-reflections at different incident angles based on Floquet harmonic analysis. On the other hand, by exciting the super-radiant mode, retrodirectivity has been achieved at three incident angles due to the coupling between the individual elements of the Fano-resonating structure. The monostatic RCS has been calculated to determine the performance of the retrodirective metasurface.

P3.091 Generation of Multi-Mode OAM Waves Through 1-Bit Direct-Radiating Programmable Metasurfaces

[Xudong Bai](#) (Shanghai Aerospace Electronics Co., Ltd, China)

A direct-radiating programmable metasurfaces is presented for generating multi-mode OAM beams. The proposed direct-radiating metasurfaces is composed of 1-bit electronically reconfigurable units, which are integrated with two PIN diodes in the radiation layer for current inversion. Compared with the traditional transmitted or reflective metasurfaces, the feeder source is integrated into the infrastructure of the metasurfaces for a lower profile.

P3.092 1-Bit Digital Coding Metasurfaces for Efficient Generation of Convergent Multi-Mode OAM Beams

[Fanwei Kong](#), [Yuntao Sun](#) and [Xudong Bai](#) (Shanghai Aerospace Electronics Co., Ltd, China)

A reconfigurable 1-bit digital coding metasurfaces are presented for generating convergent multi-mode OAM beams. The designed metasurfaces consist of reconfigurable units with 1-bit phase modulation by introducing a PIN diode to change the unit resonant property. By digitally controlling the coding distribution on the metasurfaces, the converged multi-mode OAM beams can be generated.

P3.093 Flangeless Waveguide Connection Based on Gap Waveguide Technology

[Wanzhao Cui](#) (China Academy of Space Technology Xi'an, China); [Xiang Chen](#) (Xi'an Jiaotong University & China Academy of Space Technology (Xi'an), China); [Dongquan Sun](#) (Xidian University, China); [Yongning He](#) (Xi'an Jiaotong University, China)

To reduce the size of traditional waveguide flange, a solution of pluggable flangeless waveguide connection is proposed. Artificial magnetic conductor (AMC) structure is designed surrounding the outer surface of a size-reduced end of a waveguide, called part-A. Another waveguide with stepped transition to an enlarged end is part-B, the inner surface of the enlarged end works as PEC surface. When Part-A is inserted into part-B, a tight flangeless waveguide connection is achieved under proper size conditions. Tiny air gap exists between the PEC and AMC surface, the electromagnetic leakage from the air gap is prevented by band gap of the EBG structure formed by PEC and AMC surface. A Ku-band prototype of the flangeless connection is designed and manufactured, the measured insertion and return loss are better than 0.06dB and 20dB respectively over 10GHz to 15GHz. The sectional size decreases by more than 70% comparing with traditional waveguide flange.

P3.094 Robustness in Subwavelength Locally-Resonant Metamaterial Waveguides

[Bakhtiyar Orzabayev](#) (EPFL & The Laboratory of Wave Engineering, Switzerland); [Nadège Kaina](#) and [Romain Fleury](#) (EPFL, Switzerland)

Guiding electromagnetic energy at a subwavelength scale is one of the most highly demanded functionalities in a variety of applications, including compact, lightweight satellite communications, signal and data processing, and power systems. The existing schemes for subwavelength waveguiding, including topological designs, are usually based on the use of locally resonant metamaterials and generally sensitive to the lattice imperfections and disorder-induced backscattering. We quantitatively assess here the robustness of subwavelength edge modes in different waveguide designs, including designs based on C6 symmetry or valley-Hall (VH) topological insulators (TI) and non-topological designs based on chirality or a frequency defect line. The statistical results demonstrate that all waveguiding schemes provide a different level of robustness of the edge modes for different types of disorder and superior robustness of VH and chiral metamaterial waveguides to all three types of disorder.

P3.095 Scattering-free Energy Storage in Open Cavities Bounded by Metasurfaces

[Angelica Viola Marini](#) (Università degli Studi Roma Tre, Italy); [Davide Ramaccia](#) (RomaTre University, Italy); [Alessandro Toscano](#) (University Roma Tre (IT), Italy); [Filiberto Bilotti](#) (University Roma Tre, Italy)

The storage of electromagnetic energy is a typical capability of closed cavities, whose impenetrable walls don't allow energy leakage in the form of electromagnetic radiation. Recently, the interest in open or partially-open cavities able to absorb and store the energy carried by an external illuminating field has stimulated research efforts in the exploration of special cavities exhibiting anomalous scattering properties. In this contribution, we investigate the scattering properties of a partially open cavity, bounded on one side by an infinite reflector and on the other by an infinite metasurface. We show that for a specific illumination signal, the cavity may operate in its virtual absorption state, exhibiting neither reflection nor transmission. Being the system lossless, the impinging energy is totally stored in the cavity between the metallic reflector and the metasurface. The proposed structure, which can be easily implemented, may enable the design of lossless systems with dynamic energy properties.

P3.096 Preliminary Investigation of B-dot Wire Concept

[Boris Okorn](#) (Rudjer Boskovic Institute, Croatia); [Andrey Sayanskiy](#), [Vladimir Lenets](#) and [Stanislav Glybovski](#) (ITMO University, Russia); [Silvio Hrabar](#) (University of Zagreb, Croatia)

In recent years the metatronic concept of D-dot wire (a structure that guides the electric displacement current in subwavelength channels in zero permittivity media) has been investigated. A dual concept of B-dot wire (consisting of an subwavelength air channel located in mu-near-zero material) has been analyzed numerically and quasi-magnetostatic propagation with an infinite wavelength is observed. Finally, an experimental RF replica of a B-dot wire, based on split-ring-resonators, is proposed.

P3.097 Ultrathin Zigzag Half-Wave Plate Metasurface with Near-Unity Axial Ratio and High Transmission Efficiency in Terahertz Range

[Alexia Moreno-Peñarrubia](#) (Public University of Navarre & Institute of Smart Cities (ISC), Public University of Navarre, Spain); [Sergei A. Kuznetsov](#) (IEEE Member & Novosibirsk State University, Novosibirsk, Russia); [Miguel Beruete](#) (Universidad Publica de Navarra, Spain)

In this work, a transmissive half-wave plate based on a bi-layered zigzag metasurface operating in the THz band is presented. The half-wave plate thickness is only 100 μm , less than $\lambda/20$ at the operation frequency and achieves an amplitude transmission efficiency around 92% and a cross polarization discrimination of 40 dB, ensuring almost perfect circular polarization conversion.

P3.098 Phase-Gradient Metasurfaces for Efficient Conversion of Surface Wave to Propagating Wave

[Rui Feng](#) (Xidian University, China); [Badreddine Ratni](#) (Univ Paris Nanterre, France); [Jianjia Yi](#) (Key Laboratory of Integrated Services Networks, Xidian University, China); [Alexandre Piche](#) (Airbus Defence and Space, France); [André de Lustrac](#) (Institut d'Electronique Fondamentale - Université Paris-Sud, France); [Hailin Zhang](#) (Xidian University, China); [Shah Nawaz Burokur](#) (LEME, France)

Transmission of light through subwavelength apertures surrounded by periodic structures have attracted extensive research interests since the last two decades. In this work, we propose a method to achieve directional transmission of electromagnetic waves diffracted by a subwavelength aperture using phase-gradient metasurfaces instead of grating structures. Near-field distributions from both numerical simulations and experimental measurements are presented to validate the concept. The extraordinary transmission is further maintained over a non-negligible frequency band ranging from 9 GHz to 12 GHz by modulating the phase profile of the metasurface through electronically-controlled varactor diodes inserted in the constituting unit cells of the metasurfaces.

P3.099 Tunable Terahertz Polarization Converter Based on Graphene Metasurfaces

[Behnaz Bakhtiari](#) and [Homayoon Oraizi](#) (Iran University of Science and Technology, Iran)

In this paper, a tunable Polarization Converter is proposed based on Graphene Metasurfaces in the Terahertz band. It provides a wideband polarization conversion from 6.64 to 8.53 THz with fractional bandwidth of 38% and a polarization conversion ratio (PCR) of more than 0.97. In this designed structure not only can the frequency response be controlled by localizing the plasmon resonance through altering the geometrical dimensions of its shape but it also can be controlled using the Graphene characteristics to have a tunable frequency response regardless of the variations in geometrical dimensions.

Poster3-M07: Satellite and Aerospace Antenna Characterisation

Measurements

Room: Exhibition Hall

P3.100 Impact of Lightning Diverter Strips on Antenna Radiation Patterns

[Ana Vukovic](#), [Phillip Sewell](#) and [Trevor Benson](#) (University of Nottingham, United Kingdom (Great Britain)); [Chris Jones](#) and [Simeon Earl](#) (BAE SYSTEMS, United Kingdom (Great Britain))

This paper investigates the impact of lightning segmented diverter strips on antenna performance. A fully coupled electromagnetic model is considered, where the antenna is enclosed by a realistic dielectric radome profile on which segmented diverter strips are placed. The geometric model of a radome with lightning diverter strips is generated by using a computer graphics method for seamlessly morphing two surfaces together. The antenna performance is characterised by both the S11 parameter and the far field profile.

P3.101 Proposal of GNSS Satellite Antenna Performance Evaluation Based on Reconstructed Gain Patterns

[Gerardo Allende-Alba](#) (German Aerospace Center, Germany); [Steffen Thoelet](#) (German Aerospace Center (DLR), Germany)

The evaluation of available power at user location is an important task as part of a navigation signal quality verification. This is particularly important for safety critical applications using signals from the Global Navigation Satellite Systems (GNSS). Due to a variety of factors, the performance of GNSS satellite antennas may exhibit a non-nominal performance. Efforts to characterize gain patterns of such antennas have been conducted in the past using complex observation setups. In this contribution, GNSS antenna gain patterns are reconstructed using observations from a simple measurement setup. Reconstructed patterns have been used for a characterization of performance of GNSS satellites antennas. The results may prove to be useful for safety critical and domain-specific applications, such as GNSS reflectometry.

P3.102 Deployable Helix Antennas for Nano and Micro Satellites

[Tao Huang](#), [Juan Reveles](#), [Daniel Nascimento](#) and [Vinoth Gurusamy](#) (Oxford Space Systems, United Kingdom (Great Britain)); [Benedetta Fiorelli](#) (European Space Agency, The Netherlands)

This paper presents three different deployable helix antennas developed in Oxford Space Systems for VHF/UHF telecommunications in Nano and Micro satellites. The helix antennas are of trifilar format, driven by a feed Balun and require no ground plane. Both directive high gain beam and isoflux wide beam can be achieved to meet specific mission requirements. The antenna structures are different in response to different stowage and deployment requirements. The design goal however is the same—to yield high stowage efficiency to fit into Nano and Micro satellite platforms and to provide high stiffness when the antenna is fully deployed.

P3.103 Simple and Robust Probes for Near-Field Antenna Measurements at Low UHF Bands

[Vincent Laquerbe](#), [Gwenn Le Fur](#), [Daniel Belot](#), [Lise Feat](#) and [Romain Contreres](#) (CNES, France)

This paper presents a simple and robust design of dual-linear polarized UHF antennas, based on the magnetoelectric dipole concept, for near-field measurements. Two specific probes have been designed and manufactured in order to cover the 350-750 MHz frequency bands. Measurements are currently in progress and only few preliminary results are discussed.

Poster3-M09: MIMO and OTA Testing

Measurements

Room: Exhibition Hall

P3.104 Impact of Probe Coupling on Emulation Accuracy in Massive MIMO OTA Testing

[Huiling Pei](#) and [Xiaoming Chen](#) (Xi'an Jiaotong University, China); [Wei Xue](#) (Xi'an Jiaotong University, China); [Ming Zhang](#) (Xi'an Jiaotong University, China); [Tommy Svensson](#) (Chalmers University of Technology, Sweden)

The sectored multi-probe anechoic chamber (MPAC) setup has been proposed in the literature for OTA testing of Massive MIMO base stations (BSs). However, the previous studies assume ideal isotropic probes, i.e., the radiation patterns and mutual coupling among the probe antennas have not been considered. In this paper, the impact of the mutual coupling of realistic probes on the simulation accuracy of two popular channel emulation methods, i.e. pre-faded signal synthesis (PFS) method and plane wave synthesis (PWS) method in the sectored MPAC system is investigated. Our results show that the PWS method is more robust to mutual coupling than the PFS method.

P3.105 Recent Developments in Radiated Two-Stage MIMO OTA Test Method

[Ya Jing](#) (Keysight Technologies, China); [Thorsten Hertel](#) (Keysight Technologies, USA); [Hongwei Kong](#) (Keysight Technologies (China) Co., Ltd., China); [Penghui Shen](#) (General Test Systems, China); [Yang Liu](#) (GTS, China)

This paper discusses recent developments with RTS MIMO OTA test method. It first introduces the concept of the two-stage method which is based on a first stage of antenna pattern measurement followed by a second stage of throughput measurements using a downlink signals from the communication analyzer that incorporate a convolution of the device's antenna patterns with the desired spatial channel model. The resulting signal is applied to the DUT through the radiated connection, which has the equivalent wireless cable effect. The RTS method was approved by 3GPP in Technical Report 37.977 and is considered harmonized with the Multi Probe Anechoic Chamber (MPAC) methodology. This paper will review recent RTS advancements in 3GPP and CTIA, including 4x4 MIMO OTA test on LTE devices, analyses of CTIA RTS-MPAC SNR-controlled harmonization test results, and the variable Reference Measurement Channel (RMC) MIMO OTA test for SNR-controlled and UE noise-limited environments.

P3.106 On the Measurement of Radiated Power for 5G Mobile Device with Spectrum Analyzer

[Jun Luo](#), [Edwin Mendivil](#) and [Michael Christopher](#) (ETS-Lindgren, USA)

A novel procedure to measure the radiated power of 5G mobile devices in an anechoic chamber (AC) with the spectrum analyzer is presented. In contrast to the traditional method, the new procedure improves measurement accuracy as well as measurement uncertainty (MU) and presents the proper spectrum flatness information of the device. This paper also discusses the key test parameters, such as resolution bandwidth (RBW), video bandwidth (VBW), sweep time, and detector type for 5G mobile devices radiated power measurements with spectrum analyzers.

P3.107 Measurement of OFDM Signals with PAPR Reduction in the Presence of Hardware Impairments

[Hua Wang](#) (Keysight Technologies, Denmark); [Xiaoming Chen](#) (Xi'an Jiaotong University, China); [Jiaying Zhang](#) (EM-Testing, China)

Orthogonal frequency division multiplexing (OFDM) has been selected as a 5G New Radio (NR) waveform for carrier frequency below 40 GHz. In order to satisfy the low peak-to-average power ratio (PAPR) requirement for high power amplifier (PA) efficiency, OFDM with PAPR reduction is highly desirable. In this paper, we evaluate the performance of OFDM with various receiver agnostic PAPR reduction techniques in the presence of hardware impairments. The evaluations are performed in hardware-in-the-loop trials. The measurement results showed that in case of nonlinear PA and high power transmission, OFDM with PAPR reduction schemes can effectively reduce the PAPR of OFDM signals and can achieve similar performance as compared to DFT-spread-OFDM, thus OFDM with simple PAPR reduction is a viable option for 5G NR waveform.

P3.108 Field Emulator for Wireless Communication Devices Base on Programmable Metasurface

[Bowen Hao](#), [Peng Huo](#) and [Zhiping Li](#) (Beihang University, China)

Space-time-coding metasurface provides a better method for dynamic control of electromagnetic waves. We think it can improve the test systems that used to require multiple probes in different directions. In this paper, we propose an emulator based on programmable metasurface to solve the measurement problems in wireless communication system. It can dynamically emulate the field of receiving equipment at a specific location in complex communication environment. The hologram and corresponding quantization technique are used to complete the calculation of the metasurface. We also describe the implementation and analyze the feasibility of our emulator.

Poster3-M10: General Antenna Measurements

Measurements

Room: Exhibition Hall

P3.109 Beam Optimization for 28 GHz Phased Array Utilizing Measurement Data

[Mikko Leino](#), [Jan Bergman](#) and [Juha Ala-Laurinaho](#) (Aalto University, Finland); [Ville Viikari](#) (Aalto University & School of Electrical Engineering, Finland)

This paper presents beam optimization methods for a phased array operating at 28 GHz. The phase of each antenna element is controlled with an element-specific 5-bit phase shifter. The amplitude of each element varies with the chosen phase shift state due to the antenna design. Each individual element is measured and based on the measurement data, the beam optimization for the maximum gain is done. The optimization increases the measured gain compared to the nominal case by 1.3 dB at broadside. Furthermore, the element amplitude variation allows optimization for the lower side lobes to be done by finding the correctly weighted amplitudes. Taylor distribution is used for this optimization and the side-lobe level decreases 2.4 dB for the broadside beam.

P3.110 Numerical Study of Chebyshev RF Absorber Arrangements Versus Tilted RF Absorber Pyramids

[Vince Rodriguez](#) (NSI-MI Technologies, LLC. & University of Mississippi, USA)

Driven by economics, it is common to repurpose existing indoor antenna ranges for different applications such as hardware-in-loop (HWIL) testing of systems. If the range was originally intended to have a centered line-of-sight, using it for a different use may create reflected paths with high angles on incidence onto the lateral walls. These reflected paths have angles of incidence onto the absorber that are very large and cause for the absorber to perform poorly. Two different approaches are possible to improve the range performance. One of them is to use a Chebyshev approach. The second approach is to tilt the absorber blocks to change the angle of incidence to the incoming wave. In this paper numerical methods are used to study the difference between the two approaches to see their advantages and disadvantages.

P3.111 Robot-based Calibration of Multi-GNSS Receiver Antennas Using Real Satellite Signals

[Johannes Kröger](#), [Yannick Breva](#), [Tobias Kersten](#) and [Steffen Schön](#) (Leibniz Universität Hannover, Germany)

Precise positioning and navigation based on GNSS signals require knowledge about the exact location where the signal is measured by the receiving antenna. The reception point varies with the direction of the incoming wavefront of the individual satellite. These variations can reach up to decimetre level for carrier phase measurements. Correction

values, so called phase center corrections (PCC), are determined either by anechoic chamber measurements or calibrations in the field. Currently, for geodetic antennas only PCC for GPS and GLONASS L1 and L2 frequencies are publicly available from the IGS. In this contribution, we present calibration results for these missing GNSS and frequencies obtained from field calibration with a robot using real GNSS signals and an method newly developed at the Institut für Erdmessung. The estimated PCC show an overall good repeatability (RMS<2 mm) for different GNSS receiver antennas which are frequently used in the global IGS tracking network.

P3.112 SSEEM - An Innovative Spread Spectrum System for SatCom Antenna Radiation Patterns Measurements

[Marco Andrenacci](#) (MBI, Italy); [Riccardo Andreotti](#) (MBI Srl, Italy); [Claudia Casali](#), [Michele Gammone](#) and [Leonardo Nanna](#) (M.B.I., Italy); [Alessandro Le Pera](#), [Fritz Schurig](#) and [Daniele V. Finocchiaro](#) (Eutelsat S.A., France)

This paper describes an innovative system, named SSEEM, for co-polar and cross-polar radiation pattern measurements of earth station antennas. The SSEEM system is based on highly spread spectrum waveforms and, due to its high processing gain (PG), is able to overcome the limitations of the conventional approach used by satellites operators, based on transmitting a high-power continuous wave (CW). Indeed, the SSEEM system can operate in very low carrier-to-noise plus interference ratio regions (around -56 dB for 72 MHz bandwidth). Consequently, it does not cause interference on adjacent satellites nor with a signal present within the satellite transponder used for the measurement. This means such tests can be carried out in any moment, without the need for a free satellite slot for transmission. In addition, the high PG allows for resolving even far side lobes of the antenna radiation patterns, without increasing transmission power, as in the CW case.

P3.113 L/S & C Band Medium Gain Ridge Horn Intercomparison Campaign Results

[Maria Alberica Saporetti](#) and [Lars Foged](#) (Microwave Vision Italy, Italy); [Antonis A Alexandridis](#) (NCSR Demokritos, Greece); [Isabel Expósito](#) (University of Vigo, Spain); [Cosme Culotta-Lopez](#) (RWTH Aachen University, Germany); [Bengt Svensson](#) (Saab AB, Sweden); [Ana Arboleya](#) (Universidad Rey Juan Carlos, Spain); [Martin Böttcher](#) (IMST GmbH, Germany); [Manuel Sierra-Castañer](#) (Universidad Politécnica de Madrid, Spain)

The measurements working group of the European Association on Antennas and Propagation (EurAAP), promotes cooperation to advance research and development of antenna measurements. An on-going task of this group is to support inter-comparisons of measurement facilities. The different campaigns also serve as input for a new task, recently approved in WG5, about self-evaluation from inter-comparison results. The L/S & C bands medium gain ridge horn, MVI-SH800, was selected as reference antenna for an EurAAP ACE campaign. In order to enhance the correlation in different facilities, the MVI-SH800 has been equipped with an absorber plate and employed in a new extensive comparison campaign. In [3], we described the activities and showed preliminary results. In this paper we present the complete inter-comparison and draw final conclusions. Result of the comparison is reported in terms of gain, directivity, equivalent noise level, Birge ratio and Escore considering the uncertainty declared by each facility.

P3.114 Electric Field Analysis and Measurement for a Resistively Loaded Monocone

[Jiang Tingyong](#) (EPFL, Switzerland); [Wang Xiaojia](#) (Northwest Institute of Nuclear Technology, China); [Zhou Heng](#) (Northwest Institute of Nuclear Technology, Switzerland)

A novel resistively loaded monocone was proposed to extend the application for electric field calibration. Electric field analysis and measurement was carried out to verify the design of a proposed monocone. As revealed by the results, the S11 of the monocone feed was reduced from near 0 dB to below -17 dB in the low frequency. The measured electric waveform was also consistent with the excited pulse waveform after loading. The electric field uniformity was improved by resistive loading, and the maximum variation of electric field was reduced to 1.3 dB from DC to 500MHz at the given L-line, which suggest an enhancement when compared to the unloaded monocone. The analysis and measurement results demonstrated a possible potential for electromagnetic field calibration both in time and frequency domain in the future.

Poster3-M11: Poster Session 3:Other Measurement Topics

Measurements

Room: Exhibition Hall

P3.115 Design of Constant Width Branch Line Directional Coupler for the Microwave Sensing Application

[Pramod K B Rangaiah](#) (Researcher & Uppsala University, Sweden); [Javad Ebrahimizadeh](#) (University of Uppsala, Sweden); [Jacob Velander](#) and [Roger Karlsson](#) (Uppsala University, Sweden); [Bappaditya Mandal](#) (Uppsala University, Uppsala, Sweden); [Mauricio D Perez](#) (Uppsala University, Sweden & National Technological University, Argentina); [Robin Augustine](#) (Uppsala University, Sweden)

This paper investigates the design of directional branch-line coupler using constant width multiple sections of series and open microstrip line stubs. This device is operating at the center frequency of 2.45 GHz. The designed coupler is having good performance for the frequency band 2–3 GHz. The proposed design is compared with a typical branch line coupler and shows the improved performance. The design is simulated and fabricated on the Fibreglass-resin laminate (FR4) substrate of height 1.5 mm. The results of simulated and experimented circuits are discussed and analyzed. The circuit is measured using Combination Analyzer N9918A Field Fox Handheld Microwave Analyzer. The proposed topology is easy to design and fabricate with a planar microstrip line technology. The designed coupler shows the good results at 2.45GHz i.e. S11 = - 61.26 dB, S21 = - 45 dB, S31 = - 2dB and S41 = - 4.5dB.

P3.116 Reflectometry Enhancement by Saline Injection in Microwave-based Skin Burn Injury Diagnosis

[Alireza Madannejad](#) (Research Assistant, University of Tehran, Iran); [Javad Ebrahimizadeh](#) (University of Uppsala, Sweden); [Fatemeh Ravanbakhsh](#) (Student, Islamic Azad University, Iran); [Mauricio D Perez](#) (Uppsala University, Sweden & National Technological University, Argentina); [Robin Augustine](#) (Uppsala University, Sweden)

This paper provides a novel solution for increasing the difference between the contrast of permittivity of normal skin and burnt skin using injected saline. The paper makes use of injecting saline water into healthy tissue surrounding the burnt part to increase the conductivity contrast of the healthy tissue compared to the burnt area. After 5 minutes passed by injecting the saline, it will be distributed through the normal tissues while the burnt tissues are not able to absorb the saline. Therefore, the level of permittivity contrast between the healthy tissue and burnt tissue increase drastically which is useful for microwave noninvasive diagnosis.

Thursday, 19 March 14:50 - 15:30

IS-Thu 1/1: Invited Speaker Session

Measurements

Room: A2

Chair: [Christer Larsson](#) (Lund University & Saab Dynamics, Sweden)

14:50 Antenna Measurements and Signal Processing Techniques

[Fernando Las-Heras](#) and [Yuri Alvarez-Lopez](#) (University of Oviedo, Spain); [Jaime Laviada](#) (Universidad de Oviedo, Spain); [Ana Arboleya](#) (Universidad Rey Juan Carlos, Spain); [María García Fernández](#) and [Guillermo Alvarez Narciandi](#) (University of Oviedo, Spain)

Several recent advances for in-situ antenna measurements are reviewed in this contribution. This kind of measurements are challenging as they usually require the use of phaseless techniques and non-regular acquisition grids. Thus, the main techniques for phaseless measurements as well as their last advances are firstly reviewed. Next, two novel systems for in-situ measurements are described. The first one is based on the use of Unmanned Aerial Vehicles to characterize outdoor antennas at remote places. The second one consists of a freehand portable system to characterize mm-wave antennas at accessible locations.

IS-Thu 2/1: Invited Speaker Session

Propagation

Room: A3

Chair: [George Tsoulos](#) (University of Peloponnese, Greece)

14:50 Channel Modeling at Sub-millimeter Wave and Terahertz Frequencies for Wireless Chip-to-Chip Communications

[Alenka Zajic](#) (Georgia Institute of Technology, USA)

To enable future THz wireless communication between chips in a system and between blades and racks in large-scale data center systems, it is imperative to understand propagation mechanisms and to develop good channel models to enable communication between chips on a motherboard inside a computer system, between the motherboard and an add-on card (e.g. a graphics card), between boards/blades in a rack-mounted system typical for base stations, and between racks in a data center environment (with raised floors, rows of racks, cooling ducts, etc.). Note that these propagation environments significantly differ from typical wireless channels because there might be significant propagation losses due to signal interaction with metal and plastic parts of the packaging as well as from air circulation inside the packaging/data center. This paper summarizes the latest findings from 300 GHz measurements for computer motherboard and data center environments and reviews proposed channel models for these environments.

Thursday, 19 March 15:30 - 16:10

IS-Thu 1/2: Invited Speaker Session

Antennas

Room: A2

Chair: [Christophe Fumeaux](#) (The University of Adelaide & School of Electrical and Electronic Engineering, Australia)

15:30 *Mobile Satellite Communication Terminals - State of the Art and Antenna Challenges*

[Karu Esselle](#) (University of Technology Sydney, Australia)

Established satellite operators are investing in new services and new satellite operators have committed billions of dollars to low-earth-orbit satellite constellations. Market analysts predict massive expansion of mobile satellite terminal market into new domains. Recognizing that the beam-steering antenna is the main cost item of a mobile satellite terminal and the established antenna beam-steering methods can't meet the demands of the many new markets, such as low cost and low profile, new antenna beam steering methods are being invented and developed by both industry and academics. This invited presentation outlines the challenges, and reviews the state-of-the-art antenna beam-steering methods that are commercially available at present and being developed for mobile satellite communication terminals.

IS-Thu 2/2: Invited Speaker Session

Antennas

Room: A3

Chair: [Anja K. Skrivervik](#) (EPFL, Switzerland)

15:30 *Antennas for Small Biomedical Brain Implants*

[Leena Ukkonen](#) (Tampere University of Technology, Finland)

In this paper and presentation, we will focus on different aspects of backscattering-based wireless communication and power transfer to small biomedical implants. We will present three different antenna topologies for data and power transfer through tissue, in vitro and in vivo studies on implantable intracranial pressure (ICP) sensors and give insight and analysis on wireless link reliability in tissue environment. We will also present radio frequency identification (RFID) -based implant platform and communication method. Moreover, we will focus on differences and challenges of in vivo environment compared to laboratory phantoms and tissue models. In our studies, different types of implantable antennas have been tested to investigate reliability, accuracy and sensitivity of the brain implants: a hybrid near field-far field system with a piezoresistive sensor for ICP monitoring, a UHF band split-ring resonator system and LC tank based miniature implantable antenna.

Thursday, 19 March 16:40 - 18:20

CS42: Nano and Quantum Antennas

T11 Fundamental research and emerging technologies / Convened Session / Electromagnetics

Room: A2

Chairs: [Iñigo Liberal](#) (Public University of Navarre, Spain), [Richard Ziolkowski](#) (University of Technology Sydney, Australia & University of Arizona, USA)

16:40 *Nonperturbative Dynamics of Quantum Antennas*

[Iñigo Liberal](#) (Public University of Navarre, Spain); [Richard Ziolkowski](#) (University of Technology Sydney, Australia & University of Arizona, USA)

Single-photon sources typically operate within the weak-coupling regime, where the dynamics of a quantum emitter consists of a simple exponential decay. However, advances in the fabrication of photonic nanostructures, as well as the positioning and coupling of quantum emitters to them are likely to give access to nonperturbative regimes in an increasingly large number of experimental configurations. While nonperturbative regimes are expected to provide new functionalities for nonclassical light sources, they also pose challenges to the design and modelling of such systems. Here, we theoretically investigate the nonperturbative dynamics of a quantum emitter coupled to a two-mode cavity. We demonstrate that it is characterized by a combination of coherent oscillations and an exponential decay whose rate of decrease is reduced with respect to that of the weak coupling regime at long times.

17:00 *Electromagnetic Modeling for Nanoscale Quantum Optics: Beyond the Lego-Brick Picture*

[Martijn Wubs](#) (Technical University of Denmark, Denmark)

Examples are given how the standard electromagnetic modelling of photonic environments can become inaccurate in nanoscale quantum optics. Sometimes for mundane reasons, sometimes because new physics emerges that is not captured in refractive indices alone. Aim is to make a connection between the more 'physics-based' and the more 'engineering-based' electromagnetics.

17:20 *Quantum Antenna Theory for Secure Wireless Communications*

[Said Mikki](#) (University of New Haven, USA)

We provide a very broad outline for a new research area within the domain for Future Antennas, namely quantum antenna (q-antenna) theory and their applications to building secure digital communication lines. The proposed quantum antenna theory purports to presenting a natural extension of RF antennas in classical wireless to the now established field of quantum communications. The paper provides a bird's eye view on the subject, highlighting the main themes and the expected results and benefits of such research domain.

17:40 *Modal Analysis of Deep Nanoscale Plasmonic Structures: Nonlocal Hydrodynamic Approach*

[Mario Kupresak](#) (KU Leuven, Belgium); [Xuezhi Zheng](#) (Katholieke Universiteit Leuven, Belgium); [Guy Vandenbosch](#) (Katholieke Universiteit Leuven (KU Leuven), Belgium); [Victor V. Moshchalkov](#) (Katholieke Universiteit Leuven, Belgium)

Since plasmonic structures at deep-nanometer scale cannot be fully handled by classical electromagnetics, a semiclassical hydrodynamic model has been introduced. The hydrodynamic model essentially describes the motion of the free electron gas in nonlocal metals by imposing additional boundary conditions (ABC). In this work, the hard wall hydrodynamic model with the Sauter ABC is employed, to characterize the optical features of a spherical nanoparticle. The analysis is performed for the natural (quasi-normal) modes of the nanoparticle, supported by the plane wave response of the structure. It is shown that the studied hydrodynamic model provides multiple natural frequencies and natural modes. The natural frequencies are in excellent agreement with extinction resonances.

18:00 *On the Design of Bulk Absorbers at THz Frequencies*

[Andrea Neto](#), [Ralph van Schelven](#) and [Paolo Sberna](#) (Delft University of Technology, The Netherlands)

In this contribution the design of bulk absorbers operating in the THz range is investigated and we propose to synthesize them by realizing resins with controlled percentage of metals. The resin conductivities are assumed to be obeying the Drude model for electron gas where the number of electron per unit of volume is finely tuned. Specifically the Drude model predicts the existence of two frequencies of interest, one associated to the scattering time of the electrons, and a second associated to the plasma frequency, this second largely dependent on the number of electrons. We then move on to minimize the dimensions of the absorbers, by choosing the percentage of metal composing the absorber so that the two characteristic frequencies from the Drude model are coincident. The present investigation provides new, simple and effective guidelines for the design of absorbers in the THz spectrum, based on metal.

CS49: Novel Techniques for Beam Manipulation at Millimeter

16:40 Directive Beam Radiation by A Fresnel Zone Plate Integrated Partially Reflective Surface for Millimeter-wave Applications

Qing-Yi Guo, Quan Wei Lin and Hang Wong (City University of Hong Kong, Hong Kong)

This paper introduces a high gain Fabry Perot cavity (FPC) antenna for millimeter-wave applications. By employing a Fresnel Zone Plate (FZP) integrated Partially reflective surface (PRS), 4 dB gain enhancement is realized. The proposed antenna consists of an SIW based feeding source, a quasi-curve reflector and the proposed FZP integrated PRS. All parts of the proposed antenna can be implemented by low-cost and mature printed-circuit-board (PCB) technology, which is convenient in circuitry integration. For validation, a prototype of 60 GHz FPC antenna is designed and measured. It yields a measured impedance bandwidth of 17.8% and a 3-dB gain bandwidth of 13.3 %. The measured peak gain is 21 dBi at broadside direction. The proposed antenna finds potential applications in 5G communications.

17:00 Polarization Reconfiguration of a Millimeter-Waves Antenna Using the Optical Control of Phase Change Materials

Jehison Leon-Valdes and Laure Huitema (Xlim Laboratory, France); Eric Arnaud (University of LIMOGES, France); Damien Passerieux (University of Limoges, France); Aurelian Crunteanu (XLIM, CNRS/ University of Limoges, France)

We present the integration of Germanium Telluride (GeTe), a phase change material (PCM), within a conventional patch antenna operating in the millimeter wave domain (~ 30 GHz). The GeTe is integrated within the four corners of the metallic patch, which is excited by a microstrip line. The phase changes between the insulating (OFF) and metallic (ON) states of GeTe are controlled using shorts ultraviolet (UV) laser pulses. That allows the reconfiguration of the device between a linear polarization (LP), a left hand circular polarization (LHCP) and a right hand circular polarization (RHCP). Measured results of the fabricated antenna show total efficiencies up to 75 % for the circular polarization (CP) and a 3 dB bandwidth of axial ratio (AR) over 350 MHz around 29.5 GHz.

17:20 Implementation Methods for Planar Wide-Angle Scanning Phased Array

Xiao Ding and Ren Wang (University of Electronic Science and Technology of China, China); You-Feng Cheng (Southwest Jiaotong University, China); Yan-He Lv, Wei Shao and Bing-Zhong Wang (University of Electronic Science and Technology of China, China)

Wide-angle scanning phased arrays are hotspots and difficulties in the research field of phased arrays in recent years. Since 2009, Computational Electromagnetic Laboratory (CEMLAB) at University of Electronic Science and Technology of China (UESTC) has carried out related research work, and proposed a theoretical and experimental scheme to break the bottleneck of the limitation of phased array scanning angles by using the pattern reconfigurable technique. Subsequently, CEMLAB conducted in-depth research and gradually developed theoretical methods based on the electromagnetic mirror principle, surface wave assisted method, magnetic current source technique or time reversal (TR) adaptive optimization method to realize planar phased arrays with wide-angle scanning performance. At last, the development trend of wide-angle scanning phased arrays is predicted in the conclusions.

17:40 Wideband Fixed- And Scanned-Beam Millimeter Wave Antenna Arrays for 5G Applications

Donia Oueslati (ICTEAM Institute, Université Catholique de Louvain, Belgium); Raj Mittra (Penn State University, USA)

This paper presents the design of millimeter wave (mm-Wave) antenna arrays with beam-scanning capabilities and potential use for fifth generation (5G) applications. We begin with a fixed-beam low-profile antenna array, which has a wide bandwidth and high gain in the millimeter-wave (mm-wave) band, and then go on to add the beam-scanning feature to the array. The proposed antenna covers most of the Ka-band, has a bandwidth of 10 GHz and exhibits a maximum gain of approximately 25 dB for the array dimension investigated, which exhibits good aperture efficiency. Next, the array is modified by using a beam scanning technique, which enables it to carry out a 2D beam scan at a fixed frequency, without using conventional phase shifters that are lossy as well as costly at mm waves. The issue of circular polarization (CP) is also investigated and CP is achieved by adding transverse radiating elements to the aperture array.

18:00 Fully Dielectric Phased Array for Beamsteering Using Liquid Crystal Technology at W-Band

Ersin Polat and Roland Reese (Technische Universität Darmstadt, Germany); Henning Tesmer (TU Darmstadt, Germany); Matthias Nickel (Technische Universität Darmstadt, Germany); Rolf Jakoby (Institute for Microwave Engineering and Photonics, Technische Universität Darmstadt, Germany); Holger Maune (Technische Universität Darmstadt, Germany)

In this work, we present a liquid crystal based fully dielectric phased array for beamsteering at W-Band. The array consists of 1 x 4 rod antennas including liquid crystal phase shifters and a single multimode interference power divider. With this approach, a fully dielectric approach is possible allowing a very lightweight, compact and low-loss design. Each rectangular phase shifter has a tapered dielectric rod antenna at its end. For beamsteering, dielectric subwavelength phase shifters are filled with a novel liquid crystal mixture. The realized demonstrator achieved a maximum steering range of $\pm 15^\circ$. Moreover, the measured antenna gain is ranging between 13dB to 14dB with a side lobe level below -8 dB. The input reflection coefficient is below -10 dB over the whole W-band.

T03-A11: Antennas for WLAN Applications**16:40 Dual Polarized Dual Band Collocated Beam Switching Antennas for WLAN Applications**

Halim Boutayeb (Huawei Technologies, Canada); Fayez Hyjazie (Huawei Technologies Co. Ltd., Canada); Matthew Milyavsky (Huawei Technologies, Canada); Teyan Chen (Huawei Technologies CO. Ltd, China); Tao Wu (Huawei Technologies Co., Ltd, China)

Future Access Points (APs) for Wireless Local Area Network (WLAN) systems require more streams to enhance channel capacity by using Multiple Inputs Multiple Outputs (MIMO) techniques. Furthermore, antennas with reconfigurable patterns can increase significantly the communication throughput. It is a great challenge to integrate more reconfigurable antennas elements into a limited space. We propose a technique for designing four collocated antennas in order to achieve dual bands and dual polarizations with reconfigurable patterns by using a small area. Using the proposed concept, it is possible to increase the number of streams up to 16 within the same size for conventional antenna arrays in Wireless Fidelity (WiFi) APs. Experimental results will be presented and discussed during the conference.

17:00 Adapted Low-Footprint Biasing Circuit for Switched Beam Antenna Steering Usable in Wireless Sensor Networks

Aurelien Surier and Muamba Mukendi Leingthone (Université du Québec en Abitibi-Témiscamingue, Canada); Nadir Hakem (Université du Québec en Abitibi Témiscamingue & LRTCS Research Laboratory Télec in Underground Communications, Canada); Michel Misson (Université de Clermont Auvergne, France)

Wireless Sensors Networks are of great interest for their deployment flexibility and low cost in many applications. Switched Beam Antennas can help to achieve a usable transmission range in higher frequency bands like 2.4 GHz. The switching facility may need to add a control circuitry to address adequately the antenna beam directivity. In this work, we present the integration of a steering functionality with the design of a biasing circuit to be deployed on a dipole antenna usually used by IEEE 802.15.4 standard sensors. We then compare the new configurable antenna with the former static Switched Beam Antenna design. The simulated antenna with the redesigned cells features results with a high directivity of 10.9 dBi and a 32° beam aperture that can be steered to cover 360° in azimuth plane.

17:20 Wideband Dual-polarized Antenna for Wi-Fi Communication Networks

Oleg Soykin, Alexey Artemenko, Vladimir Ssorin, Artem Kolobov and Roman Maslennikov (Radio Gigabit LLC, Russia)

The paper describes a wideband dual-polarized MIMO antenna designed for 5 GHz Wi-Fi communication networks. The antenna consists of two orthogonally polarized 4x4 antenna arrays with dipole-like elements providing enhanced bandwidth. Apertures of the two arrays are overlapped by disposal of the corresponding PCBs one above another making the MIMO antenna as compact as a single-polarized one. The antenna is integrated into an enclosure with a plastic radome and has two output connectors. Measurement results confirm good matching and high cross-polarization isolation levels in the 4.9-6.0 GHz frequency range with 17.5-18.5 dBi gain. Beamwidth of the antenna is 17-20 deg. in both azimuth and elevation planes. Achieved gain provides increased communication distance of the radios typically needed for any outdoor fixed wireless access application while the antenna is primarily developed for trackside networks in subways. Thus, it is already used in Moscow metro to provide high-throughput Internet access to passengers.

17:40 Embedded MTM-EBGs in Patch Antenna for Simultaneously Dual-Band and Dual-Polarized Operation

Braden P. Smyth and Ashwin K. Iyer (University of Alberta, Canada)

This works presents the design of a novel dual-band, dual-polarized antenna (DBDPA) enabled through the use of metamaterial-based electromagnetic bandgap structures (MTM-EBGs). The MTM-EBG is ideal for such an implementation since it is uniplanar and embedded directly into microwave devices such as patch antennas, and as such the DBDPA is compact and easily fabricated with conventional single-layer PCB fabrication methods. The antenna produces 10-dB return-loss bandwidths of 1.6% and 1.0%, with gains of 6.9 dB and 7.4 dB at 3.6 GHz and 5.8 GHz, respectively, for the two polarizations. Furthermore, the simple pin feeds for each polarization experience 30 dB isolation due to symmetry of the structure, and the general design procedure ensures that the DBDPA is practical for applications at arbitrary frequencies.

18:00 A Compact Folded Air Patch Antenna with Low Cross-Polarization

Hao Chen and Ke-Li Wu (The Chinese University of Hong Kong, Hong Kong)

In this paper, a compact folded air patch antenna with low cross-polarization radiation is proposed. The air patch antenna is folded along the E-plane so that the size of the antenna is reduced by more than 50%. Additionally, the folded structure can introduce multiple vertical current components to cancel the parasitic cross-polarization radiation from the feeding probe, leading to a low cross-polarization level in the H-plane. A prototype antenna working in the 2.4 to 2.5 GHz ISM band is designed and measured. The simulated and measured results show good agreement. The measured maximum gain at 2.45 GHz is 8.2 dBi and the measured antenna efficiency is higher than 88%. The measured beam width of the cross polarization that is 15 dB lower than the co-polarization is more than 1200.

T02-A10: Leaky-wave and Traveling-wave Antennas

T02 Millimetre wave 5G / Regular Session / Antennas

Room: B2

Chair: [David R. Jackson](#) (University of Houston, USA)

16:40 Review of Recent Advances in the Leaky-Wave Analysis of 2-D Leaky-Wave Antennas

[David R. Jackson](#) (University of Houston, USA); [Filippo Capolino](#) (University of California, Irvine, USA); [Ahmad T. Almutawa](#) (PAAET, Kuwait); [Hamidreza Kazemi](#) (University of California Irvine, USA); [Sohini Sengupta](#) (Energous Corporation, USA); [Walter Fuscaldo](#) and [Alessandro Galli](#) (Sapienza University of Rome, Italy); [Stuart A. Long](#) (University of Houston, USA)

Recent developments are reviewed in the area of leaky-wave analysis of two-dimensional (2-D) leaky-wave antennas. Recent results are reviewed in three areas: (1) new beamwidth formulas for 2-D leaky-wave antennas, (2) leaky-wave analysis of wideband Fabry-Pérot resonant cavity antennas, and (3) leaky-wave analysis of 2-D periodic leaky-wave antennas (ones that radiate from higher-order space harmonics).

17:00 Radial Line Slot Array Antenna for 5.8-GHz-Band Beam-Type Wireless Power Transmission

[Takashi Tomura](#) and [Jiro Hirokawa](#) (Tokyo Institute of Technology, Japan); [Minoru Furukawa](#) and [Teruo Fujiwara](#) (Sho Engineering Corp., Japan)

This paper presents beam-type wireless power transmission by two radial line slot array antennas (RLSA). Using electrically large antennas and their near-field region enables high-efficiency wireless power transmission. A uniformly excited RLSA is designed at 5.8-GHz-band, one of the industry science and medical (ISM) band. The two designed RLSAs are placed vis-à-vis and transmission are analyzed. At the distance of 28 cm, 67% transmission is confirmed whereas the rest is spill-over, material loss, and reflection loss.

17:20 Reducing Side-Lobe Level of Surface Mounted Printed Leaky-Wave Antenna

[Nima Javanbakht](#), [Barry Syrett](#) and [Rony E. Amaya](#) (Carleton University, Canada); [Jafar Shaker](#) (Communications Research Centre Canada, Canada)

A novel method for suppressing the undesired radiation of the feed section is introduced. Implementing the proposed method results in the side-lobe level reduction. To validate the proposed approach, we designed a leaky-wave antenna using the novel feed section. The antenna is realized based on the substrate integrated waveguide. The operating frequency is chosen as 28.5 GHz in the support of modern 5G wireless networks. The length, width, and height of the antenna are 110 mm, 31 mm, and 1.3 mm, respectively. Ease of fabrication, efficiency, and adaptability of the proposed method make it a suitable candidate for suppressing the unwanted radiation from the feed section of the printed antennas.

17:40 Multi-Beam Radiation Properties of Higher-Order Space Harmonics-Enabled Leaky-Wave Antenna

[Mohammad reza Rahimi](#) (Polytechnique Montréal, Canada); [Mohammad S. Sharawi](#) (Polytechnique Montreal, Canada); [Ke Wu](#) (Ecole Polytechnique (University of Montreal) & Center for Radiofrequency Electronics Research of Quebec, Canada)

In this work, we investigate the inherent physical behavior of higher-order space harmonics (HSH) along one-dimensional periodic leaky-wave antenna (1D-periodic LWA) structures. The interdependency of even $n \in [-2, -4]$ and odd $n \in [-1, -3]$ HSH on each other is examined in detail and a method is devised and demonstrated for analyzing their radiation properties which allow us to develop a multi-beam antenna (MBA) without using any feeding network. In addition, the scanning range of $n \in [-1, -2, -3, -4]$ space harmonics is studied and their limitation is discussed. The proposed concept is then validated by designing an LWA utilizing the substrate integrated waveguide (SIW) technology in which the $n \in [-1, -2]$ space harmonics are used for achieving a MBA exhibiting wide scanning capability. The experimental results obtained in this work shows a good agreement with the simulation and analysis counterparts.

18:00 Multi-Port Leaky-Wave Antennas as Real-Time Analog Spectral Decomposers

[Mohamed K. Emara](#) and [Shulabh Gupta](#) (Carleton University, Canada)

A novel analog and real-time spectral decomposition system for signal processing at millimeter-wave (mm-wave) frequencies is proposed and demonstrated using full-wave simulations. The system is based on a multi-port leaky-wave antennas (LWAs) structure formed using an array of N 1-D LWAs with $2N$ ports. When this structure receives a broadband time-domain signal from a single direction, the signal's various spectral components are separated in real-time. They subsequently appear at the various ports of the LWAs following their respective beam-scanning laws. The proposed concept is demonstrated using frequency- and time-domain full-wave simulations of two slot array antennas to decompose a transient pulse into four frequencies. The frequency outputs are then correlated back to the beam-scanning laws of the antennas.

CS63: State of the Art in Antenna Research in Russia

T11 Fundamental research and emerging technologies / Convened Session / Antennas

Room: B4

Chairs: [Dmitry Kholodnyak](#) (Saint Petersburg Electrotechnical University LETI, Russia), [Liubov Liubina](#) (Saint Petersburg Electrotechnical University LETI, Russia)

16:40 Circular-Polarized Antennas Far-Field Enhancement Using Round Reflectors with Curved Sidewall

[Vladimir Litun](#) (Bauman Moscow State Technical University & National Research Nuclear University MEPhI, Russia); [Daniel Semernya](#) and [Elena Komissarova](#) (Bauman Moscow State Technical University, Russia)

This report discusses the problem of wide axial ratio beamwidth and high front-to-back ratio compact antenna design problem. As a prospective solution, a system design, employing crossed dipole element and circular reflector with a curved sidewall, is proposed. In the first step of research, the reflector's influence on radiation characteristics is examined using a simplified model. Numerical analysis shows the potential front-to-back ratio value around 36 dB while the far-field radiation pattern in the upper hemisphere is close to axisymmetric and has a low cross-polarization component level for the same reflector's geometry.

17:00 A 220-300 GHz Offset Dual-Reflector Antenna for Point-to-Point Radio

[Alexey Kosogor](#) and [Yuri Tikhov](#) (Rostov-on-Don Research Institute of Radio Communication, Russia)

This paper presents a feasibility study of a classical offset dual-reflector configuration for sub-THz high gain wideband antenna demanded for radio links with multi-Gbps throughput. To the best of the authors' knowledge, this is the first demonstration of the designed, fabricated and tested offset Cassegrain antenna practical at 220-300 GHz. Antenna embodiment demonstrates notable size and weight.

17:20 Design of Wideband Reflectarray Antennas

[Yury Antonov](#), [Mikhail Sugak](#), [Svyatoslav Ballandovich](#), [Grigory Kostikov](#) and [Liubov Liubina](#) (Saint Petersburg Electrotechnical University LETI, Russia)

The method of increasing the operating frequency band of reflectarray antennas is proposed. The main idea of this method is to compensate phase errors by means of the spatial separation of layers with reflective elements. A full-metal reflectarray antenna has been designed with the use of the proposed method, manufactured and tested. The 18% relative frequency band upon a criteria of 3dB gain reduction is achieved. The peak directivity is 27.7. In addition, issues related to the excitation of slot-element self modes are considered. The excitation of these modes can significantly affect the characteristics of the reflectarray antennas.

17:40 Computer Simulations of Multiband Waveguide Filter on Modulated Metasurface

[Andrey Albertovich Yelizarov](#) and [Igor Vasilievich Nazarov](#) (Moscow Institute of Electronics and Mathematics, NRU Higher School of Economics, Russia); [Andrey Andreevich Skuridin](#) (Moscow Institute of Electronics&Mathematics, NRU Higher School of Economics, Russia)

The paper presents the results of computer simulation of electromagnetic wave propagation in a segment of rectangular waveguide that has one of its wide walls made in the form of a mushroom-shaped modulated metastructure. We used electromagnetic simulation program Ansoft HFSS to obtain the field distribution, characteristics of the complex transmission coefficient S_{21} and VSWR associated with fundamental mode H10. The results indicate that it is possible to create multiband waveguide rejection filters with improved characteristics and parameters using proposed structure.

18:00 A 3D Printed Luneburg Lens Fabricated by Fused Deposition Modelling

[Roman Orekhov](#) (Joint-Stock Company NII"Vektor", Russia); [Nikolai Pavlov](#) (Joint-Sock Company NII Vector, Russia); [Yury Salomatov](#) (Siberian Federal University, Russia); [Mikhail Sugak](#) (Saint Petersburg Electrotechnical University LETI, Russia)

CS31: GNSS Antennas and Systems for Challenged RF Environment TOP

T08 Positioning, localization & tracking / Convened Session / Antennas

Room: B5

Chairs: [Loic Bernard \(ISL, France\)](#), [Michel Clénet \(Defence Research and Development Canada, Canada\)](#)

16:40 *Interference Mitigation for Robust Automotive Satellite Navigation Achieved with Compact Distributed Antenna Sub-Arrays*

[Syed Naser Hasnain](#) and [Ralf Stephan](#) (Technische Universität Ilmenau, Germany); [Marius Brachvogel](#) (RWTH Aachen University, Germany); [Michael Meurer](#) (German Aerospace Center (DLR) & RWTH Aachen University, Germany); [Matthias Hein](#) (Ilmenau University of Technology, Germany)

Conventional distributed antenna arrays with inter-element spacing larger than half wavelength suffer from insufficient spatial sampling, and consequently unambiguous direction-of-arrival estimation of an interferer. An L-shaped inhomogeneous orthogonal distribution, with half wavelength distance between elements within each sub-array and extended distance of multiple wavelengths between sub-arrays, counteracts such drawbacks and allows for convenient installation on passenger cars. To decrease the footprint area, this paper focuses on the concept of a compact arrangement, with inter-element distance decreased to quarter wavelength within each sub-array. This introduces mutual coupling between elements affecting the received signal quality and potential interference mitigation. To cope with such destructive effect on the robustness of the arrays, a decoupling network is applied. The effects of such network on compact L-shaped arrangement, mounted on side mirrors of a car, are analyzed in terms of radiation patterns measured in automotive antenna facility, and interference mitigation performance derived from measured data.

17:00 *Comparison of Adaptive Null-Steering Algorithms for Low Power GNSS Phased Arrays*

[Elizabeth Lloyd](#) and [Robert J Watson](#) (University of Bath, United Kingdom (Great Britain))

GNSS are widely used in everyday life, for navigation, precision aircraft landing, high-frequency trading and power distribution networks. However there are always people who wish to deny access, often for reasons such as car theft or drug trafficking. As such it is of interest to many parties to be able to quickly identify and mitigate jamming. To this end, a low power, phase incoherent, detection system was designed. Exhaustive searches are inefficient and so it is proposed that bio-inspired optimisation algorithms will improve the search speed. Two algorithms were implemented and simulated, and their performance compared for both static tests and for tracking a moving jammer. It was found that both algorithms would locate a jammer faster than an exhaustive sweep. However when a moving jammer was introduced, Particle Swarm Optimisation was unable to reliably track, while Invasive Weed Optimisation could easily track both ramps and step changes in position.

17:20 *3D Printed All-GNSS Bands Miniaturized Antenna and Array for Robust Satellite Navigation*

[Stefano Caizzone](#) and [Sachit Varma](#) (German Aerospace Center (DLR), Germany)

Satellite navigation is a fundamental asset in today's mobile platforms to determine position, velocity and time. Such capability must be protected from unintentional or intentional interferences, in order to ensure availability of correct navigation information at all times. The best performing countermeasure to that threat is the use of multiantenna systems, able to mitigate interferences by placing nulls in the direction of the interferer. The present work shows the design of a 3D printed miniaturized multi-antenna array, able to operate at all GNSS bands and still fitting into a 100 mm diameter footprint, hence suitable for mobile applications, such as UAVs

17:40 *A Testing Platform for Investigation of GNSS Antenna Diversity Systems*

[Sebastian Matthie](#) (Universität der Bundeswehr München, Germany); [Stefan Lindenmeier](#) (Universität der Bundeswehr, Germany)

A new GNSS antenna diversity testing platform is presented which enables measurement, analysis and optimization of GNSS receiving conditions. The testing platform consists of a diversity antenna set, a microwave diversity circuit for phase shifting and combining, a steering unit, a GNSS receiver and an evaluation unit for data analysis. With the diversity circuit three antenna signals are decoupled and combined which are offered by two antenna structures where each of its phase centers are located in the center of a common ground plane. By steering the scan-phased diversity unit via a microcontroller various options of beamforming are possible for analysis of the reception scenario and an improvement of the reception quality. Because of its practical size and weight the testing platform is easy to handle and especially suitable for outdoor and mobile field tests. Measurement and simulation results as well as results of very first field tests are presented.

18:00 *Novel Wideband Antenna for GNSS and Satellite Communications*

[Slobodan Jović](#) (Defence R&D Canada, Canada); [Michel Clénet](#) (Defence Research and Development Canada, Canada); [Yahia Antar](#) (Royal Military College of Canada, Canada)

A novel concept of a dual-sense circularly polarized dielectric resonator antenna for the Global Navigation Satellite Systems (GNSS) and other satellite communications is presented. The concept introduces a loaded annular dielectric resonator excited using four vertical conformal strips fed in a quadrature. The most unique feature of this antenna is the resonator load, which modifies the boundary conditions of the resonator. The load is a one-dimensional array of periodic elements. The impact on the antenna performance is multifold, including improved bandwidth, radiation efficiency and reduced mutual coupling between the ports. The experimental results show this antenna effectively covers both the GNSS bands. The 0dBic gain and 3dB axial ratio (AR) bandwidth significantly exceed the 10 dB return loss (RL) bandwidth. The 0dBic gain and 3dB AR beamwidth range are greater than 105° and 135°, respectively, within the GNSS bands. The antenna also exhibits a stop-band at 1355 MHz.

T05-A12/3: Body Area Antennas and Sensor Systems TOP

T05 Biomedical and health / Regular Session / Antennas

Room: B6

Chairs: [Katsuyuki Haneda \(Aalto University, Finland\)](#), [Gaetano Marrocco \(University of Rome Tor Vergata, Italy\)](#)

16:40 *Multichip RFID Epidermal Sensor for Body Temperature Monitoring*

[Sara Parrella](#) (University of Roma "Tor Vergata", Italy); [Cecilia Occhiuzzi](#) (University of Roma Tor Vergata & DICII, Italy); [Gaetano Marrocco](#) (University of Rome Tor Vergata, Italy)

A dual chip UHF RFID epidermal sensor tag is here proposed for monitoring human body temperature. A multi-mode square loop configuration has been loaded by two orthogonal matching elements whose position and shape are such to simultaneously optimize the reading performance of both ICs. Thanks to the presence of two independent sensors, the device is able to perform differential measurements respect to the body position (the acquisition points are slightly delocalized) and to the external environment. The device is hence a concept of a single heat-flux thermometer to be used to estimate the core temperature of the body.

17:00 *Full Analysis of Wearable Textile Sensor for Biomedical Applications: Preliminary Validations Towards a Pre-Clinical Assessment*

[Sandra Costanzo](#) and [Vincenzo Cioffi](#) (University of Calabria, Italy)

A full analysis of textile wearable sensor to be adopted for the non-invasive monitoring of diabetes pathology is discussed. Simulation data are collected by adopting a stratified biological material as radiation medium, with an accurate dielectric model for the blood, properly characterizing the variation of its complex permittivity in terms of changes in the glucose concentration. Experimental results on human subject are discussed to demonstrate the validity of simulations. Furthermore, the SAR performance of the proposed sensor configuration are evaluated, and a simple increase in the textile dielectric thickness is applied to guarantee the satisfaction of the imposed maximum levels on humans. Finally, the experimental procedure leading to the preparation of biological phantoms useful for a pre-clinical assessment is described.

17:20 *Passive RFID-based Textile Touchpad*

[Han He](#), [Xiaochen Chen](#), [Leevi Raivio](#), [Heikki Huttunen](#) and [Johanna Virkki](#) (Tampere University, Finland)

This paper presents the first prototype of a passive RFID-based textile touchpad. Our unique solution takes advantage of ICs from passive UHF RFID technology. These components are combined into a textile-integrated IC array, which can be used for handwritten character recognition. As the solution is fully passive and gets all the needed energy from the RFID reader, it enables a maintenance-free and cost-effective user interface that can be integrated into clothing and into textiles around us.

17:40 *A Dual-band Repeater Antenna for On-Body Receiver Unit of Wireless Capsule Endoscope*

[Md Miah](#) and [Clemens Icheln](#) (Aalto University & School of Electrical Engineering, Finland); [Katsuyuki Haneda](#) (Aalto University, Finland)

A dual-band repeater antenna for the on-body receiver unit of a wireless capsule endoscope system is proposed at the MedRadio frequency band of 401-406 MHz and at ISM frequency band of 2.4-2.48 GHz. The radio link from the capsule transmitter to the on-body receiver utilizes the MedRadio band, whereas the on-body to off-body communication happens at the ISM band. The design utilizes two rectangular offset patches, printed on two sides of a substrate. Both the top and bottom patches are configured in such a way that wideband matching with sufficient radiation efficiency is achieved at both bands. A canonical tissue phantom and realistic human body model were used for the numerical studies. The latter was validated through ex-vivo measurements on a real human body. The measured -10 dB impedance matching bandwidths are 44% and 14.4% at the MedRadio and ISM band, respectively show a good agreement with the simulated one.

18:00 *UWB Planar Bias-switched Imaging Array for Breast-Cancer Screening*

[Natalia Nikolova](#), [Farzad Foroutan](#), [Vartika Tyagi](#), [Chih-Hung Chen](#) and [Charl Baard](#) (McMaster University, Canada)

Electronically switched arrays offer superior measurement speed and positioning certainty compared with mechanical scanning. These advantages are important in the applications of microwaves in medical imaging. However, current RF-switch architectures suffer from inherent limitations on the number of multiplexed ports, the relatively large size, the significant insertion loss, limited isolation, and high price. Here, we present a novel bias-switched architecture for microwave-imaging arrays, which eliminates the use of RF switches by shifting the burden of port multiplexing to the intermediate-frequency (IF) output. It makes full use of the dynamic range of a vector network analyzer while multiplexing hundreds of array elements. The design and performance of the system components is briefly described as well.

T06-P12: Radar, Localisation and Sensing for Aircraft and Automotive Applications

T06 Aircraft (incl. UAV, UAS, RPAS) and automotive / Regular Session / Propagation

Room: B7

Chairs: [Fernando Las-Heras](#) (University of Oviedo, Spain), [Junichi Naganawa](#) (Electronic Navigation Research Institute, Japan)

16:40 *Experimental Evaluation on TDOA-based Aircraft Position Verification*

[Junichi Naganawa](#) and [Hiromi Miyazaki](#) (Electronic Navigation Research Institute, Japan)

Automatic dependent surveillance - broadcast (ADS-B) is an emerging means of aircraft monitoring/surveillance that employs position reports periodically broadcasted by aircraft. ADS-B can provide accurate positions of aircraft with low-cost implementation of ground facilities. However, ADS-B is susceptible to false aircraft information injected by malicious emitters or generated by avionics failures. A promising countermeasure for this security issue is position verification using TDOA (Time Difference Of Arrival). In this paper, an experimental study is reported to investigate the performance of the TDOA-based position verification method. As a result, a good probability of detection was measured. The experiment also verified the theoretical model which was previously derived by the authors. The presented result is important as a rationale that supports the effectiveness of the method. In addition, the model is generic and informative to other systems that may depend on position reports, e.g. traffic management of Unmanned Aerial Vehicles (UAVs).

17:00 *Measurements of Opportunistic Aircraft Signals and Verification of a Propagation Prediction Tool in Mountainous Region*

[Junichi Naganawa](#) (Electronic Navigation Research Institute, Japan); [Karma Wangchuk](#) (Tokyo Institute of Technology, Japan); [Sangay Sangay](#) (Department of Air Transport, Japan); [Karma Gayley](#) and [Devi Adhikari](#) (Bhutan Civil Aviation Authority, Bhutan); [Hiromi Miyazaki](#) (Electronic Navigation Research Institute, Japan)

Automatic dependent surveillance - broadcast (ADS-B) is an emerging and more economically viable means of aeronautical surveillance. Aircraft periodically broadcasts surveillance information such as its own position and velocity. Although ADS-B was originally developed for air traffic control, measurement of opportunistic ADS-B signals can be applied to radio propagation study. This paper presents a comparison on the received signal strength (RSS) between measurements of opportunistic ADS-B signals and predictions by a Physical-Optics-based tool with terrain data in the Himalayan mountains of Bhutan. Two measurement scenarios were studied: one with the receiver at the airport located in the bottom of a mountainous valley and another with the receiver on the top of a mountain that surrounds the valley. The comparison is aimed at 1) investigating the ADS-B signal propagation in the mountainous region, 2) demonstrating a site-survey by opportunistic ADS-B signals, and 3) demonstrating verification of a propagation prediction tool.

17:20 *3D-SAR Processing of UAV-mounted GPR Measurements: Dealing with Non-Uniform Sampling*

[María García Fernández](#) (University of Oviedo, Spain); [Yuri Álvarez](#) (Universidad de Oviedo, Spain); [Fernando Las-Heras](#) (University of Oviedo, Spain)

This contribution is devoted to analyze the effect caused by non-uniform sampling and to present a technique for dealing with this issue in a system composed by a Ground Penetrating Radar (GPR) mounted on board an Unmanned Aerial Vehicle (UAV). Radar measurements are accurately geo-referred in order to enable the use of Synthetic Aperture Radar (SAR) techniques. The adopted SAR technique must be able to handle measurements gathered at arbitrary positions. In addition, the positioning data must be also carefully processed to cope with non-uniform sampling and flight deviation issues. A method based on defining a set of conditions that a measurement position must satisfy to be selected for processing has been proposed. Comparing the resulting 3D radar images retrieved from measurements gathered during autonomous flights, both the image artifacts and the computational time are significantly decreased, showing the feasibility of the proposed technique to overcome non-uniform sampling issues.

17:40 *Millimeter-Wave Automotive Radar Scheme with Passive Reflector for Blind Corner Conditions*

[Dmitrii Solomitckii](#) and [Carlos Baquero Barneto](#) (Tampere University, Finland); [Matias Turunen](#) (Tampere University of Technology, Finland); [Markus Allén](#) (Tampere University, Finland); [Yevgeni Koucheryav](#) (Tampere University of Technology, Finland); [Mikko Valkama](#) (Tampere University, Finland)

One of the primary functions of millimeter-wave automotive radar is collision avoidance. This application is typically realized in line-of-sight conditions. However, it does not perform well in situations, when another car suddenly come into view around the corner of a building. Hence, this paper proposes a radar scheme with a reflector, enabling the detection of an oncoming car in blind corner conditions. First, our ray tracing modelling results demonstrate the difficulties of straightforward non-line-of-sight radar application in such a scenario. Then the paper considers the installation of a planar reflector, which should solve the issue. This is verified with real-world measurements. The results also indicate that the detection performance is sensitive to the around-the-corner car position and orientation of the reflector. Specifically, +/-10 degree deviation varies the signal-to-noise ratio of more than 20 dB. Thus, the location and direction of the reflector should be adopted individually for the particular deployment.

18:00 *Metasurface-Based Radar Jammers and Deceptors Implemented Through Time-Varying Metasurfaces*

[Davide Ramaccia](#) (RomaTre University, Italy); [Dimitrios Sounas](#) (Wayne State University, USA); [Andrea Alù](#) (The University of Texas at Austin, USA); [Alessandro Toscano](#) (University Roma Tre (IT), Italy); [Filiberto Bilotti](#) (University Roma Tre, Italy)

In radar countermeasures, the terms jamming and deception are used to indicate the intentional emission of radio frequency signals whose aim is to interfere with the operation of a radar by saturating its receiver with noise or false information. Electronic radar jammers typically consist of an antenna system and a corresponding circuitry, that captures, elaborates, and re-radiates the proper interfering signals. In this contribution, we present a radar jammer implemented through a time-modulated metasurface. Such a metasurface is an electrically thin artificial structure, whose properties are dynamically changed over time to realize an elaboration of the illuminating signal. We demonstrate that such a metasurface is able to jam Doppler radars, implementing sweep jamming and velocity pull-off techniques.

T09-P13: Propagation Aspects in Remote Sensing

T09 Space (incl. cubesat) / Regular Session / Propagation

Room: B8

Chairs: [Michael Schönhuber](#) (Joanneum Research, Austria), [Franz Teschl](#) (Graz University of Technology, Austria)

16:40 *Remote Sensing of Tropical Precipitation with Radar and Radiometric Measurements*

[Animesh Maitra](#), [Soumyajyoti Jana](#) and [Gargi Rakshit](#) (University of Calcutta, India)

This paper presents the techniques and results on remote sensing of rain using radars, both space-borne and ground based, and ground based radiometers at a tropical location where precipitation has varying microstructures in terms of DSD, cloud liquid water content, radar reflectivity and atmospheric attenuation at Ka band frequencies. A technique is proposed to derive three-parameter DSDs from dual frequency radar measurements onboard GPM satellites. Time evolution of precipitation features has been studied for different types of rain using a ground based multi-frequency microwave radiometer and an MRR. Convective rain is characterized by high rain rate, high cloud liquid water content abundance of large rain drops whereas stratiform rain is characterized by radar bright band, low cloud liquid water and dominance of small rain drops. The atmospheric attenuation at 22.24 and 31.4 GHz is controlled by the relative contribution of rain and water vapour during two types of rain.

17:00 *Calibrating Ka Band Satellite Down-Link Modem Measurements for Rainfall Monitoring*

[Franz Teschl](#) and [Reinhard Teschl](#) (Graz University of Technology, Austria); [Valentin Eder](#) (Space Analyses GmbH, Austria)

The observation of the signal level in microwave satellite links for remote sensing of rainfall can be a useful complementation of existing sensors like rain gauges or weather radars. The number of very small aperture terminals (VSATs) that provide internet connectivity is constantly raising. As such terminals are more and more used in corporate networks, the VSAT density is increasing - not only in remote areas. When retrieving rain rate from signal measurements, the quality of the signal measurements has to be understood. This study compares signal measurements of two common types of co-located terminals with a reference demodulator. It shows both over- and underestimation of various modems and provides a correction function for the values. This analysis lays the foundation for using these types of VSATs for retrieving rain information and also has benefits for satcom network operators.

17:20 *Sea Surface Characterization Using Dual Polarized GNSS Reception System*

[Ankit Regmi](#) and [Aarno Pärssinen](#) (University of Oulu, Finland); [Markus Berg](#) (University of Oulu & Excellant LTd., Finland)

GNSS signal reception using Dual Circular Polarized method has been proposed to simultaneously record direct and reflected signals from the sea surface. Dual circular polarized reception (DCPR) system gives the opportunity to exploit the polarization change of the incident signal after reflection. This paper reports received signal characteristics of various GPS satellites for bare sea conditions. The received signals from various satellites are compared and are analyzed statistically to characterize the sea-state. The reflected left-hand circular polarized (LHCP) signal is used to analyze the scattering characteristics of sea surface. The statistics of LHCP signal give strong correlation with the wind speed over the sea and can be used to characterize the sea-state.

17:40 *The MEKaP Project: Measuring Tropospheric Impairments at Ka Band with MEO Satellites*

[Lorenzo Luini](#), [Carlo Riva](#) and [Alberto Panzeri](#) (Politecnico di Milano, Italy); [Armando Rocha](#) (University of Aveiro & Instituto de Telecomunicações, Portugal); [Susana Mota](#) (University of Aveiro & Institute of Telecommunications, Portugal); [Frank S. Marzano](#), [Augusto Marziani](#) and [Marianna Biscarini](#) (Sapienza University of Rome, Italy); [Fernando Consalvi](#) (FUB, Italy); [Vincenzo Schena](#) (Thales Alenia Space Italia, Italy); [Antonio Martellucci](#) (European Space Agency, The Netherlands)

The design phase of an ESA-funded project (MEKaP - MEO Ka-band Propagation) is described. The study, involving Politecnico di Milano, Sapienza Università di Roma, Instituto de Telecomunicações-Aveiro Pole and Thales Alenia Space-Italia, aims at characterizing the main properties of the atmospheric radio channel of a MEO Ka-band SatCom system. The propagation campaign, lasting at least two years and including four ground receivers, will rely on the MEO O3b Ka-band satellite constellation, which provides key characteristics for propagation measurements, such as continuous observation time (always at least one satellite is visible) and global coverage up to mid-latitudes. The experimental data collected during the campaign will be used to test and improve the available propagation models for non-geostationary systems and to extend the experimental database of radio regulatory bodies such as the ITU-R.

18:00 *The Variability of Scattering from Leaves and Its Impact on Propagation*

[Jamil Bataineh](#) and [Robert J Watson](#) (University of Bath, United Kingdom (Great Britain))

Models for the scattering of leaves is a key input into the current ITU-R recommendation P.833-9 for attenuation in vegetation. This paper examines the variability of scattering from leaves due to uncertainties in various leaf-related parameters including size, shape, curvature, inhomogeneity and moisture content. The resulting scattering amplitudes have been determined using finite-element methods at frequencies of 1.9 and 26 GHz. The modelling assumptions made in current literature, backed up by measurements are reasonable up to around 10 GHz. However, at 20 GHz and beyond it is shown that some of these assumptions begin to break down.

T10-E05/2: Imaging and Inverse Scattering

T10 EM modelling and simulation tools / Regular Session / Electromagnetics

Room: B9

Chairs: [Martina Teresa Bevacqua](#) (Università Mediterranea di Reggio Calabria, Italy), [Carey Rappaport](#) (Northeastern University, USA)

16:40 *Improving the Reconstruction Image Quality of Multiple Small Discrete Targets Using the Phase Coherence Method*

[Guanying Sun](#), [Mohammad Hossein Nemati](#) and [Carey Rappaport](#) (Northeastern University, USA)

In this work, we investigate the application of the phase coherence method for improving the quality of reconstructed images of small isolated objects with our Advanced Imaging Technique (AIT) nearfield millimeter-wave radar security scanning system. Based on the phase diversity of the reconstructed solutions for different transmitters, a phase coherence factor (PCF) is designed to weight the coherent sum. We verify its effectiveness with both numerical simulation and experimental measurement. In both simulation and experiment results, the artifacts like side-lobes, grating lobes or clutter in the original images are reduced in the processed images after applying the phase coherence method.

17:00 *A Coarse-fine Mesh Approach for Improved Solution of 3-D Inverse Problems in Unbounded Media*

[Ahmet Aydoğan](#) (Izmir Bakircay University & Istanbul Technical University, Turkey); [Emre Kilic](#) (Technische Universität München, Germany); [Mehmet Mert Taygur](#) (Technical University of Munich, Germany); [Thomas F. Eibert](#) (Technical University of Munich (TUM) & Chair of High-Frequency Engineering (HFT), Germany)

A coarse-fine mesh approach is proposed to enhance the inverse scattering method for a three-dimensional problem. The problem is decomposed into exterior and interior problems to reduce the computational cost by invoking the equivalence principle. The exterior radiation problem is formulated by a boundary integral equation which enables to estimate the unknown surface current densities. The estimated current densities form the boundary conditions of the interior problem to extract the dielectric profile. The interior problem is formulated by the finite element technique and solved by the Gauss-Newton method. The associated surfaces and volumes are respectively discretized by triangular and tetrahedral meshes in the decomposed problems. The interior problem is solved with increasingly finer meshes. The exterior problem is solved for each mesh to form the boundary conditions with the associated discretization while the extracted profile in the previous step is used as the initial solution in the interior problem.

17:20 *Inverse Scattering by Means of a New Rewriting of the Integral Equations*

[Martina Teresa Bevacqua](#) (Università Mediterranea di Reggio Calabria, Italy); [Tommaso Isernia](#) (University of Reggio Calabria, Italy)

In this contribution, the integral equations underlying the two-dimensional electromagnetic inverse scattering are conveniently rewritten in such a way to exhibit a lower degree of nonlinearity with respect to parameters embedding dielectric characteristics as compared to the traditional model. The proposed inverse scattering model is based on an original decomposition of the adopted Green's function and the use of the 'reduced scattered field', which is underlying a recently introduced qualitative method. Its adoption could allow to simplify the solution of inverse scattering problems.

17:40 *Automatic Permittivity and Thickness Characterization of Body-Borne Weak Dielectric Threats Using Wideband Radar*

[Mahshid Asri](#), [Mohammad M. Tajdini](#), [Elizabeth Wig](#) and [Carey Rappaport](#) (Northeastern University, USA)

This paper proposes a method for determining permittivity and thickness of body-borne objects automatically by processing wideband radar images. The algorithm can be used to find the explosive threats and rule out the benign objects. Having the reconstructed millimeter wave radar image of the body with an anomaly attached to it, we extract the nominal body contour, which shows the body surface in the absence of the object, then we subtract the ideal body response from the image and define the amount of body displacement observed in the radar image which is caused by the signal retardation due to presence of the weak dielectric object and look for the front surface reflection of the attached foreign object. Finally, we calculate the amount of permittivity based on body displacement and the anomaly's thickness.

18:00 *Tracking Targets from Indirect Through-The-Wall Radar Observations*

[Gabriele Incorvaia](#) (The University of Manchester, United Kingdom (Great Britain)); [Oliver Dorn](#) (University of Manchester, United Kingdom (Great Britain))

In this paper we address the practically important task of identifying and tracking moving objects (e.g. people) inside a building from through-the-wall radar data obtained outside the building. In order to solve this task, we combine modern regularization techniques for solving non-linear inverse scattering problems with a Kalman filter approach for tracking targets from (indirectly obtained) observations. A level set based shape reconstruction technique is employed in order to obtain accurate initializations for the Kalman filter iterations, and a sparsity regularized inverse scattering approach is used in the Bayesian analysis steps. Numerical simulations in 2D show for a proof-of-concept setup that this combined approach of filtering and regularized inversion is very promising for efficiently and accurately tracking moving objects (potentially) in real time.

CS48: Novel Antenna Measurement Data Analysis and Techniques

T11 Fundamental research and emerging technologies / Convened Session / Measurements

Room: B10

Chairs: [Dennis Lewis](#) (Boeing, USA), [Janet O'Neil](#) (ETS-Lindgren, USA)

16:40 *Equivalent Source Technique Processing of Broadband Antenna Measurements*

[Lucia Scialacqua](#) (Microwave Vision Italy, Italy); [Francesca Mioc](#) (Consultant, Switzerland); [Lars Foged](#) (Microwave Vision Italy, Italy); [Giorgio Giordanengo](#) (LINKS Foundation & Politecnico di Torino, Italy); [Marco Righero](#) (LINKS Foundation, Italy); [Giuseppe Vecchi](#) (Politecnico di Torino, Italy)

The equivalent source technique (EQC) has proved to be a useful aid in antenna processing, diagnostics and in the link with Computational ElectroMagnetic Tools (CEM). For broadband frequency antennas or in case of very large number of frequencies, reduction of the number of frequency points to be computed is a desirable feature, to significantly limit the global computational time. In recent applications this is a realistic need, since antennas are present in almost all commercial products, operating on a large set of frequency bands, and exhibiting a wide variety of pattern types. Therefore, they need to be analysed on a relevant number of frequency points, to finally check compliance with standards. For this purpose, in case of multifrequency processing, an interpolation technique based on radiation patterns and antenna S-parameters has been implemented in the EQC. In this paper the new implementation is applied and demonstrated on a large band antenna.

17:00 *Improved-Reliability Phase-Retrieval with Broadband Antenna Measurements*

[Alexander Paulus](#), [Josef Knapp](#), [Jonas Kornprobst](#) and [Thomas F. Eibert](#) (Technical University of Munich, Germany)

Conventional phaseless near-field measurement data is not adequate for reliable transformation into the far field. We tackle this challenge by a formulation working with multi-frequency phaseless measurements under the assumption of coherently measured spectra. Such data is, for instance, obtained with a transmitting antenna under test and standard receivers featuring a nonzero coherent bandwidth. The focus of this work is on an advanced algorithm to demonstrate that this ansatz is very promising for further research and real-world investigations. Empirical studies based on simulation data demonstrate that appropriately merging this multi-frequency data significantly increases the chance of successful phaseless near-field far-field transformation. As a by-product, this multi-frequency phase retrieval method supports also the retrieval of the phase of far-field antenna measurements.

17:20 *Direct Wave Removal in Anechoic Chamber Range Imaging from Planar Scanned Data*

[Zhong Chen](#) (ETS-Lindgren, USA); [Zubiao Xiong](#) (ETS-Lindgren, Inc., USA); [Dennis Lewis](#) (Boeing, USA)

Quiet Zone (QZ) reflectivity levels in an anechoic chamber are typically qualified using free-space VSWR method. The VSWR provides no information about the directions of the stray signals. Using a planar scanner and vector measurements, a chamber image can be developed from Fourier transform to show both signal levels and directions. It is desirable to remove the direct path signal in the image. We investigate two methods for the removal. First method is to subtract a plane wave normalized to the peak value of the spectrum. However, this approach may leave some residual effects. The second method is to apply time domain gating. Measured results are compared to show that the time domain gating method provides several advantages including a more thorough direct wave subtraction and the ability to isolate internal cable reflections or receiver leakages.

17:40 Site Validation Based on the Use of Broadband Calculable Antennas and Numerical Simulations

[Carlo Carobbi](#) (University of Florence, Italy); [Alessio Bonci](#) (ITT G. Ferraris San Giovanni Valdarno, Italy)

Semi-anechoic chambers and open area test sites validation in the frequency range between 30 MHz and 1000 MHz is typically carried out by comparing measurement results obtained by using a pair of biconical and log-periodic (broadband) dipole antennas with tabulated reference values of normalized site attenuation (NSA) provided by CISPR and ANSI standards. It is here shown, through simulations based on validated electromagnetic models of biconical and log-periodic dipole antennas, that the NSA reference values reported in the CISPR 16-1-4 and ANSI C63.4 standards may differ up to about 3 dB from those obtained by using pairs of calculable broadband antennas. Large deviations are observed both in the lower frequency range (30 MHz - 250 MHz), where the use of the biconical antenna pair is prescribed, and in the higher frequency (300 MHz - 1 GHz), where a pair of log-periodic dipole antennas is required.

18:00 An In-Depth Understanding of Salient Features of Antenna Near-Field Measurements Through Full Wave Simulations

[Vignesh Manohar](#) (University of California, Los Angeles, USA); [Yahya Rahmat-Samii](#) (University of California Los Angeles (UCLA) & UCLA, USA)

Full wave solvers today are capable of solving very complex electromagnetic problems and enable the design of complex antennas. They also allow engineers to confidently assess the antenna performance in a real-time environment prior to its fabrication and physical integration with the desired system. In this work, we use the power of full-wave simulators to understand several salient aspects of near-field antenna measurements so as to facilitate the measurement of advanced antennas for emerging technologies. The modeling of the measurement process in a fullwave solver is elaborated in detail, followed by an investigation of two representative aspects of near-field measurements, which are assessing the impact of non-ideal probe and improving the efficiency of phase retrieval algorithms.

Thursday, 19 March 16:40 - 18:40

SW05: ESA Session: Selected Papers from the 40th ESA Workshop on Antenna Developments for Terrestrial and Small-Space Platforms

T09 Space (incl. cubesat) / Regular Session / Antennas

Room: B11

Chairs: [Nelson Fonseca](#) (European Space Agency, The Netherlands), [Maarten van der Vorst](#) (European Space Agency, The Netherlands)

16:40 A Tribute to Niels Eilskov Jensen

[Antoine Roederer](#) (Technical University of Delft, The Netherlands)

Not available

17:00 A 1X3 Circular Polarized Linear Array with High-Gain near Horizon Scanning and Full Azimuth Coverage for Land Vehicles to Satellite Communications

[B. J Falkner](#) (Swansea University, United Kingdom (Great Britain))

Not available

17:20 Design of Advanced Reflectarrays for Future CubeSat Applications

[Min Zhou](#), [Erik Jørgensen](#), [Stig Sørensen](#), [Niels Vesterdal](#), [Michael F. Palvig](#), [Andreas Ericsson](#), [Oscar Borries](#), [Tonny Rubæk](#) and [Peter Meincke](#) (TICRA, Denmark)

In recent years, there have been a significant interest in reflectarray antennas and their use for CubeSat applications due to their planar nature. In this paper, we present a dedicated design tool, QUPES, that has been developed by TICRA for the design of quasi-periodic surfaces and show how it can be used to design advanced reflectarrays for future CubeSat missions. Two application examples are considered, a X-band reflectarray and a Ka-band reflectarray.

17:40 Experimental Validation of a Water Drop Geodesic Lens Design at Ka-Band

[Nelson Fonseca](#) (European Space Agency, The Netherlands)

Not available

18:00 Outdoor Unit for Satcom Next Generation Non-GEO Satellite

[Pasquale Nicolaci](#) (Space Engineering S.p.A., Italy)

Not available

18:20 Novel Design of Deployable Mesh Reflector Antenna for Mini Satellites

[Oleksandr Sushko](#) (EOS Ukraine, Ukraine)

Not available

Thursday, 19 March 18:00 - 20:00

EurAAP 4: WG Propagation (18:00-20:00, Room: B8)

EurAAP

18:00 - 20:00 Room: B8

Friday, 20 March

Friday, 20 March 8:30 - 12:20

8:30 *Integrated Doherty Power Amplifier - Antenna Element with Active Impedance Modulation: Efficiency vs. Bandwidth Trade-Offs*

[Oleg Iupikov](#) and [Jose-Ramon Perez-Cisneros](#) (Chalmers University of Technology, Sweden); [Rob Maaskant](#) (CHALMERS, Sweden); [Christian Fager](#) and [Koen Buisman](#) (Chalmers University of Technology, Sweden); [Daniel Åkesson](#) (Ericsson AB, Sweden); [Marianna Ivashina](#) (Chalmers University of Technology, Sweden)

This work presents an integrated Doherty power amplifier - antenna design at 3.5 GHz. Both power combining and matching to optimum transistor impedances at the fundamental frequency are realized on-antenna. A novel aperture-coupled cavity-backed patch antenna with a multi-port feeding is selected as the radiating element in order to provide a stable radiation pattern versus output power. The power-added efficiency (PAE) versus bandwidth trade-off of the designed integrated active antenna system is quantitatively analyzed. Simulated PAE values higher than 50% at 6 dB output power back-off within 5% bandwidth are obtained.

8:50 *Theory of Cross-Polar Beamforming for Dual Polarized Arrays in Mobile Communications*

[Björn Lindmark](#) (Commscope, Sweden)

Different theoretical aspects of cross-polarized beams in mobile communications are studied, in particular 8T8R beamforming systems. We show that closed form expressions exist for the weights of orthogonal pairs of cross-polarized beams and how the beamwidth can be changed for said beams.

9:10 *Power-Efficient Beam Pattern Synthesis via Dual Polarization Beamforming*

[Sven O. Petersson](#) (Ericsson AB, Sweden)

This paper focus on a new method, called dual polarization beamforming (DPBF), to design beam patterns. Instead of using only a single element-polarization, the traditional technique, a desired beam pattern is designed as the sum of powers for two orthogonal element-polarizations. Thus, the focus is on total radiated power beam patterns. The DPBF technique provides additional degrees of freedom to form a desired beam pattern such that amplitude variations in the beamforming vector can often be significantly reduced, potentially to uniform amplitude. This is a very interesting property, especially for active antennas, since it offers the potential of full power amplifier utilization. The method is applied to uniform linear arrays (ULAs) as well as uniform rectangular arrays (URAs). It is shown that a second beam, with identical beam pattern but orthogonal polarization in all directions compared to a first beam, can be designed with DPBF, both for ULAs and URAs.

9:30 *Full Duplex Spatial Modulation System Performance Depending on Self-interference Cancellation Accuracy*

[Yanni Zhou](#) and [Florin Hutu](#) (Univ Lyon, INSA Lyon, Inria, CITI, France); [Guillaume Villemaud](#) (Université de Lyon, INRIA, INSA-Lyon, CITI, France)

Spatial modulation (SM) as a new MIMO technique is based on transmitting part of the information by activating different emitting antennas. SM increases spectral efficiency and uses only one radio frequency chain. Moreover, for full-duplex (FD) communication systems, self-interference (SI) is always a central problem. Therefore, combining FD and SM can dramatically reduce the difficulty of SIC (Self-interference Cancellation) because of the single SI chain. A Full Duplex Spatial Modulation (FDSM) system is proposed and an active analog SIC is highlighted in this paper. Moreover, the impact of SIC accuracy on the system performance is studied. The results demonstrate that the accuracy requirement will increase as the INR (Self-interference-to-noise Ratio) increases. The FDSM system is less sensitive than the FD system, which can get a better BER (Bit Error Rate) performance as errors increase. Furthermore, an SI detector is presented to resolve the influence of the number of detect symbols.

9:50 *Signal-to-Noise Ratio Considerations for Secure Antenna Polarization Modulation*

[Cara Yang Kataria](#) and [Steven Franke](#) (University of Illinois at Urbana-Champaign, USA); [Jennifer T. Bernhard](#) (University of Illinois at Urbana-Champaign & Electromagnetics Laboratory, USA)

We investigate the impact of additive white Gaussian noise on the performance of secure antenna polarization modulation (SAPM), a technique for wireless physical layer security. The secrecy rate, calculated from the mutual information of intended versus eavesdropper channels, serves as a metric for evaluation. With increasing signal-to-noise ratio (SNR), system designers can also choose to increase spectral efficiency by using a higher order of modulation. This significantly improves the level of security provided by SAPM by narrowing the range of spatial angles for which information may be received. We use simulation data to calculate the mutual information and symbol error probability over varying SNR levels to illustrate these effects.

10:10 Coffee Break

10:40 *Array Configuration Effect on the Spatial Correlation of MU-MIMO Channels in NLoS Environments*

[Navid Amani](#) (Chalmers University of Technology, Sweden); [Amirashkan Farsaei](#) (Eindhoven University of Technology, The Netherlands); [Ulf Gustavsson](#) (Ericsson AB, Sweden); [Thomas Eriksson](#) (Chalmers University of Technology, Sweden); [Frans MJ Willems](#) (Technical University Eindhoven, The Netherlands); [Marianna Ivashina](#) (Chalmers University of Technology, Sweden); [Rob Maaskant](#) (CHALMERS, Sweden)

In this paper, three different base-station antenna (BSA) configurations are compared in terms of inter-user spatial correlation in a two dimensional (2D) non-line-of-sight (NLoS) environment. The three configurations are: (i) a regular uniform linear array (ULA); (ii) a periodic sparse array; and (iii) an aperiodic sparse array. Electromagnetic modeling of the NLoS channel is proposed where scatterers are considered as resonant dipoles confined in clusters of scatterers (CoSs). While the probability of facing highly correlated user-equipments (UEs) in a multi-user multiple-input multiple-output (MU-MIMO) system is decreasing as the richness of multipath increases, the sparsity (increased inter-element spacing) is seen to be capable of reducing this probability as well. This is due to the larger spatial variations experienced by the sparse array. Moreover, the results show that further improvement can be achieved by deploying an aperiodic distribution of antenna elements into the sparse antenna aperture.

11:00 *Efficiency Analysis in Multibeam Wideband Phased Arrays*

[Riccardo Ozzola](#) and [Daniele Cavallo](#) (Delft University of Technology, The Netherlands)

We present a study on the performance of wideband, wide scanning arrays, when the elements are fed with a set of amplitudes and phases aiming at generating multiple independent beams. The formation of multiple beams is relevant in modern wireless communication applications, when diverse data streams can be sent from a single transmitter to users located in different directions. Wideband wide-scan arrays are characterized by strong mutual coupling between antenna elements. The impact of such coupling on the capability to generate multiple beams is investigated. More specifically the active reflection coefficient of the elements and the total efficiency of the array are estimated for different beamforming configurations.

11:20 *New High-Gain Differential-Fed Dual-Polarized Filtering Microstrip Antenna for 5G Applications*

[Yasir Ismael Abdulraheem Al-Yasir](#) (University of Bradford, United Kingdom (Great Britain)); [Naser Ojaroudi Parchin](#) (University of Bradford, United Kingdom, United Kingdom (Great Britain)); [Mohammad Fares](#) (University of Basra, Iraq); [Ahmed Maan Abdulkhaleq](#) (University of Bradford & SARAS Technology, United Kingdom (Great Britain)); [Maryam Sajedin](#) (University of Aveiro, Portugal); [Issa Elfegani](#) and [Jonathan Rodriguez](#) (Instituto de Telecomunicações, Portugal); [Raed A Abd-Alhameed](#) (University of Bradford, United Kingdom (Great Britain))

In this paper, a new high-gain differential-fed dual-polarized microstrip filtering antenna with high common-mode rejection is presented. Two differential pairs of probe feeding ports are utilized to provide differentially exciting signals. The filtering response is achieved by introducing four symmetrical open-loop ring resonator slots on the top layer surrounding the four excitation ports of the patch antenna. The resonators can produce nulls at the low edge of the passband bandwidth with high gain and wide stopband characteristics. Because of the strictly symmetric configuration of the proposed antenna, the design is studied and analyzed only in one polarization configuration. Compared with other presented filtering antenna designs, the proposed design has not only high gain and dual-polarized characteristics but also introduces high efficiency and much lower cross-polarization level due to the differentially driven ports.

11:40 *On the Use of the Observable Field to Synthesize Independent Beams from a Finite Volume*

[Andrea Neto](#) and [Arturo Fiorellini Bernardis](#) (Delft University of Technology, The Netherlands); [Angelo Freni](#) (University of Florence, Italy); [Nuria LLombart](#) (Delft University of Technology, The Netherlands)

In this contribution the meaning of independent plane waves that can be received by an antenna of given volume in terms of the wavelength is addressed. To define the independency of the beams we resort to the concept of the observable field, which was developed to investigate the properties of antennas in reception, and specifically the available power for antenna. We then define two incident plane waves as independent over a given domain, if the available power associated to the two arriving simultaneously is equal to the sum of the available power for each of the two plane waves. Finally the maximum number of independent beams that can be received by an antenna of given volume in terms of the wavelength is addressed.

12:00 *High-Gain Flat-Top Antenna Sub-Arrays for Planar Arrays with Limited Field of View*

[Ronis T. Maximidis](#) (Eindhoven University of Technology, The Netherlands); [Diego Caratelli](#) (The Antenna Company, The Netherlands); [Giovanni Toso](#) (European Space Agency, ESA ESTEC, The Netherlands); A. B. (Bart) Smolders (Eindhoven University of Technology, The Netherlands)

This paper presents an antenna array which is based on a novel sub-array architecture. Each sub-array is a linear array of open-ended waveguides. The proposed sub-array structure exhibits high-gain characteristics with a flat-top distribution and is used as a unit cell in a two-dimensional array. The distance between the sub-array centers along the relevant main axis is large in terms of wavelengths, which leads to limited scanning capabilities, whereas the inter-element separation along the orthogonal plane is about half free-space wavelength at the central working frequency, this leading to a wide scan range. Using the presented approach, an array operating at 28.5 GHz was designed in such a way as to feature a maximal scanning angle of $\pm 7.4^\circ$ along the E-plane and $\pm 27.45^\circ$ along the H-plane. The specific sub-array pattern, which approximates a rectangular pulse distribution, allows to filter out the grating lobes along the E-plane.

CS37: IRACON Spectrum Sharing: Challenges and Opportunities for 5G and Beyond

T02 Millimetre wave 5G / Convened Session / Propagation

Room: A3

Chairs: [Marina Barbiroli](#) (University of Bologna, Italy), [Doriana Guiducci](#) (European Communications Office, Denmark), [Sana Salous](#) (Durham University, United Kingdom (Great Britain))

8:30 Channel Measurements and Path Loss Modeling for Indoor THz Communication

[Naveed Ahmed Abbasi](#), [Arjun Hariharan](#), [Arun Moni Nair](#) and [Andreas Molisch](#) (University of Southern California, USA)

To explore the eventual deployment of communication systems in Terahertz (THz) band (0.1-10 THz) frequencies, extensive channel measurement campaigns are essential. In this regard, we conducted an indoor line-of-sight (LoS) measurement campaign up to 5.5 m on a THz channel sounding system that covers 140-220 GHz. We use a frequency-domain channel sounder that is based on a vector network analyzer (VNA) and frequency extenders for these measurements. Using the log-distance path loss model, we estimate the values of path loss exponent and the fading distribution standard deviations. The power delay profile analysis of our measurements shows that there are negligible multipaths in the LoS channels for the current scenario. Our results provide a platform for future exploration of THz band communication in the 140-220 GHz frequency range.

8:50 Characterization of the Propagation Channel in Conference Room Scenario at 190 GHz

[Diego Dupleich](#) (Ilmenau University of Technology, Germany); [Robert Müller](#) and [Sergii Skoblikov](#) (TU Ilmenau, Germany); [Markus Landmann](#) (Fraunhofer Institute for Integrated Circuits IIS, Germany); [Giovanni Del Galdo](#) (Fraunhofer Institute for Integrated Circuits IIS & Technische Universität Ilmenau, Germany); [Reiner S. Thomä](#) (Ilmenau University of Technology, Germany)

In the present paper we introduce unique double-directional dual-polarized measurements at 190 GHz in a conference room with the aim of characterizing propagation for channel modelling and beam-forming applications. Assisted by ray-tracing, multiple scatterers have been identified, showing a rich multi-path environment. Investigations have shown that polarization diversity increases spatial diversity and a more deterministic modelling approach in polarization is needed to avoid overestimating polarization diversity gains.

9:10 Enabling RF Technologies for Spectrum Sharing

[Mark Beach](#), [Leo Laughlin](#), [Eyad Arabi](#), [Simon Wilson](#), [Sarmad Ozan](#) and [Chris Gamlath](#) (University of Bristol, United Kingdom (Great Britain))

Spectrum sharing has the potential to significantly increase spectrum utilization in underused spectrum by facilitating shared access between primary/incumbent users and new commercial and private wireless services and applications. The citizen broadband radio service in the United States implements a basic form of dynamic spectrum access and is an example of spectrum sharing becoming a reality. Numerous regulatory changes in other countries are soon to follow. To make the most efficient use of spectrum in dynamic spectrum access regimes requires transceivers with excellent frequency agility, linearity, and selectivity, in order to opportunistically exploit available spectrum, whilst reducing interference and reducing the impact of interference. This article provides a brief overview of recently introduced spectrum sharing regulations, and discusses hardware requirements for current and future dynamic spectrum access. Recent advances in relevant RF technology enablers are presented, covering transmitter power amplifiers, multi-band receivers, self-interference cancellation, and reconfigurable antennas.

9:30 Assessing the Feasibility of the Spectrum Sharing Concepts for Private Industrial Networks Operating Above 5 GHz

[Pekka Ojanen](#) (Co-Worker Technology Finland, Finland); [Seppo Yrjölä](#) (Nokia & University of Oulu, Finland); [Marja Matinmikko-Blue](#) (University of Oulu, Centre for Wireless Communications, Finland)

Ongoing 5G deployment is bringing higher speeds, higher capacity, lower latency and greater reliability into connectivity enabling data sharing amongst participating components of industrial systems. The private industrial network opportunity for serving different verticals is largely dependent on the timely availability, quality and the cost of spectrum. The growing pressure to open the wireless market for location specific networks has resulted in new regional licensing and sharing-based models for spectrum management. This paper discusses private industrial network requirements for the spectrum management through a framework that can be used to assess the feasibility of the spectrum management approaches. Specifically, recent sharing concepts above 5 GHz in the US, Europe and four selected countries: Australia, Hong Kong, Japan and UK are analyzed from the viewpoint of private industrial networks. Each of the selected sharing concepts is a unique approach to make wideband spectrum available for other network providers than traditional MNO's.

9:50 Regulatory Requirements and Characterisation of Transmitter and Receiver Parameters to Set a Novel Framework for Spectrum Sharing

[Peter Faris](#) and [Doriana Guiducci](#) (European Communications Office, Denmark)

Increase in demand for spectrum due to new radio technologies such as 5G creates challenges for regulatory bodies to enable spectrum sharing. Regulatory limits for new types of equipment need to be set to enable sharing between different systems in the same or adjacent frequency bands. A balanced approach between limits for transmitter and receiver parameters is necessary in this context. Such limits are typically derived from coexistence studies which need to be based on realistic assumptions of device performance to ensure overall efficient and interference-free use of spectrum. This paper discusses recent developments in European regulations within the Electronic Communications Committee (ECC) of the European Conference of Postal and Telecommunications Administrations (CEPT) to enable new approaches for spectrum sharing in this context.

10:10 Coffee Break

10:40 A Study of an Environment Recognition Scheme Using WLAN CSI for Dynamic Spectrum Sharing

[Tomoki Murakami](#) (NTT Corporation, Japan); [Shinya Otsuki](#) (NTT Service Integration Laboratories, Japan); [Tomoaki Ogawa](#) (NTT, Japan); [Yasushi Takatori](#) (NTT Network Innovation Laboratories, Japan)

Diversifying devices and use scenarios have been focused on spectrum sharing according to communication environments in a target area. This paper proposes an environment recognition scheme for dynamic spectrum sharing systems. Our scheme dynamically uses CSI to allocate spectrum resources by recognizing the user location and the congestion rate in a target area. Furthermore, low-cost recognition can be expected with the IEEE 802.11ac WLAN CSI. To realize our scheme in realistic environments with actual devices, we developed a CSI monitoring system that uses the commodity WLAN devices, and we evaluated the environment recognition performance in our experimental measurements. We also prove the effectiveness of our scheme in experimental results of user locations and congestion rates.

11:00 A Kirchhoff Approximation Based Spectrum Availability Prediction Method at Millimeter Wave

[Kosuke Murakami](#) (Tokyo Institute Technology, Japan); [Jun-ichi Takada](#), [Kentaro Saito](#) and [Panawit Hanpinitasak](#) (Tokyo Institute of Technology, Japan)

This paper proposes a frequency resource detection method for dynamic spectrum sharing (DSS) using the Kirchhoff approximation (KA) technique. KA is a well-known technique that can deal with the path over multiple buildings, which is the most dominant path in the suburban area. Although many researches have done for investigation of the prediction accuracy, little study has been done to clarify its applicability for frequency resource detection in millimeter wave (mmWave) band. The proposed method utilized ordinary KA with building information and elevation profile considering blockage sensitivity of mmWave band. Moreover, the proposed model was designed to calculate minimum path loss by selecting only a few building edges that significantly block the line-of-sight (LOS) ray. Through this implementation, it is possible to limit the overestimation of the path loss while keeping the value bigger than free-space path loss (FSPL) to ensure the transmission opportunity of the secondary systems.

11:20 Highly-Reconfigurable Time-based Radiating Systems and Their Optimization

[Diego Masotti](#) (University of Bologna, Italy); [Lorenzo Poli](#) (ELEDIA Research Center, University of Trento, Italy); [Mazen Al Shanawani](#) (University of Bologna, Italy); [Paolo Rocca](#) (University of Trento, Italy); [Alessandra Costanzo](#) (DEI, University of Bologna, Italy)

This work aims at underlying the high reconfiguration capability of time-modulated arrays (TMAs) and their potential use in future 5G networks, as well as at stressing the need for a rigorous design tool when the optimization of these arrays is performed. The architectural simplicity of TMAs offers, as a counterpart, a complex dynamic radiating mechanism whose accurate description can significantly impact on the optimum solution. For this reason, a review of the available simulation strategies of TMAs is provided, mainly focusing on a recently proposed tool able to take into account all the dynamic linear and nonlinear phenomena occurring during a time-based radiation.

11:40 Joint Statistics of Urban Clutter Loss and Building Entry Loss at 3.5 GHz and 27 GHz - From Measurement to Modelling

[Richard Rudd](#) (Plum Consulting Ltd, United Kingdom (Great Britain)); [Xiaomin Meng](#), [Victor Ocheri](#), [Dehao Wu](#) and [Maziar Nekovee](#) (University of Sussex, United Kingdom (Great Britain))

Empirical propagation models have been developed within the ITU-R for building entry loss and for urban clutter loss. At present these mechanisms are considered separately, but, in practice, will generally be combined. Initial measurements at 35 GHz and 27 GHz are reported here which suggest that the effects cannot be considered as multiplicative, and a simple asymptotic model is proposed for their combination.

12:00 Building Entry Loss and Clutter Loss at 26 GHz

[Sana Salous](#) (Durham University, United Kingdom (Great Britain)); [Belen Montenegro Villaceros](#) (Formerly JRC, Italy); [James Bishop](#) (Joint Research Centre of the European Commission, Italy)

This paper presents results of building entry loss measurements, clutter loss measurements and combined building entry loss with clutter loss into a modern building at 26 GHz using a custom designed channel sounder developed at Durham University. Comparative measurements indicate that the median of building entry loss is about 42.6 dB when measured over a cluttered path and 42.9 dB when measured from outside the building. This indicates that the median building entry loss can be estimated from measurements over a cluttered path.

CS33: IET Session: New Antenna Systems Involving Application of Metamaterials and Metasurfaces

8:30 A Novel Metamaterial Dual-band GPS Antenna Extendable to Space Diversity Applications

[Changhyeong Lee](#), [Heejun Park](#) and [Gwang-Gyun Namgung](#) (Incheon National University, Korea (South)); [Yejune Seo](#) (Inchoen National University, Korea (South)); [Sungtek Kahng](#) (University of Incheon, Korea (South))

In this paper, a new design method is introduced for making a very compact metamaterial dual-band circular polarization(CP) antenna for global positioning system(GPS) L1(1.575 GHz) and L2(1.227 GHz) bands. In detail, first, the dual-band resonance and radiation come from the CRLH radiator with a ring-mushroom which makes the linearly polarized broadside beam. Second, for CP at the two GPS bands, we form a tilted cross-shaped slot on the patch and tune it. Third, the proposed metamaterial dual-band antenna is applied to four multiple antennas as space diversity approach like anti-jamming. Both simulated and measured results show that the proposed antenna achieves the good impedance matching, efficiency, axial ratio at the dual-band with low correlation-coefficient as a good inter-antenna isolation.

8:50 Circularly Polarized Concentric Metaring Antenna

[Hisamatsu Nakano](#) and [Tomoki Abe](#) (Hosei University, Japan); [Amit Mehta](#) (Swansea University, United Kingdom (Great Britain)); [Junji Yamauchi](#) (Hosei University, Japan)

First, a round metaloop antenna is analyzed as the reference antenna. The reference antenna radiates a left handed (LH) circularly polarized (CP) wave at frequencies around f_{Ni} , and a right handed (RH) CP wave at frequencies around f_{Hi} ($> f_{Ni}$). Second, a metaring is concentrically added to the inside of the reference antenna. This antenna is designated as the CMRA-inside. The CMRA-inside has larger LHCP and RHCP gains than the reference antenna. These larger gains appear at frequencies around f_{Ni-in} and f_{Hi-in} , respectively, where $f_{Ni-in} < f_{Ni}$ and $f_{Hi-in} > f_{Hi}$. Third, a metaring is concentrically added to the outside of the reference antenna (CMRA-outside). The CMRA-outside has larger LHCP and RHCP gains than the CMRA-inside. Frequencies f_{Ni-out} and f_{Hi-out} , where the maximum LHCP and RHCP gains respectively appear, are shifted with relationships $f_{Ni-out} > f_{Ni}$ and $f_{Hi-out} < f_{Hi}$. Other antenna characteristics of the CMRA-outside are also discussed.

9:10 Gaussian Horn Implemented by Metasurfaces

[Valentina Sozio](#) (Istituto Superiore Mario Boella, Italy); [Enrica Martini](#) (University of Siena, Italy); [Francesco Caminita](#) (Wave-Up SRL, Italy); [Paolo De Vita](#) (IDS Ingegneria Dei Sistemi S. p. A, Italy); [Andrea Giacomini](#) (Microwave Vision Italy, Italy); [Marco Sabbadini](#) (Esa Estec, The Netherlands); [Stefano Maci](#) (University of Siena, Italy); [Giuseppe Vecchi](#) (Politecnico di Torino, Italy)

We present design, realization and measurements of a Ku-band metasurface-based horn that emulates a Gaussian corrugated horn with the use of subwavelength patches printed on the internal walls. The design method is based on the adiabatic approximate solution for the hybrid mode of a conical waveguide with balanced impedance walls. This approach results in an analytic design method that does not require any optimization. The horn has been realized and experimentally characterized showing excellent agreement with both theory and simulations, with performance comparable with those of a conventional corrugated horn.

9:30 Broadband Circularly Polarized Metasurface Antenna Fed by a Rotated L-Shaped Probe

[Wei E. I. Liu](#) and [Zhi Ning Chen](#) (National University of Singapore, Singapore); [Xianming Qing](#) (Institute for Infocomm Research, Singapore)

A broadband low-profile circularly polarized (CP) metasurface antenna fed by a single rotated L-probe is proposed. With the L-shaped probe feed, an additional surface wave resonance is excited on the finite metasurface to enhance the bandwidth of the antenna. The single rotated L-probe fed asymmetrical metasurface antenna yields an overlapped impedance/gain/axial-ratio bandwidth of 20.7% from 5.71 GHz to 7.03 GHz, a peak gain of 8.85 dBi, and FBR higher than 19 dB, covering the 6-GHz band for coming WiFi 7 applications. Experiments are carried out as well to validate the proposed CP antenna design.

9:50 Coffee Break**10:20 Metamaterials for Electromagnetic and Thermal Waves**

[Erin Donnelly](#) (Edinburgh Napier University, United Kingdom (Great Britain)); [Antoine Durant](#) (Edinburgh Napier University, United Kingdom (Great Britain) & Université Grenoble Alpes, France); [Celia Lacoste](#) (INP-ENSEEIH University of Toulouse, United Kingdom (Great Britain)); [Luigi La Spada](#) (Edinburgh Napier University, United Kingdom (Great Britain))

In the last decade, electromagnetic metamaterials, thanks to their exotic properties, become crucial building blocks to develop new technologies in several applications. Until now metamaterials have been mostly associated with electromagnetism, but the same concept can be also applied to other wave phenomena, such as thermodynamics. For this reason, here the aim is to realize a metamaterial able to control simultaneously both electromagnetic and thermal waves. The structure is manufactured by using Additive Manufacturing techniques and tested for the following applications: sensing and medical diagnostics (optical and thermal imaging), military/safety (electromagnetic and thermal guiding structures) and automotive (electrical vehicles battery electric and thermal management). Experimental results reveal that such multi-functional metamaterial can fully manipulate and control both electromagnetic and thermal waves at will. The proposed structure appears to be highly versatile and scalable, with great potential to be used also for other wave phenomena such as mechanics, acoustics and hydrodynamics.

10:40 Evaluation of Aerosol Jet Printing of Frequency Selective Surface on Glass for Building and RF Applications

[Anshuman Shastri](#), [Kumar Putta](#) and [Benito Sanz-Izquierdo](#) (University of Kent, United Kingdom (Great Britain)); [Edward Parker](#) (The University of Kent, United Kingdom (Great Britain)); [Steven Gao](#) (University of Kent, United Kingdom (Great Britain)); [Lee Winchester](#) (The Centre for Process Innovation, United Kingdom (Great Britain)); [Alan McClelland](#) (CPI, United Kingdom (Great Britain))

The use of Aerosol Jet Printing technology to fabricate frequency selective surfaces (FSS) on glass for secure WLAN building applications is presented. Aerosol Jet Printing is combined with nano-particle silver inks to produce the FSS array. A square loop design in a square lattice is employed in this demonstrator. The structure operates around the 2.5 GHz frequency band commonly used in wireless communication systems and covers a wide range frequencies. A single layer array design is studied. Aerosol Jet printing is able to produce fine tracks needed for the design and provide sufficient conductivity for the filtering performance. The aim is to demonstrate a potential solution for the development of FSS for building and radio frequency (RF) shielding applications. In particular, windows can contain these printed RF structures and enhanced their RF capabilities. CST Microwave Studio was used for the simulation of the FSS. Simulations compare well with measurements.

11:00 Direct Antenna Modulator for m-QAM Applications

[Kenneth Lee Ford](#), [Stephen Henthorn](#) and [Timothy O'Farrell](#) (University of Sheffield, United Kingdom (Great Britain))

This paper introduces a concept for direct antenna modulation using a metasurface based antenna. The antenna can be controlled with the use of an external bias to control both the amplitude and phase of the transmitted signal, in a continuous way, to provide m-QAM direct antenna modulation. The DAM comprises of five metasurfaces, four of which control the transmitted phase through the use of a varactor diode, and the fifth uses a PIN diode to control the transmitted phase. Numerical simulations are presented which show that the transmitted phase can be varied over a 360 degree range with a amplitude dynamic range of 25dB.

11:20 Electrically Small Huygens Dipole Rectennas for Wirelessly Powering Internet-of-Things Sensors

[Wei Lin](#) (University of Technology Sydney, Australia); [Richard Ziolkowski](#) (University of Technology Sydney, Australia & University of Arizona, USA)

Linearly-polarized (LP) and circularly-polarized (CP) electrically small Huygens dipole rectennas for wirelessly powering compact Internet-of-Things (IoT) sensors at 915 MHz in the ISM band are reported. They are realized through the seamless integration of electrically small near-field resonant parasitic-based Huygens LP and CP antennas with a highly efficient rectifier circuit. The Huygens LP (HLP) antenna achieves a cardioid-shaped realized gain (RG) pattern with $RG=3.8$ dBi at the targeted frequency. Similarly the Huygens CP (HCP) antenna generates a cardioid pattern with $RG=3.2$ dBi and a 1.7 dB axial ratio value. Notably, the HLP and HCP antennas have inductive input impedances that facilitate matching directly to the 50 ohm source, thus eliminating a lossy inductor in the original rectifier. The prototyped HLP and HCP rectennas achieve close to 90% AC to DC conversion efficiency. Light and temperature IoT sensors wirelessly powered with custom-designed versions of these rectennas are successfully demonstrated.

11:40 Realizing Antenna Arrays with Huygens' Metasurface Pairs Based on a Moment-Method-Like Design

[Vasileios G. Ataloglou](#), [Ayman H. Dorrah](#) and [George V. Eleftheriades](#) (University of Toronto, Canada)

Huygens' metasurfaces have demonstrated great potential at manipulating electromagnetic fields at will. While omega-bianisotropy has allowed to design a single reflectionless metasurface for transformations that conserve local power, many applications, such as antenna beamforming, require control of both the amplitude and the phase of the transmitted fields. Pairs of reflectionless omega-bianisotropic metasurfaces have been proposed to break the condition of local power conservation. However, constraints on the minimum propagation length between the two metasurfaces, often lead to bulky designs. Here, an alternative method of designing a metasurface pair for arbitrary control of the amplitude and phase of the output fields is presented. The method relies on a power-based point matching process at the two metasurfaces and allows multiple reflections in the region between them. The usefulness of multiple reflections on the compactness of the metasurface pair is investigated through the design of a Chebyshev antenna array featuring a single feedpoint.

Friday, 20 March 8:30 - 10:10**T05-M06: Dosimetry, Exposure, and SAR Assessment**

Chair: [Dragan Poljak \(University of Split, Croatia\)](#)

8:30 *Frequency Selective EMF Measurements and Exposure Assessment in Indoor Office Environments*

[Nektarios Moraitis](#) (National Technical University of Athens & Institute of Communications and Computers Systems, Greece); [Ileana Popescu](#) and [Konstantina Nikita](#) (National Technical University of Athens, Greece)

The results of an extensive radio-frequency electromagnetic field (RF-EMF) measurement campaign in indoor office locations are presented. Frequency selective EMF recordings have been carried out in different corporate buildings between 75 and 3000 MHz. Exposure levels for the general public are extracted, assessed and compared with the national and international limits. The results from the entire building dataset reveal that the total electric field varies between 0.29 and 0.75 V/m (0.24-1.90 mW/m² in terms of total power density), whereas the mean Total Exposure Ratio (TER) is on the order of (3.35±1.41)·10⁻⁴. In all cases the exposure levels in indoor environments abide by the legislated limits. Furthermore, the exposure values are found to be strongly related with the floor level, increasing linearly. Finally, broadcast and cellular emissions account for more than 57% of the total radiated levels, especially at higher floors, where they reach up to 80%.

8:50 *Human Exposure to Electromagnetic Signals with Continuous Spectra*

[Dragan Poljak](#) (University of Split, Croatia); [Marin Galić](#) (Centar za Mjerenja u Okolisu, Croatia); [Lara Pajewski](#) (Sapienza University of Rome, Italy)

This paper is focused on the assessment of human exposure to electromagnetic signals with continuous spectra. A convenient and simple approach is proposed, to compare the measured field levels with the maximum exposure levels and verify compliance with the relevant regulations. In the presence of signals with continuous spectra, the proposed method yields more accurate results than the procedure outlined by the International Commission on Non-Ionizing Radiation Protection (ICNIRP). In particular, the proposed approach is based on the classical signal theory and requires the integration in the spectral domain of the electric field amplitude, or of the square of the electric field amplitude. Illustrative computational examples are presented, dealing with human exposure to Universal Mobile Telecommunications System (UMTS), Long-Term Evolution (LTE), experimental 5G, and Ground Penetrating Radar (GPR) signals. All of these examples are based on real measured data.

9:10 *Maximum Exposure Assessment of millimeter-Wave Array Antennas*

[Sylvain Reboux](#) (ZMT Zurich MedTech AG, Switzerland); [Serge Pfeifer](#) (Foundation for Research on Information Technologies in Society (ITIS Foundation), Switzerland); [Niels Kuster](#) (Foundation for Research on Information Technologies in Society, IT'IS Foundation, Switzerland)

5G user equipment makes use of array antennas to form beams according to a predefined codebook. In this paper, we provide an algorithm to determine upper bounds of maximum power density of array antennas from a set of electromagnetic field (EMF) realized by independent configurations. The method uses only EMF of the device under test (DUT) operating at configurations taken from the actual codebook and does not require absolute reference phase to be preserved between configurations. In all cases, the algorithm provides a conservative estimate of worst-case power density with limited overestimation. The proposed method therefore provides a practical way to assess compliance of millimeter-wave array antennas with as few as $N+1$ field measurements and is a valuable step forward for the standardization of RF EMF exposure compliance procedures of 5G devices.

9:30 *On the Focusing Technique for Hyperthermia Treatment Planning*

[Morteza Ghaderi Aram](#), [Massimiliano Zanoli](#) and [Hana Dobšiček Trefná](#) (Chalmers University of Technology, Sweden)

A focusing technique based on PSO is presented and compared with other methods. The optimization problem is initialized by taking advantage of TR-based, fast focusing outcomes. This shows to enhance the quality indicator and to speed up the whole process of optimization by lowering the chance of getting trapped in local minima. Simulation results for the neck applicator developed at Chalmers are reported for both a cylindrical phantom and a realistic patient model.

9:50 *A Fast and Rigorous Assessment of the Specific Absorption Rate (SAR) for MIMO Cellular Equipment Based on Vector Near-Field Measurements*

[Mounir Teniou](#), [Ourouk Jawad](#) and [Stephane Pannetrat](#) (ART-Fi, France); [Lyazid Aberbour](#) (Art-Fi, France)

This paper introduces a rigorous and fast procedure for accurate assessment of the peak averaged specific absorption rate (SAR), quantifying the user exposure to the electromagnetic field radiation from new-radio communication devices. Focus is lent to the specific class of user equipment that exploit multiple-input multiple-output (MIMO) technology and using exclusive simultaneous excitations of the active antenna-array system, such as expected on 5G devices. In contrast with the required $N(N-1)+1$ measurements on traditional SAR systems that only take measurements of the amplitude of the electric field, it is demonstrated in this paper that only $N+1$ number of measurements are required to evaluate the true SAR of a N -antenna MIMO thanks to using a vector near-field based SAR measurement system.

Friday, 20 March 8:30 - 12:20

T11-E06: Scattering and Diffraction

T11 Fundamental research and emerging technologies / Regular Session / Electromagnetics

Room: B4

Chair: [Ala Sharaiha \(Université de Rennes 1 & IETR, France\)](#)

8:30 *Scattering Control of Wideband Phased Arrays Using Metamaterial Absorbers*

[Zhechen Zhang](#) (University of Electronic Science and Technology of China, China); [Shi Wen Yang](#) (University of Electronic Science and Technology of china, China); [Yankai Ma](#), [Yikai Chen](#) and [Shi-Wei Qu](#) (University of Electronic Science and Technology of China, China)

a novel approach for the in-band scattering cross section (SCS) reduction of tightly coupled dipole arrays (TCDAs) illuminated by incident waves with polarization mismatch is proposed in this paper. The SCS reduction of the proposed array is achieved by placing the metamaterial absorbers over the aperture of the array. The metamaterial absorbers are comprised of resistive films, dielectric layers and polarization gates. The infinite array is able to achieve 3:1 impedance bandwidth with VSWR < 2.7 for scanning up to 60° in E-/H-plane. Moreover, simulated results demonstrate that the SCS of the designed TCDA array is reduced significantly throughout the entire operating bandwidth, while good radiation efficiency is still maintained.

8:50 *A Technique for Including Edge Diffraction Effects on RCS Evaluation at Fresnel Region Ranges*

[Ilie Valentin Mihai](#) (University Politehnica of Bucharest, Romania & The Institut d'Electronique et de Télécommunications de Rennes, France); [Razvan D. Tamas](#) (Constanta Maritime University, Romania); [Ala Sharaiha](#) (Université de Rennes 1 & IETR, France)

The aim of this paper is to propose a simple and low-cost technique to measure the RCS of a complex target in the Fresnel region and in a multipath environment. The diffracted field by the target is calculated using a method based on equivalent currents. The reflected field is computed using the physical optics approach and the tangent plane approximation. The ratio between the analytical expression of the radar cross section in the far-field and Fresnel region results in a field-zone extrapolation factor for the diffracted field. The RCS resulting from the scattering parameters measured at Fresnel region distances is then corrected with that field-zone extrapolation factor. The method was validated by simulations and measurements on a rectangular, metallic target.

9:10 *Perfect Matching of Reactive-Loaded Transmission Lines Through Complex Excitation*

[Angelica Viola Marini](#) (Università degli Studi Roma Tre, Italy); [Davide Ramaccia](#) (RomaTre University, Italy); [Alessandro Toscano](#) (University Roma Tre (IT), Italy); [Filiberto Bilotti](#) (University Roma Tre, Italy)

Any lossless transmission line terminated on an arbitrary reactive load suffers from reflections, due to the high impedance mismatch between the real characteristic impedance of the transmission line and the imaginary impedance of the load. A resistive lumped component must be added at the end of the line for ensuring power dissipation and achieving the required zero reflection. Here, we present a way to achieve perfect matching condition for purely reactive loads by exploiting the properties of complex frequency excitation. By exciting the circuit with a signal having a proper time profile, we demonstrate that the amplitude of the reflected wave can be brought to zero. Being the load purely reactive, energy isn't dissipated, but stored in the load, giving rise to an interesting singularity in the transient regime, referred to as virtual absorption. The stored energy can be released at will by changing or stopping the applied complex excitation.

9:30 *Negative Reflection and Refraction and Filter Characteristics in the Leaky Wave-supportable Gratings - TE Polarization Case*

[Soonwoo Park](#), [Hongjoon Kim](#) and [Young-Ki Cho](#) (Kyungpook National University, Korea (South)); [Ji-Hwan Ko](#) (Kumoh National Institute of Technology, Korea (South))

A negative reflection corresponding to retro-reflection and negative refraction phenomena are dealt with in the leaky wave-supportable reflection grating and transmission grating respectively. The transmission grating is designed based upon geometrical parameters for the Bragg-blazing phenomena in the reflection grating structure. The applicability of the transmission grating structure to the bandpass filter for normal incidence case is examined.

9:50 *How Radiation Propagates in Random Media: Spatial Structure of Transmission Eigenchannels*

[Ping Fang](#) (Beijing University of Posts and Telecommunications, Israel); [Chushun Tian](#) (Institute for Advanced Study, Tsinghua University, China); [Liyi Zhao](#) (Tsinghua University, China); [Yury Bliokh](#) (Technion-Israel Institute of Technology, Israel); [Valentin Freilikher](#) (Bar-Ilan University, Israel); [Franco Nori](#) (Center for Emergent Matter Science (CEMS), RIKEN, Japan)

Channeling of radiation through transmission eigenchannels is the dominant mechanism of wave propagation in diffusively scattering random media. In this presentation, the physical properties of these channels are studied numerically and analytically, and possibilities of applications are discussed.

10:10 *Study on the Location of mmWave Antenna for the Autonomous Car's Detection and Ranging Sensors*

[Ali Araghi](#) (University of Surrey, United Kingdom (Great Britain)); [Mohsen Khalily](#) (University of Surrey & 5G Innovation Centre, Institute for Communication Systems (ICS), United Kingdom (Great Britain)); [Pei Xiao](#) and [Rahim Tafazolli](#) (University of Surrey, United Kingdom (Great Britain))

The effect of vehicle's proximity on the radiation pattern when the RADAR's antenna is mounted on the body of autonomous cars is analysed. Two directional radiation patterns with different specifications are placed at different locations of a realistic car body model. The simulation is performed based on ray-tracing method at 77 GHz, the standard frequency for self-driving applications. It is shown that to obtain a robust RADAR sensor, the antenna radiation pattern is better to have relatively higher gain and lower side-lobe-level (SLL), than narrower half-power-beamwidth (HPBW) and higher front-to-back (F/B) ratio. Both academia and industry can benefit from this study.

10:30 Coffee Break

11:00 *Characteristic Far-Field Analysis of Scattering Due to Plane Wave Excitations*

[Xiong Kai Benjamin Chng](#) (DSO National Laboratories, Singapore)

In the theory of characteristic modes, a set of modes was derived such that the corresponding far fields are orthogonal over the infinite sphere. We exploit the orthogonality of these far fields to derive relationships between the modal parameters, such as the modal excitation coefficients, when a plane wave is incident on the obstacle. These results provide a useful framework for visualizing how each mode contributes to the overall scattering over a range of plane wave parameters, such as the wave-vectors and polarization. Validations were performed by comparing the theoretical analysis with simulations

11:20 *Electromagnetic Scattering by an Inhomogeneous Body of Revolution: a General Approach Based on the Hybrid Projection Method*

[Sergei P. Skobelev](#) (Radiophysika, Russia); [Ekaterina Semernya](#) (Moscow Institute of Physics and Technology, Russia)

Numerical analysis of a body of revolution consisting of a homogeneous dielectric sphere and an external inhomogeneous dielectric layer with arbitrary generatrix at its excitation by external sources is carried out. A general algorithm of the analysis developed in the paper is based on the hybrid projection method involving projection of the fields on the transverse vector spherical functions combined with the one-dimensional method of finite elements in the projection form. The algorithm is realized in a MATLAB code for the case of excitation of the body by a circularly polarized plane wave propagating along the axis of revolution. Test numerical results are presented for dielectric and plasma spheres displaced from the origin of coordinates along the axis and compared with the data obtained as result of rigorous analytic solution.

11:40 *Performance of Absorbing Periodic Structures of Cylindrical Black Holes Arranged on a Perfectly Conducting Screen*

[Yana Chizhevskaya](#) (Moscow Institute of Physics and Technology, Russia); [Olga Smolnikova](#) (Company Radiophysika, Russia); [Sergei P. Skobelev](#) (Radiophysika, Russia)

The problem of electromagnetic plane wave scattering by one-dimensional periodic structures composed of cylindrical radially inhomogeneous absorbing elements of black hole type arranged on a perfectly conducting screen is considered. Two algorithms corresponding to the cases of E- and H-polarization and accounting for the features of the black holes are developed on the basis of the hybrid projection method for solution of the problem. A number of numerical results characterizing both the effectiveness of the algorithms themselves and the properties of the black-hole-based absorbing structures are presented and discussed.

12:00 *Metasurface Modeling of Periodic Diffraction Gratings Based on Generalized Sheet Transition Conditions (GSTCs)*

[Ville Tiukuvaara](#), [Tom Smy](#) and [Shulabh Gupta](#) (Carleton University, Canada)

Space-modulated diffraction gratings are modelled and analyzed using a zero thickness metasurface grating approach, and demonstrated using numerical examples. The constitutive parameters of the grating are described using surface susceptibilities of the Lorentzian form, where their resonant frequencies are sinusoidally modulated. They are then solved self-consistently with the Generalized Sheet Transition Conditions (GSTCs) to determine the scattered fields from the metasurface for specified plane-wave incident fields, for various cases of modulation periodicities and depths.

Friday, 20 March 8:30 - 10:10

T11-M05: EMI/EMC/PIM Chambers, Instrumentation, and Measurements

T11 Fundamental research and emerging technologies / Regular Session / Measurements

Room: B5

Chairs: [Philipp del Hougne](#) (Institut de Physique de Nice, France), [Antonio Sorrentino](#) (Università degli Studi di Napoli Parthenope, Italy)

8:30 *Characterization of Stirrer Performance in Reverberation Chamber Using Characteristic Modes*

[Huilin Huang](#) (Xi'an Jiaotong University, China); [Xiaoming Chen](#), [Mengting Li](#), [Juan Chen](#) and [Qinlong Li](#) (Xi'an Jiaotong University, China)

In this paper, a new method to compare the effectiveness of a stirrer by calculating the number of characteristic modes of the stirrer is proposed. We find that, for Z-shaped stirrers, the more characteristic modes a stirrer has, the better it works in the reverberation chamber. The number of characteristic modes refer to the number of modes whose characteristic angles fall between 135 and 225 degree. The effectiveness of a stirrer is measured in terms of the field uniformity in the reverberation chamber. The field uniformity is defined as the standard deviation (STD) of the average power of the total electric fields at the eight vertices of the working volume. Three types of stirrers with the same rotational volume are used for verifications.

8:50 *Diffuse Field Cross-Correlation in a Reverberation Chamber Stirred with Reconfigurable Reflectarray Metasurfaces*

[Philipp del Hougne](#) (Institut de Physique de Nice, France); [Philippe Besnier](#) (IETR, France); [Fabrice Mortessagne](#), [Ulrich Kuhl](#) and [Olivier Legrand](#) (Institut de Physique de Nice, France); [Matthieu Davy](#) (University of Rennes 1 & IETR, France)

The impulse response between two antennas operating only in receive mode can be retrieved via cross-correlation techniques leveraging thermal noise or stirred chaotic wave fields in reverberation chambers (RCs). We report an implementation of the latter using an unconventional stirring mechanism: rather than rotating a mechanical mode stirrer, we use reconfigurable reflectarray metasurfaces placed on the RC walls in different random configurations. We detail how the data processing must be adapted to this stirring mechanism and we demonstrate the convergence of the cross-correlation toward the impulse response.

9:10 *Evaluation of the Purity of OAM Modes Using the Reverberation Chamber Technique*

[Wei Xue](#) (Xi'an Jiaotong University, China); [Xiaoming Chen](#) and [Hongyu Shi](#) (Xi'an Jiaotong University, China); [Huilin Huang](#) (Xi'an Jiaotong University, China); [Juan Chen](#) and [Anxue Zhang](#) (Xi'an Jiaotong University, China)

Orbital angular momentum (OAM) waves have been applied to various applications thanks to the orthogonality between different OAM modes. OAM waves can be generated using various techniques. However, the generated OAM waves in practice are not pure, which influences the OAM orthogonality. Thus it is important to evaluate the purity of the OAM modes. The common method for purity assessment is less convenient in practical measurements. In this paper, a novel method based on reverberation chamber (RC) is proposed to evaluate the purity of the OAM mode. Extensive RC measurements show that the correlation coefficient between OAM modes can be used to evaluate the purity of the OAM mode. Moreover, in contrast to the conventional measurement in the anechoic chamber, the proposed method can conveniently evaluate the purity over the entire measurement bandwidth for one measurement set, which is helpful in determining the working bandwidth of the OAM generator.

9:30 *A Dual-Polarized Asymptotic Conical Dipole (ACD) Sensor for Ultra-Wideband E-field Measurement*

[Mingxiang Gao](#) (Xi'an Jiaotong University, China); [Yanzhao Xie](#) (Xi'an Jiaotong University, China)

In this paper, a dual-polarized E-field sensor is designed for high power ultra-wideband (UWB) pulse measurement. Based on the technique of conventional asymptotic conical dipole (ACD) sensor, two pairs of planar ACD antennas are assembled perpendicularly for measuring E-field in dual polarization. Simulation results show the working effectiveness of the designed antenna for the circularly polarized E-field and the linearly polarized E-field with different polarization directions. As a result, a sensor prototype is developed, which consists of the dual-polarized ACD antennas and wideband baluns. In the electromagnetic compatibility (EMC) anechoic chamber, the fabricated sensor is successfully tested under UWB electromagnetic radiation, with the upper frequency of nearly 2.5 GHz.

9:50 *Novel Compact Waveguide Flange Adapter for Passive Intermodulation Measurement Systems*

[Xiang Chen](#) (Xi'an Jiaotong University & China Academy of Space Technology (Xi'an), China); [Wanzhao Cui](#) (China Academy of Space Technology Xi'an, China); [Dongquan Sun](#) (Xidian University, China); [Yongning He](#) (Xi'an Jiaotong University, China)

Passive intermodulation (PIM) measurement is necessary for microwave and antenna products to evaluate their PIM performance. To achieve stable low residual PIM level of measurement system and make accurate PIM test, a compact waveguide flange adapter is proposed based on gap waveguide, dielectric filled bed of nails is adopted to construct compact double-sided artificial magnetic conductor (AMC) structure. When the adapter is connected between standard waveguide flanges, double-sided contactless electromagnetic band gap (EBG) structure with air gap is formed inside the flange connection. Electromagnetic leakage is prevented by stop band of the EBG structure. Meanwhile, metallic contact nonlinearity is almost eliminated by the contactless structure, and PIM can be therefore suppressed. A Ku band prototype of the adapter is designed for a Ku band PIM measurement system. By using the adapter, the system's residual PIM is significantly improved with a maximum improvement better than 30dB, achieving a stable low level.

10:10 *Comparison of Antenna Radiation Efficiency Measurement Techniques in Reverberation Chamber Using or Not a Reference Antenna*

[Wafa Krouka](#) (Université Paris-Est & ESYCOM, France); [Francois Sarrazin](#) (University of Paris-Est-Marne-la-Vallée & ESYCOM, France); [Jérôme Sol](#) (INSA Rennes, France); [Philippe Besnier](#) (IETR, France); [Elodie Richalot](#) (Université Paris-Est (Marne-la-Vallée), France)

Antenna characterization using reverberation chamber (RC) has become the new trend in RC measurements. In this work, we compare three antenna characterization methods in RC. These methods are applied in order to determine the radiation efficiency of a patch and a log-periodic antenna. Results are compared and show good coherence. The accuracy of the applied methods is discussed and a solution is proposed in order to enhance the accuracy of reference antenna based methods.

Friday, 20 March 8:30 - 12:20

SW06: H2020 Session ID764479 (EMERALD): Electromagnetic Imaging for a Novel Generation of Medical Devices

T05 Biomedical and health / Convened Session / Electromagnetics

Room: B6

Chairs: [Marija Nikolic \(University of Belgrade, Serbia\)](#), [Jorge A. Tobon Vasquez \(Politecnico di Torino, Italy\)](#)

8:30 *Detailed Dielectric Characterisation of the Heart and Great Vessels*

[Niko Ištuk](#) (National University of Ireland, Galway & Translational Medical Device Lab, Ireland); [Barry McDermott](#) (Translational Medical Device Lab, National University of Ireland Galway, Ireland); [Emily Porter](#) (University of Texas at Austin, USA); [Adam Santorelli](#) (National University of Ireland, Galway & Translational Medical Device Lab, Ireland); [Soroush Abedi](#) (Group of Electrical Engineering - Paris, France); [Martin O'Halloran](#) (National University of Ireland, Galway, Ireland); [Nadine Joachimowicz](#) (Group of Electrical Engineering - Paris / CentraleSupélec, France); [Hélène Roussel](#) (Sorbonne Université, France)

The dielectric properties of biological tissues play a significant role in the planning and development of electromagnetic thermal therapies. In most cases in the literature, heart is considered as a homogeneous organ and its dielectric properties values are reported as such. In this paper, the results of dielectric property measurements on nineteen different parts of four ovine hearts are presented. The results of the measurements indicate that the dielectric properties vary between the different parts of the heart and therefore, the heart should not be considered to be homogeneous for accurate electromagnetic modelling.

8:50 *Homogenization of Voxel Models Using Material Mixing Formulas*

[Tushar Singh](#) (University of Belgrade & WIPL-D, Serbia); [Mladjen Stevanetic](#) (WIPL-D, Serbia); [Marija Stevanovic](#) and [Branko Kolundzija](#) (University of Belgrade, Serbia)

In this paper, we develop a procedure for simplifying highly inhomogeneous numerical phantoms based on dielectric mixing formulas. Numerical phantoms are extremely important in designing microwave imaging systems and algorithms. However, most of the realistic phantoms, typically obtained from magnetic resonance imaging (MRI) or computerized tomography (CT) scans are unsuitable for real-time analysis due to unlikely requirements for computational power and long processing time. Hence, it is of great importance to simplify such models without sacrificing the accuracy of the electromagnetic analysis. Here, we obtain simplified models by replacing a group of voxels by an effective permittivity computed by means of Looyenga and Lichtenecker methods. To assess the accuracy of the homogenized models with different resolutions, we compare their radar cross sections as well as transmissions between the antennas placed in their vicinity.

9:10 *Electromagnetic Virtual Prototyping of a Realistic 3-D Microwave Scanner for Brain Stroke Imaging*

[David O. Rodriguez Duarte](#), [Jorge A. Tobon Vasquez](#) and [Francesca Vipiana](#) (Politecnico di Torino, Italy)

Towards a preclinical prototype for diagnostic and monitoring of cerebral pathologies, here we present the 3D electromagnetic (EM) virtual prototyping of different clinical scenarios as an instrument for studying the interaction of biological tissues with EM waves, for designing a microwave brain imaging scanner and for generating a set EM fields usually required by imaging algorithms. We employ a full-wave modelling, which uses a Method of Moment (MoM) solver with high order basis functions and includes frequency variable electrical parameters for each component. The model of the microwave imaging system consists of 24-element conformal antennas, an anthropomorphic adult human head, and a spherical shape blood-filled as stroke. Here, the simulated system and data are tested applying an imaging algorithm based on Truncated Singular Value Decomposition (TSVD) and Born approximation, but they can be combined with other microwave imaging algorithms.

9:30 *Image Improvement Through Metamaterial Technology for Brain Stroke Detection*

[Olympia Karadima](#) (King's College London, United Kingdom (Great Britain)); [Eleonora Razzicchia](#) (King's College, United Kingdom (Great Britain)); [Panagiotis Kosmas](#) (King's College London, United Kingdom (Great Britain))

In this paper we investigate the capabilities of metamaterials technology to enhance the quality of reconstructed images for the problem of brain stroke detection. We integrate the metamaterial in our headband system for brain imaging in CST, and evaluate the reconstructed images of the head model that is placed inside the microwave tomographic head system, for the cases with and without the incorporated metamaterial. For image reconstruction we apply the distorted Born iterative method (DBIM) combined with two-step iterative shrinkage/thresholding (TwIST) algorithm. Our results indicate that, the use of our metamaterial can increase the signal difference due to the presence of a blood target, which translates into more accurate reconstructions of the target.

9:50 *Investigation of S-parameter Calibration Effects on Image Reconstruction in Microwave Imaging Systems*

[Manuel Kasper](#), [Mykolas Ragulskis](#), [Ferry Kienberger](#) and [Amin Moradpour](#) (Keysight Technologies, Austria)

In Microwave imaging systems, the goal is to find the differences of dielectric properties between healthy and malignant tissue by use of microwave signals; then from the resulting contrast, an image of the target is reconstructed. In order to do this, first, region of interest is illuminated by microwaves and ratios of incident and reflected signals are obtained by measuring S-parameters (reflection and transmission coefficients) with Vector Network Analyzer. Then, we use S-parameters as inputs for inverse scattering or back-propagation methods. In the end, by processing the data, image reconstruction is possible. Since S-parameters are the first input for MWI system, with this paper, we investigate on how S-parameter calibration affects the image reconstruction and accuracy. To dive deep into the topic, the existing calibration approaches in microwave imaging system will be discussed. Finally, the application of "unknown thru" as a new calibration method in MWI system and its advantages over other methods will be presented.

10:10 Coffee Break

10:40 *Temperature Dependent Dielectric Properties of Tissue Mimicking Phantom Material in the Microwave Frequency Range*

[Alexandra Prokhorova](#) and [Sebastian Ley](#) (Technische Universität Ilmenau, Germany); [Ondrej Fiser, Jr.](#) (Czech Technical University in Prague & Faculty of Biomedical Engineering, Czech Republic); [Jan Vrba](#) (Czech Technical University, Czech Republic); [Jürgen Sachs](#) (Ilmenau University of Technology, Germany); [Marko Helbig](#) (Technische Universität Ilmenau, Germany)

Microwave sensing represents a promising approach for non-invasive tissue temperature monitoring during hyperthermia treatment. Tissue mimicking phantom materials with corresponding dielectric properties and are suitable for heating experiments are essential for preliminary methodical investigations as well as for the development of the measurement hardware. In the present paper, a fat tissue mimicking phantom material is investigated depending on the temperature in the range between 30 °C and 50 °C and the frequency range between 0.5 GHz and 7 GHz. The measured data are modeled by means of a two-pole Cole-Cole model and the temperature dependence of the Cole-Cole parameters is fitted by means of a second-order polynomial.

11:00 *Monitoring Tumor Response During Chemotherapy Treatment with Microwave Imaging*

[Aleksandar Janjic](#), [Tuba Yilmaz](#), [Mehmet Çayören](#) and [Ibrahim Akduman](#) (Istanbul Technical University, Turkey); [Lorenzo Crocco](#) (CNR - National Research Council of Italy, Italy)

Chemotherapy treatment is a commonly used approach for treatment of localized malignant breast tumors. Ensuring accurate and reliable monitoring of the malignant tumor response to therapy can lead to the better follow-up care; thus, it would aid to increase the patient survival rate. In this paper, we introduce a microwave imaging system that can be used for breast cancer diagnostics and monitoring. The system is modeled in CST Microwave Studio and homogeneous breast model was used in order to assess its performance. Additionally, we propose a qualitative inverse scattering approach based on factorization method which allows us to monitor disease's evolution during and after the treatment. Results reported present preliminary assessment of proposed imaging approach and serve as a guideline for future work considerations.

11:20 *Development of a Transmission-Based Open-Ended Coaxial-Probe Suitable for Axillary Lymph Node Dielectric Measurements*

[Matteo Savazzi](#) (Universidade de Lisboa, Portugal); [Emily Porter](#) (University of Texas at Austin, USA); [Martin O'Halloran](#) (National University of Ireland, Galway, Ireland); [Jorge R. Costa](#) (Instituto de Telecomunicações / ISCTE-IUL, Portugal); [Carlos A. Fernandes](#) (Instituto de Telecomunicações, Instituto Superior Técnico, Portugal); [Joao M. Felicio](#) (Instituto de Telecomunicações, Portugal); [Raquel C. Conceição](#) (Instituto de Biofísica e Engenharia Biomédica, Faculdade de Ciências, Universidade de Lisboa, Portugal)

We assess the feasibility of a transmission-based open-ended coaxial-probe, which we intend to use for axillary lymph node dielectric measurement. The method consists in placing the material under test between two opposite open-ended coaxial-probes and measure the transmission coefficient. Numerical tests guided us in the choice of the probe design. The developed setup allows for enough propagation through a 5mm sample (which will be sufficient for the measurements of axillary lymph nodes), while confining the sensing volume to the region of interest. Moreover, we evaluate the viability of a comparative approach (simulations vs experiments) for the de-embedding of the dielectric properties. Experimental tests on phantoms showed good agreement between the measured and numerical transmission coefficient. Finally, we observed that the transmission coefficient can highlight the contrast between materials with different dielectric properties. The promising initial results motivate extending the application of the method to the case of axillary lymph nodes.

T06-A11: Aircraft Antennas

T06 Aircraft (incl. UAV, UAS, RPAS) and automotive / Regular Session / Antennas

Room: B7

Chairs: [Daniele Cavallo \(Delft University of Technology, The Netherlands\)](#), [Atif Shamim \(King Abdullah University of Science and Technology, Saudi Arabia\)](#)

8:30 *Bandwidth Enhanced Flexible UAV Antenna with 360 Azimuth Coverage for Air to Ground Communication*

[Azamat Bakytbekov](#) and [Atif Shamim](#) (King Abdullah University of Science and Technology, Saudi Arabia)

Utility of UAVs, particularly in hi-tech industries, is massive today and it is predicted to grow more. High data rate, air-to-ground, long range communication is still a bottleneck. UAV antenna is one of the most important part of the system and ideally it must be planar and conformal so that it does not create aerodynamics issues. Moreover, it must have omnidirectional radiation pattern to achieve 360 azimuthal coverage while maneuvering with decent gain and bandwidth. It is also required that the antenna performance is not deteriorated due to placement on UAV body. In this paper, an annular slot antenna has been designed which meets all the above-mentioned requirements. The antenna has omnidirectional radiation pattern with ~5 dB gain. Bandwidth enhancement has been achieved from 0.9% to 3% at 2.4 GHz on a thin substrate through additional parasitic slots. Flexibility analysis showed that the antenna works well in different bending conditions.

8:50 *Asymmetric Metasurface Antenna with Opposite Currents for Wide Beam and Low Profile Wide-Angle Scanning Phased Array*

[Yan-He Lv](#), [Xiao Ding](#) and [Bing-Zhong Wang](#) (University of Electronic Science and Technology of China, China)

We propose a novel and simple method based on an efficient asymmetric metasurface antenna (AMSA) to achieve a low-profile phased array for wide-angle scanning. The designed AMSA is constructed by asymmetrically loading MS of spiral unit cells on one side of a compact parasitic patch antenna. Due to the proposed MS, two opposite current layers are induced on adjacent patches, which results in a wide beam pattern instead of the narrow beam of a conventional parasitic patch antenna. Based on the AMSA with a wide beam, a one-dimensional phased array has been designed and simulated. The simulated results demonstrate that the AMSA phased array has a wide angle scanning range about $\pm 70^\circ$ and a low profile of 0.058 λ . With the advantages of simple structure, no back cavity, no floor slotting, and low profile, the proposed novel method provides an efficient alternate for wide beam and wide-angle scanning.

9:10 *Study of a Low-Loss Planar Radome for a Wide-Coverage Antenna*

[Hiromasa Nakajima](#) (Mitsubishi Electric Corporation, Japan); [Shin-ichi Yamamoto](#) (Mitsubishi Electric Corporation, Japan); [Michio Takikawa](#) (Mitsubishi Electric Corporation, Japan); [Naofumi Yoneda](#) (Mitsubishi Electric Corporation, Japan)

In this paper a multilayer radome with low-loss over a wide angle for Active Electronically Scanned Array (AESA) is proposed. The proposed radome is divided into some regions and the layer configuration of each region is optimized, depending on the incident angle from the antenna to the radome. This design approach leads to low transmission loss over a wide incident angle. In addition, the validity of the proposed radome is also shown in measurements.

9:30 *A Novel U-slot Aperture Coupled Annular-Ring Microstrip Patch Antenna for Multiband GNSS Applications*

[Kush Parikh](#) (Entuple Technologies, India)

A multiband circularly polarized novel U-slot aperture coupled annular ring antenna is proposed in this paper. The antenna covers the bands of IRNSS - L1; GPS - L1, L2 and GLONASS - L1. The antenna has a stacked structure with two substrates separated by an air gap. The top substrate has two annular rings and the bottom substrate has the U-slots and the power divider network. The transmission and radiation characteristics were simulated and measured for the above mentioned bands. Measured S11 is less than -10dB and axial ratio is better than 2.2dB over the proposed bands.

9:50 *Dual Band GNSS Antenna with High Back Lobe Suppression*

[Sachit Varma](#) and [Stefano Caizzone](#) (German Aerospace Center (DLR), Germany)

This paper presents the study of a novel design of a miniaturized GNSS antenna for E5a and E1 bands (i.e. at the central operating frequencies of 1.176 and 1.575 GHz) with high gain and very low back lobe for multipath reduction in high end static (e.g. geodesy) or dynamic (e.g. UAV) environments. The antenna itself is 56 mm in diameter and has a vertically stacked appurtenance of approximately 160 mm diameter that forces the cancellation of electromagnetic fields underneath the ground plane, thereby drastically improving the cross polarization discrimination and allowing for multipath suppression in both bands of operation.

10:10 Coffee Break

10:40 *Skewed Dipole Linear Array for Angular Filtering*

[Cristina Yepes](#) (Delft University of Technology, The Netherlands); [Erio Gandini](#) (ESA - European Space Agency, The Netherlands); [Stefania Monni](#) and [Frank van Vliet](#) (TNO Defence Security and Safety, The Netherlands); [Andrea Neto](#) and [Daniele Cavallo](#) (Delft University of Technology, The Netherlands)

In this work, we present a design of a linear array of tilted dipoles to achieve radiation patterns with asymmetric angular filtering characteristics. To realize the asymmetric radiation, the dipole elements are spaced by a distance larger than half a wavelength and loaded with artificial dielectrics to increase the front-to-back ratio and consequently to enable higher gain in certain desired angular regions. Based on the design, a linear array with 10 elements is manufactured and tested. The measured results show the ability of such an array to achieve stable gain from broadside up to 90 degrees scanning, while implementing a stop-band angular filter for negative scanning angles.

11:00 *A Wideband 122 GHz Cavity-Backed Dipole Antenna for Millimeter-Wave Radar Altimetry*

[Tobias Chaloun](#) and [Philipp Hügler](#) (Ulm University, Germany); [Christian Waldschmidt](#) (University of Ulm, Germany)

A wideband and robust design of a cavity-backed dipole antenna at D-band for radar altimeter applications is presented. The proposed antenna is based on a planar multilayer arrangement using standard PCB technology which enables the seamless integration into a affordable millimeter-wave sensor system. The antenna performance has been investigated by full wave simulations and validated through the fabrication and measurement of the antenna prototype. The experimental results of the realized antenna element shows excellent agreement to the simulated values. The dipole antenna covers a 10 dB impedance bandwidth from 119 GHz to 126.6 GHz and achieves a maximum gain of 6.9 dBi. The measured 3D radiation patterns at various frequencies across the operational band are provided.

11:20 *Edge Truncation Effects in a Wide-Scan Phased Array of Connected Bowtie Antenna Elements*

[Prabhat Khanal](#), [Jian Yang](#) and [Marianna Ivashina](#) (Chalmers University of Technology, Sweden); [Anders Höök](#) and [Ruoshan Luo](#) (SAAB AB, Sweden)

Edge truncation effects are critical when designing a phased array, as these can lead to the variation of the active antenna impedance and radiation pattern between individual array elements. This paper investigates edge truncation effects in an array of connected Bowtie antenna elements that has been initially designed through an infinite array approach. This design represents a novel implementation of the connected-array concept that offers a wide-scan performance with up to +/- 80-degree scan range in the E-plane (in the infinite array). The goal of this study is to estimate the minimum size of a realistic finite array of such connected Bowtie antennas.

11:40 *Amended Design of Travelling-Wave Slot Arrays*

[Soumya Sheel](#) and [Jacob Coetzee](#) (Queensland University of Technology, Australia)

Travelling wave slot arrays provide wider bandwidth in comparison to slot arrays implemented in standing wave configurations. Conventional travelling wave design techniques utilise Chebyshev excitations to achieve a desired radiation pattern, however, this results in increased sidelobe levels. This paper presents a 21-element travelling wave slot array implemented in substrate integrated waveguide (SIW) operating at 12 GHz. Design technique to calculate accurate slot excitations is presented and the proposed design is compared with those using the conventional technique. The proposed design achieves a pattern that closely resembles the required Chebyshev pattern with -25 dB sidelobe level and has less than 4 percent power dissipated into the load. The propose antenna has a bandwidth of 1 GHz.

12:00 *Design of Airborne Small Ultra-Wideband Spinning Direction Finding Antennas*

[YoungJu Park](#) (Agency for Defense Development, Korea (South))

Design, fabrication and measurement of a novel rotating direction finding antenna system for aviation use is presented. It can detect various radar signals in the ultra-wideband frequency region of 0.5-40 GHz. The whole antenna system is composed of antennas for low frequency band of 0.5-2 GHz and high frequency band of 2-40 GHz. Each antenna is designed to be small and lightweight. An array of log-periodic dipole array (LPDA) antennas on a lightweight support structure for aviation is proposed for the low frequency band. For the higher one, a reflector antenna using a single LPDA antenna as a feeder is designed. The designed each antenna is combined on a pedestal. All the simulation results are verified experimentally.

CS59: Reconfigurable Reflectarray and Transmitarrays

T09 Space (incl. cubesat) / Convened Session / Antennas

Room: B8

Chairs: [Nader Behdad](#) (University of Wisconsin-Madison, USA), [Nima Ghalichechian](#) (The Ohio State University, USA)

8:30 *On the Design of Multiband Antenna Employing AFSR Structure as Ground Plane for Low Out-of-Band RCS*

[Ahmed Abdelmottaleb Omar](#) (Pohang University of Science and Technology (POSTECH), Korea (South)); [Zhongxiang Shen](#) (Nanyang Technological University, Singapore); [Wonbin Hong](#) (Pohang University of Science and Technology (POSTECH), Korea (South))

Two design parameters of a multiband antenna with low radar cross-section (RCS) are studied in this paper. A dual-band absorptive frequency-selective reflection (AFSR) structure is utilized as the ground plane for a dual-band antenna to achieve low out-of-band RCS. The first parameter is the separation between the bandstop frequency-selective structure (FSS) and the absorber. Even-odd mode analysis is utilized to investigate the physical mechanism of the absorption occurring at the lower reflection band. Flat reflection band, which is important to maintain the radiation characteristics of the antenna, is realized based on this analysis. The second design parameter is the size of the metal ground

plane of the dual-band stacked patch antenna with the AFSR ground. The lower limit is bounded by achieving good antenna impedance matching at the low-frequency band while the upper limit is characterized by the RCS reduction performance.

8:50 *Steerable Reflectarray Using Tunable Height Dielectric for High-Power Applications*

[Kendrick Q Henderson](#) (The Ohio State University - The ElectroScience Lab, USA); [Nima Ghalichechian](#) (The Ohio State University, USA)

A reconfigurable reflectarray using a tunable height dielectric was designed for high-power applications. Each unit cell consists of a spiral slot etched into a metal sheet. The unit cell was able to support both linear and circular polarization without a change in the phase response. The design was able to achieve 330 degrees of phase range with a loss of 0.3 dB. Unlike other architectures that use semiconductor devices such as PIN diodes for tuning, the proposed mechanical reconfiguration of the dielectric layer beneath the slot enables high-power applications in radar and communication. A full-wave model was constructed for $10\lambda_0 \times 10\lambda_0$ square aperture consisting of 20×20 elements. The simulated reflectarray was able to steer the beam from -30 to 30 degrees with a 2.2 dB drop in the peak gain. The axial ratio was below 1.8 dB for both left-hand and right-hand circular polarizations at 20 GHz.

9:10 *A 2-Bit Phase-Shifting Unit Cell Design for Beam-Steerable Reflectarrays*

[Hung Luyen](#), [John Booske](#) and [Nader Behdad](#) (University of Wisconsin-Madison, USA)

This paper presents a 2-bit, 20% bandwidth, switch-controlled phase-shifting unit cell design for beam-steerable reflectarrays. The unit cell uses four single-junction connections, which can be replaced with single-pole single-throw switches, for selecting between four distinct reflection modes. Two of the four modes reflect an x- or y-polarized incident wave with a $+90^\circ$ and -90° polarization rotation while the other two provide non-polarization-rotating reflection. The dominant reflection coefficients of the four modes have relative phase values of 0, π , $\pi/2$, and $3\pi/2$, respectively. This results in 2-bit phase shifts for the reflected wave when the unit cell is illuminated with an incident wave polarized along either of its two diagonal lines. The proposed unit cell was used to construct a beam-steerable reflectarray operating at X-band. Full-wave simulation results predict an aperture efficiency of 42% at 10 GHz and a 3-dB gain bandwidth of 9-11 GHz (20%) for a $\pm 45^\circ$ scan range.

9:30 *Design of Multilayer, Dualband Metasurface Reflectarrays*

[Jordan Budhu](#) (University of Michigan, USA); [Anthony Grbic](#) (University of Michigan, Ann Arbor, USA); [Eric Michielssen](#) (University of Michigan, USA)

Reflectarray antennas are typically designed under the local periodicity approximation. Thus, mutual coupling is modeled as though the array is infinite in extent and made of identical elements. In dualband reflectarrays, elements are typically designed separately, with those at one frequency band operating with elements at the other band in the background. Elements are typically tuned to find the best compromise between the reflectarray's performance at one frequency versus the other. Such a design process leads to non-optimal designs. Here, we present an algorithm to design both layers of the reflectarray at both frequencies simultaneously. The reflectarray consists of two metasurfaces above a ground plane. The method accurately accounts for mutual coupling within the homogenized reflectarray, without resorting to local periodicity approximations. The design process produces practically realizable structures fabricable with standard printed circuit technologies. Subwavelength element patterning of the reflectarray surfaces also give rise to higher bandwidth.

9:50 Coffee Break

10:20 *Time Modulated Reflectarray Unit-Cells with Nonreciprocal Polarization Control*

[Santiago Spatola](#) (Universidad Politecnica de Madrid, Spain); [Juan Sebastián Gomez-Diaz](#) (University of California, Davis, USA); [Eduardo Carrasco](#) (Universidad Politecnica de Madrid, Spain)

This contribution explores nonreciprocal and reconfigurable reflectarray unit-cells with full polarization control based on time-modulated resonators. To this purpose, a unit-cell operating in the X-band is designed to aperture-couple each polarization of the impinging fields through a patch into a substrate integrated waveguide (SIW). The SIWs are loaded with varactor diodes which are biased using coplanar waveguides printed on the back side of the ground plane. There, upon adequate modulation parameters, waves undergo an efficient conversion process towards a desired harmonic and are then radiated back to free space. The photonic Aharonov-Bohm effect is exploited on each cells through modulation signals to independently control the phase and amplitude of the fields radiated with each polarization, thus allowing to obtain any polarization state and achieve nonreciprocity at the polarization level. We envision that this technology will have important implications in wireless terrestrial and satellite communication systems.

10:40 *P-i-n Diode Based Electronically Steerable Transmitarrays for SOTM at Ka-band*

[Francesco Foglia Manzillo](#) (CEA-LETI, France); [Maciej Smierzchalski](#) (CEA, France); [Antonio Clemente](#) (CEA-LETI Minatec, France); [Ronan Sauleau](#) (University of Rennes 1, France)

In this contribution, we present a preliminary assessment of the capabilities of electronically steerable transmitarray antennas for Ka-band satellite communications, with emphasis on SatCom-on-the-move (SOTM) up-link terminals. These studies build on a novel linearly-polarized four-state unit cell (UC) comprising four p-i-n diodes. The enhanced phase resolution allows one to increase the directivity by 2.5 dB with respect to state-of-the-art 1-bit TA designs and to reduce the sidelobe levels (SLLs). Several configurations based on a 50×50 -element transmitarray are analyzed to show the design trade-offs in terms of gain, bandwidth, scanning performance and size, in the case of linear polarization. The achieved gain patterns are also compared to stringent radiation envelopes defined by regulations for SOTM. Switchable circular polarization is demonstrated combining two sets of unit cells radiating orthogonal linear polarizations. As per simulations, the -3dB gain bandwidth spans from 28 to 31 GHz, with peak gain of 31.3 dBIC at broadside.

11:00 *Design of Microwave Imaging System Based on Reconfigurable Transmitarray with Variable Focuses*

[Xiaotian Pan](#), [Fan Yang](#), [Shenheng Xu](#) and [Maokun Li](#) (Tsinghua University, China)

The microwave imaging system based on vari-focal reconfigurable transmitarray (RTA) is presented and analyzed in this paper. Structure of the imaging system is presented, containing a focal-plane array and a vari-focal RTA. This imaging system can achieve flexible imaging distance, compared with conventional microwave front-view imaging method. Furthermore, by using cascaded RTAs, the image distance can be fixed, which is desirable for practical imaging system construction. This paper shows that the RTAs have promising potential in imaging systems.

11:20 *A Design Methodology for Reconfigurable Reflectarrays with a Deformable Ground*

[Claire Benteyn](#) (Heriot watt University, France); [Raphael Gillard](#) (IETR & INSA, France); [Erwan Fourn](#) (INSA of Rennes & IETR, France); [George Goussetis](#) (Heriot-Watt University, United Kingdom (Great Britain)); [Hervé Legay](#) (Thalès Alenia Space, France); [Leri Datashvili](#) (Large Space Structures (LSS) GmbH, Germany)

This article presents a new reconfigurable reflectarray concept involving mechanical actuators that modify the shape of an RF conductive flexible ground plane. The distance between the ground plane and the cells is used to control their reflected phase. A dedicated design methodology is proposed to optimize the performance while minimizing the number of actuators. As a first illustration, a 1D panel providing three different shaped beams with only four actuators is studied. Full-wave simulations with HFSS are used for validation.

11:40 *Performance Assessment of a Reconfigurable Circularly Polarized Reflectarray at K-Band*

[Roger Farias](#) (Instituto Superior Técnico, Portugal); [Custodio Peixeiro](#) (IST-University of Lisbon, Portugal); [Marcos V. T. Heckler](#) (Universidade Federal do Pampa, Brazil)

The performance assessment of a two-beam electronically switchable circularly polarized reflectarray antenna based on single-layer circular microstrip patches with phase delay line stubs is presented. Preliminary numerical analysis demonstrates the reflectarray capability to switch its main beam between 9.1° and 18.2° from the boresight in K-band (17.7-20.2 GHz). A very simple preliminary model is used for the envisaged PIN diode switches. For an array with 20×20 unit-cells, the achieved gain is above 27.2 dBic and the side-lobe level is below -18.2 dB at f_0 . Moreover, a remarkably low axial ratio of 1.1 dB is obtained for the whole frequency band of operation.

12:00 *Bandwidth and Efficiency Enhancement for 2-D Beamscanning Reflectarray Operating at X Band*

[Michael Trampler](#) (L3Harris, USA); [Ricardo Lovato](#) and [Xun Gong](#) (University of Central Florida, USA)

Continuous beamscanning reflectarrays can be realized by loading unit cell antenna elements with tunable devices. In a single-resonance unit cell, there is a fundamental limit in terms of phase range, loss and bandwidth. In order to enhance the frequency bandwidth without sacrificing the phase range and loss performance, dual-resonance unit cells are implemented to achieve >360 degree phase range with lower loss compared to single-resonance designs. A 7×7 beamscanning reflectarray using dual-resonance antenna elements is designed, fabricated and measured, exhibiting 7.81% 3dB gain fractional bandwidth, 15.02 dBi gain, and up to $\pm 50^\circ$ beamscanning angles operating at 10.1 GHz. This reflectarray is able to scan the beam in two dimensions.

T10-P02: Propagation Modelling and Simulation TOP

T10 EM modelling and simulation tools / Regular Session / Propagation

Room: B9

Chairs: [Rafael F. S. Caldeirinha](#) (Polytechnic Institute of Leiria & Instituto de Telecomunicações, Portugal), [Yang Miao](#) (University of Twente, The Netherlands)

8:30 *Deterministic Radio Channel Characterization for Near-Ground Wireless Sensor Networks Deployment Optimization in Smart Agriculture*

[Hicham Klaina](#) (University of Vigo, Spain); [Imanol Picallo](#) (Universidad Pública de Navarra, Spain); [Peio Lopez Iturri](#) (Universidad Publica de Navarra, Spain); [Leyre Azpilicueta](#) and [Mikel Celaya-Echarri](#) (Tecnologico de Monterrey, Mexico); [Otman Aghzout](#) (ENSA Tetouan - UAE, Morocco); [Francisco Falcone](#) (Universidad Publica de Navarra, Spain); [Ana Alejos](#) (Universidade de Vigo, Spain)

In this paper, a deterministic propagation modeling for wireless sensor networks in agriculture fields is presented. The impact of corn and potato fields on near-ground radio propagation is analyzed by means of an in-house 3D Ray Launching Simulator. Corn and Potato fields models have been developed taking into account the dielectric properties of each and every component of the field, as well as its morphology. Analyzing and understanding the influence of these fields on the wireless propagation is one of the important keys to the deployment of an optimal low cost WSN in smart agriculture.

8:50 *Indoor Channel Estimation Using Single-Snapshot Wideband Measurement*

[Yun Ai](#), [Michael Cheffena](#), [Marshad Mohamed](#) and [Ahmed Al-Saman](#) (Norwegian University of Science and Technology, Norway)

The successful design of communication systems generally requires knowledge of various channel characteristic parameters. This paper utilizes the reverberation time extracted from single-snapshot wideband measurement to estimate different indoor propagation parameters based on the room electromagnetics theory. The indoor room environment is conceived as a lossy cavity that is characterized by the diffuse scattering components resulting from the surrounding walls and objects and possibly a line-of-sight (LoS) component. The main advantages of the room electromagnetics based approach are simplicity and good accuracy. The approach needs only one wideband measurement in order to extract the reverberation time in addition to some dimensional information on the investigated room to predict various important channel parameter of great importance. The measurements show good agreement with the theoretical predicted results.

9:10 *Terahertz MIMO Fading Analysis and Doppler Modeling in a Data Center Environment*

[Chia-Lin Cheng](#) (Georgia Tech, USA); [Seun Sangodoyin](#) and [Alenka Zajic](#) (Georgia Institute of Technology, USA)

In this paper, we present results from a Terahertz (THz) channel measurement campaign in a data center environment. We analyze propagation parameters, such as pathloss, shadowing gain, and RMS delay spread. Amplitude fading statistics in a 4×4 Multiple-Input-Multiple-Output (MIMO) channel are also investigated. Furthermore, Doppler shift in THz bands due to the effect of cooling airflow turbulence, which causes cables (lying in the wireless propagation path) to vibrate is also measured. A two-dimensional (2-D) geometrical propagation model that includes moving scatterers (cables) is introduced. From the 2-D model, a corresponding Doppler power spectrum (DPS) is derived and validated with measured data. This work is pertinent to THz wireless systems design for a data center environment.

9:30 *Radiowave Propagation Modelling in the Presence of Wildfires: Initial Results*

[Stefânia Faria](#) and [Nuno R. Leonor](#) (Instituto de Telecomunicações, Portugal); [Carlos A. Fernandes](#) (Instituto de Telecomunicacoes, Instituto Superior Tecnico, Portugal); [Joao M. Felicio](#) (Instituto de Telecomunicações, Portugal); [Carlos Salema](#) (I.S.T. - Technical U. Lisbon / IT Lisbon, Portugal); [Rafael F. S. Caldeirinha](#) (Polytechnic Institute of Leiria & Instituto de Telecomunicações, Portugal)

In this paper, a thorough study of radiowave propagation phenomena in the presence of wildfires, is presented. Electrical modelling of a fire environment based on computational fluid dynamics is revisited. Modelling of the fire phenomena in terms of its refractive index and combustion of cold plasma lays the foundation for considering the fire environment as a propagation medium. Electrical models are formulated that are used to provide means of calculating propagation characteristics based on thermal-ionisation to create a plasma surface under fire environments and, thus, to determine of the excess loss arising in the burning area. The paper presents initial results for single trees under fire at 385 MHz, envisaged to assist in the identification of radio exclusion zones in real-time during wildfires, in mission critical applications.

9:50 *Implementation and Evaluation of Ray-Tracing Acceleration Methods in Wireless Communication*

[Hang Mi](#) (Beijing Jiaotong University & State Key Laboratory of Rail Traffic Control and Safety, China); [Danping He](#), [Ke Guan](#) and [Bo Ai](#) (Beijing Jiaotong University, China); [Chenji Liu](#), [Tianyun Shui](#), [Liju Zhu](#) and [Hui Mei](#) (Jiangxi Mobile Communication Company Limited, China)

Accurate channel modeling is critical to support the design and deployment of wireless communication systems. Ray-tracing (RT) based deterministic channel modeling has been considered as a key candidate to generate accurate channels for specified scenarios. However, the efficiency of RT decreases as the complexity of the environment increases. This factor significantly limits the applicability of RT, thus the acceleration technologies are highly demanded. In this paper, two space partitioning methods, including the uniform grid and the k-dimensional (k-D) tree, are implemented to accelerate RT by changing the storage structure of the environment. The efficiencies of both methods are compared in different environments with different configurations. As expected, the efficiency of RT has been improved considerably after being accelerated, and the application scenarios for both acceleration methods are derived. Finally, by comparing with the measurement and simulation, it is found that the accuracy of RT is not influenced after being accelerated.

10:10 Coffee Break

10:40 *A Speed Up of Split-Step Wavelet for the Computation of Long Range Propagation*

[Thomas Bonnafont](#), [Rémi Douvenot](#) and [Alexandre Chabory](#) (ENAC, France)

The atmospheric long-range propagation above the ground is of major importance for many ground systems as radars. The split-step wavelet method allows to compute efficiently this propagation using a pre-computed library for the wavelet-to-wavelet propagation. In this paper we propose a new method to efficiently compute the library needed for the propagation. From numerical experiments, we show that this novel method is faster to compute the library and as efficient in terms of precision and memory storage as the previous version.

11:00 *3D Simulation of Infinite Baffle Diffraction*

[Christopher G Hynes](#), [Roshanak Zabihi](#) and [Rodney Vaughan](#) (Simon Fraser University, Canada)

Diffraction formulations have infinite boundaries whereas simulations are solved with strictly limited dimensions. Consequently, the simulation of diffraction effects is challenging. Here, 3D electromagnetic simulations are described and compared against theoretical results for the diffraction of normally incident plane waves onto semi-infinite and infinite strip baffles. A detailed description is provided of the 3D simulation configuration necessary to successfully simulate the model. A simple expression is presented for the diffraction of an infinite strip. We show that it is possible to achieve excellent agreement between the Uniform Geometrical Theory of Diffraction and simulations. Accurate simulation results were only achieved by using the frequency domain with periodic boundary conditions and appropriately handling the bottom boundary for semi-infinite baffle diffraction.

11:20 *Simulation-based Investigation on Massive Multi-Antenna System as to Spatial Channel Hardening for Mobile Single User in a Controlled Multipath Environment*

[Yang Miao](#) (University of Twente, The Netherlands); [Sofie Pollin](#) (KU Leuven, Belgium); [Andrés Alayón Glazunov](#) (University of Twente, The Netherlands & Chalmers University of Technology, Sweden)

This paper brings up the concept of spatial hardening of massive MIMO radio channel in a controlled multipath cavity. The motivation is that, for a mobile user being active in certain area, the massive multi-antenna system shall guarantee the channel hardening in that area. This paper simulates the radio channel confined in a controllable indoor cavity using ray tracing, where the propagation environment contains reflecting and absorbing walls. The multipath channels composing of direct paths and specularly reflected paths up to a second order are analyzed as function of the large scale array topology and configuration in the cavity. We analyze the area focusing performance using a novel spatial channel hardening metric. This study is instructive for massive MIMO system design targeting at steadily hardened channel in an area for user with mobility.

11:40 *A Gamma Beta Mixture Model for Channel Multipath Components Clustering*

[Cheng Sun](#), [Yupeng Li](#), [Pan Tang](#) and [Jianhua Zhang](#) (Beijing University of Posts and Telecommunications, China); [Lei Tian](#) (Beijing University of Posts and Telecommunications & Wireless Technology Innovation Institute, China)

In this paper, a Gamma Beta Mixture Model (GBMM) is proposed to cluster channel multipath components (MPCs) where the gamma distribution is utilized to fit the delay data and angle data is fitted with beta distribution. We optimize the GBMM parameters with the expectation-maximization (EM) algorithm. Specially, in the M step of the EM algorithm, the Newton-Raphson method is utilized to optimize the GBMM parameters since we could not get closed solutions. To verify the clustering effect, an outdoor-to-indoor (O2I) measurement activity at 3.5 GHz was conducted. Simulation results based on real channel measurement data indicate that, compared with Gaussian mixture model (GMM), GBMM has better clustering performance.

12:00 *Time-Domain Modelling of Solid State RF Receiver Protection Systems*

[Luke J K Matthews](#) (The University of Nottingham, United Kingdom (Great Britain)); [Ana Vukovic](#) (University of Nottingham, United Kingdom (Great Britain)); [Christopher Mellor](#) (Nottingham University, United Kingdom (Great Britain)); [Phillip Sewell](#) and [Trevor Benson](#) (University of Nottingham, United Kingdom (Great Britain))

We investigate the effects of switching the state of a PIN diode from insulating to conducting as a component within a Solid State Receiver Protection (SSRP) system. The investigation follows a component adding process, ultimately arriving at a full configuration of a metallic post insulated from the waveguide by two dielectric blocks in the Off-state, which is then connected at one end in the on state. The effects of the diameter of the post are also studied. The S-parameters of the system are calculated from the voltage and current transmission line observations sampled directly with a single time-domain numerical method based upon an unstructured mesh.

CS11: Antenna Design and Fundamental Bounds with External Constraints

T11 Fundamental research and emerging technologies / Convened Session / Antennas

Room: B10

Chairs: [Fabien Ferrero](#) (University Nice Sophia Antipolis, CNRS, LEAT & CREMANT, France), [Lars Jonsson](#) (KTH Royal Institute of Technology, Sweden)

8:30 *Physical Bounds on Antennas with Feed Constraints*

[Mats Gustafsson](#) (Lund University, Sweden); [Miloslav Capek](#) (Czech Technical University in Prague, Czech Republic)

Antenna current optimization has been used to derive physical bounds on antenna parameters such as Q-factor, efficiency, gain, directivity, capacity, and radiation patterns. The success of the methodology is partly due to the assumption of perfect control of the antenna current in the antenna region which in practice producing an array antenna with multiple feeds. Details of the feed such as input impedance and placement are however essential in antenna synthesis and there has so far been no successful approach to include these types of constraints. In this presentation, we illustrate how feed constraints can be included in current optimization and discuss its associated challenges.

8:50 *Characteristic Mode Analysis of Mobile and Wearable Antennas in Lossy Environment*

[Pasi Ylä-Oijala](#), [Anu Lehtovuori](#) and [Rasmus Luomaniemi](#) (Aalto University, Finland)

Performing characteristic mode analysis for lossy structures is a new research theme, which can offer novel insights into the mobile and wearable antenna design. In this paper, we study two cases where lossy environment has a significant effect on the performance of an antenna: a mobile device in the user's hand and a smart watch in the wrist. We show how introducing lossy objects into the model changes the characteristic modes and makes interpretation of the results and their usability in practical antenna design more challenging.

9:10 **Adapting Frequency Domain Physical Bounds for the Analysis of Time-Varying Transmitters**

[Kurt Schab](#) (Santa Clara University, USA)

Based on recent theoretical and experimental results, a class of ideal transmitters based on time-varying matching networks (direct antenna modulation) is modeled using time domain distortion and classical models of ohmic conduction losses. This model is compared against classical bandwidth-efficiency bounds on linear time-invariant transmitters. Results show that optimal performance gains using direct antenna modulation is highly dependent on resonance conditions and matching network loss models.

9:30 **High Directivity, Omnidirectional Horizontally Polarized Antenna Array for Wireless Power Transfer in Internet-of-Things Applications**

[Wei Lin](#) (University of Technology Sydney, Australia); [Richard Ziolkowski](#) (University of Technology Sydney, Australia & University of Arizona, USA)

A high directivity, compact, omnidirectional horizontally polarized (OHP) antenna array is developed for wirelessly powering internet-of-things (IoT) devices. The antenna array is realized by seamlessly inserting several phase inverters inside an electrically long TE_{0,5,0} mode open waveguide. The phase inverter consists of a meandered slot and eight shorting vias. The meandered slot creates an interdigitated structure on the top surface of the waveguide; it introduces capacitance. The eight shorting vias are placed in an alternating pattern on the two sides of the slot; they produce inductance. The combination of the slot and vias forms a bandpass effect and inverts the electric fields in the waveguide. Consequently, a collinear and in-phase magnetic dipole array is realized. A compact eight-element OHP magnetic dipole array is designed, fabricated and measured. The measured results confirm the design concept and high directivity (10.4 dBi), omnidirectional HP radiation pattern has been achieved.

9:50 **Fundamental Bounds for Volumetric Structures and Their Feasibility**

[Miloslav Capek](#) and [Lukas Jelinek](#) (Czech Technical University in Prague, Czech Republic); [Mats Gustafsson](#) (Lund University, Sweden); [Kurt Schab](#) (Santa Clara University, USA)

Fundamental bounds on antenna and scattering metrics are presented in this paper utilizing volumetric method of moments. This makes it possible to investigate scenarios not solvable with classical surface method of moments which assumes that good conductors as used. One practical example is the study of plasmonic devices whose operation relies on the interaction between material properties and radiation mechanisms. The implementation of the code is briefly summarized, including some implementation hints which allow for fast evaluation of necessary matrix operators. Two optimization problems are introduced and solved for scattering and antenna problems. Feasibility of the bounds will be investigated with topology optimization and the results will be presented during the conference.

10:10 **Coffee Break**

10:40 **Nesting Dual Tapered Additively Manufactured Helical Antennas for Size Reduction Constraints**

[Youssef Tawk](#) and [Joseph Costantine](#) (American University of Beirut, Lebanon)

This paper presents novel dual tapered helical antenna structures that are 3D printed and nested within each other for size reduction. Each tapered helical antenna element is designed to operate at a distinct span of frequencies. The two helical antennas are nested together and wrapped in opposite direction to each other in order to satisfy orthogonal polarization. The two helical elements are fabricated using a laser based 3- D printing process where good measured radiation behavior is obtained.

11:00 **Experimental Assessment of Q-factor Bounds for Miniature Embedded Antenna**

[Fabien Ferrero](#) (University Nice Sophia Antipolis, CNRS, LEAT & CREMANT, France); [Lars Jonsson](#) (KTH Royal Institute of Technology, Sweden); [Philippe Ratajczak](#) (Orange Labs, France)

This work present the experimental assessment of frequency bandwidth limits on 2x2cm² antenna embedded in a 5x5cm² terminal at 900MHz. A meander Inverted F antenna is synthesized, prototyped and measured. Frequency bandwidth and radiation efficiency are extracted from radiation measurement. Comparison with optimal bounds on Q-factor show that this structure can reach the bandwidth fundamental limit.

11:20 **Optimal Bounds and Matching Networks of Fixed Degree and for Frequency Varying Impedances**

[David Martinez Martinez](#) (Inria Sophia Antipolis, France); [Adam Cooman](#) (Ampleon, The Netherlands); [Fabien Seyfert](#) and [Martine Olivi](#) (Inria Sophia Antipolis, France); [Stéphane Bila](#) (XLIM UMR 7252 Université de Limoges/CNRS, France)

In this paper, matching networks of finite degree are computed. Additionally the presented results are compared with the lower fundamental bounds available in the literature. These bounds are used to certify the optimality of the provided matching networks in function of the attained matching tolerance. To illustrate the presented results, two different examples of matching problems are presented.

11:40 **Q-factor Bounds for MIMO Antennas**

[Casimir Ehrenborg](#) and [Mats Gustafsson](#) (Lund University, Sweden); [Miloslav Capek](#) (Czech Technical University in Prague, Czech Republic)

The optimal spectral efficiency of MIMO antennas operating in an ideal channel with bandwidth requirements is analyzed in this paper. An optimization problem formulated in the input ports of a MIMO antenna is relaxed and solved to find an upper bound on the spectral efficiency using current optimization. It is shown that the solution depends only on the restricting Q-factor and a set of modes known as energy modes. A simple and useful method for using these modes to evaluate the quality of different shapes and design strategies is presented. It is shown that characteristic modes naturally maximize spectral efficiency by comparison to the energy modes. The ratio of spectral efficiency over Q-factor is studied and the existence of a Pareto optimal Q-factor for the trade off between them is shown.

12:00 **Transparent mm-Wave Array on a Glass Substrate with Surface Wave Reduction**

[Rocio Rodriguez-Cano](#), [Shuai Zhang](#) and [Gert Pedersen](#) (Aalborg University, Denmark)

In this paper, a transparent dual-element millimeter-wave (mm-wave) array for handsets is proposed. The antenna is mounted on top of a glass display and it is made by diamond grid cells that provide a transparency of 86 %. In order to reduce the surface waves generated and make the radiation pattern more directive, several rows of meshed patches have been placed in front of the mm-wave bow-tie array. The antenna array operates from 26.5 to 29.5 GHz and has a total efficiency of more than 70 % in the operating bandwidth. The array is able to steer the beam 70° with a realized gain higher than 7 dBi.

CS20: Assessment and Modeling of Antennas and Radio Channels Jointly

T10 EM modelling and simulation tools / Convened Session / Antennas

Room: B11

Chairs: [Danping He](#) (Beijing Jiaotong University, China), [Alain Sibille](#) (Telecom ParisTech, France), [Raffaele D'Errico](#) (CEA, LETI, Minatec Campus & Univ\ Grenoble-Alpes, France)

8:30 **Including the Aircraft and the Antenna in a Wide Band Aeronautical LMS Channel Model**

[Capucine Amielh](#), [Alexandre Chabory](#) and [Christophe Macabiau](#) (ENAC, France); [Laurent Azoulai](#) (Airbus Commercial Aircraft, France)

During airport ground navigation, aircraft pass close to obstacles such as buildings, other aircraft... These obstacles may be few meters from the antenna. In this context, modeling the antenna plus aircraft system as a radiation pattern is not justified due to the far-field hypothesis. To overcome this issue, the idea proposed here is to reduce the size of the radiating element to the antenna itself and to account for the aircraft structure in another way. To do so, the antenna plus aircraft is divided into 3 zones which contributions are dealt separately: the antenna is seen as gain, phase and group delay patterns, the fuselage in the near field of the antenna is modeled as a single multipath and the rest of the aircraft is considered as a source of multipath. By means of the theorem of superposition, the different contributions are gathered to get the complete antenna+aircraft model.

8:50 **Antenna Perturbation Modelling and Impact on Radio Channel**

[Laura Pometcu](#) and [Raffaele D'Errico](#) (CEA, LETI, Minatec Campus & Univ\ Grenoble-Alpes, France)

In this paper we investigate a joint antenna-channel model, considering stochastic variability on the radiating element. We considered a wide-band monopole antenna with a nearby metallic perturbation, whose position is random. The perturbed antenna characteristics are described through spherical wave expansion modes coefficient distribution in order to produce a stochastic antenna model. This model is then considered in a classical single cluster and indoor industrial channel, in order to evaluate the impact on delay and angular spread.

9:10 **The Influence of Self-User Shadowing in the Intra-Metro Communication Scenario at 28 GHz**

[Yuxuan Xu](#), [Danping He](#), [Haofan Yi](#) and [Ke Guan](#) (Beijing Jiaotong University, China); [Mikko Heino](#) (Aalto University, Finland); [Marko Sonkki](#) (University of Oulu, Finland)

Nowadays metro plays an important role in people's daily life. It is significant to realize a high-data-rate wireless connectivity in metro carriages. In this paper, the intra-metro channels with the consideration of self-user shadowing at 28 GHz are characterized by ray-tracing (RT) simulation. The three-dimensional metro model is reconstructed according to the actual size of Madrid Metro. Based on the RT simulation results, totally six cases (three transmitter deployments, with and without self-user shadowing) are characterized in terms of angular spreads, received power, root-mean-square (RMS) delay spread. Once the user shadows the channel, the received power will be approximately 15-25 dB less than that of unshadowed. Compared with the parameters of angular spreads and RMS delay spread without shadowing, the wireless link is established by Non-LOS due to the self-user shadowing effect. These results provide valuable insights into the system design and evaluation for wireless communications inside the metro scenario.

9:30 *Joint Antenna-Channel Modelling for in-to-out-Body Propagation of Dairy Cows at 868 MHz*

[Said Benaissa](#) (Ghent University/imec, Belgium); [Leen Verloock](#) (IBBT - Ghent University, Belgium); [Denys Nikolayev](#) (Institut d'Électronique et de Télécommunications de Rennes (UMR CNRS 6164), France); [Margot Deruyck](#) (Ghent University - IMEC, Belgium); [Gunter Vermeeren](#) and [Luc Martens](#) (Ghent University, Belgium); [Frank Tuytens](#) and [Bart Sonck](#) (Institute for Agricultural and Fisheries Research (ILVO), Belgium); [David Plets](#) (Ghent University - imec, Belgium); [Wout Joseph](#) (Ghent University/IMEC, Belgium)

In this paper, for the first time, the in-to-out-body path loss between a capsule antenna placed inside the cows' rumen and a distant gateway was characterized at 868 MHz. Measurements were conducted on five different fistulated cows in a dairy barn. The in-body antenna gain was then de-embedded from the wireless channel. The difference between free space measurements and in-to-out-body path loss assessment was used to quantify the path loss increase due to the cows' body. Results have shown an increase of the path loss on average (all cows) by 50.6 dB, with a variation between 43.7 and 55.3 dB. The obtained results were used to calculate the range of a LoRa (Long range) based network accounting for the antenna channel. With an input transmit power of 14 dBm, ranges up to 175 m in indoor and 364 m in outdoor were obtained depending on the used bit rate.

9:50 *A Practical Deconvolution Antenna Method to Retrieve Scattering Profile in Complex Random Media - A Vegetation Case Study at 28 GHz*

[Nuno R. Leonor](#) (Instituto de Telecomunicações, Portugal); [Telmo R. Fernandes](#) (IPLeiria / Institute of Telecommunications & ESTG/IT-DL, Portugal); [Rafael F. S. Caldeirinha](#) (Polytechnic Institute of Leiria & Instituto de Telecomunicações, Portugal)

This paper presents a method to improve the extraction the Radiative Energy Transfer (RET) theory input parameters for application in vegetation attenuation modeling. The input parameters for this model, which are extracted from specific measurement data, are normally influenced by the radiation pattern of the receiver antenna. A new method to improve the accuracy of the scattering function parameters obtained from measurements is presented. This method is based on the prior analysis of the antenna's radiation pattern distortion while measuring the scattering function, allowing the development of calibration curves, to correct the distorted propagation parameters. The proposed method was tested with measurements conducted inside an anechoic chamber, using real small indoor trees, mimicking a forest scenario using various different receiver antennas at 28 GHz, and the model accuracy improvement was assessed at various vegetation depths.

10:10 Coffee Break

10:40 *Towards Hybrid Statistical-Deterministic Wireless Channel Modelling of Multiroom Environments*

[Valon Blakaj](#) (Research Associate, United Kingdom (Great Britain)); [Shukai Ma](#) (University of Maryland, USA); [Steven Anlage](#) (Center for Nanophysics and Advanced Materials, USA); [Gabriele Gradoni](#) (University of Nottingham, United Kingdom (Great Britain)); [Thomas Antonsen](#) (University of Maryland, USA); [Stephen Creagh](#) and [Gregor Tanner](#) (University of Nottingham, United Kingdom (Great Britain))

The fluctuation of wireless signals propagating through a linear chain of cavities deviates from Gaussian. In multiply-connected environments, fluctuation statistics can be computed only in the room hosting the receiving terminal and can be used to establish fading margins independently from deterministic simulations performed for power coverage predictions. If the room hosting the detector is complex enough to support wave chaos and coupling with neighboring rooms is strong, those margins stand on the assumption of having Gaussian random signals. The signal fading induced at the receiving antenna critically depend on topology of and strength of coupling across the multiply connected environment. A simple formula for the kurtosis index of antenna currents that captures number of rooms and average number of channels coupling two contiguous rooms is obtained through the impedance-based random coupling model, which can be used to assist the fusion between deterministic and statistical coverage prediction tools.

11:00 *Directionally Resolved UWB Channel Modeling for Environment-Aware Positioning*

[Michael Rath](#) and [Erik Leitinger](#) (Graz University of Technology, Austria); [Anh Nguyen](#) (Hanoi University of Science and Technology, Vietnam); [Klaus Witrisal](#) (Graz University of Technology, Austria)

In this paper, we formulate a radio channel model for directionally resolved ultra-wideband radio measurements, which takes the directionality of a steerable antenna frontend into account. We outline a figure of merit to assess the quality of specular multipath components (SMCs) for positioning applications, the signal-to-noise-and-interference-ratio (SINR), and perform an analysis thereof for a practical environment on the basis of a measurement campaign conducted in a parking house. The angle resolved analysis of the SINRs of various SMCs establishes a site specific model of the radio environment that can be leveraged for location-aware radio positioning and communication systems.

11:20 *Millimeter-Wave Indoor Channel Measurement and Intra-Cluster Modelling*

[Minseok Kim](#), [Satoru Kishimoto](#) and [Keita Akasaka](#) (Niigata University, Japan)

A quasi-deterministic (Q-D) channel is an approach that considers the millimeter-wave propagation properties and has been adopted in IEEE 802.11ay. This study conducted the measurement campaigns in a conference room environment to develop and validate the Q-D channel modeling for indoor use scenarios. Using a super-resolution path parameter estimation algorithm, the multi-path clusters were extracted from the measurement data via the scattering process identification and clustering algorithm. This paper presents the stochastic model parameters (intra-cluster parameters) obtained from the clusters generated by the first-order specular reflection over the plasterboard wall which is a typical interior wall material. Moreover, they were experimentally validated via measuring small-scale fading due to specular reflection and diffuse scattering.

11:40 *Massive Radio Channel Sounder Architecture for 5G Mobility Scenarios: MaMIMOSA*

[Pierre Laly](#), [Davy P Gaillot](#) and [Gauthier Delbarre](#) (University of Lille, France); [Matthias Van den Bossche](#) and [Gunter Vermeeren](#) (Ghent University, Belgium); [Frédéric Challita](#) (University of Lille & IEMN Lab, France); [Emmeric Tanghe](#) (Ghent University, Belgium); [Eric P. Simon](#) (University of Lille, France); [Wout Joseph](#) (Ghent University/IMEC, Belgium); [Luc Martens](#) (Ghent University, Belgium); [Martine Liénard](#) (University of Lille, France)

This paper presents a real-time 64 x 16 massive MIMO channel sounder based on space-frequency division multiplexing and antenna subarray switching, giving a large possibility of antenna allocation and frequency tone between 2 and 12 GHz. This channel sounder called Massive MIMOSA or MaMIMOSA belongs to the new generation of software radio design based systems. The architecture of the proposed approach was designed with the highest flexibility thus opening a wide range of applications depending upon the investigated scenarios. Currently, the system is being setup using a massive 10 x 10 antenna array operating around 6 GHz with 80 MHz bandwidth for 5G V2X applications. The channel sounder can be powered with vehicle batteries to perform day long measurements when electrical outlets are not available. The output file gives the measured Massive MIMO matrix in a friendly compact binary format. It will be operational in early 2020.

12:00 *Smart Dipole Arrays for Radio Channel Enhancement*

[Juan Bucheli Garcia](#) (Huawei Technologies & Telecom Paristech, France); [Alain Sibille](#) (Telecom ParisTech, France); [Mohamed Kamoun](#) (Huawei France, France)

In this work we address the use of smart mirrors and smart scatterers as a way to enhance the radio channel properties from the point of view of the wireless link performance. The difference between both depends on their size, resulting in the 2nd or 4th power of the distance to the transmitter and the receiver, respectively, as explained on the basis of elementary electromagnetics. The performance of a smart device made of an array of dipoles in front of a perfectly conducting background reflector is subsequently analyzed, when operated as a scatterer. A simple model explains well the scattering behavior, provided the size of the reflector is sufficient, resulting in a performance as scatterer varying as the square of the number of dipoles.

SW09: Integration Challenges for Low-cost Mm-wave Phased Arrays

T12 Scientific / Industrial Workshops

Room: B3

Friday, 20 March 10:40 - 12:20

T02-M08: Mm-wave, THz, and Quasi-optical Antenna Measurements

T02 Millimetre wave 5G / Regular Session / Measurements

Room: B2

Chairs: [Marta Arias Campo](#) (IMST GmbH, Germany & Delft University of Technology, The Netherlands), [Dragan Poljak](#) (University of Split, Croatia)

10:40 *Experimental Characterization of a Wideband G-Band Circularly Polarized Lens Antenna*

[Marta Arias Campo](#) (IMST GmbH, Germany & Delft University of Technology, The Netherlands); [Giorgio Carluccio](#) (Delft University of Technology, The Netherlands); [Darwin Blanco](#) (Ericsson, Sweden); [Oliver Litschke](#) and [Simona Bruni](#) (IMST GmbH, Germany); [Nuria LLombart](#) (Delft University of Technology, The Netherlands)

The interest for mm- and sub-mm-wave systems has grown in the last years, mostly driven by communications and radar industries. In this context, not only new wideband high-gain antenna concepts are needed, but also advances in the applied antenna measurement procedures. In particular, the characterization of circularly polarized antennas represents a challenge in the higher frequencies, as the difficulty of achieving accurate phase measurements increases. In this work, the experimental characterization of a circularly polarized lens antenna in G-band (140-220GHz) is presented. Accurate measurement results are reached for the circularly polarized fields, showing excellent agreement with simulations.

11:00 *Experimental Validation of System NEP of a Single-Pixel THz Imaging Camera in CMOS*

[Sven van Berkel](#), [Satoshi Malotaux](#), [Carmine De Martino](#), [Marco Spirito](#), [Daniele Cavallo](#), [Andrea Neto](#) and [Nuria LLombart](#) (Delft University of Technology, The Netherlands)

CMOS technologies show great potential for realizing fully passive multi-pixel THz imagers without cooling the system. In order to achieve such high performance, system NEPs in the order of a few pW/sqrtHz are required, which are difficult to achieve in CMOS technologies. Accurate high-frequency models of the detectors, and an antenna-detector co-design are vital but not always readily available. This work presents the experimental derivation of a high-frequency model of the smallest Schottky Barrier Diode that is allowed for in a CMOS technology and the experimental validation of that model by means of a single-pixel THz imaging camera operating from 200 GHz to 600 GHz. The camera consists of a double bow-tie slot antenna in combination with a dielectric lens and offers an average system NEP of 50 pW/sqrtHz in the WR2 band.

11:20 *Measurement and Calculation of Exposure Level to 5G Base Station Antenna*

[Marin Galić](#) (Centar za Mjerenja u Okolisu, Croatia); [Dragan Poljak](#) (University of Split, Croatia); [Tajmin Tadic](#) (Environmental Measurement Center, Croatia)

The paper deals with the measurement and theoretical estimation of field levels generated by 5G base station antenna. The 5G base station antenna of interest operates in the frequency range between 3.4 GHz and 3.6 GHz. Both measurement and calculation of the field level have been carried out at 6 different points. The measurement has been undertaken using the Rohde&Schwarz measurement equipment including spectrum analyzer, isotropic antenna and suitable optical cables. The electric field calculation has been undertaken by free space and Modified Image Theory (MIT) approach, respectively. The exposure assessment has been estimated in accordance to well-known ICNIRP guidelines and by means of spectra integrals approach.

11:40 *Analysis of Substrate Parameters' Variations in a PCB-based 60 GHz GCPW Marchand Balun Design*

[Muhammad Umar](#) (Technische Universität Dresden, Germany); [Martin Laabs](#) (Dresden University of Technology, Germany); [Jacqueline Damas](#) (Technical University of Dresden, Germany); [Niels Neumann](#) (Technische Universität Dresden, Germany); [Dirk Plettemeier](#) (Dresden University of Technology, Germany)

A 60 GHz grounded coplanar-waveguide Marchand balun that is robust against variations of substrate height or dielectric constant is presented. The via-free design and minimum trace-width and trace-to-trace clearance of 0.1 mm makes it compatible for fabrication with economical PCB development technology. For optimal choice of height for a given substrate with known dielectric constant, EM-simulation results show 33% bandwidth with maximum amplitude and phase imbalance of 0.2 dB and 13 degree, respectively. The substrate dependency analysis in terms of height and dielectric constant show the possibility of implementing this GCPW balun on substrates with deviations in height or dielectric constant with tolerable performance degradation. It provides a cost-effective solution of measuring differential antennas and differential mmWave ICs using single-ended laboratory equipment. Simulation results are verified through fabrication and measurements of two baluns back-to-back connected through their differential ports. The measured results are in accordance with the simulated results.

12:00 *Echo Reduction Properties of Fast Non-Redundant Planar NF Sampling Methodologies*

Francesco D'Agostino, [Flaminio Ferrara](#), [Claudio Gennarelli](#) and [Rocco Guerriero](#) (University of Salerno, Italy); [Maria Alberica Saporetti](#), [Francesco Saccardi](#) and [Lars Foged](#) (Microwave Vision Italy, Italy); [Damiano Trenta](#) (European Space Agency, ESTEC, Italy)

The optimal sampling interpolation expansion is employed in near field measurements to reconstruct the field at any point of the observation surface starting from a non-redundant scanning scheme [1]-[3]. Such schemes allow faster measurements than classical Nyquist-compliant acquisitions. The methodology has no accuracy loss and has been validated at different bands and with different antennas [5], [6]. As the metrology restricts the source region to a surface conformal to the measured antenna, it intrinsically acts as low-pass spatial filter and thus possess echo reduction properties [7]. In this paper, the echo reduction benefits of the optimal sampling interpolation expansion applied to Planar Near Field measurements is investigated for the first time. A standard gain horn, MVG SGH4000 has been measured at V-band in an environment with controlled echoes. The results obtained with non-redundant methodology are compared against classical measurements post-processed with standard echo reduction techniques [8].

T11-M01: Material Characterisation and Non-destructive Testing

T11 Fundamental research and emerging technologies / Regular Session / Measurements

Room: B5

Chairs: [Zhirun Hu](#) (University of Manchester, United Kingdom (Great Britain)), [Alberto Toccafondi](#) (University of Siena, Italy)

10:40 *Bioinspired Sensor for the Electrical Permittivity Characterization of Dielectric Materials*

[João Guilherme Domingos de Oliveira](#) and [Samuel Paiva](#) (Universidade Federal do Rio Grande do Norte, Brazil); [Jose Garibaldi Duarte, Jr.](#) and [Luis Felipe V. T. Costa](#) (Federal University of Rio Grande do Norte, Brazil); [Valdemir S. Neto](#) and [Adaildo D´Assunção](#) (Universidade Federal do Rio Grande do Norte, Brazil)

A new bioinspired microstrip antenna is proposed to determine the electrical permittivity of dielectric materials. The antenna patch shape is inspired on the Shiso leaf, whose scientific name is Perilla Frutescens. A complementary interdigital capacitor (CIDC) is inserted in the patch antenna geometry. The antenna is simulated and designed using the Ansoft HFSS software. For validation purpose, a prototype of the proposed antenna is fabricated and measured. Thereafter, measurements are carried out to determine the electrical permittivity of three different dielectric materials samples based on the antenna resonant frequency variation in each case. A good agreement is observed between measured and simulated results, including those available in the literature for the considered materials.

11:00 *UHF and L-Band Microwave Measurements of the Antarctic Firn-Layer Complex Permittivity Depth Profile*

[Roberto Olmi](#) (National Research Council, Italy); [Saverio Priori](#) (IFAC CNR, Italy); [Federico Puggelli](#) and [Alberto Toccafondi](#) (University of Siena, Italy)

In order to characterize the complex permittivity depth profile of the firn constituting the Antarctic ice sheet, a microwave sensor, based on the open-coaxial re-entrant cavity method, is presented. Preliminary results of the measurements of firn permittivity depth profile, taken during an Antarctic campaign, are also presented, highlighting very good agreement with expected values.

11:20 *Broadband Microwave Dielectric Property Comparison of Human Fetal Osteoblastic (hFOB) and Osteosarcoma (SaOS-2) Cell Lines*

[Zeynep Macit](#), [Cemanur Aydinalp](#), [Tuba Yilmaz](#), [Ayse Buse Ozdabak Sert](#) and [Fatma Nese Kok](#) (Istanbul Technical University, Turkey)

This study investigates whether the dielectric property discrepancy is consistent on cell level between the malignant and normal cell samples to identify sources for dielectric property discrepancy in tissues and to enable microwave pathological applications. To this end, the dielectric properties of human fetal osteoblastic (hFOB) and osteosarcoma (SaOS-2) cell lines were measured in the frequency range of 500 MHz to 10 GHz using an open-ended coaxial probe. The measurements were conducted on pellet form and suspension form of cells, since there is no consensus on the protocol of cell line broadband dielectric property measurement. The discrepancy between hFOB and SaOS-2 cell suspensions at the whole measurement frequency are 0.1480% and 2.8267% for relative permittivity and conductivity, respectively. In pellet measurements, calculated percent discrepancy are to 2.1895% for relative permittivity and 3.6766% for conductivity.

11:40 *Non-invasive Blood Glucose Measurement Based on Microwave Resonator*

[Ayodunni Oloyo](#) and [Zhirun Hu](#) (University of Manchester, United Kingdom (Great Britain))

This paper presents a novel method for non-invasive continuous monitoring of blood glucose level using a microwave resonator. The technique has been tested on 8 participants for three days to determine the correlation between the standard invasive method of measuring blood glucose level and proposed novel non-invasive method. The results show a good correlation (R2=0.9967) between the novel non-invasive method and the standard invasive method with a percentage error of 2%, experimentally verifying that microwave resonator is capable of measuring the blood glucose level in a non-invasive way with minimum error and has the potential to replace the standard invasive method of measurement. The non-invasive measurement of blood glucose level has vital advantages for the management of diabetes and would significantly improve the health of diabetes patients. This approach would also help the NHS by reducing £1.5m spent every 10 minutes on diabetes. Index Terms- Diabetes, Non-Invasive Measurement, Permittivity.

12:00 *Dielectric Spectroscopy Characterization Within a Microfluidic Device Based on Open-Ended Coplanar Waveguide*

[Houssein Mariam](#) (Université Paris-Est Marne-la-Vallée, France); [Patrick Poulichet](#) (ESIEE, France); [Hakim Takhedmit](#) (Paris-Est Marne-la-Vallée University, France); [Elodie Richalot](#) (Université Paris-Est (Marne-la-Vallée), France); [Olivier Français](#) (ESIEE Paris, France)

This is paper reports a new instrumented microdevice which allows the characterization of liquid media by dielectric spectroscopy. Coplanar waveguides (CPW) in an open-ended configuration are used within a microfluidic channel and compared according to the shape of the aperture: single open-end or interdigitated capacitor. These microdevices are used in order to extract dielectric permittivity properties of liquid media. The proposed CPW sensors are analyzed and characterized in reflection within the frequency band ranging from 0.15 to 5 GHz. Microtechnologies are used to fabricate the devices which are coupled with microfluidic capability. The microfluidic channel is 100 µm thick and typical size of the interdigital capacitor is associated to an area of 150 µm length x 90 µm width. The volume under test is in the nanoliter range which is compatible with biological cells characterization and represents a progress in this field of interest.

Friday, 20 March 12:30 - 13:30

CC: Closing Ceremony

Room: A2

Chairs: [Olav Breinbjerg](#) (Technical University of Denmark, Denmark), [Cyril Mangenot](#) (Api-Space, France)